CROP BREEDING FOR DROUGHT RESISTANCE

EDITED BY: Lijun Luo, Hanwei Mei, Hui Xia, Roberto Tuberosa, Henry T. Nguyen and Baorong Lu

PUBLISHED IN: Frontiers in Plant Science

frontiers Research Topics

ISSN 1664-8714
ISBN 978-2-88945-861-5
DOI 10.3389/978-2-88945-861-5

About Frontiers

Frontiers is more than just an open-access publisher of scholarly articles: it is a pioneering approach to the world of academia, radically improving the way scholarly research is managed. The grand vision of Frontiers is a world where all people have an equal opportunity to seek, share and generate knowledge. Frontiers provides immediate and permanent online open access to all its publications, but this alone is not enough to realize our grand goals.

Frontiers Journal Series

The Frontiers Journal Series is a multi-tier and interdisciplinary set of open-access, online journals, promising a paradigm shift from the current review, selection and dissemination processes in academic publishing. All Frontiers journals are driven by researchers for researchers; therefore, they constitute a service to the scholarly community. At the same time, the Frontiers Journal Series operates on a revolutionary invention, the tiered publishing system, initially addressing specific communities of scholars, and gradually climbing up to broader public understanding, thus serving the interests of the lay society, too.

Dedication to Quality

Each Frontiers article is a landmark of the highest quality, thanks to genuinely collaborative interactions between authors and review editors, who include some of the world's best academicians. Research must be certified by peers before entering a stream of knowledge that may eventually reach the public - and shape society; therefore, Frontiers only applies the most rigorous and unbiased reviews.
Frontiers revolutionizes research publishing by freely delivering the most outstanding research, evaluated with no bias from both the academic and social point of view. By applying the most advanced information technologies, Frontiers is catapulting scholarly publishing into a new generation.

What are Frontiers Research Topics?

Frontiers Research Topics are very popular trademarks of the Frontiers Journals Series: they are collections of at least ten articles, all centered on a particular subject. With their unique mix of varied contributions from Original Research to Review Articles, Frontiers Research Topics unify the most influential researchers, the latest key findings and historical advances in a hot research area! Find out more on how to host your own Frontiers Research Topic or contribute to one as an author by contacting the Frontiers Editorial Office: researchtopics@frontiersin.org

CROP BREEDING FOR DROUGHT RESISTANCE

Topic Editors:
Lijun Luo, Shanghai Agrobiological Gene Center, China
Hanwei Mei, Shanghai Agrobiological Gene Center, China
Hui Xia, Shanghai Agrobiological Gene Center, China
Roberto Tuberosa, University of Bologna, Italy
Henry T. Nguyen, University of Missouri, United States
Baorong Lu, Ministry of Education Key Laboratory for Biodiversity and Ecological Engineering, Fudan University, China

Citation: Luo, L., Mei, H., Xia, H., Tuberosa, R., Nguyen, H. T., Lu, B., eds. (2019). Crop Breeding for Drought Resistance. Lausanne: Frontiers Media.
doi: 10.3389/978-2-88945-861-5

Table of Contents

4. OMICS

5. BREEDING IN FIELDS

6. REVIEWS

frontiers in Plant Science

EDITORIAL
published: 20 March 2019
doi: 10.3389/fpls.2019.00314

Editorial: Crop Breeding for Drought Resistance

Lijun Luo[1], *Hui Xia*[1]* *and Bao-Rong Lu*[2]

[1] Shanghai Agrobiological Gene Center, Shanghai, China, [2] Ministry of Education Key Laboratory for Biodiversity and Ecological Engineering, Fudan University, Shanghai, China

Keywords: drought-resistance, crop breeding, GWAS - genome-wide association study, transcriptome, phenotyping

Editorial on the Research Topic

Crop Breeding for Drought Resistance

The increased water shortage and frequent drought in agricultural ecosystems have caused tremendous problems worldwide, owning to the resulted yield losses for many crops. It is therefore essential to breed water-saving and drought-resistant crops to ensure world food security. Great progress has been made in the last decade in plant drought-resistance because of the novel findings and fast development of many new techniques and methodologies. However, accumulated knowledge about drought-resistance in crops is quite limited so far, particularly on the following questions: (1) How does drought-resistance evolve in crop during domestication; (2) How to identify drought-resistance genes and assess their potentials in breeding; (3) How to bridge the gap between theoretical research and crop breeding. To address these scientific questions, we need to establish the research topic, aiming to reveal the genetic, epigenetic, transcriptomic, and metabolomic bases of any trait associated with drought-resistance in crops, which can be applied in crop breeding.

During the last year or so, we have received more than 30 manuscripts focused on this topic and selected 13 research articles and two review articles for publication after rigorous peer review. These articles reported studies on eight crops, including rice, maize, barley, durum wheat, winter wheat, chickpea, cotton, and sweet pepper. Due to common interests in drought-resistance of different crops, any finding in a crop may provide informative references for another crop. We hope that studies on drought-resistance in different crops on this topic could benefit each other. Meanwhile, these articles apply various methodologies, including breeding and selection in the field, QTL mapping or genome wide association study (GWAS), comparative transcriptome, precise high-throughput phenotyping, and characterization of the drought-resistance genes, to study drought-resistance in different crops. To the benefit of our potential readers, we highlighted the key points of the 15 contributed articles in this research topic as follows:

Root architecture is the most promising characteristic for drought avoidance to be used in breeding. Such characteristics can greatly improve drought-resistance of crops by introducing or manipulating a single gene (e.g., *DRO1*). Lou et al. investigated transcriptomic divergences between deep-rooting and shallow-rooting rice genotypes. Based on the consistent results from a series of analyses and experimental validation, they conclude that the ATP synthesis should be a key factor to influence the root architecture. Their finding is novel and can provide valuable cues for other researchers to study genetic bases of deep-rooting in rice.

Identification of drought-resistance QTLs is essential to provide valuable targets in crop breeding. Li et al. identified four genetic regions containing SNPs significantly associated with several different traits in chickpea under drought by GWAS. This result indicated pleiotropic effects of drought-resistance associated QTLs. Gudys et al. identify 11 candidate QTLs of physiological and biochemical traits associated with drought-tolerance in Barley on a high-density function map. They further prioritize 143 candidate genes by their potential involvements in certain biological processes based on Gene Ontology annotation. Meanwhile, Cui et al. provided a new method

OPEN ACCESS

Edited and reviewed by:
Elena Prats,
Spanish National Research Council (CSIC), Spain

***Correspondence:**
Hui Xia
hxia@sagc.org.cn

Specialty section:
This article was submitted to Plant Breeding, a section of the journal Frontiers in Plant Science

Received: *30 January 2019*
Accepted: *26 February 2019*
Published: *20 March 2019*

Citation:
Luo L, Xia H and Lu B-R (2019) Editorial: Crop Breeding for Drought Resistance. Front. Plant Sci. 10:314. doi: 10.3389/fpls.2019.00314

to identify QTLs for drought-tolerance. They compared the allele frequency between drought-resistant introgression lines (resulted from strong selection in the field) and random populations and identified 13 major QTLs of drought-tolerance using the joint segregation distortion method. The most exciting result from their study is that the detected large-effect QTLs locate upstream of the genetic networks as putative regulators, which means that these QTLs could contribute significantly to drought-tolerance in breeding. In addition, they also suggest the designed QTL pyramiding strategy that is feasible for improving drought-tolerance in rice breeding.

One common difficulty for researchers to study drought-resistance is the precise evaluation of drought-resistance under field condition for a great number of genotypes. It is therefore essential to involve a high-throughput phenotyping technology in studying drought-resistance, which has drown researchers' attentions recently. Condorelli et al. described a high-throughput phenotyping platform by which the Normalized Difference Vegetation Index (NDVI) was used to precisely estimate drought-resistance traits in 248 durum wheat genotypes. Meanwhile, dozens of NDVI-based QTLs related to drought-resistance were identified by GWAS, indicating that this high-throughput phenotyping platform is valuable in the theoretical research and breeding practices.

The ABA-dependent pathway is very important for plants in responses to drought. In this volume, five articles characterized seven drought-resistance genes (*OsJAZ1*, *GhPLY9-11*, *OsDRAP1*, *ZmPLY8/9/12*, and *OsNAC14*) in various crops (Fu et al.; Liang et al.; He et al.; Huang et al.; Shim et al.) These genes could improve drought-resistance at seedling stage in different crops or transgenic *Arabidopsis*. However, the authors did not mention impacts of these genes on yield under drought. It is common that genes showing drought-tolerance only have minor effects in field. We consider pyramiding drought-tolerance genes, which may be a solution for the applications of these genes in production. However, such a strategy requires deep understanding in interactions among drought-resistance genes.

We appreciate the contribution from Lopes et al. who conduct large-scale field experiments to test the genotype-environment interactions in winter wheat in different experimental locations and seasons. Based on the results, they suggest that the narrow range of variation for phenology in families may facilitate the discovery and selection of new drought-resistant and -avoidant wheat lines targeting specific locations. Their proposal is valuable for the improvement of drought-resistant winter-wheat varieties.

Direct-seeding is an important method for water-saving agriculture in rice. Zhao et al. identify 13 of deep-sowing tolerance QTLs related to mesocotyl length by Non-syn GWAS (GWAS using non-synonyomous SNP). Although it is not directly related to drought-resistance, deep-sowing tolerance has a particular significance in promoting water-saving and drought-resistance rice production in China.

In one review article, Nepolean et al. reviewed the proceedings of research and breeding in maize drought-resistance, referringto precise phenotyping, genetic resources, breeding systems, drought-resistance genes, breeding informatics, etc. In the section of "MAIZE GENOMIC RESOURCES," the authors emphasized the importance of genetic resources for drought-resistance improvement. In another review article, Ding et al. discussed the cross-talk between drought-resistance, water transport, and nitrogen uptake in higher plants. They suggest that a good management of ammonium fertilization in the field could promote water-saving agriculture and improve drought-resistance in rice. In fact, potential associations between nutrition and drought-resistance become a hot spot recently, which is also discussed in the research article by Serret et al. It requires the efforts from both biologists and agronomists to determine the associations.

From the above contributions of this research topic, some valuable cues for better understanding of drought-resistance can be found. We hope that the knowledge can facilitate further success of new studies and breeding for drought-resistance crops. For better understanding of drought-resistance in crops, combined efforts among theoretical research, variety improvement, and field management are required. Finally, we greatly appreciate the efforts of the journal editors, peer reviewers, and authors. This volume would not be available without their great contribution. We hope that our readers can identify valuable information from this volume and also find appropriate collaborators to promote their great success.

AUTHOR CONTRIBUTIONS

All authors listed have made a substantial, direct and intellectual contribution to the work, and approved it for publication.

FUNDING

This work is supported by Shanghai Agriculture Applied Technology Development Program, China (Grant No. G2016060107), Shanghai Natural Science Foundation (17ZR1425500).

ACKNOWLEDGMENTS

We greatly appreciate the efforts of the journal editors, peer reviewers, and authors.

Conflict of Interest Statement: The authors declare that the research was conducted in the absence of any commercial or financial relationships that could be construed as a potential conflict of interest.

frontiers in Plant Science

ORIGINAL RESEARCH
published: 19 February 2018
doi: 10.3389/fpls.2018.00190

Investigating Drought Tolerance in Chickpea Using Genome-Wide Association Mapping and Genomic Selection Based on Whole-Genome Resequencing Data

Yongle Li[1], Pradeep Ruperao[2], Jacqueline Batley[3,4,5], David Edwards[3,4,5], Tanveer Khan[4,5], Timothy D. Colmer[4,5], Jiayin Pang[4,5], Kadambot H. M. Siddique[4,5] and Tim Sutton[1,6]*

[1] School of Agriculture, Food and Wine, The University of Adelaide, Adelaide, SA, Australia, [2] School of Agriculture and Food Sciences, The University of Queensland, Brisbane, QLD, Australia, [3] School of Biological Sciences, The University of Western Australia, Perth, WA, Australia, [4] The UWA Institute of Agriculture, The University of Western Australia, Perth, WA, Australia, [5] UWA School of Agriculture and Environment, The University of Western Australia, Perth, WA, Australia, [6] South Australian Research and Development Institute, Adelaide, SA, Australia

OPEN ACCESS

Edited by:
Hanwei Mei, Shanghai Agrobiological Gene Center, China

Reviewed by:
Liezhao Liu, Southwest University, China
Kevin E. McPhee, Montana State University, United States

***Correspondence:**
Yongle Li
yongle.li@adelaide.edu.au

Specialty section:
This article was submitted to Plant Breeding, a section of the journal Frontiers in Plant Science

Received: *12 October 2017*
Accepted: *01 February 2018*
Published: *19 February 2018*

Citation:
Li Y, Ruperao P, Batley J, Edwards D, Khan T, Colmer TD, Pang J, Siddique KHM and Sutton T (2018) Investigating Drought Tolerance in Chickpea Using Genome-Wide Association Mapping and Genomic Selection Based on Whole-Genome Resequencing Data. Front. Plant Sci. 9:190. doi: 10.3389/fpls.2018.00190

Drought tolerance is a complex trait that involves numerous genes. Identifying key causal genes or linked molecular markers can facilitate the fast development of drought tolerant varieties. Using a whole-genome resequencing approach, we sequenced 132 chickpea varieties and advanced breeding lines and found more than 144,000 single nucleotide polymorphisms (SNPs). We measured 13 yield and yield-related traits in three drought-prone environments of Western Australia. The genotypic effects were significant for all traits, and many traits showed highly significant correlations, ranging from 0.83 between grain yield and biomass to −0.67 between seed weight and seed emergence rate. To identify candidate genes, the SNP and trait data were incorporated into the SUPER genome-wide association study (GWAS) model, a modified version of the linear mixed model. We found that several SNPs from auxin-related genes, including auxin efflux carrier protein (PIN3), p-glycoprotein, and nodulin MtN21/EamA-like transporter, were significantly associated with yield and yield-related traits under drought-prone environments. We identified four genetic regions containing SNPs significantly associated with several different traits, which was an indication of pleiotropic effects. We also investigated the possibility of incorporating the GWAS results into a genomic selection (GS) model, which is another approach to deal with complex traits. Compared to using all SNPs, application of the GS model using subsets of SNPs significantly associated with the traits under investigation increased the prediction accuracies of three yield and yield-related traits by more than twofold. This has important implication for implementing GS in plant breeding programs.

Keywords: drought tolerance, genome-wide association mapping, genomic selection, chickpea, whole-genome resequencing, auxin

INTRODUCTION

Chickpea (*Cicer arietinum* L.) is ranked second after soybean in terms of global legume production, reaching ∼13 million tons in 2014 (FAOSTAT 2017). Consisting of 25% of the total exports worldwide, Australia was the second-largest producer and the largest exporter of chickpea in 2014 (FAOSTAT 2017). Chickpea is an important component of the farming system in Australia, serving as a disease break crop and nitrogen fixer (Knights et al., 2009; Siddique et al., 2013). Chickpea seed is a rich source of protein, essential minerals, and dietary fiber (Bar-El Dadon et al., 2017).

Drought is one of the most important constraints limiting yield potential in cereal and legume crops. Significant differences in terms of drought tolerance, measured by yield reduction, were observed among legume species in a meta-analysis of over 100 studies with chickpea ranking seventh among 13 legume species (Daryanto et al., 2015). There are generally two types of drought: transient drought and terminal drought. Transient drought is a short-term water deficit that can be relieved by precipitation and can occur at any stages of the growing season. Terminal drought is an unrelieved water deficit that terminates the reproductive growth of the plant. Terminal drought is very common in semi-arid tropics (South Asia, north-east Australia) and Mediterranean-type climates such as southern Australia. More than 80% of the world chickpea production is located in South Asia and north-east Australia. Australia has experienced severe drought events from the late 1990s to mid 2000s known as "the Millennium drought." As a consequence, the total production of irrigated rice and cotton fell by 99 and 84% during 2002 and 2009, respectively (van Dijk et al., 2013).

With current climate change projections, extremely hot weather will become more frequent and rainfall will be more erratic in Australia and other regions of the world (Hennesy et al., 2010; Foyer et al., 2016). The reproductive stage of growth is usually the most critical phase influencing grain yield in crops. It is well documented that drought stress during pod filling can lead to pod abortion thus reducing the number of seeds per plant (Leport et al., 1999; Fang et al., 2010; Pang et al., 2017). In a glasshouse experiment, seed yield declined by 85% in chickpea plants exposed to terminal drought at the early podding stage, relative to well-watered plants (Pang et al., 2017). There is an urgent need to develop chickpea varieties that are drought resilient.

Chickpea has a relatively small genome size of 730 Mb, compared to other food legumes such as lentil (*Lens culinaris* L.) and faba bean (*Vicia faba* L.). Thanks to the advance of next-generation sequencing (NGS) technology and a relatively small genome size, chickpea has well-developed genomic resources. Chickpea reference genomes for kabuli, desi, and wild *Cicer* species are available and there are ongoing efforts to improve the assemblies and annotation of the genomes (Jain et al., 2013; Varshney et al., 2013; Ruperao et al., 2014; Parween et al., 2015; Gupta et al., 2017). Whole-genome resequencing (WGRS) has emerged as one of the best methods for genome-wide association studies (GWAS) due to its potential to discover a large amount of sequence variants [single nucleotide polymorphisms (SNPs), Indel, CNV] in a cost effective manner. A recent study using this method narrowed down a major QTL for ascochyta blight resistance in chickpea (Li et al., 2017). Using WGRS data, several genomic regions were identified under positive selection for plasticity for yield, nitrogen fixation, and δ13C in chickpea under drought and/or heat conditions in the field (Sadras et al., 2016).

To identify QTL/genes associated with drought tolerance in chickpea, different forward-genetic approaches using various molecular markers have been used. A recent study using bi-parental mapping population (ILC588 × ILC 3279) and sparse simple sequence repeat (SSR) markers, identified 15 and 93 QTL associated with different drought-related traits (Rehman et al., 2011; Hamwieh et al., 2013). However, the resulting large QTL intervals have limited practical application in breeding. A "QTL-hotspot" region on chromosome 4 was identified using traditional QTL analysis with SSR and GBS (genotyping-by-sequencing) markers (Varshney et al., 2014b; Jaganathan et al., 2015). This region was further fine mapped to a ∼300 kb region, which contains 26 genes using a QTL bin-mapping approach and gene enrichment analysis by adding more SNPs (Kale et al., 2015). The authors also tested 12 genes for differential gene-expression profiling using real-time PCR. Under drought condition, several genes had higher gene-expression levels in the resistant line than in susceptible lines, including E3 ubiquitin ligase, serine/threonine protein kinases, and homocysteine S-methyltransferase. Another study, employing the GWAS approach, discovered over 200 markers associated with drought-related traits using SSR, DArT, and SNP markers (Thudi et al., 2014). The results, albeit needing further validation, are promising for marker-assisted selection. However, the development of these molecular markers is labor-intensive and not cost-effective.

One of the challenges of marker-assisted selection is how to pyramid numerous markers with small effect size, particularly for complex traits such as yield under drought environments (Collins et al., 2008). As such, genomic selection (GS), also known as genome-wide selection, was proposed as an alternative method for marker-assisted selection for complex traits (Meuwissen et al., 2001). GS uses information from all of the markers to estimate the breeding value of plants, thus eliminating the complicated pyramiding process in marker-assisted selection. This approach is more relevant to breeding programs as it can help select the best parents for crossing and reduce the cost and time of a standard breeding cycle; thus it has been adopted rapidly by many livestock and crop breeding programs (Hayes et al., 2009a; Meuwissen and Goddard, 2010; Crossa et al., 2014). Traditionally, animal scientists estimated breeding values by best linear unbiased prediction (BLUP) using the additive-genetic relationship matrix obtained from pedigree information (Henderson, 1975). Thanks to advances in genotyping and NGS technology, a large amount of molecular markers can be obtained at a relatively low cost (Davey et al., 2011; Elshire et al., 2011; Poland and Rife, 2012). The genomic estimated breeding values can be estimated more accurately using the ridge regression BLUP (RR-BLUP) model which replaces the pedigree matrix (**A** matrix) with the genomic relationship matrix (**G** matrix), which is obtained from genome-wide markers (VanRaden, 2008; Hayes et al.,

2009b). A simulation study in barley showed that GS was better than phenotypic selection when the traits had low heritability and the training population was large enough. Ziyomo and Bernardo (2013) demonstrated in a real experiment that GS is superior to indirect phenotypic selection using secondary traits for improving drought tolerance of maize. However, a recent GS study in chickpea showed that prediction accuracies of yield under rainfed environments were much lower than under irrigated environments (Roorkiwal et al., 2016). A similar observation was reported in synthetic wheat, posing a challenge to improving drought tolerance using GS (Jafarzadeh et al., 2016). A new method is needed to increase prediction accuracy, particularly when applied to drought-stressed environments. The objectives of this study were to: (1) identify candidate genes/SNPs significantly associated with yield and yield-related traits under drought stressed environments using GWAS approaches; and (2) investigate whether incorporation of the GWAS result can increase prediction accuracy.

MATERIALS AND METHODS

Plant Materials and Field Experiments

Plant materials included 13 Australian released varieties and 119 Australian and Indian-derived breeding lines, which were selected for yield potential and adaptation to drought-prone environments. The field experiments are described in detail by Pang et al. (2017). Briefly, chickpea accessions were planted in plots (6 × 1.5 m) in Western Australia at one site in 2012 and two sites in 2013. There were three replicates for each site. Rainfall at the three sites during the growing seasons ranged from 196 to 230 mm, and no irrigation was supplied. Twelve traits were measured: grain yield per ha (GY), hundred seed weight (100SW), seed number per plant (SN), empty pod ratio (EPR), harvest index (HI), biomass dry weight (DW), flowering time score (FT), podding time score (PT), maturity score (MA), emergence score (EM), early vigor score (EV), and plant height (PH). Five plants per plot were randomly cut at ground level to measure SN, EPR, HI, and DW. Scores for FT, PT, MA, EM, and EV were on a 1–9 scale.

Phenotypic Analysis

The three sites were first analyzed separately for each trait by fitting a linear mixed model (LMM), which included spatial effects (row and column effects). The resulting best linear unbiased estimator (BLUE) values for each genotype were used to fit a multiple-environment LMM in which environments were treated as random effects. Statistical significance of fixed and random effects were assessed using Wald's test (Wald, 1943) and the likelihood ratio test, respectively (Van Belle et al., 2004). The resulting BLUE values were subsequently used for GWAS analysis. Broad-sense heritability (h^2) was estimated using the following formula:

$$\hat{h}^2 = \hat{\sigma}_g^2/(\hat{\sigma}_g^2+\hat{\sigma}_{ge}^2/t+\hat{\sigma}_e^2/rt)$$

where $\hat{\sigma}_g^2$, $\hat{\sigma}_{ge}^2$, and $\hat{\sigma}_e^2$ denote genotypic variance, genotype × environment interaction variance, and experimental error variance, respectively. t and r are the numbers of environments and replications within an environment, respectively. All phenotypic analysis was done using GenStat, 16th edition.

WGRS and SNP Discovery

DNA of the 132 genotypes was extracted from young leaf tissues using the Qiagen DNeasy Plant Mini Kit following the manufacturer's instruction. Paired-end sequencing libraries were constructed using the TruSeq library kit for each genotype with an insert size of 500 bp. The procedure was implemented according to the Illumina manufacturer's instruction. Paired-end short reads (150 bp) were generated using the Illumina HiSeq 2000 platform. Sequence data is available from the NCBI Short Read Archive under BioProject accession PRJNA375953. Paired-end reads for each genotype were trimmed, filtered, and mapped to the kabuli reference genome 2.6.3[1] using SOAP2. Homozygous SNPs were called using the SGSautoSNP pipeline (Lorenc et al., 2012).

Population Structure and Linkage Disequilibrium

To correct for confounding effects in the association studies, population structure was estimated based on 144,777 SNPs (MAF > 0.05) using ADMIXTURE (v1.23) software (Alexander and Lange, 2011). Similar to the popular software STRUCTURE, ADMIXTURE uses a model-based algorithm to estimate the ancestry of unrelated individuals. The number of underlying population groups (K) was estimated from 1 to 10 using the maximum likelihood estimation approach with a fast numerical optimization algorithm. Cross-validation method of Alexander and Lange (2011) was used to determine the most likely number of population group (K). Linkage disequilibrium (LD) was measured by the parameter r^2 using SNPs with high confidence (minimum five reads per genotype). An $r^2 = 0.2$ was used as a threshold to determine LD extent. The method to estimate the LD-decay curve under the mutation-drift-equilibrium model was described in detail in Li et al. (2011).

Genome-Wide Association Mapping

Genome-wide association analysis was done using BLUE values of the 132 genotypes with 12 traits and 144,777 SNPs (MAF > 0.05). Adjusting the confounding effects of population structure and kinship, the SUPER GWAS method, implemented in the GAPIT software, was used to estimate each SNP effect (Lipka et al., 2012; Tang et al., 2016). This method can increase statistical power by estimating kinship matrix with a subset of markers which are not in LD with the testing marker (Wang et al., 2014). The kinship matrix was estimated using the VanRaden method and later compressed to its optimum groups using the P3D method to speed up computation time. Default parameters of the SUPER model were used: sangwich.top = "MLM,"

[1] http://www.cicer.info/databases.php

sangwich.bottom = "SUPER," LD = 0.1. The significant *p*-value cut-off was set as $p = 3.45e\text{-}07$, equivalent to the α level of 0.05 after Bonferroni correction. The two genes flanking the significant SNP are reported.

Genomic Selection

Genomic predictions were performed using three different models: RR-BLUP, Bayesian least absolute shrinkage and selection operator (Bayesian LASSO or BL), and Bayesian ridge regression (BRR). The RR-BLUP model is written as:

$$y = \mu 1_n + Zg + e, \quad e \sim \mathrm{N}(0, \mathrm{I}\sigma^2), ,$$

where y is the adjusted entry means of phenotypes, μ is the overall mean, $1n$ denotes $n \times 1$ vector of 1s, **Z** is an incident matrix for random genotype effect, and g is genotype effect with normal distribution N (0, $\mathbf{G}\sigma_g^2$), where **G** is the genomic relationship matrix obtained from markers (VanRaden, 2008). The markers included all 147,777 markers or a subset of markers selected based on different levels of *p*-value from GWAS.

The general structure of the two Bayesian linear regressions BL and BRR can be written as,

$$\mathrm{p}(\mu, \boldsymbol{\beta}, \sigma^2 | \mathbf{y}, \boldsymbol{\theta}),$$

the posterior probability of unknown parameters includes overall mean μ, marker effect β, and its variance σ^2, given the data y and hyperparameters **θ**. Estimates of these unknown parameters are obtained by solving the optimization problem and adding a penalty function to **β**. For BRR, the same Gaussian prior was assigned to **β**, resulting in the same shrinkage for all markers. For BL, a Bayesian version of the least absolute shrinkage and selection operation (Tibshirani, 1996) was introduced in the penalty function of **β**, resulting in greater shrinkage of markers with small effects and less shrinkage of markers with large effects. BL has a special feature of both variables selection and shrinkage, whereas BRR only shrinks variables. The detailed similarities and differences between genomic prediction models are reviewed by de Los Campos et al. (2013). The R package synbreed was used to fit the three models (Wimmer et al., 2012).

A fivefold cross-validation was performed to evaluate the prediction performance of the three models. The whole dataset was randomly divided into five mutually exclusive subsets, four of which formed the training set for fitting the model and the fifth was used as a test set. This process was repeated ten times, resulting in 50 cross-validations. Predictive abilities were calculated as Pearson's correlation coefficient between the predicted values and observed phenotypic values of the test set. An average predictive ability of 50 cross-validations was reported.

RESULTS

Yield and Yield-Related Traits

In total, 12 traits including phenology, yield, and yield components were measured. Multiple-environment linear mixed-models were fitted to obtain BLUE values for each genotype (**Table 1** and Supplementary Figure S1). The genotypic effect of SN was significant at an alpha level of 0.05 while the other 11 traits were highly significant at an alpha level of 0.001 (**Table 1**). Heritabilities (h^2) of the 12 traits ranged from 0.11 for GY to 0.91 for 100SW. Many traits showed highly significant correlations, ranging from 0.83 between GY and DW to −0.67 between 100SW and EM (**Table 2**). GY was positively correlated with 100SW, SN, DW, FT, PT, EM, EV and negatively correlated with EPR, MA, and PH. 100SW was positively correlated with FT, DW, MA and negatively correlated with SN, PT, and EM. GY has a highly positive correlation with DW ($r = 0.83$), which is not surprising, given that a strong and healthy plant with sufficient biomass is advantageous under drought to retain yield (Hamwieh et al., 2013; Kashiwagi et al., 2013). PT and MA were negatively correlated (−0.64), which appears counterintuitive. Due to the low temperatures in early spring in Australian environments, some genotypes originating from India with an early podding trait, aborted their early onset pods which is reflected in the negative correlation between PT and EPR (i.e., the earlier the podding time, the higher the EPR). This supports the observation that chickpea plants need to set pods within a fairly narrow window to optimize yield in Australian environment.

SNP, Linkage Disequilibrium, and Population Structure

A total of 144,777 homozygous SNPs were discovered in 132 genotypes (**Table 3**). The number of SNPs on each chromosome ranged from 25,323 on Ca4 to 4,740 on Ca8, partially reflecting the length of the chromosomes in the Kabuli 2.6.3 reference assembly. The extent of LD on each chromosome ranged from 4,000 kb on Ca3 to 150 kb on Ca6 with an average of 700 kb (**Table 3** and Supplementary Figure S2). The average extent of LD is almost seven times smaller than a previous study, in which mainly Australian-released chickpea varieties were used (Li et al., 2017). The short extent of LD in the 132 genotypes has the potential to enable higher mapping resolution. To avoid false positive results in association analysis, the population structure was investigated using 144,777 SNPs (**Figure 1**). The most likely number of groups (K) in the 132 genotypes was estimated to be two using a cross-validation method from the ADMIXTURE software. The red group in **Figure 1** is mainly the DICC lines (selected from ICRISAT breeding lines) consisting of progenies from the crosses of ICCV98503 × Moti, ICCV96836 × PBG5, ICCV96836 × ICC12004, and ICCV96836 × ICC3996. The green group in **Figure 1** consists of Australian-released varieties and advanced lines. Genotypes with a mixture of red and green have mixed ancestry from ICRISAT, ICARDA, and Australia.

Genome-Wide Association Mapping

In total, 38 SNPs were significantly ($p < 3.45e\text{-}07$) associated with six traits: GY, 100SW, EPR, PT, EM, and EV (Supplementary Table S1 and **Figures 2**, **3**). One SNP, located in Ca3: 18,924,965, was significantly associated with GY (**Figure 2**). The closest gene near this SNP encodes a protein belonging to the ABC transporter B family/p-glycoprotein (PGP). Nine SNPs, located on Ca3, Ca4, Ca5, and Ca6, were significantly associated with 100SW (Supplementary Table S1 and **Figure 2**). Candidate

TABLE 1 | BLUE values (minimum–maximum), genotypic effect, and heritabilities (h^2) of 12 traits obtained from a multi-environment LMM.

Traits	No. of genotypes	Mean	Minimum	Maximum	Wald's test for genotypic effect	H^2
GY (kg)	132	1027.11	623.19	1264.75	$p < 0.001$	0.11
100SW (g)	132	20.00	15.00	37.61	$p < 0.001$	0.91
SN	93	21.96	11.91	32.28	$p = 0.015$	0.32
EPR	59	0.31	0.14	0.46	$p < 0.001$	0.52
HI	93	0.38	0.28	0.46	$p < 0.001$	0.51
DW (g)	93	9.81	6.14	18.02	$p < 0.001$	0.49
FT	132	5.36	1.98	9.56	$p < 0.001$	0.70
PT	132	5.31	0.55	9.27	$p < 0.001$	0.72
MA	132	5.97	4.61	10.04	$p < 0.001$	0.25
EM	132	7.95	5.68	8.88	$p < 0.001$	0.49
EV	132	6.13	3.65	7.93	$p < 0.001$	0.65
PH (cm)	62	53.62	42.88	61.84	$p < 0.001$	0.64

GY, grain yield per ha; 100SW, hundred seed weight; SN, seed number per plant; EPR, empty pod ratio; HI, harvest index; DW, biomass dry weight; FT, flowering time score; PT, podding time score; MA, maturity score; EM, seed-emergence score; EV, early vigor score; PH, plant height.

TABLE 2 | Correlation matrix of the 12 traits.

	GY	100SW	SN	EPR	HI	DW	FT	PT	MA	EM	EV	PH
GY	–											
100SW	0.45***	–										
SN	0.47***	−0.36**	–									
EPR	−0.37**	−0.12	−0.22	–								
HI	0.13	−0.27*	0.56***	0.02	–							
DW	0.83***	0.67***	0.15	−0.33*	−0.35**	–						
FT	−0.43***	0.42***	−0.14	−0.55***	−0.28*	0.43***	–					
PT	0.58***	−0.42***	0.27*	0.58***	0.41**	−0.40**	−0.65***	–				
MA	−0.53***	0.70***	−0.17	−0.35**	−0.47***	0.73***	0.54***	−0.64***	–			
EM	0.42***	−0.67***	0.20	0.25	0.27*	−0.59***	−0.29*	0.38**	−0.59***	–		
EV	0.29*	−0.20	−0.03	0.65***	0.03	−0.29*	−0.60***	0.55***	−0.37**	0.25	–	
PH	−0.22	0.25	−0.56***	0.18	−0.58***	0.08	0.11	−0.10	0.28*	−0.27*	0.25	–

*GY, grain yield; 100SW, hundred seed weight; SN, seed number; EPR, empty pod ratio; HI, harvest index; DW, biomass dry weight; FT, flowering time score; PT, podding time score; MA, maturity score; EM, emergence score; EV, early vigor score; PH, plant height. *$p < 0.05$, **$p < 0.01$, ***$p < 0.001$.*

TABLE 3 | Summary of LD and SNPs used to estimate LD.

Chromosome	No. of SNPs	Density of SNPs (No. of SNPs/10 kb)	No. of SNPs used to estimate LD[1]	Mean r^2	LD extent (kb)
Ca1	20,837	4.25	2,979	0.06	400
Ca2	11,181	3.01	2,826	0.03	200
Ca3	19,487	2.92	1,674	0.15	4,000
Ca4	25,323	4.30	7,106	0.02	200
Ca5	18,313	2.64	1,428	0.07	200
Ca6	15,620	2.37	2,469	0.05	150
Ca7	13,272	2.36	2,070	0.03	200
Ca8	4,740	2.38	933	0.06	200
Unassembled contigs	16,004	3.25	NA	NA	NA
Total/average	144,777		21,485	0.06	700

[1] *SNPs with high confidence (minimum five reads per genotype).*

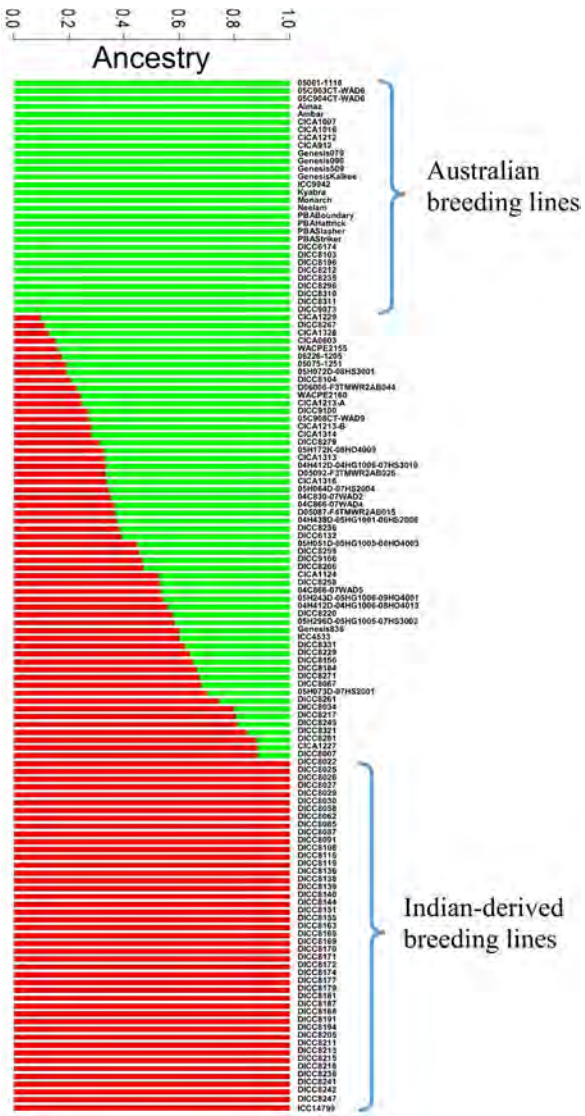

FIGURE 1 | Population structure diagrams of the 132 genotypes. Results of population structure are shown when the numbers of estimated clusters is $k = 2$. The vertical bar is partitioned into red and green segments that represent the genotype's estimated membership fractions.

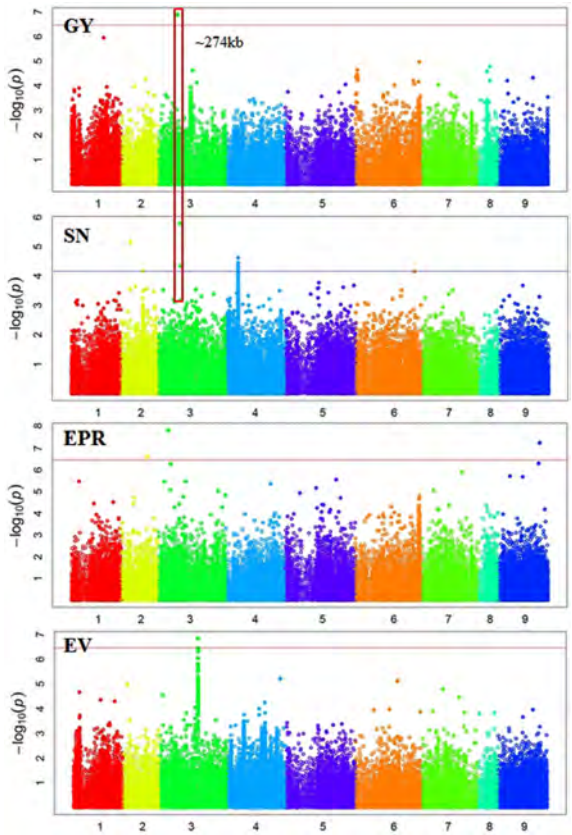

FIGURE 2 | Manhattan plots showing GWAS results of grain yield (GY), seed number (SN), empty pod ratio (EPR), and early vigor score (EV). Each dot represents a SNP. The *x*-axis is the physical position of the SNP. Chromosomes are numbered from 1 to 8 while 9 represents all unassembled contigs. The red line is a significant threshold of *p*-value = 3.47e-07, equal to a level of 0.05 after Bonferroni correction. The blue line is a suggestive threshold of *p*-value = 1.0e-04. Regions containing SNPs significantly associated with different traits are highlighted with red rectangles.

genes located near these SNPs include two sugar transporters, two nodulin MtN21/EamA-like transporters, one Lateral Organ Boundaries (LOB) domain protein and several uncharacterized genes.

There were five SNPs significantly associated with PT, including two SNPs on Ca1, one SNP on Ca3, and two SNPs on Ca4 (Supplementary Table S1 and **Figure 3**). One was located on Ca4: 35,589,599 near a gene encoding a major latex protein (MLP), which promotes vegetative growth and delays flowering in Arabidopsis (Guo et al., 2011). Another significant SNP was located on Ca3: 38,173,722 close to a transcriptional factor squamosa promoter-binding-like protein 9 (SPL9). It was shown that SPL9 and SPL15 act redundantly in promoting the juvenile-to-adult phase transition in Arabidopsis (Schwarz et al., 2008).

There were 12 SNPs significantly associated with MA, including one SNP on Ca2, three SNPs on Ca4, six SNPs on Ca5, and two SNPs on Ca6 (Supplementary Table S1 and **Figure 3**). One of the significant SNPs was located on Ca5: 11,580,061, near the nodulin MtN21/EamA-like transporter which has been shown to be involved in auxin homoeostasis (Ranocha et al., 2013). Another significant SNP was located on Ca5: 12,166,907, near a sugar transporter gene with an important role in plant growth (Wobus and Weber, 1999). Six SNPs were significantly associated with EM, including one SNP on Ca3, three SNPs on Ca4, and two SNP on Ca5 (Supplementary Table S1 and **Figure 3**). One of the significant SNPs (Ca4: 35,589,599) was located near a gene encoding MLP, which promotes vegetative growth in Arabidopsis as described above (Guo et al., 2011). Two SNPs were significantly associated with EV (Supplementary Table S1 and **Figure 2**). One of the significant SNPs (Ca3: 38,177,160) was located near a gene encoding the transcriptional

factor SPL9. It has been shown that SPL9 regulates leaf initiation negatively in Arabidopsis, leading to a shorter leaf plastochron, which is the time interval between two successive events of plant growth (Schwarz et al., 2008). There were no SNPs significantly (p < 3.45e-07) associated with SN, HI, DW, FT, or PH. This could be attributed to the lack of statistical power due to the small sample size (62–93 genotypes) employed in this study.

Some regions contain SNPs significantly associated with several different traits, which is an indication of a pleiotropic effect (**Figures 2**, **3**). For example, a genomic region of ∼274 kb on Ca3 (18,924,965 to 21,660,191) contains a SNP significantly associated with GY and two SNPs weakly (p-value = 1.59e-06 and 4.49e-05) associated with SN. A ∼437 kb genomic region on Ca4 (35,589,599 to 36,026,910) contains eight SNPs, significantly associated with four traits: EM, maturity, PT, and 100SW. Four auxin-related genes, encoding one auxin efflux carrier protein (PIN3) and three nodulin MtN21/EamA-like transporters, are located in this region on Ca4. Another ∼587 kb genomic region on Ca5 (11,580,061 to 12,166,907) contains two SNPs, which were significantly associated with 100SW and MA. Five auxin-related genes, including one auxin influx transporter (LAX3) and four nodulin MtN21/EamA-like transporters, are located in this region. Two SNPs, significantly associated with both 100SW and maturity, were located in a 197 kb region on Ca6 (39,200,356 to 39,397,897) which contains two sugar transporters.

Genomic Prediction

Prediction accuracies for GY, 100SW, SN, and EV were estimated using RR-BLUP and different subsets of the SNPs based on p-values from GWAS results. Prediction accuracies increased when subsets of the SNPs based on a more stringent level of p-value were used (**Figure 4**). The increments plateaued in all four traits using subsets of SNPs with p-values between 0.05 and 0.01 and dropped dramatically at p-values of 3.45e-07 (equal to 0.05 after Bonferroni correction). The lowest prediction accuracies in three traits occurred when using all SNPs, which was probably due to noise introduced by non-causal variants as RR-BLUP shrikes each marker effect equally (de Los Campos et al., 2013). We also used BL and BRR to estimate prediction accuracies using subsets of SNPs. The results were similar to the RR-BLUP model.

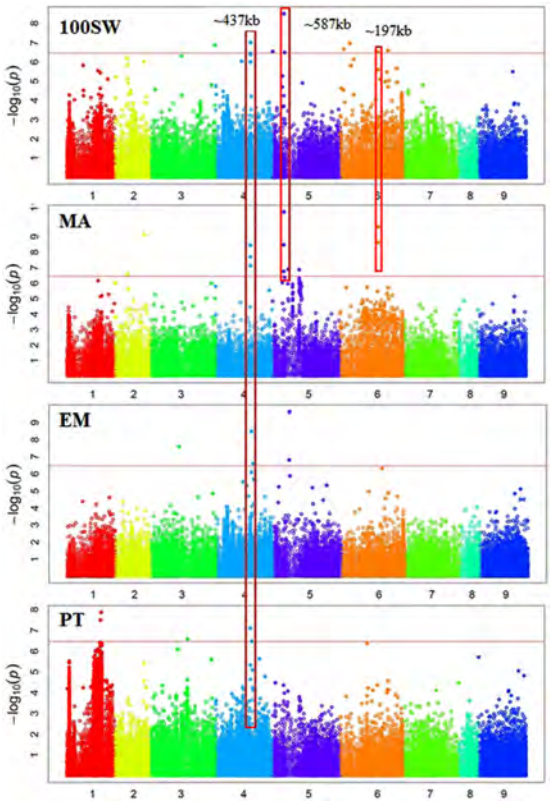

FIGURE 3 | Manhattan plots showing GWAS results of hundred seed weight (100SW), maturity score (MA), emergence score (EM), and podding time score (PT). Each dot represents an SNP. The x-axis is the physical position of the SNP. Chromosomes are numbered from 1 to 8 while 9 represents all unassembled contigs. The red line is a significant threshold of p-value = 3.47e-07, equal to a level of 0.05 after Bonferroni correction. Regions containing SNPs significantly associated with different traits are highlighted with red rectangles.

DISCUSSION

Previous effort on breeding drought-tolerant chickpea has concentrated on accelerating flowering to escape terminal drought (Upadhyaya et al., 2012). This study showed that some India-derived genotypes with early podding trait aborted early onset pods in the Australian environments due to low temperatures in early spring. This suggests that it may be more relevant to focus on breeding for drought tolerance *per se* under Australia environments, traits such as water-use efficiency (Zaman-Allah et al., 2011; Kashiwagi et al., 2013), beneficial root traits (Zaman-Allah et al., 2011), stomatal conductance (Rehman et al., 2011), and osmotic adjustment (Morgan et al., 1991). As pointed out by Berger et al. (2016), the selection pressure for drought escape and drought tolerance *per se* is very different. Excessive use of the drought escape mechanism can compromise yield potential due to shorter life cycles to accumulate water and light resources. Thus a new breeding strategy is warranted, such as the integrated framework proposed by Berger et al. (2016).

Auxin-Related Genes and Sugar Transporters Play an Important Role in Yield-Related Traits under Drought-Prone Environments

Several auxin-related genes, including PIN3, ABC transporter B family/PGP, and nodulin MtN21/EamA-like transporters, were found to be near SNPs significantly associated with GY, 100SW, PT, EM, and MA. Auxin (primarily indole-3-acetic acid) is a well-known phytohormone that plays a pivotal

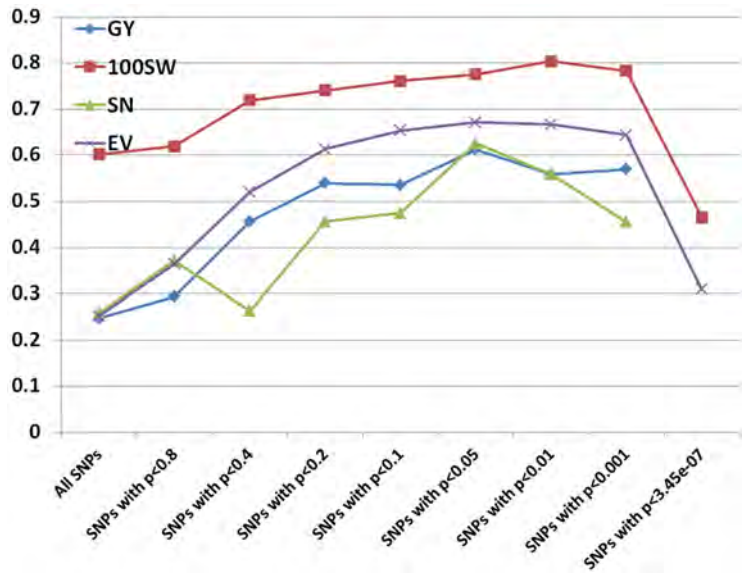

FIGURE 4 | Prediction accuracies for grain yield (GY), hundred seed weight (100SW), seed number (SN), and early vigor score (EV) using different subsets of SNPs based on *p*-values from GWAS results.

role in plant growth, seed development, and abiotic stress response (Zhao, 2010; Kazan, 2013; Locascio et al., 2014). A recent review paper summarized how plants coordinate auxin biosynthesis, transport, perception under osmotic stresses induced be drought, salinity (Naser and Shani, 2016). Auxin was found to enhance drought tolerance via the regulation of root architecture, expression of abiotic stress genes (*DREB2A* and *DREB2B*), ROS metabolism, and metabolic homeostasis in Arabidopsis (Shi et al., 2014). PIN3, belonging to the auxin efflux carrier protein family, have been characterized as important regulators involved in plant growth, phototropic response, and drought stress response (Ding et al., 2011; Zhang et al., 2012, 2013). A study in rice showed that drought, cold and heat stress affected the expression of genes involved in auxin signaling and polar transport, such as the PIN protein family (Du et al., 2013). Several studies have shown that PGP is involved in auxin transport through the plasma membrane and can stabilize the PIN protein family (Geisler and Murphy, 2006; Blakeslee et al., 2007; Titapiwatanakun et al., 2009; Zazimalova et al., 2010). Arabidopsis WAT1, a homolog of the nodulin MtN21/EamA-like transporter, was recently identified as a vacuolar auxin transporter required for auxin homoeostasis, a process that maintains an endogenous steady-state concentration of primary auxin (Ranocha et al., 2013). Several sugar transporters were found to be near SNPs significantly associated with 100SW and MA. Comprising hexose and sucrose transport proteins, the sugar transporters are members of the major facilitator superfamily. Sugar transporters play a key role in plant growth, source–sink partitioning, molecular signaling, and seed development, and are therefore important for optimal plant development and crop yield (Wobus and Weber, 1999; Wingenter et al., 2010; Doidy et al., 2012).

Using a bi-parental QTL mapping population, a "QTL-hotspot" region on Ca4 13,239,546 to 13,547,009 (based on the kabuli reference genome v1.0) was associated with at least seven traits including root traits, 100SW, PH, and days to flowering (Varshney et al., 2014b; Jaganathan et al., 2015; Kale et al., 2015). In this study, we did not identify SNPs from the "QTL-hotspot" region significantly associated with any traits. We identified a ∼437 kb genomic region on Ca4: 35,589,599 to 36,026,910 (Ca4: 37,933,355 to 38,412,853 based on the kabuli reference genome v1.0) containing eight SNPs significantly associated with four traits: EM, maturity, PT, and 100SW. Different 100SW QTL were identified between the two studies, which may be attributed to the different mapping populations examined.

Confounding Effects of Self-Incompatibility with Pod Abortion under Drought

Three SNPs, located on Ca2, Ca3, and an unassembled contig, were significantly associated with EPR (Supplementary Table S1 and **Figure 2**). The kinesin-4 and self-incompatibility (SI) proteins were adjacent to two of the three significant SNPs. The kinesin-4 family plays an important role in cell elongation and has been shown to affect the length of siliques and seeds produced per silique in Arabidopsis (Kong et al., 2015). The SI protein (IPR010264) is highly homologous (with a total score of 141 and E value of 2e-32 using NCBI blastn) to a Medicago gene Medtr1g057250.1, which was well characterized in *Papaver rhoeas* (Foote et al., 1994; Wilkins et al., 2014). SI is a mechanism used by many flowering plants to prevent self-fertilization and inbreeding depression. Pollen from SI plants, carrying the same haplotype as the pistil, was rejected via the program cell death

mechanism (Wilkins et al., 2014). Chickpea is generally a self-pollinating crop with an outcrossing rate of less than 2% (Toker et al., 2006); however, SI plants with empty pods yet viable pollen were observed in an F2 segregating population from a cross (H 82-5 × E100 ym) × Bhim with ∼22% of F2 SI plants (Lather and Dahiya, 1992). Pod abortion has long been thought to be introduced mainly by abiotic stress (Fang et al., 2010; Pang et al., 2017). Our findings, however, indicated that SI might have confounding effects with pod abortion under drought.

Incorporating the Results of GWAS Increased Prediction Accuracy

Prediction models, employing variable selection procedures such as the LASSO, are considered to be better than RR-BLUP theoretically because they remove non-causal variants and variants not in LD with causal variants (Daetwyler et al., 2010; Meuwissen and Goddard, 2010). However, Wimmer et al. (2013) showed that LASSO failed to achieve its superiority and thus suggested to "*preselect markers according to biological prior information*." Our study supports this assumption by showing that prediction accuracies were significantly improved using a subset of SNPs significantly (between $p < 0.05$ and $p < 0.01$) associated with traits. Several computer simulation studies (Meuwissen and Goddard, 2010; Ober et al., 2012) speculated that using large amounts of markers from WGRS may increase prediction accuracy, particularly in cases where the training population is distantly related to the prediction population. We argue that having more markers alone may not help to increase prediction accuracy, but it may help to identify the causal variants. If the prediction is done subsequent to the identification of causal variants, then the prediction may increase, as demonstrated in the current study, and thus the advantage of employing WGRS in GS can be realized.

Many studies have been published on the effect of marker density on prediction accuracy (Lorenzana and Bernardo, 2009; Vazquez et al., 2010; Weigel et al., 2010; Hoffstetter et al., 2016). Most have selected markers randomly or based on equal space and found that prediction accuracy increased when the number of markers increased, but reached a plateau depending on the extent of LD and the population size (Vazquez et al., 2010). A few studies selected markers based on biological prior information (Hoffstetter et al., 2016; Kooke et al., 2016; Spindel et al., 2016). Compared to using all markers in the RR-BLUP model, prediction accuracies doubled by using a subset of markers with significant association with grain yield in wheat (Hoffstetter et al., 2016). Another GS study in rice also showed that prediction accuracies were 7.0%–29.8% higher based on RR-BLUP with all markers and markers (selected from GWAS) fitted as fixed effects compared to that based on RR-BLUP with all markers alone (Spindel et al., 2016). Using different models, a recent GS study in chickpea indicated that prediction accuracies of yield under rainfed environments ranged from 0.148 to 0.186, which is similar (0.25) to this study using all 144,777 SNPs, but much smaller (0.56–0.61) than when using a subset of SNPs significantly associated with yield. We speculate that prediction accuracy may increase if an approach described here is adopted.

Training population size is an important factor in GS. Several studies have been conducted to investigate the optimum size for a training population in plants. Generally, the accuracy of estimated marker effects increases as the sample size increases (Albrecht et al., 2011; Endelman et al., 2014). Compared to other prediction models, one simulation study showed that RR-BLUP is robust with a small training population size even as low as $n = 75$, with diminishing benefits between $n = 125$ and $n = 300$ (Lorenz, 2013). Riedelsheimer and Melchinger (2013) reached a similar observation and recommended to allocate more resources to the selection candidates (prediction set) instead of the training population when budget is fix. Compared to a GS study in chickpea conducted by Roorkiwal et al. (2016), the training population size in this study is relatively small. Because the main objective of this study is to test the prediction accuracy based on subsets of significant SNPs. The result of this study should hold since the size of the training population was the same in different subsets of SNPs. For real breeding application, such as selecting candidate genotypes without phenotypic data, larger training populations should be used to increase prediction accuracy. Additionally, the training population needs to be updated regularly to maintain a close relationship with selection candidates (Neyhart et al., 2017).

Grain yield is a complex trait controlled by numerous genes with small effect. We found only one SNP significantly associated with grain yield in this study, probably due to limited statistical power to identify genes which underline complex traits. Even if all yield-related genes could be identified using a larger sample size, pyramiding favorable alleles from all genes into a single genotype using traditional marker-assisted selection or transgenic approaches would be extremely difficult. The superiority of the GS approach is that it can use all marker information simultaneously and thus circumvent the complex process of pyramiding. That is not to say that GWAS and marker-assisted selection do not have a place in molecular breeding; for example these approaches are useful for targeting simple traits (Mendelian traits) such as disease resistance (Varshney et al., 2014a; Li et al., 2017). This study also shows that incorporating the results of GWAS into the prediction model can significantly increase prediction accuracy. However, this gain of prediction accuracy is only examined in a cross-validation scheme. Further study is needed to investigate whether this result holds true when this approach is applied to selection candidates.

AUTHOR CONTRIBUTIONS

YL and TS conceived the study; YL performed the GWAS and GS analysis; JB contributed to sequencing; PR analyzed the sequencing data; DE supervised sequencing-data analysis; KS, JP, TK, and TC contributed to phenotyping; YL wrote the manuscript and all the authors read and approved the manuscript.

FUNDING

This study was supported by grant GCF010013 through the Australia-India Strategic Research Fund (AISRF), Australian Government Department of Industry, Innovation and Science.

ACKNOWLEDGMENTS

This work was supported with supercomputing resources provided by the Phoenix HPC service at the University of Adelaide. We thank Alison Hay for extracting DNA, Satomi Hayashi for NGS library preparation, and Kenneth Chan for bioinformatics support.

SUPPLEMENTARY MATERIAL

The Supplementary Material for this article can be found online at: https://www.frontiersin.org/articles/10.3389/fpls.2018.00190/full#supplementary-material

REFERENCES

Albrecht, T., Wimmer, V., Auinger, H. J., Erbe, M., Knaak, C., Ouzunova, M., et al. (2011). Genome-based prediction of testcross values in maize. *Theor. Appl. Genet.* 123, 339–350. doi: 10.1007/s00122-011-1587-7

Alexander, D. H., and Lange, K. (2011). Enhancements to the ADMIXTURE algorithm for individual ancestry estimation. *BMC Bioinformatics* 12:246. doi: 10.1186/1471-2105-12-246

Bar-El Dadon, S., Abbo, S., and Reifen, R. (2017). Leveraging traditional crops for better nutrition and health - The case of chickpea. *Trends Food Sci. Technol.* 64, 39–47. doi: 10.1016/j.tifs.2017.04.002

Berger, J., Palta, J., and Vadez, V. (2016). Review: an integrated framework for crop adaptation to dry environments: responses to transient and terminal drought. *Plant Sci.* 253, 58–67. doi: 10.1016/j.plantsci.2016.09.007

Blakeslee, J. J., Bandyopadhyay, A., Lee, O. R., Mravec, J., Titapiwatanakun, B., Sauer, M., et al. (2007). Interactions among PIN-FORMED and P-glycoprotein auxin transporters in *Arabidopsis*. *Plant Cell* 19, 131–147. doi: 10.1105/tpc.106.040782

Collins, N. C., Tardieu, F., and Tuberosa, R. (2008). Quantitative trait loci and crop performance under abiotic stress: Where do we stand? *Plant Physiol.* 147, 469–486. doi: 10.1104/pp.108.118117

Crossa, J., Perez, P., Hickey, J., Burgueno, J., Ornella, L., Ceron-Rojas, J., et al. (2014). Genomic prediction in CIMMYT maize and wheat breeding programs. *Heredity* 112, 48–60. doi: 10.1038/hdy.2013.16

Daetwyler, H. D., Pong-Wong, R., Villanueva, B., and Woolliams, J. A. (2010). The impact of genetic architecture on genome-wide evaluation methods. *Genetics* 185, 1021–1031. doi: 10.1534/genetics.110.116855

Daryanto, S., Wang, L., and Jacinthe, P. A. (2015). Global synthesis of drought effects on food legume production. *PLoS One* 10:e0127401. doi: 10.1371/journal.pone.0127401

Davey, J. W., Hohenlohe, P. A., Etter, P. D., Boone, J. Q., Catchen, J. M., and Blaxter, M. L. (2011). Genome-wide genetic marker discovery and genotyping using next-generation sequencing. *Nat. Rev. Genet.* 12, 499–510. doi: 10.1038/nrg3012

de Los Campos, G., Hickey, J. M., Pong-Wong, R., Daetwyler, H. D., and Calus, M. P. (2013). Whole-genome regression and prediction methods applied to plant and animal breeding. *Genetics* 193, 327–345. doi: 10.1534/genetics.112.143313

Ding, Z., Galvan-Ampudia, C. S., Demarsy, E., Langowski, L., Kleine-Vehn, J., Fan, Y., et al. (2011). Light-mediated polarization of the PIN3 auxin transporter for the phototropic response in *Arabidopsis*. *Nat. Cell Biol.* 13, 447–452. doi: 10.1038/ncb2208

Doidy, J., Grace, E., Kuehn, C., Simon-Plas, F., Casieri, L., and Wipf, D. (2012). Sugar transporters in plants and in their interactions with fungi. *Trends Plant Sci.* 17, 413–422. doi: 10.1016/j.tplants.2012.03.009

Du, H., Liu, H., and Xiong, L. (2013). Endogenous auxin and jasmonic acid levels are differentially modulated by abiotic stresses in rice. *Front. Plant Sci.* 4:397. doi: 10.3389/fpls.2013.00397

Elshire, R. J., Glaubitz, J. C., Sun, Q., Poland, J. A., Kawamoto, K., Buckler, E. S., et al. (2011). A robust, simple genotyping-by-sequencing (GBS) approach for high diversity species. *PLoS One* 6:e19379. doi: 10.1371/journal.pone.0019379

Endelman, J. B., Atlin, G. N., Beyene, Y., Semagn, K., Zhang, X. C., Sorrells, M. E., et al. (2014). Optimal design of preliminary yield trials with genome-wide markers. *Crop Sci.* 54, 48–59. doi: 10.2135/cropsci2013.03.0154

Fang, X. W., Turner, N. C., Yan, G. J., Li, F. M., and Siddique, K. H. M. (2010). Flower numbers, pod production, pollen viability, and pistil function are reduced and flower and pod abortion increased in chickpea (*Cicer arietinum* L.) under terminal drought. *J. Exp. Bot.* 61, 335–345. doi: 10.1093/jxb/erp307.

Foote, H. C. C., Ride, J. P., Franklin-Tong, V. E., Walker, E. A., Lawrence, M. J., and Franklin, F. C. H. (1994). Cloning and expression of a distinctive class of self-incompatibility (S) gene from *Papaver rhoeas* L. *Proc. Natl. Acad. Sci. U.S.A.* 91, 2265–2269. doi: 10.1073/pnas.91.6.2265

Foyer, C. H., Lam, H. M., Nguyen, H. T., Siddique, K. H. M., Varshney, R. K., Colmer, T. D., et al. (2016). Neglecting legumes has compromised human health and sustainable food production. *Nat. Plants* 2:16112. doi: 10.1038/nplants.2016.112

Geisler, M., and Murphy, A. S. (2006). The ABC of auxin transport: the role of p-glycoproteins in plant development. *FEBS Lett.* 580, 1094–1102. doi: 10.1016/j.febslet.2005.11.054.

Guo, D., Wong, W. S., Xu, W. Z., Sun, F. F., Qing, D. J., and Li, N. (2011). *Cis-cinnamic acid-enhanced* 1 gene plays a role in regulation of Arabidopsis bolting. *Plant Mol. Biol.* 75, 481–495. doi: 10.1007/s11103-011-9746-4

Gupta, S., Nawaz, K., Parween, S., Roy, R., Sahu, K., Pole, A. K., et al. (2017). Draft genome sequence of *Cicer reticulatum* L., the wild progenitor of chickpea provides a resource for agronomic trait improvement. *DNA Res.* 24, 1–10. doi: 10.1093/dnares/dsw042

Hamwieh, A., Imtiaz, M., and Malhotra, R. S. (2013). Multi-environment QTL analyses for drought-related traits in a recombinant inbred population of chickpea (*Cicer arientinum* L.). *Theor. Appl. Genet.* 126, 1025–1038. doi: 10.1007/s00122-012-2034-0

Hayes, B. J., Bowman, P. J., Chamberlain, A. J., and Goddard, M. E. (2009a). Invited review: Genomic selection in dairy cattle: progress and challenges. *J. Dairy Sci.* 92, 433–443. doi: 10.3168/jds.2008-1646

Hayes, B. J., Visscher, P. M., and Goddard, M. E. (2009b). Increased accuracy of artificial selection by using the realized relationship matrix. *Genet. Res.* 91, 47–60. doi: 10.1017/s0016672308009981

Henderson, C. R. (1975). Best linear unbiased estimation and prediction under a selection model. *Biometrics* 31, 423–447. doi: 10.2307/2529430

Hennesy, K., Whetton, P., and Preston, B. (2010). "Climate projection," in *Adapting Agriculture to Climate Change: Preparing Australian Agriculture, Forestry and Fisheries for the Future*, eds C. Stokes, and M. Howden (Canberra: CSIRO), 13–20.

Hoffstetter, A., Cabrera, A., Huang, M., and Sneller, C. (2016). Optimizing training population data and validation of genomic selection for economic traits in soft winter wheat. *G3* 6, 2919–2928. doi: 10.1534/g3.116.032532

Jafarzadeh, J., Bonnett, D., Jannink, J. L., Akdemir, D., Dreisigacker, S., and Sorrells, M. E. (2016). Breeding value of primary synthetic wheat genotypes for grain yield. *PLoS One* 11:e0162860. doi: 10.1371/journal.pone.0162860

Jaganathan, D., Thudi, M., Kale, S., Azam, S., Roorkiwal, M., Gaur, P. M., et al. (2015). Genotyping-by-sequencing based intra-specific genetic map refines a "QTL-hotspot" region for drought tolerance in chickpea. *Mol. Genet. Genomics* 290, 559–571. doi: 10.1007/s00438-014-0932-3

Jain, M., Misra, G., Patel, R. K., Priya, P., Jhanwar, S., Khan, A. W., et al. (2013). A draft genome sequence of the pulse crop chickpea (*Cicer arietinum* L.). *Plant J.* 74, 715–729. doi: 10.1111/tpj.12173

Kale, S. M., Jaganathan, D., Ruperao, P., Chen, C., Punna, R., Kudapa, H., et al. (2015). Prioritization of candidate genes in "QTL-hotspot" region for drought

tolerance in chickpea (*Cicer arietinum* L.). *Sci. Rep.* 5:15296. doi: 10.1038/srep15296

Kashiwagi, J., Krishnamurthy, L., Gaur, P. M., Upadhyaya, H. D., Varshney, R. K., and Tobita, S. (2013). Traits of relevance to improve yield under terminal drought stress in chickpea (*C. arietinum* L.). *Field Crops Res* 145, 88–95. doi: 10.1016/j.fcr.2013.02.011

Kazan, K. (2013). Auxin and the integration of environmental signals into plant root development. *Ann. Bot.* 112, 1655–1665. doi: 10.1093/aob/mct229

Knights, E. J., Siddique, K. H. M., Khan, T. N., and Hobson, K. B. (2009). "Development of the Australian chickpea industry: booms and blights," in *Milestones in Food Legumes Research*, eds M. Ali, and M. Kumar (Kanpur: Indian Institute of Pulses Research), 36–57.

Kong, Z., Ioki, M., Braybrook, S., Li, S., Ye, Z. H., Julie Lee, Y. R., et al. (2015). Kinesin-4 functions in vesicular transport on cortical microtubules and regulates cell wall mechanics during cell elongation in plants. *Mol. Plant* 8, 1011–1023. doi: 10.1016/j.molp.2015.01.004

Kooke, R., Kruijer, W., Bours, R., Becker, F., Kuhn, A., van de Geest, H., et al. (2016). Genome-wide association mapping and genomic prediction elucidate the genetic architecture of morphological traits in Arabidopsis. *Plant Physiol.* 170, 2187–2203. doi: 10.1104/pp.15.00997

Lather, V. S., and Dahiya, B. S. (1992). Self-incompatibility in Chickpea. *Int. Chickpea Pigeonpea Newsl.* 14, 4–5.

Leport, L., Turner, N. C., French, R. J., Barr, M. D., Duda, R., Daves, S. L., et al. (1999). Physiological responses of chickpea genotypes to terminal drought in a Mediterranean-type environment. *Eur. J. Agron.* 11, 279–291. doi: 10.1016/s1161-0301(99)00039-8

Li, Y., Haseneyer, G., Schön, C. C., Ankerst, D., Korzun, V., Wilde, P., et al. (2011). High levels of nucleotide diversity and fast decline of linkage disequilibrium in rye (*Secale cereale* L.) genes involved in frost response. *BMC Plant Biol.* 11:6. doi: 10.1186/1471-2229-11-6

Li, Y. L., Ruperao, P., Batley, J., Edwards, D., Davidson, J., Hobson, K., et al. (2017). Genome analysis identified novel candidate genes for *Ascochyta* blight resistance in chickpea using whole genome re-sequencing data. *Front. Plant Sci.* 8:369. doi: 10.3389/fpls.2017.00359

Lipka, A. E., Tian, F., Wang, Q., Peiffer, J., Li, M., Bradbury, P. J., et al. (2012). GAPIT: genome association and prediction integrated tool. *Bioinformatics* 28, 2397–2399. doi: 10.1093/bioinformatics/bts444

Locascio, A., Roig-Villanova, I., Bernardi, J., and Varotto, S. (2014). Current perspectives on the hormonal control of seed development in Arabidopsis and maize: a focus on auxin. *Front. Plant Sci.* 5:412. doi: 10.3389/fpls.2014.00412

Lorenc, M. T., Hayashi, S., Stiller, J., Lee, H., Manoli, S., Ruperao, P., et al. (2012). Discovery of single nucleotide polymorphisms in complex genomes using SGSautoSNP. *Biology* 1, 370–382. doi: 10.3390/biology1020370

Lorenz, A. J. (2013). Resource allocation for maximizing prediction accuracy and genetic gain of genomic selection in plant breeding: a simulation experiment. *G3* 3, 481–491. doi: 10.1534/g3.112.004911

Lorenzana, R. E., and Bernardo, R. (2009). Accuracy of genotypic value predictions for marker-based selection in biparental plant populations. *Theor. Appl. Genet.* 120, 151–161. doi: 10.1007/s00122-009-1166-3

Meuwissen, T., and Goddard, M. (2010). Accurate prediction of genetic values for complex traits by whole-genome resequencing. *Genetics* 185, 623–631. doi: 10.1534/genetics.110.116590

Meuwissen, T. H. E., Hayes, B. J., and Goddard, M. E. (2001). Prediction of total genetic value using genome-wide dense marker maps. *Genetics* 157, 1819–1829.

Morgan, J. M., Rodriguezmaribona, B., and Knights, E. J. (1991). Adaptation to water-deficit in chickpea breeding lines by osomoregulation: relationship to grain-yields in field. *Field Crops Res.* 27, 61–70. doi: 10.1016/0378-4290(91)90022-n

Naser, V., and Shani, E. (2016). Auxin response under osmotic stress. *Plant Mol. Biol.* 91, 661–672. doi: 10.1007/s11103-016-0476-5

Neyhart, J. L., Tiede, T., Lorenz, A. J., and Smith, K. P. (2017). Evaluating methods of updating training data in long-term genomewide selection. *G3* 7, 1499–1510. doi: 10.1534/g3.117.040550

Ober, U., Ayroles, J. F., Stone, E. A., Richards, S., Zhu, D. H., Gibbs, R. A., et al. (2012). Using whole-genome sequence data to predict quantitative trait phenotypes in drosophila melanogaster. *PLoS Genet.* 8:e1002685. doi: 10.1371/journal.pgen.1002685

Pang, J., Turner, N. C., Khan, T., Du, Y. L., Xiong, J. L., Colmer, T. D., et al. (2017). Response of chickpea (*Cicer arietinum* L.) to terminal drought: leaf stomatal conductance, pod abscisic acid concentration, and seed set. *J. Exp. Bot.* 68, 1973–1985 doi: 10.1093/jxb/erw153

Parween, S., Nawaz, K., Roy, R., Pole, A. K., Suresh, B. V., Misra, G., et al. (2015). An advanced draft genome assembly of a desi type chickpea (*Cicer arietinum* L.). *Sci. Rep.* 5:12806. doi: 10.1038/srep12806

Poland, J. A., and Rife, T. W. (2012). Genotyping-by-sequencing for plant breeding and genetics. *Plant Genome* 5, 92–102. doi: 10.3835/plantgenome2012.05.0005

Ranocha, P., Dima, O., Nagy, R., Felten, J., Corratge-Faillie, C., Novak, O., et al. (2013). *Arabidopsis* WAT1 is a vacuolar auxin transport facilitator required for auxin homoeostasis. *Nat. Commun.* 4:2625. doi: 10.1038/ncomms3625

Rehman, A. U., Malhotra, R. S., Bett, K., Tar'an, B., Bueckert, R., and Warkentin, T. D. (2011). Mapping QTL associated with traits affecting grain yield in chickpea (*Cicer arietinum* L.) under terminal drought stress. *Crop Sci.* 51, 450–463. doi: 10.2135/cropsci2010.03.0129

Riedelsheimer, C., and Melchinger, A. E. (2013). Optimizing the allocation of resources for genomic selection in one breeding cycle. *Theor. Appl. Genet.* 126, 2835–2848. doi: 10.1007/s00122-013-2175-9

Roorkiwal, M., Rathore, A., Das, R. R., Singh, M. K., Jain, A., Srinivasan, S., et al. (2016). Genome-enabled prediction models for yield related traits in chickpea. *Front. Plant Sci.* 7:1666. doi: 10.3389/fpls.2016.01666.

Ruperao, P., Chan, C. K. K., Azam, S., Karafiatova, M., Hayashi, S., Cizkova, J., et al. (2014). A chromosomal genomics approach to assess and validate the desi and kabuli draft chickpea genome assemblies. *Plant Biotechnol. J.* 12, 778–786. doi: 10.1111/pbi.12182

Sadras, V. O., Lake, L., Li, Y., Farquharson, E. A., and Sutton, T. (2016). Phenotypic plasticity and its genetic regulation for yield, nitrogen fixation and delta13C in chickpea crops under varying water regimes. *J. Exp. Bot.* 67, 4339–4351. doi: 10.1093/jxb/erw221

Schwarz, S., Grande, A. V., Bujdoso, N., Saedler, H., and Huijser, P. (2008). The microRNA regulated SBP-box genes *SPL9* and *SPL15* control shoot maturation in Arabidopsis. *Plant Mol. Biol.* 67, 183–195. doi: 10.1007/s11103-008-9310-z

Shi, H., Chen, L., Ye, T., Liu, X., Ding, K., and Chan, Z. (2014). Modulation of auxin content in Arabidopsis confers improved drought stress resistance. *Plant Physiol. Biochem.* 82, 209–217. doi: 10.1016/j.plaphy.2014.06.008

Siddique, K. H. M., Erskine, W., Hobson, K., Knights, E. J., Leonforte, A., Khan, T. N., et al. (2013). Cool-season grain legume improvement in Australia-use of genetic resources. *Crop Pasture Sci.* 64, 347–360. doi: 10.1071/cp13071

Spindel, J. E., Begum, H., Akdemir, D., Collard, B., Redona, E., Jannink, J. L., et al. (2016). Genome-wide prediction models that incorporate de novo GWAS are a powerful new tool for tropical rice improvement. *Heredity* 116, 395–408. doi: 10.1038/hdy.2015.113

Tang, Y., Liu, X., Wang, J., Li, M., Wang, Q., Tian, F., et al. (2016). GAPIT version 2: an enhanced integrated tool for genomic association and prediction. *Plant Genome* 9, 1–9. doi: 10.3835/plantgenome2015.11.0120

Thudi, M., Upadhyaya, H. D., Rathore, A., Gaur, P. M., Krishnamurthy, L., Roorkiwal, M., et al. (2014). Genetic dissection of drought and heat tolerance in chickpea through genome-wide and candidate gene-based association mapping approaches. *PLoS One* 9:e96758. doi: 10.1371/journal.pone.0096758

Tibshirani, R. (1996). Regression shrinkage and selection via the Lasso. *J. R. Stat. Soc. Ser. B Methodol.* 58, 267–288.

Titapiwatanakun, B., Blakeslee, J. J., Bandyopadhyay, A., Yang, H., Mravec, J., Sauer, M., et al. (2009). ABCB19/PGP19 stabilises PIN1 in membrane microdomains in Arabidopsis. *Plant J.* 57, 27–44. doi: 10.1111/j.1365-313X.2008.03668.x

Toker, C., Canci, H., and Ceylan, F. O. (2006). Estimation of outcrossing rate in chickpea (*Cicer arietinum* L.) sown in autumn. *Euphytica* 151, 201–205. doi: 10.1007/s10681-006-9140-5

Upadhyaya, H. D., Kashiwagi, J., Varshney, R. K., Gaur, P. M., Saxena, K. B., Krishnamurthy, L., et al. (2012). Phenotyping chickpeas and pigeonpeas for adaptation to drought. *Front. Physiol.* 3:179. doi: 10.3389/fphys.2012.00179

Van Belle, G., Fisher, L., Heagerty, P., and Lumley, T. (2004). *Biostatistics: A Methodology for the Health Sciences*. Hoboken, NJ: John Wiley & Sons. doi: 10.1002/0471602396

van Dijk, A., Beck, H. E., Crosbie, R. S., de Jeu, R. A. M., Liu, Y. Y., Podger, G. M., et al. (2013). The millennium drought in southeast Australia (2001-2009):

natural and human causes and implications for water resources, ecosystems, economy, and society. *Water Resour. Res.* 49, 1040–1057. doi: 10.1002/wrcr.20123

VanRaden, P. M. (2008). Efficient methods to compute genomic predictions. *J. Dairy Sci.* 91, 4414–4423. doi: 10.3168/jds.2007-0980

Varshney, R. K., Mohan, S. M., Gaur, P. M., Chamarthi, S. K., Singh, V. K., Srinivasan, S., et al. (2014a). Marker-assisted backcrossing to introgress resistance to fusarium wilt race 1 and Ascochyta Blight in C 214, an elite cultivar of chickpea. *Plant Genome* 7. doi: 10.3835/plantgenome2013.10.0035.

Varshney, R. K., Song, C., Saxena, R. K., Azam, S., Yu, S., Sharpe, A. G., et al. (2013). Draft genome sequence of chickpea (*Cicer arietinum*) provides a resource for trait improvement. *Nat. Biotechnol.* 31, 240–246. doi: 10.1038/nbt.2491

Varshney, R. K., Thudi, M., Nayak, S. N., Gaur, P. M., Kashiwagi, J., Krishnamurthy, L., et al. (2014b). Genetic dissection of drought tolerance in chickpea (*Cicer arietinum* L.). *Theor. Appl. Genet.* 127, 445–462. doi: 10.1007/s00122-013-2230-6

Vazquez, A. I., Rosa, G. J., Weigel, K. A., de los Campos, G., Gianola, D., and Allison, D. B. (2010). Predictive ability of subsets of single nucleotide polymorphisms with and without parent average in US Holsteins. *J. Dairy Sci.* 93, 5942–5949. doi: 10.3168/jds.2010-3335

Wald, A. (1943). Tests of statistical hypotheses concerning several parameters when the number of observations is large. *Trans. Am. Math. Soc.* 54, 426–482. doi: 10.1093/biostatistics/kxs015

Wang, Q., Tian, F., Pan, Y., Buckler, E. S., and Zhang, Z. (2014). A SUPER powerful method for genome wide association study. *PLoS One* 9: e107684. doi: 10.1371/journal.pone.0107684

Weigel, K. A., de los Campos, G., Vazquez, A. I., Rosa, G. J. M., Gianola, D., and Van Tassell, C. P. (2010). Accuracy of direct genomic values derived from imputed single nucleotide polymorphism genotypes in Jersey cattle. *J. Dairy Sci.* 93, 5423–5435. doi: 10.3168/jds.2010-3149

Wilkins, K. A., Poulter, N. S., and Franklin-Tong, V. E. (2014). Taking one for the team: self-recognition and cell suicide in pollen. *J. Exp. Bot.* 65, 1331–1342. doi: 10.1093/jxb/ert468

Wimmer, V., Albrecht, T., Auinger, H. J., and Schon, C. C. (2012). synbreed: a framework for the analysis of genomic prediction data using R. *Bioinformatics* 28, 2086–2087. doi: 10.1093/bioinformatics/bts335

Wimmer, V., Lehermeier, C., Albrecht, T., Auinger, H. J., Wang, Y., and Schon, C. C. (2013). Genome-wide prediction of traits with different genetic architecture through efficient variable selection. *Genetics* 195, 573–587. doi: 10.1534/genetics.113.150078

Wingenter, K., Schulz, A., Wormit, A., Wic, S., Trentmann, O., and Hoermiller, II, et al. (2010). Increased activity of the vacuolar monosaccharide transporter TMT1 alters cellular sugar partitioning, sugar signaling, and seed yield in Arabidopsis. *Plant Physiol.* 154, 665–677. doi: 10.1104/pp.110.162040

Wobus, U., and Weber, H. (1999). Sugars as signal molecules in plant seed development. *Biol. Chem.* 380, 937–944. doi: 10.1515/bc.1999.116

Zaman-Allah, M., Jenkinson, D. M., and Vadez, V. (2011). A conservative pattern of water use, rather than deep or profuse rooting, is critical for the terminal drought tolerance of chickpea. *J. Exp. Bot.* 62, 4239–4252. doi: 10.1093/jxb/err139

Zazimalova, E., Murphy, A. S., Yang, H. B., Hoyerova, K., and Hosek, P. (2010). Auxin transporters - Why so many? *Cold Spring Harb. Perspect. Biol.* 2:a001552. doi: 10.1101/cshperspect.a001552

Zhang, K. X., Xu, H. H., Yuan, T. T., Zhang, L., and Lu, Y. T. (2013). Blue-light-induced PIN3 polarization for root negative phototropic response in Arabidopsis. *Plant J.* 76, 308–321. doi: 10.1111/tpj.12298

Zhang, Q., Li, J., Zhang, W., Yan, S., Wang, R., Zhao, J., et al. (2012). The putative auxin efflux carrier OsPIN3t is involved in the drought stress response and drought tolerance. *Plant J.* 72, 805–816. doi: 10.1111/j.1365-313X.2012.05121.x

Zhao, Y. (2010). Auxin biosynthesis and its role in plant development. *Annu. Rev. Plant Biol.* 61, 49–64. doi: 10.1146/annurev-arplant-042809-112308

Ziyomo, C., and Bernardo, R. (2013). Drought tolerance in maize: indirect selection through secondary traits versus genomewide selection. *Crop Sci.* 53, 1269–1275. doi: 10.2135/cropsci2012.11.0651

Conflict of Interest Statement: The authors declare that the research was conducted in the absence of any commercial or financial relationships that could be construed as a potential conflict of interest.

frontiers in Plant Science

ORIGINAL RESEARCH
published: 15 March 2018
doi: 10.3389/fpls.2018.00320

Simultaneous Improvement and Genetic Dissection of Drought Tolerance Using Selected Breeding Populations of Rice

Yanru Cui[1†], Wenying Zhang[2†], Xiuyun Lin[3], Shizhong Xu[4], Jianlong Xu[1,5] and Zhikang Li[1,5*]*

[1] Institute of Crop Sciences, National Key Facility for Crop Gene Resources and Genetic Improvement, Chinese Academy of Agricultural Sciences, Beijing, China, [2] Ningxia Academy of Agriculture and Forestry Sciences, Yinchuan, China, [3] Rice Research Institute, Jilin Academy of Agricultural Sciences, Changchun, China, [4] Department of Botany and Plant Sciences, University of California, Riverside, CA, United States, [5] Shenzhen Institute of Breeding and Innovation, Chinese Academy of Agricultural Sciences, Shenzhen, China

OPEN ACCESS

Edited by:
Hui Xia,
Shanghai Agrobiological Gene Center, China

Reviewed by:
Hamid Khazaei,
University of Saskatchewan, Canada
Hongjun Liu,
Shandong Agricultural University, China

***Correspondence:**
Jianlong Xu
xujlcaas@126.com
Zhikang Li
zhkli1953@126.com

[†]*These authors have contributed equally to this work.*

Specialty section:
This article was submitted to Plant Breeding, a section of the journal Frontiers in Plant Science

Received: *04 December 2017*
Accepted: *27 February 2018*
Published: *15 March 2018*

Citation:
Cui Y, Zhang W, Lin X, Xu S, Xu J and Li Z (2018) Simultaneous Improvement and Genetic Dissection of Drought Tolerance Using Selected Breeding Populations of Rice. Front. Plant Sci. 9:320. doi: 10.3389/fpls.2018.00320

Drought is the most important factor limiting rice yield in most rainfed areas of Asia and Africa. Four large BC_2F_2 populations consisted of 3,200 individuals, which were derived from crosses between an elite *Geng* variety, Jigeng88, and four donors from three different countries, were screened and progeny tested under severe drought stress, resulting in the development of 72 introgression lines (ILs) with significantly improved yield compared to the recurrent parent Jigeng88. These DT ILs plus four random populations (without drought selection population) from the same crosses were evaluated in replicated trials under both drought stress and non-stress conditions in two environments, and characterized with simple sequence repeat (SSR) markers to understand how directional selection was operating on the genetic variation of DT of rice. Thirteen DT QTLs of large effect were identified based on the significant allelic and genotypic frequency shits in the DT ILs by using the joint segregation distortion method. The 13 QTLs were validated by the genotypic differences at individual QTL in the random populations. Putative genetic networks consisting of 30 loci in 29 functional genetic units underlying DT were detected by X^2 tests and non-random associations between or among DT loci in DT ILs from the four populations. Most large-effect DT QTLs were previously reported and located in the upstream of the genetic networks as putative regulators, and were either mapped to important regulatory genes for DT or drought responsiveness reported previously. In our study, five promising ILs with significantly improved yield were selected under both drought and normal irrigated conditions. The QTLs and their genetic networks underlying DT detected provided useful genetic information for further improving DT and yield using designed QTL pyramiding.

Keywords: QTL, drought tolerance, functional genetic units, non-random associations, hidden genetic diversity

INTRODUCTION

Rice (*Oryza sativa* L.) is the major food crop for more than 700 million people and more than 90% of rice in the world is grown and consumed in Asia (Ji et al., 2012; Palanog et al., 2014). However, with the deterioration of environment, area with severe water shortage is expected to increase. In Asia, about 50% of the rice land is rainfed rice area where the water supply is unpredictable and droughts are common. Rice is sensitive to drought stress at the reproductive stage, when a slight drought stress can cause drastic yield loss (Kamoshita et al., 2008; Palanog et al., 2014). Drought has been a major abiotic stress factor for limiting rice production in rainfed ecosystem. Developing drought tolerance (DT) rice cultivars is the direct and effective way to reduce crop loss.

Developing DT rice varieties is often challenging because of the complexity of DT. In nature, drought stress may occur at any stage of rice growth, and the effect of drought stress on rice are various at different growth stage. The rice species has 12 chromosomes with the whole genome size of 430 Mb. In rice breeding, direct selection for improving DT was often ineffective because rice DT often show a considerable degree of genotype by environment interaction (Fukai and Cooper, 1995). As a result, tremendous efforts have been devoted to genetically dissect DT related secondary traits such as root architecture, leaf water potential and relative water content, etc. Unfortunately, indirect selection for secondary traits have not been effective to improve DT in rice due to poor correlation between the secondary traits and grain yield under drought stress (Palanog et al., 2014). Recent studies showed that direct selection for grain yield (GY) in artificial or natural drought stress conditions is the most effective way for developing DT rice with high yield potential under non-tress conditions (Venuprasad et al., 2007, 2008; Guan et al., 2010). However, it often takes long time for cultivar development using traditional methods of rice breeding on the basis of simple cross making and phenotypic selection. An alternative method of improving breeding effectiveness is to identify quantitative trait loci (QTLs) with large and consistent effects in different populations under drought stress conditions. The identified QTL can be used for marker assistant breeding (MAB) (Venuprasad et al., 2011). Thus, many efforts have been made to identify large-effect QTL affecting DT and develop marker assisted selection systems for improving rice DT (Xu et al., 2005; Yue et al., 2005; Palanog et al., 2014). Again, despite larger numbers of QTL related to DT have been detected, relatively few of them have large and consistent effects for an efficient MAS program.

In order to fill the gap between basic genetic/molecular dissection of DT and improving DT in breeding, a new strategy has been proposed for simultaneous improvement and genetic dissection of complex traits using backcross breeding and marker-facilitated tracking of gene flow from donors to recipients from selection (Li et al., 2005b). In other words, selected breeding progeny will be used to conduct QTL mapping, which have three major advantages over the classical QTL mapping. The first one is the small size of selected breeding populations and thus requires low costs in both genotyping and phenotyping. Second, selected population often has greatly increased power in detecting QTL for the target traits under selection, but much reduced power in detecting QTL for non-target traits. The third and most important one is that mapping QTL using selected population is part of breeding and lines from selected populations are expected to carry beneficial alleles of QTL. Thus, selected lines can potentially become new varieties, but more likely can be used directly as parents in making crosses of "designed QTL pyramiding," an important step toward breeding by design (Ali et al., 2017).

In this study, we demonstrated again the strategy for simultaneous improvement and genetic dissection of DT of rice in the process of breeding. We reported the development of superior lines with significantly improved grain yield under both drought stress and irrigated conditions as well as providing useful breeding lines and genetic information for further improving rice yield and DT using designed QTL pyramiding.

MATERIALS AND METHODS

Development of the Plant Materials

A superior high yield *Geng* (*japonica*) variety, Jigeng88, which is an elite cultivar commercially grown in Jilin province of China, was used as the recurrent parent (RP) and four varieties collected from China, Malaysia, and IRRI as donors. These donors contained three *Xian* (*indicas*) and one *Geng* variety (**Table 1**). In the summer of 2005, Jigeng88 (JG88) was crossed with all donors to produce F_1s on the experimental farm of Ningxia Academy of Agriculture and Forestry Sciences (NAAFS) in Yinchuan (38.5° N, 106.2° E). The F_1 plants were backcrossed with the RP to produce BC_1F_1 population in Sanya (18.3° N, 109.3° E), Hainan Province of China during the winter season of 2005–2006. In the summer of 2006, 25–30 randomly selected plants from each of the BC_1F_1 populations were backcrossed with the RP to produce 25–30 BC_2F_1 lines. From each of the crosses, 25 BC_2F_1 lines were planted (36 plants of each line in a single row) in 2007. Selfed seeds from individual plants of 25 BC_2F_1 lines of each cross were bulk harvested to produce a single bulk BC_2F_2 population.

The Screening of the BC_2F_2 Bulk Populations for DT at the Reproductive Stage

The screening of the BC_2F_2 bulk populations was conducted on the experimental farm of NAAFS. The soil of the test field was a sandy clay. In the initial screen for DT, 800 25-day old seedlings of each BC_2F_2 population were transplanted into a big 80-row plot with 10 plants per row and a spacing of 20 × 25 cm between plants and rows flanked by two rows of the RP in the summer of 2008 at the NAAFS. **Figure 1A** shows the field screening of drought tolerance (DT) at reproductive stage. The field was managed under the normal irrigation until the peak tillering stage 50 days after transplanting. Then, the field was drained. Flush irrigation was applied twice when drought stress became very severe due to large evaporation capacity, at an interval of 10 days (total water applied 1,600 m^3 ha^{-1}), to create severe water stress at the reproductive stage. The resulting soil water

TABLE 1 | The information of 4 rice backcross populations used for improving drought tolerance in this study.

Donor (code)	Subspecies[a]	Origin	DT selected ILs						Random ILs		
			N_1[b]	N_2	SI (%)[c]	N_3	DG%[d]	H[e]	N_4	DG%	H
							Mean ± *SD*			Mean ± *SD*	
IR66897B (I)	*Xian(X)*	IRRI	800	28	3.5	17	13.5 ± 16.8	2.1 ± 3.3	60	10.4 ± 9.8	2.8 ± 3.3
MR77 (II)	*Xian(X)*	Malaysia	800	40	5.0	21	10.2 ± 8.1	1.4 ± 3.0	55	5.9 ± 6.5	1.0 ± 2.6
MR167 (III)	*Xian(X)*	Malaysia	800	29	3.6	10	8.9 ± 16.8	0.0	60	6.4 ± 7.2	0.6 ± 1.5
SN265 (IV)	*Geng(G)*	China	800	38	4.8	24	19.9 ± 11.5	3.6 ± 4.8	60	13.9 ± 8.1	0.9 ± 1.3
Mean				33.8	4.2	19.8	11.5	1.8	58.8	9.2	1.3

[a] *Subspecies X = Xian (indica) and G = Geng (japonica).*

[b] *N_1 is the original size of the BC_2F_2 population used for screening drought tolerance. N_2 is the number of surviving plants initially selected from each population after drought stress treatment at the reproductive stage. N_3 is the number of selected BC progeny with significantly improved DT as confirmed by progeny testing of their derived $BC_2F_{2:3}$ ILs under drought stress at the reproductive stage. N_4 is the size of each of the BC_2F_2 random populations used for validation.*

[c] *SI is the initial selection intensity (proportion of plants selected) in the BC_2F_2 populations.*

[d] *Percentage of the donor genome of the BC_2F_2 ILs was calculated based all polymorphic SSR markers used in genotyping.*

[e] *H, heterozygosity.*

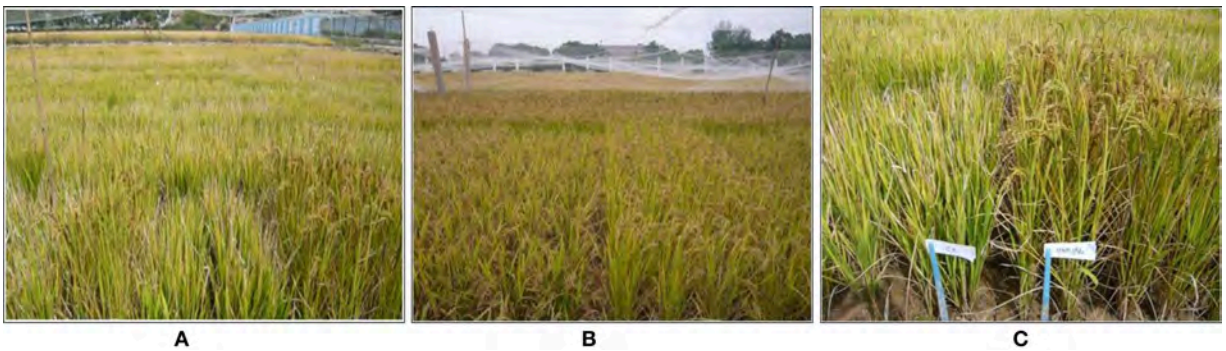

FIGURE 1 | Field screening and performance of drought tolerance under drought stress. **(A)** The field screening of DT at the reproductive stage. **(B)** Performance of the DT ILs under drought stress. **(C)** Comparison of DT IL and JG88 under drought stress (The left side are JG88 and right side are DT ILs).

content was ∼16–19% (v/v) based on constant monitoring using the time domain reflectometry method (TRIME-FM moisture meter; IMKO GmbH, Ettlingen, Germany) at a soil depth of 0–30 cm. No rainfall occurred during this period at the study site. Out of 3,200 plants from the four BC_2F_2 populations, total of 135 plants survived under the severe drought stress, and then were harvested individually at the maturing stage. All selected BC_2F_3 lines were progeny tested under the similar drought stress (DS) conditions in the summer of 2009, and 72 BC_2F_3 lines with significantly higher yield were selected, ranging from 10 lines from the Jigeng88/MR167 population to 24 lines from the Jigeng88/SN265 population (**Table 1** and **Figures 1B,C**). The flowchart shows the population development for identification of QTL in selected population and validation of QTL in random population (**Figure 2**).

Phenotypic Data Collection

In the summers of 2012 and 2013, all selected 72 BC_2F_4 lines plus 235 random BC_2F_4 lines from the same four populations were evaluated under the drought stress and irrigated conditions in the experimental farms of NAAFS and Chinese Academy of Agricultural Sciences (CAAS) in Beijing (BJ). The soil of the test field was a sandy loam in Beijing. In each experiment, 30-day old seedlings of each ILs were transplanted into a five-row plot with 30 plants in each plot and a spacing of 20 × 25 cm between plants and rows. A completely randomized block design was used with two replications per line. Under the irrigated control condition, water was applied whenever necessary until most lines had reached the grain-filling stage (total water applied 4,800 m^3 ha^{-1}). For drought stress, moderate stress condition was performed to validate the DT lines at the NAAFS. A water sheltered facility was adopted in CAAS for creating drought stress. Normal irrigation was maintained for 1 month after transplanting, then the plots were drained and irrigation was withheld completely till harvest. Thus, all tested lines were subjected to severe drought at the reproductive stage. During the periods of drought stress, water levels of the fields were monitored daily at a soil depth of 0–30 cm based on constant monitoring using the time domain reflectometry method (TRIME-FM moisture meter; IMKO GmbH, Ettlingen, Germany). At maturity, all plants were harvested and measured for grain yield and five plants in each plot were sampled and measured for following yield related traits: heading date (HD), plant height (PH), effective panicle number per plant (PN),

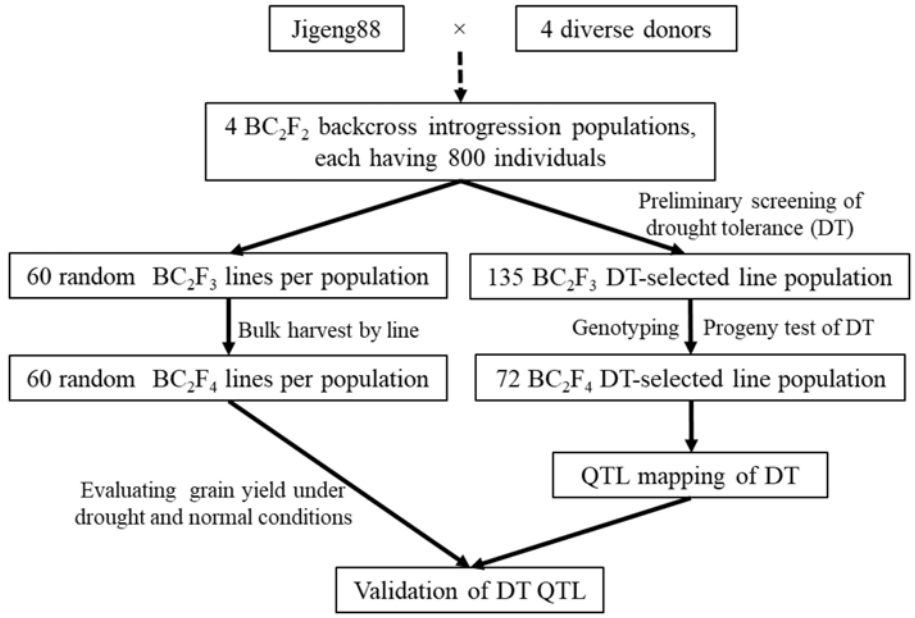

FIGURE 2 | Flowchart of the population development for identification and validation of QTL for drought tolerance in rice.

thousand-grain weight (GW), filled grain number per panicle (GN), grain weight per plant (GY), and spikelet number per panicle (SN). HD was recorded when the panicle was exerted ∼50% of the plants in a plot.

Genotyping Experiments

Genomic DNA was extracted using the CTAB method (Ahmadikhah, 2009). The DNA was isolated from bulk fresh leaf tissues of each $BC_2F_{2:3}$ IL. More than 600 rice anchor simple sequence repeat (SSR) markers were used to survey the parental lines, resulting in 181, 201, 197, and 38 polymorphic SSR markers, respectively, for the four populations. The markers were used to genotype the selected ILs and random ILs.

Statistical Analysis

Because of the greatly reduced variation among lines within each of the selected IL population, normal statistical methods for identifying QTL in random segregating populations are not appropriate for detecting QTL in selected populations. Therefore, we took a segregation distortion approach to map segregation distortion markers (Cui et al., 2015). In addition, we combined the four selected breeding populations together to perform a joint QTL mapping following the method developed by Cui et al. (2015). However, the four selected populations in this study have different markers. Some markers in some populations were not genotyped. We first developed a consensus map using the multipoint method under the Markov model (Cui et al., 2015). As Cui et al developed, an individual survived from the drought stress with an underlying quantitative trait $y_j$called liability which can be described by the liner model

$$y_j = Z_j a + \xi_j \tag{1}$$

where Z_j is the genotype indicator for individual j, a is the genetic effect of locus, ξ_j is the residual error follow the normal distribution $\xi_j \sim N(0,1)$. Assume all the individuals survived are selected based on the $y_j > 0$ criterion. The probability of surviving is $\Pr(y_j > 0) = \Phi(Z_j a)$. Using the Bayes' theorem, the posterior probability of survival for each genotype are $\pi_{j(11)} = \phi_{11}\Phi(a)/\bar{\pi}_j$, $\pi_{j(12)} = \phi_{12}\Phi(0)/\bar{\pi}_j$, $\pi_{j(22)} = \phi_{22}\Phi(-a)/\bar{\pi}_j$, where $\bar{\pi}_j = \phi_{11}\Phi(a) + \phi_{12}\Phi(0) + \phi_{22}\Phi(-a)$ and $\phi_{11} = 13/16$, $\phi_{12} = 2/16$, $\phi_{22} = 1/16$ are the expected Mendelian frequencies for the three genotypes in BC_2F_2. When $a = 0$, the posterior probabilities are equal to the expected Mendelian frequencies and we will not be able to detect segregation distortion. If $a \neq 0$ the posterior probabilities of genotypes will deviate from the expected Mendelian Segregation ratios. The segregation distortion loci could be identified. For each population, we estimated the effect of each marker and calculated the variance of the estimated effect. Let $\hat{a}_k$ be the estimated effect and $\text{var}(\hat{a}_k)$ be the variance of the estimate for a marker under consideration. The Wald test for $H_0 : a_k = 0$ in the kth population was obtained using $\hat{a}_k^2/\text{var}(\hat{a}_k)$. The joint test for all populations for $H_0 : a_1 = a_2 = ... = a_p = 0$ is

$$\text{Wald} = \sum_{k=1}^{p} \frac{\hat{a}_k^2}{\text{var}(\hat{a}_k)} \tag{2}$$

where $p = 4$ is the number of populations. When there are multiple populations, the Wald test simply takes the sum of the Wald test of each individual population. In fact, the random model approach was developed by treating each a_k as a normally distributed random variable with a common variance across populations, i.e., $a_k \sim N(0, \sigma_a^2)$ for $k = 1, ..., p$. The shared variance

justified the joint mapping (Cui et al., 2015). The critical value for genome-wide significance at the 0.05 level was drawn from 1,000 permuted samples (Churchill and Doerge, 1994).

Construction of Genetic Networks Underlying Drought Tolerance

According to the molecular quantitative genetic theory (Zhang et al., 2011; Wang et al., 2015), segregating loci at different levels of signaling pathways contributing to DT in the selected ILs from each BC population were expected to show significant frequency shifts and non-random associations in a strictly hierarchical manner. Here, a functional genetic unit (FGU) is defined either as a single locus of significant excess introgression or an associate group (AG) of r ($r \geq 2$) unlinked but perfectly associated loci of equal introgression in the DT ILs selected from each BC population. Single FGUs of excessive introgression could be detected by the segregation distortion method described above, or by simple X^2 tests for detecting significant deviations of the donor and genotypic frequencies at individual loci across the genome from the expected allelic and genotypic frequencies estimated from all genotyped markers of the random populations. In addition, DT loci involved in epistasis (the same signaling pathways) were expected to show strong non-random associations in response to selection, and thus could be detected as association groups (AGs) each consisting of r ($r \geq 2$) unlinked but perfectly associated loci of equal introgression in DT ILs selected from each BC population. Thus, a multi-locus probability test:

$$P_{(AG)} = (p_i)^{rm} \times (1 - p_i)^{r(n-m)} \quad (3)$$

where p_i is the frequency of the donor introgression in the random ILs from each BC population, $n$is the number of the selected ILs, $m$is the number of ILs that have co-introgression of the donor alleles, and $(n - m)$ is the number of ILs having no introgression at the r unlinked loci in the AG. Here $(p_i)^m$ is the probability of m ILs having co-introgression of the donor alleles and $(1 - p_i)^{n-m}$ is the probability of $(n - m)$ ILs having no introgression at r unlinked loci. The threshold to claim a significant case was $P \leq 0.005$ (Zhang et al., 2014). For each AG consisting of r ($r \geq 2$) unlinked but perfectly associated loci, $r \times (r - 1)/2$ significant pairwise associations would be existed between the $r$loci, which were also confirmed by the linkage disequilibrium (LD) analyses. To reveal the multi-locus structure or putative genetic network underlying DT in the ILs from each BC population, pairwise gametic LD analyses were performed to characterize the relationship between alleles at all DT FGUs detected in the DT ILs from each BC population. The equation of LD statistic

$$\tilde{D}_{AB} = \tilde{p}_{AB} - \tilde{p}_A\tilde{p}_B \quad (4)$$

where $\tilde{p}_{AB}$, $\tilde{p}_A$, and $\tilde{p}_B$were the frequencies of co-introgression functional AB and functional genotypes at FGUs A and FGUs B, respectively. A multi-locus genetic network including all detected FGUs in the confirmed drought-tolerance ILs was constructed in two steps based on the principle hierarchy: (1) All the FGUs detected in the DT ILs from a single population were divided into major groups according to the LD results. The individual FGUs of different IF within each group were all significantly and positively associated with $\widehat{Ds}_{AB'} = 1.0$, and FGUs in different groups were either independent or negatively associated; (2) Based on the principle of hierarchy, all associated FGUs within each group were connected and formed multiple layers according to their progressively reduced functional genotypes (FG) frequencies and inclusive relationships (Zhang et al., 2011). The underlying assumption for the network construction is that all FGUs in a network are genetically independent (unlinked) from one another, which was true in our cases because all redundant loci due to linkage (recombination frequency $\leq$0.4) associated with each of the FGUs detected in DT ILs of each population were removed.

RESULTS

Developing ILs With Significantly Improved DT and Yields

From a total of 3,200 plants in the four BC_2F_2 populations, 135 plants survived the drought stress and were selected in the first round screening. The number of selected individuals ranged from 28 in population I to 40 in population II (**Table 1**). After progeny testing of the 135 DT BC_2F_3 lines, 17, 21, 10, and 24 DT ILs from the four populations showed significantly higher GY than the recurrent parent (JG88) under drought stress at the reproductive stage. In the phenotyping experiment, all BC_2F_4 IL populations showed significantly improved GY under drought stress when compared to JG88, at Ningxia and/or Beijing (**Table 2**). The ANOVA results show that there was a statistically significant difference in all traits between the normal and drought stress conditions. The location factor for trait PH, PN, SN, GW, and HD were found to be statistically significant with $P < 0.01$. There was a significantly difference for PH, PN, GW, and HD between the different lines. The G by E interactions were existed in the trait PH and PN (Supplementary Table 1). The mean yield advantage of the IL populations over the RP ranged from 12.7 to 22.5% under the moderate drought stress (JG88 suffered 58.5% yield loss) in Ningxia, and from 89.4 to 178.9% under the severe drought (JG88 suffered 91.0% yield loss) in Beijing, even though there was some residual variation for DT among ILs from each population (**Table 2**). Clearly, the more severe of drought stress was, the greater the yield advantage over the RP the selected DT ILs had. When the yield related traits of the IL populations were examined, almost all populations had similar mean trait values as JG88 except for population I which had significantly higher trait values for PH, SN, and GN. Under the irrigated conditions, no significant differences were detected for yield and related traits between the selected IL populations and JG88 (**Table 2**). Nevertheless, we were able to identify five promising ILs which had significant higher yields than JG88 under both drought

TABLE 2 | Mean performances of the DT introgression lines for grain yield and related traits selected from 4 backcross populations and their recurrent parent (JG88) in Ningxia (2013) and Beijing (2012) under the drought stress and non-stress irrigated conditions.

	Population	Location	N	GY(g)	HD(d)	PH(cm)	PN	GN	SN	GW(g)
Drought stress	I	NX	17	8.4 ± 1.8*	108.1 ± 6.1	84.5 ± 13.3*	4.7 ± 0.6	121.3 ± 17.0**	151.1 ± 20.0**	17.8 ± 1.5
	II	NX	21	8.1 ± 1.0*	101.6 ± 3.7	67.5 ± 6.7	5.3 ± 0.7*	94.0 ± 14.8	126.5 ± 18.9	18.0 ± 1.2
	III	NX	10	8.7 ± 1.5**	103.3 ± 4.1	69.8 ± 4.8	5.7 ± 0.8**	93.3 ± 16.1	119.4 ± 15.9	19.0 ± 1.7
	IV	NX	24	8.0 ± 1.2*	106.4 ± 1.4	74.2 ± 3.3	5.2 ± 0.6	97.4 ± 10.2	111.6 ± 10.6	18.8 ± 1.8
	JG88(RP)	NX		7.1 ± 0.4	105.1 ± 1.9	73.6 ± 2.1	4.7 ± 0.4	87.9 ± 3.3	113.4 ± 15.1	20.3 ± 2.4
	I	BJ	17	4.5 ± 2.1	96.9 ± 8.8*	89.1 ± 12.4*	2.1 ± 1.2	114.8 ± 46.7	150.4 ± 50.9	14.9 ± 1.9
	II	BJ	21	5.3 ± 1.8	93.3 ± 3.9	79.0 ± 7.1	3.0 ± 1.4	119.0 ± 54.8	170.9 ± 123.4	16.7 ± 1.4
	III	BJ	10	4.6 ± 2.5	91.7 ± 3.3	81.2 ± 5.6	2.2 ± 1.4	130.1 ± 60.7*	155.4 ± 62.9	16.1 ± 2.4
	IV	BJ	24	3.6 ± 1.6	98.0 ± 3.0**	89.1 ± 5.4*	1.9 ± 0.9	111.2 ± 52.8	141.0 ± 66.6	16.1 ± 1.9
	JG88(RP)	BJ		1.9 ± 0.5	92.5 ± 3.2	78.5 ± 6.6	2.2 ± 1.0	97.7 ± 56.2	138.7 ± 60.2	15.7 ± 1.9
Non-stress irrigated conditions	I	NX	17	17.4 ± 3.9	102.5 ± 5.0	95.8 ± 10.7	5.9 ± 1.0	184.1 ± 22.0	204.5 ± 21.7	20.3 ± 1.3
	II	NX	21	18.5 ± 2.7	96.9 ± 2.3	93.3 ± 7.4	6.2 ± 1.2	175.7 ± 26.2	192.5 ± 27.7	21.5 ± 1.4
	III	NX	10	16.9 ± 3.8	99.4 ± 3.9	87.4 ± 6.4	5.9 ± 0.9	157.7 ± 30.5	169.1 ± 31.8	22.3 ± 1.9
	IV	NX	24	18.9 ± 3.1	101.6 ± 1.8	99.4 ± 3.4	6.3 ± 0.9	175.7 ± 20.0	187.3 ± 19.7	21.3 ± 1.2
	JG88(RP)	NX		17.1 ± 1.4	99.0 ± 2.6	91.0 ± 4.8	6.0 ± 0.6	175.1 ± 28.7	186.6 ± 31.8	21.5 ± 2.1
	I	BJ	17	22.6 ± 4.5	93.3 ± 6.8	114.2 ± 14.1**	7.3 ± 1.1	217.3 ± 31.9	245.8 ± 29.0	19.1 ± 1.2
	II	BJ	21	20.0 ± 2.4	90.9 ± 5.1	104.4 ± 6.1	6.2 ± 0.8	206.4 ± 37.9	237.2 ± 44.9	19.6 ± 1.2
	III	BJ	10	21.6 ± 6.3	91.5 ± 4.8	100.2 ± 7.1	6.8 ± 1.2	192.6 ± 32.6	208.2 ± 31.5	20.6 ± 1.0
	IV	BJ	24	22.1 ± 2.4	96.2 ± 1.7	109.8 ± 3.6	6.7 ± 0.8	214.4 ± 19.3	226.2 ± 20.3	20.0 ± 1.3
	JG88(RP)	BJ		21.1 ± 4.7	94.9 ± 4.5	106.5 ± 2.1	7.4 ± 1.7	222.0 ± 25.8	241.0 ± 29.3	19.6 ± 2.2

*GY, grain yield; PH, plant height; PN, effective panicle number per plant; GN, filled grain number per panicle; SN, spike number per panicle; GW, thousand grain weight; HD, head date. * and ** indicate the significance levels of P = 0.05 and 0.01, respectively, based on Duncan's multiple comparisons in ANOVA.*

stress and normal irrigated conditions in both and/or either environments (**Table 3**).

Detection and Validation of DT QTL in the Selected and Random IL Populations

Using a critical value of Wald test of 16.97 drawn from 1,000 permutated samples, 13 QTLs on seven rice chromosomes were detected in 72 ILs selected from the four BC populations (**Table 4**). These included 7 QTL (*QDT1.3*, *QDT2.4*, *QDT2.9*, *QDT7.1*, *QDT7.2*, *QDT7.4*, and *QDT11.5*) in the 17 ILs from population JG88/IR66897B(I), 7 QTL (*QDT1.4*, *QDT6.3*, *QDT2.9*, *QDT6.3*, *QDT6.5*, and *QDT10.3*) from 21 ILs from population JG88/MR77(II), 3 QTL (*QDT2.9*, *QDT6.3,* and *QDT6.5*) from 10 ILs from population JG88/MR167 (III), and 4 QTL (*QDT1.3*, *QDT2.4*, *QDT6.3,* and *QDT6.5*) from the 24 ILs of JG88/SN265(IV). Of these, 2 QTL (*QDT2.9* and *QDT6.3*) each was detected in three of the populations, 4 QTL (*QDT1.3*, *QDT1.4*, *QDT6.5,* and *QDT7.1*) each was detected in two of the populations, and the 7 remaining QTL each was detected in a single population. Two QTL, *QDT1.4* near marker RM449 on chromosome 1 and *QDT2.9* near MR266 on chromosome 2 were identified with the highest Wald values of 65.8 and 41.54.

In order to validate the detected DT QTL, the four random (unselected) populations each with ∼60 BC_2F_4 lines from the same four crosses were evaluated under drought stress in the replicated trials. Based on the genotypic differences in mean yields under drought at each of the detected QTL in the random BC_2F_4 lines from each population, 11 of the 13 detected QTL could be validated in the random populations evaluated in the Ningxia experiment and 8 of the DT QTL could be validated in the random populations in the Beijing experiment (**Table 5**). In all cases, significantly increased GY under drought stress in both Ningxia and Beijing were associated with the donor homozygote genotype, indicating that the donor alleles at all these detected QTL were associated with DT. The average yield advantage under drought from the donor homozygote at individual QTL ranged from 4.1% for *QDT8.3* to 45.9% for *QDT10.3*.

Putative Genetic Networks (Multi-Locus Structures) Underlying DT

Table 6 shows 29 FGUs (28 single loci and 1 association group or AG) for DT detected by χ^2 tests (single loci) and multi-locus linkage disequilibrium analyses in 72 drought-tolerant introgression lines (ILs) selected from the four populations. These included 10 FGUs detected in 17 ILs of JG88/IR66897B (I), 9 loci in eight FGUs in 21 ILs of JG88/MR77 (II), 4 FGUs in 10 ILs of JG88/MR167 (III), and 7 FGUs in 24 ILs of JG88/SN265(IV), respectively (**Table 6** and **Figure 3**). The average introgression frequency (IF) of the donor alleles at the 30 DT loci ranged from 0.147 to 0.81.

Figure 3 shows the four putative genetic networks or multi-locus structures each containing all DT FGUs identified in

TABLE 3 | Five promising JG88 introgression lines with significantly improved yields under both drought stress and irrigated conditions compare with recurrent parent (JG88) in either Ningxia (2013) and/or Beijing (2012) under the drought stress and non-stress irrigated conditions.

ILs	Env.	Under drought							Irrigated conditions					
		GY (g)	HD (d)	PH(cm)	PN	FGN	SN	GW (g)	GY (g)	HD(d)	PH (cm)	PN	FGN	SN	GW (g)
BJC9	BJ	6.9 ± 1.8*	97.5 ± 1.5	83.2 ± 1.5	3.3 ± 2.2	97.8 ± 23.8	124.5 ± 10.5	15.5 ± 0.8	21.8 ± 1.9	97.0 ± 0.1	108.3 ± 2.5	6.9 ± 1.5	204.4 ± 20.8	218.7 ± 23.3	20.8 ± 0.2
	NX	10.0 ± 0.7*	107.5 ± 1.5	74.6 ± 0.4	4.5 ± 0.1	126.1 ± 0.7**	143.0 ± 3.6*	19.6 ± 0.1	21.6 ± 3.1	104.1 ± 2.0	91.9 ± 0.3	6.8 ± 1.0	197.3 ± 1.9*	220.6 ± 0.6*	21.6 ± 0.3
BJC85	BJ	4.2 ± 1.9	89.5 ± 2.5	79.8 ± 1.1	4.7 ± 1.7	120.2 ± 30.1	134.3 ± 31.8	16.2 ± 0.1	24.4 ± 0.6	92.5 ± 0.5	100.8 ± 1.6	7.6 ± 0.8	177.8 ± 3.4	195.1 ± 11.7	20.9 ± 1.3
	NX	8.8 ± 0.3*	99.0 ± 0.1**	65.3 ± 0.7*	5.4 ± 0.1**	92.5 ± 6.1	113.7 ± 2.5	19.1 ± 0.5	18.2 ± 2.2	96.1 ± 0.1*	92.8 ± 1.0	6.1 ± 1.0	171.1 ± 5.3	180.5 ± 1.7	21.3 ± 0.6
BJC101	BJ	3.1 ± 1.1	97.0 ± 1.3	90.3 ± 0.5*	4.3 ± 0.5*	103.3 ± 28.3	115.8 ± 36.8	17.5 ± 1.8	21.6 ± 3.0	97.5 ± 1.5	108.9 ± 0.7	6.6 ± 1.0	185.9 ± 2.1	221.9 ± 28.5	21.1 ± 1.3
	NX	10.8 ± 0.7*	106.0 ± 0.1	75.5 ± 1.5	6.1 ± 1.1	107.9 ± 5.1	114.0 ± 7.2	20.9 ± 0.1*	24.7 ± 6.4	102.0 ± 0.1*	101.5 ± 4.3	7.6 ± 1.8	168.1 ± 6.7	174.9 ± 8.1	22.3 ± 0.4
BJC105	BJ	2.5 ± 0.2*	98.0 ± 1.7	86.7 ± 0.1	4.1 ± 2.0	166.7 ± 16.5	198.2 ± 7.0	18.4 ± 0.8*	25.6 ± 5.9	97.5 ± 0.5	109.1 ± 0.3	8.5 ± 2.3	214.3 ± 3.3	220.1 ± 1.9	19.8 ± 0.7
	NX	8.6 ± 0.5*	106.5 ± 0.5	73.0 ± 1.2	4.4 ± 0.1*	104.6 ± 6.8	117.2 ± 9.8	19.4 ± 0.1	19.9 ± 2.6	100.5 ± 2.5	99.1 ± 3.3	6.1 ± 0.9	188.2 ± 1.6	198.4 ± 4.4	21.6 ± 0.8
BJC112	BJ	6.3 ± 1.0*	98.0 ± 0.5	94.2 ± 2.0*	2.5 ± 7.0	113.7 ± 8.7	131.0 ± 47.3	16.1 ± 1.5	22.2 ± 4.5	96.1 ± 1.0	115.3 ± 1.5*	5.8 ± 1.0	236.5 ± 11.7	246.4 ± 17.6	20.9 ± 0.3
	NX	8.6 ± 0.7*	106.5 ± 0.5	75.9 ± 1.5	5.1 ± 0.5	99.9 ± 3.5	110.4 ± 3.2	19.6 ± 0.2	25.2 ± 7.7	105.5 ± 4.5	105.8 ± 7.8	8.2 ± 2.2	194.1 ± 23.2	207.8 ± 30.0	21.1 ± 1.4
JG88	BJ	1.9 ± 0.5	92.5 ± 3.2	78.5 ± 6.6	2.2 ± 1.0	97.7 ± 56.2	138.7 ± 60.2	15.7 ± 1.9	21.1 ± 4.7	94.9 ± 4.5	106.5 ± 2.1	7.4 ± 1.7	222.1 ± 25.8	241.1 ± 29.3	19.6 ± 2.2
	NX	7.1 ± 0.4	105.0 ± 1.9	73.6 ± 2.1	4.7 ± 0.4	87.9 ± 3.3	113.4 ± 15.1	20.3 ± 2.4	17.1 ± 1.4	99.1 ± 2.6	91.1 ± 4.8	6.0 ± 0.6	175.1 ± 28.7	186.6 ± 31.8	21.5 ± 2.1

The trait abbreviations are the same as ***Table 2****.*

andindicate the significance levels of P = 0.05 and 0.01, respectively, based on Duncan's multiple comparisons in ANOVA.*

the selected DT ILs from populations I–IV. Genetic network I contains 10 FGUs (10 loci) in five largely independent branches detected in the 17 DT ILs from population Jigeng88/IR66897B. Branch I-1 consisted of two unlinked but perfectly associated loci, with RM542 (bin 7.4) of high introgression placed in the upstream (IF = 0.588) and RM480 (bin 5.8) of lower introgression (IF = 0.294) in the downstream. Similarly, branches I-2, I-3, and I-4 each also consisted of two unlinked but perfectly associated loci with a locus of high introgression placed in the upstream and a locus of low introgression placed in the downstream. Branch I-5 contains a single locus near RM141 (bin 6.7). Genetic network II consisted of eight FGUs (9 loci) with two major branches plus two independent loci detected in the 21 DT ILs from population Jigeng88/MR77. Branch II-1 had RM449 (Bin1.1) of very high introgression (IF = 0.810) in the upstream as the putative regulator connected with three sub-branches, RM286 (bin11.1) (IF = 0.333), RM470 (bin 4.6) (IF = 0.214), and $agDT_{II-1}$ consisting of two unlinked but perfectly associated loci at RM336 (Bin7.6) and RM331 (Bin8.3) of low introgression (IF = 0.286) in the downstream. Branch II-2 consisted of 3 unlinked but highly associated FGUs with RM406 of high introgression placed at the top as the putative regulator and 2 FGUs (RM276 in Bin6.3 and RM311 in Bin10.3) of lower introgression in the downstream. The independent FGUs included RM541 at bin 6.5 of high introgression (IF = 0.429) which were detected as DT QTL using the segregation distortion method (**Table 3**). Genetic network III detected in the 10 ILs of JG88/MR167 consisted of 4 FGUs (4 loci) with a single branch plus two independent loci (MR518 in bin4.2 and MR253 in bin6.3). Branch III-1 containing 2 unlinked but highly associated loci with MR339 (bin8.3) in the upstream and MR406 (bin2.9) in the downstream. The genetic network of JG88/SN265 contained only 7 independent loci (FGUs). This was not surprising since both JG88 and SN265 are closely related *Geng* varieties from Northeast China.

DISCUSSION

In this study, we have shown that most selected ILs from the four BC populations had significantly improved GY under drought stress without yield penalty under the normal irrigated conditions (**Table 2**). This result plus the development of five promising ILs that had significantly higher yields under both drought stress and normal irrigated conditions indicated that backcross breeding was effective for improving DT of high yielding *Geng* varieties. We noted that the improved yield performances of ILs under drought stress were associated primarily with increased PN and GN, but not with increased TGW. This is consistent with the effect of natural selection which tends to act on the number instead of size of rice grains (Ashikari et al., 2005; Lu et al., 2013). It should be pointed out that none of the four donors in our BC breeding has good DT, but they apparently all have genes contributing to DT, indicating the presence of rich "hidden" genetic diversity in the primary gene pool of rice for DT, as reported previously (Lafitte et al., 2006; He et al., 2010; Wang et al., 2013a,b; Ali et al., 2017). This is true for tolerances to other abiotic stresses such as salinity, submergence,

TABLE 4 | Thirteen QTL associated with drought tolerance identified by the segregation distortion mapping method in DT introgression lines selected from four backcross populations.

QTL	Marker	Position (cM)[a]	Wald value[b]	Population[c]	QTL and drought-responsive genes
QDT1.3	RM572	66.4	22.15	I, II	*rfw1b* (Li et al., 2005a)
QDT1.4	RM449	78.4	65.8	II, IV	*brt1d* (Li et al., 2005a)
QDT2.4	RM424	66	17.5	I	*qDTY2.1* (Dixit et al., 2012); *qLRS-2* (You et al., 2006)
QDT2.8	RM425	166	32.72	II	
QDT2.9	RM266	192.2	41.54	I, II, III	*OsPIP1;3* (Lian et al., 2004; Liu et al., 2007)
QDT6.3	RM276	40.3	37.87	II, III, IV	
QDT6.5	RM541	75.5	27.82	II, IV	*qgy6.1* (Palanog et al., 2014)
QDT7.1	RM427	1.1	20.74	I, IV	*OsCIPK23* (Yang et al., 2008)
QDT7.2	RM125	24.8	25.12	I	*OsNAC3/ONAC067* (Ooka et al., 2003)
QDT7.4	RM542	34.7	30.42	I	*rn7a* (Li et al., 2005a)
QDT8.3	RM339	72.2	22.05	III	*QGy8* (Xu et al., 2005); *QPn8,QTgw8, QSf8* (Wang et al., 2012)
QDT10.3	RM311	25.2	19.82	II	*trdw10.1* (Nguyen et al., 2004)
QDT11.5	RM229	77.8	21.75	I	

[a] *cM means centimorgan, a unit of genetic distance.*
[b] *Wald value = 16.97 and 20.35 at P = 0.05 and 0.01, respectively.*
[c] *The designations of the populations are the same as* ***Table 1****.*

TABLE 5 | Phenotype validation of DT QTLs by comparing mean grain yields of QTL genotypes of the four random populations in Ningxia (2013) and Beijing (2012) under the drought condition.

QTL	Marker	Population	Mean grain yield (g/plant) in Ningxia			Mean grain yield (g/plant) in Beijing			Yield improvement[a] (%)
			Donor homozygote	JG88 homozygote	Jg88	Donor homozygote	JG88 homozygote	Jg88	
QDT1.4	RM449	IV	9.22	8.47	7.71	7.54	6.60	6.89	14.5
QDT2.4	RM424	I	10.30	8.8	7.38				39.6
QDT2.8	RM425	II	10.25	8.46	7.63	8.38	6.87	6.52	31.4
QDT2.9	RM266	I	10.23	9.05	7.38	6.39	5.91	5.41	28.4
		II	9.92	8.68	8.82				12.5
QDT6.3	RM276	II	9.83	9.04	8.82	8.23	7.00	6.52	18.8
QDT6.5	RM541	II	10.10	8.58	7.63	8.60	6.81	6.42	24.2
		IV				8.20	6.70	6.89	19.0
QDT7.1	RM427	I	11.56	8.72	8.82	6.86	6.10	5.41	28.9
		IV	9.03	8.31	7.71				17.1
QDT7.4	RM542	I	9.52	9.10	8.82				8.0
QDT8.3	RM339	III	9.18	8.26	8.82				4.1
QDT10.3	RM311	II	11.13	9.05	7.63				45.9
QDT11.5	RM229	I	10.00	9.10	7.38	7.04	6.07	5.41	32.8

[a] *Yield improvement (%) = (mean GY of ILs carrying the donor allele – mean GY of JG88)/mean GY of JG88.*

high and low temperatures, etc. (Ali et al., 2006; Cheng et al., 2011; Zhang et al., 2014) as well as for almost all complex traits in rice (Li and Rutger, 2000; Zhang, 2012).

Rice responses to drought and other abiotic stresses are known to be controlled by complex gene networks consisting of many signaling pathways (Wang et al., 2011, 2015). However, it remains a great challenge to link results from the classic QTL mapping with those of molecular and transcriptomic analyses. Resembling the previously reported genetic networks underlying rice tolerances to cold and submergence (Zhang et al., 2014; Wang et al., 2015), the genetic networks underlying DT detected in this study each consisted of multiple independent branches, each might represent a signaling pathway involved in rice DT based on the following pieces of evidence. First, all DT QTL of large effects (high introgression) detected in this study (**Table 4**) appeared to be real ones as they were all validated in the random BC populations of small population sizes that are known to be less powerful in detecting QTL. Secondly, seven of the major DT QTL (*QDT1.3*, *QDT1.4*, *QDT2.4*, *QDT6.5*, *QDT7.4*, *QDT8.3,* and *QDT11.5*) had high introgression and were placed as putative regulators in the upstream positions of the genetic networks (**Figure 3**), as predicted by the theory (Zhang et al., 2011). Two other putative regulators at bins 1.3 (branch I-4) and 2.8 (branch II-2) were also in the approximate vicinity

TABLE 6 | Genomic information for 29 functional genetic units (FGUs) (28 single loci and 1 association groups or AGs) for drought tolerance (DT) detected by χ^2 tests (single loci) and multi-locus linkage disequilibrium analyses in 72 drought-tolerant introgression lines (ILs) selected from four populations.

Donor	Code	AG[a]	Branch	Marker	Bin[b]	Position (cM)[c]	B[d]	H	IF	*P*-value
IR66897B	I		I-1	RM542	**7.4**	34.7	10	0	0.588	1.40E-11
IR66897B	I		I-1	RM480	5.8	130.6	5	0	0.294	1.49E-02
IR66897B	I		I-2	RM229	**11.5**	77.8	8	2	0.529	2.66E-10
IR66897B	I		I-2	RM427	**7.1**	1.1	8	0	0.471	4.70E-07
IR66897B	I		I-3	RM424	**2.4**	66	7	1	0.441	6.66E-06
IR66897B	I		I-3	RM276	**6.3**	40.3	4	0	0.235	1.67E-02
IR66897B	I		I-4	RM572	**1.3**	61.2	7	0	0.412	3.38E-05
IR66897B	I		I-4	RM266	**2.9**	192.2	5	0	0.294	1.67E-02
IR66897B	I		I-4	RM167	11.2	37.5	1	3	0.147	6.35E-08
IR66897B	I			RM141	6.7	143.7	6	0	0.353	9.50E-04
MR77	II		II-1	RM449	**1.1**	78.4	17	0	0.81	9.56E-29
MR77	II	$agDT_{II-1}$	II-1	RM336	7.6	61	6	0	0.286	8.36E-03
MR77	II	$agDT_{II-1}$	II-1	RM331	8.3	69	6	0	0.286	8.36E-03
MR77	II		II-1	RM286	**11.1**	0	7	0	0.333	6.32E-04
MR77	II		II-1	RM470	4.6	115.5	4	1	0.214	1.14E-01
MR77	II		II-2	RM406	2.8	186.4	12	0	0.571	3.03E-13
MR77	II		II-2	RM276	**6.3**	40.3	9	1	0.452	9.35E-06
MR77	II		II-2	RM311	**10.3**	25.2	9	1	0.452	2.14E-07
MR77	II			RM541	**6.5**	75.5	9	0	0.429	6.53E-07
MR167	III		III-1	RM339	**8.3**	72.2	6	0	0.6	2.04E-07
MR167	III			RM406	2.9	186.4	4	0	0.4	3.39E-03
MR167	III			RM518	4.2	25.5	4	0	0.4	3.39E-03
MR167	III			RM253	6.3	37	4	0	0.4	3.39E-03
SN265	IV			RM449	**1.4**	78.4	8	3	0.396	4.95E-08
SN265	IV			RM506	8.1	0	8	1	0.354	1.81E-04
SN265	IV			RM541	**6.5**	75.5	7	2	0.333	5.77E-05
SN265	IV			RM585	6.3	25.1	7	2	0.333	5.77E-05
SN265	IV			RM426	3.9	157.3	7	0	0.292	4.42E-03
SN265	IV			RM481	**7.1**	3.2	6	0	0.25	3.28E-02
SN265	IV			RM283	1.2	31.4	6	0	0.25	3.28E-02

[a] *AGs are defined as a group unlinked but perfectly associated loci of equal introgression in the selected DT ILs from each BC population, detected by multi-locus probability tests. P-value is the probabilities for the null hypothesis that the genotypic frequencies fit the Mendelian segregation based on single locus X^2 tests.*

[b] *Bold ones were DT QTLs detected by the segregation distortion approach in* ***Table 2****.*

[c] *cM means centimorgan, a unit of genetic distance.*

[d] *B, H, and IF are the frequencies of the donor homozygote, heterozygote, and donor introgression frequency in the selected DT ILs from each population.*

to *QDT1.4* and *QDT2.9*, suggesting they were likely due to linkage. Thirdly, according to the QTLs/genes located in the region within 200 kb are the same QTL/gene, we found that most of the major QTL identified in this study were mapped to approximately the same locations as previously reported QTL or important regulatory genes for DT (**Table 4**). For example, *QDT7.2* (near RM125) was mapped to the genomic location harboring *ONAC067/OsNAC3,* a member of plant-specific NAC family that is known to regulate plant responses to drought, cold and high salinity (Kikuchi et al., 2003; Takasaki et al., 2010). This region also harbor two previously reported DT QTL in rice detected in a set of recombinant inbred lines developed from the cross between Zhenshan 97 (*Xian*) and a upland rice cultivar IRAT109 (*tropical Geng*; Yue et al., 2005, 2008). Similarly, *QDT2.9* was mapped together with *OsPIP1-3*, a gene that showed increased transcription in response to drought and probably played an important role in drought avoidance in rice (Lian et al., 2004). The *QDT7.1* was mapped in the region with a cloned gene *OsCIPK23* which is a multi-stress induced gene mediates a signaling pathway commonly shared by both pollination and drought stress. The *QDTY2.4* was mapped to the same location as most a previously reported DT QTL, *qDTY2.1,* and *qLRS-2* (Dixit et al., 2012). The *QDT1.3* and *QDT1.3* located on chromosome 1 were mapped in the adjacent region harboring *rfw1b* and *brt1d* (Li et al., 2005a). The *QDT8.3* was mapped in the same region of *QGy8* for grain yield, *QPn8* for panicle number, *QTgw8* for thousand grain weight and *QSf8* for seed fertility (Wang et al., 2012) under drought stresses. The *QDT10.3* was mapped to the same region as the *trdw10.1* was reported by Nguyen et al. (2004). The *QDT2.8*, *QDT6.3,* and *QDT11.5* are probably new DT QTLs which have been validated in random population of this study. All these results strongly suggested that most main-effect

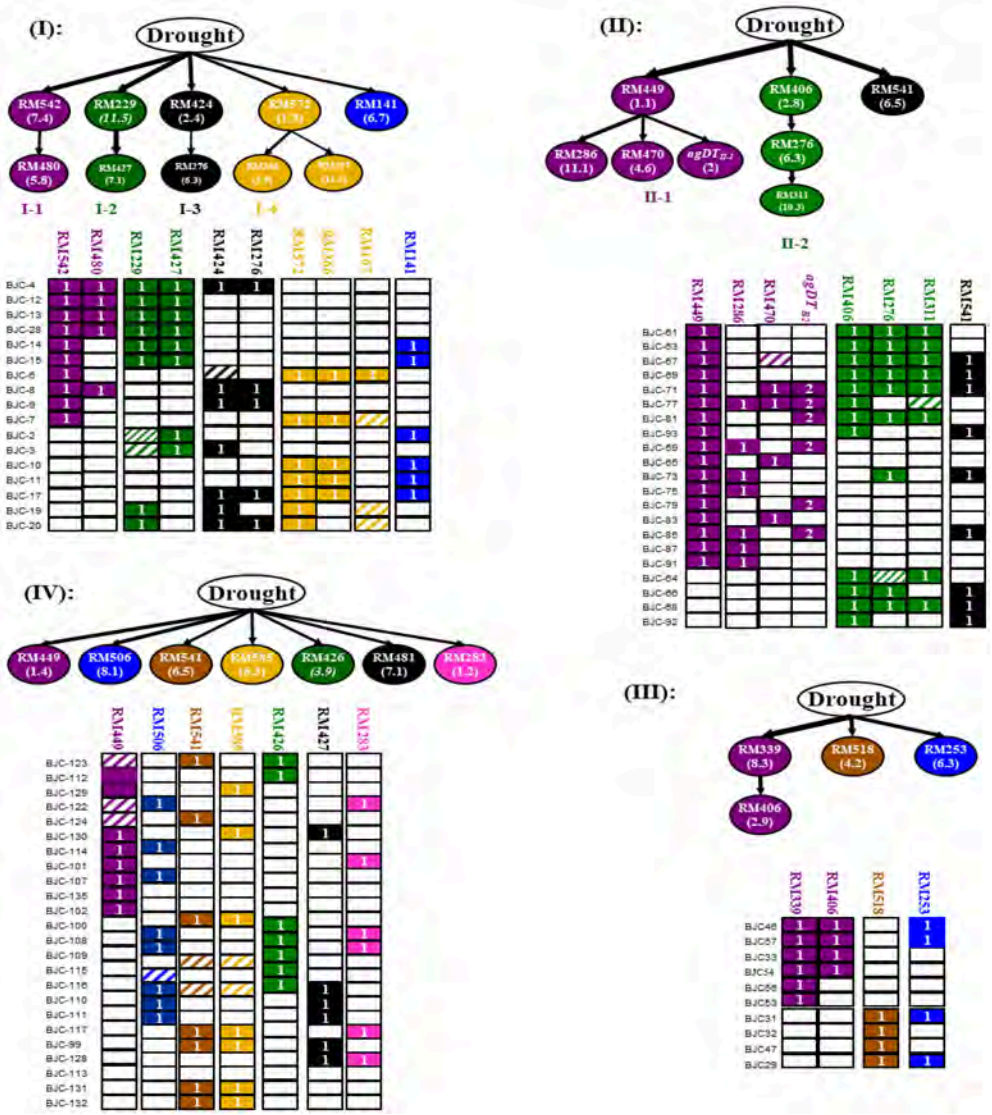

FIGURE 3 | Putative genetic networks (multi-locus structures) underlying drought tolerance (DT) of rice detected in JG88 backcross introgression lines (BILs) from four populations. In the corresponding graphical genotypes of each network, the unfilled, fully colored, and patched cells represent the recipient homozygote, donor homozygote, and heterozygote genotypes. The numbers in the cells of each FGU are the number of loci included in the FGUs. The loci (markers) included in each of the detected association groups (AGs) are shown in **Table 6**. Solid arrow lines connected two FGUs in each branch of a network represent putative functional relationships with those of high introgression as putative regulators in the upstream and those of low introgression in the downstream, and the thickness of an arrow line was proportional to the introgression frequency of the downstream FGU in **Table 6**.

QTL detected in this study were most likely regulatory genes that play important roles in regulating rice responses to DT and probably other abiotic stresses. We noted that 8 additional downstream FGUs by our non-random association analyses were undetectable by the segregation distortion method (SDM). This was due partially to the fact that SDM considers only allelic frequency shifts but not on the deviation of genotypic frequency shifts from direction selection, and primarily to its inability to detect epistasis (Cui et al., 2015).

Finally, the DT ILs and the genetic information regarding the DT QTL and the network (Supplementary Table 2) they carry provide useful materials and information for further improving rice DT and yield by designed QTL pyramiding (Zhang et al., 2014; Ali et al., 2017). As we noted in **Table 2**, there were considerable residual variation among individual ILs for GY and related traits, and so were for different QTL from different donors in their genetic compositions (**Figure 1**). According to our experiences, it is hoped that better and promising progeny that combine higher levels of DT and grain yield can be readily achieved using this breeding strategy with relatively short period of time and limited breeding effort (Ali et al., 2017).

AUTHOR CONTRIBUTIONS

YC analyzed the data and wrote the manuscript; WZ and XL were in charge of the field experiment management; SX developed the statistical model; JX designed and performed the experiment; ZL conceived the study and were in charge of the direction and planning.

ACKNOWLEDGMENTS

The project was supported by the National Natural Science Foundation of China-Consultative Group on International Agriculture Research (31261140369) to JX, Fundamental Research Funds for Central Non-profit Scientific Institution (Y2016PT53) to JX, The 863 GSR grants (2014AA10A601) to JX and Shenzhen Peacock Plan and BMGF grants (GD1393) to ZL. YC was supported by the Beachell-Borlaug International Student Fellowship from Monsanto.

SUPPLEMENTARY MATERIAL

The Supplementary Material for this article can be found online at: https://www.frontiersin.org/articles/10.3389/fpls.2018.00320/full#supplementary-material

REFERENCES

Ahmadikhah, A. (2009). A rapid mini-prep DNA extraction method in rice (*Oryza sativa*). *Afr. J. Biotechnol.* 8, 234–238.

Ali, A. J., Xu, J. L., Ismail, A. M., Fu, B. Y., Vijaykumar, C. H. M., Gao, Y. M., et al. (2006). Hidden diversity for abiotic and biotic stress tolerances in the primary gene pool of rice revealed by a large backcross breeding program. *Field Crops Res.* 97, 66–76. doi: 10.1016/j.fcr.2005.08.016

Ali, J., Xu, J. L., Gao, Y. M., Ma, X. F., Meng, L. J., Wang, Y., et al. (2017). Harnessing the hidden genetic diversity for improving multiple abiotic stress tolerance in rice (*Oryza sativa* L.). *PLoS ONE* 12:e0172515. doi: 10.1371/journal.pone.0172515

Ashikari, M., Sakakibara, H., Lin, S., Yamamoto, T., Takashi, T., Nishimura, A., et al. (2005). Cytokinin oxidase regulates rice grain production. *Science* 309, 741–745. doi: 10.1126/science.1113373

Cheng, L., Wang, Y., Meng, L., Hu, X., Cui, Y., Sun, Y., et al. (2011). Identification of salt-tolerant QTLs with strong genetic background effect using two sets of reciprocal introgression lines in rice. *Genome* 55, 45–55. doi: 10.1139/g11-075

Churchill, G. A., and Doerge, R. W. (1994). Empirical threshold values for quantitative trait mapping. *Genetics* 138, 963–971.

Cui, Y., Zhang, F., Xu, J., Li, Z., and Xu, S. (2015). Mapping quantitative trait loci in selected breeding populations: a segregation distortion approach. *Heredity* 115, 538–546. doi: 10.1038/hdy.2015.56

Dixit, S., Swamy, B. P., Vikram, P., Ahmed, H. U., Sta Cruz, M. T., Amante, M., et al. (2012). Fine mapping of QTLs for rice grain yield under drought reveals sub-QTLs conferring a response to variable drought severities. *Theor. Appl. Genet.* 125, 155–169. doi: 10.1007/s00122-012-1823-9

Fukai, S., and Cooper, M. (1995). Development of drought-resistant cultivars using physiomorphological traits in rice. *Field Crops Res.* 40, 67–86. doi: 10.1016/0378-4290(94)00096-U

Guan, Y. S., Serraj, R., Liu, S. H., Xu, J. L., Ali, J., Wang, W. S., et al. (2010). Simultaneously improving yield under drought stress and non-stress conditions: a case study of rice (*Oryza sativa* L.). *J. Exp. Bot.* 61, 4145–4156. doi: 10.1093/jxb/erq212

He, Y., Zheng, T., Hao, X., Wang, L., Gao, Y., Hua, Z., et al. (2010). Yield performances of japonica introgression lines selected for drought tolerance in a BC breeding programme. *Plant Breed.* 129, 167–175. doi: 10.1111/j.1439-0523.2009.01683.x

Ji, K., Wang, Y., Sun, W., Lou, Q., Mei, H., Shen, S., et al. (2012). Drought-responsive mechanisms in rice genotypes with contrasting drought tolerance during reproductive stage. *J. Plant Physiol.* 169, 336–344. doi: 10.1016/j.jplph.2011.10.010

Kamoshita, A., Babu, R. C., Boopathi, N. M., and Fukai, S. (2008). Phenotypic and genotypic analysis of drought-resistance traits for development of rice cultivars adapted to rainfed environments. *Field Crop Res.* 109, 1–23. doi: 10.1016/j.fcr.2008.06.010

Kikuchi, S., Satoh, K., Nagata, T., Kawagashira, N., Doi, K., Kishimoto, N., et al. (2003). Collection, mapping, and annotation of over 28,000 cDNA clones from japonica rice. *Science* 301, 376–379. doi: 10.1126/science.1081288

Lafitte, H., Li, Z., Vijayakumar, C., Gao, Y., Shi, Y., Xu, J., et al. (2006). Improvement of rice drought tolerance through backcross breeding: evaluation of donors and selection in drought nurseries. *Field Crop Res.* 97, 77–86. doi: 10.1016/j.fcr.2005.08.017

Li, Z., Mu, P., Li, C., Zhang, H., Li, Z., Gao, Y., et al. (2005a). QTL mapping of root traits in a doubled haploid population from a cross between upland and lowland japonica rice in three environments. *Theor. Appl. Genet.* 110, 1244–1252. doi: 10.1007/s00122-005-1958-z

Li, Z., and Rutger, J. (2000). Geographic distribution and multilocus organization of isozyme variation of rice (*Oryza sativa* L.). *Theor. Appl. Genet.* 101, 379–387. doi: 10.1007/s001220051494

Li, Z., Fu, B., Gao, Y., Xu, J., Ali, J., Lafitte, H., et al. (2005b). Genomewide introgression lines and their use in genetic and molecular dissection of complex phenotypes in rice (*Oryza sativa* L.). *Plant Mol. Biol.* 59, 33–52. doi: 10.1007/s11103-005-8519-3

Lian, H., Yu, X., Ye, Q., Ding, X., Kitagawa, Y., Kwak, S., et al. (2004). The role of aquaporin RWC3 in drought avoidance in rice. *Plant Cell Physiol.* 45, 481–489. doi: 10.1093/pcp/pch058

Liu, H. Y., Yu, X., Cui, D. Y., Sun, M. H., Sun, W. N., Tang, Z. C., et al. (2007). The role of water channel proteins and nitric oxide signaling in rice seed germination. *Cell Res.* 17, 638–649. doi: 10.1038/cr.2007.34

Lu, L., Shao, D., Qiu, X., Sun, L., Yan, W., Zhou, X., et al. (2013). Natural variation and artificial selection in four genes determine grain shape in rice. *New Phytol.* 200, 1269–1280. doi: 10.1111/nph.12430

Nguyen, T., Klueva, N., Chamareck, V., Aarti, A., Magpantay, G., Millena, A., et al. (2004). Saturation mapping of QTL regions and identification of putative candidate genes for drought tolerance in rice. *Mol. Genet. Genomics* 272, 35–46. doi: 10.1007/s00438-004-1025-5

Ooka, H., Satoh, K., Doi, K., Nagata, T., Otomo, Y., Murakami, K., et al. (2003). Comprehensive analysis of NAC family genes in oryza sativa and arabidopsis thaliana. *DNA Res.* 10, 239–247. doi: 10.1093/dnares/10.6.239

Palanog, A. D., Swamy, B. P. M., Shamsudin, N. A. A., Dixit, S., Hernandez, J. E., Boromeo, T. H., et al. (2014). Grain yield QTLs with consistent-effect under reproductive-stage drought stress in rice. *Field Crop Res.* 161, 46–54. doi: 10.1016/j.fcr.2014.01.004

Takasaki, H., Maruyama, K., Kidokoro, S., Ito, Y., Fujita, Y., Shinozaki, K., et al. (2010). The abiotic stress-responsive NAC-type transcription factor OsNAC5 regulates stress-inducible genes and stress tolerance in rice. *Mol. Genet. Genomics* 284, 173–183. doi: 10.1007/s00438-010-0557-0

Venuprasad, R., Bool, M. E., Quiatchon, L., Sta Cruz, M. T., Amante, M., and Atlin, G. N. (2011). A large-effect QTL for rice grain yield under upland drought stress on chromosome 1. *Mol. Breed.* 30, 535–547. doi: 10.1007/s11032-011-9642-2

Venuprasad, R., Lafitte, H. R., and Atlin, G. N. (2007). Response to direct selection for grain yield under drought stress in rice. *Crop Sci.* 47:285. doi: 10.2135/cropsci2006.03.0181

Venuprasad, R., Sta Cruz, M. T., Amante, M., Magbanua, R., Kumar, A., and Atlin, G. N. (2008). Response to two cycles of divergent selection for grain yield under drought stress in four rice breeding populations. *Field Crop Res.* 107, 232–244. doi: 10.1016/j.fcr.2008.02.004

Wang, D., Pan, Y., Zhao, X., Zhu, L., Fu, B., and Li, Z. (2011). Genome-wide temporal-spatial gene expression profiling of drought responsiveness in rice. *BMC Genomics* 12:149. doi: 10.1186/1471-2164-12-149

Wang, Y., Zang, J., Yong, S., Jauhar, A., Xu, J., and Li, Z. (2012). Identification of genetic overlaps for salt and drought tolerance using simple sequence repeat markers on an advanced backcross population in rice. *Crop. Sci.* 52, 1583–1592. doi: 10.2135/cropsci2011.12.062

Wang, W.-S., Zhao, X.-Q., Li, M., Huang, L.-Y., Xu, J.-L., Zhang, F., et al. (2015). Complex molecular mechanisms underlying seedling salt tolerance in rice revealed by comparative transcriptome and metabolomic profiling. *J. Exp. Bot.* 67, 405–419. doi: 10.1093/jxb/erv476

Wang, Y., Zang, J., Sun, Y., Ali, J., Xu, J., and Li, Z. (2013a). Background-independent quantitative trait loci for drought tolerance identified using advanced backcross introgression lines in rice. *Crop Sci.* 53, 430–441. doi: 10.2135/cropsci2012.06.0361

Wang, Y., Zhang, L. B., Nafisah, A., Zhu, L. H., Xu, J. L., and Li, Z. K. (2013b). Selection efficiencies for improving drought/salt tolerance yield using introgression breeding in rice (*Oryza sativa* L.). *Crop J.* 1, 134–142. doi: 10.1016/j.cj.2013.07.006

Xu, J., Lafitte, H., Gao, Y., Fu, B., Torres, R., and Li, Z. (2005). QTLs for drought escape and tolerance identified in a set of random introgression lines of rice. *Theor. Appl. Genet.* 111, 1642–1650. doi: 10.1007/s00122-005-0099-8

Yang, W., Kong, Z., Omo-Ikerodah, E., Xu, W., Li, Q., and Xue, Y. (2008). Calcineurin B-like interacting protein kinase OsCIPK23 functions in pollination and drought stress responses in rice (*Oryza sativa* L.). *J. Genet. Genomics.* 35, 531–543. doi: 10.1016/S1673-8527(08)60073-9

You, J., Li, Q., Yue, B., Xue, W.Y., Luo, L. J., and Xiong, L. Z. (2006). Identification of quantitative trait loci for ABA sensitivity at seed germination and seedling stages in rice. *Yi. Chuan Xue. Bao.* 33, 532–541. doi: 10.1016/S0379-4172(06)60082-6

Yue, B., Xiong, L., Xue, W., Xing, Y., Luo, L., and Xu, C. (2005). Genetic analysis for drought resistance of rice at reproductive stage in field with different types of soil. *Theor. Appl. Genet.* 111, 1127–1136. doi: 10.1007/s00122-005-0040-1

Yue, B., Xue, W., Luo, L., and Xing, Y. (2008). Identification of quantitative trait loci for four morphologic traits under water stress in rice (*Oryza sativa* L.). *J. Genet. Genomics* 35, 569–575. doi: 10.1016/S1673-8527(08)60077-6

Zhang, F., Ma, X. F., Gao, Y. M., Hao, X. B., and Li, Z. K. (2014). Genome-wide response to selection and genetic basis of cold tolerance in rice (*Oryza sativa* L.). *BMC Genet.* 15:55. doi: 10.1186/1471-2156-15-55

Zhang, F., Zhai, H.-Q., Paterson, A. H., Xu, J.-L., Gao, Y.-M., Zheng, T.-Q., et al. (2011). Dissecting genetic networks underlying complex phenotypes: the theoretical framework. *PLoS ONE* 6:e14541. doi: 10.1371/journal.pone.0014541

Zhang, L. (2012). Identification of gene modules associated with drought Response in rice by network-based analysis. *PLoS ONE* 7:e33748. doi: 10.1371/journal.pone.0033748

Conflict of Interest Statement: The authors declare that the research was conducted in the absence of any commercial or financial relationships that could be construed as a potential conflict of interest.

frontiers in Plant Science

ORIGINAL RESEARCH
published: 16 March 2018
doi: 10.3389/fpls.2018.00332

Genetic Architecture and Candidate Genes for Deep-Sowing Tolerance in Rice Revealed by Non-syn GWAS

Yan Zhao[1†], Weipeng Zhao[1†], Conghui Jiang[1†], Xiaoning Wang[2], Huaiyang Xiong[2], Elena G. Todorovska[3], Zhigang Yin[1], Yanfa Chen[1], Xin Wang[1], Jianyin Xie[1], Yinghua Pan[1,4], Muhammad A. R. Rashid[1,5], Hongliang Zhang[1], Jinjie Li[1] and Zichao Li[1]**

[1] Key Lab of Crop Heterosis and Utilization of Ministry of Education and Beijing Key Lab of Crop Genetic Improvement, China Agricultural University, Beijing, China, [2] Institute of Food Crops, Hainan Academy of Agricultural Sciences, Haikou, China, [3] AgroBioInstitute, Bulgarian Agricultural Academy, Sofia, Bulgaria, [4] Rice Research Institute, Guangxi Academy of Agricultural Sciences, Nanning, China, [5] Plant Breeding and Genetics Lab, University of Agriculture Faisalabad, Vehari, Pakistan

OPEN ACCESS

Edited by:
Hanwei Mei, Shanghai Agrobiological Gene Center, China

Reviewed by:
Xinghua Wei, China National Rice Research Institute (CAAS), China
Yongzhong Xing, Huazhong Agricultural University, China

***Correspondence:**
Jinjie Li
lijinjie@cau.edu.cn
Zichao Li
lizichao@cau.edu.cn

[†]*These authors have contributed equally to this work.*

Specialty section:
This article was submitted to Plant Breeding, a section of the journal Frontiers in Plant Science

Received: *16 November 2017*
Accepted: *28 February 2018*
Published: *16 March 2018*

Citation:
Zhao Y, Zhao W, Jiang C, Wang X, Xiong H, Todorovska EG, Yin Z, Chen Y, Wang X, Xie J, Pan Y, Rashid MAR, Zhang H, Li J and Li Z (2018) Genetic Architecture and Candidate Genes for Deep-Sowing Tolerance in Rice Revealed by Non-syn GWAS. Front. Plant Sci. 9:332. doi: 10.3389/fpls.2018.00332

Dry direct-seeding of rice is rapidly increasing in China, but variable planting depth associated with machine sowing can lead to low seedling emergence rates. Phenotype analysis of 621 rice accessions showed that mesocotyl length (ML) was induced by deep soil covering and was important in deep-sowing tolerance in the field. Here, we performed and compared GWAS using three types of SNPs (non-synonymous SNP, non-synonymous SNPs and SNPs within promoters and 3 million randomly selected SNPs from the entire set of SNPs) and found that Non-Syn GWAS (GWAS using non-synonyomous SNP) decreased computation time and eliminated confounding by other loci relative to GWAS using randomly selected SNPs. Thirteen QTLs were finally detected, and two new major-effect genes, named *OsML1* and *OsML2*, were identified by an integrated analysis. There were 2 and 7 non-synonymous SNPs in *OsML1* and *OsML2*, respectively, from which 3 and 4 haplotypes were detected in cultivated rice. Combinations of superior haplotypes of *OsML1* and *OsML2* increased ML by up to 4 cm, representing high emergence rate (85%) in the field with 10 cm of soil cover. The studies provide key loci and naturally occurring alleles of ML that can be used in improving tolerance to dry direct-seeding.

Keywords: deep-sowing tolerance, genome-wide association study, mesocotyl length, non-synonymous SNP, *Oryza sativa*

INTRODUCTION

Rice is one of the most important food crops, feeding more than one-half of the world population. Rice planting is currently carried out in two ways, namely transplanting and direct-seeding (Farooq et al., 2011). Transplanting is a traditional system based on transplanting of seedlings from seedbeds to paddy fields, and is used to ensure high seedling emergence and uniform plant density (Farooq et al., 2011; Wu et al., 2015). Transplanting by hand remains the predominant method in China, accounting for more than 90% of the total area. Direct-seeding is the major cultivation method in Europe and the United States due to mechanized farming practices, and savings in labor and time (Farooq et al., 2011). Recently, dry direct-seeding is increasing rapidly in China, but variable planting depths associated with machine sowing cause agronomic problems that prevent the achievement of optimum plant populations (Farooq et al., 2006a,b). Poor emergence and

weak seedling establishment caused by deep soil greatly restrict the application of direct-seedling technology. Thus, an understanding of the genetic mechanisms affecting the plant establishment by dry direct-seeding is needed to support breeding solutions.

The mesocotyl is an embryonic structure between the scutellar node and coleoptilar node, and it can directly push the shoot tip above the soil surface during germination (Lee H. S. et al., 2012). Thus, mesocotyl length (ML) is an important trait affecting plant establishment under deep sown conditions in rice (Turner et al., 1982; Wu et al., 2015; Lu et al., 2016). Earlier studies showed that drill-seeded semi-dwarf rice genotypes emerge more slowly and less uniformly than non-dwarf types with long mesocotyls (Turner et al., 1982). However, further study indicated there was no correlation between ML and mature plant traits such as plant height and internode length (Mgonja et al., 1993). Thus, it should be possible to breed semi-dwarf accessions with long mesocotyls and to identify genes determining ML. Mesocotyls can elongate in dark and water-covered situations as well as under deep sown conditions (Feng et al., 2017). Under dark and water-covered conditions, elite germplasm with long mesocotyls were identified in different subpopulations and ecotypes (Redoña and Mackill, 1996a; Wu et al., 2005; Luo et al., 2007). The previous studies generally showed that accessions with long mesocotyls were rare in cultivated rice. Some elite *indica* accessions with long mesocotyls were identified under direct-seeding conditions of 5 cm depth of sand cover (Lu et al., 2016). Given that mesocotyl elongation in soil-sand culture differs from elongation under dark and water-covered conditions (Simon et al., 2011), further deep-sowing field experiments were needed to identify germplasm with long mesocotyls and to determine the relationship between ML and emergence rate (ER).

Traditional bi-parental linkage mapping has been fully applied to detect QTL for complex traits, including ML. Five QTLs for ML were first identified using an F_2 population of 204 plants from a cross between a low-vigor *japonica* "Labelle" and a high-vigor *indica* "Black Gora" (Redoña and Mackill, 1996b). Using a DH population crossed between *indica* and *japonica*, eight QTLs for ML were detected (Cao et al., 2002). Additionally, 11, 8, and 27 QTLs for ML were identified by using RIL population, respectively (Cai and Morishima, 2002; Ouyang et al., 2005; Huang C. et al., 2010). In a subsequent study, linkage mapping of ML was conducted by using BIL population from a cross between the cultivated rice and weedy rice with long ML (Lee H. et al., 2012). These identified genomic regions that were associated with ML, and were conducive to breeding for deep-sowing tolerance and gene cloning.

Previous studies demonstrated that genes *OsBRI1*, *D10*, *D17*, *D27*, *D3*, *D14*, *PTOX1,* and *OsTCP5* were involved in ML by comparison of mutants and wild type (Hu et al., 2010, 2014; Gao et al., 2014; Tamiru et al., 2014; Kameoka and Kyozuka, 2015). Studies showed that the elongation of mesocotyls were regulated by strigolactones and cytokinins during germination of rice seeds in darkness (Hu et al., 2010, 2014; Chen et al., 2014; Tamiru et al., 2014; Kameoka and Kyozuka, 2015). Other reports indicated that brassinosteroids, ethephon and gibberellic acid were also involved (Watanabe et al., 2015; Liang et al., 2016). Dynamic transcriptome analysis suggested plant hormone signal transduction, α-linolenic acid metabolism and diterpenoid biosynthesis were critical processes of mesocotyl growth that were inhibited by light (Feng et al., 2017). Importantly, a single natural variation of the *GY1* gene for ML was identified from 3,000 accessions, and was investigated by map-based cloning (Xiong et al., 2017). The gene functioned at the initial step of jasmonic acid biosynthesis to repress mesocotyl and coleoptile elongation. Despite these reports, identification of natural variation in ML may be a better way to find genes associated with ML for breeding and for gaining insights into the molecular basis of variation in ML.

The advent of the next-generation sequencing technology offers abundant genetic information and a solid basis for genome-wide association studies (GWAS). Compared with conventional linkage mapping, GWAS explores a wider range of natural variation and enables a greater number of significant SNPs to be identified. By GWAS of 1,019,883 SNPs in 270 rice accessions, 13 SNPs were identified to be highly associated with ML of rice plants grown in water (Wu et al., 2015). Another GWAS of 4,136 SNPs in 469 *indica* rice accessions identified 17 loci for ML, explaining 19.31% of the phenotypic variation (Lu et al., 2016). These two preliminary GWAS provided reliable QTL regions for ML, although it was hard to distinguish functional loci. High density sequencing and GWAS of a large representative collection of germplasm was necessary to gain further insights into loci and naturally occurring alleles for ML.

To breed rice accessions for dry direct-seeding, the following problems needed to be solved: (1) identification of germplasm with long mesocotyls and investigation of the relationship between ML and seedling ER under deep-sowing conditions in the field; and (2) exploration of QTLs or candidate genes for ML that can be further used in molecular breeding by marker assisted selection. In this study, we evaluated ML and ER of a large population of germplasm under deep sown conditions in the field and identified several accessions with long mesocotyls as possible breeding parents. More than 15 million SNPs were identified in the germplasm following sequencing at an average depth of 15X. We first screened for non-synonymous SNPs linked to ML and performed GWAS between ML and non-synonymous SNPs. Candidate genes/loci for ML were verified by an integrated analysis of GWAS, linkage mapping, allelic frequency differences between phenotypic pools, expression, and sequence alignment.

MATERIALS AND METHODS

Materials and Sequencing

A total of 621 cultivated rice accessions from the 3000 Rice Genome Project (3KRGP) (Li J. Y. et al., 2014; Alexandrov et al., 2015) formed the materials for identification of ML QTLs. The collection was based on broadly genetic diversity, and comprised mini-core collections selected from an original core set of 4,310 primary accessions of Chinese cultivated rice (Zhang et al., 2011), and 402 lines in the International Rice Molecular Breeding Network (Yu et al., 2003). The sequencing data of the 621 accessions were directly from the 3KRGP, which have an average sequencing depth of 15X and generated >15 million SNPs when

compared with the Nipponbare reference genome (Li Z. et al., 2014).

Phenotyping

Based on previous studies (Turner et al., 1982; Lu et al., 2016), we chose 10 cm depth of soil cover to measure MLs of different accessions, which could exceed the maximum capacity of mesocotyl elongation in rice. We then designed field experiments with 10 cm depth of soil cover at the Experiment Station of China Agricultural University, Beijing. Ten full and uniformed seeds of each accession were planted in the field. A 10 cm soil layer was placed over the seeds followed by sprinkling with adequate water. The field experiment was conducted in summer of 2014 in two fields as two replications (Figure S1). After 10 days, MLs of all seedlings were measured with a ruler.

For an experiment in plastic boxes, three groups of five accessions with ML in the range of 0–0.5, 2–3, and 5–6 cm were planted on a thick soil layer (Figure S2). Each accession was planted in one column with 30 plants as repetition. The seeds in separate boxes were covered with 1, 3, 5, and 7 cm of soil followed by sprinkling with adequate water. MLs of all seedlings were measured after 10 days.

Non-synonymous SNPs and Population Genetic Analysis

Based on information on coding sequence (CDS) coordinates and transcript from MSU-RGAP 7, we separated the non-synonymous SNPs from a total of 15 million SNPs using an in-house Perl script. A neighbor-joining (N-J) tree was generated from more than 75,000 randomly selected SNPs using Tassel 5 and Mega 6 software. Principal components (PC) and kinship matrix were calculated by software GAPIT to verify population structure using more than 3 million SNPs with minor allele frequency > 0.05 and missing rates < 0.5. LD heatmaps of two important QTLs identified in GWAS were generated using the R package "LD heatmaps." Candidate regions were identified using an $r^2 > 0.6$. Nucleotide diversity (π) (Nei, 1987) and Tajima's D (Tajima, 1989) were calculated using an in-house Perl script.

Screening of SDSs and ESDSs for Mesocotyl Length

For screening of the SDSs (SNPs with significant differences in allele frequency between polar pools, $p < 0.05$) and ESDSs (SNPs with extremely significant differences in allele frequency between polar pools, $p < 0.01$) associated with ML by bulked segregant analysis, we selected accessions with polar ML from typical *indica* and *japonica* accessions, followed by chi-squared tests of allele frequency for each non-synonymous SNP. To identify the SDS- and ESDS-enriched windows, we performed a permutation test to obtain significant thresholds by random shuffling of 10,000 iterations of SNP numbers of all 500 kb sliding windows along the entire genome. We finally set 99th percentiles of SDS and ESDS numbers of permutation tests as threshold values.

Comparison of GWAS Using Three Types of SNPs for Mesocotyl Length

To perform GWAS efficiently it is important to eliminate false positives from the population structure and to identify family relationships in natural population. The first three PCs were used to construct the PC matrix. We performed GWAS using CMLM with PC and kinship, which accounts for population structure and identifies the optimal group kinship matrix (Zhang et al., 2010a). Previous studies indicated that a trait-specific kinship derived from weighted SNPs has better genomic prediction accuracy than kinship derived from all SNPs (Zhang et al., 2010b; Wang et al., 2014). Thus, we performed and compared GWAS of the CMLM using 3 groups of SNPs to search for target genes for ML. Group I included non-synonymous SNPs; group II included non-synonymous SNPs and SNPs located in 5′ flanking sequences of genes ($\leq$1 Kb upstream of the first ATG); and group III included 3 million randomly selected SNPs from the entire SNP set.

Given that the default parameters were too strict for detecting significant associations when the threshold was derived from the total number of markers, we used the formula "$-\log_{10}$(0.01/effective number of SNPs with a p-value less than 0.01)," i.e., the threshold at a significance level of 1% after Bonferroni-adjusted multiple test correction (Pan et al., 2015). False discovery rate (FDR) was performed to compare with the threshold value (Benjamini and Hochberg, 1995). All signals at a significance level of 0.01 after Bonferroni-adjusted multiple test corrections were up to a significance level of FDR ($p < 0.05$).

RNA Extraction and qRT-PCR

Total RNA was extracted from mesocotyls of 6 rice accessions using RNAiso Plus (Takara). The cDNA was generated in 25 μl reaction mixtures containing 2 μg Dnase I-treated RNA, 200 U M-MLV reverse transcriptase (Takara), 40 U Recombinant RNase Inhibitor (Takara) and 0.1 μM oligo $(dT)_{18}$ primer. qRT-PCR was performed in total volumes of 10 μl containing 5 μl SYBR premix EX Taq (Takara), 0.2 μl Rox Reference Dye II (Takara), 0.4 mM gene-specific primers and 0.5 ul of cDNA on an ABI 7500 Real time PCR system (Applied Bio-systems). The gene LOC_Os03g50885 was used as an internal reference.

RESULTS

Population Characterization and Phenotypic Variation in Mesocotyl Length

The PC analysis showed that PC1 could explain more than 90% genetic variation, suggesting the 621 accessions could be classified in two major subpopulations (**Figure 1A** and Figure S3). The result was also supported by the N-J tree and kinship plot (**Figure 1B** and Figure S3). Therefore, referring to the reported classification information of the sample (Yu et al., 2003; Zhang et al., 2011), we divided the population into two subgroups, including 390 *indica* and 231 *japonica* accessions. Large variations in ML and ER were observed in repeated phenotypic assays in the field with 10 cm of soil cover, with ML ranging from 0.1 to 6.19 cm and ER ranging from 0 to 85%

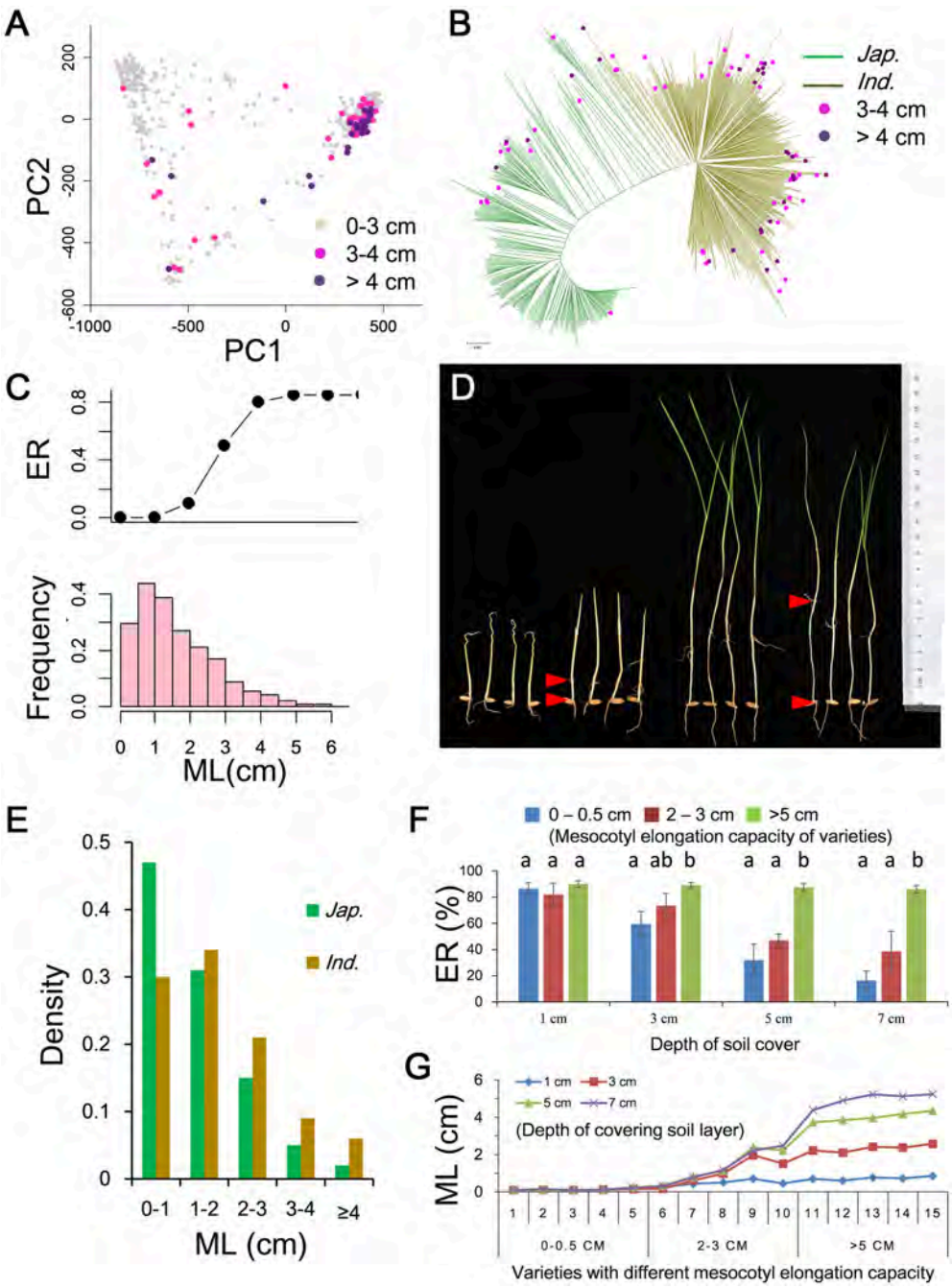

FIGURE 1 | Mesocotyl lengths (MLs) in 621 cultivated rice and relationship among ML, emergence rate (ER) and planting depth. **(A)** Principal component plot and distribution of accessions with different ML. **(B)** Neighbor-joining tree and distribution of accessions with ML of more than 3 cm on the tree. **(C)** Relationship between ER and ML (upper) and histogram of ML (lower) in field plantings with 10 cm of soil cover. **(D)** Differentiation of MLs in cultivated accessions. **(E)** Comparison of MLs of *indica* and *japonica*. **(F)** Relationship between ER and ML in box plantings with different depths of soil cover. Different letters above bars indicate significant differences ($p < 0.05$) detected by Duncan's multiple range test. **(G)** Relationship between ML and depth of soil cover for accessions with different mesocotyl elongation capacities.

(**Figures 1C,D** and Table S1). Generally, variation in ML in rice fitted a negative binomial distribution, and most of accessions had short mesocotyls ranging from 0 to 1 cm (**Figure 1C**). There was high ER (85%) when ML exceeded 4 cm in the field with 10 cm of soil cover (**Figure 1C** and Figure S4). Whereas most accessions had short ML there were significant differences in ML between *indica* and *japonica* (Table S2). There was a higher proportion of accessions with ML of 0–1 cm in *japonica*

(46.7%) than in *indica* (30.2%) (**Figure 1E**). However, more *indica* accessions had long mesocotyls of 4 cm or more than in *japonica* (**Figure 1E**). Finally, we identified 23 *indica* and 4 *japonica* accessions having deep-sowing tolerance with ER of about 80% and with ML of more than 4 cm (**Figures 1A,B** and Table S3). The average plant height of these accessions was about 104 cm. Considering the weak correlations between ML and plant height in rice (Table S4), these accessions were considered to be potentially useful parental germplasm for breeding.

To gain further insight into the relationship among ML, ER and depth of soil cover we measured the ER of accessions with different ML at different depths of soil cover (Figure S2). Three groups of five accessions were selected according to ML in the range of 0–0.5, 2–3, and 5–6 cm in the field. The 15 accessions were planted on a thick soil layer in plastic boxes. The seeds in separate boxes were covered with 1, 3, 5, and 7 cm of soil. Under shallow sowing conditions (covered with 1 and 3 cm of soil), the three groups accessions had higher ER of 60–90% (**Figure 1F**) and shorter ML of 0.1–2.6 cm (**Figure 1G**). There were no significant correlations between ML and ER in boxes covered with 1 or 3 cm of soil. Under deep sowing (covered with 5 and 7 cm of soil), only five accessions with long ML (>5 cm) had higher ER (≈87%) (**Figure 1F**), and the other two groups with ML in the range of 0–0.5 and 2–3 cm showed lower ER of 16 and 39%, respectively (**Figure 1F**). There were highly significant correlations between ML and ER with Pearson correlation coefficients of 0.81 and 0.78 in boxes covered with 5 and 7 cm of soil, respectively. The results showed that ML was induced by the depth of soil cover, and greater ML led to improved ER under deep sowing conditions.

Characteristics of Non-synonymous SNPs Along the Entire Genome and Screening of SDSs and ESDSs

Polymorphisms causing protein-coding differences are most likely to be important functional loci associated with agronomic traits (Yano et al., 2016). Here, we focused on non-synonymous SNPs in all 50,086 annotated genes from MSU-RGAP 7 except transposons and retrotransposons. The 572,511 non-synonymous SNPs were screened from 15 million SNPs across the whole genomes of all accessions. Among them 73,000 SNPs were found to cause premature terminations (**Figures 2A,B**). The analysis of minor allele frequencies (MAFs) indicated that 54, 55, and 60% of the non-synonymous SNPs could be considered as rare variants in the full population, and *indica* and *japonica* for groups with low MAF (<0.05) (**Figures 2C–E**).

To explore non-synonymous SNPs associated to ML, we constructed separate pools with extreme differences in ML based on conventional bulked segregant analysis for *indica* and *japonica*. To reduce genetic differences unrelated to ML between polar pools, we took no account of accessions at PC1 values ranging from −400 to 300. The accessions with PC1 < −400 were defined as typical *indica*, and those with PC1 > 300 were considered to be typical *japonica*. Each pool included 20 accessions of each subgroup (Table S5). On the basis of chi-squared tests of allele frequency between the polar pools, we selected out the SDSs and ESDSs associated with ML (**Figures 2F,G** and Figure S5). As a result we obtained 35,911, and 40,615 SDSs in *indica* and *japonica*, respectively. Among them, there were 19,073 and 26,055 ESDSs associated with ML in each subgroup. These SNPs appeared to be randomly distributed over the entire genome except for a few enriched peaks. Using thresholds of extreme significance for each window established by permutation tests we selected the regions with peaks higher than the threshold as candidate loci associated with ML (**Figures 2F,G** and Figure S5).

Comparison of GWAS Using Three Types of SNPs for Mesocotyl Length

Quantile-quantile (Q-Q) plots for ML showed that CMLM accounted for false positives arising from the population structure and family relationships in our population on the basis of GLM (**Figures 3A–C**). By performing GWAS using each group separately, we identified 23, 53, and 91 SNPs for ML at significance levels of 0.01 after Bonferroni-adjusted multiple test correction in the full population (**Figures 3A–C** and **Table 1** and Tables S6, S7). Due to lower genome-wide linkage disequilibrium (LD) decay rates in *indica* and *japonica* at 123 and 167 kb (Huang X. et al., 2010), adjacent significant SNP with distances <170 kb were merged into an independent QTL. Thirteen, 11 and 20 QTLs were identified by GWAS using the separate groups (**Table 1** and Tables S6, S7). We also performed GWAS of ML in *indica* with its wider phenotypic variation (Figure S6). Here we identified 3, 5, and 4 QTLs, including 11, 21, and 17 SNPs associated with ML, respectively (Tables S8–S10). With GLM, these SNPs and QTLs showed higher $-\log(p)$ values as well (Figures S7, S8 and **Table 1** and Tables S6–S10). By comparison of GWAS results using the three sets of SNPs, five QTL in the full population (named as *qFML3-2*, *qFML7-2*, *qFML7-3*, *qFML7-4,* and *qFML11-1*) from GWAS using group I were detected in GWAS using groups II and III; one QTL in *indica* (named as *qIML7-2*) from GWAS using group I were also detected in GWAS of groups II and III. The results demonstrated that Non-Syn GWAS (GWAS using SNPs from group I) was a feasible method to identify QTL regions as well as GWAS of 3 million randomly selected SNPs.

Due to PC and kinship derived from genetic markers different sets of markers result in different PC and kinship. That is the biggest difference among GWAS using three groups of SNPs. To assess the effect of the original GWAS using groups I and II, we performed complementary GWAS between ML and SNPs in these groups using PC and kinship data derived from group III. As shown by the Q-Q and Manhattan plots, similar GWAS results were obtained using PC and kinships derived from groups I, II ,and III in CMLM (**Figure 3** and Figures S6, S9). By further comparing peak $-\log(p)$ values of each QTL between the original and complementary GWAS using the full population 9 of 13 and 8 of 11 QTLs in the original GWAS of the full population had higher signals than in the complementary GWAS using groups I and II, respectively (**Table 1** and Table S6). Furthermore, all 3 and 5 QTLs in the original GWAS in *indica* also had higher signals than the complementary GWAS using groups I and II (Tables S8, S9). These results indicated that PC and kinship derived from

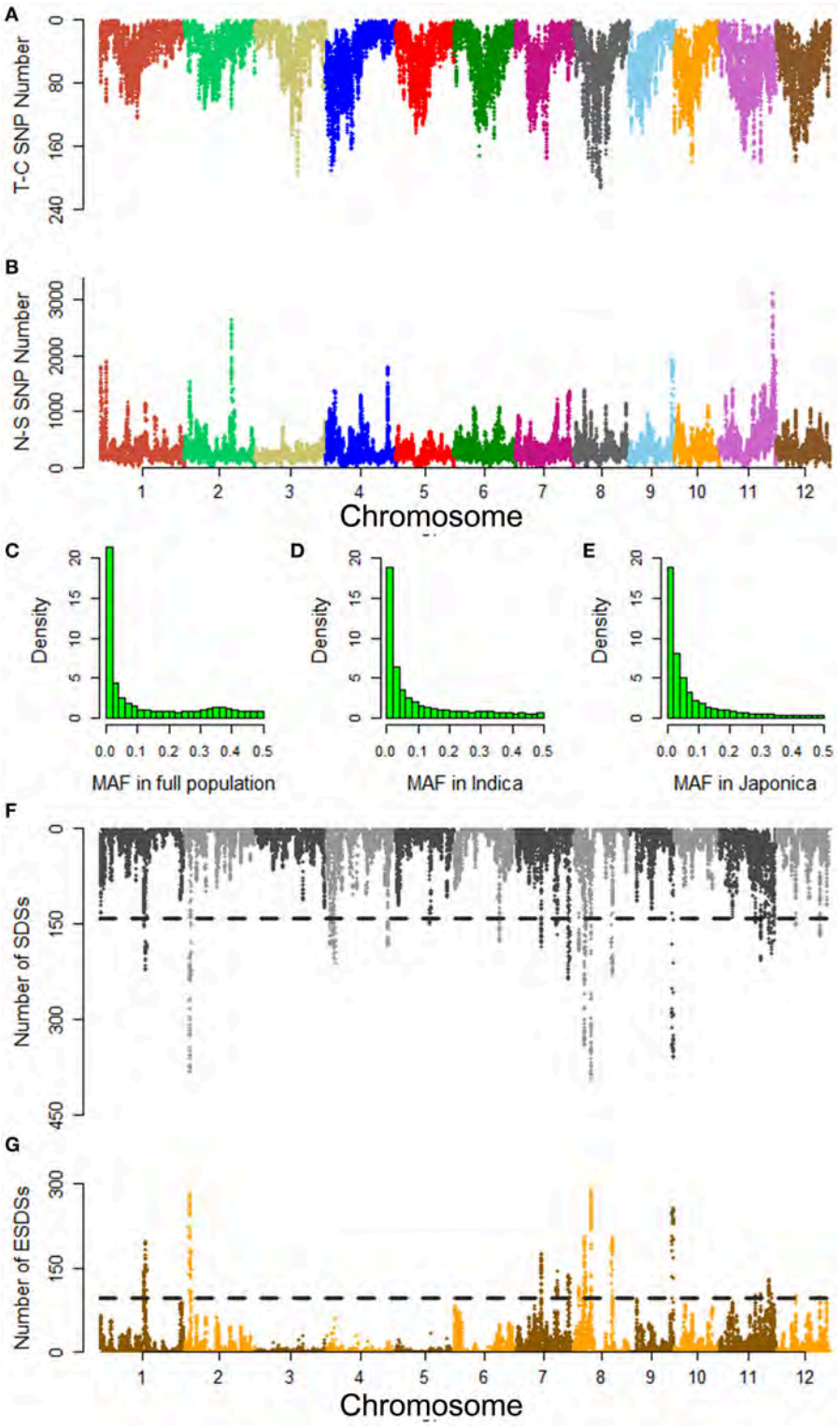

FIGURE 2 | Summary of non-synonymous SNPs detected in the full population and their distribution associated with mesocotyl length in the *indica* genome. **(A)** Termination codon SNP (T-C SNP) along the genome. **(B)** Non-synonymous SNPs (N-S SNP) along the genome. Histograms of minor allele frequencies (MAFs) of non-synonymous SNPs in the **(C)** full population, **(D)** *indica*, and **(E)** *japonica*. Distributions of **(F)** SDSs and **(G)** ESDSs along the *indica* genome. SDS and ESDS show SNPs with significant and extremely significant differences ($p < 0.05$; $p < 0.01$) in allele frequency between polar pools. For each 500 kb sliding window, the numbers of SDSs and ESDSs were plotted on the entire genome. The sliding step is 50 kb. Adjacent chromosomes are delineated using different colors. Horizontal black lines show the thresholds for the 99th percentile of 10,000 permutations of the SDS and ESDS numbers.

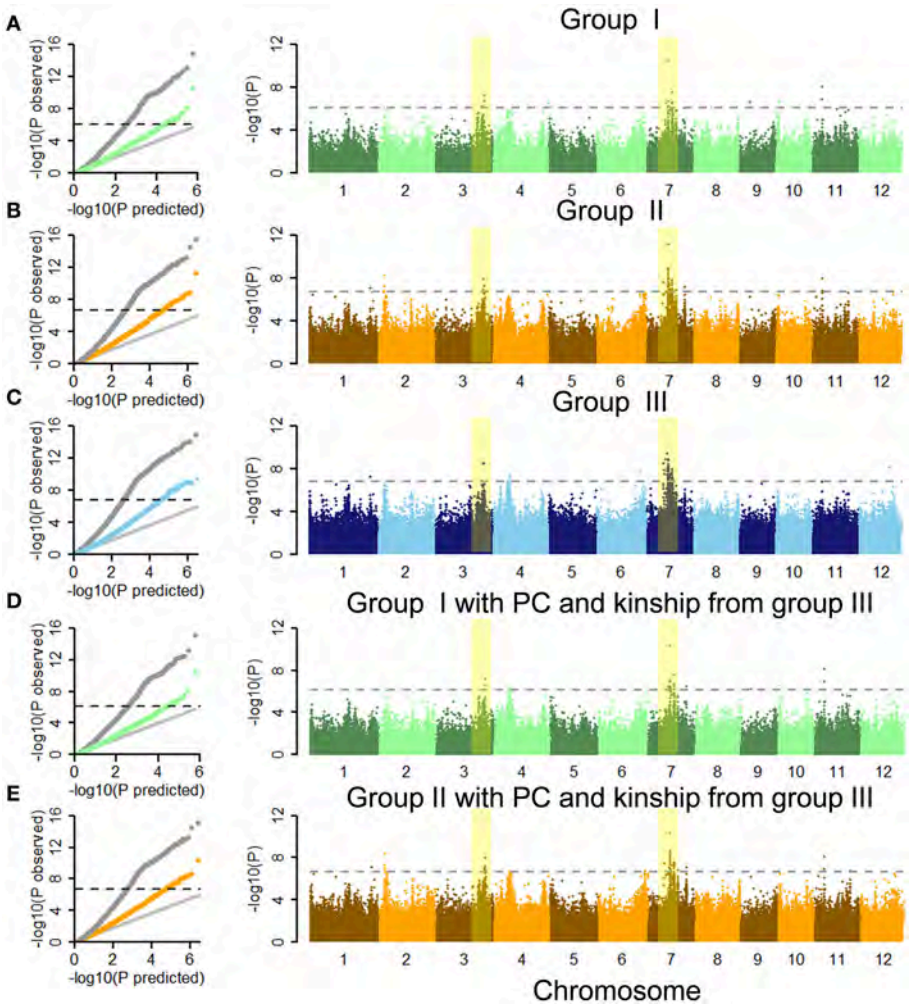

FIGURE 3 | Genome-wide association studies of mesocotyl length under CMLM in full population using three sets of SNPs and different PC and kinship. Quantile-quantile plots and Manhattan plots of the CMLM using groups **(A)** I, **(B)** II, and **(C)** III in full population. Quantile-quantile plots and Manhattan plots of CMLM using groups **(D)** I and **(E)** II with PC and kinship derived from group III in full population. In quantile-quantile plots, gray dots show GLM, and other colored points show CMLM. The horizontal black dashed lines in Manhattan plots of CMLM show thresholds at $p = 0.01$ after Bonferroni-adjusted multiple test correction. Yellow stripes show two important signals in three GWAS using three sets of SNPs in the full population.

groups I and II effectively reduced the frequency of false positives. Moreover, Non-Syn GWAS markedly reduced the computational burden.

Exploration of Candidate Gene *OsML1*

By comparing Non-Syn GWAS to previous bi-parental mapping results (Redoña and Mackill, 1996b; Cai and Morishima, 2002; Cao et al., 2002; Ouyang et al., 2005; Huang C. et al., 2010; Lee H. et al., 2012; Lee H. S. et al., 2012; Eizenga et al., 2016), we confirmed 4 QTL for ML, including *qFML2-1*, *qFML3-1*, *qFML3-2*, and *qFML11-1*. Among them, QTL *qFML3-2* was previously identified for four times (Table S11). Based on high-density sequencing of four parental accessions in two of the bi-parental mapping studies (Table S11), we identified 28 non-synonymous SNPs with different alleles between the parents in the range of 300 kb around peak SNP (Chr3_30603087). LD analysis showed that 9 of 28 non-synonymous SNPs were in the same LD block with $r^2 > 0.6$, including 2 non-synonymous SNPs (Chr3_30603087, Chr3_30606285) above the threshold with $-\log(p)$ values of 7.31 and 6.74, respectively (**Figure 4A** and (**Table 1**). The both loci were ESDSs with χ^2-values of 20.72 and 19.12 in *indica* (**Table 1**). The analysis of association and linkage mapping and screening of ESDSs indicates that one or both non-synonymous SNPs could be functional loci located in candidate genes LOC_Os03g53320 and LOC_Os03g53340, respectively.

To confirm the functional gene for ML, we further investigated the relationship between ML and other polymorphic protein-coding differences in the two genes. There were three InDel (Chr3_30605444, Chr3_30605446 and Chr3_30606411) in the CDS of LOC_Os03g53340 in 621 accessions but none in LOC_Os03g53320 (Table S12). However, no significant difference in ML was detected between alleles of each InDel of

TABLE 1 | Summary of SNPs associated with ML by GWAS using CMLM and group I in the full population.

QTL	Gene	Position	−log(*p*)[a]	−log(*p*)[b]	−log(*p*)[c]	x^2-value[d]	x^2-value[e]	SNP variation	Amino acid variation	MAF	Functional annotation
qFML2-1	LOC_Os02g07480	Chr2_3858289	6.12	8.13	6.07	1.39	0	G/T	T/N	0.011	Transglycosylase SLT domain containing protein, expressed
qFML3-1	LOC_Os03g51340	Chr3_29376315	6.26	9.65	4.66	11.86	0.51	C/T	P/L	0.074	Expressed protein
qFML3-2	LOC_Os03g53320	Chr3_30603087	7.31	12.69	7.24	20.72	0.51	G/A	A/V	0.069	Hypothetical protein
	LOC_Os03g53340	Chr3_30606285	6.74	11.89	6.6	19.12	0.51	G/T	D/E	0.076	HSF-type DNA-binding domain containing protein, expressed
qFML4-1	LOC_Os04g58590	Chr4_34837207	6.53	3.52	3.54	0	2.37	A/T	L/P	0.01	RNA recognition motif containing protein, putative, expressed
qFML7-1	LOC_Os07g22360	Chr7_12552125	6.53	5.78	6.54	9.26	0	G/A	V/I	0.047	Expressed protein
qFML7-2	LOC_Os07g23990	Chr7_13602658	6.77	9.71	7.04	26.52	0.51	A/T	M/L	0.366	Tetratricopeptide repeat domain containing protein, putative, expressed
	LOC_Os07g24010	Chr7_13611491	10.51	14.9	10.35	31	0	A/T	S/T	0.26	Hypothetical protein
	LOC_Os07g24170	Chr7_13728692	6.73	9.66	6.95	28.82	0.51	T/A	N/K	0.39	Expressed protein
		Chr7_13728704	6.27	9.1	6.43	26.45	0.51	G/T	Q/H	0.388	
		Chr7_13729329	6.18	9.26	6.32	31.25	0	G/A	V/M	0.393	
	LOC_Os07g24190	Chr7_13746039	6.32	9.05	6.53	24.22	0	C/T	M/I	0.385	CESA3 - cellulose synthase, expressed
qFML7-3	LOC_Os07g25460	Chr7_14579544	6.11	9.06	5.96	22.65	0.51	G/A	R/C	0.394	Ankyrin repeat domain containing protein, expressed
qFML7-4	LOC_Os07g27610	Chr7_16129890	7.58	13.11	7.56	33.63	0	G/A	R/Q	0.438	Expressed protein
	LOC_Os07g27630	Chr7_16135146	6.57	12	6.5	29.53	0	G/A	S/L	0.185	Expressed protein
	LOC_Os07g27680	Chr7_16151805	6.65	12.31	6.65	33.63	0	T/C	T/A	0.457	Expressed protein
qFML7-5	LOC_Os07g39660	Chr7_23772528	6.14	9.65	6.47	27.42	0	A/T	H/L	0.221	Hypothetical protein
qFML8-1	LOC_Os08g17350	Chr8_10613231	6.17	6.24	6.18	0	0	G/A	S/F	0.004	Expressed protein
qFML9-1	LOC_Os09g11800	Chr9_6598055	6.63	8.52	6.25	2.37	0	T/A	V/E	0.009	Expressed protein
qFML10-1	LOC_Os10g03730	Chr10_1681425	6.64	9.13	6.63	4.8	0	T/C	E/G	0.024	OsFBX347 - F-box domain containing protein, expressed
	LOC_Os10g03780	Chr10_1713500	6.69	9.5	6.59	5.64	0	G/A	Q/*	0.02	OsFBX351 - F-box domain containing protein, expressed
qFML11-1	LOC_Os11g10920	Chr11_6031396	8.07	9.64	8.18	2.37	0	A/C	V/G	0.011	Carboxyl-terminal proteinase, putative, expressed
	LOC_Os11g10990	Chr11_6065939	6.91	8.42	6.92	2.37	0	C/T	G/R	0.01	Heat shock protein DnaJ, putative, expressed

[a] *−log(p) are association signals of CMLM using PC and kinship derived from non-synonymous SNPs (group I).*
[b] *−log(p) are association signals of GLM using PC derived from group I.*
[c] *−log(p) are association signals of CMLM using PC and kinship derived from group III.*
[d] *x^2-value are chi-squared tests between polar pools in indica.*
[e] *x^2-value are chi-squared tests between polar pools in japonica.*

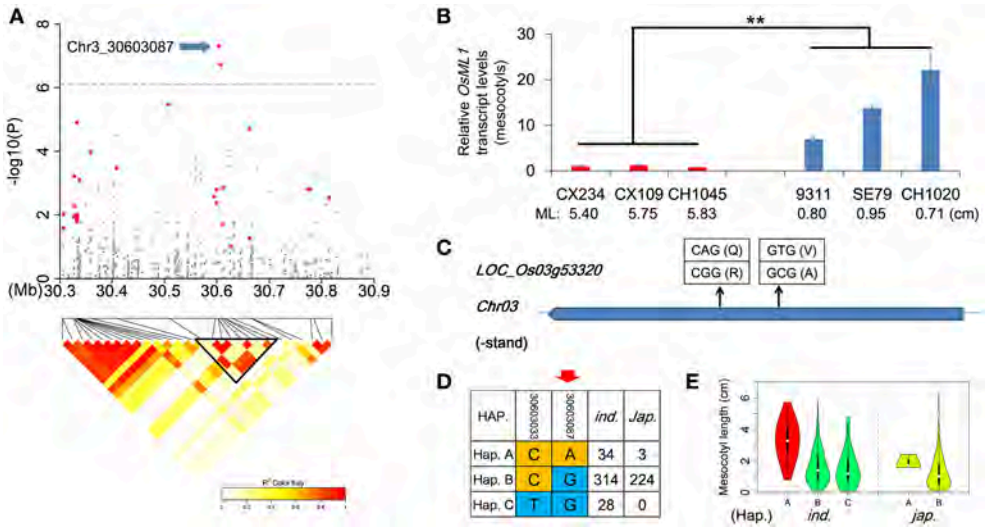

FIGURE 4 | Identification of *OsML1* for mesocotyl length in *qFML3-2*. **(A)** Genome-wide association signals in the region at 30.3–30.9 Mb on chromosome 3 and LD heatmap (bottom) for 28 non-synonymous SNPs (colored red) with different alleles between parents of known bi-parental maps. Blue arrow indicates possible functional locus in *OsML1* (LOC_Os03g53320). Triangular block shows region with strong local LD ($r^2 > 0.6$). **(B)** Expression analysis of *OsML1* in the mesocotyls from 6 accessions with long- and short-mesocotyls. Names and ML of accessions are plotted on the *X*-axis. Red and blue bars show long- and short-mesocotyl accessions, respectively. Data represent means ±s.d ($n = 3$). Asterisks represent significant differences between accessions with long- and short-mesocotyls (**$p < 0.01$, Student's *t* test). **(C)** Structure of *OsML1* showing non-synonymous SNPs and amino acid polymorphisms. **(D)** Haplotype analysis of two non-synonymous SNPs in *OsML1*. Red arrow indicates possible functional locus. **(E)** Comparison of ML among haplotypes of *OsML1* in *indica* and *japonica*. Accessions with haplotype colored red had significantly longer mesocotyls than members of haplotypes colored green.

LOC_Os03g53340. We also measured expression levels of the two candidate genes in mesocotyls using accessions with long- and short-mesocotyls by qRT-PCR. One (LOC_Os03g53320) showed more than 13.8-fold higher expression in short-mesocotyl accessions compared to long-mesocotyl accessions (**Figure 4B**), whereas the other (LOC_Os03g53340) showed no difference in expression levels in mesocotyls between long-mesocotyl and short-mesocotyl genotypes (Figure S10). Since there were not obvious differences in ML between alleles of 3 InDel as well as expression level between long- and short-mesocotyl accessions in LOC_Os03g53340, we suggest that LOC_Os03g53320 is the most likely functional gene for ML.

Here, we rename gene LOC_Os03g53320, which encodes a hypothetical protein, as *OsML1*. There were two non-synonymous SNPs in *OsML1* among the 621 accessions; only one of these (Chr3_30603087) showed an obvious signal in the integrated analysis (**Figure 4C**). Based on the two non-synonymous SNPs, we identified three haplotypes of *OsML1* in *indica* with distinct phenotypes. Accessions with haplotype A produced significantly longer mesocotyls than those containing haplotypes B or C (**Figures 4D,E**). Further sequence alignment between the long mesocotyl haplotype A and short mesocotyl haplotypes B and C showed that SNP (Chr3_30603087) could be the functional locus of *OsML1*.

Exploration of Candidate Gene *OsML2*

We focused on *qFML7-2* with the highest signal in the whole genome. In view of the short physical distance covering *qFML7-2*, *qFML7-3,* and *qFML7-4* we redefined the QTL region based on local LD. As indicated in the LD heatmap seven non-synonymous SNPs above threshold in *qFML7-2* and *qFML7-3* are in the same LD block (named as Block 1) (**Figure 5A**). We also found strong LDs with r^2 of ≈0.9 among the seven SNPs, except for the peak non-synonymous SNP (Chr7_13611491) with r^2 of ≈0.5. These results indicated that one of the seven non-synonymous SNPs within Block 1 could be the functional locus for ML.

After comparisons with previous bi-parental mapping studies we established that the QTL was a new locus for ML. We checked the alleles of all 7 non-synonymous SNPs between the parental accessions of the previous bi-parental mapping populations (Table S13) and no allelic difference could explain why this QTL was not identified in previous mapping studies.

To search for functional SNPs and genes for ML in Block 1, we performed a sequence alignment analysis of the 7 non-synonymous SNPs in the LD block. In the full population there were four main haplotypes (A–D) involving more than three accessions. Three (B, C, and D) and all four haplotypes were detected in *japonica* and *indica*, respectively (**Figure 5B**). Accessions carrying haplotype C had shorter ML than those carrying B or D, with significant differences in *indica*. The peak non-synonymous SNP (Chr7_13611491) was the only locus with a consistent allele (A) in long mesocotyl haplotypes B and D, whereas allele (T) was present in short mesocotyl haplotype C (**Figure 5B**). We suggest that the peak non-synonymous SNP might be the functional locus for ML in Block 1.

To check the inference we divided the population into groups carrying alleles (A) and (T) of the peak locus, and re-examined the relationship between ML and each of other 6 non-synonymous SNPs above threshold in Block 1. In 222 and 151 accessions carrying allele (A) in *indica* and *japonica*, respectively,

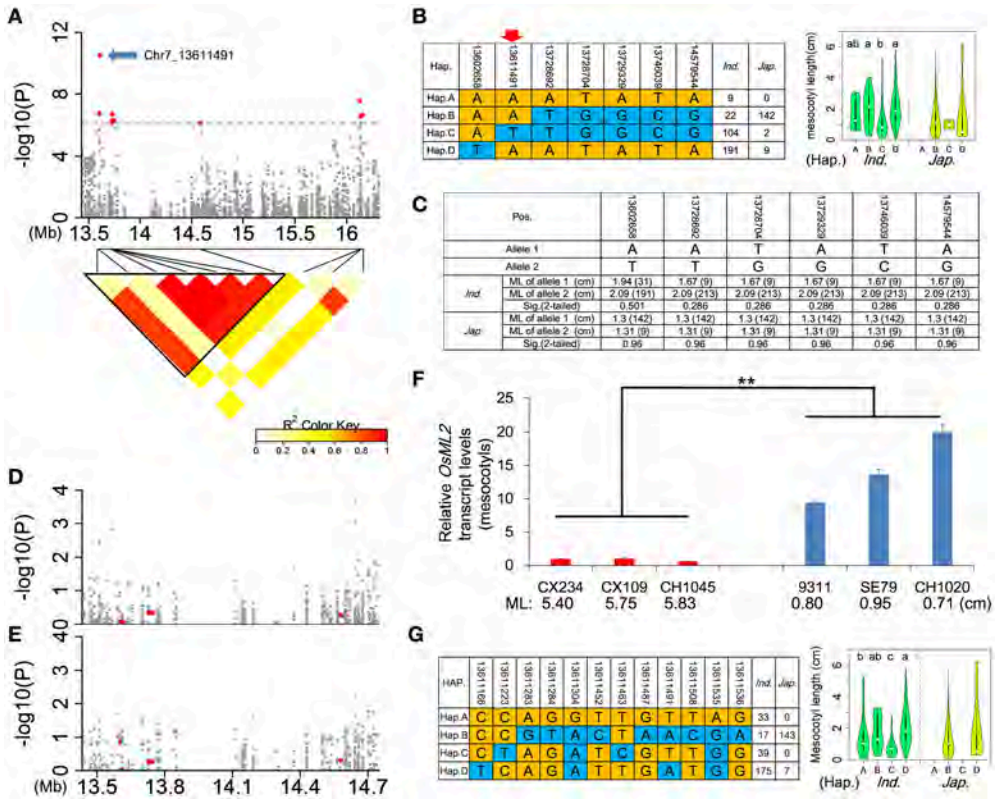

FIGURE 5 | Identification of *OsML2* for mesocotyl length. **(A)** Genome-wide association signals (top) in the region 13.4–16.4 Mb on chromosome 7 and LD heatmap (bottom) of 10 non-synonymous SNPs above the threshold. A total of 10 red points show non-synonymous SNPs above threshold in *qFML7-2*, *qFML7-3* and *qFML7-4*, and blue arrow indicates possible functional locus in *OsML2* (LOC_Os07g24010). Triangular block (named Block 1) shows region with strong local LD ($r^2 > 0.6$). **(B)** Haplotype analysis (left) of 7 non-synonymous SNPs above threshold in Block 1 and comparison of ML (right) among haplotypes in *indica* and *japonica*. Different letters above the violins indicate significant differences ($p < 0.05$) when analyzed by Duncan's test. Red arrow indicates possible functional locus. **(C)** Independent-sample *T*-tests for ML differences between alleles of each of the 6 non-synonymous SNPs in Block 1 using accessions carrying allele **(A)** of the peak signal (Chr7_13611491). Data in parentheses show number of accessions. Manhattan plots for ML in Block 1 using **(D)** 373 accessions and **(E)** 222 *indica* accessions carrying allele **(A)** of the peak signal. Red points show 6 non-synonymous SNPs in Block 1. **(F)** Expression analysis of *OsML2* in the mesocotyls from 6 accessions with long- and short-mesocotyls. Names and ML of accessions are plotted on the *X*-axis. Red and blue bars show long- and short-mesocotyl accessions, respectively. Data represent means ± s.d ($n = 3$). Asterisks represent significant differences between accessions with long- and short-mesocotyls (**$p < 0.01$, Student's *t* test). **(G)** Haplotype analysis (left) of 12 non-synonymous SNPs in *OsML2* and comparison of ML (right) among haplotypes of *OsML2* in *indica* and *japonica*, respectively. Different letters above the violins indicate significant differences ($p < 0.05$) detected by Duncan's test.

there was no significant difference in ML between alleles of each non-synonymous SNP (**Figure 5C**). In 104 and 2 accessions carrying allele (T) in *indica* and *japonica*, we detected no allelic diversity in the other 6 non-synonymous SNPs (**Figure 5B**). We performed another complementary GWAS using accessions carrying allele (A) of the peak SNP in the full population and *indica*, respectively. There was no signal for ML in Block 1, and the 6 non-synonymous SNPs showed *p*-values $< -\log(p) = 1$ in the full population and *indica* (**Figures 5D,E**). These results showed that the other 6 non-synonymous SNPs were not functional loci associated with ML, despite the higher $-\log(p)$ values in the original Non-Syn GWAS of the full population and *indica* (**Tables 1** and Table S8). We suggest that the signals in the other 6 non-synonymous SNPs were produced in accessions carrying allele (T) of the peak SNP (Chr7_13611491).

We checked the expression level of the candidate LOC_Os07g24010 including non-synonymous SNP Chr7_13611491. There was about a 15.9-fold higher expression in short-mesocotyl accessions compared to long-mesocotyl accessions (**Figure 5F**). We renamed LOC_Os07g24010 as *OsML2*; it also encoded a hypothetical protein. There were 12 non-synonymous SNPs in *OsML2*. Among them, six (13611166, 13611223, 13611304, 13611463, 13611491, and 13611535) showed high signals with $-\log(p) > 4$ in the Non-Syn GWAS using the full population (Table S14). Based on the 12 non-synonymous SNPs in *OsML2*, four and two haplotypes were identified in *indica* and *japonica*, respectively. There were clear differences in ML among accessions carrying haplotypes A, B, C, or D (**Figure 5G**). The results showed that *OsML2* was an important expressed gene in regulating mesocotyl elongation, and several non-synonymous SNPs were associated with ML.

Cross-Validation of Two Genes for Mesocotyl Length

For efficient utilization of *OsML1* and *OsML2* in breeding for deep-sowing tolerance, it is important to uncover the genotypic

effect of each haplotype and the combined haplotypes of two genes. Based on the above sequence alignment analysis of each gene, we focused on *OsML1*-A, *OsML2*-A, *OsML2*-B, and *OsML2*-D as long ML haplotypes, whereas *OsML1*-B, *OsML1*-C, and *OsML2*-C were considered to be short ML haplotypes. Among 12 possible allelic combinations of the two genes, eleven could be detected in 621 rice accessions. There were more genetic diversity in *indica*, including 11 allelic combinations, but only 3 allelic combinations were identified in *japonica* (**Figure 6A**). Considering the complexity of population structure and genetic background, we performed statistical analysis in *indica* by one-way ANOVA. The MLs were the shortest in accessions without long ML genotypes, *OsML1*-C + *OsML2*-C (0.62 cm) and *OsML1*-B + *OsML2*-C (0.87 cm), followed by accessions with only one long ML genotypes, *OsML1*-C + *OsML2*-A (1.12 cm), *OsML1*-C + *OsML2*-B (1.15 cm), *OsML1*-B + *OsML2*-A (1.35 cm), *OsML1*-B + *OsML2*-B (1.66 cm), *OsML1*-B + *OsML2*-D (1.91 cm), *OsML1*-C + *OsML2*-D (2.27 cm), while accessions with both long ML genotypes had longest ML, *OsML1*-A + *OsML2*-B (3.07 cm), *OsML1*-A + *OsML2*-A (3.69 cm), and *OsML1*-A + *OsML2*-D (3.76 cm) (**Figure 6A**). Haplotypes *OsML1*-A and *OsML2*-D formed the best combination with longest ML and should be the best genotype for use in molecular marker assisted breeding for long ML.

For validation, we identified accessions with long ML haplotypes for each gene from 3,024 cultivated rice accessions (Li J. Y. et al., 2014; Alexandrov et al., 2015). Three hundred and sixty seven and 982 accessions were detected with *OsML1*-A and *OsML2*-D, respectively, and 110 had both alleles. We selected 7 lines with *OsML2*-D, 2 lines with *OsML1*-A and *OsML2*-A and 1 line with *OsML1*-A and *OsML2*-D, and grew them in a plastic box with 10 cm of soil cover. The mean MLs were 4.57, 4.70, and 3.74 cm, respectively (**Figure 6B**). Unfortunately no seed of other accessions was available, but the results supported the hypothesis that *OsML1* and *OsML2* are functional genes and that the long ML haplotypes acting in an additive manner can be used in molecular marker assisted breeding. Additionally, we demonstrated a powerful strategy for efficient cloning of complex trait QTL that combines Non-Syn GWAS, known linkage map information, allelic frequencies differences between phenotypic pools, expression analyses and haplotype analyses.

Evidence of Positive Selection on *OsML1* in *Japonica*

To explore whether the two genes were targeted by natural or human selection during rice domestication, we performed signature identification of selection using 621 cultivated and 446 wild rice accessions (Huang et al., 2012a). We extracted the sequencing data including the gene and a 2 kb promoter region, respectively, within *OsML1* and *OsML2*. Selective signal scan were performed within the both genes using the ratio of the genetic diversity in wild rice to that in *indica* and *japonica* (π_W/π_I and π_W/π_J), respectively (**Table 2**). High selective signal was detected within *OsML1* in *japonica* ($\pi_W/\pi_J = 4.59$). The Tajima's *D* was lowest at the value of −2.19, suggesting strong positive selection across *OsML1* in *japonica*.

DISCUSSION

Mesocotyl Elongation Is a Key Trait for Deep-Sowing Tolerance

Rice accessions for dry direct-seeding need have the ability to withstand deep planting for access to moisture or to tolerate

TABLE 2 | Nucleotide diversity and Tajima's *D* Test.

Gene_Population	π	Tajima's *D*
*OsML1*_Wild	0.00224	−0.65
*OsML1*_Cultivated	0.00301	0.20
OsML1_Ind.	0.00365	1.97
OsML1_Jap.	0.00049	−2.20
*OsML2*_Wild	0.0061	1.31
*OsML2*_Cultivated	0.01671	1.27
OsML2_Ind.	0.01093	0.30
OsML2_Jap.	0.00604	−1.02

A

Hap.	*Jap.*		*Ind.*	
	Num.	ML (cm)	Num.	ML (cm)
OsML1-A + *OsML2*-A	0	-	3	3.69^{a}
OsML1-A + *OsML2*-B	1	1.57	2	3.07^{ab}
OsML1-A + *OsML2*-C	0	-	0	-
OsML1-A + *OsML2*-D	0	-	14	3.76^{a}
OsML1-B + *OsML2*-A	0	-	23	1.35^{cde}
OsML1-B + *OsML2*-B	141	1.28	14	1.66^{cde}
OsML1-B + *OsML2*-C	0	-	31	0.87^{de}
OsML1-B + *OsML2*-D	7	1.59	145	1.91^{bcd}
OsML1-C + *OsML2*-A	0	-	7	1.12^{cde}
OsML1-C + *OsML2*-B	0	-	1	1.15
OsML1-C + *OsML2*-C	0	-	7	0.62^{e}
OsML1-C + *OsML2*-D	0	-	9	2.27^{bc}

B

HAP.	Variety	Subpop.	ML (cm)
OsML2-D (Mean: 4.57 cm)	IRIS_313-9032	*Indica*	4.3
	IRIS_313-11144	*Indica*	3.38
	IRIS_313-8731	*Indica*	6.67
	IRIS_313-10134	*Indica*	4.64
	IRIS_313-10929	*Indica*	5.55
	IRIS_313-10971	*Indica*	2.68
	IRIS_313-10978	*Indica*	4.78
OsML1-A+*OsML2*-A (Mean: 4.70 cm)	IRIS_313-11204	*Indica*	4.14
	IRIS_313-8283	*Aus/boro*	5.25
OsML1-A+*OsML2*-D	IRIS_313-10980	*Indica*	3.74

FIGURE 6 | Functional validation of haplotype combinations of *OsML1* and *OsML2*. **(A)** ML of different combinations of haplotypes in *OsML1* and *OsML2*. Different letters indicate significant differences ($p < 0.05$) detected by one-way ANOVA. **(B)** Cross-validation by phenotyping of 10 accessions representing different genotypes of *OsML1* and *OsML2*.

variable planting depth associated with machine sowing. Many studies have been carried out to identify deep-sowing tolerant cereal genotypes and to examine the relationship between mesocotyl and/or coleoptile length and deep-sowing tolerance (Turner et al., 1982; Kirby, 1993; Luo et al., 2007; Chung, 2010; Wu et al., 2015; Lu et al., 2016). Here a diverse set of 621 cultivars was tested for deep-sowing tolerance under field conditions and in subsequent depth-of-sowing experiments in plastic boxes. Our results, like previous studies, confirmed two points: (1) ML is induced by deeper soil covering (Wu et al., 2015; Lu et al., 2016), (2) and variation in ML fits a negative binomial distribution and there are few elite cultivated rice genotypes with long mesocotyls (Luo et al., 2007). Moreover, our results showed that ER was not affected greatly until the sowing depth reached 3 cm. Therefore, we suggest that new accessions for dry direct-seeding should have ML of more than 3 cm.

Comparison of ML between the two main rice subgroups showed that average ML in *indica* was significantly longer than in *japonica*. Given that *indica* rice was originally developed from crosses between *japonica* and local wild rice (Huang et al., 2012a) and that weedy and wild rice have longer ML (Cai and Morishima, 2002; Chung, 2010; Eizenga et al., 2016), we suggest that short mesocotyls are probably the result of an evolutionary change due to the long period of traditional rice cultivation by transplantation. Weedy and wild rice could be elite genetic resources for solving the problem of poor seedling establishment in direct-seeded rice (Chung, 2010). However, in the present work we also identified several germplasm with long mesocotyls and good seedling emergence under deep sown conditions and those elite germplasm can be used as parents in breeding rice accessions for dry direct-seeding.

Non-syn GWAS Was Conducive in Identifying Functional Loci and Alleles

GWAS has become a common method in searching for candidate genes underlying target traits in rice (Huang X. et al., 2010; Huang et al., 2012b; Si et al., 2016; Yano et al., 2016). The Mixed Linear Model (MLM) with PC and kinship is efficient in decreasing false positives due to population structure and relationships among individuals (Yu et al., 2006). However, for complex traits affected by population structure, MLM weakens the real association and reduces signal strength of known genes. CMLM improves the statistical power by using group kinship (Zhang et al., 2010a). Constructing a trait-specific kinship derived from weighted SNP analysis is another strategy to improve MLM, as achieved by SUPER and FarmCPU (Wang et al., 2014; Liu et al., 2016). We derived two sets of SNPs (groups I and II) from 15 million polymorphisms according to annotated gene locations and possible influence on gene function, and then we obtained 572,511 non-synonymous SNPs and 1,801,421 SNPs located in the 5′ sequences of genes ($\leq$1 Kb upstream of the first ATG) by this approach. Finally, we performed and compared GWAS using these groups to search for candidate genes affecting ML. this provides an alternative solution for constructing a trait-specific kinship derived from polymorphisms that can be screened out according to biological function of target traits. Additionally, this greatly reduced the computational burden by performing GWAS using these SNPs that accounted for amino acid sequence and expression.

There were two differences between Non-Syn GWAS and GWAS using a random sample of genetic markers (group III), one was the loci, the other was PC and kinship matrix derived from these loci. In our studies, we assessed their impact on the GWAS results. By comparison of GWAS between ML and SNPs in group I using different PC and kinship, Non-Syn GWAS detected the same SNPs for ML as GWAS with PC and kinship derived from group III. The results suggested that CMLM using PC and kinship derived from group I had same efficiency as CMLM using PC and kinship from group III. Further comparison of Non-Syn GWAS and GWAS using group III indicated that there were less loci in QTL regions (local LD block of peak SNP) identified by Non-Syn GWAS. Thus, we were able to quickly and conveniently identify functional loci by the integrated analysis without confounding by other loci with little likelihood of biological function.

OsML1 and *OsML2* Are Natural Variants for Mesocotyl Length, and Could Be Useful in Breeding for Deep-Sowing Tolerance

Four of 13 QTLs in Non-Syn GWAS of the full population overlapped with loci identified in previous linkage mapping studies (Cai and Morishima, 2002; Ouyang et al., 2005; Huang C. et al., 2010; Lee H. S. et al., 2012). Among them, *qFML3-2* located in chromosome 3 was previously detected four times in bi-parental mapping studies. However, none QTL in Non-Syn GWAS overlapped with association signal in previous GWAS (Wu et al., 2015; Lu et al., 2016). The most likely reason for this finding was that different depths of soil cover were applied in these GWAS (Wu et al., 2015; Lu et al., 2016).

Interestingly, both genes showed higher expression in short-mesocotyl accessions compared to long-mesocotyl accessions. Furthermore, long ML haplotypes of both genes (*OsML1*-A, *OsML2*-A, *OsML2*-B, and *OsML2*-D) could be loss-of-function or partial loss-of-function variations. Nucleotide diversity analysis and Tajima's *D* Test showed that *OsML1* was strongly directly selected in *japonica* accessions. These results supported that short ML was a target of selection during the long term process of conversion from wild rice to *japonica* under the traditional transplanting system.

Sequence alignment of two genes also showed that there was less genetic diversity of *OsML1* and *OsML2* in *japonica*, and most of *japonica* rice had haplotypes *OsML1*-B and *OsML2*-B associated with short mesocotyls. However, there were significant differences among *OsML1* and *OsML2* haplotypes in *indica*. Superior haplotypes with long mesocotyls (*OsML1*-A and *OsML2*-D) can be used for molecular marker assistant selection, and those two genes can also be further cloned and analyzed, then used for gene transformation and breeding of rice accessions for deep-sowing tolerance.

AUTHOR CONTRIBUTIONS

YZ, WZ, CJ, JL, and ZL designed the research, performed most of experiments and analyzed the data. XiaW, HX, ET, ZY, YC, and

XinW performed part of the experiments. JX, YP, MR, and HZ conceived and supervised the project. YZ and ZL conceived the experiment and wrote the manuscript.

ACKNOWLEDGMENTS

This work was supported by Program of Science and Technology cooperation (2015DFG31900), Key Program of Hainan Department of Science and Technology (ZDYF2016217), and the China National Key Technologies Research and Developments Program (2015BAD02B01, 2013BAD01B02-15 and 2016YFD0100101).

SUPPLEMENTARY MATERIAL

The Supplementary Material for this article can be found online at: https://www.frontiersin.org/articles/10.3389/fpls.2018.00332/full#supplementary-material

REFERENCES

Alexandrov, N., Tai, S., Wang, W., Mansueto, L., Palis, K., Fuentes, R. R., et al. (2015). SNP-seek database of SNPs derived from 3000 rice genomes. *Nucleic Acids Res.* 43, 1023–1027. doi: 10.1093/nar/gku1039

Benjamini, Y., and Hochberg, Y. (1995). Controlling the false discovery rate: a practical and powerful approach to multiple testing. *J. R. Stat. Soc.* 57, 289–300.

Cai, W., and Morishima, H. (2002). QTL clusters reflect character associations in wild and cultivated rice. *Theor. Appl. Genet.* 104, 1217–1228. doi: 10.1007/s00122-001-0819-7

Cao, L., Zhu, J., Yan, Q., He, L., Wei, X., and Cheng, S. (2002). Mapping QTLs with epistasis for mesocotyl length in a DH population from *indica-japonica* cross of rice (*Oryza sativa*). *Chin. J. Rice Sci.* 16, 221–224.

Chen, F., Jiang, L., Zheng, J., Huang, R., Wang, H., Hong, Z., et al. (2014). Identification of differentially expressed proteins and phosphorylated proteins in rice seedlings in response to strigolactone treatment. *PLoS ONE* 9:e93947. doi: 10.1371/journal.pone.0093947

Chung, N. J. (2010). Elongation habit of mesocotyls and coleoptiles in weedy rice with high emergence ability in direct-seeding on dry paddy fields. *Crop Pas. Sci.* 61, 911–917. doi: 10.1071/CP10099

Eizenga, G. C., Neves, P. C. F., Bryant, R. J., Agrama, H. A., and Mackill, D. J. (2016). Evaluation of a M-202 × *Oryza nivara* advanced backcross mapping population for seedling vigor, yield components and quality. *Euphytica* 208, 157–171. doi: 10.1007/s10681-015-1613-y

Farooq, M., Barsa, S. M. A., and Wahid, A. (2006a). Priming of field-sown rice seed enhances germination, seedling establishment, allometry and yield. *Plant Growth Regul.* 49, 285–294. doi: 10.1007/s10725-006-9138-y

Farooq, M., Basra, S. M. A., Tabassum, R., and Afzal, I. (2006b). Enhancing the performance of direct seeded fine rice by seed priming. *Plant Prod. Sci.* 9, 446–456. doi: 10.1626/pps.9.446

Farooq, M., Siddique, K. H. M., Rehman, H., Aziz, T., Lee, D. J., and Wahid, A. (2011). Rice direct seeding: experiences, challenges and opportunities. *Soil Tillage Res.* 111, 87–98. doi: 10.1016/j.still.2010.10.008

Feng, F., Mei, H., Fan, P., Li, Y., Xu, X., Wei, H., et al. (2017). Dynamic transcriptome and phytohormone profiling along the time of light exposure in the mesocotyl of rice seedling. *Sci. Rep.* 7:11961. doi: 10.1038/s41598-017-12326-2

Gao, Y., Wang, G., Yuan, S., Qin, Y., Zhao, J., Zhang, Y., et al. (2014). Phenotypic analysis and molecular characterization of an allelic mutant of the *D61* gene in rice. *Crop J.* 2, 175–182. doi: 10.1016/j.cj.2014.04.003

Hu, Z., Yamauchi, T., Yang, J., Jikumaru, Y., Tsuchida-Mayama, T., Ichikawa, H., et al. (2014). Strigolactone and cytokinin act antagonistically in regulating rice mesocotyl elongation in darkness. *Plant Cell Physiol.* 55, 30–41. doi: 10.1093/pcp/pct150

Hu, Z., Yan, H., Yang, J., Yamaguchi, S., Masahiko, M., Takamure I., et al. (2010). Strigolactones negatively regulate mesocotyl elongation in rice during germination and growth in darkness. *Plant Cell Physiol.* 51, 1136–1142. doi: 10.1093/pcp/pcq075

Huang, C., Jiang, S. K., Feng, L. L., Xu, Z. J., and Chen, W. F. (2010). QTL analysis for mesocotyl length in rice (*Oryza sativa* L.). *Acta Agron. Sin.* 36, 1108–1113. doi: 10.1016/S1875-2780(09)60060-2

Huang, X., Kurata, N., Wei, X., Wang, Z. X., Wang, A., Zhao, Q., et al. (2012a). A map of rice genome variation reveals the origin of cultivated rice. *Nature* 490, 497–501. doi: 10.1038/nature11532

Huang, X., Wei, X., Sang, T., Zhao, Q., Feng, Q., Zhao, Y., et al. (2010). Genome-wide association studies of 14 agronomic traits in rice landraces. *Nat. Genet.* 42, 961–967. doi: 10.1038/ng.695

Huang, X., Zhao, Y., Wei, X., Li, C., Wang, A., Zhao, Q., et al. (2012b). Genome-wide association study of flowering time and grain yield traits in a worldwide collection of rice germplasm. *Nat. Genet.* 44, 32–39. doi: 10.1038/ng.1018

Kameoka, H., and Kyozuka, J. (2015). Downregulation of rice *DWARF 14 LIKE* suppress mesocotyl elongation via a strigolactone independent pathway in the dark. *J. Genet. Genomics* 42, 119–124. doi: 10.1016/j.jgg.2014.12.003

Kirby, E. J. M. (1993). Effect of sowing depth on seedling emergence, growth and development in barley and wheat. *Field Crops Res.* 35, 101–111. doi: 10.1016/0378-4290(93)90143-B

Lee, H., Kang, J., Chung, N., Choi, K., and Ahn, S. (2012). Identification of molecular markers for mesocotyl elongation in weedy rice. *Korean J. Breed. Sci.* 44, 238–244.

Lee, H. S., Sasaki, K., Higashitani, A., Ahn, S. N., and Sato, T. (2012). Mapping and characterization of quantitative trait loci for mesocotyl elongation in rice (*Oryza sativa* L.). *Rice* 5, 1–10. doi: 10.1186/1939-8433-5-13

Li, J. Y., Wang, J., and Zeigler, R. S. (2014). The 3,000 rice genomes project: new opportunities and challenges for future rice research. *Gigascience* 3:8. doi: 10.1186/2047-217X-3-8

Li, Z., Fu, B., Gao, Y., Wang, W., Xu, J., Zhang, F., et al. (2014). The 3,000 rice genomes project. *Gigascience* 3:7. doi: 10.1186/2047-217X-3-7

Liang, Q., Wang, C., Ma, D., Li, L., Cui, Z., Wang, X., et al. (2016). Cortical microtubule disorganized related to an endogenous gibberellin increase plays an important role in rice mesocotyl elongation. *Plant Biotechnol.* 33, 59–69. doi: 10.5511/plantbiotechnology.16.0205a

Liu, X., Huang, M., Fan, B., Buckler, E. S., and Zhang, Z. (2016). Iterative usage of fixed and random effect models for powerful and efficient genome-wide association studies. *PLoS Genet.* 12:e1005767. doi: 10.1371/journal.pgen.1005767

Lu, Q., Zhang, M., Niu, X., Wang, C., Xu, Q., Feng, Y., et al. (2016). Uncovering novel loci for mesocotyl elongation and shoot length in *indica* rice through genome-wide association mapping. *Planta* 243, 645–657. doi: 10.1007/s00425-015-2434-x

Luo, J., Tang, S., Hu, P., Aleman, L., Jiao, G., and Tang, J. (2007). Analysis on factors affecting seedling establishment in rice. *Rice Sci.* 14, 27–32. doi: 10.1016/S1672-6308(07)60005-5

Mgonja, M. A., Ladeinde, T. A. O., and Aken'Ova, M. E. (1993). Genetic analysis of mesocotyl length and its relationship with other agronomic characters in rice (*Oryza sativa* L.). *Euphytica* 72, 189–195. doi: 10.1007/BF00034157

Nei, M. (1987). *Molecular Evolutionary Genetics*. Manhattan: Columbia University Press.

Ouyang, Y. N., Zhang, Q. Y., Zhang, K. Q., Yu, S. M., Zhuang, J. Y., Jin, Q. Y., et al. (2005). QTL mapping and interaction analysis of genotype x environment (Fe^{2+}-concentrations) for mesocotyl length in rice (*Oryza sativa* L.). *Acta Genet. Sin.* 32, 712–718.

Pan, Y., Zhang, H., Zhang, D., Li, J., Xiong, H., Yu, J., et al. (2015). Genetic analysis of cold tolerance at the germination and booting stages in rice by association mapping. *PLoS ONE* 10:e0120590. doi: 10.1371/journal.pone.0120590

Redoña, E. D., and Mackill, D. J. (1996a). Genetic variation for seedling vigor traits in rice. *Crop Sci.* 36, 285–290. doi: 10.2135/cropsci1996.0011183X003600020012x

Redoña, E. D., and Mackill, D. J. (1996b). Mapping quantitative trait loci for seedling vigor in rice using RFLPs. *Theor. Appl. Genet.* 92, 395–402. doi: 10.1007/BF00223685

Si, L., Chen, J., Huang, X., Gong, H., Luo, J., Hou, Q., et al. (2016). *OsSPL13* controls grain size in cultivated rice. *Nat. Genet.* 48, 447–458. doi: 10.1038/ng.3518

Simon, A., Yuri, S., Hironobu, S., and Kenji, I. (2011). Relationship between coleoptile and mesocotyl elongation of upland rice (*Oryza sativa* L.) seedlings under submergence and soil-sand culture. *Afr. J. Agric. Res.* 6, 6463–6472. doi: 10.5897/AJAR11.1506

Tajima, F. (1989). Statistical method for testing the neutral mutation hypothesis by DNA polymorphism. *Genetics* 123, 585–595.

Tamiru, M., Abe, A., Utsushi, H., Yoshida, K., Takagi, H., Fujisaki, K., et al. (2014). The tillering phenotype of the rice plastid terminal oxidase (PTOX) loss-of-function mutant is associated with strigolactone deficiency. *New Phytol.* 202, 116–131. doi: 10.1111/nph.12630

Turner, F. T., Chen, C. C., and Bollich, C. N. (1982). Coleoptile and mesocotyl lengths in semidwarf rice seedlings. *Crop Sci.* 22, 43–46. doi: 10.2135/cropsci1982.0011183X002200010010x

Wang, Q., Tian, F., Pan, Y., Buckler, E. S., and Zhang, Z. (2014). A SUPER powerful method for genome wide association study. *PLoS ONE* 9:e107684. doi: 10.1371/journal.pone.0107684

Watanabe, H., Adachi, Y., and Saigusa, M. (2015). Synergistic effects of ethephon and gibberellic acid on the growth of rice seedlings grown under field and environmentally controlled conditions. *J. Agron.* 14, 87–92. doi: 10.3923/ja.2015.87.92

Wu, J., Feng, F., Lian, X., Teng, X., Wei, H., Yu, H., et al. (2015). Genome-wide Association Study (GWAS) of mesocotyl elongation based on re-sequencing approach in rice. *BMC Plant Biol.* 15:218. doi: 10.1186/s12870-015-0608-0

Wu, M., Zhang, G., Lin, J., and Cheng, S. (2005). Screening for rice germplasms with specially-elongated mesocotyl. *Rice Sci.* 12, 226–228.

Xiong, Q., Ma, B., Lu, X., Huang, Y. H., He, S. J., Yang, C., et al. (2017). Ethylene-inhibited jasmonic acid biosynthesis promotes mesocotyl/coleoptile elongation of etiolated rice seedlings. *Plant Cell* 29, 1053–1072. doi: 10.1105/tpc.16.00981

Yano, K., Yamamoto, E., Aya, K., Takeuchi, H., Lo, P. C., Hu, L., et al. (2016). Genome-wide association study using whole-genome sequencing rapidly identifies new genes influencing agronomic traits in rice. *Nat. Genet.* 48, 927–934. doi: 10.1038/ng.3596

Yu, J., Pressoir, G., Briggs, W. H., Vroh, B. I., Yamasaki, M., Doebley, J. F., et al. (2006). A unified mixed-model method for association mapping that accounts for multiple levels of relatedness. *Nat. Genet.* 38, 203–208. doi: 10.1038/ng1702

Yu, S. B., Xu, W. J., Vijayakumar, C. H., Ali, J., Fu, B. Y., Xu, J. L., et al. (2003). Molecular diversity and multilocus organization of the parental lines used in the International Rice Molecular Breeding Program. *Theor. Appl. Genet.* 108, 131–140. doi: 10.1007/s00122-003-1400-3

Zhang, H., Zhang, D., Wang, M., Sun, J., Qi, Y., Li, J., et al. (2011). A core collection and mini core collection of *Oryza sativa* L. in China. *Theor. Appl. Genet.* 122, 49–61. doi: 10.1007/s00122-010-1421-7

Zhang, Z., Ersoz, E., Lai, C. Q., Todhunter, R. J., Tiwari, H. K., Gore, M. A., et al. (2010a). Mixed linear model approach adapted for genome-wide association studies. *Nat. Genet.* 42, 355–360. doi: 10.1038/ng.546

Zhang, Z., Liu, J., Ding, X., Bijma, P., de Koning, D. J., and Zhang, Q. (2010b). Best linear unbiased prediction of genomic breeding values using a trait-specific marker-derived relationship matrix. *PLoS ONE* 5:e12648. doi: 10.1371/journal.pone.0012648

Conflict of Interest Statement: The authors declare that the research was conducted in the absence of any commercial or financial relationships that could be construed as a potential conflict of interest.

frontiers in Plant Science

ORIGINAL RESEARCH
published: 12 June 2018
doi: 10.3389/fpls.2018.00769

Prioritization of Candidate Genes in QTL Regions for Physiological and Biochemical Traits Underlying Drought Response in Barley (*Hordeum vulgare* L.)

Kornelia Gudys[1,2], Justyna Guzy-Wrobelska[1], Agnieszka Janiak[1], Michał A. Dziurka[3], Agnieszka Ostrowska[3], Katarzyna Hura[4], Barbara Jurczyk[4], Katarzyna Żmuda[4], Daria Grzybkowska[1], Joanna Śróbka[1], Wojciech Urban[1], Jolanta Biesaga-Koscielniak[3], Maria Filek[3], Janusz Koscielniak[4], Krzysztof Mikołajczak[5], Piotr Ogrodowicz[5], Karolina Krystkowiak[5,6], Anetta Kuczyńska[5], Paweł Krajewski[7] and Iwona Szarejko[1]*

[1] Department of Genetics, Faculty of Biology and Environmental Protection, University of Silesia, Katowice, Poland, [2] Department of Botany and Nature Protection, Faculty of Biology and Environmental Protection, University of Silesia, Katowice, Poland, [3] Department of Developmental Biology, Institute of Plant Physiology, Polish Academy of Sciences, Krakow, Poland, [4] Department of Plant Physiology, Faculty of Agriculture and Economics, University of Agriculture, Krakow, Poland, [5] Department of Biotechnology, Institute of Plant Genetics, Polish Academy of Sciences, Poznan, Poland, [6] Department of Plant Functional Metabolomics, Institute of Bioorganic Chemistry, Polish Academy of Sciences, Poznan, Poland, [7] Department of Biometry and Bioinformatics, Institute of Plant Genetics, Polish Academy of Sciences, Poznan, Poland

OPEN ACCESS

Edited by:
Hanwei Mei,
Shanghai Agrobiological Gene Center, China

Reviewed by:
Enrico Francia,
Università degli Studi di Modena e Reggio Emilia, Italy
Shabir Hussain Wani,
Sher-e-Kashmir University of Agricultural Sciences and Technology, India

***Correspondence:**
Justyna Guzy-Wrobelska
justyna.guzy-wrobelska@us.edu.pl

Specialty section:
This article was submitted to Plant Breeding, a section of the journal Frontiers in Plant Science

Received: 31 October 2017
Accepted: 18 May 2018
Published: 12 June 2018

Citation:
Gudys K, Guzy-Wrobelska J, Janiak A, Dziurka MA, Ostrowska A, Hura K, Jurczyk B, Żmuda K, Grzybkowska D, Śróbka J, Urban W, Biesaga-Koscielniak J, Filek M, Koscielniak J, Mikołajczak K, Ogrodowicz P, Krystkowiak K, Kuczyńska A, Krajewski P and Szarejko I (2018) Prioritization of Candidate Genes in QTL Regions for Physiological and Biochemical Traits Underlying Drought Response in Barley (Hordeum vulgare L.). Front. Plant Sci. 9:769. doi: 10.3389/fpls.2018.00769

Drought is one of the most adverse abiotic factors limiting growth and productivity of crops. Among them is barley, ranked fourth cereal worldwide in terms of harvested acreage and production. Plants have evolved various mechanisms to cope with water deficit at different biological levels, but there is an enormous challenge to decipher genes responsible for particular complex phenotypic traits, in order to develop drought tolerant crops. This work presents a comprehensive approach for elucidation of molecular mechanisms of drought tolerance in barley at the seedling stage of development. The study includes mapping of QTLs for physiological and biochemical traits associated with drought tolerance on a high-density function map, projection of QTL confidence intervals on barley physical map, and the retrievement of positional candidate genes (CGs), followed by their prioritization based on Gene Ontology (GO) enrichment analysis. A total of 64 QTLs for 25 physiological and biochemical traits that describe plant water status, photosynthetic efficiency, osmoprotectant and hormone content, as well as antioxidant activity, were positioned on a consensus map, constructed using RIL populations developed from the crosses between European and Syrian genotypes. The map contained a total of 875 SNP, SSR and CGs, spanning 941.86 cM with resolution of 1.1 cM. For the first time, QTLs for ethylene, glucose, sucrose, maltose, raffinose, α-tocopherol, γ-tocotrienol content, and catalase activity, have been mapped in barley. Based on overlapping confidence intervals of QTLs, 11 hotspots were identified that enclosed more than 60% of mapped QTLs. Genetic and physical map integration allowed the identification of 1,101 positional CGs within the confidence intervals of drought response-specific QTLs. Prioritization resulted in the designation of 143 CGs, among

them were genes encoding antioxidants, carboxylic acid biosynthesis enzymes, heat shock proteins, small auxin up-regulated RNAs, nitric oxide synthase, ATP sulfurylases, and proteins involved in regulation of flowering time. This global approach may be proposed for identification of new CGs that underlies QTLs responsible for complex traits.

Keywords: barley, drought tolerance, function map, QTL, QTL hotspot, CG prioritization, GO enrichment

INTRODUCTION

Drought is one of the most devastating abiotic stresses which limits strongly crops growth and productivity. It varies in occurrence, duration and severity, and also from location to location, and in the same location from year to year. Increases in the frequency, severity, and affected areas of droughts are projected due to global climate changes (Baum et al., 2007; Cattivelli et al., 2011; Fang and Xiong, 2015). Plant water deficit occurs when the rate of transpiration exceeds water uptake, and is a component of several different stresses including drought (Bray, 1997). In order to survive and reduce stress damage, plants respond to drought stress with a variety of defense reactions, including stomata closure, limitation of transpiration, repression of photosynthesis and cell growth, activation of respiration, accumulation of osmoprotectants, or antioxidants, although their growth, development, and yield are usually negatively affected (Shinozaki and Yamaguchi-Shinozaki, 2007; Farooq et al., 2009; Cattivelli et al., 2011).

To adapt to water deficit conditions, plants have evolved complex strategies of drought resistance, which integrate multiple adaptations, from the cellular to the whole plant level, and often are specific for particular genotype × environment relationships. Thanks to extensive research, four major drought resistance mechanisms have been described and their indicators dissected: drought escape manifested by a short life cycle, photoperiod sensitivity and plasticity of development; drought avoidance through reduced water loss or increased water uptake; drought tolerance through osmotic adjustment and antioxidant capacity; and drought recovery related to capability to resume the growth after a complete loss of turgor pressure and leaf dehydration (Bray, 2007; Farooq et al., 2009; Chen et al., 2010; Fang and Xiong, 2015). Despite the efforts, much slower progress has been made in understanding genetic basis of drought resistance and in developing more tolerant genotypes, owing to the genetic complexity of this trait and its quantitative inheritance with hundreds of genes of small, often epistatic and/or pleiotropic effects and low heritability (Tuberosa and Salvi, 2007; Cattivelli et al., 2011; Fan et al., 2015).

Barley (*Hordeum vulgare* L.) is the fourth most widely cultivated cereal in terms of harvested acreage and production (FAO, 2016). It is an excellent model plant to decipher genetic background of drought resistance as it has considerable genetic adaptability to a wide range of environments and a high level of drought tolerance showed by local landraces and wild barley (*H. vulgare* spp. *spontaneum)*. Being a valuable resource of alleles for adaptive traits, drought tolerant genotypes have been increasingly exploited in quantitative trait loci (QTL) studies to uncover the genetic control of multiple adaptations to drought stress (Baum et al., 2007; Cattivelli et al., 2011). Over last two decades numerous QTLs controlling agronomic performance and yield components under drought stress have been identified for barley (Teulat et al., 2001b; Baum et al., 2003; Talamé et al., 2004; von Korff et al., 2008; Cuesta-Marcos et al., 2009; Kalladan et al., 2013; Mansour et al., 2014; Tondelli et al., 2014). While these studies were oriented to decipher genomic regions important for barley breeding in order to maintain crop yield and grain quality under drought stress, they have seldom been used to elucidate the mechanisms of drought resistance at the genetic and molecular level (Baum et al., 2007; Fang and Xiong, 2015).

To fulfill this purpose, various indicator traits of physiological/biochemical processes occurring under drought have been investigated in barley using diverse mapping populations and drought stress conditions. Most studies concentrated on the parameters related to plant water status, resulting primarily in the identification of QTLs for relative water content (RWC), and then, for osmotic adjustment (OA), osmotic potential (OP), water content (WC), or carbon isotope discrimination (Teulat et al., 1997, 1998, 2001a, 2003; Diab et al., 2004; Chen et al., 2010; Szira et al., 2011; Wójcik-Jagła et al., 2013; Honsdorf et al., 2014; Fan et al., 2015; Mora et al., 2016). In contrast, only individual studies have detected QTLs for water-soluble carbohydrates (WSC, Teulat et al., 2001a; Diab et al., 2004) and proline content (Sayed et al., 2012; Fan et al., 2015). Additionally, some studies on the photosynthetic efficiency under drought stress conditions have identified QTLs related to chlorophyll fluorescence parameters, chlorophyll content or PSII (photosystem II) photochemical activity (Guo et al., 2008; von Korff et al., 2008; Wójcik-Jagła et al., 2013; Honsdorf et al., 2014; Mora et al., 2016) and plasma membrane integrity (Wójcik-Jagła et al., 2013). Recently, QTLs for multiple metabolites accumulation under drought stress (Piasecka et al., 2017), including QTLs for the content of fat-soluble antioxidants: α- and γ-tocopherols (Templer et al., 2017), have been detected.

These papers present a valuable source of data on the chromosomal regions potentially involved in drought response in barley, however, the comprehensive integration of the majority of these results and the anchoring of the identified QTLs on barley genome to decipher genes and networks for QTLs underlying particular physiological traits could be challenging. The difficulties arise not only from inherent limitations associated with particular mapping populations and applied methods but foremost from a lack of the information on the proper genomic localization of these QTLs which preclude their precise positioning on physical maps (Mir et al., 2012; Salvi and Tuberosa, 2015). Today, more comprehensive and effective

approach to decipher the genetic basis of QTLs (Monclus et al., 2012; Bargsten et al., 2014; Kumar et al., 2017) may be applied also in barley. The availability of SNP (single nucleotide polymorphism) markers based on within-gene polymorphisms (Close et al., 2009) together with high-throughput genotyping methods enable production of function maps with high density genome coverage for QTL mapping (Potokina et al., 2008; Mammadov et al., 2012). Such maps provide straight-forward connection of the identified QTL intervals to the reference barley genome sequence (Mayer et al., 2012), which could be followed by the analysis of large candidate gene assemblies and their biological interpretation using public databases (e.g., Gene Ontology; GO) and bioinformatics high-throughput enrichment tools.

This study present a first comprehensive approach for elucidation of genetic basis of physiological mechanisms of drought response/tolerance in barley based on the identification of the positional candidate gene (CG) assembly within the QTL confidence intervals, followed by the exploration of their putative functions related to drought tolerance. The study aimed particularly (1) to identify QTLs for a wide range of physiological/biochemical traits representative for plant water status, photosynthetic efficiency, osmoprotectant and hormone content, as well as activity or accumulation of antioxidants under drought stress on a created high-density function map; (2) to project QTL confidence intervals on physical barley genome map; and (3) to retrieve a set of potentially causative CGs, underlying the analyzed traits using a Gene Ontology (GO) enrichment approach.

MATERIALS AND METHODS

Plant Material

Barley (*H. vulgare* L.) population of 100 recombinant inbred lines (RIL), named MCam, produced by the single-seed descent (SSD) method from the cross between spring genotypes "Maresi" and Cam/B1/CI08887//CI05761 (here after referred as CamB), was used in this study to phenotype a set of physiological and biochemical traits under drought stress and control conditions, followed by their QTL mapping on a high-density function map. "Maresi" is a German advanced cultivar (semidwarf, two-rowed, malting type), of high and stable yielding under the European environmental conditions (pedigree and seed source: http://genbank.vurv.cz/genetic/resources/asp2/default_a.htm), whereas CamB is a Syrian breeding line (two-rowed, early heading), kindly obtained from ICARDA (International Center for Agricultural Research in the Dry Areas), adapted to dry environments (detailed characteristics of parental genotypes: Górny, 2001; Filek et al., 2015, 2016; Chmielewska et al., 2016).

Plant Growth Conditions and Drought Stress Treatment

The experiment was carried out in a phytotron (growth chamber). Seeds of each RIL were sterilized and sown separately in a box (22 L; 10 RIL per day), filled with a mixture of sandy loam and sand (7/2, v/v). In this substrate, a pF range of 2.2–3.0 indicated easily available water whereas pF > 4.2 was the permanent wilting point, as calculated based on the water retention curve (Filek et al., 2015). The pF-value is defined as a logarithm of the pressure p (expressed in centimeters of water head) necessary for removal of water from soil capillaries (Mikołajczak et al., 2017). Soil moisture was regulated two times a day. After germination (4 days, at 25°C), the boxes containing 30 plants were kept at 5°C (day/night) during the next 10 days, then the following parameters were settled in phytotron growth chamber: photoperiod 16/8 h (day/night), the temperature of 20/17°C (day/night), irradiance of 520 μmol(photon)$m^{-2}s^{-1}$. After 10 days, the number of plants in a box was reduced to 25. The substrate humidity was determined by monitoring boxes weight, and it was kept at 11% water content (VWC), i.e., pF = 2.8. After 13 days (at the moment of the emergence of the 4th leaf) the temperature was set to 25/16°C and soil drought (3.65% VWC, i.e., pF = 4.0) was applied to plants for 10 days. Plants grown in boxes with 11% VWC were used as the control (optimal condition growth). The boxes were randomly distributed in the growth chamber, and their location was changed twice a day. Measurements of the physiological/biochemical traits were performed at the seedling stage, on the third leaf for the plants from both (control and drought stress) conditions after 10 days of drought. Depending on the trait, the measurements were performed in 4–25 biological replications.

Phenotyping

Altogether, 40 different physiological/biochemical traits were measured at the seedling stage for RILs and the parents (described below and in **Table 1**). To facilitate the analysis, the traits were grouped into four categories according to their roles in drought stress response: plant water status (5 traits), photosynthetic efficiency (19 traits), osmoprotectant and hormone content (7 traits), activity and accumulation of antioxidants (9 traits).

Plant Water Status

Relative water content (RWC), water content (WC), water loss (WL) rate, water use efficiency (WUE), and electrolyte leakage (EL) were determined in this category. RWC was calculated according to Barrs (1968), where RWC = (FW – DW)/(TW – DW) × 100%, and where FW, DW and TW, respectively, are fresh, dry and turgid weight. To measure TW, leaf samples were placed in water (7°C) in darkness for 24 h, for the complete rehydration. WC was calculated as (DW/FW) × 100%. WL rate was calculated on the basis of the depletion of leaf FW during 24 h under the appropriate growing conditions. WUE was calculated as Pn/E, where Pn and E are net photosynthesis and transpiration rates, respectively, estimated by the measurement of gas exchange (next section). EL test was used to determine the plasma membrane integrity. For each genotype, samples were prepared as described by Płazek et al. (2014).

Photosynthetic Efficiency

Photochemical efficiency was estimated by means of chlorophyll *a* fluorescence registration. Measurements were taken using a fast chlorophyll fluorescence induction kinetics fluorometer Handy PEA and modulated fluorescence system FMS2 (Hansatech,

TABLE 1 | Physiological and biochemical traits used in QTL analysis.

Trait category	Abbrev.	Physiological/biochemical trait	Units
Plant water status	WC	Water content	g H_2O/g DW
	WL	Water loss rate	g H_2O/g DW
	RWC	Relative water content	%
	WUE	Water use efficiency	μmol CO_2/mmol H_2O
	EL	Electrolyte leakage	%%
Photosynthetic efficiency	ABS/RC	Light absorption flux (ABS) per PSII reaction center (RC)	%
	TR_0/RC	Trapped energy flux per PSII reaction center (RC)	%
	ET_0/RC	Electron transport flux per PSII reaction center (RC)	%
	DI_0/RC	Dissipated energy flux per PSII reaction center (RC)	%
	ABS/CS	Light absorption flux per excited leaf cross-section at $t = 0$ (CS)	%
	TR_0/CS	Trapped energy flux per excited leaf cross-section at $t = 0$ (CS)	%
	ET_0/CS	Electron transport flux per excited leaf cross-section at $t = 0$ (CS)	%
	DI_0/CS	Dissipated energy flux per excited leaf cross-section at $t = 0$ (CS)	%
	RC/CS	The maximum number of active reaction center (RC) per excited leaf cross-section at $t = 0$ (CS)	%
	ϕ_{po}	Maximal quantum yield of primary photochemistry (TR_0/ABS)	%%
	ψ_o	Exciton transfer efficiency to the electron transport chain (ET_0/TR_0)	%%
	ϕ_{eo}	Electron transport yield (ET_0/ABS)	%%
	(1-B)av	The average fraction of open RC during the time needed to complete the closure of all RCs	%
	PI_{abs}	The performance index per absorption	%
	F_v'/F_m'	Efficiency of excitation energy capture by open PSII RC	%%
	qP	Photochemical quenching	%%
	Φ_{PSII}	Photochemical quantum yield of PSII	%%
	Pn	Net photosynthesis rate	μmol CO_2/m^2s
	E	Transpiration rate	mmol H_2O/m^2s
Osmoprotectant and hormone content	Pro	Free proline content	μg/g FW
	Glu	Glucose content	μg/mg DW
	Fru	Fructose content	μg/mg DW
	Suc	Sucrose content	μg/mg DW
	Raf	Raffinose content	μg/mg DW
	Mal	Maltose content	μg/mg DW
	Eth	Ethylene content	nl/g FW
Activity and accumulation of antioxidants	SOD	Superoxide dismutase activity	U
	CAT	Catalase activity	U
	POX	Peroxidase activity	U
	GTt	γ-tocotrienol content	μg/mg DW
	ATt	α-tocotrienol content	μg/mg DW
	DTf	δ-tocopherol content	μg/mg DW
	GTf	γ-tocopherol content	μg/mg DW
	ATf	α-tocopherol content	μg/mg DW
	BC	β-carotene content	μg/mg DW

DW, dry weight; FW, fresh weight; U, arbitrary unit of enzyme activity per mg of total soluble protein.

Kings Lynn, UK). The induction of a chlorophyll fluorescence signal was measured after 30 min of leaf dark adaptation in clips (Hansatech). Before measurements, the LED-light source of the fluorometer was calibrated using an SQS light meter (Hansatech, Kings Lynn, UK). The conditions used to determine polyphasic chlorophyll *a* fluorescence transients were: excitation irradiance of 3,000 μmol $m^{-2}s^{-1}$, a pulse duration of 1 s, and fixed gain of 0.7 (Handy PEA ver. 1.3 software, Hansatech). Fourteen parameters were calculated (Kalaji et al., 2011): ABS/RC and ABS/CS—light absorption flux, respectively, per PSII reaction center (RC) and per excited leaf cross-section at $t = 0$ (CS); ET_0/RC and ET_0/CS (electron transport flux per RC and CS); TR_0/RC and TR_0/CS (trapped energy flux per RC and CS); DI_0/RC and DI_0/CS (dissipated energy flux per RC and CS); RC/CS (the maximum number of active RC per CS); ϕ_{po} (TR_0/ABS—maximal quantum yield of primary photochemistry); ψ_o (ET_0/TR_0—exciton transfer efficiency to the electron transport chain); ϕ_{eo} (ET_0/ABS—electron transport

yield); PI_{abs} (the performance index per absorption); (1-B)av (the average fraction of open RC during the time needed to complete the closure of all RCs). FMS2 measurements were made after light adaptation of the leaf (usually 2–5 min at 500 μmol (quanta) $m^{-2}s^{-1}$) when the fluorescence signal (Fs) became constant. Three parameters: the photochemical quantum yield of PSII (Φ_{PSII}), the photochemical quenching (qP) and the efficiency of excitation energy capture by open PSII RC (F_v'/F_m') were calculated according to Genty et al. (1989). The gas exchange rate (Pn; E) was measured using an infrared gas analyzer (Ciras-1, PP Systems, Hitchin, UK) and Parkinson leaf chamber (PLC6). The controlled measuring conditions were: CO_2 concentration of 400 μmol (CO_2) mol^{-1} (air), 30% relative humidity, irradiance of 800 μmol (quanta) $m^{-2}s^{-1}$ and the leaf temperature of 25°C. The measurements of chlorophyll fluorescence and gas exchange were carried out from 10 a.m. to 2 p.m. (beginning of day 6 a.m., day length 16 h), and until stable measurement values were obtained. The order of plants measurements (photosynthesis and fluorescence) during each day of was random.

Osmoprotectant and Hormone Content

Seven compounds were quantified in this category. Soluble carbohydrates (glucose, fructose, sucrose, raffinose, and maltose) were identified by their retention times and quantified by integrating peak areas against the internal standard according to the procedure by Janeczko et al. (2010). Measurements were made using a high performance liquid chromatography consisting of the following modules: a gradient pump (Agilent 1200, Santa Clara, CA, USA), autosampler (Agilent 1200), the thermostat STH 585 (Dionex, Sunnyvale, CA, USA), ESA detector Coulochem II Analitical Cell 5040 with a gold working electrode and a palladium reference electrode, an analog/digital converter (Agilent), program control and data collector software ChemStation Rev.B.04.01 (Agilent).

The content of free proline was determined spectrophotometrically (at λ = 520 nm) according to the methods by Bates et al. (1973) and Marin et al. (2009), with the use of UV/VIS spectrophotometer (UV-1800, Rayleigh, Beijing, China) and it was calculated from the standard curve.

For ethylene production, each sample (0.1 g FW) was homogenized in 70% ethanol. Following the centrifugation, the supernatant was evaporated (at 40°C) and the pellet was dissolved in H_2O (1 ml), and 1 pmol $HgCl_2$ was added. Then, the sample was transferred into a new vial and incubated on ice (for 5 min) with a mixture of 5% NaOCl and saturated NaOH (2/1, v/v). The gas sample was taken from the vial, and ethylene was quantified by gas chromatography (Hewlett Packard 5890 Series II, Palo Alto, CA, USA) with Porapak R column (80/100 mesh, Agilent, Santa Clara, CA, USA) and detector (flame ionization) as described by Grzesiak et al. (2013).

Activity and Accumulation of Antioxidants

Antioxidant enzymes (3), fat-soluble antioxidants (5) and β-carotene were quantified in this category. To measure the activity of antioxidant enzymes: superoxide dismutase (SOD), catalase (CAT), and peroxidase (POD), the plant material was homogenized at 4°C in 0.05 mM potassium phosphate buffer (KP) with 0.1 mM EDTA. The supernatant was divided into three subsamples after centrifugation. The activity of SOD [EC 1.15.1.1.] was determined spectrophotometrically by the cytochrome reduction method (McCord and Fridovich, 1969) with the modifications by Szechyńska-Hebda et al. (2012). Changes in absorbance were followed with a Biochrom Ultrospec II spectrophotometer (LKB, Sweden) at λ = 550 nm. The inhibition of oxidized cytochrome c absorbance was monitored. The activity of CAT [EC 1.11.1.6] was measured spectrophotometrically according to Aebi (1984) with the modifications by Wojtania et al. (2016). The decrease in H_2O_2 absorbance was measured at λ = 240 nm. The activity of POD [EC 1.11.1.11] was measured spectrophotometrically using the method by Lück (1962) with the modifications by Wojtania et al. (2016). The increase in oxidized p-phenylenediamine absorbance was monitored at λ = 485 nm.

Tocochromanols (α- γ- δ-tocopherols and α- γ-tocotrienols) and β-carotene were measured based on the modified method by Surówka et al. (2016). Briefly, lyophilized samples were extracted in 0.1% solution of butylated hydroxytoluene (BHT) in ethanol/acetone/methanol/2-propanol (8/3/3/1 v/v) at 70°C in shaking water bath for 15 min, then 80% KOH was added, and the extraction was continued for 30 min. Next, samples were diluted with H_2O (1/1 v/v) and cleaned on Chromabond XTR cartridge (Macherey-Nagel, Germany). Compounds of interest were eluted by n-hexane, vacuum evaporated (Rota Vapor, Switzerland) and reconstituted in 1% BHT in methanol/dichloromethane (3/1 v/v) prior HPLC separation. The Agilent 1260 (Santa Clara, CA, USA) UHPLC binary system with diode array (DAD) and fluorescence (FLD) detectors was used. Separation was achieved on Ascentis Express C-18 (Supelco Analytical, Sigma Aldrich, USA) analytical columns at 0.8 ml/min, 60°C and linear gradient of A) 0.5% formic acid (FA) in acetonitrile (ACN)/H_2O (6/4 v/v) and B) 0.5% FA in 2-propanol/ACN (9/1 v/v), from 40 to 100% of B in 15 min. Tocochromanols were detected by FLD, whereas β-carotene by DAD. Identity and quantity of compounds were confirmed by the comparison with data obtained for the pure standards under identical conditions.

Statistical Analysis

All physiological traits data were analyzed with Statistica 12.0 software (Stat. Soft Inc., USA). The normality of trait distributions was verified using the Shapiro–Wilk test. Linear correlation coefficients (Pearson's) were calculated between all the analyzed traits separately for drought and control conditions. The *F*-test was used to assess the homogeneity of variance and the Student's *t*-test to compare the statistical significance of differences of the analyzed traits between control and drought conditions.

In the QTL analysis absolute values of all physiological/biochemical traits were used which described the drought response/tolerance level of RILs, and drought stress indices (DSI), which are relative values, were also calculated for all measured traits to compare among RILs (Bouslama and Schapaugh, 1984; Wójcik-Jagła et al., 2013) according to the formula: DSI (%) = $(d/c) \times 100\%$, where d and c are the absolute values obtained under drought and control conditions,

respectively. DSI data were included into QTL mapping as a set of additional phenotypic traits.

Genotyping

Mapping Functional CGs on a Consensus Barley Map

A consensus barley linkage map of SNP markers from BOPA1 (barley oligonucleotide pool assay 1; Close et al., 2009) and simple sequence repeat (SSR) markers, published earlier (Mikołajczak et al., 2016), was used in this study for the map enrichment with functional candidate genes (CG) and the construction of a new high-density, function barley map for the QTL analysis. Briefly, the consensus map was constructed for the MCam population and two other bi-parental RILs: LCam (derived from "Lubuski" × CamB) and GH (derived from "Georgie" × "Harmal"), produced from the crosses between European (drought susceptible) and Syrian (drought tolerant) spring barley cultivars. The map consisted of 819 markers, spanned 953.8 cM (an average resolution of 1.2 cM) and comprised of 13 linkage groups attributed to barley chromosomes 1H-7H. The map was uniformly covered with the markers, and was in good agreement with other integrated barley maps (Varshney et al., 2007; Close et al., 2009). The number of linkage groups exceeding the number of barley chromosomes was probably the effect of a diverse genetic background of parental genotypes, but it did not affect the marker order within the linkage groups, nor the CGs mapping and the overall quality of the map.

For the enrichment of the map, a group of 41 CGs potentially involved in drought response was selected based on the transcriptome analysis of "Maresi" and CamB genotypes under drought stress (Janiak et al., 2018). In addition, 23 genes encoding barley orthologs of drought tolerance-related genes, described in model species, were chosen (Supplementary Material S1). Publicly available genomic sequence information in GenBank (http://www.ncbi.nlm.nih.gov/genbank/) was utilized to identify barley genomic sequences of these CGs, so called functional CGs (Pflieger et al., 2001). The information on the structure and the chromosomal localizations of the CGs was derived from Ensembl Plants (http://plants.ensembl.org/index.html; ver. 082214v1).

For polymorphisms identification in the functional CG sequences, total genomic DNAs of two RIL populations, MCam and GH, and their parental forms, were extracted using a method by Doyle and Doyle (1987) with minor modifications. Primer pairs (Supplementary Material S2) for the PCR amplifications of CG fragments (800–1,200 bp) from genomic DNA of parental genotypes were designed with the software Primer 3 (http://bioinfo.ut.ee/primer3-0.4.0/). PCR products were sequenced from both ends at Genomed company (Warsaw, Poland; www.genomed.pl). The sequences assembly was done with the CodonCode Aligner software (CodonCode Corporation, Centerville, MA, USA).

Sequence polymorphisms (SNPs or insertions/deletions) identified in the CG sequences between the parental genotypes of RILs ("Maresi" vs. CamB or "Georgie" vs. "Harmal") were subsequently genotyped within the adequate RIL population using one of the following methods: CAPS (cleaved amplified polymorphisms) or dCAPS (derived CAPS) for SNPs, and PCR for indels. In case of CAPS, the same primer pairs were used for the PCR amplification, then PCR products were cleaved with the appropriate restriction enzymes and visualized by 2.0% agarose gel electrophoresis. In the dCAPS, mismatch primers were designed with the dCAPS Finder 2.0. software (http://helix.wustl.edu/dcaps/dcaps.html) for nested-PCR amplification step, which followed the standard PCR amplification, then PCR products were cleaved with the appropriate restriction enzymes and visualized by 4.0% agarose gel electrophoresis. The indels were genotyped using the PCR amplifications with a newly designed primer pairs, followed by 4.0% agarose gel electrophoresis of the PCR products. Primer pairs designed for the methods of genotyping polymorphisms are given in Supplementary Material S2.

The functional CG linkage analysis was performed on the individual maps of the adequate mapping populations (MCam or GH), and was followed by construction of a new consensus, function map with the use all three maps and the software JoinMap 3.0 (Van Ooijen and Voorrips, 2001), according the procedure described previously (Mikołajczak et al., 2016). Marker order within each linkage group was check for the accordance with the other consensus barley maps (Varshney et al., 2007; Close et al., 2009). Final chromosome maps were drawn with the MapChart software (Voorrips, 2002).

QTL Analysis

QTL analysis was performed with the MapQTL 5.0 software (Van Ooijen, 2004) for 40 physiological/biochemical traits measured under both water regimes (optimal water supply and drought) and for their DSI. QTLs were first mapped by interval mapping (IM), followed by multiple-QTL model (MQM), using the marker closest to the peak at each putative QTL as a cofactor. After performing a genome-wide permutation test with 1,000 iterations (Churchill and Doerge, 1994), a LOD (logarithm of the odds) thresholds from 2.8 to 3.5 (depending on the trait) were used to establish the presence of significant QTLs ($p < 0.05$). Confidence intervals for the QTLs were estimated based on two-LOD support interval, by taking two positions around the peak of the LOD profile, which had LOD-values by 2.0 lower than the maximum. The percentage of phenotypic variation (R^2) explained by each QTL was calculated and a QTL was considered as major when it explained >10% of the phenotypic variation. The additive genetic effects were also calculated for the QTLs, and positive value indicated that the "Maresi" allele increased the trait value, whereas negative value indicated the decrease in the trait value caused by the "Maresi" allele. The QTLs which showed overlapping confidence intervals were clustered into hotspots.

Identification of Positional Candidate Genes Within QTL Confidence Intervals

In order to identify the positional candidate genes (CG; i.e., closely linked genes localized within QTL regions; Pflieger et al., 2001), genetic and physical map integration was performed based on the positions of markers defining the boundaries of QTL confidence intervals (or the closest to them) in the genome. Nucleotide sequences of markers were mapped to the barley reference genomic sequence deposited in Ensembl Plants database (version 082214v1; http://plants.ensembl.org/index.

html) using BLAST tool in order to project QTLs on the physical map (maximum *E*-value = 1E-100, minimum 95% identity of the sequence). Gene models found within the physical QTL intervals were retrieved using BioMart tool and grouped into the same four gene categories as the physiological/biochemical traits and corresponding QTL regions. This classification was based on the assumption that positional CGs identified within QTL regions related to a given trait category should be involved in the biological processes relevant to this trait category under the analyzed water regime.

GO Enrichment Analysis

With the aim to identify GO terms (Biological Processes; BPs) associated with positional CGs and to determine the over-representation of a given GO term in an analyzed set of genes compared to the genome-wide background frequency, the GO enrichment analysis was performed using the PLAZA Monocots database version 3.0 (http://bioinformatics.psb.ugent.be/plaza/versions/plaza_v3_monocots; Proost et al., 2015). The significance of over-representation was determined using the hyper geometric distribution followed by the Bonferroni correction for multiple testing (corrected $p \leq 0.05$). Furthermore, PLAZA was used to barley/Arabidopsis cross-species analysis in order to identify putative barley orthologs in the *Arabidopsis thaliana* genome. It was motivated by the extensive annotation features available for this model species.

RESULTS

Phenotypic Variation and Correlations Among Traits

Descriptive statistics for physiological/biochemical traits evaluated in the MCam RIL population and parental genotypes is shown in Supplementary Material S3. The mean values of most of the measured parameters under both conditions: optimal water supply (C) and drought stress (D) as well as their stress indices (DSI), significantly differentiated both parental genotypes and varied among the RILs. Almost all traits were distributed normally within RIL population, and lines which exceeded the parental range of variation for different traits were observed. Significant transgressive segregation suggests a broad genetic diversity of parental genotypes and the polygenic inheritance of the investigated traits. Drought stress conditions caused a significant decrease of mean values for the majority of physiological parameters describing plant water status, specific energy fluxes, quantum efficiency ratios, photochemical activity of PSII and efficiency of gas exchange. On the other hand, an increase in proline and ethylene content, as well as in the activity of antioxidant enzymes and fat-soluble antioxidants, was observed. Analyzed genotypes varied in terms of carbohydrates content, both under control and drought conditions. Drought stress increased the accumulation of glucose, fructose and sucrose, whereas maltose and raffinose contents were diminished.

Under control conditions, strong significant correlations ($|r| \geq 0.5$, $p < 0.05$) were exclusively observed among photosynthesis-related traits and parameters describing plant water status (**Figure 1**). The strongest positive correlations were revealed between: net photosynthesis (Pn) and transpiration (E); the photochemical quantum yield of PSII (Φ_{PSII}) and the photochemical quenching (qP); the performance index per absorption (PI_{abs}) and quantum efficiency ratios (ϕ_{po}, ψ_o, ϕ_{eo}). Furthermore, three groups of parameters were found with significant internal correlations: specific energy fluxes (ABS, TR_0, ET_0, DI_0) per excited leaf cross-section (CS), specific energy fluxes per reaction centre (RC), and quantum efficiency ratios (ϕ_{po}, ψ_o, ϕ_{eo}). The strongest negative correlations were observed between: transpiration (E) and water use efficiency (WUE); and between ABS/RC, TR_0RC, DI_0/RC and the efficiency of excitation energy capture by open PSII reaction centres (F_v'/F_m'), PI_{abs}, ϕ_{po}, and ϕ_{eo}.

Interestingly, the increasing number and magnitude of significant correlations, both among physiological parameters and between physiological and biochemical traits, was revealed under drought stress conditions (**Figure 1**). Photosynthetic efficiency parameters and plant water status traits were positively correlated in the majority of cases. The strongest relationships, not identified under control conditions, were observed between: the RWC and Φ_{PSII}, Pn, E, F_v'/F_m'; as well as Φ_{PSII} and the number of active RCs per CS (RC/CS), specific energy fluxes (ABS, TR_0, ET_0,) per CS, PI_{abs}, and (1-B)av. Only three parameters, i.e., electrolyte leakage (EL), ABS/RC, and DI_0/RC were strongly and negatively correlated with all of the other physiological traits. This indicates drought-induced increase of the permeability of cell membranes, inactivation of a part of RC pool and increase of the antenna size. Under drought stress, in contrast to optimal water supply, we observed numerous and mainly negative correlations between the physiological and biochemical parameters (in particular, for SOD, POX, γ- and α-tocopherols activities). Taken together, these results revealed the changes in cellular metabolism during water deficit which activated the processes enhancing barley adaptation capacity to unfavorable conditions and prevented from a negative impact of drought stress on photosynthesis efficiency.

Quantitative Trait Loci Identification

QTL analysis was performed using our previously published high-density SNP and SSR-based consensus genetic map (Mikołajczak et al., 2016) which was enriched with 64 functional CGs including differentially expressed genes (DEGs) derived from the transcriptome analysis of parental genotypes under drought stress and barley orthologs of drought tolerance-related genes described in model species (Supplementary Material S1). The newly constructed barley function map consists of 875 loci and spans 941.86 cM with an average resolution of 1.1 cM. Based on comparison with physical map we estimated that it covers about 95% of the barley genome. This provides an excellent framework for QTL identification. In order to extensively evaluate the response of the analyzed genotypes to drought, both, the direct values of the 40 physiological and biochemical parameters measured under control conditions and drought stress, as well as the relative values (DSI) for each trait, were used in QTL mapping.

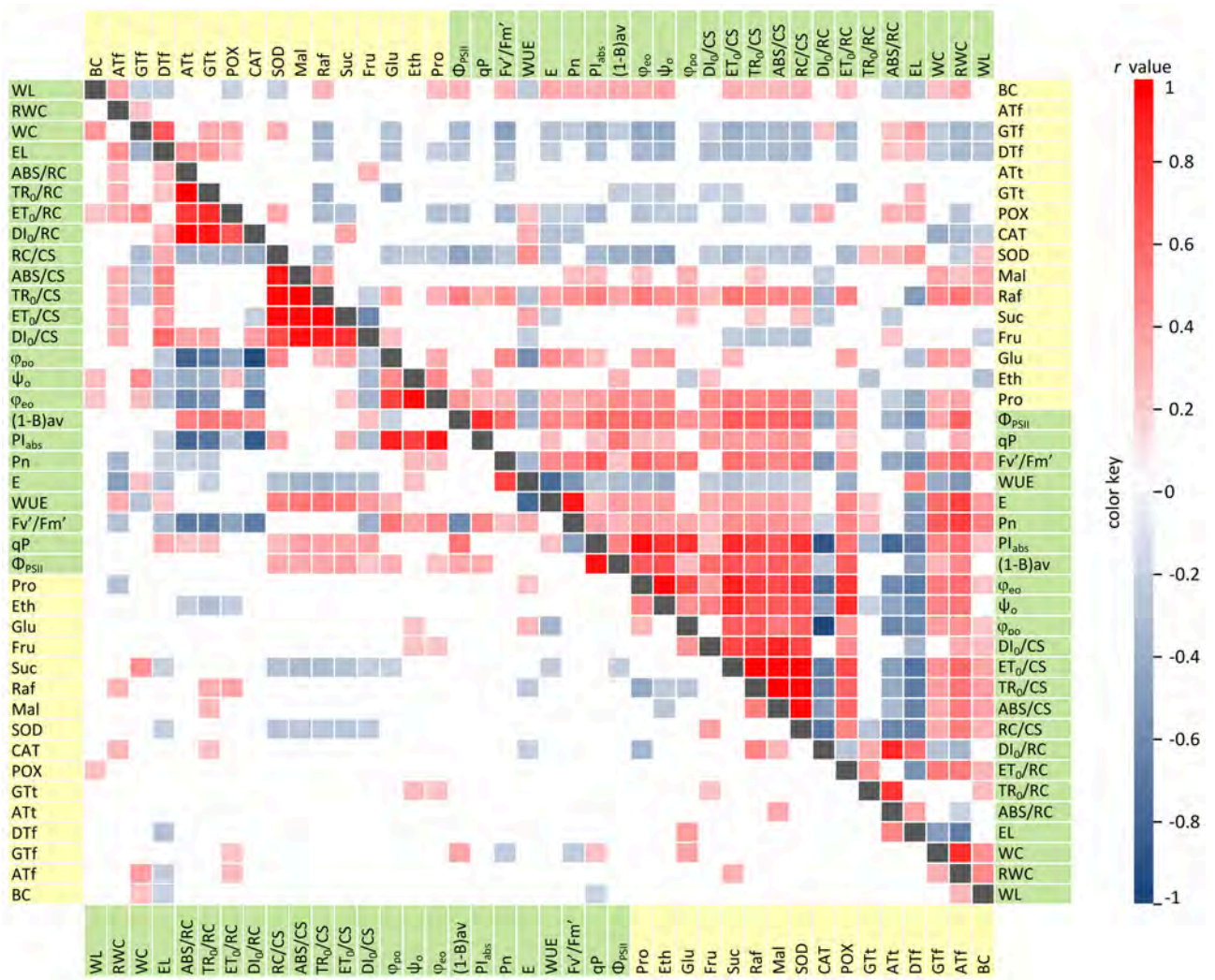

FIGURE 1 | Correlation diagram for physiological (green) and biochemical (yellow) traits evaluated among RILs. Correlations under control conditions and drought stress are presented, respectively, in the lower and upper triangular. Statistically significant Pearson's coefficients (r, $p<0.05$) are represented by colored matrix cells.

A total of 64 QTLs for 25 drought tolerance-related traits that describe plant water status, photosynthetic efficiency, osmoprotectant, and hormone content, as well as activity and accumulation of antioxidants were identified among all of the chromosomes, except 4H (**Figure 2**). The number of detected QTLs varied from 1 to 4, depending on the trait and the experiment variant (C/D/DSI). The highest number of QTLs were positioned on chromosomes 2H and 3H (18 and 17, respectively), and 5H (12). Eight regions for QTLs were mapped on chromosomes 6H and 7H, whereas chromosome 1H contained a single QTL. The maximum LOD scores estimated in the QTL confidence intervals ranged from 3.0 to 20.76, while the phenotypic variation explained by an individual QTL varied from 6.7 to 87.5%. Chromosome 3H contained regions that accounted for most of the observed phenotypic variation in the investigated parameters (14 QTLs with at least 30% of R^2). Favorable alleles which had positive effects on the variation in analyzed traits came from both parental genotypes, "Maresi" and CamB.

Under control conditions, the QTL analysis revealed 32 chromosomal regions for 17 traits (**Table 2**). Most (22) QTLs were found to determine photosynthetic efficiency. The others were related to the plant water status traits (4), raffinose content (2), maltose content (2), sucrose content (1), and catalase activity (1). About a half of the identified QTLs under control conditions explained a large proportion of the observed phenotypic variation ($R^2 \geq 30\%$). Chromosomal regions with the highest R^2 values (exceeding 60%) were mapped for RWC, TR_0/CS, DI_0/CS and maltose content. Furthermore, two QTLs located on chromosome 7H, which explained more than 85% of the observed phenotypic variation in maltose content, were characterized by the highest LOD scores (>20.0) among all the QTLs revealed in the analyzed RIL population. Three functional CGs, co-segregating with the maximum LOD scores

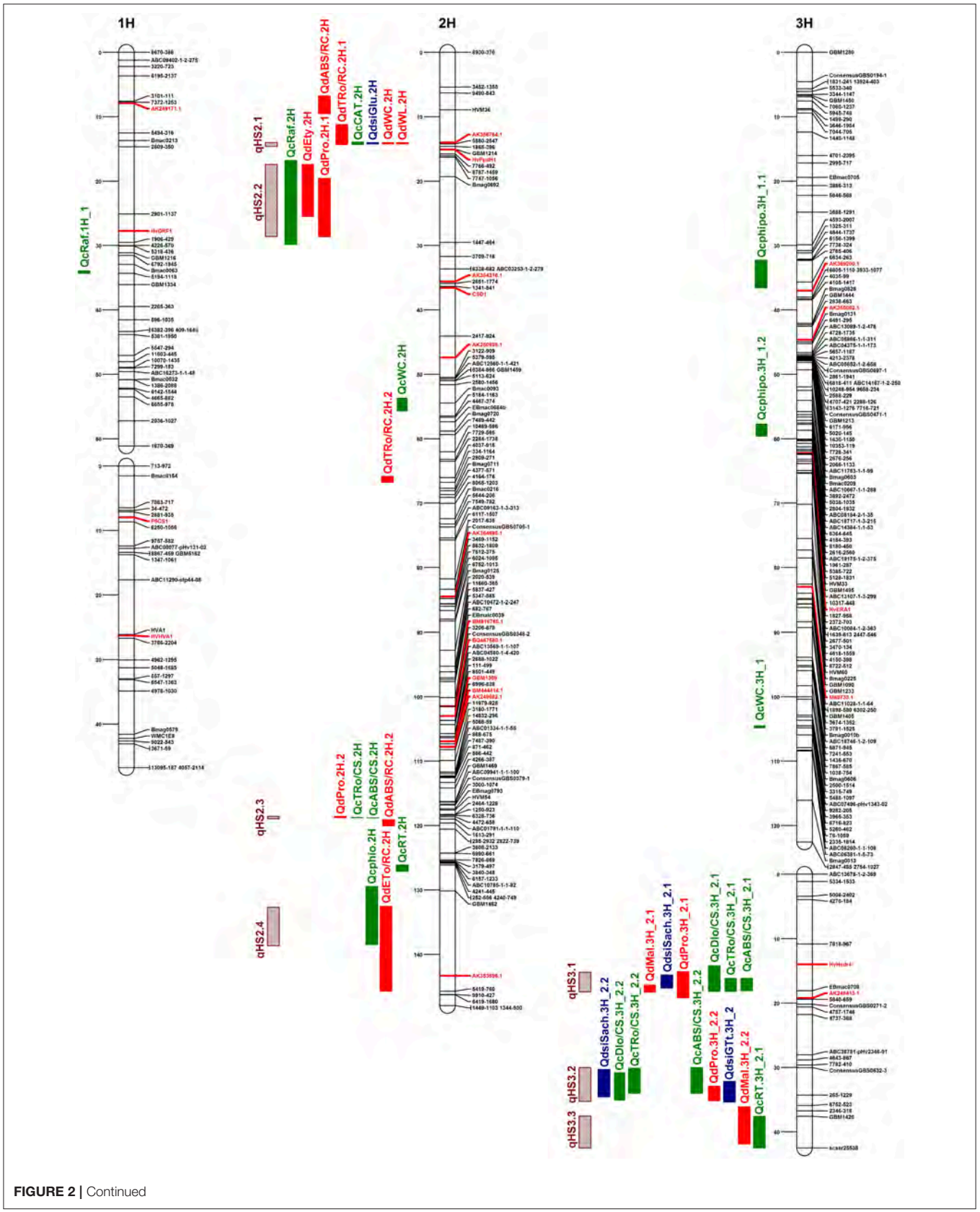

FIGURE 2 | Continued

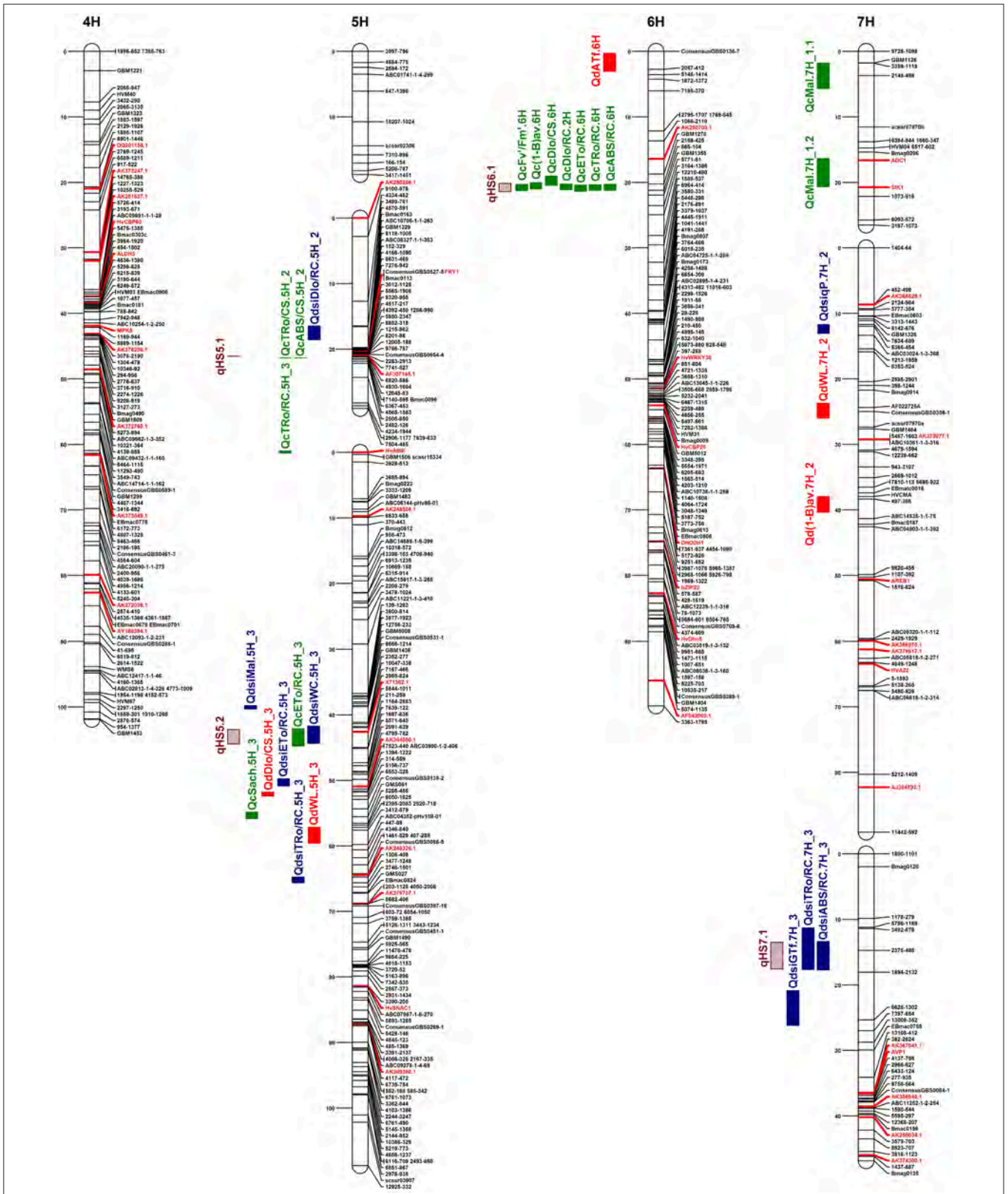

FIGURE 2 | High-density consensus function map of barley with the positions of QTLs for physiological and biochemical traits related to the drought stress response. Markers are given on the right side of the linkage groups. Functional candidate genes are given in red. Bars represent intervals associated with QTLs for: drought stress (red), control conditions (green), stress indices (blue), and QTL hotspots (patterned).

TABLE 2 | Summary of QTLs detected for 17 physiological and biochemical traits in the MCam population under control conditions.

Trait	Control conditions						
	QTL name	Chr.	Nearest marker	LOD	Confidence interval [cM]	Additive effect	R^2 [%]
PLANT WATER STATUS							
RWC	QcRWC.2H	2H	252-556	7.44	126.13–127.13	−0.463	**84.4**
	QcRWC.3H_2.1	3H	scssr25538	7.34	37.59–42.52	9.432	**83.8**
WC	QcWC.2H	2H	5184-1163	3.34	54.46–56.46	−0.338	13.1
	QcWC.3H_1	3H	5260-462	3.11	104.52–104.83	0.358	12.1
PHOTOSYNTHETIC EFFICIENCY							
ABS/RC	QcABS/RC.6H	6H	885-104	7.01	20.25–21.22	−0.182	**34.8**
TR_0/RC	QcTRo/RC.5H_3	5H	HvABI5	3.46	0–0.32	0.051	10.5
	QcTRo/RC.6H	6H	2188-425	8.53	20.25–21.22	−0.108	**30.7**
ET_0/RC	QcETo/RC.5H_3	5H	X71362.1	3.75	41.96–44.59	−0.024	11.9
	QcETo/RC.6H	6H	885-104	7.55	20.25–21.22	−0.048	**30.0**
DI_0/RC	QcDIo/RC.2H	6H	885-104	5.62	20.25–21.22	−0.072	**30.0**
ABS/CS	QcABS/CS.2H	2H	2464-1228	3.35	118.27–118.27	787.930	10.0
	QcABS/CS.3H_2.1	3H	EBmac0708	6.51	16.02–18.08	1907.390	**55.6**
	QcABS/CS.3H_2.2	3H	ConsensusGBS0632-3	**11.09**	30.01–34.01	−1722.250	**59.1**
	QcABS/CS.5H_2	5H	Bmac0096	4.05	21.56–21.56	−192.893	11.6
TR_0/CS	QcTRo/CS.2H	2H	2464-1228	4.28	118.27–118.32	637.155	10.7
	QcTRo/CS.3H_2.1	3H	EBmac0708	7.59	16.02–18.08	1558.190	**57.8**
	QcTRo/CS.3H_2.2	3H	ConsensusGBS0632-3	**12.39**	30.01–34.01	−1448.690	**60.5**
	QcTRo/CS.5H_2	5H	Bmac0096	4.25	21.56–21.56	−152.128	6.7
DI_0/CS	QcDIo/CS.3H_2.1	3H	EBmac0708	9.04	14.02–18.08	331.108	**63.8**
	QcDIo/CS.3H_2.2	3H	265-1229	7.99	31.01–35.29	−359.451	**64.3**
	QcDIo/CS.6H	6H	2188-425	3.03	18.74–20.25	−55.813	6.7
ϕ_{po}	Qcphi_po.3H_1.1	3H	6634-263	4.43	32.33–36.69	−0.006	17.0
	Qcphi_po.3H_1.2	3H	ABC19175-1-2-375	5.66	57.79–59.70	0.008	23.5
ψ_o	Qcpsi_o.2H	2H	GBM1462	3.15	129.13–138.17	0.009	17.2
(1-B)av	Qc(1-B)av.6H	6H	885-104	5.8	20.25–21.22	−0.470	**30.0**
F_v'/F_m'	QcFv'/Fm'.6H	6H	885-104	3.85	20.25–21.22	0.018	23.3
OSMOPROTECTANT AND HORMONE CONTENT							
Suc	QcSuc.5H_3	5H	GMS061	4.68	55.55–56.54	−6.558	21.1
Raf	QcRaf.1H_1	1H	5194-1118	3.84	33.95–34.34	−0.339	16.2
	QcRaf.2H	2H	Bmag0692	9.01	16.28–29.33	−0.458	**34.8**
Mal	QcMal.7H_1.1	7H	2148-498	**20.76**	1.79–5.69	−14.320	**87.5**
	QcMal.7H_1.2	7H	ADC1	**20.75**	16.36–20.66	14.387	**85.4**
ACTIVITY AND ACCUMULATION OF ANTIOXIDANTS							
Cat	QcCAT.2H	2H	1865-396	7.29	14.23–14.63	−0.003	**30.3**

Functional candidate genes that co-segregated with the maximum LOD scores within confidence intervals of mapped QTLs are underlined; LOD ≥ 10 and R^2 ≥ 30 are in bold. R^2, percentage of phenotypic variation explained by individual QTL.

within confidence intervals of the QTLs mapped under control conditions, were found. X71362.1 gene, encoding a member of the dehydrin family, was associated with the QTL for ET_0/RC on chromosome 5H. On the same chromosome, *HvABI5* gene, involved in plant response to abscisic acid, was located in the QTL confidence interval for TR_0/RC. Finally, the QTL for maltose content mapped on chromosome 7H co-segregated with barley ortholog of *ADC1* gene which encodes arginine decarboxylase.

The QTL analysis performed for the same physiological/biochemical parameters of RILs grown under drought stress conditions showed the presence of 19 QTL regions for 11 traits (**Table 3**). All detected QTLs were declared as the major ones, as they explained more than 10% of the phenotypic variation of the particular traits. The highest number of QTLs was identified for photosynthetic efficiency parameters (7), as well as osmoprotectant content (6). The remaining QTLs were found to determine plant water status (4), ethylene content (1), and α-tocopherol activity (1). The highest R^2 values and LOD scores described the chromosomal regions involved in the proline and maltose accumulation. Drought-induced proline level was found to be controlled by three major QTLs mapped on chromosomes 2H and 3H, which explained between 73.6 and

TABLE 3 | Summary of QTLs detected for 11 physiological and biochemical traits in the MCam population under drought stress.

Trait	Drought stress conditions						
	QTL name	Chr.	Nearest marker	LOD	Confidence interval [cM]	Additive effect	R^2 [%]
PLANT WATER STATUS							
WL	QdWL.2H	2H	5880-2547	6.84	14.03–14.23	−0.202	21.9
	QdWL.5H_3	5H	3412-579	4.15	57.16–9.59	0.136	12.9
	QdWL.7H_2	7H	ConsensusGBS0356-1	3.15	23.72–25.99	−0.121	10.6
WC	QdWC.2H	2H	5880-2547	3.82	14.03–14.23	−0.323	17.2
PHOTOSYNTHETIC EFFICIENCY							
ABS/RC	QdABS/RC.2H.1	2H	9490-843	3.97	5.42–8.31	−0.085	17.3
	QdABS/RC.2H.2	2H	285-2932	4.09	119.60–120.57	−0.166	17.7
TR_0/RC	QdTRo/RC.2H.1	2H	AK356764.1	3.55	10.92–14.03	−0.051	13.4
	QdTRo/RC.2H.2	2H	2809-271	4.69	66.78–67.71	−0.047	16.9
ET_0/RC	QdETo/RC.2H	2H	AK353596.1	3.85	132.17–145.34	0.041	20.5
DI_0/CS	QdDIo/CS.5H_3	5H	5156-737	3.89	51.79–52.38	44.152	17.5
(1-B)av	Qd(1-B)av.7H_2	7H	497-386	3.33	37.97–40.35	−0.354	18.7
OSMOPROTECTANT AND HORMONE CONTENT							
Pro	QdPro.2H.1	2H	Bmag0692	6.36	19.28–28.33	3.114	12.2
	QdPro.2H.2	2H	6328-736	**10.62**	118.44–118.63	−7.080	**75.2**
	QdPro.3H_2.1	3H	EBmac0708	**10.53**	15.02–19.08	−11.964	**73.6**
	QdPro.3H_2.2	3H	265-1229	**11.58**	33.01–35.29	20.832	**77.5**
Mal	QdMal.3H_2.1	3H	EBmac0708	**18.38**	17.02–18.08	1.370	**85.8**
	QdMal.3H_2.2	3H	GBM1420	**18.44**	36.75–42.52	−1.533	**85.9**
Eth	QdEth.2H	2H	Bmag0692	3.66	18.28–26.33	0.084	18.5
ACTIVITY AND ACCUMULATION OF ANTIOXIDANTS							
ATf	QdATf.6H	6H	ConsensusGBS0136-7	4.36	0–2.75	−0.019	20.0

Functional candidate genes that co-segregated with the maximum LOD scores within confidence intervals of mapped QTLs are underlined; LOD ≥ 10 and R^2 ≥ 30 are in bold. R^2, percentage of phenotypic variation explained by individual QTL.

77.5% of the observed phenotypic variation, but an additional locus with a smaller effect was identified on chromosome 2H. In addition, two QTLs located on chromosome 3H, involved in maltose content regulation, were characterized by LOD scores above 18.0 and R^2 values that exceeded 85%. Two differently expressed functional CGs were found to be associated with the chromosomal regions for fast kinetics of chlorophyll *a* fluorescence parameters, located on chromosome 2H. Gene AK356764.1 that encodes transketolase co-localized with the QTL for TR_0/RC, whereas gene AK353596.1 encoding a member of the peroxidase family showed coincidence with the LOD peak region for ET_0/RC.

All 13 QTLs mapped for stress indices (DSI) of 11 parameters were classified as the major ones (**Table 4**). Most of them were detected for photosynthetic efficiency and osmoprotectant content (6 and 4, respectively), similarly to the drought stress conditions. The other QTLs were identified for leaf water content (1) and tocochromanols activity (2). The highest proportion of observed phenotypic variation, ranging from 60.8 to 82.1%, was explained by two QTLs positioned on chromosome 3H: for sucrose and for γ-tocotrienol stress indices. Two functional CGs from the transcriptome analysis of "Maresi" and CamB co-segregated with maximum LOD scores within the QTL confidence intervals, identified on chromosome 5H. Dehydrin gene (X71362.1) co-localized with the QTLs for leaf water content stress index, while AK356764.1 gene that encodes cysteine protease was associated with the QTL for TR_0/RC stress index.

Co-location of QTLs for Different Traits

The positioned QTLs were not distributed evenly in the barley genome, and they clearly tend to be clustered in the particular chromosome regions. Based on their overlapping confidence intervals, 11 hotspots were identified that contained together more than 60% of mapped QTLs for different traits (**Table 5**, **Figure 2**). The highest number of hotspots (4), that combined the QTLs from all investigated trait categories analyzed in all experiment variants (C/D/DSI), was located on chromosome 2H, followed by three hotspots which contained 2–6 overlapping QTL confidence intervals detected on chromosome 3H. Two hotspots were localized on chromosome 5H, each of them for two physiological parameters. Then, a single genomic region on chromosome 6H enclosed 7 QTLs for photosynthetic efficiency under control water conditions. The last hotspot, that included 2 overlapping QTLs for DSI of fast kinetics of chlorophyll *a* fluorescence parameters, was identified on chromosome 7H.

QTL Projection on Barley Genome

One of the main goals of this study was to identify the positional candidate genes (CGs) within QTL confidence intervals, followed

TABLE 4 | Summary of QTLs for stress indices (DSI) for 11 physiological and biochemical traits in the MCam population.

Trait	Stress indices (DSI)						
	QTL name	Chr.	Nearest marker	LOD	Confidence interval [cM]	Additive effect	R^2 [%]
PLANT WATER STATUS							
WC	QdsiWC.5H_3	5H	X71362.1	4.98	41.96–44.59	6.097	23.6
PHOTOSYNTHETIC EFFICIENCY							
ABS/RC	QdsiABS/RC.7H_3	7H	2378-498	3.68	13.39–17.73	3.663	16.7
TR_0/RC	QdsiTRo/RC.5H_3	5H	3477-1248	3.84	64.75–65.63	−2.242	14.4
	QdsiTRo/RC.7H_3	7H	2378-498	4.19	11.39–17.73	2.399	16.5
ET_0/RC	QdsiETo/RC.5H_3	5H	AK364080.1	3.57	49.85–50.94	3.310	16.2
DI_0/RC	QdsiDIo/RC.5H_2	5H	4570-591	3.61	16.46–18.57	15.007	18.1
qP	QdsiqP.7H_2	7H	ABC03024-1-3-368	3.00	11.98–13.36	4.848	15.5
OSMOPROTECTANT AND HORMONE CONTENT							
Glu	QdsiGlu.2H	2H	5880-2547	5.81	14.03–14.23	−107.193	25.7
Suc	QdsiSuc.3H_2.1	3H	EBmac0708	4.88	16.02–18.08	405.162	**60.8**
	QdsiSuc.3H_2.2	3H	265-1229	4.29	31.01–35.29	−400.512	**54.6**
Mal	QdsiMal.5H_3	5H	GBM5008	3.28	37.50–38.03	17.274	15.5
ACTIVITY AND ACCUMULATION OF ANTIOXIDANTS							
GTf	QdsiGTf.7H_3	7H	6628-1302	3.09	21.05–26.34	60.182	16.0
GTt	QdsiGTt.3H_2	3H	265-1229	**14.1**	32.01–35.29	−248.340	**82.1**

Functional candidate genes that co-segregated with the maximum LOD scores within confidence intervals of mapped QTLs are underlined; LOD ≥ 10 and R^2 ≥ 30 are in bold. R^2, percentage of phenotypic variation explained by individual QTL.

by the exploration of their putative functions related to drought tolerance. We used the availability of the barley reference genome sequence to search for positional CGs in the chromosomal regions corresponding to the confidence intervals of the QTLs determined on the consensus map. The integration of the genetic and physical map led to the identification of overall 3,198 positional candidate genes that could be responsible for the variation in the analyzed traits (Supplementary Material S4; **Figure 3A**). Among them, there were the CGs (1,101) underlying the drought response-specific QTLs, i.e., those QTLs which were detected under drought stress conditions and for the stress indices. The number of genes included in a particular QTL region for all analyzed traits varied between 1 and 550, and was correlated with the confidence interval size, whereas the total ratio between physical and genetic distances was 2.11 Mbp/cM.

Comparative analysis of the number of the positional CGs classified into four trait categories, as well as three analyzed experiment variants (C/D/DSI) was shown on **Figures 3B–E**. When considering plant water status and antioxidant activity, 699 and 172 genes, respectively, were specific to the analyzed experiment variants. Altogether, 2,004 positional CGs were identified for photosynthetic efficiency, and approximately 30% of CGs involved in this process under drought stress (192 out of 665) were also detected in the control conditions. Even larger overlap was observed among 933 genes corresponding to the osmoprotectant and hormone content. Approximately 30% of positional CGs identified under drought stress (88 out of 289) were also detected under control conditions, while as much as 66% (192) were common with stress indices of the analyzed traits. Only 9 genes were identified exclusively under drought stress within this trait category.

QTL Candidate Genes Prioritization

Due to the limited resolution of QTL mapping which resulted in a high number of identified positional candidate genes, we applied Gene Ontology (GO) enrichment approach to: (1) predict the functional ontologies associated with positional CGs, (2) to determine the over-representation of certain GO terms in the analyzed gene sets compared to the genome-wide background frequency, (3) to reduce the number of CGs to potentially casual genes responsible for the variation in the considered traits.

As for the gene sets detected for the analyzed trait categories under optimal water supply, the functional annotation showed their participation in Biological Processes (BP) clearly relevant for the proper shaping of plant growth and development at the morphological, anatomical and physiological levels. They included e.g., post-embryonic organ development, carbohydrate mediated signaling, pentose metabolic process, protein phosphorylation, stomatal movement, defense response, as well as biosynthesis and transport of various compounds (Supplementary Material S5). In order to gain an insight into molecular mechanisms of drought stress response in barley, the special attention was paid to 1,101 positional CGs underlying drought response-specific QTLs. The GO enrichment analysis resulted in narrowing down this number to 143 prime candidates involved in the significantly over-represented BPs which were closely related to the exposition of the analyzed genotypes to drought stress (**Figure 4**). Some of them are described as unknown in existing annotations and assessment of their potential engagement in drought response in barley requires further exploration of their biological functions.

TABLE 5 | Main characteristics of QTL hotspot regions.

Hotspot	Trait	Experiment variant	QTL name	Chromosome	Confidence interval [cM]
qHS2.1	TR_0/RC	D	QdTRo/RC.2H.1	2H	10.92–14.63
	WC	D	QdWC.2H		
	WL	D	QdWL.2H		
	CAT	C	QcCAT.2H		
	Glucose	DSI	QdsiGlu.2H		
qHS2.2	Proline	D	QdPro.2H.1	2H	16.28–29.33
	Ethylene	D	QdEth.2H		
	Raffinose	C	QcRaf.2H		
qHS2.3	Proline	D	QdPro.2H.2	2H	118.27–118.63
	TR_0/CS	C	QcTRo/CS.2H		
	ABS/CS	C	QcABS/CS.2H		
qHS2.4	ET_0/RC	D	QdETo/RC.2H	2H	129.13–145.34
	ψ_o	C	Qcpsi_o.2H		
qHS3.1	Maltose	D	QdMal.3H_2.1	3H	14.02–19.08
	Proline	D	QdPro.3H_2.1		
	DI_0/CS	C	QcDIo/CS.3H_2.1		
	TR_0/CS	C	QcTRo/CS.3H_2.1		
	ABS/CS	C	QcABS/CS.3H_2.1		
	Sucrose	DSI	QdsiSuc.3H_2.1		
qHS3.2	Proline	D	QdPro.3H_2.2	3H	30.01–35.29
	DI_0/CS	C	QcDIo/CS.3H_2.2		
	TR_0/CS	C	QcTRo/CS.3H_2.2		
	ABS/CS	C	QcABS/CS.3H_2.2		
	γ-tocotrienol	DSI	QdsiGTte.3H_2		
	Sucrose	DSI	QdsiSuc.3H_2.2		
qHS3.3	Maltose	D	QdMal.3H_2.2	3H	36.75–42.52
	RWC	C	QcRWC.3H_2.1		
qHS5.1	TR_0/CS	C	QcTRo/CS.5H_2	5H	21.56
	ABS/CS	C	QcABS/CS.5H_2		
qHS5.2	ET_0/RC	C	QcETo/RC.5H_3	5H	41.96–44.59
	WC	DSI	QdsiWC.5H_3		
qHS6.1	F_v'/F_m'	C	QcFv'/Fm'.6H	6H	18.74–21.22
	(1-B)av	C	Qc(1-B)av.6H		
	DI_0/CS	C	QcDIo/CS.6H		
	DI_0/RC	C	QcDIo/RC.2H		
	ET_0/RC	C	QcETo/RC.6H		
	TR_0/RC	C	QcTRo/RC.6H		
	ABS/RC	C	QcABS/RC.6H		
qHS7.1	TR_0/RC	DSI	QdsiTRo/RC.7H_3	7H	11.39–17.73
	ABS/RC	DSI	QdsiABS/RC.7H_3		

D, drought stress; C, control conditions; DSI, stress index.

CGs for Plant Water Status

The GO enrichment in the set of positional CGs identified for plant water status under drought stress, revealed 17% of them to be involved in the oxidation-reduction process (Supplementary Material S6). A detailed analysis showed that two barley genes, MLOC_5505 and MLOC_69302, encoding enzymes belonging to the dehydrogenase and peroxidase families, respectively, were identified in qHS2.1 hotspot which included the overlapping QTLs for leaf water content and water loss under drought, as well as glucose content stress index and catalase activity under control water conditions. The other genes of this GO category are: MLOC_6299 (an ortholog of Arabidopsis AT5G65110, involved in biosynthesis of long chain fatty acid), MLOC_4579 (flavonol synthase), and MLOC_71498 (an ortholog of Arabidopsis gene AT4G25650, encoding translocation channel at the inner envelope membrane of chloroplasts). All these genes were detected in the QTL confidence interval for water loss, on chromosome 7H. The remaining highly enriched

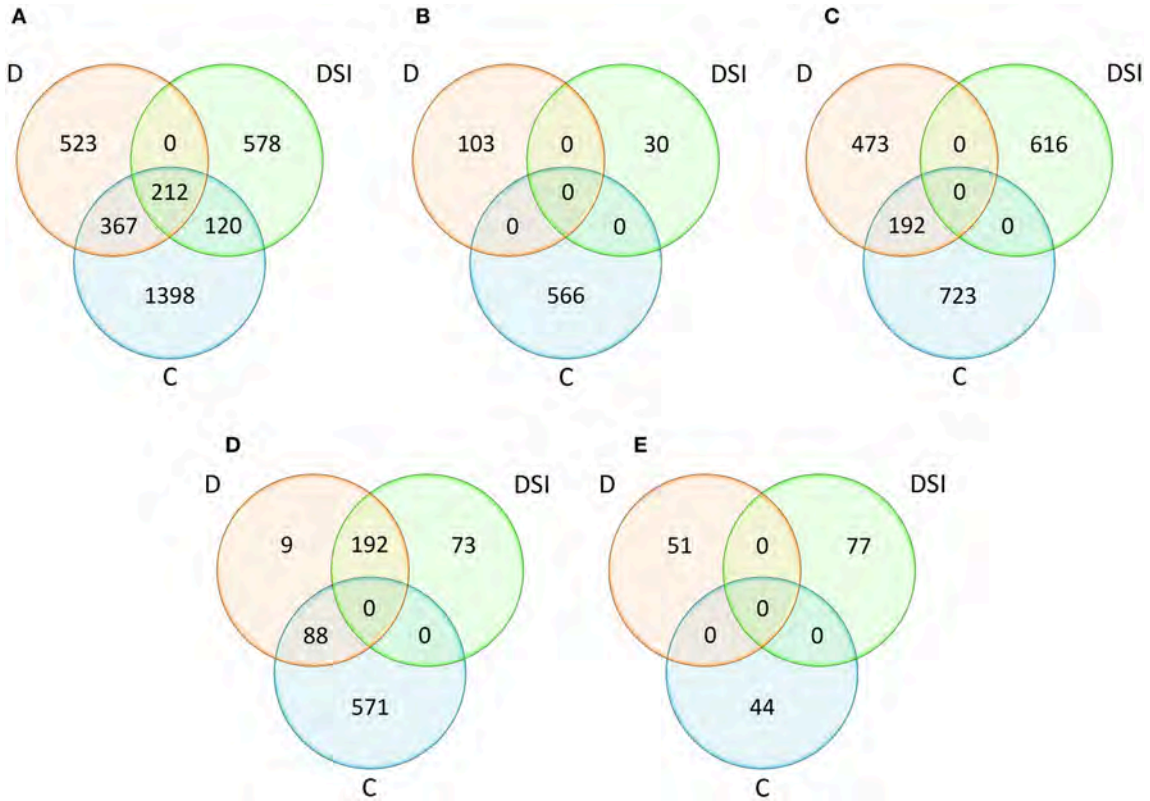

FIGURE 3 | Comparative analysis of the numbers of positional candidate genes identified within QTL confidence intervals with respect to the experiment variants (C, D, DSI) for all traits **(A)** and for the considered trait categories: plant water status **(B)**, photosynthetic efficiency **(C)**, osmoprotectant and hormone content **(D)**, activity and accumulation of antioxidants **(E)**. D, drought stress; C, control conditions; DSI, stress index.

group of genes were annotated as intermembrane transport (MLOC_52403 encoding vesicle-associated membrane protein), homoserine metabolic process and "*de novo*" L-methionine biosynthetic process (MLOC_71910, cystathionine gamma), cyanidin 3-O-glucoside metabolic process and beta-glucoside metabolic process (MLOC_36976, UDP-glucosyl transferase), and regulation of brassinosteroid mediated signaling pathway (MLOC_72613, L-type lectin-domain containing receptor kinase III). Among the CGs for water content stress index, the most enriched Biological Process was carboxylic acid biosynthesis. A detailed analysis of the genes classified into this BP category revealed two barley genes: MLOC_18300 (a member of NCED-related gene family) encoding the key enzyme involved in ABA biosynthesis, and MLOC_53947 for putative plastid pyruvate dehydrogenase. The others significantly over-represented GO terms were: proline biosynthesis process, ornithine catabolic process, arginine catabolic process to glutamate (MLOC_35821, ornithine aminotransferase), regulation of ATPase activity, and response to heat (MLOC_37449, protein DnaJ).

CGs for Photosynthetic Efficiency

The functional annotation analysis of the positional CGs identified for photosynthetic efficiency under drought stress showed that the majority of genes belong to the GO categories of protein folding, response to heat, response to high light intensity, and response to hydrogen peroxide (Supplementary Material S7). They include genes located mostly on chromosomes 2H and 7H that encoded heat shock proteins (MLOC_568, MLOC_31567, MLOC_41281) and chaperonins (MLOC_51927 and MLOC_54083). Some of them are involved in folding of RuBisCO, the major enzyme at the first step of carbon fixation in the Calvin cycle. A particularly interesting GO category comprised three genes mapped on chromosomes 2H and 5H (MLOC_15256, MLOC_19075, MLOC_38928), encoding ATP sulfurylases involved in the sulfate assimilation pathway. The other highly enriched Biological Process among CGs for photosynthetic efficiency in response to drought was detection of abiotic stimulus. Two genes, one encoding phytochrome A (MLOC_824) and the other involved in the chromatin remodeling in the response to environmental cues (MLOC_60235) were found within this category. The most enriched GO terms of the CGs for photosynthetic efficiency DSI included three groups. The first group consisted of the over-represented BPs related to DNA dealkylation and DNA demethylation (MLOC_53029 and MLOC_11707, encoding DNA repair proteins). Another highly represented GO category was lipid transport. Here, MLOC_51456 encoding a non-specific lipid-transfer protein was found. The BPs belonging

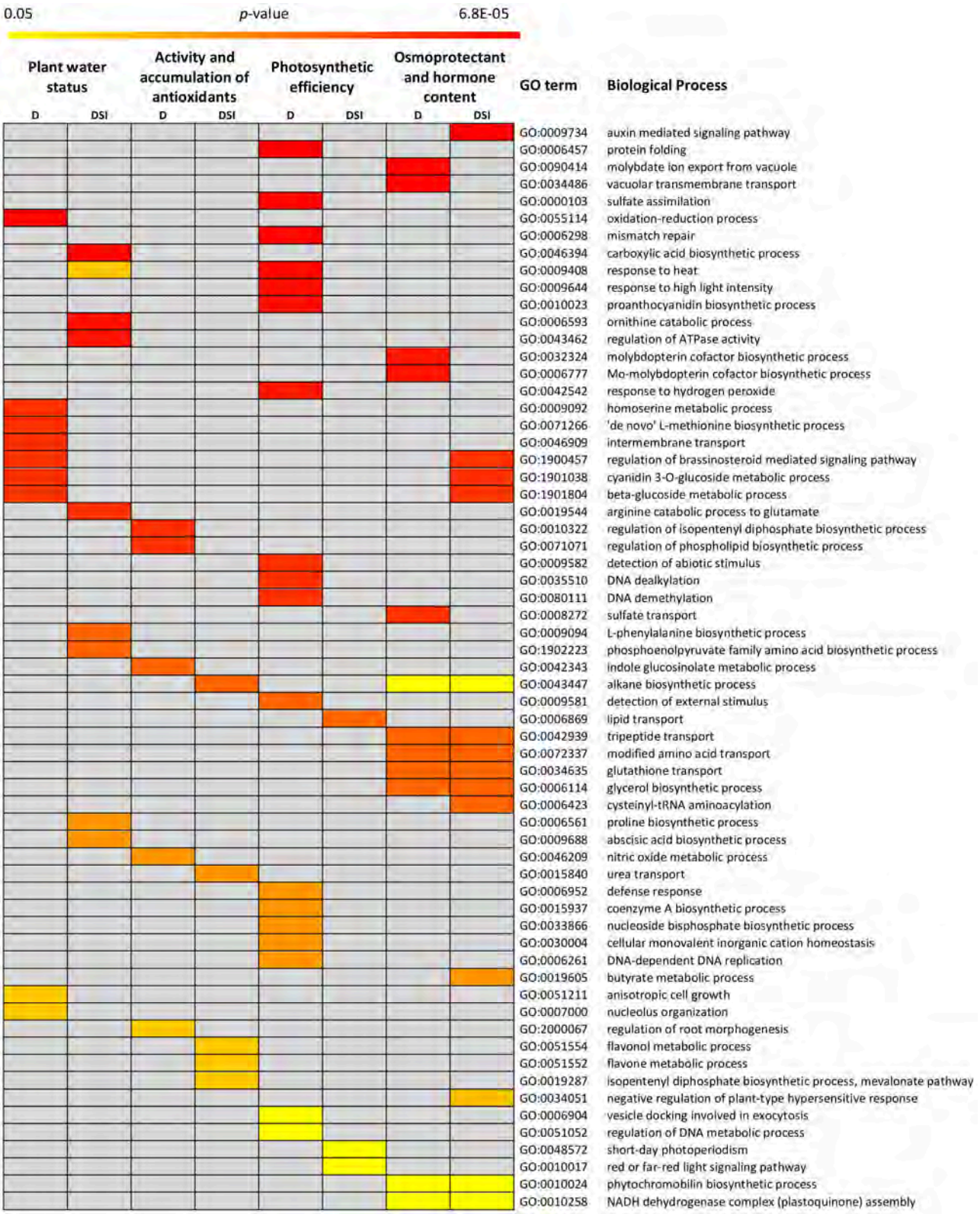

FIGURE 4 | Biological processes significantly over-represented in the gene sets for the analyzed trait categories: under drought stress (D) and for stress indices (DSI).

to the last group were related to short-day photoperiodism that included MLOC_6879 (an ortholog of Arabidopsis gene AT3G24440, *VERNALIZATION INSENSITIVE 3-LIKE 1*) and MLOC_19228 (an ortholog of Arabidopsis gene AT5G46210, *CULLIN4*). Red or far-red light signaling pathway was another overrepresented BP from this group, including MLOC_20045, encoding nucleoside diphosphate kinase and MLOC_53845, an ortholog of Arabidopsis gene *PFT1*, encoding phytochrome and flowering time regulatory protein).

CGs for Osmoprotectant and Hormone Content

The majority of drought-specific CGs for the osmoprotectant and hormone content category were common for drought stress conditions and stress indices (DSI). According to the GO enrichment, they are involved in tripeptide and modified amino acid transport, glutathione transport (MLOC_174, a member of Crt-like transporters), glycerol biosynthetic process (MLOC_40292, glycerol-3-phosphatase 1), and phytochromobilin metabolic process (MLOC_70465, phytochromobilin oxidoreductase; Supplementary Material S8). These genes encode proteins located in chloroplasts and they were mapped in qHS3.1 hotspot which included the overlapping QTLs for sucrose content stress index, as well as for proline and maltose content under drought stress. Among CGs for this category, GO enrichment analysis led to the identification of two barley genes exclusive for drought stress, which were positioned in qHS3.2 hotspot. MLOC_65646 is a putative ortholog of Arabidopsis gene AT5G20990, encoding molybdopterin biosynthesis protein, which is involved in molybdenum cofactor biosynthesis, whereas MLOC_22343, encoding molybdate transporter showed enrichment in BP categories related to vacuolar transmembrane transport, molybdate ion export from vacuole, and sulfate transport. The most represented category of BPs among the CGs for osmoprotectant and hormone content stress indices was auxin mediated signaling pathway. One of the genes involved in this process was MLOC_58506, encoding a member of the small auxin up-regulated RNA family. It was mapped on chromosome 5H in QTL confidence interval for maltose content stress index. Other highly enriched GO categories were the same as for the plant water status under drought stress: cyanidin 3-O-glucoside metabolic process, beta-glucoside metabolic process (MLOC_36976, UDP-glucosyl transferase), and regulation of brassinosteroid mediated pathway (MLOC_72613, L-type lectin-domain containing receptor kinase III).

CGs for Activity and Accumulation of Antioxidants

For the activity and accumulation of antioxidants trait category, a single QTL for α-tocopherol content under water-deficiency conditions was identified on chromosome 6H. The GO enrichment analysis among CGs for α-tocopherol led to the identification of over-represented BP categories, such as: regulation of isopentenyl diphosphate biosynthetic process, regulation of phospholipid biosynthetic process, nitric oxide metabolic process, and indole glucosinolate metabolic process (Supplementary Material S9). In-depth analysis showed MLOC_63263, encoding a chloroplastic/mitochondrial NO-associated protein, and MLOC_57100, encoding O-methyltransferase which is involved in flavonol biosynthesis. The analysis of the GO annotations of the positional CGs for antioxidant activity DSI revealed their involvement in: flavonol metabolic process, flavone metabolic process (MLOC_73233, O-methyltransferase), and urea transport (MLOC_58872, an ortholog of Arabidopsis gene AT4G01470, encoding tonoplast intrinsic protein functions as water and urea channel). Furthermore, the both selected genes for antioxidant activity stress indices were identified in qHS3.2 hotspot which overlapped 6 QTLs, among them for γ-tocotrienol and sucrose stress indices, as well as proline content under drought stress.

DISCUSSION

The identification of genes underlying particular QTLs, followed by the elucidation of their molecular functions, is one of the paramount challenges in the modern plant genetics, as more than 2500 studies on QTL analysis in crop plants have been published so far (Kumar et al., 2017). Most studies have focused on exploiting the highly saturated molecular function maps to co-localize QTL regions with the genetic markers, based on within-gene polymorphisms (Diab et al., 2008; Sehgal et al., 2012; Li W. T. et al., 2013; de Miguel et al., 2014; Mikołajczak et al., 2016). In a standard strategy, after fine mapping of a QTL, a positional cloning of the QTL has been proposed to identify a gene or genes underlying a complex trait (Kumar et al., 2017). Although, there are examples of successful positional cloning of QTLs (Salvi and Tuberosa, 2007; Collins et al., 2008; Mir et al., 2012), this procedure remains difficult and cumbersome, especially for large genomes. This could explain a small number of cloned QTLs in barley with only a few examples related to abiotic stress tolerance, such as boron (Sutton et al., 2007), and aluminum toxicity (Furukawa et al., 2007) or freezing tolerances (Francia et al., 2007).

Recently, the availability of complete genome sequences for a growing number of plant species gave the opportunity to gain an insight into the physical gene space, resulting in the straightforward searching for all possible positional candidate genes associated with QTL confidence intervals (Monclus et al., 2012; Bargsten et al., 2014; Correa et al., 2014). Therefore, an inherent bottleneck is an effective selection of the most promising CGs within QTL regions, typically including tens to hundreds of genes, most of them unrelated to the trait of interest. Various methods to prioritize CGs within the QTL regions for the target trait can be combined, including the approach based on CGs overrepresentation in the biological processes, the analysis of their differential expression at transcriptome and/or proteome levels or functional annotation of CGs based on their orthologs in related or model species (Monclus et al., 2012; Bargsten et al., 2014; Kumar et al., 2017).

Our study presents the comprehensive multistep approach for elucidation of the genetic basis of drought response mechanisms in barley. Firstly, the identification of precise chromosomal regions underlying physiological and biochemical indicators of the drought tolerance was accomplished by merging the

extensive analysis of these parameters under drought stress and classical quantitative genetic approach, performed with the use of strict threshold criteria and a high-density function map. Next, the anchoring of drought response-specific QTLs to the reference barley genome sequence was performed, after the thorough evaluation of QTL data. Finally, a huge number of identified positional CGs was reduced to potentially causative genes underlying the analyzed traits, using a Gene Ontology enrichment approach, followed by additional prioritization tools. Below, the most important results of the particular steps of the study are discussed.

Reliability and Accuracy of QTL Mapping

QTL analysis in this study identified a total of 64 QTLs for 25 out of 40 physiological and biochemical traits measured under the optimal and drought stress conditions (absolute values), as well as for their DSI (relative values). The identified QTLs showed LOD scores ranging from 3.0 to 20.8, and explained 6.7 to 87.5% of observed variation (R^2). The applied LOD threshold of 3.0 to declare a presence of the QTL ensured the detection of reliable and significant QTLs involved in the formation of analyzed traits and the exclusion of small effect, tentative QTLs (Salvi and Tuberosa, 2015; Kumar et al., 2017). Using the same criterion (LOD $>$ 3.0), Liu et al. (2017) identified 11 significant QTLs for 6 traits, out of a total of 15 stomatal and photosynthetic traits related to salinity tolerance in barley, while with a lower LOD score (2.5 $<$ LOD $<$ 3.0), the authors added 11 tentative QTLs for 11 traits to this list. Similarly, Wójcik-Jagła et al. (2013), in two barley mapping populations identified in total 33 QTLs (LOD $>$ 2.5) for physiological parameters measured under short-time drought, but only 11 QTLs were detected with a LOD score $>$3.0. In the present study, with the aim to search for positional candidate genes associated with QTL confidence intervals, we decided to consider only significant QTLs with a high LOD score.

The QTLs detected in our study are characterized by a large phenotypic effect and a high accuracy of mapping (Mir et al., 2012; Kumar et al., 2017). Assuming that the proportion of phenotype variation explained by a major QTL should be above 10% (Kumar et al., 2017), as much as 95% of the QTLs identified in our study can be considered as the major ones, including all 32 QTLs detected under drought stress and for DSI. Similarly, the 11 significant QTLs detected by Liu et al. (2017), mentioned above, can be classified as the major QTLs, as each of them explained at least 11.2% of variation. On the contrary, in the work of Wójcik-Jagła et al. (2013) only 4 out of 33 QTLs detected in two mapping populations could be considered as the major ones using the above criterion. Moreover, the majority of the QTLs (92.2%) of our study were precisely positioned on the linkage map within confidence intervals below 6.0 cM. It is not a common situation as usually the linkage analysis locates QTLs within the confidence intervals of 10–30 cM (Chander et al., 2008; Li et al., 2008; Capelle et al., 2010; Chen et al., 2010; Kumar et al., 2017). However, in accordance with our results, Bertholdsson et al. (2015) showed a group of 5 QTLs including 3 major QTLs for quantum yield of electron transport of PSII under waterlogging in barley, and all of them but one, were mapped within confidence intervals below 5.0 cM.

Co-locations of Present and Known QTL Regions

Over the last two decades, QTL for a wide range of traits related to the drought tolerance, including physiological/biochemical characteristics, have been mapped to all seven barley chromosomes (Mir et al., 2012). A precise comparison among these results is not possible owing to the differences in used plant materials and maps, various traits analyzed and diverse methodology applied, however, some interesting observation can be made in regard to the results of the present study. The QTLs identified in our study were mapped to all barley chromosomes, except 4H, with the highest number of QTLs located on chromosomes 2H, 3H and 5H. Based on the overlapping confidence intervals, 11 hotspots were identified that contained together over 60% of mapped QTLs for all the traits, most on 2H (4) and 3H (3). In the previous studies with the same mapping population, aimed at the detection of QTLs underlying yield-related agronomic traits under drought and control conditions (Mikołajczak et al., 2016, 2017; Ogrodowicz et al., 2017), the important role of the regions on chromosomes 2H and 3H was also reported. Moreover, the most significant QTL hotspot on 2H, clustering QTLs for the length of main stem and yield traits (Mikołajczak et al., 2017), as well as heading date (Ogrodowicz et al., 2017), co-localized with a hotspot region (qHS2.1) of the present study. The other region of overlapping QTL hotspots between these studies was found on chromosome 5H. Similarly, Mora et al. (2016) revealed the highest number of QTLs for drought-related morphological and physiological traits on chromosomes 2H and 3H, using a distinct barley gene-pool and environmental conditions. Recently, meta-QTL analysis approach has been developed which is aimed in the integration of data from multiple QTLs studies and has a greater statistical power for the detection of, so called, meta-QTLs (MQTL), and more precise estimation of their genetic effects (Wu and Hu, 2012). Zhang et al. (2017) performed a meta-QTL analysis of drought tolerance in barley using 72 major QTLs described in several studies, and most of QTLs were located on chromosomes 2H, 3H, 5H, and 7H. As a result, MQTLs, integrating QTLs for barley drought tolerance, have been positioned on chromosomes, with some particularly important regions, common to drought and salinity tolerance on 2H (2), 3H (1), and 5H (1).

In the present study no overlapping QTLs identified for a given trait under different water regimes were found. A similar situation was observed by Wang et al. (2014) in QTL mapping for yield-related traits in barley in six diverse environments. Mora et al. (2016) also showed that 80% of the identified QTLs for analyzed traits were specific for a particular environment. According to this observation, we used only the QTLs detected under drought stress conditions and QTLs for adequate DSI, to be subjected for the co-location analysis, projection to barley genome sequence and positional CGs identification.

For the plant water status related traits, a total of 5 QTLs were detected under drought stress conditions and for adequate DSI in our study. Among them, two neighboring regions from chromosome 5H have been pointed in previous studies: QdsiWC.5H_3 for the water content DSI and QdWL.5H_3 for

water loss under drought stress co-located with QTL region for RWC determined by Teulat et al. (2001a, 2003), in the close vicinity of *dhn1* and *dhn9* genes encoding dehydrins. This co-location is further confirmed as QdsiWC.5H_3 ($R^2 = 23.6\%$) was mapped into the position of X7136.1 gene, a functional CG which encodes a dehydrin protein. This gene was chosen for mapping based on the transcriptome analysis of parental genotypes of MCam population under drought stress.

For the photosynthetic efficiency category 13 QTLs were detected under drought stress conditions and for adequate DSI. The analysis revealed that two QTL regions from the distal part of a long arm of chromosome 2H: QdABS/RC.2H.2 for PSII light absorption flux per RC and $QdET_0$/RC.2H (from hotspot qHS2.4) for electron transport flux in PSII per RC co-localize with two hotspots for chlorophyll *a* fluorescence parameters detected by Guo et al. (2008). These two chromosomal regions were also identified by Wójcik-Jagła et al. (2013) with QTLs for photochemical quantum yield of PSII (Φ_{PSII}) DSI, and for photochemical quenching (qP). The region of $QdET_0$/RC.2H seems to be especially significant as it explained the highest proportion of the variation (20.5%) and was mapped in the position of AK353596.1 gene (MLOC_65477), a functional CG used for map construction. This gene encodes for an enzyme from the peroxidase class engaged in reactive oxygen species (ROS) detoxification. Different ROS are excessively formatted under drought stress, but they are also produced during the light phase of photosynthesis where about 10% of the pool of electrons is transferred to oxygen forming superoxide anion radical (Foyer and Noctor, 2000). The AK353596.1 gene was selected for mapping based on its differential expression between parental genotypes of MCam under drought (Janiak et al., 2018). Thus, the relationship between this gene and the identified QTL seems to be well-supported. Additionally, two other QTLs related to photosynthetic efficiency of PSII showed the co-locations with QTLs detected previously. The region of Qd(1-B)av.7H_2 from 7H co-located with the QTL for initial fluorescence (F_0) from the study of Guo et al. (2008) and $QdsiDI_0$/RC.5H_2 from 5H overlapped with the chromosomal region of four QTLs for DSI for PSII photosynthetic efficiency and water content (Wójcik-Jagła et al., 2013).

In the osmoprotectant and hormone content category, altogether 11 drought response-specific QTLs were detected. It should be underscored that our study for the first time identified the QTLs for glucose, maltose, sucrose and ethylene content under drought stress conditions in barley. Among them, the QTL from the short arm of 2H, QdsiGlu.2H, for glucose content DSI, overlapped with three other QTLs for WC, WL, and TR_0/RC (hotspot qHS2.1, around SNP marker 5880-2547) and was mapped near the position of another functional CG, AK356764 (MLOC_21709, an ortholog of Arabidopsis AT3G60750), encoding transketolase. This enzyme is involved in the Calvin-Benson cycle during the light-independent phase of photosynthesis, and according to GO terms, might be also involved in salinity tolerance, gluconeogenesis and water transport. The QdsiGlu.2H region showed the co-location with QTL for WSC concentration at full turgor under drought stress (WSC_{100}) designated by Diab et al. (2004). The most interesting result was obtained in the case of six, partially overlapping QTLs for proline, maltose and sucrose content, located in the distal part of a long arm of chromosome 3H. These QTLs explained the highest amount of phenotype variation (54.6–85.9%), were divided among three neighboring hotspots (qHS3.1, qHS3.2, qHS3.3), and coincided with the QTL regions for proline content under drought and salinity stresses identified by Sayed et al. (2012) and Fan et al. (2015), respectively.

In the activity and accumulation of antioxidants category, 3 QTLs were detected under drought stress conditions and for adequate DSI. Here again, for the first time our study determined the QTLs for α-tocopherol (QdATf.6H on 6H) and γ-tocotrienol (QdsiGTt.3H_2) content under drought stress in barley. The region QdsiGTt.3H_2 for γ-tocotrienol content DSI explained 82.1% of phenotype variation for this trait and was included into the hotspot qHS3.2 together with QTLs for proline and sucrose content (co-locations presented above). A third QTL region, QdsiGTf.7H_3 for γ-tocopherol content DSI was mapped on chromosome 7H near SNP marker 6628-1302 and showed the co-location with the QTL for γ-tocopherol content under drought stress detected recently by Templer et al. (2017).

Prioritization of Positional CGs Related to Drought Response-Specific QTLs

Although the sequence assembly of the barley genome has been accessible since 2012 (Mayer et al., 2012), only a few studies demonstrated the genetic and physical map integration resulting in numerous putative CG identification (Fan et al., 2015; Piasecka et al., 2017; Templer et al., 2017; Zhang et al., 2017). In the present work, the QTL projection on the genome was extended by the GO enrichment analysis. This allowed an efficient selection of CGs on the basis of their relevance to biological processes related to analyzed trait categories. To the best of our knowledge, it was the first attempt to apply the Gene Ontology-based prioritization to barley QTL analysis. The resulting reduction in the number of genes was almost eight-fold: out of the 1,101 CGs corresponding to the drought response-specific QTLs, we selected 143 significant candidates predicted to be responsible for the variation in the considered traits. Similar findings have been reported by Bargsten et al. (2014) who prioritized rice QTL data leading to the ten-fold reduction in the number of candidate genes. The GO enrichment was also successfully applied to select CGs participating in the genetic determination of the grapevine cluster architecture (Correa et al., 2014), as well as the productivity, growth, and water-use efficiency in poplar (Monclus et al., 2012).

Unquestionably, the thorough examination of CGs revealed in the present study is necessary to confirm their exact role in drought stress response in barley. However, we want to point out that our findings have been supported by results of the global gene expression profiling of parental genotypes that had been used for QTL mapping in our study (Janiak et al., 2018). The differentiated expression due to drought stress was confirmed for 34 CGs from the set of 143 genes selected based on prioritization approach. In the following paragraphs, we characterize the best candidates for further experimental

validation of their role in driving drought response. The genes have been carefully chosen based on one of the following criteria: (1) differentiated expression under drought stress, (2) location within overlapping QTL confidence intervals (hotspots), (3) well-documented engagement of their orthologs in model species in drought stress response.

The majority of CGs identified within drought response-specific QTLs for plant water status corresponded to the oxidation-reduction process. It is well-recognized that accumulation of reactive oxygen species (ROS) in the chloroplasts and mitochondria is an early response of plants to decreased water potential inside the cells during adverse stress conditions (Xiong et al., 2002; Choudhury et al., 2013). Many studies have revealed the ROS-mediated retrograde signaling pathway from chloroplasts to nucleus, which results in substantial changes in the expression of the nuclear genes that maintain chloroplasts function and other aspects of plant adaptation to environmental cues (reviewed in Chi et al., 2015). In contrast, an attention has been drawn to the role of ROS as major drivers of cellular oxidative damages (Noctor et al., 2014). Among the barley genes that correlated with the oxidation-reduction process, we highlighted MLOC_69302 encoding ascorbate peroxidase (APX) as a key player involved in the hydrogen peroxide removal. It was reported that *APX* loss-of-function Arabidopsis mutants accumulated more hydrogen peroxide and were significantly more sensitive to different abiotic stresses than the wild type (Koussevitzky et al., 2008). Another gene identified in our study that may be important for barley drought response, MLOC_4579, encodes a flavonol synthase. Flavonols are members of secondary metabolites highly accumulated under various stresses which are involved in ROS scavenging leading to the enhancement of oxidative tolerance (Nakabayashi et al., 2014). Therefore, it can be suspected that the identified barley redox-linked genes contribute to regulation of ROS homeostasis under water deprivation.

The carboxylic acid biosynthesis was the second over-represented process among CGs identified in intervals of QTLs for plant water status. Within this group, MLOC_18300 encoding a member of 9-cis-epoxycarotenoid dioxygenase family (NCED), which catalyzes an essential regulatory step in ABA biosynthesis, was found (Seo and Koshiba, 2002). Drought stress-stimulated accumulation of ABA modulates root hydraulic conductivity and regulates shoot vs. root growth, as well as alters guard cell ion transport, promoting stomatal closure and reducing water loss by transpiration (Roychoudhury et al., 2013; Sah et al., 2016). Another identified gene, MLOC_53947, encodes a putative plastid pyruvate dehydrogenase which contributes to transforming pyruvate to Acetyl-CoA, the precursor for fatty acid biosynthesis (Johnston et al., 1997; Mentzen et al., 2008). It was shown that prolonged drought exerts phospholipid bilayer destabilization and increases its permeability leading to the ion leakage (Bajji et al., 2002; Fang and Xiong, 2015). Therefore, an enhanced biosynthesis of fatty acids may be a crucial strategy of protecting plasma membrane integrity against the damage under drought stress, maintaining osmotic homeostasis and cell turgor pressure, as well as controlling transcellular water and ion transport.

Our analysis clearly showed a putative involvement of numerous genes encoding the heat shock proteins (HSP) in the regulation of photosynthetic efficiency under drought stress in barley. Members of different HSP families perform the molecular chaperone function by participation in the proper protein folding and assembly. Furthermore, they enable disposal of non-functional and aggregated stress-labile proteins (Santhanagopalan et al., 2015). It is well-recognized that HSP proteins play a pivotal role in the protection of photosynthetic components against stress injuries. Recent studies have revealed that stress-induced impairment of photosynthesis results in the reduction of carbon fixation and oxygen evolution, as well as disruption of the linear electron flow. One of the main effects of photoinhibition is the exposure of chloroplasts to excess excitation energy. This increases the generation of ROS by the incomplete reduction of molecular oxygen, which in turn induce remarkable damages in chloroplast proteins, lipids, and pigments (Filek et al., 2015; Pospisil, 2016). The components of photosynthetic apparatus particularly sensitive to oxidative stress are: PSII with its oxygen-evolving complex, the carbon assimilation process driven by RuBisCO, and the ATP generating system (Allakhverdiev et al., 2008). Among genes for HSP identified in this work, the most represented group was orthologs of Arabidopsis AT5G51440 encoding HSP20-like chaperone (MLOC_568 and MLOC_31567). HSP20 proteins are encoded by nuclear multigenic families and are located in different cellular compartments (Lopes-Caitar et al., 2013). In Arabidopsis, 19 genes encoding HSP20 were identified, whereas 36 and 23 *HSP20* genes were described in poplar and rice, respectively (Scharf et al., 2001; Waters et al., 2008; Sarkar et al., 2009). An intriguing over-represented biological process among CGs for photosynthetic efficiency under drought stress was the sulfate assimilation, represented by MLOC_19075, an ortholog of Arabidopsis gene AT4G14680 encoding ATP sulfurylase. Many studies indicate the importance of sulfur as the component of a wide range of compounds with fundamental biological functions, including tolerance to various abiotic stresses (Prioretti et al., 2014). ATP sulfurylases catalyze the first step in the sulfate assimilation pathway. They activate sulfate (SO_4^{2-}; a metabolically inert form of sulfur taken up by roots), yielding a high-energy adenosine-5′-phosphosulfate (APS) that is reduced to sulfide (S^{2-}) and incorporated into cysteine. In turn, cysteine acts as a donor of highly reactive thiol group (-SH) for numerous S-compounds (Prioretti et al., 2014; Anjum et al., 2015). One of them is glutathione, whose contribution to drought stress tolerance by ROS detoxification and stress-induced signal transduction has been extensively evidenced (Munemasa et al., 2013; Pyngrope et al., 2013; Nahar et al., 2015).

Other relevant biological processes related to the photosynthetic efficiency, over-represented among CGs analyzed in this work, were: short day photoperiodism and red or far red light signaling pathway. Within this group, we highlighted two barley genes, MLOC_6879 and MLOC_53845, orthologs of Arabidopsis *VERNALIZATION INSENSITIVE 3-LIKE 1* (*VIN3-LIKE1*) and *PHYTOCHROME AND FLOWERING TIME 1* (*PFT1*), respectively, involved in the control of flowering time. Many studies have reported a limiting effect of drought

stress on plant yield, including early arrest of floral development leading to the interruption of plant reproduction. One of the mechanisms to cope with the water deficit adopted by plants is an acceleration of the flowering process to shorten plant life cycle *via* drought escape. In Arabidopsis, the *FLOWERING LOCUS T* (*FT*) is a master regulator of flowering promotion. It activates the expression of meristem identity genes which control the reprogramming of shoot apical meristem to form flowers (Turck et al., 2008; Kazan and Lyons, 2016). *FT* gene is up-regulated by a transcription factor CONSTANS (CO) and repressed by the product of *FLOWERING LOCUS C* (*FC*). Furthermore, *PFT1* gene was shown to activate expression of *FT* through CO- dependent and independent manner. In contrary, *FC* is epigenetically down-regulated by the vernalization response genes (e.g., *VIN3-LIKE1*; Inigo et al., 2012; Kazan and Lyons, 2016). Taking these data into account, it could be suggested that drought stress occurring at the seedling stage may trigger the up-regulation of MLOC_6879 and MLOC_53845 genes to switch on a drought escape adaptive mechanism by promotion of flowering. This suggestion is supported by a distinctly early flowering of one of the parental genotypes used for QTL mapping, the Syrian line CamB (Ogrodowicz et al., 2017).

We identified several CGs for accumulation of osmoprotectants and hormones within the hotspot regions: qHS2.1, qHS2.3, qHS3.1, and qHS3.2, which suggests their engagement in the complex metabolic networks, probably common to different drought-responsive compounds. As an example, MLOC_174 [a CRT (chloroquine-resistance transporter)-like transporter 3, involved in modified amino acid and glutathione transport], MLOC_40292 (glycerol-3-phosphatase), and MLOC_20354 (gamma-secretase subunit, involved in Notch signaling pathway) were candidate genes for the proline, sucrose, and maltose accumulation. Furthermore, a special attention was given to five genes (MLOC_58506, MLOC_58508, MLOC_58507, MLOC_65368, MLOC_65978) encoding SAUR-like auxin-responsive proteins. Many findings suggest participation of auxin in the plant response to stresses, including drought (Du et al., 2013; Krishnamurthy and Rathinasabapathi, 2013; Rahman, 2013; Shi et al., 2014). It is well-documented, that small auxin up-regulated RNAs (SAUR) are the most numerous family among early auxin response genes, found to be tandemly duplicated in plant genomes (Wu et al., 2012). Accordingly, the SAUR genes identified in this work are clustered within single QTL chromosomal region for maltose content on chromosome 5H. Despite of progressive identification of SAUR genes in different plant species, the functions of most of them, especially in the stress response, remained elusive due to their large genetic redundancy (Ren and Gray, 2015). However, recent studies revealed the role of SAUR genes in hypocotyl elongation and leaf senescence in Arabidopsis, bacterial blight resistance in rice, and drought tolerance in wheat (Chae et al., 2012; Kai et al., 2013; Aoki et al., 2016; Guo et al., 2018). Therefore, it can be hypothesized that observed decrease in maltose content under drought stress conditions, may be regulated by auxin-mediated SAUR genes, but this requires further verification.

The most striking result of GO enrichment was the identification of two genes: MLOC_65646 (encoding molybdopterin biosynthesis protein) and MLOC_22343 (encoding molybdate transporter) involved in the formation of molybdenum cofactor (Moco), which acts as an active compound at the catalytic center of a wide range of oxidation-reduction enzymes (Mendel, 2013). One of these enzymes is aldehyde oxidase which converts abscisic aldehyde to ABA in the last step of the ABA biosynthesis pathway. It was shown that aldehyde oxidase requires the sulfurylated form of Moco for providing its activity (Mendel and Haensch, 2002). This reaction is catalyzed by Moco sulfurase encoded in Arabidopsis by *LOS5/ABI3* gene (Xiong et al., 2001). The study of Li Y. et al. (2013) have revealed that soybean transgenic lines with overexpression of *LOS5/ABI3* showed a reduced electrolyte leakage, enhanced accumulation of proline and antioxidant enzymes, as well as significant increase in ABA content and drought tolerance. The identification on the aforementioned barley genes in the QTL hotspot qHS2.3 for ABS/RC and proline content suggests an interplay between the decreasing photosynthetic efficiency and expression of genes engaged in molybdenum cofactor synthesis, which results in ABA-mediated proline accumulation.

Considering CGs related to the activity and accumulation of antioxidants, we distinguished two genes, MLOC_57100 and MLOC_73233, orthologs of Arabidopsis AT5G54160 (*AtOMT1*), encoding O-methyltransferase. Enzymes belonging to the OMT family catalyze transfer of methyl group to the oxygen atom of the wide range of low molecular weight organic compounds, including flavonoids, alkaloids, and phenylpropanoids. Their methylated products are involved in lignin biosynthesis and response to environmental cues (Lam et al., 2007). Furthermore, it has already been shown that drought stress increased *OMT* transcription in maize, soybean, and grape (Yamaguchi et al., 2010; Liu et al., 2013; Giordano et al., 2016). Since MLOC_73233 was located in the hotspot qHS3.2 that includes QTLs for γ-tocotrienol, proline and sucrose content, it can be hypothesized that O-methylation of intermediate products in the metabolic pathways of these drought-response compounds plays an important role in improving barley tolerance to water deficit.

A putative candidate gene for α-tocopherol accumulation is MLOC_63263 encoding an ortholog of Arabidopsis AT3G47450 (*NITRIC OXIDE SYNTHASE1*; *AtNOS1*). Nitric oxide (NO) is a short-lived, highly membrane permeable, inorganic free radical. It is a crucial signaling molecule mediating diverse physiological processes and defense mechanisms in plants, likewise ROS (Siddiqui et al., 2011). The increased accumulation of NO was reported in wheat and pea under osmotic stress, in parsley under water deficit conditions, and in tobacco under various types of abiotic stimuli (Gould et al., 2003; Kolbert et al., 2005). It is worth noting that NO participates in the ABA-mediated control of stomatal aperture by negative feedback regulation (Wang et al., 2015). The recent study of Yang et al. (2015) showed an interplay between NO and ROS homeostasis. They demonstrated that NO positively regulates the activity of Arabidopsis ascorbate peroxidase APX1 by S-nitrosylation of cysteine residue, which increases its enzymatic activity of hydrogen peroxide detoxification.

CONCLUSION

To dissect complex drought tolerance traits and decipher genes underlying resistance mechanisms in barley we employed multidisciplinary approach integrating the latest achievements and tools of physiology, genetics and genomics. Our study proved that thorough physiological/biochemical analysis merged with precisely performed QTL mapping, followed by the use of prioritization tools to dissect genes within physical QTL confidence intervals, is an effective approach to designate the most relevant CGs underlying quantitatively inherited traits. The list of CGs selected on the basis of GO prioritization can be further narrowed down by identifying those that are differentially expressed under drought stress, located within overlapping QTL confidence intervals (hotspots), or have orthologs in model species with well-documented engagement in drought stress response. However, further detailed experimentation using mutants and/or overexpression lines is required to confirm the individual CG relation to the studied trait, before breeding application.

AUTHOR CONTRIBUTIONS

IS and PK conceived and designed the study; MF, JB-K, and JK designed and coordinated drought stress experiment, contributed to the analysis of the physiological data; KZ and AO performed drought stress experiment; MD, JK, BJ, KH, and KZ generated and elaborated data on physiological and biochemical traits; JG-W and IS coordinated genetic part of the study; KG, JG-W, and DG identified SSRs for mapping; AJ, KG, and JG-W performed selection of functional CGs for mapping; KG, JG-W, JS, and WU genotyped two RIL populations; KG analyzed all genotyping data and constructed two RILs maps and the consensus function map; AK, KM, PO, KK, and PK performed LCam population genotyping and constructed LCam genetic map; KG performed QTL mapping, integration QTLs to physical map, GO enrichment analysis, and together with IS and JG-W performed analysis and interpretation of data; KG, JG-W, and IS wrote the manuscript; All authors commented on the manuscript.

FUNDING

This work was supported by the European Regional Development Fund through the Innovative Economy Program for Poland 2007–2013, project WND-POIG.01.03.01-00-101/08 POLAPGEN-BD, Biotechnological tools for breeding cereals with increased resistance to drought. All information about the project can be found at www.polapgen.pl.

ACKNOWLEDGMENTS

The authors thank Dr. Robbie Waugh of the James Hutton Institute (JHI) for the possibility of the usage of Barley Oligonucleotide Pool Assays (BOPA1), and Dr. Joseph DeYoung of the Southern California Genotyping Consortium (SCGC) at the University of California Los Angeles (UCLA) for genotyping the RIL populations with BOPA1 and providing the SNP marker data.

SUPPLEMENTARY MATERIAL

The Supplementary Material for this article can be found online at: https://www.frontiersin.org/articles/10.3389/fpls.2018.00769/full#supplementary-material

REFERENCES

Aebi, H. (1984). Catalase *in vitro*. *Methods Enzymol.* 105, 121–126. doi: 10.1016/S0076-6879(84)05016-3

Allakhverdiev, S. I., Kreslavski, V. D., Klimov, V. V., Los, D. A., Carpentier, R., and Mohanty, P. (2008). Heat stress: an overview of molecular responses in photosynthesis. *Photosyn. Res.* 98, 541–550. doi: 10.1007/s11120-008-9331-0

Anjum, N. A., Gill, R., Kaushik, M., Hasanuzzaman, M., Pereira, E., Ahmad, I., et al. (2015). ATP-sulfurylase, sulfur-compounds, and plant stress tolerance. *Front. Plant Sci.* 6:210. doi: 10.3389/fpls.2015.00210

Aoki, H., Onishi, A., Miyashita, M., Miyagawa, H., Yatou, O., and Saito, K. (2016). Involvement of the rice *OsSAUR51* gene in the auxin related field resistance mechanism against bacterial blight disease. *Japan Agric. Res. Q.* 50, 219–227. doi: 10.6090/jarq.50.219

Bajji, M., Kinet, J. M., and Lutts, S. (2002). The use of the electrolyte leakage method for assessing cell membrane stability as a water stress tolerance test in durum wheat. *Plant Growth Reg.* 36, 61–70. doi: 10.1023/A:1014732714549

Bargsten, J. W., Nap, J. P., Sanchez-Perez, G. F., and van Dijk, A. D. (2014). Prioritization of candidate genes in QTL regions based on associations between traits and biological processes. *BMC Plant Biol.* 14:330. doi: 10.1186/s12870-014-0330-3

Barrs, H. D. (1968). "Determination of water deficits in plant tissues," in *Water Deficits and Plant Growth*, ed T. T. Kozlowski (New York, NY: Academic Press), 235–368.

Bates, L., Waldren, R. P., and Teare, I. D. (1973). Rapid determination of free proline for water-stress studies. *Plant Soil* 39, 205–207. doi: 10.1007/BF00018060

Baum, M., Grando, S., Backes, G., Jahoor, A., Sabbagh, A., and Ceccarelli, S. (2003). QTLs for agronomic traits in the Mediterranean environment identified in recombinant inbred lines of the cross 'Arta' x*H. spontaneum* 41–1. *Theor. Appl. Genet.* 107, 1215–1225. doi: 10.1007/s00122-003-1357-2

Baum, M., von Korff, M., Guo, P., Lakew, B., Udupa, S. M., Sayed, H., et al. (2007). "Molecular approaches and breeding strategies for drought tolerance in barley," in *Genomic Assisted Crop Improvement: Vol 2. Genomics Applications in Crops*, eds R. Varshney, R. Tuberosa (Dordrecht: Springer), 51–79. doi: 10.1007/978-1-4020-6297-1

Bertholdsson, N., Holefors, A., Macaulay, M., and Crespo-Herrera, L. A. (2015). QTL for chlorophyll fluorescence of barley plants grown at low oxygen concentration in hydroponics to simulate waterlogging. *Euphytica* 201, 357–365. doi: 10.1007/s10681-014-1215-0

Bouslama, M., and Schapaugh, W. T. Jr. (1984). Stress tolerance in soybeans. I. Evaluation of three screening techniques for heat and drought tolerance. *Crop Sci.* 24, 933–937. doi: 10.2135/cropsci1984.0011183X002400050026x

Bray, E. A. (1997). Plant responses to water deficit. *Trends Plant Sci.* 2, 48-54. doi: 10.1016/S1360-1385(97)82562-9

Bray, E. A. (2007). "Molecular and physiological responses to water-deficit stress," in *Advances in Molecular Breeding Toward Drought and Salt Tolerant Crops*, eds M. A. Jenks, P. M. Hasegawa, and S. M. Jain (Dordrecht: Springer), 121–140.

Capelle, V., Remoué, C., Moreau, L., Reyss, A., Mahé, A., Massonneau, A., et al. (2010). QTLs and candidate genes for desiccation and abscisic acid content in maize kernels. *BMC Plant Biol.* 10:2. doi: 10.1186/1471-2229-10-2

Cattivelli, L., Ceccarelli, S., Romagosa, I., and Stanca, M. (2011). "Abiotic stresses in barley: problems and solutions," in *Barley: Production, Improvement, and Uses*, ed S. E. Ullrich (Oxford, UK: Blackwell Publishing Ltd.), 282–306.

Chae, K., Isaacs, C. G., Reeves, P. H., Maloney, G. S., Muday, G. K., Nagpal, P., et al. (2012). Arabidopsis SMALL AUXIN UP RNA63 promotes hypocotyl and stamen filament elongation. *Plant J.* 71, 684–697. doi: 10.1111/j.1365-313X.2012.05024.x

Chander, S., Guo, Y. Q., Yang, X. H., Yan, J. B., Zhang, Y. R., Song, T. M., et al. (2008). Genetic dissection of tocopherol content and composition in maize grain using quantitative trait loci analysis and the candidate gene approach. *Mol. Breed.* 22, 353–365. doi: 10.1007/s11032-008-9180-8

Chen, G., Krugman, T., Fahima, T., Chen, K., Hu, Y., Roder, M., et al. (2010). Chromosomal regions controlling seedling drought resistance in Israeli wild barley, *Hordeum spontaneum* C. Koch. *Genet. Resour. Crop Evol.* 57, 85–99. doi: 10.1007/s10722-009-9453-z

Chi, W., Fang, P., Ma, J., and Zhang, L. (2015). Metabolites and chloroplast retrograde signaling. *Curr. Opin. Plant Biol.* 25, 32–38. doi: 10.1016/j.pbi.2015.04.006

Chmielewska, K., Rodziewicz, P., Swarcewicz, B., Sawikowska, A., Krajewski, P., Marczak, Ł., et al. (2016). Analysis of Drought-induced proteomic and metabolomic changes in barley (*Hordeum vulgare* L.) leaves and roots unravels some aspects of biochemical mechanisms involved in drought tolerance. *Front. Plant Sci.* 7:1108. doi: 10.3389/fpls.2016.01108

Choudhury, S., Panda, P., Sahoo, L., and Panda, S. K. (2013). Reactive oxygen species signaling in plants under abiotic stress. *Plant Signal. Behav.* 8:e23681. doi: 10.4161/psb.23681

Churchill, G. A., and Doerge, R. W. (1994). Empirical threshold values for quantitative trait mapping. *Genetics* 138, 963–971.

Close, T. J., Bhat, P. R., Lonardi, S., Wu, Y., Rostoks, N., Ramsay, L., et al. (2009). Development and implementation of high-throughput SNP genotyping in barley. *BMC Genomics* 10:582. doi: 10.1186/1471-2164-10-582

Collins, N. C., Tardieu, F., and Tuberosa, R. (2008). QTL approaches for improving crop performance under abiotic stress conditions: where do we stand? *Plant Physiol.* 147, 469–486. doi: 10.1104/pp.108.118117

Correa, J., Mamani, M., Muñoz-Espinoza, C., Laborie, D., Muñoz, C., Pinto, M., et al. (2014). Heritability and identification of QTLs and underlying candidate genes associated with the architecture of the grapevine cluster (*Vitis vinifera* L.). *Theor. Appl. Genet.* 127, 1143–1162. doi: 10.1007/s00122-014-2286-y

Cuesta-Marcos, A., Casas, A. M., Hayes, P. M., Gracia, M. P., Lasa, J. M., Ciudad, F., et al. (2009). Yield QTL affected by heading date in Mediterranean grown barley. *Plant Breed.* 128, 46–53. doi: 10.1111/j.1439-0523.2008.01510.x

de Miguel, M., Cabezas, J. A., de María, N., Sánchez-Gómez, D., Guevara, M. A., Vélez, M. D., et al. (2014). Genetic control of functional traits related to photosynthesis and water use efficiency in *Pinus pinaster* Ait. drought response: integration of genome annotation, allele association and QTL detection for candidate gene identification. *BMC Genomics* 15:464. doi: 10.1186/1471-2164-15-464

Diab, A. A., Kantety, R. V., Ozturk, N. Z., Benscher, D., Nachit, M. M., and Sorrells, M. E. (2008). Drought-inducible genes and differentially expressed sequence tags associated with components of drought tolerance in durum wheat. *Sci. Res. Essay* 3, 9–26.

Diab, A. A., Teulat-Merah, B., This, D., Ozturk, N. Z., Benscher, D., and Sorrells, M. E. (2004). Identification of drought-inducible genes and differentially expressed sequence tags in barley. *Theor. Appl. Genet.* 109, 1417–1425. doi: 10.1007/s00122-004-1755-0

Doyle, J. J., and Doyle, J. L. (1987). A rapid DNA isolation procedure for small quantities of fresh leaf tissue. *Phytochem. Bull.* 19, 11–15.

Du, H., Liu, H., and Xiong, L. (2013). Endogenous auxin and jasmonic acid levels are differentially modulated by abiotic stresses in rice. *Front. Plant Sci.* 4:397. doi: 10.3389/fpls.2013.00397

Fan, Y., Shabala, S., Ma, Y., Xu, R., and Zhou, M. (2015). Using QTL mapping to investigate the relationships between abiotic stress tolerance (drought and salinity) and agronomic and physiological traits. *BMC Genomics* 16:43. doi: 10.1186/s12864-015-1243-8

Fang, Y., and Xiong, L. (2015). General mechanisms of drought response and their application in drought resistance improvement in plants. *Cell Mol. Life Sci.* 72, 673–689. doi: 10.1007/s00018-014-1767-0

FAO (2016). *FAOSTAT Database Collections. Food and Agriculture Organization of the United Nations*. Available online at: http://faostat3.fao.org/ (Accessed September 12, 2017).

Farooq, M., Wahid, A., Kobayashi, N., Fujita, D., and Basra, S. M. A. (2009). Plant drought stress: effects, mechanisms and management. *Agron. Sustain. Dev.* 29, 185–212. doi: 10.1051/agro:2008021

Filek, M., Łabanowska, M., Kościelniak, J., Biesaga-Kościelniak, J., Kurdziel, M., Szarejko, I., et al. (2015). Characterization of barley leaf tolerance to drought stress by chlorophyll fluorescence and electron paramagnetic resonance studies. *J. Agro. Crop Sci.* 201, 228–240. doi: 10.1111/jac.12063

Filek, M., Łabanowska, M., Kurdziel, M., Wesełucha-Birczynska, A., and Bednarska-Kozakiewicz, E. (2016). Structural and biochemical response of chloroplasts in tolerant and sensitive barley genotypes to drought stress. *J. Plant Physiol.* 207, 61–72. doi: 10.1016/j.jplph.2016.09.012

Foyer, C. H., and Noctor, G. (2000). Oxygen processing in photosynthesis: regulation and signalling. *New Phytol.* 146, 359–388. doi: 10.1046/j.1469-8137.2000.00667.x

Francia, E., Barabaschi, D., Tondelli, A., Laidò, G., Rizza, F., Stanca, A. M., et al. (2007). Fine mapping of a *HvCBF* gene cluster at the frost resistance locus *Fr-H2* in barley. *Theor. Appl. Genet.* 115, 1083–1091. doi: 10.1007/s00122-007-0634-x

Furukawa, J., Yamaji, N., Wang, H., Mitani, N., Murata, Y., Sato, K., et al. (2007). An aluminum-activated citrate transporter in barley. *Plant Cell Physiol.* 48, 1081–1091. doi: 10.1093/pcp/pcm091

Genty, B., Briantais, J.-M., and Baker, N. R. (1989). The relationship between the quantum yield of photosynthetic electron transport and quenching of chlorophyll fluorescence. *Biochem. Biophys. Acta* 990, 87–92. doi: 10.1016/S0304-4165(89)80016-9

Giordano, D., Provenzano, S., Ferrandino, A., Vitali, M., Pagliarani, C., Roman, F., et al. (2016). Characterization of a multifunctional caffeoyl-CoA O-methyltransferase activated in grape berries upon drought stress. *Plant Physiol. Biochem.* 101, 23–32. doi: 10.1016/j.plaphy.2016.01.015

Górny, A. G. (2001). Variation in utilization efficiency and tolerance to reduced water and nitrogen supply among wild and cultivated barleys. *Euphytica* 117, 59–66. doi: 10.1023/A:1004061709964

Gould, K. S., Lamotte, O., Klinguer, A., Pugin, A., and Wendehenne, D. (2003). Nitric oxide production in tobacco leaf cells: a generalized stress response? *Plant Cell Environ.* 26, 1851–1862. doi: 10.1046/j.1365-3040.2003.01101.x

Grzesiak, M., Filek, M., Barbasz, A., Kreczmer, B., and Hartikainen, H. (2013). Relationships between polyamines, ethylene, osmoprotectants and antioxidant enzymes activities in wheat seedlings after short-term PEG- and NaCl-induced stresses. *Plant Growth Regul.* 69, 177–189. doi: 10.1007/s10725-012-9760-9

Guo, P., Baum, M., Varshney, R. K., Graner, A., Grando, S., and Ceccarvelli, S. (2008). QTLs for chlorophyll and chlorophyll fluorescence parameters in barley under post-flowering drought. *Euphytica* 163, 203–214. doi: 10.1007/s10681-007-9629-6

Guo, Y., Jiang, Q., Hu, Z., Sun, X., Fan, S., and Zhang, H. (2018). Function of the auxin-responsive gene TaSAUR75 under salt and drought stress. *The Crop Journal.* 6, 181–190. doi: 10.1016/j.cj.2017.08.005

Honsdorf, N., March, T. J., Hecht, A., Eglinton, J., and Pillen, K. (2014). Evaluation of juvenile drought stress tolerance and genotyping by sequencing with wild barley introgression lines. *Mol. Breed.* 34, 1475–1495. doi: 10.1007/s11032-014-0131-2

Inigo, S., Alvarez, M. J., Strasser, B., Califano, A., and Cerdán, P. D. (2012). PFT1, the MED25 subunit of the plant mediator complex, promotes flowering through CONSTANS dependent and independent mechanisms in Arabidopsis. *Plant J.* 69, 601–612. doi: 10.1111/j.1365-313X.2011.04815.x

Janeczko, A., Biesaga-Kościelniak, J., Oklestkova, J., Filek, M., Dziurka, M., Szarek-Łukaszewska, G., et al. (2010). Role of 24-Epibrassinolide in wheat production: physiological activity and uptake. *J. Agron. Crop Sci.* 196, 311–321. doi: 10.1111/j.1439-037X.2009.00413.x

Janiak, A., Kwasniewski, M., Sowa, M., Gajek, K., Zmuda, K., Kościelniak, J., et al. (2018). No time to waste: transcriptome study reveals that drought tolerance in barley may be attributed to stressed-like expression patterns that exist before the occurrence of stress. *Front. Plant Sci.* 8:2212. doi: 10.3389/fpls.2017.02212

Johnston, M. L., Luethy, M. H., Miernyk, J. A., and Randall, D. D. (1997). Cloning and molecular analyses of the *Arabidopsis thaliana* plastid pyruvate dehydrogenase subunits. *Biochim. Biophys. Acta* 1321, 200–206. doi: 10.1016/S0005-2728(97)00059-5

Kai, H., Wu, W., and Gan, S. S. (2013). *SAUR36*, a small auxin up RNA gene, is involved in the promotion of leaf senescence in Arabidopsis. *Plant Physiol.* 161, 1002–1009. doi: 10.1104/pp.112.212787

Kalaji, M. H., Bosa, K., Kościelniak, J., and Hossain, Z. (2011). Chlorophyll *a* fluorescence - a useful tool for the early detection of temperature stress in spring barley (*Hordeum vulgare* L.). *OMICS* 15, 925–934. doi: 10.1089/omi.2011.0070

Kalladan, R., Worch, S., Roletschek, H., Harshavardhan, V. T., Kuntze, L., Seiler, C., et al. (2013). Identification of quantitative trait loci contributing to yield and seed quality parameters under terminal drought in barley advanced backcross lines. *Mol. Breed.* 32, 71–90. doi: 10.1007/s11032-013-9853-9

Kazan, K., and Lyons, R. (2016). The link between flowering time and stress tolerance. *J. Exp. Bot.* 67, 47–60. doi: 10.1093/jxb/erv441

Kolbert, Z., Bartha, B., and Erdei, L. (2005). Generation of nitric oxide in roots of *Pisum sativum*, *Triticum aestivum* and *Petroselinum crispum* plants under osmotic and drought stress. *Acta Biol. Szegediensis* 49, 13–16.

Koussevitzky, S., Suzuki, N., Huntington, S., Armijo, L., Sha, W., Cortes, D., et al. (2008). Ascorbate peroxidase 1 plays a key role in the response of *Arabidopsis thaliana* to stress combination. *J. Biol. Chem.* 283, 34197–34203. doi: 10.1074/jbc.M806337200

Krishnamurthy, A., and Rathinasabapathi, B. (2013). Oxidative stress tolerance in plants: novel interplay between auxin and reactive oxygen species signaling. *Plant Signal. Behav.* 8:e25761. doi: 10.4161/psb.25761

Kumar, J., Gupta, D. S., Gupta, S., Dubey, S., Gupta, P., and Kumar, S. (2017). Quantitative trait loci from identification to exploitation for crop improvement. *Plant Cell Rep*. 36, 1187–1213. doi: 10.1007/s00299-017-2127-y

Lam, K. C., Ibrahim, R. K., Behdad, B., and Dayanandan, S. (2007). Structure, function, and evolution of plant O-methyltransferases. *Genome* 50, 1001–1013. doi: 10.1139/G07-077

Li, H. B., Vaillancourt, R., Mendham, N., and Zhou, M. X. (2008). Comparative mapping of quantitative trait loci associated with waterlogging tolerance in barley (*Hordeum vulgare* L.). *BMC Genomics* 9:401. doi: 10.1186/1471-2164-9-401

Li, W. T., Liu, C., Liu, Y. X., Pu, Z. E., Dai, S. F., Wang, J. R., et al. (2013). Meta-analysis of QTL associated with tolerance to abiotic stresses in barley. *Euphytica* 189, 31–49. doi: 10.1007/s10681-012-0683-3

Li, Y., Zhang, J., Zhang, J., Hao, L., Hua, J., Duan, L., et al. (2013). Expression of an Arabidopsis molybdenum cofactor sulphurase gene in soybean enhances drought tolerance and increases yield under field conditions. *Plant Biotech. J.* 11, 747–758. doi: 10.1111/pbi.12066

Liu, T., Zhang, L., Yuan, Z., Hu, X., Lu, M., Wang, W., et al. (2013). Identification of proteins regulated by ABA in response to combined drought and heat stress in maize roots. *Acta Physiol. Plant* 35, 501–513. doi: 10.1007/s11738-012-1092-x

Liu, X., Fan, Y., Mak, M., Babla, M., Holford, P., Wang, F., et al. (2017). QTLs for stomatal and photosynthetic traits related to salinity tolerance in barley. *BMC Genomics* 18:9. doi: 10.1186/s12864-016-3380-0

Lopes-Caitar, V. S., de Carvalho, M. C., Darben, L. M., Kuwahara, M. K., Nepomuceno, A. L., Dias, W. P., et al. (2013). Genome-wide analysis of the *Hsp20* gene family in soybean: comprehensive sequence, genomic organization and expression profile analysis under abiotic and biotic stresses. *BMC Genomics* 14:577. doi: 10.1186/1471-2164-14-577

Lück, H. (1962). "Peroxydase," in *Methoden der Enzymatischen Analyse*, ed H. U. Bergmeyer (Weinheim; Verlag Chemie: GmbH), 895–897.

Mammadov, J., Aggarwal, R., Buyyarapu, R., and Kumpatla, S. (2012). SNP markers and their impact on plant breeding. *Int. J. Plant Genome* 2012:728398. doi: 10.1155/2012/728398

Mansour, E., Casas, A. M., Gracia, M. P., Molina-Cano, J. L., Moralejo, M., Cattivelli, L., et al. (2014). Quantitative trait loci for agronomic traits in an elite barley population for Mediterranean conditions. *Mol. Breed.* 33, 249–265. doi: 10.1007/s11032-013-9946-5

Marin, J. A., Andreu, P., Carrasco, A., and Arbeloa, A. (2009). Proline content in root tissues and root exudates as a response to salt stress of excised root cultures of *Prunus* fruit tree rootstocks. *Información Técnica Económica Agraria* 105, 282–290.

Mayer, K. F. X., Waugh, R., Langridge, P., Close, T. J., Wise, R. P., Graner, A., et al. (2012). A physical, genetic and functional sequence assembly of the barley genome. *Nature* 491, 711–716. doi: 10.1038/nature11543

McCord, J. M., and Fridovich, I. (1969). Superoxide dismutase: an enzymatic function for erythrocuprein (hemocuprein). *J. Biol. Chem.* 244, 6049–6055

Mendel, R. R. (2013). The molybdenum cofactor. *J. Biol. Chem.* 288, 13165–13172. doi: 10.1074/jbc.R113.455311

Mendel, R. R., and Haensch, R. (2002). Molybdoenzymes and molybdenum cofactor in plants. *J. Exp. Bot.* 53, 1689–1698. doi: 10.1093/jxb/erf038

Mentzen, W. I., Peng, J., Ransom, N., Nikolau, B. J., and Wurtele, E. S. (2008). Articulation of three core metabolic processes in Arabidopsis: fatty acid biosynthesis, leucine catabolism and starch metabolism. *BMC Plant Biol.* 8:76. doi: 10.1186/1471-2229-8-76

Mikołajczak, K., Kuczynska, A., Krajewski, P., Sawikowska, A., Surma, M., Ogrodowicz, P., et al. (2017). Quantitative trait loci for plant height in Maresi × CamB barley population and their associations with yield-related traits under different water regimes. *J. Appl. Genet.* 58, 23–35.doi: 10.1007/s13353-016-0358-1

Mikołajczak, K., Ogrodowicz, P., Gudyś, K., Krystkowiak, K., Sawikowska, A., Frohmberg, W., et al. (2016). Quantitative trait loci for yield and yield- related traits in spring barley populations derived from crosses between European and Syrian cultivars. *PLoS ONE* 11:e0155938. doi: 10.1371/journal.pone.0155938

Mir, R. R., Zaman-Allah, M., Sreenivasulu, N., Trethowan, R., and Varshney, R. K. (2012). Integrated genomics, physiology and breeding approaches for improving drought tolerance in crops. *Theor. Appl. Genet.* 125, 625–645. doi: 10.1007/s00122-012-1904-9

Monclus, R., Leple, J. C., Bastien, C., Bert, P. F., Villar, M., Marron, N., et al. (2012). Integrating genome annotation and QTL position to identify candidate genes for productivity, architecture and water-use efficiency in *Populus* spp. *BMC Plant Biol.* 12:173. doi: 10.1186/1471-2229-12-173

Mora, F., Quitral, Y. A., Matus, I., Russell, J., Waugh, R., and del Pozo, A. (2016). SNP-based QTL mapping of 15 complex traits in barley under rain-fed and well-watered conditions by a mixed modeling approach. *Front. Plant Sci.* 7:909. doi: 10.3389/fpls.2016.00909

Munemasa, S., Muroyama, D., Nagahashi, H., Nakamura, Y., Mori, I. C., and Murata, Y. (2013). Regulation of reactive oxygen species-mediated abscisic acid signalling in guard cells and drought tolerance by glutathione. *Front. Plant Sci.* 4:472. doi: 10.3389/fpls.2013.00472

Nahar, K., Hasanuzzaman, M., Alam, M. M., and Fujita, M. (2015). Glutathione-induced drought stress tolerance in mung bean: coordinated roles of the antioxidant defence and methylglyoxal detoxification systems. *AoB Plants* 7:plv069. doi: 10.1093/aobpla/plv069

Nakabayashi, R., Yonekura-Sakakibara, K., Urano, K., Suzuki, M., Yamada, Y., Nishizawa, T., et al. (2014). Enhancement of oxidative and drought tolerance in Arabidopsis by overaccumulation of antioxidant flavonoids. *Plant J.* 77, 367–379. doi: 10.1111/tpj.12388

Noctor, G., Mhamdi, A., and Foyer, C. H. (2014). *Plant Physiol.* 164, 1636–1648. doi: 10.1104/pp.113.233478

Ogrodowicz, P., Adamski, T., Mikołajczak, K., Kuczynska, A., Surma, M., Krajewski, P., et al. (2017). QTLs for earliness and yield-forming traits in the Lubuski × CamB barley RIL population under various water regimes. *J. Appl. Genet.* 58, 49–65. doi: 10.1007/s13353-016-0363-4

Pflieger, S., Lefebvre, V., and Causse, M. (2001). The candidate gene approach in plant genetics: a review. *Mol. Breed.* 7:275. doi: 10.1023/A:1011605013259

Piasecka, A., Sawikowska, A., Kuczynska,A., Ogrodowicz, P., Mikolajczak, K., Krystkowiak, K., et al. (2017). Drought-related secondary metabolites of barley (*Hordeum vulgare* L.) leaves and their metabolomic quantitative trait loci. *Plant J.* 89, 898–913. doi: 10.1111/tpj.13430

Płazek, A., Dubert, F., Kościelniak, J., Tatrzanska, M., Maciejewski, M., Gondek, K., and Zurek, G. (2014). Tolerance of *Miscanthus×giganteus* to salinity depends on initial weight of rhizomes as well as high accumulation of potassium and proline in leaves. *Ind. Crops Prod.* 52, 278–285. doi: 10.1016/j.indcrop.2013.10.041

Pospisil, P. (2016). Production of reactive oxygen species by photosystem II as a response to light and temperature stress. *Front. Plant Sci.* 7:1950. doi: 10.3389/fpls.2016.01950

Potokina, E., Druka, A., Luo, Z., Wise, R., Waugh, R., and Kearsey, M. (2008). Gene expression quantitative trait locus analysis of 16000 barley genes reveals

a complex pattern of genome-wide transcriptional regulation. *Plant, J.* 53, 90–101. doi: 10.1111/j.1365-313X.2007.03315.x

Prioretti, L., Gontero, B., Hell, R., and Giordano, M. (2014). Diversity and regulation of ATP sulfurylase in photosynthetic organisms. *Front. Plant Sci.* 5:597. doi: 10.3389/fpls.2014.00597

Proost, S., Van Bel, M., Vaneechoutte, D., Van de Peer, Y., Inzé, D., Mueller-Roeber, B., et al. (2015). PLAZA 3.0: an access point for plant comparative genomics. *Nucleic Acids Res.* 43, D974–D981. doi: 10.1093/nar/gku986

Pyngrope, S., Bhoomika, K., and Dubey, R. S. (2013). Reactive oxygen species, ascorbate-glutathione pool, and enzymes of their metabolism in drought-sensitive and tolerant indica rice (*Oryza sativa* L.) seedlings subjected to progressing levels of water deficit. *Protoplasma* 250, 585–600. doi: 10.1007/s00709-012-0444-0

Rahman, A. (2013). Auxin: a regulator of cold stress response. *Physiol. Plant.* 147, 28–35. doi: 10.1111/j.1399-3054.2012.01617.x

Ren, H., and Gray, W. M. (2015). SAUR proteins as effectors of hormonal and environmental signals in plant growth. *Mol. Plant* 8, 1153–1164. doi: 10.1016/j.molp.2015.05.003

Roychoudhury, A., Paul, S., and Basu, S. (2013). Cross-talk between abscisic acid-dependent and abscisic acid-independent pathways during abiotic stress. *Plant Cell Rep.* 32, 985–1006. doi: 10.1007/s00299-013-1414-5

Sah, S. K., Reddy, K. R., and Li, J. (2016). Abscisic acid and abiotic stress tolerance in crop plants. *Front. Plant Sci.* 7:571. doi: 10.3389/fpls.2016.00571

Salvi, S., and Tuberosa, R. (2007). "Cloning QTLs in plants," *in Genomics-Assisted Crop Improvement, Vol. 1, Genomics Approaches and Platforms*, eds R. K. Varshney and R. Tuberosa (Berlin; Heidelberg: Springer), 207–225.

Salvi, S., and Tuberosa, R. (2015). The crop QTLome comes of age. *Curr. Opin. Biotechnol.* 32, 179–185.doi: 10.1016/j.copbio.2015.01.001

Santhanagopalan, I., Basha, E., Ballard, K. N., Bopp, N. E., and Vierling, E. (2015). "Model chaperones: small heat shock proteins from plants," in *The Big Book on Small Heat Shock Proteins*, eds R. M. Tanguay and L. E. Hightower (Berlin; Heidelberg: Springer), 119–153.

Sarkar, N. K., Kim, Y. K., and Grover, A. (2009). Rice *sHsp* genes: genomic organization and expression profiling under stress and development. *BMC Genomics* 10:393. doi: 10.1186/1471-2164-10-393

Sayed, M. A., Schumann, H., Pillen, K., Naz, A. A., and Léon, J. (2012). AB-QTL analysis reveals new alleles associated to proline accumulation and leaf wilting under drought stress conditions in barley (*Hordeum vulgare* L.). *BMC Genet.* 13:61. doi: 10.1186/1471-2156-13-61

Scharf, K. D., Siddique, M., and Vierling, E. (2001). The expanding family of *Arabidopsis thaliana* small heat stress proteins and a new family of proteins containing alpha-crystallin domains (Acd proteins). *Cell Stress Chaperones* 6, 225–237. doi: 10.1379/1466-1268(2001)006<0225:TEFOAT>2.0.CO;2

Sehgal, D., Rajaram, V., Armstead, I. P., Vadez, V., Yadav, Y. P., Hash, C. T., et al. (2012). Integration of gene-based markers in a pearl millet genetic map for identification of candidate genes underlying drought tolerance quantitative trait loci. *BMC Plant Biol.* 12:9. doi: 10.1186/1471-2229-12-9

Seo, M., and Koshiba, T. (2002). Complex regulation of ABA biosynthesis in plants. *Trends Plant Sci.* 7, 41–48. doi: 10.1016/S1360-1385(01)02187-2

Shi, H., Chen, L., Ye, T., Liu, X., Ding, K., and Chan, Z. (2014). Modulation of auxin content in Arabidopsis confers improved drought stress resistance. *Plant Physiol. Biochem.* 82, 209–217. doi: 10.1016/j.plaphy.2014.06.008

Shinozaki, K., and Yamaguchi-Shinozaki, K. (2007). Gene networks involved in drought stress response and tolerance. *J. Exp. Bot.* 58, 221–227. doi: 10.1093/jxb/erl164

Siddiqui, M. H., Al-Whaibi, M. H., and Basalah, M. O. (2011). Role of nitric oxide in tolerance of plants to abiotic stress. *Protoplasma* 248, 447–455. doi: 10.1007/s00709-010-0206-9

Surówka, E., Dziurka, M., Kocurek, M., Goraj, S., Rapacz, M., and Miszalski, M. (2016). Effects of exogenously applied hydrogen peroxide on antioxidant and osmoprotectant profiles and the C_3-CAM shift in the halophyte *Mesembryanthemum crystallinum* L. *J. Plant Physiol.* 200, 102–110. doi: 10.1016/j.jplph.2016.05.021

Sutton, T., Baumann, U., Hayes, J., Collins, N. C., Shi, B. J., Schnurbusch, T., et al. (2007). Boron-toxicity tolerance in barley arising from efflux transporter amplification. *Science* 318, 1446–1449. doi: 10.1126/science.1146853

Szechyńska-Hebda, M., Skrzypek, E., Dabrowska, G., Wedzony, M., and van Lammeren, A. (2012). The effect of endogenous hydrogen peroxide induced by cold treatment in the improvement of tissue regeneration efficiency. *Acta Physiol. Plant.* 34, 547–560. doi: 10.1007/s11738-011-0852-3

Szira, F., Börner, A., Neumann, K., Nezhad, K. Z., Galiba, G., and Balint, A. F. (2011). Could EST-based markers be used for the marker-assisted selection of drought tolerant barley (*Hordeum vulgare*) lines? *Euphytica* 178, 373–391. doi: 10.1007/s10681-010-0317-6

Talamé, V., Sanguineti, M. C., Chiapparino, E., Bahri, H., Salem, M. B., Forster, B. P., et al. (2004). Identification of *Hordeum spontaneum* QTL alleles improving field performance of barley grown under rainfed conditions. *Ann. Appl. Biol.* 144, 309–319. doi: 10.1111/j.1744-7348.2004.tb00346.x

Templer, S. E., Ammon, A., Pscheidt, D., Ciobotea, O., Schuy, C., McCollum, C., et al. (2017). Metabolite profiling of barley flag leaves under drought and combined heat and drought stress reveals metabolic QTLs for metabolites associated with antioxidant defense. *J. Exp. Bot.* 68, 1697–1713. doi: 10.1093/jxb/erx038

Teulat, B., Borries, C., and This, D. (2001a). New QTLs identified for plant water-status, water soluble carbohydrate and osmotic adjustment in a barley population grown in a growth-chamber under two water regimes. *Theor. Appl. Genet.* 103, 161–170. doi: 10.1007/s001220000503

Teulat, B., Merah, O., Souyris, I., and This, D. (2001b). QTLs for agronomic traits from Mediterranean barley progeny grown in several environments. *Theor. Appl. Genet.* 103, 774–787. doi: 10.1007/s001220100619

Teulat, B., Monneveux, P., Wery, J., Borries, C., Souyris, I., Charrier, A., et al. (1997). Relationships between relative water content and growth parameters under water stress in barley: a QTL study. *New Phytol.* 137, 99–107. doi: 10.1046/j.1469-8137.1997.00815.x

Teulat, B., This, D., Khairallah, M., Borries, C., Ragot, C., Sourdille, P., et al. (1998). Several QTLs involved in osmotic-adjustment trait variation in barley (*Hordeum vulgare* L.). *Theor. Appl. Genet.* 96, 688–698. doi: 10.1007/s001220050790

Teulat, B., Zoumarou-Wallis, N., Rotter, B., Salem, M. B., Bahri, H., and This, D. (2003). QTL for relative water content in field-grown barley and their stability across Mediterranean environments. *Theor. Appl. Genet.* 108, 181–188. doi: 10.1007/s00122-003-1417-7

Tondelli, A., Francia, E., Visioni, A., Comadran, J., Mastrangelo, A. M., Akar, T., et al. (2014). QTLs for barley yield adaptation to Mediterranean environments in the 'Nure' × 'Tremois' biparental population. *Euphytica* 197, 73–86. doi: 10.1007/s10681-013-1053-5

Tuberosa, R., and Salvi, S. (2007). "Dissecting QTLs for tolerance to drought and salinity," in: *Advances in Molecular Breeding Toward Drought And Salt Tolerant Crops*, eds M. A. Jenks, P. M. Hasegawa, and S. M. Jain (Dordrecht: Springer), 381–411.

Turck, F., Fornara, F., and Coupland, G. (2008). Regulation and identity of florigen: *FLOWERING LOCUS T* moves center stage. *Annu. Rev. Plant Biol.* 59, 573–594. doi: 10.1146/annurev.arplant.59.032607.092755

Van Ooijen, J. W. (2004). MapQTL® 5, *Software for the Mapping of Quantitative Trait loci in Experimental Populations*. Wageningen: Plant Research International.

Van Ooijen, J. W., and Voorrips, R. E. (2001). *JoinMap® 3.0, Software for the Calculation of Genetic Linkage Maps.* Wageningen: Plant Research International.

Varshney, R. K., Marcel, T. C., Ramsay, L., Russell, J., Röder, M. S., Stein, N., et al. (2007). A high density barley microsattelite consensus map with 775 SSR loci. *Theor. Appl. Genet.* 114, 1091–1103. doi: 10.1007/s00122-007-0503-7

von Korff, M., Grando, S., Del Greco, A., This, D., Baum, M., and Ceccarelli, S. (2008). Quantitative trait loci associated with adaptation to Mediterranean dryland conditions in barley. *Theor. Appl. Genet.* 117, 653–669. doi: 10.1007/s00122-008-0787-2

Voorrips, R. E. (2002). MapChart: software for the graphical presentation of linkage maps and QTLs. *J. Hered.* 93, 77–78. doi: 10.1093/jhered/93.1.77

Wang, J., Yang, J., Jia, Q., Zhu, J., Shang, Y., Hua, W., et al. (2014). A new QTL for plant height in barley (*Hordeum vulgare* L.) showing no negative effects on grain yield. *PLoS ONE* 9:e90144. doi: 10.1371/journal.pone.0090144. eCollection 2014.

Wang, P., Du, Y., Hou, Y. J., Zhao, Y., Hsu, C. C., Yuan, F., et al. (2015). Nitric oxide negatively regulates abscisic acid signaling in guard cells by S-nitrosylation of OST1. *Proc. Natl. Acad. Sci. U.S.A.* 112, 613–618. doi: 10.1073/pnas.1423481112

Waters, E. R., Aevermann, B. D., and Sanders-Reed, Z. (2008). Comparative analysis of the small heat shock proteins in three angiosperm genomes identifies new subfamilies and reveals diverse evolutionary patterns. *Cell Stress Chaperones.* 13, 127–142. doi: 10.1007/s12192-008-0023-7

Wójcik-Jagła, M., Rapacz, M., Tyrka, M., Kościelniak, J., Crissy, K., and Zmuda, K. (2013). Comparative QTL analysis of early short time drought tolerance in Polish fodder and malting spring barleys. *Theor. Appl. Genet.* 126, 3021–3034. doi: 10.1007/s00122-013-2190-x

Wojtania, A., Skrzypek, E., and Gabryszewska, E. (2016). Morphological and biochemical responses to gibberellic acid in *Magnolia* × *'Spectrum' in vitro*. *Acta Biol. Cracov. Ser. Bot.* 58, 103–111. doi: 10.1515/abcsb-2016-0010

Wu, J., Liu, S., He, Y., Guan, X., Zhu, X., Cheng, L., et al. (2012). Genome-wide analysis of SAUR gene family in Solanaceae species. *Gene* 509, 38–50. doi: 10.1016/j.gene.2012.08.002

Wu, X. L., and Hu, Z. L. (2012). Meta-analysis of QTL mapping experiments. *Methods Mol. Biol.* 871, 145–171. doi: 10.1007/978-1-61779-785-9_8

Xiong, L., Ishitani, M., Lee, H., and Zhu, J. K. (2001).The Arabidopsis *los5/aba3* locus encodes amolybdenum cofactor sulfurase and modulates cold stress- and osmotic stress-responsive gene expression. *Plant Cell* 13, 2063–2083. doi: 10.1105/tpc.13.9.2063

Xiong, L., Schumaker, K. S., and Zhu, J. K. (2002). Cell signaling during cold, drought, and salt stress. *Plant Cell* 14, 165–183. doi: 10.1105/tpc.000596

Yamaguchi, M., Valliyodan, B., Zhang, J., Lenoble, M. E., Yu, O., Rogers, E. E., et al. (2010). Regulation of growth response to water stress in the soybean primary root. I. Proteomic analysis reveals region-specific regulation of phenylpropanoid metabolism and control of free iron in the elongation zone. *Plant Cell Environ.* 33, 223–243. doi: 10.1111/j.1365-3040.2009.02073.x

Yang, H., Mu, J., Chen, L., Feng, J., Hu, J., Li, L., et al. (2015). S-nitrosylation positively regulates ascorbate peroxidase activity during plant stress responses. *Plant Physiol.* 167, 1604–1615. doi: 10.1104/pp.114.255216

Zhang, X., Shabala, S., Koutoulis, A., Shabala, L., and Zhou, M. (2017). Meta-analysis of major QTL for abiotic stress tolerance in barley and implications for barley breeding. *Planta* 245, 283–295. doi: 10.1007/s00425-016-2605-4

Conflict of Interest Statement: The authors declare that the research was conducted in the absence of any commercial or financial relationships that could be construed as a potential conflict of interest.

frontiers in Plant Science

ORIGINAL RESEARCH
published: 23 August 2017
doi: 10.3389/fpls.2017.01453

Activation of ABA Receptors Gene *GhPYL9-11A* Is Positively Correlated with Cotton Drought Tolerance in Transgenic *Arabidopsis*

Chengzhen Liang[1†], Yan Liu[1†], Yanyan Li[1†], Zhigang Meng[1], Rong Yan[1,2], Tao Zhu[1], Yuan Wang[1], Shujing Kang[1], Muhammad Ali Abid[1], Waqas Malik[1,3], Guoqing Sun[1], Sandui Guo[1] and Rui Zhang[1]**

[1] Biotechnology Research Institute, Chinese Academy of Agricultural Sciences, Beijing, China, [2] College of Agronomy and Biotechnology, Southwest University, Chongqing, China, [3] Genomics Lab, Department of Plant Breeding and Genetics, Bahauddin Zakariya University, Multan, Pakistan

OPEN ACCESS

Edited by:
Hui Xia,
Shanghai Agrobiological Gene Center, China

Reviewed by:
Abid Ali,
University of Agriculture, Faisalabad, Pakistan
Andrew Wood,
Southern Illinois University Carbondale, United States

***Correspondence:**
Rui Zhang
zhangrui@caas.cn
Sandui Guo
guosandui@caas.cn

[†] *These authors have contributed equally to this work.*

Specialty section:
This article was submitted to Crop Science and Horticulture, a section of the journal Frontiers in Plant Science

Received: *11 May 2017*
Accepted: *04 August 2017*
Published: *23 August 2017*

Citation:
Liang C, Liu Y, Li Y, Meng Z, Yan R, Zhu T, Wang Y, Kang S, Ali Abid M, Malik W, Sun G, Guo S and Zhang R (2017) Activation of ABA Receptors Gene GhPYL9-11A Is Positively Correlated with Cotton Drought Tolerance in Transgenic Arabidopsis. Front. Plant Sci. 8:1453. doi: 10.3389/fpls.2017.01453

The sensitivity to abscisic acid (ABA) by its receptors, pyrabactin resistance-like proteins (PYLs), is considered a most important factor in activating the ABA signal pathway in response to abiotic stress. However, it is still unknown which PYL is the crucial ABA receptor mediating response to drought stress in cotton (*Gossypium hirsutum* L.). Here, we reported the identification and characterization of highly induced ABA receptor GhPYL9-11A in response to drought in cotton. It is observed that *GhPYL9-11A* was highly induced by ABA treatment. GhPYL9-11A binds to protein phosphatase 2Cs (PP2Cs) in an ABA-independent manner. Moreover, the GhPYL-11A-PP2C interactions are partially disrupted by mutations, proline (P84) and histidine (H111), in the gate-latch region. Transgenic *Arabidopsis* overexpressing *GhPYL9-11A* plants were hypersensitive to ABA during seed germination and early seedling stage. Further, the increased in root growth and up regulation of drought stress-related genes in transgenic *Arabidopsis* as compared to wild type confirmed the potential role of *GhPYL9-11A* in abiotic stress tolerance. Consistently, the expression level of *GhPYL9-11A* is on average higher in drought-tolerant cotton cultivars than in drought-sensitive cottons under drought treatment. In conclusion, the manipulation of *GhPYL9-11A* expression could be a useful strategy for developing drought-tolerant cotton cultivars.

Keywords: ABA, ABA receptor, GhPYL9, PP2C, seed germination, drought stress, cotton

INTRODUCTION

Abscisic acid (ABA) is a multifunctional phytohormone that regulates multiple aspects of plant growth and development, including seed dormancy and germination (Fang et al., 2008), vegetative development (Finkelstein et al., 2002), root elongation (Xing et al., 2016), leaf senescence (Liang et al., 2014), and fruit ripening (Zhang et al., 2009). ABA has also long been known to be a key endogenous messenger in the response to abiotic and biotic stresses, such as drought, salinity, cold, and pathogen infection (Choi et al., 2000; Xiong et al., 2002; Zhu, 2002; Sheard and Zheng, 2009; Yoshida et al., 2014). ABA-regulated stress responses include changes in gene expression, increased

stomatal closure, reduced transpiration rate, protection of photosynthesis, and regulation of plant growth.

Previous studies have demonstrated that pyrabactin resistance-like (PYL), clade A protein phosphatase 2C (PP2C), and sucrose non-fermenting 1- related protein kinase 2 (SnRK2) proteins are the three core components of the ABA signaling cascade (Park et al., 2009; Sheard and Zheng, 2009; Zhu, 2016). The primary step in initiating the ABA signaling pathway is triggered by the PYL ABA receptors (Sheard and Zheng, 2009), which contain a central hydrophobic ligand-binding pocket (Iyer et al., 2001). In the absence of ABA, two β-loops, termed the gate and latch, together with several nearby structural elements form a large open pocket for ligand binding. When ABA is present, ABA binds to this pocket, leading to a series of conformational rearrangements, including gate and latch closure, which sequester ABA within the pocket. The ABA-bound PYL receptor physically interacts with and sequesters the constitutive SnRK2 repressor, PP2C, allowing SnRK2 kinases autophosphorylation. ABA-activated SnRK2 kinases subsequently phosphorylate and activate downstream ABA-responsive element-binding transcription factors that induce the expression of ABA-responsive genes (Melcher et al., 2009; Miyazono et al., 2009; Nishimura et al., 2009).

The PYL proteins belong to the START/Bet V1 superfamily (Iyer et al., 2001). There are fourteen PYL members in *Arabidopsis*, and this family is divided into three subfamilies based on amino acid sequences similarity (Zhao et al., 2013, 2016). All PYL proteins have highly conserved amino-acid residues in key interaction domains, including ABA-binding pocket, and the two entrance loops. Despite these similar structural features, PYLs have distinct properties and different expression patterns that explain the versatility of ABA signaling in plant growth and development. For example, *Arabidopsis* PYR1, PYL1, and PYL2 are able to form dimers in solution, whereas PYL proteins 4–10 exist as monomers (Hao et al., 2011). PYR1, PYL1, PYL2, and PYL3 interact with several clade A PP2Cs in an ABA-dependent manner. In contrast, most other PYL proteins except for PYL7 inhibit PP2Cs independently of ABA (Bai et al., 2013; Li et al., 2013; Zhao et al., 2013). Recently, several genetic studies have elucidated the significance of these receptors in ABA response; *pyr1 pyl1 pyl2 pyl4* quadruple mutants show ABA insensitivity (Park et al., 2009; Nishimura et al., 2010; Gonzalez-Guzman et al., 2012), and a *pyl8* single mutant has altered ABA responses during seed germination and seedling growth, as well as decreased drought resistance (Antoni et al., 2013; Zhao et al., 2014). PYL9 enhances drought resistance by limiting transpiration water loss and regulating senescence in old leaves and growth in young tissues (Zhao et al., 2016). Moreover, both PYL9 and PYL8 act as critical regulators of lateral root formation in response to ABA (Xing et al., 2016).

Upland cotton (*Gossypium hirsutum* L.) is an important economic crop and is an important source of fiber and oil (Wang et al., 2012, 2017; Shan et al., 2014). Compared with the model plants *Arabidopsis* and rice, cotton has higher tolerance to drought and salt stress (Liang et al., 2016). However, its growth and development, as well as fiber yield and quality are also significantly affected by severe environmental conditions, especially drought stress (He et al., 2016). To date, a number of candidate genes for drought tolerance in cotton have been identified. Several stress-related genes, including *GhABF2* (Liang et al., 2016), *GhNAC2* (Gunapati et al., 2016), *GhATAF1* (He et al., 2016), *GhbHLH130* (Guang et al., 2014), *GhSARP1* (Liu et al., 2016), *GhMKK3* (Wang C. et al., 2016), *Di19-1* and *Di19-2* (Qin et al., 2016), have been shown to regulate stress response in an ABA-dependent manner. Therefore, understanding ABA signal transduction in cotton will accelerate the molecular breeding of stress-tolerant cotton cultivars.

Because ABA has an essential role in plant growth and development, understanding how each PYL protein affects plant physiology has both basic and applied agricultural significance. Although there have been a number of studies of ABA receptors in the model plant *Arabidopsis* and other crops, such as rice and soybean, functional analysis of PYLs in upland cotton has not been reported. Upland cotton is a typical allotetraploid crop that was formed about 1–2 MYA by hybridization between an A-genome ancestor and a D-genome ancestor (Chen et al., 2007; Lin et al., 2010; Paterson et al., 2012; Li et al., 2014; Cao, 2015; Yuan et al., 2015), and the *PYL* gene family expanded in this process. In this study, we carried out genome-wide analysis to identify all *PYL* genes in the two diploid progenitor species, *G. raimondii* and *G. arboretum*, and two tetraploids *G. hirsutum* and *G. barbadense*. Genome-wide expression profiling analysis revealed that *GhPYL9-11A* was the most highly expressed PYL gene during drought stress in upland cotton. Consistent with a function in drought stress response, overexpression of *GhPYL9-11A* in *Arabidopsis* remarkably increases ABA sensitivity and enhances drought tolerance. The future characterization of *GhPYL9-11A* will further our understanding of ABA-mediated stress response in cotton, and facilitate its application in breeding drought tolerant cotton cultivars.

MATERIALS AND METHODS

Plant Materials and Growth Conditions

Upland cotton (*G. hirsutum*) seeds of cultivar Y18R, a restores variety developed by our lab (Shi et al., 2012), were planted during the regular cotton cultivation season in 2015 and 2016 in the experimental farm at the Biotechnology Research Institute, Chinese Academy of Agricultural Sciences (Beijing, China). The recommended cultural and plant measures were adopted during the growth of cotton crop. For expression analysis, various organs including leaf, root, stem, and seed, were collected after 1 week of the onset of flowering stage. For analysis of ABA-induced *GhPYL9-11A* expression, cotton plants were grown in the Greenhouse with a 12-h-light (30°C)/12-h-dark (26°C) photoperiod with about 300 μM $m^{-2}s^{-1}$ photon density and 45% humidity, and the leaves of 3-weeks old plants were sprayed with 100 μM ABA (Sigma–Aldrich, United States). Ten plants were collected at 0, 1, 3, and 6 h after treatment and stored at −70°C for RNA isolation.

Arabidopsis thaliana Col-0 seed and *GhPYL9-11A* transgenic plants were sterilized for approximately 10 min in 10% bleach

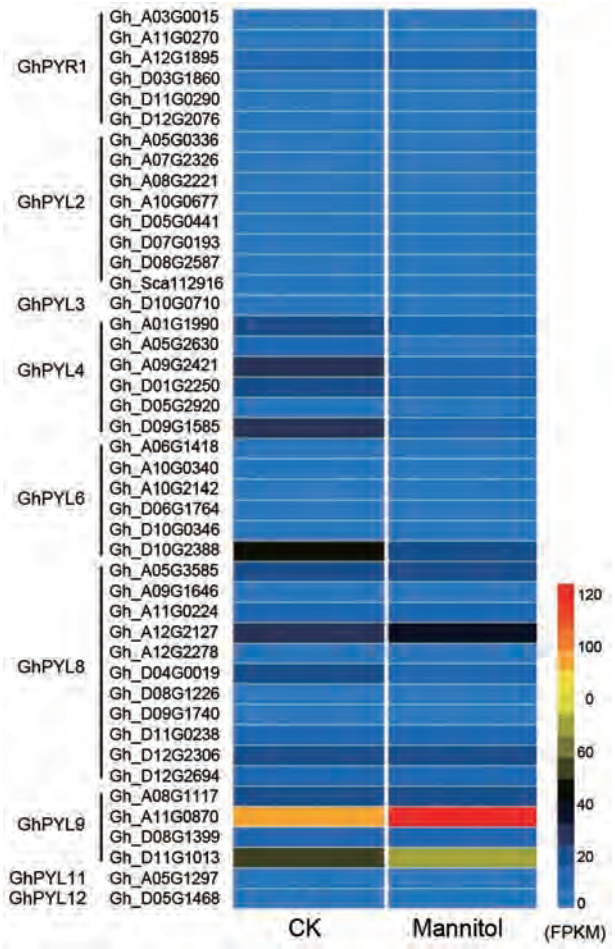

FIGURE 1 | Heat map of pyrabactin resistance-like (PYL) family genes in upland cotton. Detailed information about gene annotations can be found in **Table S1**. Gene annotation data were obtained from the Cotton Functional Genomics Database (https://cottonfgd.org/).

and then rinsed in sterile deionized water three times. Sterilized seeds were sown on petri dishes containing 0.8% agar media with ½ MS nutrients and 1% sucrose. After stratification at 4°C for 2 days, the dishes were moved to a growth chamber at 22°C with a 16-h light/8-h dark cycle and 70% humidity. All seedlings were grown vertically before transplanting to media supplemented different concentrations of ABA and mannitol.

Gene Cloning and Expression Analysis

The full-length open reading frame of *GhPYL9-11A* was amplified from *G. hirsutum* L. using the Invitrogen RACE system (Invitrogen, United States). Total RNA was extracted using the EASYspin reagent (YPHBio, China). After DNase treatment, approximately 2 μg total RNA was reverse-transcribed using the ReverTra Ace qPCR RT Master Kit (Toyobo, Japan). Quantitative RT-PCR (qRT-PCR) analysis was performed using SYBR Green I PCR mix (SSoFast EvaGreen Supermix, Bio-Rad, United States) and the Bio-Rad CFX96 real time PCR system. Data were analyzed with Opticon monitor software (Bio-Rad). The cotton *GhHISTON3* (*GhHIS3*) and *Arabidopsis Actin 8* genes, both with stability expression in the different tissues, developmental stages and environmental conditions (Zhu et al., 2017), were used as internal controls. Primers used are listed in **Table S1**. Values are means ± SD of three biological repeats. Student's *t*-test was used for statistical analysis.

Vector Construction and *Arabidopsis* Transformation

The *GhPYL9-11A* full-length coding sequence was cloned into *pBI121-35S* to generate the *pBI121-35S:GhPYL9-11A* overexpression construct. The constructs were transfected into *Agrobacterium tumefaciens* GV3101 by electroporation, and then transformed into *Arabidopsis* Col-0 pants using the floral dipping method (Liu L. et al., 2015). Homozygous transgenic *Arabidopsis* lines were obtained, and the lines GO16, GO21, and GO22, which have high levels of *GhPYL9-11A* expression, were selected for further analysis. The primers used for vector construction are listed in **Table S1**.

Yeast Two-Hybrid Assay

The Y2H assay was performed using the Matchmaker™ Gold Yeast Two-hybrid System (Clontech, United States). Full length cDNA of *GhPYL9-11A* was amplified and cloned into the pGBKT7 vector, and *AtABI1*, *AtABI2*, *GhPP2C1*, and *GhPP2C2* full length cDNAs were amplified and cloned into the pGADT7 vector. *GhPYL9-11A* point mutations were introduced by site-directed mutagenesis using *pBI121-35S:GhPYL9-11A* as a template, and *GhPYL9-11A*^{P84S} and *GhPYL9-11A*^{H111A} were cloned into the pGBKT7 vector. Each pair of AD and BD constructs was co-transformed according to the manufacturer's protocol. The positive yeast liquid culture was serially diluted to OD600 = 0.6 and 3 μL of dilutions 1:10, 1:100, 1:1,000, and 1:10,000 were inoculated onto various plates [Synthetic Dropout Medium (SD) -leucine (Leu)/tryptophan (Trp), SD-Leu/Trp/histidine (His), and SD-Leu/Trp/His supplemented with 10 μM ABA]. All plates were incubated at 28°C for 2 days and then photographed.

Germination Assay

Surface-sterilized seeds were sown on ½ MS without or with ABA (0.3 and 0.5 μM) or mannitol (150 and 300 μM). After 5 days seeds with green shoots were scored as germinated.

Drought Stress Treatment

To test the drought tolerance of *35S:GhPYL9-11A* transgenic *Arabidopsis*, the homozygous F2 generation was subjected to drought stress in soil in a growth chamber. Seed from GO1, GO2, GO3, and wild type lines were imbibed at 4°C for 2 days and directly planted in soil in the same pots (30 cm

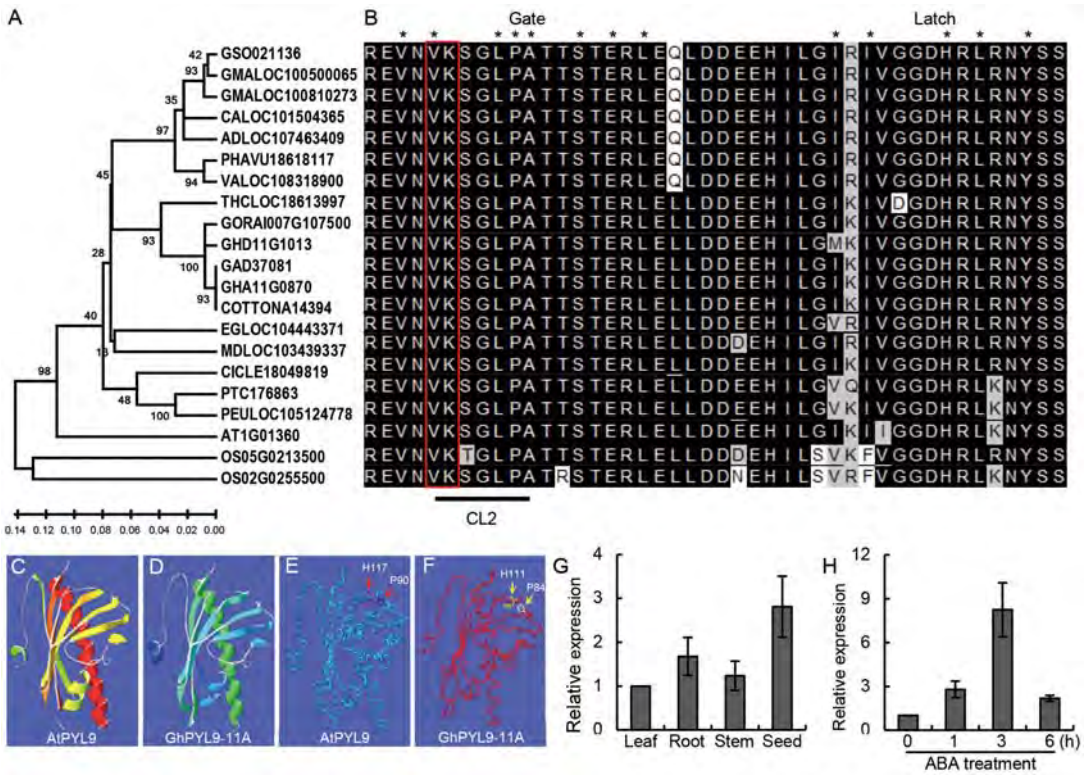

FIGURE 2 | Phylogenetic analyses of *GhPYL9-11A* homologs and organic-specific expression of *GhPYL9-11A*. **(A)** Phylogenetic relationship of *GhPYL9-11A* homologs in plants. AT (*Arabidopsis thaliana*), OS (*Oryza sativa*), GSO (*Glycine soja*), GMA (*Glycine max*), CAL (*Citrus clementina*), AD (*Arachis duranensis*), PHAVU (*Phaseolus vulgaris*), VA (*Vigna angularis*), THC (*Theobroma cacao*), GORA (*Gossypium raimondii*), GH (*Gossypium hirsutum*), GA (*Gossypium arboreum*), EG (*Eucalyptus grandis*), MD (*Malus domestica*), ClCLE (*Citrus clementine*), PT (*Populus trichocarpa*), PEU (*Populus euphratica*). **(B)** Amino acid alignment of the PYL9 CL2/gate-latch region for the proteins shown in **(A)**. The black line indicates the CL2 domain. Two amino acid residues 'VK' are marked with a red open rectangle. The residues in contact with the ABA molecule are designated by asterisk. **(C–F)** Comparison of the predicted 3-D structures of AtPYL9 and *GhPYL9-11A*. The conserved proline and histidine residues in the gate and latch region are marked with red arrows in AtPYL9 **(E)** and yellow arrows in *GhPYL9-11A* **(F)**. **(G)** Expression of *GhPYL9-11A* in various organs determined by quantitative real time (qRT)-PCR analysis. Roots, leaves, and stems were harvested from 3-week-old plants. **(H)** Time-course of the response of *GhPYL-11A* to 100 μM ABA treatment.

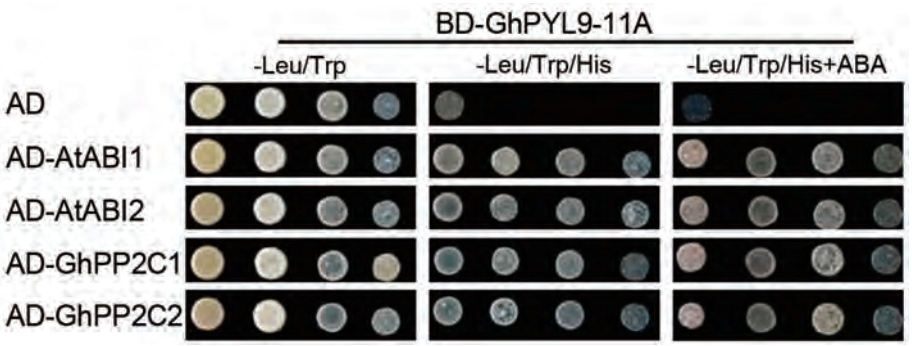

FIGURE 3 | Interactions between *GhPYL9-11A* and PP2C proteins in yeast. The BD-GhPYL9-11A fusion was co-expressed with AD-AtABI1, AD-AtABI2, AD-GhPP2C1, or AD-GhPP2C2 in yeast. Interactions were determined by growth assays on media lacking leucine (Leu), tryptophan (Trp), and histidine (His) in the presence and absence of 10 μM ABA.

in diameter). All plants were grown at room temperature (22–25°C) under long-day conditions (16 h light/8 h dark) in the culture room. After 2 weeks of seedling emergence, drought treatment was established by withholding the water for 4 weeks. The experiment was comprised of five replications. Watering was resumed 1 day after the 4 weeks of drought

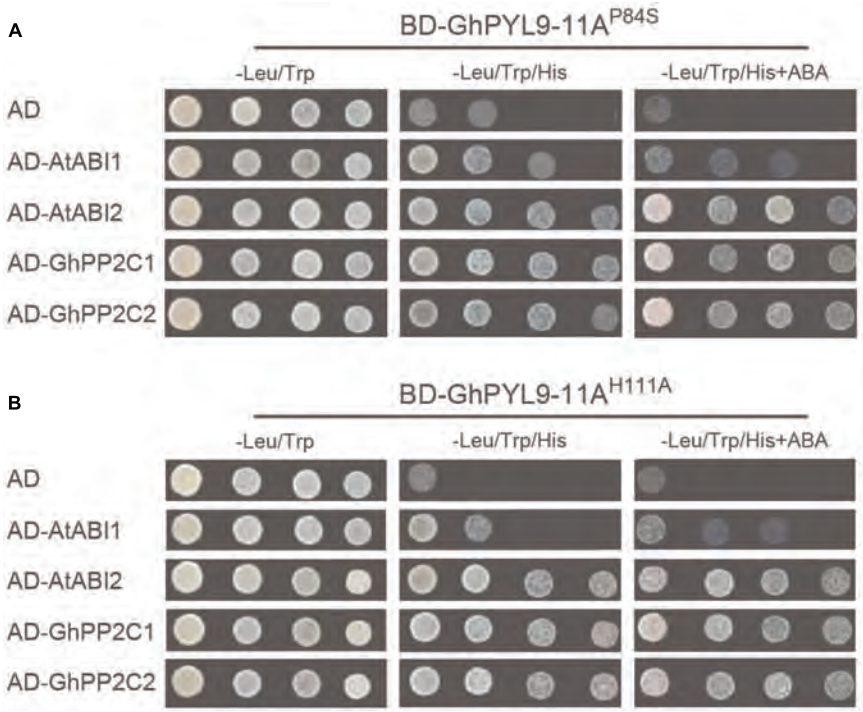

FIGURE 4 | GhPYL-11A-PP2C interactions are partially mediated by proline (P84) and histidine (H111) in the gate-latch region of *GhPYL9-11A*. Replacement of P84 by serine (GhPYL9-11A^{P84S}) **(A)** and H111 by alanine (GhPYL9-11A^{H111A}) **(B)** abolished binding to AtABI1 both in the absence and presence of 10 μM ABA. However, these mutations partially affected binding to AtABI2, GhPP2C1, and GhPP2C2 both in the presence and absence of 10 μM ABA.

treatment, and the survival rate (SR) was calculated 3 days later.

Chlorophyll Measurement

After measuring the fresh weight of the samples, five seedlings for each sample were used to calculated the total chlorophyll contents as the absorbance at 652 nm following (Liang et al., 2014).

Photosynthesis Parameters and Water Loss Measurement

For measurement of photosynthesis parameters, water was withheld for 7 days beginning when plants were 14-days old. Ten independent plants were used for each *GhPYL9-11A* overexpression line. Photosynthesis parameters were measured as previously described by (Liang et al., 2015). For determination of water loss, the whole aboveground rosettes of 21-day-old plants were cut from the base and weighed at different time points.

Electrolyte Leakage Measurement

The measurement of electrolyte leakage was performed according to a previously described method (Lin A. et al., 2012). Ten different leaf disks from wild-type and *GhPYL9-11A* overexpression plants were placed into a flask containing 10 mL distilled deionized water. After shaking at room temperature for 6 h at approximately 120 rpm, the conductivity (C_i) was measured with a conductivity meter (Leici-DDS-307A). Then, the disks were boiled for 20 min to kill the leaf tissues and shaken for 1 h to completely release the electrolytes into the solution. The conductivity (C_m) was measured again. The electrolyte leakage was calculated according to the equation $(C_i/C_m) \times 100\%$.

Hydrogen Peroxide Production and Measurement of Antioxidant Enzyme Activities

For hydrogen peroxide production and measurement of antioxidant enzyme activities, *Arabidopsis* plants were grown on soil for 14 days and leaves were collected from the plants after water was withheld for 7 days. Measurement of H_2O_2 production was performed according to a previously described method (Liang et al., 2015), and quantified using the Hydrogen peroxidase assay kit (Beyotime, China) according to the manufacturer's instructions. The quantification of CAT, SOD, and POD activity was performed according to a previously described method (Liang et al., 2016). Total protein was measured using Bradford protein assay kit (Sangon Biotech, China).

Protein Sequence and Phylogenetic Analysis

For phylogenetic analysis of GhPYL9-11A homologs in plants, 20 protein sequences were obtained through National Center for Biotechnology Information database using BLASTp searches

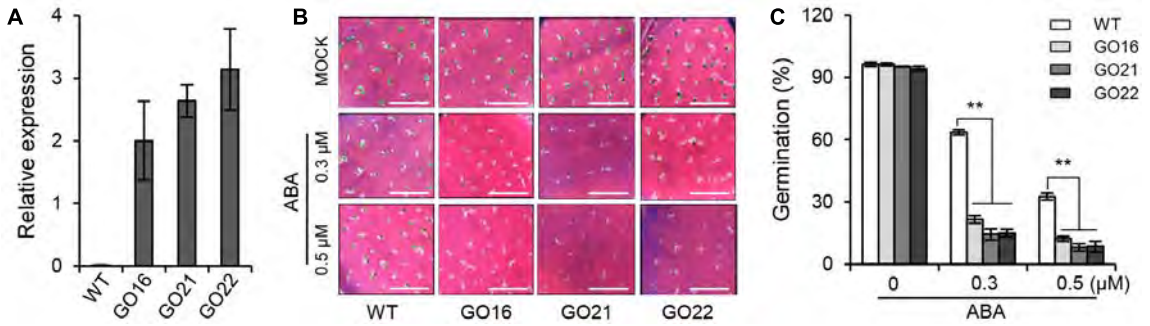

FIGURE 5 | The effect of *GhPYL9-11A* overexpression on *Arabidopsis* seed germination. **(A)** The expression levels of *GhPYL9-11A* in transgenic *Arabidopsis* plants determined by qRT-PCR. GO, *GhPYL9-11A* overexpression lines. Values are means ± SD of three biological repeats. **(B)** Germinated seeds from wild-type plants and GO lines grown for 5 days on half-strength Murashige and Skoog (½ MS) in the presence or absence of ABA. **(C)** Seed germination rate under the different growth conditions in **(B)**. Values are means ± SD of five measurements. $^{**}P \leq 0.01$; Student's *t*-test.

with the GhPYL9-11A protein as a query. All sequences were aligned using Clustal W. Phylogenetic trees were constructed using MEGA 6.0 based on the neighbor-joining method. Topological robustness was assessed by bootstrap analysis with 1,000 replicates (Liu L. et al., 2015).

RESULTS

Transcriptome Analysis of Cotton PYL ABA Receptor

Pyrabactin resistance-like protein coding sequences were identified in upland cotton species, *G. hirsute*, *G. barbadense, G. raimondii*, and *G. arboretum*, with complete genomes or genome assemblies. We then compared the expression profiles of the *PYL* genes under drought stress. Twenty-two PYL proteins were identified from each of the two diploid progenitor species *G. raimondii* and *G. arboretum*, and 44 and 36 members were identified in the tetraploids *G. hirsutum* and *G. barbadense*, respectively (**Table S2**). High-resolution temporal expression profiling revealed that two *GhPYL* genes, *Gh_A11G08070* and *Gh_D11G1013,* were most highly expressed during drought stress in upland cotton (*G. hirsutum*) (**Figure 1** and **Table S2**). The proteins encoded by *Gh_A11G0870* and *Gh_D11G1013* share approximately 80 and 79% amino acid identity with AtPYL9, an ABA receptor, respectively.

Both Gh_A11G0870 and Gh_D11G1013 belong to the PYL9 subfamily of PYL proteins. There are two members each in *G. raimondii* and *G. arboretum,* and four members each in *G. hirsutum* and *G. barbadense*. Based on phylogenetic analysis, the PYL proteins could be further divided into two distinct subgroups, PYL9-I and PLY9-II (**Figure S1**). Interestingly, all members of PYL9-I in both diploid and tetraploid cotton were highly expressed during seed germination and drought stress, whereas PLY9-II members were with low expression level (**Table S2**). These results suggest that PYL9-I proteins may play important roles in the regulation of seed germination and drought responses in cotton. Because Gh_A11G08070 (hereafter referred to as GhPYL9-11A) belongs to the drought stress-responsive PYL9-I subfamily, its function was investigated in detail.

Structural Features of GhPYL9-11A

Using protein database searches, we identified a number of putative GhPYL9-11A orthologs in various higher plants. GhPYL9-11A homologs were only found in the plant kingdom, indicating that PYL9 proteins are plant-specific. The identification of PYL proteins in both monocots and dicots suggests that PYL proteins are evolutionally conserved across plant species. The existence of PYL9 in different plant species might also suggest that its function in drought stress response is also conserved. Phylogenetic analysis of the cotton GhPYL9-11A protein and its 20 homologs showed that GyhPYL9-11A is most closely related to LOC18613997 of *Theobroma cacao,* and shares approximately 80% amino acid sequence identity with related proteins in **Figure 2A**.

PYL9 family proteins have a pyrabactin resistance1/pyr1-like/regulatory component of ABA receptor (PYR/PYL/RCAC)-like structure (amino acids 28–172) typical of ABA receptors (**Figure 2B**). We analyzed the 3D structure of this conserved motif in GhPYL9-11A using SWISSMODEL. The predicted structure is a common helix-grip structural feature consisting of four α-helixes and seven antiparallel β-sheets and is highly similar to the *Arabidopsis* AtPYL9 PYR/PYL/RCAC motif (**Figures 2C,D**).

Expression Pattern of *GhPYL9-11A*

Quantitative RT-PCR analysis showed that *GhPYL9-11A* is expressed preferentially in seeds and roots, with a low level of expression in the leaf and stem (**Figure 2E**). Moreover, time-course analysis revealed that *GhPYL9-11A* was rapidly induced by ABA, with expression levels increasing approximately 2.8-fold after 1 h of ABA application (**Figure 2F**). Levels of *GhPYL9-11A* transcription reached a maximum after 4 h of treatment, and were approximately eightfold higher than without hormone treatment. These

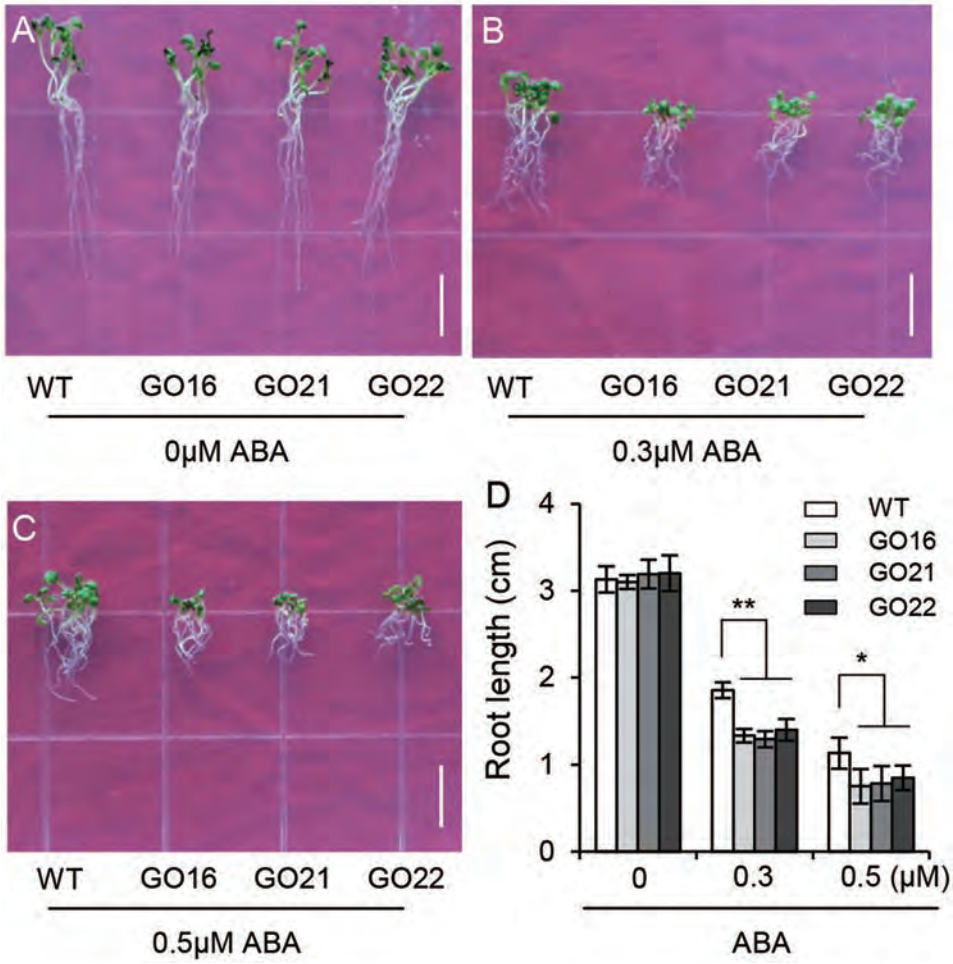

FIGURE 6 | Differential ABA responsiveness of *GhPYL9-11A* overexpression and wild-type *Arabidopsis* seedlings. **(A–C)** Phenotypes of wild type and three independent *35S:GhPYL9-11A* transgenic *Arabidopsis* lines, GO16, GO21, and GO22, grown in ½ MS medium supplemented with 0 μM **(A)**, 0.3 μM **(B)**, and 0.5 μM **(C)** ABA. Bar = 1 cm. **(D)** Seedling primary roots lengths under the different growth conditions in **(A–C)**. Measurements were performed for least 30 independent seedlings. Results are shown as mean ± SD of three replicates; Student's *t*-test. $^{*}P \leq 0.05$, $^{**}P \leq 0.01$.

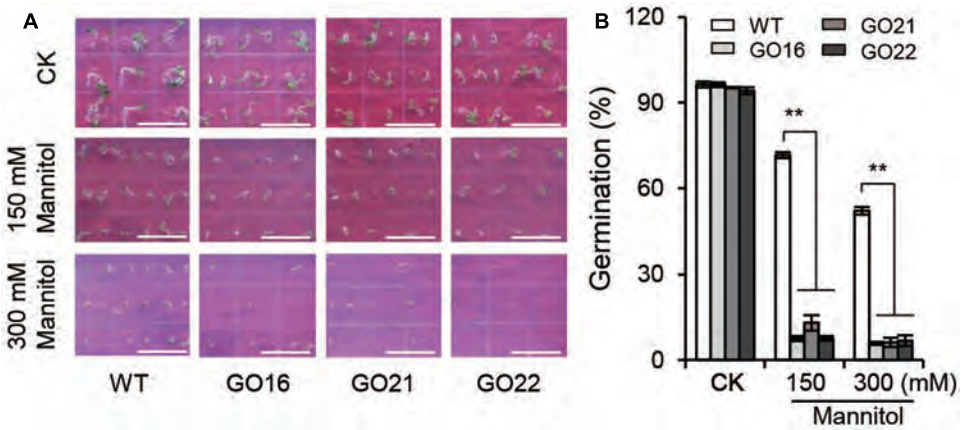

FIGURE 7 | Effect of *GhPYL9-11A* overexpression on *Arabidopsis* seed germination under mannitol treatment. **(A)** Germinated seeds from wild-type and *GhPYL9-11A* overexpression plants grown for 5 days on 1/2 MS with or without mannitol. **(B)** Seed germination rate under the different growth conditions in **(A)**. Values are means ± SD of five measurements. $^{**}P \leq 0.01$; Student's *t*-test.

results clearly demonstrate that this gene is transcribed in response to ABA and thus is potentially involved in ABA response.

GhPYL9-11A Interacts with Clade A PP2Cs in an ABA-Independent Manner

It has been shown that PYL proteins can interact with PP2Cs in yeast two-hybrid (Y2H) assays in an ABA-dependent or ABA-independent manner (Bai et al., 2013; Zhao et al., 2013). To investigate whether GhPYL9-11A binds clade A PP2Cs, we tested the interaction of GhPYL9-11A with two *Arabidopsis* PP2C proteins, *A. thaliana* ABSCISIC ACID INSENSITIVE1 (AtABI1) and AtABI2, in Y2H assays in the presence or absence of ABA. As shown in **Figure 3**, GhPYL9-11A interacted with both AtABI1 and AtABI2 in an ABA-independent manner. We further tested the interaction between GhPYL9-11A and two cotton PP2Cproteins, GhPP2C1 (Gh_A05G0308) and GhPP2C2 (Gh_A07G0123), that share high similarity with AtABI1 (63% for GhPP2C1 and 71% for GhPP2C2, **Figure S2**). GhPYL9-11A also binds to both GhPP2C1 and GhPP2C2 in an ABA-independent manner (**Figure 3**).

The mutated conserved proline (P88S) in the gate region and histidine (H111A) in the latch region of GhPYL9-11A, and tested the ability of the mutated proteins, GhPYL9-11A^{P84S} and GhPYL9-11A^{H111A}, to interact with AtABI1, AtABI2, GhPP2C1, and GhPP2C2 in Y2H assays. Both the GhPYL9-11A^{P84S} and GhPYL9-11A^{H111A} mutations reduced the level of interaction with AtABI1, AtABI2, GhPP2C1, and GhPP2C2 both in the presence and absence of ABA (**Figure 4**). These data suggest that GhPYL-11A-PP2C interactions are partially mediated by P84 and H111 in the gate-latch region of GhPYL9-11A.

Overexpression of *GhPYL9-11A* in *Arabidopsis* Leads to an ABA-Hypersensitive Phenotype during Germination

To investigate the biological function of *GhPYL9-11A* in plants, the *GhPYL9-11A* coding sequence was cloned into the plant binary vector pBI121 in front of the 35S promoter and transformed into *Arabidopsis* though *Agrobacterium tumefaciens*-mediated transformation. A set of 27 positive independent transgenic lines had up-regulated expression of *GhPYL9-11A*. Among them, three independent homozygous T3 *GhPYL9-11A*-overexpressing (GO) lines, GO16, GO21, and GO22, with high levels of *GhPYL9-11A* transcript, were selected for further analysis (**Figure 5A**).

To determine whether GhPYL9-11A is a functional ABA receptor, we treated three GO plants and wild type with 0.3 and 0.5 μM ABA and then compared their seed germination phenotypes. Under control conditions, there was no significant difference in seed germination rate between GO plants and wild type. However, the seed germination rates of the three GO transgenic *Arabidopsis* lines were less than 20 and 10% in the presence of 0.3 μM ABA and 0.5 μ M ABA, respectively, whereas the germination rates of wild type were 63.5 and 32.6%, respectively (**Figures 5B,C**). These observations suggest that overexpression of *GhPYL9-11A* represses seed germination in the presence of ABA in *Arabidopsis*.

GhPYL9-11A Overexpression in *Arabidopsis* Results in ABA-Hypersensitive Phenotypes during Seedling Growth

We further examined the effects of *GhPYL9-11A*-overexpression on *Arabidopsis* seedling root growth. We found no obvious difference in root development between GO transgenic plants and wild type at different stages of seedling growth. However, ABA treatment repressed root growth to a larger extent in the GO lines compared with wild type; in the presence of 0.3 M ABA the root lengths of in the three GO lines were reduced by 37.5–47.9% compared with control conditions, but in wild type root lengths were only reduced by 28.8%. In the absence of ABA, and in the presence of 0.5 μM ABA, root lengths were 44.8–52.6% of GO plants while 34.8% of wild type (**Figures 6A–D**). These results suggest that overexpression of *GhPLY9-11A* in *Arabidopsis* significantly increases sensitivity to ABA. Thus, we deduced that GhPYL9-11A may act as an ABA receptor in cotton.

The Seeds of *Arabidopsis* GO Lines Are Hypersensitive to Osmotic Stress

Keeping in view the ability of ABA to regulate seed germination, we examined the effects of *GhPYL9-11A* overexpression on seed germination under osmotic stress imposed by adding 150 and 300 mM mannitol to ½ MS media. Compared with wild-type *Arabidopsis*, GO plants had a significantly decreased ratio of seed germination under osmotic stress (**Figure 7**), but no difference in seed germination rate between GO plants and wild type was observed under control conditions. The repression of seed germination under osmotic stress in the *GhPYL9-11A* overexpression lines is consistent with hypersensitivity to ABA.

GhPYL9-11A Overexpression in *Arabidopsis* Enhances Tolerance to Drought Stress

The ABA-dependent signaling pathway has an essential role in response to drought stress therefore, we examined whether overexpression of *GhPYL9-11A* was sufficient to confer drought stress tolerance to *Arabidopsis*. The *Arabidopsis 35S:GhPYL9-11A* plants, GO16, GO21, and GO22, exhibited significantly increased drought tolerance during the vegetative stage (**Figures 8A–F**). GO plants also had reduced chlorophyll degradation (**Figure 8G**), reduced water loss (**Figure 8H**), enhanced photosynthetic rate (**Figure 8I**), reduced electrolyte leakage (**Figure 8J**), reduced accumulation of toxic hydrogen peroxide (**Figure 8K**), and enhanced activities of antioxidant enzymes including catalase (CAT, **Figure 8L**), superoxide dismutase (SOD, **Figure 8M**) and peroxidase (POD, **Figure 8N**). Consistent with these observations, the SR and total biomass were significantly increased after drought treatment in GO lines compared with

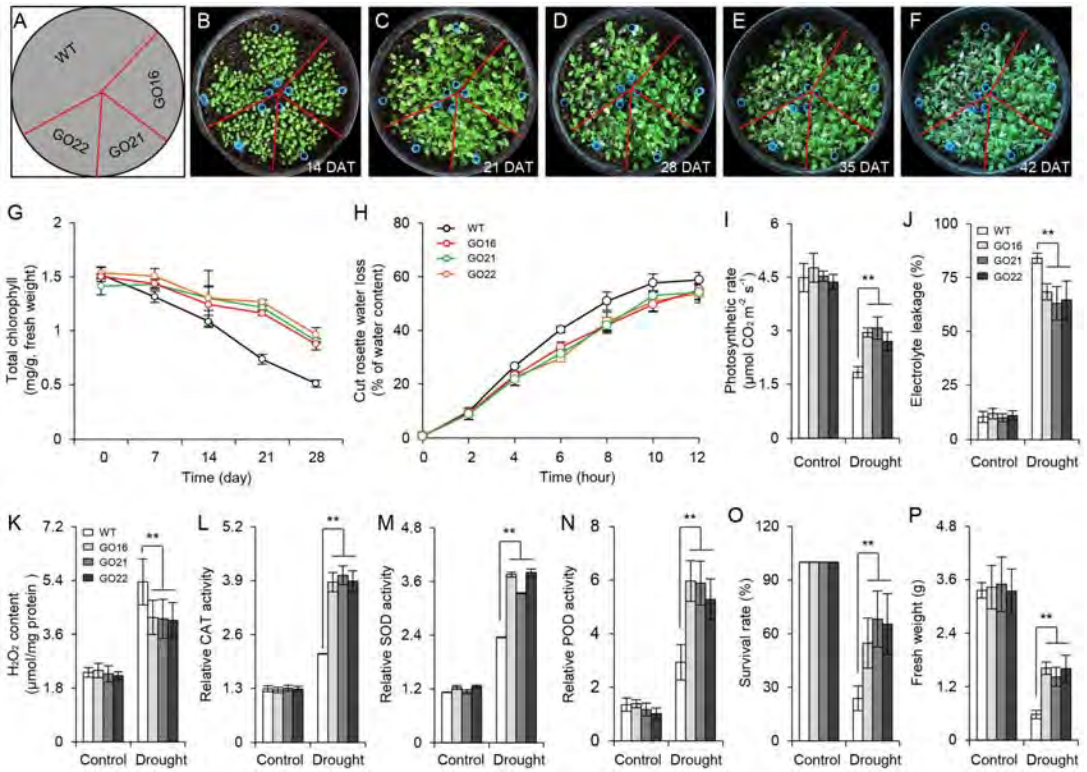

FIGURE 8 | Transgenic *Arabidopsis* harboring *35S:GhPYL9-11A* exhibit increased drought tolerance. **(A–F)** *35S:GhPYL9-11A* confers drought tolerance to *Arabidopsis*. After 2 weeks of growth, water was withheld for 28 days under short-day conditions before watering was resumed. Representative images of plants taken 7, 14, 21, and 28 days after watering was withheld. DAT, day after transplanting. **(G)** Chlorophyll content of mature leaves in wild type and GO plants at the indicated times after watering were withheld. Values are means ± SD of 20 measurements; Student's *t*-test. **(H)** Cumulative transpirational water loss from the rosettes of wild-type and GO *Arabidopsis* at the indicated times after detachment. Values are means ± SD of 20 measurements; Student's *t*-test. **(I–N)** Physiological parameters of GO plants under drought stress treatment. Parameters were measured after water was withheld for 7 days. Overexpression of *GhPYL9-11A* in *Arabidopsis* increased the photosynthetic rate **(I)**, reduced electrolyte leakage **(J)**, reduced H_2O_2 content **(K)**, and increased the activities of antioxidant enzymes, including CAT **(L)**, SOD **(M)**, and POD **(N)**. Error bars indicate SD ($n = 5$). $^{**}P \leq 0.01$; Student's *t*-test. **(O)** Survival rate (SR) of the wild-type and GO *Arabidopsis*. After 2 weeks of growth, plants were subjected to drought stress by withholding water for 4 weeks. Survival was scored 3 days after watering was resumed. Error bars indicate SD ($n = 3$); Student's *t*-test. **(P)** Relative fresh weights of wild type and GO lines. After watering was withheld for 28 days, the rosettes were collected and weighted. Plants grown under well-watered conditions served as the control. Error bars indicate SD ($n = 3$). $^{**}P \leq 0.01$; Student's *t*-test.

the wild type (**Figures 8O,P**). Moreover, four ABA-dependent drought stress-associated genes, *ABF2*, *RAB18*, *RD29A*, and *RD29B*, were more strongly induced after drought treatment in the rosette leaves of *Arabidopsis* GO lines than in wild type (**Figures 9A–D**). Taken together, these data provide strong evidence that *GhPYL9-11A* overexpression confers drought tolerance in plants by activating the ABA-dependent signaling pathway.

GhPYL9-11A Expression Level Associates with Drought Stress Tolerance in Different Cultivated Cotton Cultivars

Our results clearly demonstrate that overexpression of *GhPYL9-11A* in *Arabidopsis* enhances drought stress tolerance. Thus, we speculated that the expression level of *GhPLY-11A* may be correlated with drought tolerance in cultivated cotton varieties. To test this hypothesis, we phenotyped the drought tolerance of 226 cotton varieties. These varieties were indexed by plant SR under severe drought stress, and 20 drought-tolerant (with SR ranging from 17.0 to 49.3%) and 20 drought-sensitive (with SR ranging from 65.2 to 95.9%) cotton varieties were selected for further analysis (**Table S3**). We next compared the seedling-stage expression levels of *GhPYL9-11A* in drought-tolerant and drought-sensitive cultivated cotton accessions under drought treatment. The average expression levels of *GhPYL9-11A* in the 20 drought-tolerant cotton varieties were significantly higher than in the drought-sensitive varieties under drought treatment (**Figure 10B**). However, the expression level did not differ under control conditions (**Figure 10A**). We further examined the relationship between the *GhPYL9-11A* expression levels and SR in 20 drought-tolerant and 20 drought-sensitive cultivated cotton varieties under drought stress and found that *GhPYL9-11A* expression is positively correlated with drought tolerance ($R = 0.483$; **Figure 10C**). These results further suggest that *GhPYL9-11A* plays an important role in drought tolerance in cultivated cotton.

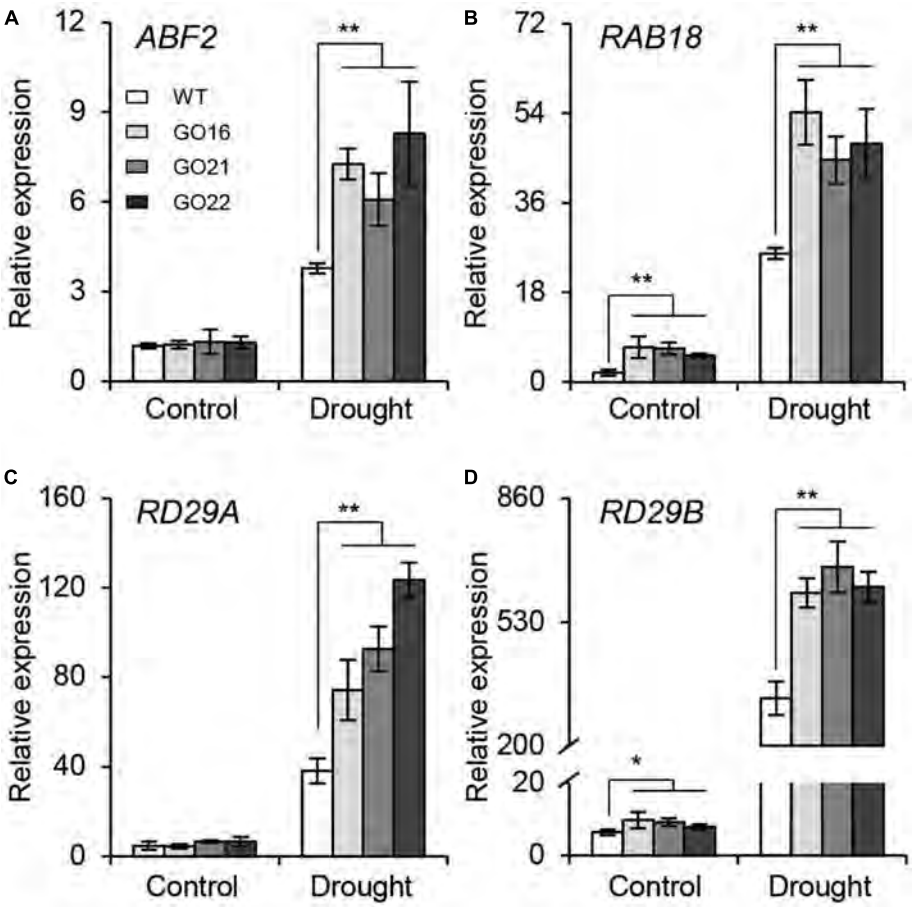

FIGURE 9 | Expression of ABA-responsive genes in *GhPYL9-11A* overexpression plants under control and drought conditions. QRT-PCR analysis of ABA-responsive genes, including *ABF2* **(A)**, *RAB18* **(B)**, *DR29A* **(C)**, and *RD29B* **(D)**, in wild type and *Arabidopsis GhPYL9-11A* overexpression lines treated with 400 μM mannitol for 24 h. Values are means ± SD of three biological repeats. $^{*}P \leq 0.05$, $^{**}P \leq 0.01$; Student's *t*-test.

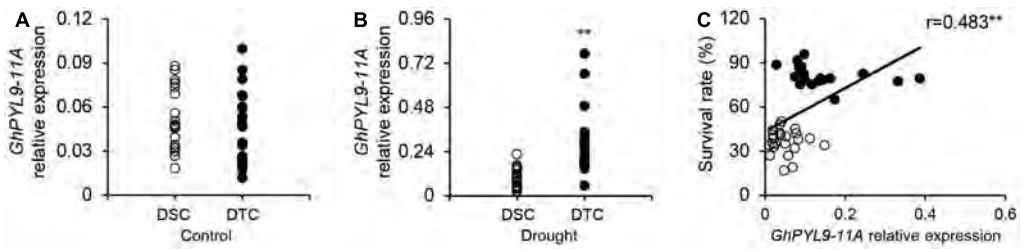

FIGURE 10 | Expression level of *GhPYL-11A* in drought-tolerant and drought-sensitive cultivated cotton varieties is correlated with SR under severe drought stress. **(A,B)** The expression level of *GhPYL9-11A* in drought-tolerant and drought-sensitive cultivated cotton varieties treated with H_2O **(A)** and 400 mM mannitol **(B)** for 24 h was determined by qRT-PCR. DSC, drought-sensitive cultivated cotton. DTC, drought-tolerant cultivated cotton. In **(A,B)**, asterisks indicate significant differences ($^{**}P < 0.01$). **(C)** Correlation between the SR of cotton seedlings grown under severe drought conditions and the expression level of *GhPYL9-11A*.

DISCUSSION

Recently, significant progress has been made in the identification and characterization of the PYL ABA receptors in several plants (Sheard and Zheng, 2009; Bai et al., 2013). However, to our knowledge, up to now, no ABA receptors from upland cotton, which is widely grown in over 80 countries and provides the material for about 90% of the world's cotton lint production (Wang et al., 2012; Wang Y. et al., 2016; Paterson and Wendel, 2015; Liang et al., 2016), have been reported. Owing to allopolyploidization, the number of *PYL* genes has doubled in upland cotton compared with diploid cotton. However, to

date, it remains largely unknown which PYL members is the crucial ABA receptor mediating response to drought stress in tetraploid cotton. Therefore, it is interesting and important to determine the functions and regulatory mechanisms of the ABA receptors in tetraploid cotton. In this study, we identified 22 ABA receptors orthologous to *Arabidopsis* PYLs in both the A- and D-genomes of the tetraploid cotton *G. hirsutum* using the recently released cotton genome sequence (Wang et al., 2012; Li et al., 2014, 2015; Liu X. et al., 2015). We further demonstrated that GhPYL9-11A is a functional ABA receptor, and similar to AtPYL9, interacts with PP2Cs in ABA-independent manner and regulates drought resistance and leaf senescence in *Arabidopsis* (Zhao et al., 2016). We found that *GhPYL9-11A* overexpression in *Arabidopsis* results in ABA-hypersensitive seed germination and root development phenotypes. Moreover, overexpression of *GhPYL9-11A* also significantly enhances drought and osmotic stress tolerance.

Abscisic acid was discovered in the 1960s, and to date, numerous biochemical and genetic studies have revealed that ABA is a vital regulator of multiple stress responses (Hurst, 1995; Finkelstein et al., 2002; Zhu, 2002; Sheard and Zheng, 2009; Zhao et al., 2014). ABA enhances plant survival under stress conditions by inducing seed and bud dormancy, inhibiting germination, closing stomata, and accelerating old leaf senescence and abscission. A variety of abiotic stresses sharply increase endogenous ABA levels and activates ABA signaling pathways leading to elevated plant survival. Furthermore, exogenously applied ABA has been shown to induce the expression of genes known to enhance stress tolerance. Our previous studies have demonstrated that several ABA-responsive genes, such as *GhABF2* (Liang et al., 2016), *GhDr1* (Ding et al., 2011), and *GhSRK2D* (Lin F. et al., 2012), play important roles in ABA signal transduction in response to drought stress in cotton. In this study, through comparative analysis of the transcript levels of 44 *PYL* genes, we found that *GhPYL9-11A* (*Gh_A11G08070*) is the most highly expressed during both seed germination and drought stress (**Figure 1** and **Table S2**). Consistently, the homologs of *GhPYL9-11A*, *Gorai_007G107500* and *Cotton_A14394*, in diploid cotton *G. raimondii* and *G. arboreum*, respectively, also show highly expressed pattern during seed germination and drought stress (**Table S2**). Moreover, the expression level of *GhPYL9-11A* is associated with drought stress in different cultivated cotton cultivars (**Figure 10**). We also confirmed that expression of *GhPYL9-11A* is indeed significantly induced by exogenous ABA treatment (**Figure 2**). These findings suggest that among the cotton PYLs, *GhPYL9-11A* may be the most important regulator of ABA signaling during seed germination and under drought stress.

Pyrabactin resistance-likes are ABA receptors that act at the apex of a negative regulatory pathway and regulate ABA signaling by binding and inhibiting PP2Cs (Melcher et al., 2009; Miyazono et al., 2009; Nishimura et al., 2009; Park et al., 2009; Santiago et al., 2009; Sheard and Zheng, 2009). Similar to AtPYL-PP2C interactions in *Arabidopsis*, GhPYL9-11A interacts with AtABI1 and AtABI2, as well as with GhPP2C1 and GhPP2C2 in Y2H assays (**Figure 3**). Moreover, the interaction between GhPL9-11A and PP2C proteins does not depend on ABA. Previous studies have revealed that PYL-PP2C interactions are partially associated with two conserved amino acid residues preceding the CL2/gate-latch domain (**Figure 4**), and there are several polymorphisms in these residues, including VI, VV, VK, VQ, VT, VR, VN, IT, LV, and LK, in *Arabidopsis*, rice, soybean, poplar, and maize (Bai et al., 2013; Zhao et al., 2013). These polymorphisms are closely correlated with ABA-dependent or -independent interactions with PP2C. GhPYL9-11A belong to subgroup II of the GhPYL family, and have the typical VK combination in the CL2/gate-latch domain (**Figure 2B**). Consistent with the ABA-independent interaction between GhPYL0-11A and PP2Cs, VK is correlated with ABA-independent PYL-PP2C interactions. Intriguingly, *GhPYL9-11A* and AtPYL9 share high amino acid sequence identity and 3D structures, and both proteins contain the conserved proline (P84) and histidine (H111) residues in the gate-latch domain (**Figure 2C**). However, the site-directed mutants GhPYL9-11A^{P84S} and GhPYL9-11A^{H111A} are able to interact with AtABI2, GhPP2C1, and GhPP2C2, but not AtABI1 in an ABA-independent manner (**Figures 3**, **4**), suggesting that residues in other regions of GhPYL9-11A also regulate the ABA-independent interactions with PP2Cs in cotton.

To escape unfavorable environmental conditions at unusual times or of atypical severity, plants increase seed dormancy and inhibit growth by elevating ABA content and activating core ABA signaling pathways (Zhu, 2002; Zhao et al., 2016). Although recent studies have greatly improved our knowledge about the PYL family in several plants, the basic biological functions of PYLs in tetraploid cotton remain largely unknown. Here, we clearly demonstrate that *GhPYL9-11A* overexpression in *Arabidopsis* has multiple physiological effects, including enhanced ABA sensitivity and inhibition of seed germination under mannitol treatment (**Figures 3**, **4**). *GhPYL9-11A* overexpression also significantly increased seedling drought and osmotic tolerance, enhanced antioxidant enzyme activities, reduced the change in photosynthetic rate, reduced chlorophyll degradation, water loss, and electrolyte leakage, and induced the expression of a subset of ABA-regulated genes (**Figures 8**, **9**). The combination of inhibition of seed germination and enhanced seedling abiotic stress tolerance in *GhPYL9-11A* overexpression lines is consistent with plant survival. These results and the observation that drought tolerant cotton varieties have higher *GhPYL9-11A* expression levels suggests that *GhPYL9-11A* may have played a role in the evolution of drought and osmotic tolerance in cotton.

CONCLUSION

GhPYL9-11A acts as a positive regulator of the ABA signaling pathway by binding to type PP2C protein phosphatases in an ABA-independent manner. Our study provides valuable insight into the function of GhPYL9-11A in the regulation of ABA signaling. In addition, the improved drought and osmotic tolerance of both seeds and seedlings of *Arabidopsis GhPYL9-11A* overexpression lines is encouraging for future efforts to genetically engineer plant drought and osmotic tolerance.

Further manipulation of *GhPYL-11A* expression in cotton could aid the development of drought and osmotic tolerant cultivars.

AUTHOR CONTRIBUTIONS

CL, SG, and RZ designed research. CL, YLiu, YLi, ZM, RY, YW, SK, MA, and GS performed research. CL, TZ, and RZ analyzed data. CL, WM, SG, and RZ wrote the paper.

FUNDING

This work was supported by grants from the National Natural Science Foundation of China (Grant No. 31601349 to CL) and the Ministry of Agriculture (Grant No. 2016ZX08005004 to RZ, Grant No. 2016ZX08009003-003-004 to CL), and the Innovation Program of Chinese Academy of Agricultural Sciences.

SUPPLEMENTARY MATERIAL

The Supplementary Material for this article can be found online at: http://journal.frontiersin.org/article/10.3389/fpls.2017.01453/full#supplementary-material

FIGURE S1 | Phylogenetic analysis of PYL9 proteins in two diploid progenitor species *G. raimondii* and *G. arboretum*, and 4 two tetraploids *G. hirsutum* and *G. barbadense*. The scale bar indicates 0.1 amino acid substitution per site.

FIGURE S2 | Protein sequence alignment of PP2C protein, AtABI1, AtABI2 GhPP2C1, and GhPP2C2 in *Arabidopsis* and cotton using Cluster X. Conserved amino acid are highlighted in shades of black and gray. White letter with black background (100% identity), white letter with gray background (60%).

TABLE S1 | Primers used in this study.

TABLE S2 | Expression pattern of PYL genes in cotton.

TABLE S3 | Drought-tolerance and drought-sensitive cotton varieties used for correlation analysis between survival rate and *GhPYL9-11A* expression level.

REFERENCES

Antoni, R., Gonzalez-Guzman, M., Rodriguez, L., Peirats-Llobet, M., Pizzio, G. A., Fernandez, M. A., et al. (2013). PYRABACTIN RESISTANCE1-LIKE8 plays an important role for the regulation of abscisic acid signaling in root. *Plant Physiol.* 161, 931–941. doi: 10.1104/pp.112.208678

Bai, G., Yang, D. H., Zhao, Y., Ha, S., Yang, F., Ma, J., et al. (2013). Interactions between soybean ABA receptors and type 2C protein phosphatases. *Plant Mol. Biol.* 83, 651–664. doi: 10.1007/s11103-013-0114-4

Cao, X. (2015). Whole genome sequencing of cotton–a new chapter in cotton genomics. *Sci. China Life Sci.* 58, 515–516. doi: 10.1007/s11427-015-4862-z

Chen, Z. J., Scheffler, B. E., Dennis, E., Triplett, B. A., Zhang, T., Guo, W., et al. (2007). Toward sequencing cotton (*Gossypium*) genomes. *Plant Physiol.* 145, 1303–1310. doi: 10.1104/pp.107.107672

Choi, H., Hong, J., Ha, J., Kang, J., and Kim, S. Y. (2000). ABFs, a family of ABA-responsive element binding factors. *J. Biol. Chem.* 275, 1723–1730. doi: 10.1074/jbc.275.3.1723

Ding, Z., Zhang, R., and Guo, S. (2011). Cloning and bioinformatics analysis of cotton gene *GhDr1* related to resistance to abiotic stress. *Biotechnol. Bull.* 1, 99–106. doi: 10.1093/pcp/pcw090

Fang, J., Chai, C., Qian, Q., Li, C., Tang, J., Sun, L., et al. (2008). Mutations of genes in synthesis of the carotenoid precursors of ABA lead to pre-harvest sprouting and photo-oxidation in rice. *Plant J.* 54, 177–189. doi: 10.1111/j.1365-313X.2008.03411.x

Finkelstein, R. R., Gampala, S. S., and Rock, C. D. (2002). Abscisic acid signaling in seeds and seedlings. *Plant Cell* 14(Suppl.), S15–S45. doi: 10.1105/tpc.010441

Gonzalez-Guzman, M., Pizzio, G. A., Antoni, R., Vera-Sirera, F., Merilo, E., Bassel, G. W., et al. (2012). Arabidopsis PYR/PYL/RCAR receptors play a major role in quantitative regulation of stomatal aperture and transcriptional response to abscisic acid. *Plant Cell* 24, 2483–2496. doi: 10.1105/tpc.112.098574

Guang, Y., Song, G., Zhang, J., Wang, X., and Tan, C. (2014). Molecular cloning and expression analysis of *GhbHLH130*, encoding a novel bHLH transcription factor in uplant cotton (*Gossypium hirsutum* L.). *Cotton Sci.* 26, 363–370. doi: 10.1126/scisignal.2005051

Gunapati, S., Naresh, R., Ranjan, S., Nigam, D., Hans, A., Verma, P. C., et al. (2016). Expression of *GhNAC2* from *G. herbaceum*, improves root growth and imparts tolerance to drought in transgenic cotton and Arabidopsis. *Sci. Rep.* 6:24978. doi: 10.1038/srep24978

Hao, Q., Yin, P., Li, W., Wang, L., Yan, C., Lin, Z., et al. (2011). The molecular basis of ABA-independent inhibition of PP2Cs by a subclass of PYL proteins. *Mol. Cell* 42, 662–672. doi: 10.1016/j.molcel.2011.05.011

He, X., Zhu, L., Xu, L., Guo, W., and Zhang, X. (2016). GhATAF1, a NAC transcription factor, confers abiotic and biotic stress responses by regulating phytohormonal signaling networks. *Plant Cell Rep.* 35, 2167–2179. doi: 10.1007/s00299-016-20276

Hurst, H. C. (1995). Transcription factors 1: bZIP proteins. *Protein Profile* 2, 101–168.

Iyer, L. M., Koonin, E. V., and Aravind, L. (2001). Adaptations of the helix-grip fold for ligand binding and catalysis in the START domain superfamily. *Proteins* 43, 134–144. doi: 10.1002/1097-0134(20010501)43:2<134::AID-PROT1025>3.0.CO;2-I

Li, F., Fan, G., Lu, C., Xiao, G., Zou, C., Kohel, R. J., et al. (2015). Genome sequence of cultivated Upland cotton (*Gossypium hirsutum* TM-1) provides insights into genome evolution. *Nat. Biotechnol.* 33, 524–530. doi: 10.1038/nbt.3208

Li, F., Fan, G., Wang, K., Sun, F., Yuan, Y., Song, G., et al. (2014). Genome sequence of the cultivated cotton *Gossypium arboreum*. *Nat. Genet.* 46, 567–572. doi: 10.1038/ng.2987

Li, W., Wang, L., Sheng, X., Yan, C., Zhou, R., Hang, J., et al. (2013). Molecular basis for the selective and ABA-independent inhibition of PP2CA by PYL13. *Cell Res.* 23, 1369–1379. doi: 10.1038/cr.2013.143

Liang, C., Meng, Z., Meng, Z., Malik, W., Yan, R., Lwin, K. M., et al. (2016). GhABF2, a bZIP transcription factor, confers drought and salinity tolerance in cotton (*Gossypium hirsutum* L.). *Sci. Rep.* 6:35040. doi: 10.1038/srep35040

Liang, C., Wang, Y., Zhu, Y., Tang, J., Hu, B., Liu, L., et al. (2014). OsNAP connects abscisic acid and leaf senescence by fine-tuning abscisic acid biosynthesis and directly targeting senescence-associated genes in rice. *Proc. Natl. Acad. Sci. U.S.A.* 111, 10013–10018. doi: 10.1073/pnas.1321568111

Liang, C., Zheng, G., Li, W., Wang, Y., Hu, B., Wang, H., et al. (2015). Melatonin delays leaf senescence and enhances salt stress tolerance in rice. *J. Pineal Res.* 59, 91–101. doi: 10.1111/jpi.12243

Lin, A., Wang, Y., Tang, J., Xue, P., Li, C., Liu, L., et al. (2012). Nitric oxide and protein S-nitrosylation are integral to hydrogen peroxide-induced leaf cell death in rice. *Plant Physiol.* 158, 451–464. doi: 10.1104/pp.111.184531

Lin, F., Zhang, R., Sun, G., Sun, B., and Guo, S. (2012). Molecular cloning and its functional analysis of *GhSRK20* gene from cotton. *J. Agric. Sci. Technol.* 14, 36–42.

Lin, L., Pierce, G. J., Bowers, J. E., Estill, J. C., Compton, R. O., Rainville, L. K., et al. (2010). A draft physical map of a D-genome cotton species (*Gossypium raimondii*). *BMC Genomics* 11:395. doi: 10.1186/1471-2164-11-395

Liu, L., Tong, H., Xiao, Y., Che, R., Xu, F., Hu, B., et al. (2015). Activation of *Big Grain1* significantly improves grain size by regulating auxin transport in rice. *Proc. Natl. Acad. Sci. U.S.A.* 112, 11102–11107. doi: 10.1073/pnas.1512748112

Liu, X., Zhao, B., Zheng, H. J., Hu, Y., Lu, G., Yang, C. Q., et al. (2015). *Gossypium barbadense* genome sequence provides insight into the evolution of extra-long staple fiber and specialized metabolites. *Sci. Rep.* 5:14139. doi: 10.1038/srep14139

Liu, Y., Zhang, X., Zhu, S., Zhang, H., Li, Y., Zhang, T., et al. (2016). Overexpression of *GhSARP1* encoding a E3 ligase from cotton reduce the tolerance to salt

in transgenic *Arabidopsis*. *Biochem. Biophys. Res. Commun.* 478, 1491–1496. doi: 10.1016/j.bbrc.2016.07.033

Melcher, K., Ng, L. M., Zhou, X. E., Soon, F. F., Xu, Y., Suino-Powell, K. M., et al. (2009). A gate-latch-lock mechanism for hormone signalling by abscisic acid receptors. *Nature* 462, 602–608. doi: 10.1038/nature08613

Miyazono, K., Miyakawa, T., Sawano, Y., Kubota, K., Kang, H. J., Asano, A., et al. (2009). Structural basis of abscisic acid signalling. *Nature* 462, 609–614. doi: 10.1038/nature08583

Nishimura, N., Hitomi, K., Arvai, A. S., Rambo, R. P., Hitomi, C., Cutler, S. R., et al. (2009). Structural mechanism of abscisic acid binding and signaling by dimeric PYR1. *Science* 326, 1373–1379. doi: 10.1126/science.1181829

Nishimura, N., Sarkeshik, A., Nito, K., Park, S. Y., Wang, A., Carvalho, P. C., et al. (2010). PYR/PYL/RCAR family members are major *in-vivo* ABI1 protein phosphatase 2C-interacting proteins in Arabidopsis. *Plant J.* 61, 290–299. doi: 10.1111/j.1365-313X.2009.04054.x

Park, S. Y., Fung, P., Nishimura, N., Jensen, D. R., Fujii, H., Zhao, Y., et al. (2009). Abscisic acid inhibits type 2C protein phosphatases via the PYR/PYL family of START proteins. *Science* 324, 1068–1071. doi: 10.1126/science.1173041

Paterson, A. H., and Wendel, J. F. (2015). Unraveling the fabric of polyploidy. *Nat. Biotechnol.* 33, 491–493. doi: 10.1038/nbt.3217

Paterson, A. H., Wendel, J. F., Gundlach, H., Guo, H., Jenkins, J., Jin, D., et al. (2012). Repeated polyploidization of *Gossypium genomes* and the evolution of spinnable cotton fibres. *Nature* 492, 423–427. doi: 10.1038/nature11798

Qin, L. X., Nie, X. Y., Hu, R., Li, G., Xu, W. L., and Li, X. B. (2016). Phosphorylation of serine residue modulates cotton Di19-1 and Di19-2 activities for responding to high salinity stress and abscisic acid signaling. *Sci. Rep*. 6:20371. doi: 10.1038/srep20371

Santiago, J., Dupeux, F., Round, A., Antoni, R., Park, S. Y., Jamin, M., et al. (2009). The abscisic acid receptor PYR1 in complex with abscisic acid. *Nature* 462, 665–668. doi: 10.1038/nature08591

Shan, C. M., Shangguan, X. X., Zhao, B., Zhang, X. F., Chao, L. M., Yang, C. Q., et al. (2014). Control of cotton fibre elongation by a homeodomain transcription factor GhHOX3. *Nat. Commun.* 5:5519. doi: 10.1038/ncomms6519

Sheard, L. B., and Zheng, N. (2009). Signal advance for abscisic acid. *Nature* 462, 575–576. doi: 10.1038/462575a

Shi, Y., Zhang, R., Wu, X. P., Meng, Z., and Guo, S. (2012). Cloning and characterization of a somatic embryogenesis receptor-like kinase gene in cotton (*Gossypium hirsutum*). *J. Integr. Agric.* 11, 898–909. doi: 10.1016/S2095-3119(12)60080-X

Wang, C., Lu, W., He, X., Wang, F., Zhou, Y., Guo, X., et al. (2016). The cotton *mitogen-activated protein kinase kinase 3* functions in drought tolerance by regulating stomatal responses and root growth. *Plant Cell Physiol.* 57, 1629–1642. doi: 10.1093/pcp/pcw090

Wang, M., Tu, L., Lin, M., Lin, Z., Wang, P., Yang, Q., et al. (2017). Asymmetric subgenome selection and *cis*-regulatory divergence during cotton domestication. *Nat. Genet.* 49, 579–587. doi: 10.1038/ng.3807

Wang, K., Wang, Z., Li, F., Ye, W., Wang, J., Song, G., et al. (2012). The draft genome of a diploid cotton *Gossypium raimondii*. *Nat. Genet.* 44, 1098–1103. doi: 10.1038/ng.2371

Wang, Y., Liang, C., Wu, S., Zhang, X., Tang, J., Jian, G., et al. (2016). Significant improvement of cotton *Verticillium* wilt resistance by manipulating the expression of *Gastrodia* antifungal proteins. *Mol. Plant* 9, 1436–1439. doi: 10.1016/j.molp.2016.06.013

Xing, L., Zhao, Y., Gao, J., Xiang, C., and Zhu, J. K. (2016). The ABA receptor PYL9 together with PYL8 plays an important role in regulating lateral root growth. *Sci. Rep.* 6:27177. doi: 10.1038/srep27177

Xiong, L., Schumaker, K. S., and Zhu, J. K. (2002). Cell signaling during cold, drought, and salt stress. *Plant Cell* 14(Suppl.), S165–S183.

Yoshida, T., Mogami, J., and Yamaguchi-Shinozaki, K. (2014). ABA-dependent and ABA-independent signaling in response to osmotic stress in plants. *Curr. Opin. Plant Biol.* 21, 133–139. doi: 10.1016/j.pbi.2014.07.009

Yuan, D., Tang, Z., Wang, M., Gao, W., Tu, L., Jin, X., et al. (2015). The genome sequence of Sea-Island cotton (*Gossypium barbadense*) provides insights into the allopolyploidization and development of superior spinnable fibres. *Sci. Rep.* 5:17662. doi: 10.1038/srep17662

Zhang, M., Yuan, B., and Leng, P. (2009). The role of ABA in triggering ethylene biosynthesis and ripening of tomato fruit. *J. Exp. Bot.* 60, 1579–1588. doi: 10.1093/jxb/erp026

Zhao, Y., Chan, Z., Gao, J., Xing, L., Cao, M., Yu, C., et al. (2016). ABA receptor PYL9 promotes drought resistance and leaf senescence. *Proc. Natl. Acad. Sci. U.S.A.* 113, 1949–1954. doi: 10.1073/pnas.1522840113

Zhao, Y., Chan, Z., Xing, L., Liu, X., Hou, Y. J., Chinnusamy, V., et al. (2013). The unique mode of action of a divergent member of the ABA-receptor protein family in ABA and stress signaling. *Cell Res.* 23, 1380–1395. doi: 10.1038/cr.2013.149

Zhao, Y., Xing, L., Wang, X., Hou, Y. J., Gao, J., Wang, P., et al. (2014). The ABA receptor PYL8 promotes lateral root growth by enhancing MYB77-dependent transcription of auxin-responsive genes. *Sci. Signal.* 7, ra53. doi: 10.1126/scisignal.2005051

Zhu, J. K. (2002). Salt and drought stress signal transduction in plants. *Annu. Rev. Plant Biol.* 53, 247–273. doi: 10.1146/annurev.arplant.53.091401.143329

Zhu, J. K. (2016). Abiotic stress signaling and responses in plants. *Cell* 167, 313–324. doi: 10.1016/j.cell.2016.08.029

Zhu, T., Liang, C., Meng, Z., Sun, G., Meng, Z., Guo, S., et al. (2017). CottonFGD: an integrated functional genomics database for cotton. *BMC Plant Biol.* 17:101. doi: 10.1186/s12870-017-1039-x

Conflict of Interest Statement: The authors declare that the research was conducted in the absence of any commercial or financial relationships that could be construed as a potential conflict of interest.

frontiers in Plant Science

ORIGINAL RESEARCH
published: 11 December 2017
doi: 10.3389/fpls.2017.02108

OsJAZ1 Attenuates Drought Resistance by Regulating JA and ABA Signaling in Rice

*Jie Fu, Hua Wu, Siqi Ma, Denghao Xiang, Ruyi Liu and Lizhong Xiong**

National Key Laboratory of Crop Genetic Improvement and National Center of Plant Gene Research (Wuhan), Huazhong Agricultural University, Wuhan, China

Jasmonates (JAs) and abscisic acid (ABA) are phytohormones known play important roles in plant response and adaptation to various abiotic stresses including salinity, drought, wounding, and cold. JAZ (JASMONATE ZIM-domain) proteins have been reported to play negative roles in JA signaling. However, direct evidence is still lacking that JAZ proteins regulate drought resistance. In this study, OsJAZ1 was investigated for its role in drought resistance in rice. Expression of *OsJAZ1* was strongly responsive to JA treatment, and it was slightly responsive to ABA, salicylic acid, and abiotic stresses including drought, salinity, and cold. The *OsJAZ1*-overexpression rice plants were more sensitive to drought stress treatment than the wild-type (WT) rice Zhonghua 11 (ZH11) at both the seedling and reproductive stages, while the *jaz1* T-DNA insertion mutant plants showed increased drought tolerance compared to the WT plants. The *OsJAZ1*-overexpression plants were hyposensitive to MeJA and ABA, whereas the *jaz1* mutant plants were hypersensitive to MeJA and ABA. In addition, there were significant differences in shoot and root length between the OsJAZ1 transgenic and WT plants under the MeJA and ABA treatments. A subcellular localization assay indicated that OsJAZ1 was localized in both the nucleus and cytoplasm. Transcriptome profiling analysis by RNA-seq revealed that the expression levels of many genes in the ABA and JA signaling pathways exhibited significant differences between the *OsJAZ1*-overexpression plants and WT ZH11 under drought stress treatment. Quantitative real-time PCR confirmed the expression profiles of some of the differentially expressed genes, including *OsNCED4*, *OsLEA3*, *RAB21*, *OsbHLH006*, *OsbHLH148*, *OsDREB1A*, *OsDREB1B*, *SNAC1*, and *OsCCD1*. These results together suggest that OsJAZ1 plays a role in regulating the drought resistance of rice partially via the ABA and JA pathways.

Keywords: jasmonates, abscisic acid, JAZ protein, crosstalk, drought resistance

OPEN ACCESS

Edited by:
Hanwei Mei,
Shanghai Agrobiological Gene Center, China

Reviewed by:
Tibor Janda,
Centre for Agricultural Research (MTA), Hungary
Guangxiao Yang,
Huazhong University of Science and Technology, China

***Correspondence:**
Lizhong Xiong
lizhongx@mail.hzau.edu.cn

Specialty section:
This article was submitted to Plant Breeding, a section of the journal Frontiers in Plant Science

Received: *17 October 2017*
Accepted: *27 November 2017*
Published: *11 December 2017*

Citation:
Fu J, Wu H, Ma S, Xiang D, Liu R and Xiong L (2017) OsJAZ1 Attenuates Drought Resistance by Regulating JA and ABA Signaling in Rice. Front. Plant Sci. 8:2108. doi: 10.3389/fpls.2017.02108

INTRODUCTION

Due to their sessile nature, plants have to face variable environmental stresses including drought, high salinity, cold, and heat during their growth and development. Plants respond and adapt to the adverse cues throughout their life cycle by coordinating an array of biochemical and physiological changes. Phytohormones, such as abscisic acid (ABA) and jasmonates (fatty acid-derived oxylipins, JAs), play important roles in promoting plant defense against abiotic stresses (Verma et al., 2016).

To date, key components of JA perception and signaling have been extensively studied in numerous plant species, particularly in *Arabidopsis*, tomato (*Solanum lycopersicum*), and rice (*Oryza sativa*) (Cheong and Choi, 2003; Goossens et al., 2016; Wasternack and Song, 2017). According to the updated model of JA perception and the regulation of JA-responsive genes (Xu, 2002; Chini et al., 2007; Sheard et al., 2010; Zhu et al., 2011), the COI1-JAZ complex acts as JA co-receptor and transcriptional repressor in JA signaling. Under normal or JA-absent conditions, JAZ proteins bind to transcription factors (TFs) and inhibit their activities by recruiting the TOPLESS (TPL) co-repressor or by directly recruiting histone-modifying proteins such as HDA6. These TFs can bind to the G-box of JA- and JA-Ile-responsive genes. Under any stress conditions or developmental processes in which the levels of endogenous JA-Ile (bioactive jasmonyl-isoleucine) are increased, the binding of JA-Ile to the COI1-JAZ co-receptor will lead to the degradation of JAZs via the 26S proteasome, and the JA signaling responses and downstream genes are activated.

JASMONATE ZIM-domain (JAZ) proteins, belonging to the group II of the TIFY family, have been identified as important regulators of JA signaling in numerous plants, including *Arabidopsis thaliana*, *Solanum lycopersicum*, and rice, etc. There are 20 and 18 members of the TIFY family in rice and *Arabidopsis*, respectively (Vanholme et al., 2007; Ye et al., 2009). In previous studies, overexpression of *JAZ1* lacking the Jas domain in *Arabidopsis* showed an obvious JA-hyposensitive phenotype, and a similar phenotype was observed in a *JAI3/JAZ* mutant (Chini et al., 2007; Thines et al., 2007). Furthermore, JAZ proteins have been well characterized for their interaction with bHLH TFs to repress the transcriptional activities of bHLH, which are the core transcriptional activators of JA signaling mediated gene expression. For example, MYC2, MYC3, and MYC4, which are core bHLH factors in the regulation of JA signaling in rice and *Arabidopsis*, have been reported to interact with almost all the JAZ proteins (Cheng et al., 2011; Fernandez-Calvo et al., 2011; Sasaki-Sekimoto et al., 2014). JAZ proteins are also found to interact with the F-box protein COI1, leading to the degradation of the JAZ proteins (Song et al., 2011). The *coi1* mutants in *Arabidopsis* were defective in the JA response. In addition, expression of the JA-induced genes *AtVSP*, *Thi2.0*, and *PDF1.2*, which encode defense-related proteins, were suppressed in the *coi1* mutant (Penninckx et al., 1998; Xu et al., 2001), indicating that *COI1* is a core player in the JA signaling pathway. JAZ proteins have been reported to be involved in the regulation of trichome formation, anthocyanin synthesis, and male fertility by interacting with various TFs and affecting their transcriptional function (Kirik et al., 2005; Gonzalez et al., 2008; Qi et al., 2011; Song et al., 2011). JAZ proteins directly interacted with a wide array of TFs (such as GL3, EGL3, TT8, and the MYB factor MYB75), repressed their transcriptional function, and then suppressed JA-induced anthocyanin biosynthesis and trichome initiation (Kirik et al., 2005; Gonzalez et al., 2008; Qi et al., 2011). In addition, JAZ proteins (JAZ1, JAZ8, and JAZ11) in *Arabidopsis* were reported to interact with two R2R3-MYB TFs MYB21 and MYB24, which inhibited the expression of downstream genes essential for JA-mediated stamen development (Song et al., 2011). JAZ proteins also have been reported to be involved in the regulation of abiotic stresses including cold, salinity, drought, wounding, and ozone (Savchenko et al., 2014; Wu et al., 2015). Hu et al. (2013) suggested that JAZ proteins (JAZ1 and JAZ4) physically interact with ICE1, resulting in a blockage in the ICE-CBF pathway in *Arabidopsis*. JAZ9, a transcriptional regulator in JA signaling, is known to modulate salt tolerance in rice (Wu et al., 2015).

Abscisic acid also plays an important role in regulating various stress responses and the expression of stress responsive genes (Stone et al., 2006; Nilson and Assmann, 2007; Sirichandra et al., 2009). A number of studies have shown that JA signaling can interact with ABA signaling (Lackman et al., 2011; Chen et al., 2012; Aleman et al., 2016). *MED25* plays a positive role in JA signaling via *OsMYC2*, while it negatively regulates the protein abundance of ABI5, which plays a core role in ABA signaling (Chen et al., 2012). In addition, *HDA6*, an RPD3-type histone deacetylase, was found to be involved in the JA and ABA response (Wu et al., 2008; Chen and Wu, 2010). PYL4, an ABA receptor, is involved in the crosstalk between JA and the ABA pathway to regulate plant metabolism and growth (Lackman et al., 2011). The ABA-dependent signaling pathway is partially controlled by MYC/MYB TFs, which are target proteins of JAZ proteins. It has been demonstrated that ATMYC2 (JIN1) in *Arabidopsis*, an important player in JA signaling, can function as a positive activator in the expression of ABA and the drought inducible gene *RD22* (Abe et al., 2003). Recently, several publications have demonstrated that JAs are involved in the regulation of numerous stress-responsive genes which are also regulated by ABA. The expression levels of *SNAC1* and *OsbHLH148*, involved in the regulation of drought-responsive genes, were both increased by MeJA and ABA treatments (Takasaki et al., 2010; Seo et al., 2011). The crosstalk between JA and ABA signaling was also observed in guard cells. CPK6, an *Arabidopsis* calcium dependent protein kinase, was involved in both ABA and JA signaling in guard cells (Munemasa et al., 2011). Moreover, de Ollas et al. (2015) suggested that the ABA concentration was increased fourfold to sevenfold in an exogenous JA treatment, while a JA deficiency mutant *jarl* showed reduced ABA accumulation.

Although previous studies clearly suggest that JA is involved in drought responses, direct evidence for JAZ proteins in regulating drought resistance is lacking. In this study, we aimed to investigate whether and how a stress-responsive JAZ gene, *OsJAZ1*, regulates drought resistance in rice. The *OsJAZ1*-overexpression (*OsJAZ1*-OE) plants showed increased sensitivity to drought stress, while the *jaz1* mutant plants were more hyposensitive to drought stress compared to the wild-type (WT) plants. Moreover, the *jaz1* mutant plants were more hypersensitive to MeJA and ABA, indicating that JAZ1 may play a negative role in modulating JA and ABA signaling. Consistent with this, many genes in the JA and ABA signaling pathways were affected by *OsJAZ1* overexpression under drought stress conditions. Our results suggest that OsJAZ1 plays a negative role

in drought resistance, partially through regulation of the JA and ABA pathways.

MATERIALS AND METHODS

Plant Materials and Growth Conditions

The *OsJAZ1* mutant line 4A-00845 in the background of the rice variety Dongjin (*Oryza sativa* L. ssp. *japonica*) was obtained from the POSTECH RISD[1]. Homozygous mutant lines (mut-1 and mut-2) were segregated from the heterozygous mutant 4A-00845. Genotyping was performed using the *OsJAZ1* genomic primers and the T-DNA left-border primer (Supplementary Table 1). The full coding sequence of *OsJAZ1* (LOC_Os04g55920.1) was amplified from the total cDNA of rice leaves. The amplified fragment of *OsJAZ1* was cloned into pCAMBIA1301H, which was driven by the *OsLEA3* promoter (Xiao et al., 2007). The plasmid was then introduced into the *japonica* rice cultivar Zhonghua11 (ZH11) via *Agrobacterium*-mediated transformation (Hiei and Komari, 2008). The rice plants used for drought resistance testing were grown in pots or paddy field under the natural conditions at Wuhan (114.36°E, 30.48°N), China. The seedlings for phytohormone treatments were grown in a phytotron (PPFD 75 $\mu mol/m^2.s$) with a 14 h light/10 h dark cycle for 7 days with a temperature at 28°C and 25°C, for the light and dark conditions, respectively.

Drought Resistance Testing

To investigate the drought stress resistance of *OsJAZ1*-OE plants and *jaz1* mutant plants at the seedling stage, WT and transgenic seeds were germinated on 1/2 strength MS medium for 3 days in the dark and 4 days in a greenhouse. WT and transgenic lines were transplanted into barrels (30 cm in diameter and 25 cm in height) filled with a mixture of sand and soil (1:1). Each barrel was planted with about 10 transgenic seedlings and 10 WT seedlings in a half-and-half manner. Seedlings at the four-leaf stage were subjected to drought stress treatment for 4 days with the water content of the soil maintained at 5–10%. After recovery by watering for 7 days, the plants were photographed and the survival rates were recorded. Each of the OE or mutant lines were tested with three biological repeats for drought resistance. Drought stress treatment was also performed in the barrels at the reproductive stage. In this testing, each barrel was planted with a single plant. A rice automatic phenotyping (RAP) platform (Yang et al., 2014) was used to extract phenotypic traits of the plants in the barrels. At the booting stage, the WT and transgenic plants were subjected to drought stress treatment for 7 days with the soil moisture content maintained at 15%. All the materials in this had three repeats under both normal growth and drought stress conditions. To reflect the morphological changes of plants in response to drought stress treatment, we adopted an image index called PAR, which was defined as the plant perimeter divided by the projected plant area. Since rice leaves exhibit rolling under moderate and severe drought stress conditions, the projected area will decrease, but the plant perimeter will not change too much. Therefore, the change in PAR will largely reflect the degree of leaf rolling and plant architecture. Drought stress treatment at the reproductive stage was performed in a refined paddy field facilitated with a movable rain-off shelter. Each material was planted in a plot of 10 plants with three repeats. The transgenic plants and WT plants at the booting stage were subjected to drought stress treatment for about 3 weeks with the soil moisture content maintained at 15% for the final 5 days. Then the field was fully irrigated for recovery. The relative water content (RWC) in plant leaves were determined as follows: RWC % = 100% × (fresh weight – dry weight)/(turgid weight – dry weight). The dry weight was determined by placing the samples at 80°C for 24 h. Turgid weight was obtained after placing the samples in ddH_2O at room temperature for 3 h.

[1]http://www.postech.ac.kr/life/pfg/risd/

Phytohormone Treatment

To test the phytohormones (ABA and JA) sensitivity of the *OsJAZ1*-OE transgenic plants and T-DNA mutant plants at the seedling stage, WT plants and transgenic lines were germinated on 1/2 strength MS medium for 3 days in the dark. After germination, seedlings with similar shoot length and root length were transplanted to transparent plastic plates (13 cm × 13 cm, seven plants half by half, at least three repeats) with 1/2 strength MS medium containing phytohormones (3 μM for ABA, 10 μM for MeJA) or water as a control. Finally, the phenotypes were recorded and shoot length and root length of these seedling were measured. To check the expression level of *OsJAZ1* under phytohormone treatments, the seedlings at four-leaf stage were sprayed with ABA (100 μmol/L), MeJA (100 μmol/L), and SA (100 μmol/L), respectively, each with three replicates. Then seedling leaves were sampled in a designed time course indicated in **Figure 1**. The concentration for testing MeJA and ABA sensitivity of OsJAZ1-OE and T-DNA mutant plants were selected by referring to Cai et al. (2014) and Tang et al. (2016).

Subcellular Localization

For investigating the subcellular localization of the OsJAZ1 protein, the coding region of *OsJAZ1* was cloned into the PM999-35 vector with C-terminal YFP tag by a one-step *in vitro* recombination method (Gibson et al., 2009). The resulting construct (35S: JAZ1-YFP) and the nuclear marker 35S: CFP-GHD7 (Xue et al., 2008) were used for transient transformation of protoplasts. The protocol for isolation and transformation of rice protoplasts was described previously (Xie and Yang, 2013). The fluorescence signal was observed with a confocal laser-scanning microscope (FV1200) at 16–18 h after transformation. To confirm the nuclear signal of JAZ1, the protoplasts were treated with 100 μM MeJA for 3 h in the dark before collection for microscope observation.

RNA Extraction and Quantification of Gene Expression

All the harvested leaf samples were frozen in liquid nitrogen, and RNA was extracted using TRIzol® reagent (Ambion™, Lot No.15596018) according to the manufacturer's instructions.

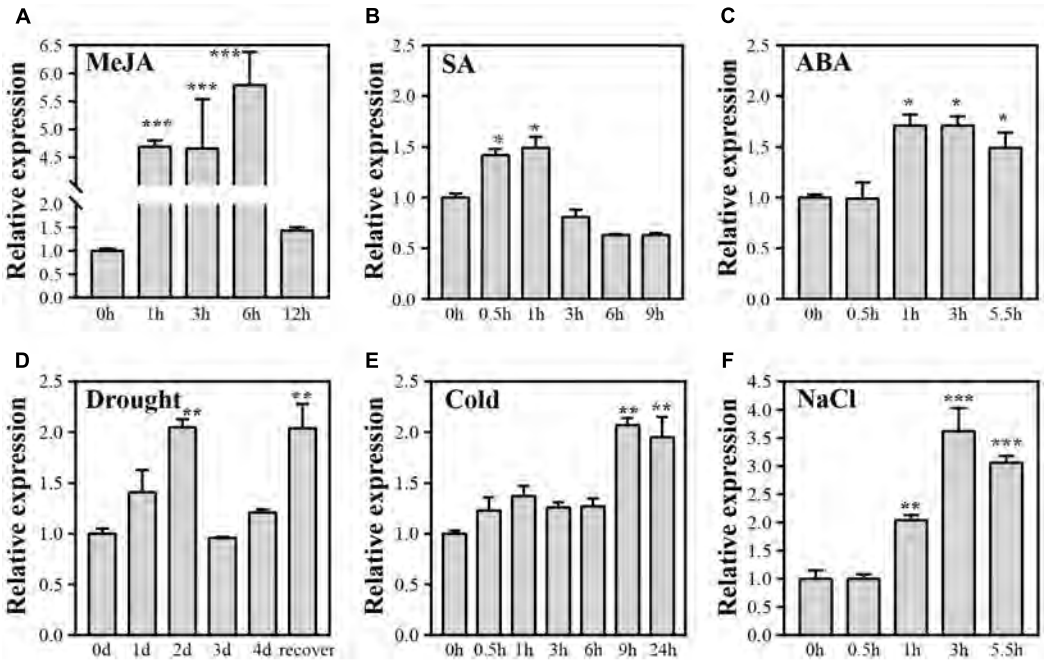

FIGURE 1 | Expression levels of *OsJAZ1* under various abiotic stresses and phytohormone treatments. **(A–F)** Seedlings at the four-leaf stage were subjected to treatment with drought stress, NaCl (200 mmol/L), cold (4°C), ABA (100 μmol/L), MeJA (100 μmol/L), and SA (100 μmol/L), respectively. Error bars represent the SE of three replicates. Significance was determined by Student's *t*-test (***$P < 0.001$, **$P < 0.01$, *$P < 0.05$).

RNA was reverse transcribed using the EasyScript One-Step gDNA Removal and cDNA Synthesis Kit (TRANS) according to the manufacturer's protocol. The quality of cDNA product was checked by amplifying *OsActin* (LOC_Os03g50885), which was used as an internal control and then the cDNA sample was 10-fold diluted with ddH_2O for qRT-PCR. Real-time PCR was performed using a Quant Studio 6 Flex Real-time system with a SYBR Green Master Mix kit (Applied Biosystems^{TM}). Three repeated reactions were routinely performed for each sample. The PCR reactions were performed as follows: 50°C for 2 min, 95°C for 2 min, followed by 40 cycles of 95°C for 1 s, 60°C for 30 s. All primers used in this study for qPCR are shown in Supplementary Table 1. The quantification of the relative expression level followed the reported $2^{-\Delta\Delta C_T}$ method (Livak and Schmittgen, 2001).

RNA-Seq and Transcriptome Profiling Analysis

Total RNA was extracted from WT Zhonghua 11 (ZH11) and the *OsJAZ1*-OE plants at the four-leaf stage under normal and drought stress conditions with three biological replicates. The RNA samples were sequenced by Novogene (Tianjin, China) with Hiseq-PE150 and the raw data was analyzed using the customized RNA-seq data processing platform at the BMKCloud cloud server[2]. According to the results of Pearson's correlation coefficient (Schulze et al., 2012), the third biological replicate of WT ZH11 and *OsJAZ1*-OE under drought stress was excluded from further analysis because of a low correlation coefficient. The expression levels of the genes were quantified by FPKM (fragments per kilobase of transcript per million fragments mapped) (Florea et al., 2013). The fold change of the expression level of the stressed sample over the corresponding non-stressed sample was calculated, and the genes with an absolute value of $|\log_2(\text{fold change})| \geq 1$ and FDR < 0.05 were selected as differentially expressed genes (DEGs) (Anders and Huber, 2010). The Gene Ontology Consortium and Kyoto Encyclopedia of Genes and Genomes were referenced by GO enrichment analysis and the functional associated pathways, respectively, for the DEGs.

The RNA-Seq data were deposited in the Gene Expression Omnibus under accession number GSE107425.

Statistical Analysis

The Student's *t*-test was used for statistical analysis. Statistical significance was determined at $P^{*} < 0.05$, $P^{**} < 0.01$, and $P^{***} < 0.001$.

RESULTS

Expression Analysis of *OsJAZ1*

To investigate if *OsJAZ1* is involved in stress response, we applied quantitative real-time PCR (qPCR) to check the expression profiles of *OsJAZ1* under various phytohormone treatments and abiotic stresses at the four-leaf stage of rice. The results showed that *OsJAZ1* was strongly induced by MeJA (**Figure 1A**),

[2]http://www.biocloud.net/

suggesting that JAZ1 may be involved in JA signaling. *OsJAZ1* was slightly up-regulated by exogenous SA and ABA (**Figures 1B,C**). *OsJAZ1* was also induced by multiple abiotic stresses including drought, cold, and salinity (**Figures 1D–F**). Considering the biochemical function of JAZ proteins, these results suggest that OsJAZ1 may participate in the regulation of the responses to abiotic stresses and multiple phytohormones.

OsJAZ1 Negatively Regulates Drought Resistance at the Seedling Stage

To answer whether OsJAZ1 is involved in drought resistance regulation, we requested and obtained a heterozygous mutant 4A-00845 (Dongjin rice background) from the POSTECH RISD[3]. As shown in **Figure 2A**, the T-DNA was inserted in the promoter of *OsJAZ1*, and homozygous mutant plants (mut-1 and mut-2) were identified by PCR analysis using the primers Z1-mutF, Z1-mutR, and PGAR (Supplementary Table 1). The expression level of *OsJAZ1* in the mutant was dramatically repressed (**Figure 2B**). The primers JAZ1rtF and JAZ1rtR (Supplementary Table 1) were used for *OsJAZ1* expression analysis. For testing drought resistance at the seedling stage, the jaz1 mutant plants and the WT Dongjin plants of 3–4 cm length were transplanted to a blue barrel which was filled with a mixture of sand and soil (1:1). The mutant lines and WT seedlings were subjected to drought stress at the four-leaf stage. The water content of the soil was maintained at 5–10% for 3–4 days, and then watered for recovery. All the *jaz1* mutant lines (mut-1 and mut-2) showed increased tolerance to drought stress treatment (**Figure 2D**). After recovery for 7 days, about 80% of the *jaz1* mutant plants survived, while only 10–20% of the WT plants survived (**Figure 2F**). This result suggested that JAZ1 may have a negative role in drought resistance.

To further confirm the negative role of JAZ1 in drought resistance, we constructed an overexpression vector of *OsJAZ1* which was driven by the drought-inducible *OsLEA3-1* promoter (Xiao et al., 2007). We selected two independent *OsJAZ1*-OE transgenic lines (ZH11 background) with the expression levels of *OsJAZ1* in the transgenic plants confirmed by quantitative real-time PCR (**Figure 2C**). The *OsJAZ1*-OE plants and WT ZH11 were treated with drought stress at the four-leaf stage. During the drought stress treatment, the *OsJAZ1*-OE lines were more sensitive to the stress compared to the WT ZH11 (**Figure 2E**). After recovery, the survival rate of the *OsJAZ1*-OE lines (20%) was significantly lower than that of ZH11 (80%) (**Figure 2G**). These results together further supported that JAZ1 may act as a negative regulator in drought resistance.

OsJAZ1 Negatively Affects Drought Resistance at the Reproductive Stage

Our results described above indicated that OsJAZ1 has a negative effect on drought resistance at the seedling stage. Therefore, we wondered whether JAZ1 affects drought resistance at the reproductive stage. We conducted a drought resistance phenotyping of the *OsJAZ1*-OE lines and T-DNA mutant lines along with their WT controls (ZH11 and Dongjin) at the panicle development reproductive stage by using the high-throughput rice phenotyping facility (HRPF) (Yang et al., 2014). The dynamic changes of the plants to drought stress treatment were recorded by RGB digital cameras (**Figures 3A,D**) installed in the facility. As shown in **Figure 3B**, an image index named PAR (plant perimeter divided by projected area), which mainly reflects the degree of leaf-rolling (see description in Materials and Methods), was significantly greater in the *OsJAZ1*-OE plants than the WT ZH11 under drought stress conditions. This result indicated that the OE plants were more sensitive to drought stress treatment. The RWC is a commonly used indicator for the evaluation of the degree of cell and tissue hydration. As shown in **Figure 3C**, the RWC values of the *OsJAZ1*-OE plants (OE-1 and OE-2) were significantly lower (59.36% and 65.21%) than the WT ZH11 (82.15%) under drought stress conditions. This result further supported the negative effect of *OsJAZ1* in drought resistance. For the *jaz1* mutant lines, the PAR was significantly lower compared to the WT Dongjin under drought stress conditions, while the RWC values of the *jaz1* mutant lines (mut-1 and mut-2) were significantly greater (83.38% and 79.44%) than the WT (61.88%) under drought stress conditions (**Figures 3E,F**). At the same time, we performed drought testing in a paddy field facilitated with a movable rain-off shelter. We found that the green leaves of the *OsJAZ1*-OE plants were significantly fewer than that of ZH11 after severe drought stress treatment. However, we did not observe a significant difference in the drought sensitivity phenotype between the *jaz1* mutant and the WT in the field at the reproductive stage (Supplementary Figure 1). However, there were no differences in yield-related traits between the transgenic and WT plants under drought stress conditions, which may be mainly due to the fact that OsJAZ1/EG2 has been reported with a role in the regulation of spikelet development (Cai et al., 2014), and so the ectopic expression or mutation of this gene may lead to abnormal fertility.

Sensitivity of *OsJAZ1*-Overexpression and Mutant Plants to ABA and MeJA Treatment

To investigate the possible roles of OsJAZ1 in ABA and JA signaling, the *OsJAZ1*-OE plants were treated with 10 μM MeJA and 3 μM ABA. As shown in **Figure 4A**, the *OsJAZ1*-OE lines exhibited hyposensitivity to MeJA and ABA. This result was consistent with a previous study that showed *Arabidopsis* JAZ9-OE plants were insensitive to MeJA (Yang et al., 2012). Moreover, the shoot and root length of the *OsJAZ1*-OE lines were significantly longer than that of WT ZH11 under MeJA and ABA treatments (**Figures 4C,D**), but there was no significant difference under normal conditions. Therefore, we proposed that JAZ1 might repress ABA and JA signaling. To further confirm this, the *jaz1* mutant seeds were germinated for MeJA and ABA sensitivity analysis. We found that the germination of *jaz1* mutant seeds were more sensitive to MeJA and ABA compared to the WT Dongjin (**Figure 4B**). In addition, the shoot and root length of the *jaz1* mutant lines were much shorter than that of the WT Dongjin under the MeJA and ABA treatments (**Figures 4E,F**). Nevertheless, there was no significant difference

[3]http://www.postech.ac.kr/life/pfg/risd/

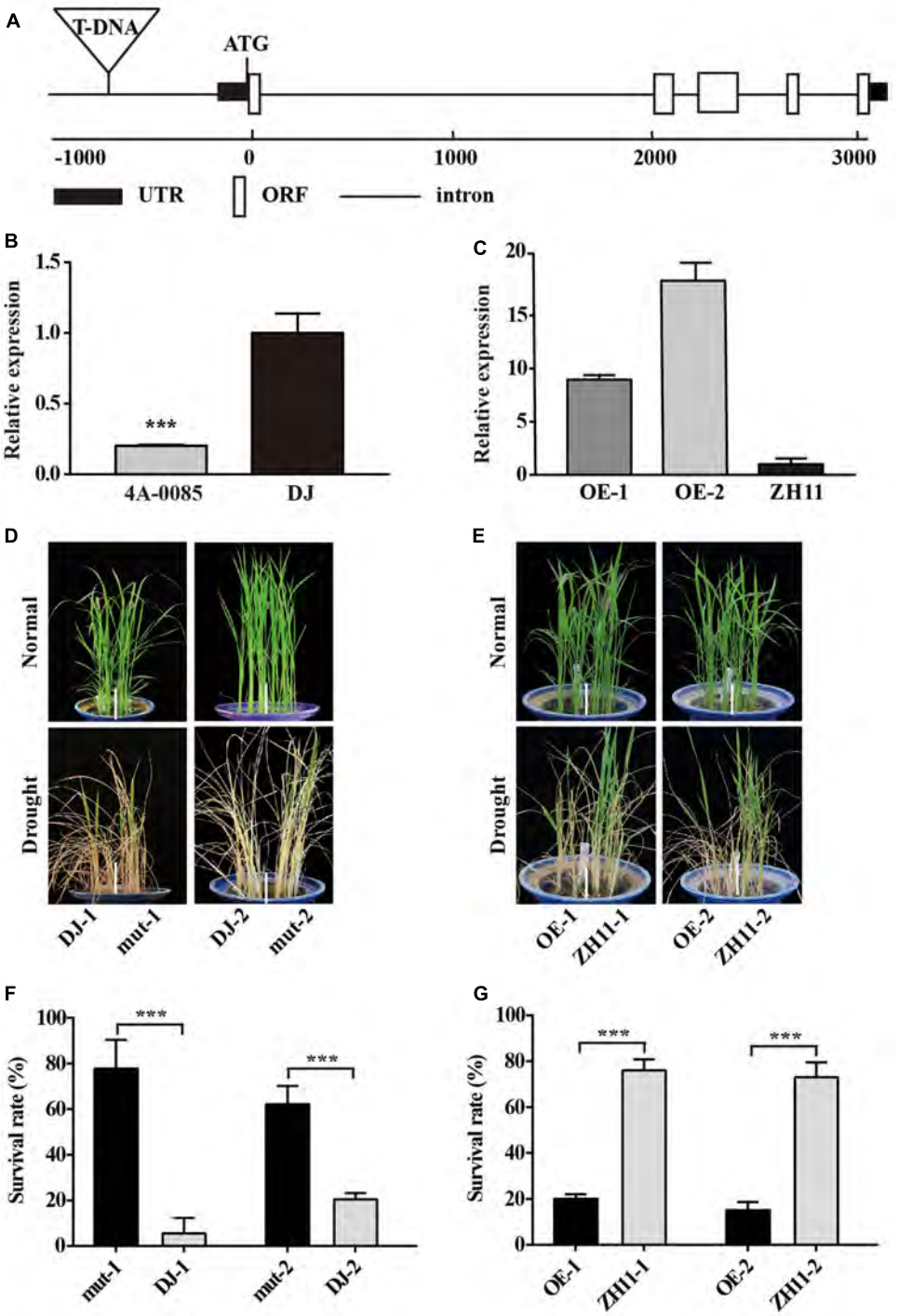

FIGURE 2 | Phenotypes of the *OsJAZ1*-OE plants and the *jaz1* T-DNA insertion mutant plants under drought stress treatment at the seedling stage. **(A)** Schematic diagram of the *OsJAZ1* gene and 4A-00845 T-DNA insertion mutant. UTR, ORF, and introns are indicated in the black box, white box, and line, respectively. **(B)** Expression levels of *OsJAZ1* in the 4A-00845 homozygous line and Dongjin. **(C)** The expression levels of *OsJAZ1* in the OE lines and WT ZH11. **(D,E)** Drought tolerance testing of *jaz1* T-DNA mutant plants and over-expression plants. **(D)** The *jaz1* mutant lines showed increased drought resistance. **(E)** The *OsJAZ1*-OE plants were more sensitive to drought stress treatment compared to WT ZH11. **(F,G)** The survival rates of the transgenic and WT plants after recovery from drought stress treatment for 7 days. Mut-1 and mut-2 were heterozygous mutants segregated from 4A-00845. Error bars represent the SE of three replicates (***$P < 0.005$, Student's *t*-test).

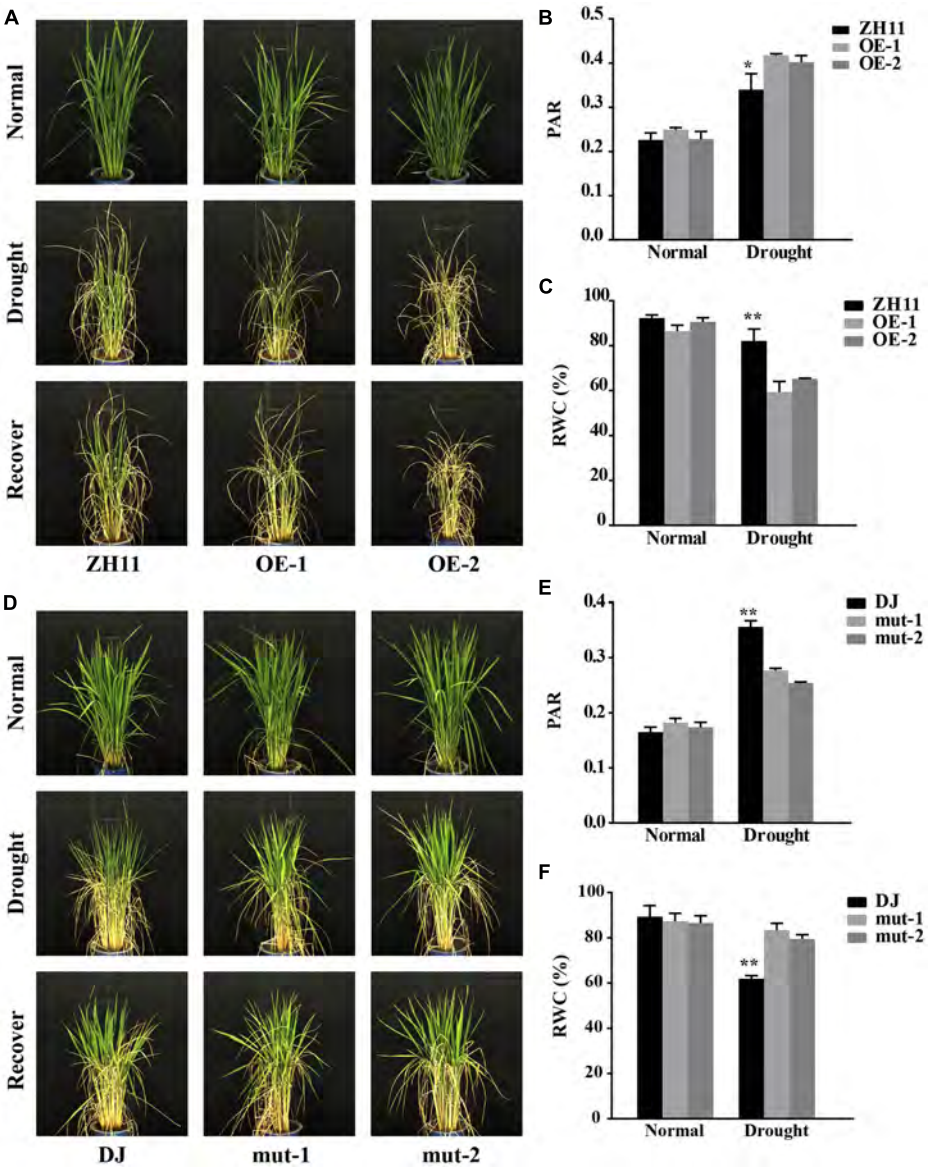

FIGURE 3 | Drought resistance testing of the *OsJAZ1*-OE and mutant lines at the reproductive stage. **(A)** The *OsJAZ1*-OE lines and the WT plants grown in barrels at the booting stage were subjected to drought stress treatment for 7 days with the soil moisture content maintained at 15%. The degree of leaf rolling is indicated by the PAR **(B)** and the relative water content (RWC) **(C)** of the *OsJAZ1*-OE lines under normal and drought stress conditions. PAR = plant perimeter/plant projected area. **(D)** The *jaz1* mutant lines showed increased drought resistance. PAR **(E)** and RWC **(F)** of the *jaz1* mutant lines and Dongjin under normal and drought stress conditions. Error bars represent the SE of three replicates (**$P < 0.01$, *$P < 0.05$, Student's *t*-test).

in these phenotypes under normal germination conditions. Taken together, our results suggest that JAZ1 may negatively modulate ABA and JA signaling.

Subcellular Localization of OsJAZ1

In previous studies, JAZ proteins, such as JAZ9 and JAZ10, were reported to locate in nucleus (Chung and Howe, 2009; Ye et al., 2009; Withers et al., 2012). Therefore, we wondered whether OsJAZ1 is also a nuclear protein. To investigate the subcellular localization of the OsJAZ1, the coding region of *OsJAZ1* was cloned into PM999-35 vector with C-terminal YFP tag. The tag-fused construct (35S: JAZ1-YFP) and the nuclear marker 35S: CFP-GHD7 (Xue et al., 2008) were used for transient transformation of protoplast in rice (Xie and Yang, 2013). To our surprise, OsJAZ1-YFP was found to be localized in cytoplasm (**Figure 5A**), and the YFP signal of OsJAZ1 was completely separated from the nuclear signal. In addition, YFP alone was observed in both nucleus and cytoplasm in a diffuse manner (**Figure 5C**). As we know, MYC2, a bHLH TFs, interacts with JAZ1 in nucleus (Cai et al., 2014). To further examine whether OsJAZ1 is also localized in nucleus in presence JA signaling, the protoplasts contained the construct 35S: OsJAZ1-YFP were

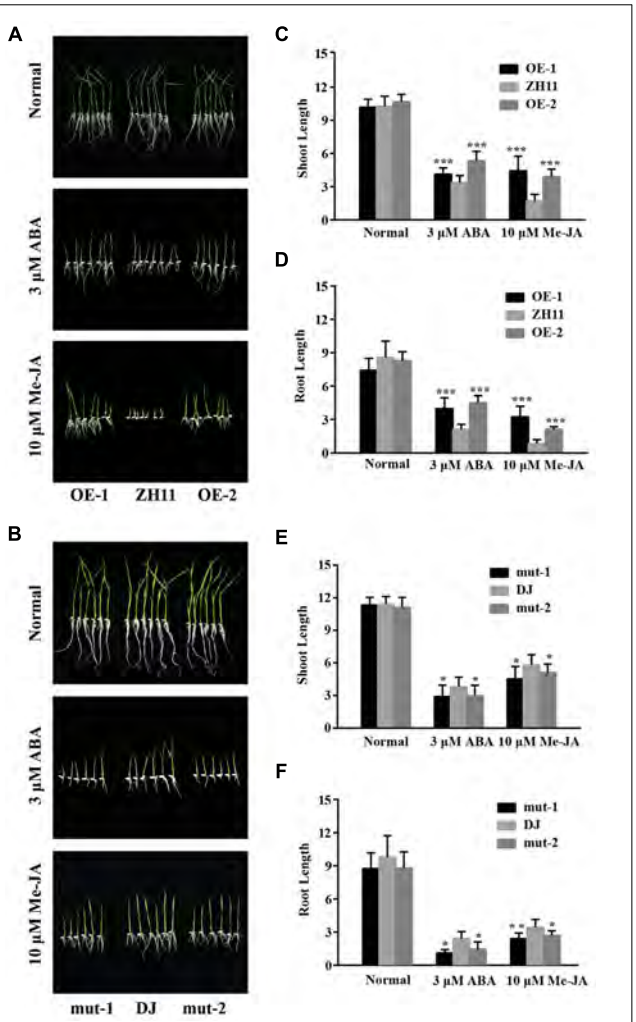

FIGURE 4 | ABA and MeJA sensitivity assay of the *OsJAZ1*-OE and T-DNA mutant plants. **(A,B)** The OE lines and the mutant lines were treated with 3 μM ABA and 10 μM MeJA, under normal conditions (no addition of ABA or MeJA) as a control. **(C–F)** Shoot and root length of the seedlings were measured to estimate the sensitivity of the WT and transgenic plants. Error bars represent the SE of three replicates (***$P < 0.005$, **$P < 0.01$, *$P < 0.05$, Student's *t*-test).

treated with 100 μM MeJA for 3 h. As shown in **Figure 5B**, OsJAZ1-YFP was obviously observed in the nucleus and was co-localized with Ghd7 which has been reported as nuclear protein in rice. These results indicate that OsJAZ1 can function as a nuclear protein in the presence JA signaling.

Transcriptome Analysis of the *OsJAZ1*-Overexpressed Plants

To investigate the transcriptomic changes that may explain the drought-hypersensitive phenotype of the *OsJAZ1*-OE plants, the whole genome expression profiles of *OsJAZ1*-OE and WT ZH11 plants under normal and drought stress conditions were analyzed by RNA-seq. Each sample was collected with three biological replicates. We set the threshold as FDR < 0.05 between sample replicates, and $|\log_2(\text{fold change})| \geq 1$ relative to the respective control. As a result, 2,206 and 2,519 DEGs were detected in the *OsJAZ1* OE and WT ZH11 plants, respectively, under drought stress conditions compared to normal conditions (Supplementary Files 2, 3). As shown in **Figure 6A**, the heat map revealed the different expression patterns of the DEGs (Supplementary File 1) in the *OsJAZ1*-OE and ZH11 plants. There were 899 and 946 up-regulated DEGs, and 1,307 and 1,573 down-regulated DEGs in the *OsJAZ1*-OE and WT ZH11 plants, respectively. Gene ontology (GO) enrichment analysis was conducted to identify the major functional gene groups of the DEGs. We found that most GO enrichments of the DEGs belonged to the 'biological function' super-group, both in the *OsJAZ1*-OE and WT ZH11 plants (Supplementary Files 2, 3). As shown in **Figure 6B**, there were 484 (Group II) and 797 (Group I) DEGs (Supplementary Files 4, 5) specifically in *OsJAZ1*-OE and WT ZH11, respectively, and the expression levels of most genes (1,722) were changed both in *OsJAZ1*-OE and WT ZH11. Among the *OsJAZ1*-OE or WT ZH11-specific DEGs, 197 and 244 DEGs were up-regulated, and 287 and 553 DEGs were down-regulated in the *OsJAZ1*-OE and WT ZH11 plants, respectively. It is noticeable that the number of up-regulated and down-regulated DEGs in the *OsJAZ1*-OE plants were much less than that in the WT ZH11, indicating that JAZ1 may repress some of the expression levels of drought-responsive genes.

To gain insights into the putative functions of the specific DEGs, GO enrichment and KEGG analyses were conducted for the DEGs in Group I and Group II. According to the GO term enrichment, the top three terms in Group I were 'response to oxygen-containing compound' (GO:1901700), 'response to nitrate' (GO:0010167), and 'response to oxidative stress' (GO:0006979), while the top three categories in Group II were 'cell proliferation' (GO:0008283), 'regulation of DNA replication' (GO:0006275), and 'histone H3-K9 methylation' (GO:0051567) (Supplementary Files 4, 5). In addition, there were 49 DEGs and 32 DEGs, respectively, in the WT ZH11 and *OsJAZ1*-OE plants belonging to the GO of 'water deprivation' (GO:0009414). According to the results of the KEGG analysis (Supplementary Files 4, 5), 58 and 99 DEGs were identified, respectively, in Group II and Group I. According to the KEGG analysis, 62% and 7% of the DEGs in Group I belong to 'metabolism' and 'environmental information processing' (Plant hormone signal transduction), while 39% and 15% of the DEGs in Group II belong to these two classifications, respectively (**Figure 6C**). These results suggested that the DEGs in the plant metabolism and hormone signaling pathways may mainly contribute to the hypersensitive phenotype of the *OsJAZ1*-OE plants. To further confirm this speculation, we performed quantitative real-time PCR to examine the expression profiles of some DEGs belonging to plant hormone metabolism and signaling pathways. As shown in **Figure 6D**, we found that the expressions levels of *OsNCED4* (ABA biosynthesis), *RAB21* and *OsLEA3* (typical downstream genes of ABA signaling), *OsbHLH006* and *OsbHLH148* (related to JA signaling), and *OsDREB1A*, *OsDREB1B*, *SNAC1*, and *OsCCD1* (well-known drought responsive genes) were significantly lower in the *OsJAZ1*-OE plants than in the WT ZH11 under drought

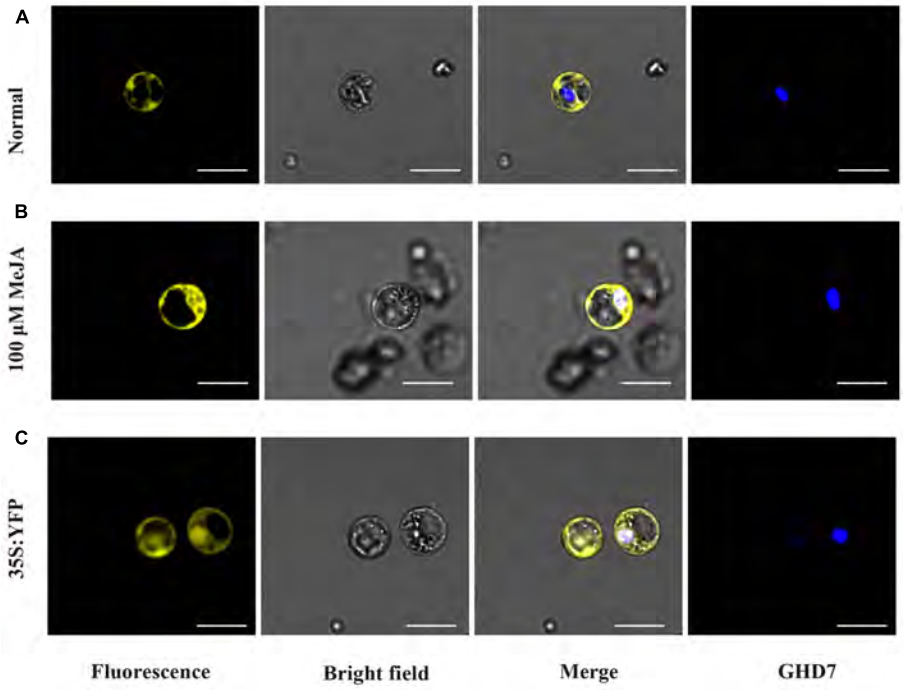

FIGURE 5 | OsJAZ1 subcellular localization. **(A,B)** Confocal microscopy of OsJAZ1-YFP localization in rice protoplasts under normal conditions and 100 μM MeJA treatment, respectively. **(C)** 35S: YFP (PM999-YFP) was transformed into rice protoplasts as a control. GHD7 was used as a nucleus marker. Bars = 20 μm.

stress conditions. These results indicate that the JA and ABA signaling pathways might be attenuated in the *OsJAZ1*-OE plants under drought stress conditions, and the expression levels of some drought resistance-related genes were also repressed to some extent. Together with the hyposensitive and hypersenstive phenotypes for the *OsJAZ1*-OE and the *jaz1* mutant, respectively, under MeJA and ABA treatments, these results suggest that JAZ1 may affect drought resistance partially in an ABA and JA-dependent manner.

DISCUSSION

Phytohormones play important roles in promoting the adaptation of plants to various abiotic stresses. The roles of JA and ABA under abiotic stress have been intensively studied. However, JAZ proteins act as a repressor of JA signaling, and there are only a few reports about the roles of JAZ proteins under abiotic stress treatment in rice (Hu et al., 2013; Wu et al., 2015; Lv et al., 2017). Here, we found that the *jaz1* mutant plants showed increased drought resistance at the seedling and reproductive stages, while the *OsJAZ1*-OE plants were more sensitive to drought stress treatment compared to the WT plants.

OsJAZ1 Negatively Regulates JA and ABA Signaling

According to previous studies, JAZ proteins play a negative role for JA perception and the regulation of JA responsive genes. JA-insensitive and hypersensitive mutants contributed to confirming the negative role of JAZ proteins in JA signaling. MeJA treatment was performed to examine the JA responsiveness of *OsJAZ1* (**Figure 1A**). The changed expression level of *OsJAZ1* showed that *OsJAZ1* was responsive to JA. A MeJA sensitivity test for the *OsJAZ1*-OE lines and *jaz1* mutant lines suggests that the *OsJAZ1*-OE plants were hyposensitive to MeJA (**Figure 4A**), whereas the *jaz1* mutant plants were hypersensitive to MeJA (**Figure 4B**). The result is consistent with previous results that the JAZ overexpression plants showed a hyposensitive phenotype under MeJA treatment (Chini et al., 2007; Thines et al., 2007). The expression level of *OsJAZ1* was much greater in the overexpression plants than that in WT ZH11, resulting in stronger repression on the activation of JA-responsive TFs. Therefore, we propose that *OsJAZ1* acts as a repressor in the JA signaling pathway.

Previous studies have reported that the ABA-dependent signaling pathway and the JA dependent pathway have common TFs (MYB/MYC), such as OsMYC2 (Abe et al., 2003; Adie et al., 2007). However, crosstalk between the JA and ABA signaling pathways is still ambiguous, since both synergistic and antagonistic interactions have been reported. In our study, we found that *OsJAZ1* is also significantly induced by ABA (**Figure 1C**), and a hyposensitive phenotype is present in the *OsJAZ1*-OE plants under ABA treatment (**Figure 4A**). What's more, the *jaz1* mutant lines were hypersensitive to ABA (**Figure 4B**), indicating that *OsJAZ1* plays a negative role in the ABA signaling pathway. Our finding that *OsJAZ1* negatively regulates both the JA and ABA signaling pathways

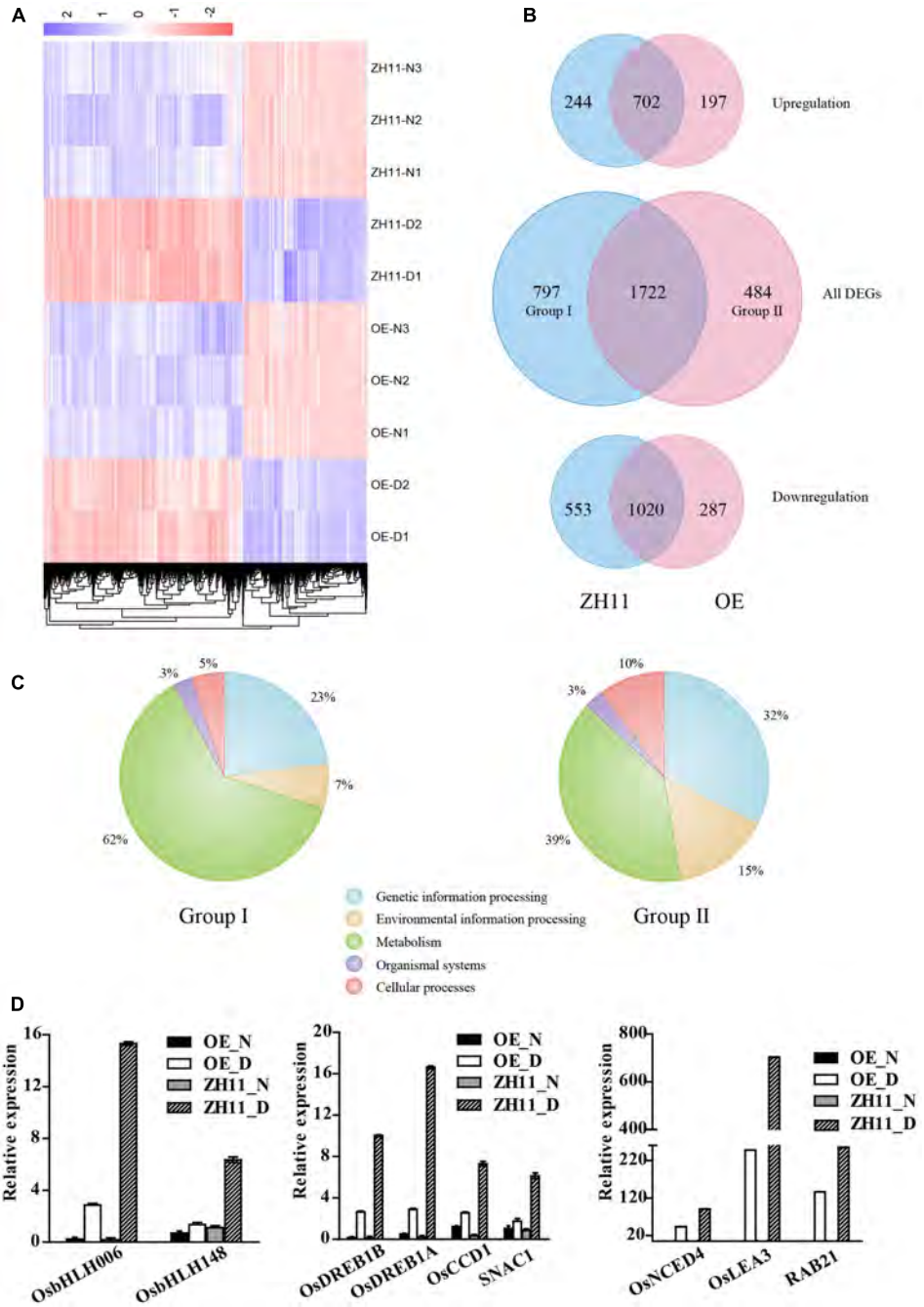

FIGURE 6 | Transcriptome profiling of *OsJAZ1*-OE plants. **(A)** The expression patterns of the DEGs under normal (–N) and drought stress conditions (–D). Color scale is in $\log_2$ of the fold change. **(B)** Number of specific and common drought-responsive DEGs in the WT and OE plants. **(C)** KEGG classification of the specific drought-responsive DEGs (Group I and Group II) in the WT and *OsJAZ1*-OE plants. **(D)** Confirmation of several genes involved in the ABA and JA pathways and stress resistance showing lower drought-induced levels in the *OsJAZ1*-OE plants than in WT ZH11. Error bars represent the SE of three replicates.

may contribute to the study of crosstalk between JA and ABA signaling. Nevertheless, the phenotypic changes of the *jaz1* mutant lines under the MeJA and ABA treatments were less obvious than that of the *OsJAZ1*-OE plants, which may be due to potential functional redundancy of OsJAZ1 homologs in rice.

OsJAZ1 Negatively Modulates Drought Resistance

Plant adaptation to variable environmental stresses relies on arrays of signaling networks. JAs play important roles in plant adaptation and mediate several biotic responses, plant growth

and developmental processes, and recently they have been reported to regulate tolerance to abiotic stresses. The JAZ proteins, belonging to the TIFY plant-specific family, are key components of the JA signaling pathway. A previous study indicated that JAZ9 repressed the expression of *OsbHLH062* and *OsMYB30*, resulting in increased salt and cold tolerance (Wu et al., 2015; Lv et al., 2017). However, there is no direct evidence that JAZ proteins can affect drought resistance. In this study, we found that the *jaz1* mutant lines showed increased drought resistance compared to the Dongjin control rice at both the seedling and reproductive stages (**Figures 2D**, **3D**). As expected, the *OsJAZ1*-OE plants exhibited decreased drought resistance at both the seedling and reproductive stages (**Figures 2E**, **3A**). In addition, we also tested the drought resistance of the *OsJAZ1* transgenic rice in the field. The results showed that the *OsJAZ*1-OE lines were more sensitive to drought stress treatment in terms of the green leaves which remained after drought recovery, which is consistent with the increased drought sensitivity of the *OsJAZ*1-OE lines observed at the seedling stage. However, the *jaz1* mutant lines in the field did not show an obvious hyposensitive phenotype as we expected (Supplementary Figure 1). One of the possible reasons may be that the suppression of *OsJAZ*1 only has a relatively small genetic effect in changing drought resistance, especially under the severe drought stress treatment we applied in this experiment. Nevertheless, it cannot be excluded that other homologs of OsJAZ1 may have similar functions in regulating drought resistance. In addition, we suspect that the overexpression or mutation of *OsJAZ1* may cause fertility abnormalities, since this gene has been reported with a role in the control of spikelet development (Cai et al., 2014). Therefore, the relative yield or spikelet fertility are not suitable traits to evaluate the effect of this gene on drought resistance at the reproductive stage.

We conducted transcriptome profiling to find clues to the mechanisms responsible for the drought-hypersensitive phenotype of the *OsJAZ1*-OE plants. According to the profiling results, we speculate that the hypersensitive phenotype of the *OsJAZ1*-OE plants under drought stress treatment may be partially attributed to the significantly decreased expression levels of abiotic stress and ABA and JA signaling and stress-responsive genes. These include *OsNCED4*, *OsLEA3*, *RAB21*, *OsbHLH006*, *OsbHLH148*, *OsDREB1A*, *OsDREB1B*, *SNAC1*, and *OsCCD1* which were confirmed by qRT-PCR analysis. *OsNCED4*, *OsLEA3*, and *RAB21* are well known ABA and abiotic stress responsive genes (Ganguly et al., 2012). Furthermore, *OsNCED4* is a key gene in ABA biosynthesis and involved in the regulation of drought resistance (Zong et al., 2016). *OsLEA3* encodes a group 3 late-embryogenesis abundant protein and plays an important role in drought and salt stress responses (Hu, 2008). The suppressed expression of *OsNCED4*, *OsLEA3*, and *RAB21* may result in an attenuation of the ABA pathway and subsequently lead to the drought-hypersensitive phenotype of the *OsJAZ1*-OE plants. Furthermore, no DEGs in Group II were enriched in the GO terms related to ABA signaling (Supplementary File 4), such as 'response to ABA' (GO:0009737) and 'regulation of ABA biosynthetic process' (GO:0010115). These results further suggest that ABA signaling was suppressed to some extent in the process of OsJAZ1-regulated drought resistance.

Previous studies have shown that JA also plays an important role in abiotic stress resistance. In this study, the expression levels of *OsbHLH006* and *OsbHLH148* were repressed in the *OsJAZ1*-OE plants under drought stress treatment. OsbHLH006 and OsbHLH148 are both basic helix-loop-helix proteins that regulate drought resistance via the JA-dependent pathway (Seo et al., 2011; Miyamoto et al., 2013). Previous studies have reported that *OsDREB1A*, *OsDREB1B*, *SNAC1*, and *OsCCD1* positively regulate drought resistance in rice (Dubouzet et al., 2003; Figueiredo et al., 2012; Redillas et al., 2012; Jing et al., 2016). *OsDREB1A* and *OsDREB1B* regulate the expression of abiotic stress-related genes via an ABA-independent pathway. Here, we showed that the expression levels of *OsDREB1A*, *OsDREB1B*, *SNAC1*, and *OsCCD1* were suppressed in the *OsJAZ1*-OE plants under drought stress conditions, which further supported the hypersensitive phenotype in the *OsJAZ1*-OE plants under drought stress treatment. Besides these reported genes related to the JA and ABA pathways or drought resistance, there are many DEGs in Group I enriched in several GO terms related to other stress responses, such as 'response to oxidative stress' (GO:0006979), 'response to water deprivation' (GO:0009414), and 'response to salt stress' (GO:0009651), while there were none or fewer DEGs in Group II enriched in these GO terms.

CONCLUSION

We have demonstrated that OsJAZ1 functions as a negative regulator in the drought resistance of rice, partially in an ABA-dependent and JA-dependent manner.

AUTHOR CONTRIBUTIONS

JF designed and performed the experiments and wrote the manuscript. HW generated the transgenic materials and performed the experiments. SM, DX, and RL provided assistance with subcellular localization and data analysis. LX designed the experiments and wrote the manuscript.

ACKNOWLEDGMENTS

This work was supported by the National Program of China for Transgenic Research (2016ZX08009003-002 and 2016ZX08001-003), National Program on High Technology Development (2016YFD0100604), and the Fundamental Research Funds for the Central Universities to LX.

SUPPLEMENTARY MATERIAL

The Supplementary Material for this article can be found online at: https://www.frontiersin.org/articles/10.3389/fpls.2017.02108/full#supplementary-material.

REFERENCES

Abe, H., Urao, T., Ito, T., Seki, M., Shinozaki, K., and Yamaguchi-Shinozaki, K. (2003). Arabidopsis AtMYC2 (bHLH) and AtMYB2 (MYB) function as transcriptional activators in abscisic acid signaling. *Plant Cell* 15, 63–78. doi: 10.1105/tpc.006130

Adie, B. A., Perez-Perez, J., Perez-Perez, M. M., Godoy, M., Sanchez-Serrano, J. J., Schmelz, E. A., et al. (2007). ABA is an essential signal for plant resistance to pathogens affecting JA biosynthesis and the activation of defenses in *Arabidopsis*. *Plant Cell* 19, 1665–1681. doi: 10.1105/tpc.106.048041

Aleman, F., Yazaki, J., Lee, M., Takahashi, Y., Kim, A. Y., Li, Z., et al. (2016). An ABA-increased interaction of the PYL6 ABA receptor with MYC2 transcription factor: a putative link of ABA and JA signaling. *Sci. Rep.* 6:28941. doi: 10.1038/srep28941

Anders, S., and Huber, W. (2010). Differential expression analysis for sequence count data. *Genome Biol.* 11:R106. doi: 10.1186/gb-2010-11-10-r106

Cai, Q., Yuan, Z., Chen, M., Yin, C., Luo, Z., Zhao, X., et al. (2014). Jasmonic acid regulates spikelet development in rice. *Nat. Commun.* 5:3476. doi: 10.1038/ncomms4476

Chen, L. T., and Wu, K. (2010). Role of histone deacetylases HDA6 and HDA19 in ABA and abiotic stress response. *Plant Signal. Behav.* 5, 1318–1320. doi: 10.4161/psb.5.10.13168

Chen, R., Jiang, H., Li, L., Zhai, Q., Qi, L., Zhou, W., et al. (2012). The *Arabidopsis* mediator subunit MED25 differentially regulates jasmonate and abscisic acid signaling through interacting with the MYC2 and ABI5 transcription factors. *Plant Cell* 24, 2898–2916. doi: 10.1105/tpc.112.098277

Cheng, Z., Sun, L., Qi, T., Zhang, B., Peng, W., Liu, Y., et al. (2011). The bHLH transcription factor MYC3 interacts with the Jasmonate ZIM-domain proteins to mediate jasmonate response in *Arabidopsis*. *Mol. Plant* 4, 279–288. doi: 10.1093/mp/ssq073

Cheong, J.-J., and Choi, Y. D. (2003). Methyl jasmonate as a vital substance in plants. *Trends Genet.* 19, 409–413. doi: 10.1016/s0168-9525(03)00138-0

Chini, A., Fonseca, S., Fernandez, G., Adie, B., Chico, J. M., Lorenzo, O., et al. (2007). The JAZ family of repressors is the missing link in jasmonate signalling. *Nature* 448, 666–671. doi: 10.1038/nature06006

Chung, H. S., and Howe, G. A. (2009). A critical role for the TIFY motif in repression of jasmonate signaling by a stabilized splice variant of the JASMONATE ZIM-domain protein JAZ10 in *Arabidopsis*. *Plant Cell* 21, 131–145. doi: 10.1105/tpc.108.064097

de Ollas, C., Arbona, V., and Gomez-Cadenas, A. (2015). Jasmonoyl isoleucine accumulation is needed for abscisic acid build-up in roots of Arabidopsis under water stress conditions. *Plant Cell Environ.* 38, 2157–2170. doi: 10.1111/pce.12536

Dubouzet, J. G., Sakuma, Y., Ito, Y., Kasuga, M., Dubouzet, E. G., Miura, S., et al. (2003). OsDREB genes in rice, *Oryza sativa* L., encode transcription activators that function in drought-, high-salt- and cold-responsive gene expression. *Plant J.* 33, 751–763. doi: 10.1046/j.1365-313X.2003.01661.x

Fernandez-Calvo, P., Chini, A., Fernandez-Barbero, G., Chico, J. M., Gimenez-Ibanez, S., Geerinck, J., et al. (2011). The *Arabidopsis* bHLH transcription factors MYC3 and MYC4 are targets of JAZ repressors and act additively with MYC2 in the activation of jasmonate responses. *Plant Cell* 23, 701–715. doi: 10.1105/tpc.110.080788

Figueiredo, D. D., Barros, P. M., Cordeiro, A. M., Serra, T. S., Lourenco, T., Chander, S., et al. (2012). Seven zinc-finger transcription factors are novel regulators of the stress responsive gene OsDREB1B. *J. Exp. Bot.* 63, 3643–3656. doi: 10.1093/jxb/ers035

Florea, L., Song, L., and Salzberg, S. L. (2013). Thousands of exon skipping events differentiate among splicing patterns in sixteen human tissues. *F1000Res.* 2:188. doi: 10.12688/f1000research.2-188.v2

Ganguly, M., Datta, K., Roychoudhury, A., Gayen, D., Sengupta, D. N., and Datta, S. K. (2012). Overexpression of Rab16A gene in indica rice variety for generating enhanced salt tolerance. *Plant Signal. Behav.* 7, 502–509. doi: 10.4161/psb.19646

Gibson, D. G., Young, L., Chuang, R. Y., Venter, J. C., Hutchison, C. A. III, and Smith, H. O. (2009). Enzymatic assembly of DNA molecules up to several hundred kilobases. *Nat. Methods* 6, 343–345. doi: 10.1038/NMETH.1318

Gonzalez, A., Zhao, M., Leavitt, J. M., and Lloyd, A. M. (2008). Regulation of the anthocyanin biosynthetic pathway by the TTG1/bHLH/Myb transcriptional complex in Arabidopsis seedlings. *Plant J.* 53, 814–827. doi: 10.1111/j.1365-313X.2007.03373.x

Goossens, J., Fernandez-Calvo, P., Schweizer, F., and Goossens, A. (2016). Jasmonates: signal transduction components and their roles in environmental stress responses. *Plant Mol. Biol.* 91, 673–689. doi: 10.1007/s11103-016-0480-9

Hiei, Y., and Komari, T. (2008). *Agrobacterium*-mediated transformation of rice using immature embryos or calli induced from mature seed. *Nat. Protoc.* 3, 824–834. doi: 10.1038/nprot.2008.46

Hu, T. Z. (2008). OsLEA3, a late embryogenesis abundant protein gene from rice, confers tolerance to water deficit and salt stress to transgenic rice. *Russ. J. Plant Physiol.* 55, 530–537. doi: 10.1134/s1021443708040158

Hu, Y., Jiang, L., Wang, F., and Yu, D. (2013). Jasmonate regulates the inducer of cbf expression-C-repeat binding factor/DRE binding factor1 cascade and freezing tolerance in *Arabidopsis*. *Plant Cell* 25, 2907–2924. doi: 10.1105/tpc.113.112631

Jing, P., Zou, J., Kong, L., Hu, S., Wang, B., Yang, J., et al. (2016). OsCCD1, a novel small calcium-binding protein with one EF-hand motif, positively regulates osmotic and salt tolerance in rice. *Plant Sci.* 247, 104–114. doi: 10.1016/j.plantsci.2016.03.011

Kirik, V., Lee, M. M., Wester, K., Herrmann, U., Zheng, Z., Oppenheimer, D., et al. (2005). Functional diversification of MYB23 and GL1 genes in trichome morphogenesis and initiation. *Development* 132, 1477–1485. doi: 10.1242/dev.01708

Lackman, P., Gonzalez-Guzman, M., Tilleman, S., Carqueijeiro, I., Perez, A. C., Moses, T., et al. (2011). Jasmonate signaling involves the abscisic acid receptor PYL4 to regulate metabolic reprogramming in *Arabidopsis* and tobacco. *Proc. Natl. Acad. Sci. U.S.A.* 108, 5891–5896. doi: 10.1073/pnas.1103010108

Livak, K. J., and Schmittgen, T. D. (2001). Analysis of relative gene expression data using real-time quantitative PCR and the $2^{-\Delta\Delta C_T}$ method. *Methods* 25, 402–408. doi: 10.1006/meth.2001.1262

Lv, Y., Yang, M., Hu, D., Yang, Z., Ma, S., Li, X., et al. (2017). The OsMYB30 transcription factor suppresses cold tolerance by interacting with a JAZ protein and suppressing beta-amylase expression. *Plant Physiol.* 173, 1475–1491. doi: 10.1104/pp.16.01725

Miyamoto, K., Shimizu, T., Mochizuki, S., Nishizawa, Y., Minami, E., Nojiri, H., et al. (2013). Stress-induced expression of the transcription factor RERJ1 is tightly regulated in response to jasmonic acid accumulation in rice. *Protoplasma* 250, 241–249. doi: 10.1007/s00709-012-0400-z

Munemasa, S., Hossain, M. A., Nakamura, Y., Mori, I. C., and Murata, Y. (2011). The Arabidopsis calcium-dependent protein kinase, CPK6, functions as a positive regulator of methyl jasmonate signaling in guard cells. *Plant Physiol.* 155, 553–561. doi: 10.1104/pp.110.162750

Nilson, S. E., and Assmann, S. M. (2007). The control of transpiration. Insights from Arabidopsis. *Plant Physiol.* 143, 19–27. doi: 10.1104/pp.106.093161

Penninckx, I. A., Thomma, B. P., Buchala, A., Metraux, J. P., and Broekaert, W. F. (1998). Concomitant activation of jasmonate and ethylene response pathways is required for induction of a plant defensin gene in Arabidopsis. *Plant Cell* 10, 2103–2113.

Qi, T., Song, S., Ren, Q., Wu, D., Huang, H., Chen, Y., et al. (2011). The Jasmonate-ZIM-domain proteins interact with the WD-Repeat/bHLH/MYB complexes to regulate Jasmonate-mediated anthocyanin accumulation and trichome initiation in *Arabidopsis thaliana*. *Plant Cell* 23, 1795–1814. doi: 10.1105/tpc.111.083261

Redillas, M. C., Jeong, J. S., Kim, Y. S., Jung, H., Bang, S. W., Choi, Y. D., et al. (2012). The overexpression of OsNAC9 alters the root architecture of rice plants enhancing drought resistance and grain yield under field conditions. *Plant Biotechnol. J.* 10, 792–805. doi: 10.1111/j.1467-7652.2012.00697.x

Sasaki-Sekimoto, Y., Saito, H., Masuda, S., Shirasu, K., and Ohta, H. (2014). Comprehensive analysis of protein interactions between JAZ proteins and bHLH transcription factors that negatively regulate jasmonate signaling. *Plant Signal. Behav.* 9:e27639. doi: 10.4161/psb.27639

Savchenko, T., Kolla, V. A., Wang, C. Q., Nasafi, Z., Hicks, D. R., Phadungchob, B., et al. (2014). Functional convergence of oxylipin and abscisic acid pathways controls stomatal closure in response to drought. *Plant Physiol.* 164, 1151–1160. doi: 10.1104/pp.113.234310

Schulze, S. K., Kanwar, R., Golzenleuchter, M., Therneau, T. M., and Beutler, A. S. (2012). SERE: single-parameter quality control and sample comparison for RNA-Seq. *BMC Genomics* 13:524. doi: 10.1186/1471-2164-13-524

Seo, J. S., Joo, J., Kim, M. J., Kim, Y. K., Nahm, B. H., Song, S. I., et al. (2011). OsbHLH148, a basic helix-loop-helix protein, interacts with OsJAZ proteins in a jasmonate signaling pathway leading to drought tolerance in rice. *Plant J.* 65, 907–921. doi: 10.1111/j.1365-313X.2010.04477.x

Sheard, L. B., Tan, X., Mao, H., Withers, J., Ben-Nissan, G., Hinds, T. R., et al. (2010). Jasmonate perception by inositol-phosphate-potentiated COI1-JAZ co-receptor. *Nature* 468, 400–405. doi: 10.1038/nature09430

Sirichandra, C., Wasilewska, A., Vlad, F., Valon, C., and Leung, J. (2009). The guard cell as a single-cell model towards understanding drought tolerance and abscisic acid action. *J. Exp. Bot.* 60, 1439–1463. doi: 10.1093/jxb/ern340

Song, S., Qi, T., Huang, H., Ren, Q., Wu, D., Chang, C., et al. (2011). The Jasmonate-ZIM domain proteins interact with the R2R3-MYB transcription factors MYB21 and MYB24 to affect Jasmonate-regulated stamen development in *Arabidopsis*. *Plant Cell* 23, 1000–1013. doi: 10.1105/tpc.111.083089

Stone, S. L., Williams, L. A., Farmer, L. M., Vierstra, R. D., and Callis, J. (2006). KEEP ON GOING, a RING E3 ligase essential for *Arabidopsis* growth and development, is involved in abscisic acid signaling. *Plant Cell* 18, 3415–3428. doi: 10.1105/tpc.106.046532

Takasaki, H., Maruyama, K., Kidokoro, S., Ito, Y., Fujita, Y., Shinozaki, K., et al. (2010). The abiotic stress-responsive NAC-type transcription factor OsNAC5 regulates stress-inducible genes and stress tolerance in rice. *Mol. Genet. Genomics* 284, 173–183. doi: 10.1007/s00438-010-0557-0

Tang, N., Ma, S., Zong, W., Yang, N., Lv, Y., Yan, C., et al. (2016). MODD mediates deactivation and degradation of OsbZIP46 to negatively regulate ABA signaling and drought resistance in rice. *Plant Cell* 28, 2161–2177. doi: 10.1105/tpc.16.00171

Thines, B., Katsir, L., Melotto, M., Niu, Y., Mandaokar, A., Liu, G., et al. (2007). JAZ repressor proteins are targets of the SCF(COI1) complex during jasmonate signalling. *Nature* 448, 661–665. doi: 10.1038/nature05960

Vanholme, B., Grunewald, W., Bateman, A., Kohchi, T., and Gheysen, G. (2007). The tify family previously known as ZIM. *Trends Plant Sci.* 12, 239–244. doi: 10.1016/j.tplants.2007.04.004

Verma, V., Ravindran, P., and Kumar, P. P. (2016). Plant hormone-mediated regulation of stress responses. *BMC Plant Biol.* 16:86. doi: 10.1186/s12870-016-0771-y

Wasternack, C., and Song, S. (2017). Jasmonates: biosynthesis, metabolism, and signaling by proteins activating and repressing transcription. *J. Exp. Bot.* 68, 1303–1321. doi: 10.1093/jxb/erw443

Withers, J., Yao, J., Mecey, C., Howe, G. A., Melotto, M., and He, S. Y. (2012). Transcription factor-dependent nuclear localization of a transcriptional repressor in jasmonate hormone signaling. *Proc. Natl. Acad. Sci. U.S.A.* 109, 20148–20153. doi: 10.1073/pnas.1210054109

Wu, H., Ye, H., Yao, R., Zhang, T., and Xiong, L. (2015). OsJAZ9 acts as a transcriptional regulator in jasmonate signaling and modulates salt stress tolerance in rice. *Plant Sci.* 232, 1–12. doi: 10.1016/j.plantsci.2014.12.010

Wu, K., Zhang, L., Zhou, C., Yu, C. W., and Chaikam, V. (2008). HDA6 is required for jasmonate response, senescence and flowering in *Arabidopsis*. *J. Exp. Bot.* 59, 225–234. doi: 10.1093/jxb/erm300

Xiao, B., Huang, Y., Tang, N., and Xiong, L. (2007). Over-expression of a LEA gene in rice improves drought resistance under the field conditions. *Theor. Appl. Genet.* 115, 35–46. doi: 10.1007/s00122-007-0538-9

Xie, K., and Yang, Y. (2013). RNA-guided genome editing in plants using a CRISPR-Cas system. *Mol. Plant* 6, 1975–1983. doi: 10.1093/mp/sst119

Xu, L. (2002). The SCF^{COI1} ubiquitin-ligase complexes are required for jasmonate response in Arabidopsis. *Plant Cell* 14, 1919–1935. doi: 10.1105/tpc.003368

Xu, L., Liu, F., Wang, Z., Peng, W., Huang, R., Huang, D., et al. (2001). An *Arabidopsis* mutant cex1 exhibits constant accumulation of jasmonate-regulated *AtVSP*, *Thi2.1* and *PDF1.2*. *FEBS Lett.* 494, 161–164. doi: 10.1016/S0014-5793(01)02331-6

Xue, W., Xing, Y., Weng, X., Zhao, Y., Tang, W., Wang, L., et al. (2008). Natural variation in Ghd7 is an important regulator of heading date and yield potential in rice. *Nat. Genet.* 40, 761–767. doi: 10.1038/ng.143

Yang, D. L., Yao, J., Mei, C. S., Tong, X. H., Zeng, L. J., Li, Q., et al. (2012). Plant hormone jasmonate prioritizes defense over growth by interfering with gibberellin signaling cascade. *Proc. Natl. Acad. Sci. U.S.A.* 109, E1192–E1200. doi: 10.1073/pnas.1201616109

Yang, W., Guo, Z., Huang, C., Duan, L., Chen, G., Jiang, N., et al. (2014). Combining high-throughput phenotyping and genome-wide association studies to reveal natural genetic variation in rice. *Nat. Commun.* 5:5087. doi: 10.1038/ncomms6087

Ye, H., Du, H., Tang, N., Li, X., and Xiong, L. (2009). Identification and expression profiling analysis of TIFY family genes involved in stress and phytohormone responses in rice. *Plant Mol. Biol.* 71, 291–305. doi: 10.1007/s11103-009-9524-8

Zhu, Z., An, F., Feng, Y., Li, P., Xue, L. A. M., Jiang, Z., et al. (2011). Derepression of ethylene-stabilized transcription factors (EIN3/EIL1) mediates jasmonate and ethylene signaling synergy in *Arabidopsis*. *Proc. Natl. Acad. Sci. U.S.A.* 108, 12539–12544. doi: 10.1073/pnas.1103959108

Zong, W., Tang, N., Yang, J., Peng, L., Ma, S., Xu, Y., et al. (2016). Feedback regulation of ABA signaling and biosynthesis by a bZIP transcription factor targets drought-resistance-related genes. *Plant Physiol.* 171, 2810–2825. doi: 10.1104/pp.16.00469

Conflict of Interest Statement: The authors declare that the research was conducted in the absence of any commercial or financial relationships that could be construed as a potential conflict of interest.

frontiers in Plant Science

ORIGINAL RESEARCH
published: 01 February 2018
doi: 10.3389/fpls.2018.00094

Characterization of Transcription Factor Gene *OsDRAP1* Conferring Drought Tolerance in Rice

Liyu Huang[1,2†], Yinxiao Wang[1†], Wensheng Wang[1], Xiuqin Zhao[1], Qiao Qin[1], Fan Sun[1], Fengyi Hu[2], Yan Zhao[3], Zichao Li[3], Binying Fu[1,4] and Zhikang Li[1,4*]*

[1] National Key Facility for Crop Gene Resources and Genetic Improvement, Institute of Crop Sciences, Chinese Academy of Agricultural Sciences, Beijing, China, [2] School of Agriculture, Yunnan University, Yunnan, China, [3] Key Lab of Crop Heterosis and Utilization of Ministry of Education, Beijing Key Lab of Crop Genetic Improvement, China Agricultural University, Beijing, China, [4] Shenzhen Institute for Innovative Breeding, Chinese Academy of Agricultural Sciences, Shenzhen, China

HIGHLIGHTS

- Overexpressing and RNA interfering *OsDRAP1* transgenic rice plants exhibited significantly improved and reduced drought tolerance, but accompanied with negative effects on development and yield.

The dehydration responsive element binding (DREBs) genes are important transcription factors which play a crucial role in plant abiotic stress tolerances. In this study, we functionally characterized a DREB2-like gene, *OsDRAP1* conferring drought tolerance (DT) in rice. *OsDRAP1*, containing many *cis*-elements in its promoter region, was expressed in all organs (mainly expressed in vascular tissues) of rice, and induced by a variety of environmental stresses and plant hormones. Overexpressing *OsDRAP1* transgenic plants exhibited significantly improved DT; while *OsDRAP1* RNA interfering plants exhibited significantly reduced DT which also accompanied with significant negative effects on development and yield. Overexpression of *OsDRAP1* has a positive impact on maintaining water balance, redox homeostasis and vascular development in transgenic rice plants under drought stress. *OsDRAP1* interacted with many genes/proteins and could activate many downstream DT related genes, including important transcription factors such as *OsCBSX3* to response drought stress, indicating the *OsDRAP1*-mediated pathways for DT involve complex genes networks. All these results provide a basis for further complete understanding of the *OsDRAP1* mediated gene networks and their related phenotypic effects.

Keywords: DREB, drought tolerance, *OsDRAP1*, overexpression, rice, transcription factor

OPEN ACCESS

Edited by:
Hanwei Mei,
Shanghai Agrobiological Gene Center, China

Reviewed by:
Lizhong Xiong,
Huazhong Agricultural University, China
Gabriella Szalai,
Agricultural Institute, Centre for Agricultural Research (MTA), Hungary

****Correspondence:***
Binying Fu
fubinying@caas.cn
Zhikang Li
lizhikang@caas.cn

† These authors have contributed equally to this work.

Specialty section:
This article was submitted to Plant Breeding, a section of the journal Frontiers in Plant Science

Received: *11 December 2017*
Accepted: *17 January 2018*
Published: *01 February 2018*

Citation:
Huang L, Wang Y, Wang W, Zhao X, Qin Q, Sun F, Hu F, Zhao Y, Li Z, Fu B and Li Z (2018) Characterization of Transcription Factor Gene OsDRAP1 Conferring Drought Tolerance in Rice. Front. Plant Sci. 9:94. doi: 10.3389/fpls.2018.00094

INTRODUCTION

Rice (*Oryza sativa*. L) is the staple food for half of the world's population. Rice production normally requires large amounts of water. Water availability and drought are becoming major constraints for rice cultivation because of greatly fluctuated and generally reduced rainfall in the majority of rice growing areas worldwide resulting from the global climate change. Rice production was dramatically affected by severe drought occurred every year in rainfed rice-growing areas worldwide (Pandey, 2009; Lenka et al., 2011). To ensure food security, it is imperative to develop drought tolerant high-yielding rice varieties.

DT is a complex trait controlled by many genes and shows significant genotype by environment interaction (Babu, 2010). Genetically, many QTLs affecting DT in rice has been identified (Li et al., 2005; Xu and Vision, 2005; Kumar et al., 2014), but few of them have been cloned and functionally characterized (Uga et al., 2013; Li et al., 2015). At the transcriptomic level, it is well known that drought can induce differential expression of large numbers of genes in rice (Wang D. et al., 2011). Of these drought responsive genes, several families of transcription factor (TF) such as AP2/ERFs, NAC, bZIPs and MYBs were found to play an important role in drought responses via regulating large numbers of downstream genes and pathways through complex transcriptional networks (Hadiarto and Tran, 2011; Todaka et al., 2015). Many TF families typically each contains many member genes, but only a portion of a TF family are functionally involved in plant responses to abiotic stresses (Joshi et al., 2016). Genes of the AP2/ERF family are characterized by a conserved AP2/ERF DNA binding domain (Riechmann and Meyerowitz, 1998; Sakuma et al., 2002). This TF family is further classified as four major subfamilies including AP2 (Apetala), RAV (related to ABI3/VP1), DREB (dehydration responsive element-binding protein), and ERF (ethylene responsive factor). There are 163 AP2/ERF genes in the rice genome (including 57 DREB members), and 70 of them were differentially regulated under different abiotic stresses (Sharoni et al., 2011). Most DREB member genes have been found to manipulate downstream stress-responsive genes by binding their drought responsive element (DRE) and GCC-box *cis*-element (Liu et al., 1998; Dubouzet et al., 2003). The DREB TFs could be further divided into DREB1 and DREB2, which were reportedly involved in two separate signal transduction pathways in plants in response to low temperature and dehydration stresses, respectively (Lata and Prasad, 2011). Four DREB1 genes (*OsDREB1A*, *OsDREB1B*, *OsDREB1C*, and *OsDREB1D*) were firstly identified in rice. Overexpression of *OsDREB1A* could enhance abiotic stress tolerance in *Arabidopsis* (Dubouzet et al., 2003) *OsDREB1F* is highly induced by drought stress and exogenous ABA application and overexpression of *OsDREB1F* is reportedly to lead to enhanced tolerance to salt, drought, and low temperature in both rice and *Arabidopsis* (Wang et al., 2008). In addition, higher expression of *OsDREB1G* in transgenic rice plants could significantly improve their tolerance to water deficit stress (Chen et al., 2008). Similarly, DREB2-type TFs are involved in a conserved regulatory mechanism in several crop plants in response to drought, salinity, and heat stresses (Lata and Prasad, 2011; Mizoi et al., 2012). There are five DREB2 genes (*OsDREB2A*, *OsDREB2B*, *OsDREB2C*, *OsDREB2E*, and *OsABI4*) in the rice genome (Matsukura et al., 2010; Srivastav et al., 2010). *OsDREB2A* expression in rice was evidently induced by water deficit and exogenous ABA application, which could result in improved DT (Cui et al., 2011). The transcript of *OsDREB2B* has both functional and non-functional forms. The former was markedly increased during stress conditions and was able to enhance DT by drought-induced alternative splicing of its pre-mRNA (Matsukura et al., 2010). All these results indicated that *OsDREB2s* also play important roles in plant DT.

In our breeding program, we developed a DT pyramiding line-DK151 from an F_2 population of a cross between two IR64 introgression lines (Wang W. S. et al., 2011). In the following transcriptomic experiment using DK151 and its background parent, IR64, we found that large numbers of genes were specifically up-regulated in DK151 when compared with IR64 (Wang D. et al., 2011). Of these drought up-regulated genes in DK151, we identified a new rice DREB2-like TF gene, *OsDRAP1* (Drought Responsive AP2/EREBP gene) located in an introgressed segment on chromosome 8 of DK151 and whose expression was greatly up-regulated in DK151 by drought, suggesting its potential role in rice DT. Here, we report the functional characterization of *OsDRAP1* and evidence for its important role in improving rice DT.

MATERIALS AND METHODS

Plant Materials, Growth Conditions, and Stress Treatments

Seeds of three rice genotypes, including Nipponbare, its transgenic plants overexpressing coding region of *OsDRAP1* and RNAi knock-down transgenic plants generated by *Agrobacterium*-mediated transformation, were grown under the controlled conditions in the growth chamber. For stress and hormones treatments, 2-week-old rice plants were transferred from the basal nutrient solution to nutrient solution containing 20% PEG (PEG6000), 150 mM NaCl, 100 μM ABA, 100 μM methyl jasmonate (MeJA) or 20 mM H_2O_2 and exposed to low temperature (4°C). Leaf tissues were then harvested as the indicated times and stored at −80°C for further analysis.

The transgenic rice plants and their background parent, Nipponbare, were evaluated for their DT performances in a pot experiment in the greenhouse of Chinese Academy of Agricultural Sciences (Beijing, China). Three healthy seedlings were transplanted equidistantly into a strip pot (50 cm in length, 15 cm in width and 15 cm in height) filled with 2 kg of sterilized field soil. Seedlings of each genotype were planted in six pots. The pots were maintained under controlled conditions with 14 h daylight at 28°C and a 10 h dark period at 25°C. In the stress treatment, drought stress was initiated at seedling and tillering stages by withholding watering at precisely determined time intervals when the soil water content reached 15, 10, and 7.5% at 1, 3, and 5 days after the drought treatment, respectively, as measured by soil moisture meters (TZS-W, Zhejiang Top Instrument Co. Ltd).

RNA Extraction, Quantitative Real-Time PCR (qRT-PCR)

Total RNA was extracted from rice tissues of the three genotypes using TRIzol Reagent (Invitrogen, USA). cDNA synthesis was performed using EasyScript First-strand cDNA Synthesis SuperMix (TransGene, Beijing, China) according to the manufacturer's instructions. qRT-PCR analysis was carried out using TaKaRa SYBR premix Ex Taq™ according to the

manufacturer's instructions. The relative expression of each gene was calculated according to the method of $2^{-\Delta\Delta Ct}$ (Livak and Schmittgen, 2001). Primers used for qRT-PCR were subsequently tested in a dissociation curve analysis and verified for the absence of nonspecific amplification. All analyses were performed with three biological replicates.

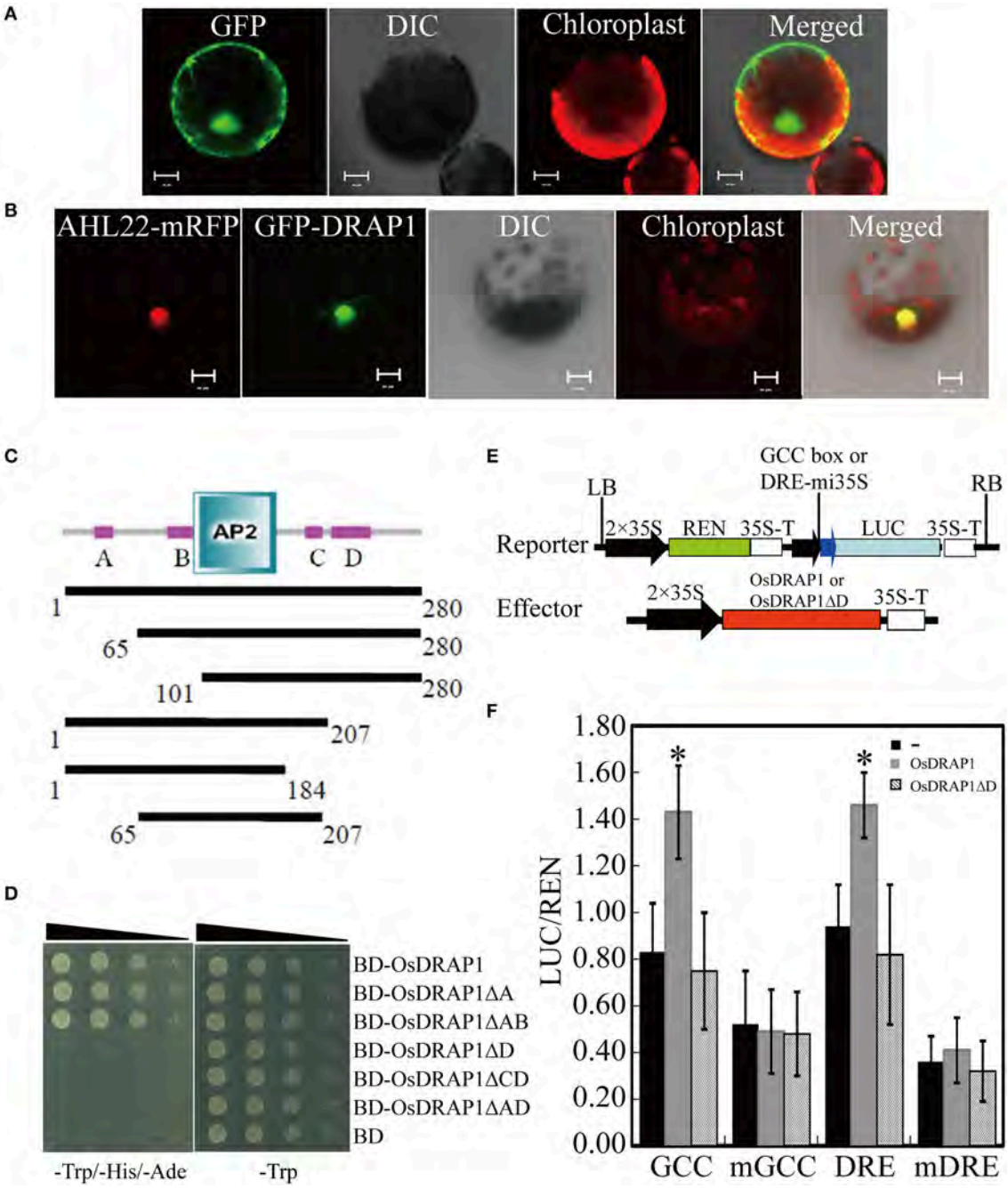

FIGURE 1 | OsDRAP1 is a typical transcription activator. **(A)** GFP extensively localized in both nucleus andcytoplasm in the *N. benthamiana* protoplast; **(B)** GFP-*OsDRAP1* positively localized in the nucleus, in which AHL22 used as the nucleus marker protein, DIC indicating its differential interference contrast transmission, chlorophyll fluorescence in red and the merged image, with the scale bars in 5 μm. **(C)** The structure of the *OsDRAP1* protein and analysis of its transcription activating domains in yeast; Domains of the *OsDRAP1* protein and different lengths of bait proteins with different domain deletions; **A–D** indicate four unknown domains. **(D)** Transcription activating domain identification of *OsDRAP1* in yeast in which Yeast suspension was diluted to 10^{-1}, 10^{-2}, 10^{-3} times and dripped to the SD (-Trp/-His/-Ade) and SD (-Trp) medium, with pGKBT7 (BD) used as the negative control. **(E)** The schematic diagram of the reporters and effectors; **(F)** The transcription activation assay of *OsDRAP1* and *OsDRAP1*ΔD in *N. benthamiana*, with "-," *OsDRAP1* and *OsDRAP1*ΔD indicating no effector control, full length and D domain deletion of the *OsDRAP1* proteins, respectively, with the asterisks indicating significant differences at $p < 0.05$ in *t*-tests (vs. no effector control, $n > 10$).

Vector Construction and Genetic Transformation

The coding region of *OsDRAP1*, was amplified from the rice cDNA by PCR using *Kpn*I and *Bam*HI linker primers. The resulting *OsDRAP1* fragment was inserted into the *Kpn*I and *Bam*HI site of pCUbi1390 (Peng et al., 2009), generating Ubipro::OsDRAP1. 275-bp *OsDRAP1* specific sequence was amplified from the rice cDNA and inserted into RNAi vector pH7GWIWG2 (II) (Karimi et al., 2005) using the Gateway technology in end-to-end orientations by using an intron as spacer. 1.8 kb-fragments of the *OsDRAP1* promoter were amplified from rice genomic DNA (Nipponbare) by PCR and inserted into the vector pMDC162 (Curtis and Grossniklaus, 2003), respectively using the Gateway technology, generating OsDRAP1-pro::GUS. All the vectors were introduced into *Agrobacterium tumefaciens* strain *EHA105*, and then transferred into Nipponbare plants via *Agrobacterium*-mediated transformation following the protocol described by Duan (Duan et al., 2012).

Histological Analyses

To determine the localization of *OsDRAP1* in rice plant tissues, the transverse sections (100 μm thick) of the OsDRAP1-pro1::GUS transgenic seedlings and roots with GUS stained were fixed for over 12 h in 2.5% glutaraldehyde buffered with 0.2 M phosphate buffer (pH 7.2). The sections were treated as described by Takemoto et al. (2002). For histological analyses, freshly collected leaves at the tillering stage were fixed immediately in FAA (3.7% formaldehyde, 5% acetic acid, 50% absolute ethanol). Plant tissues were then dehydrated, embedded, sliced, and pre-treated. Transverse section slices were ultimately stained with Haematoxylin and eosin (HE) and viewed and photographed on a microscope (DM-LS2, Leica, http://www.leica.com/).

Physiological Traits of the Three Genotypes under Drought Stress

Relative Water Content (RWC) was calculated using the following formula: RWC (%) = [(FM−DM)/(TM−DM)] × 100, where FM, DM, and TM were the fresh, dry, and turgid masses of the leaves weighed, respectively. Monitoring the fresh weight loss at the indicated time points (per hour) measured the WLRs (water loss rates) of the detached leaves (You et al., 2013). Relative electrolyte leakage (REL) or solute leakage from the sampled rice leaves were evaluated using the method of Arora et al. (1998). Percent injury arising from each treatment was calculated from the conductivity data using the equation: % injury = [(% L(t)-% L(c))/(100-% L(c))] × 100), where % L (t) and % L(c) are percent conductivity for treated and control samples, respectively. Antioxidant enzyme activity such as catalase (CAT), was determined following previously reported methods (Bonnecarrère et al., 2011). Proline and MDA concentrations of the sampled leaves were measured according to the protocol of Shukla et al. (2012).

TABLE 1 | *Cis*-elements analysis of the *OsDRAP1* promoter sequence.

Cis-Element	Number	Function
ABRE	6	*cis*-acting element involved in the abscisic acid responsiveness
MBS	5	MYB binding site involved in drought-inducibility
CGTCA-motif	1	*cis*-acting regulatory element involved in the MeJA-responsiveness
GARE-motif	2	gibberellin-responsive element
TC-rich repeats	1	*cis*-acting element involved in the defense and stress responsiveness
motif I	1	*cis*-acting regulatory element root specific

Subcellular Localization of GFP-OsDRAP1 Fusion Proteins

The open reading frames (ORFs) of *OsDRAP1* were inserted into pMDC43 as C-terminal fusions to the green fluorescent protein (GFP) reporter gene driven by the CaMV 35S promoter (Curtis and Grossniklaus, 2003). For transient expression, the GFP-OsDRAP1 fusion vector constructs were transformed into *Nicotiana benthamiana* protoplasts. Protoplast isolation from tobacco leaf tissues and PEG-mediated transformation were performed according to Bart et al. (2006). Cells were incubated at 28°C in the dark overnight. The resulting green fluorescence of protoplasts expressing GFP-OsDRAP1 was observed using a confocal laser scanning microscope (LSM700, Zeiss, Jena, Germany). The 35S::GFP construct was used as a control. AHL22 was used as a nucleus marker protein (Xiao et al., 2009).

Histochemical GUS Assay

For GUS staining analysis, sample tissues or whole seedlings were submerged in the GUS staining buffer (containing 2 mM 5-bromo-4-chloro-3-indolyl glucuronide, 0.1 M sodium phosphate buffer [pH 7.0], 0.1% [v/v] Triton X-100, 1 mM potassium ferricyanide, 1 mM potassium ferrocyanide, and 10 mM EDTA), vacuum infiltrated for 10 min, and then incubated overnight at 37°C. The staining buffer was removed before the samples were cleared with 95% (v/v) ethanol and then observed using a stereoscope (LEICA, 10447157, Germany).

Transactivation Analysis in Yeast

OsDRAP1 in transgenic plants was examined for the presence of one of its activation domains using a yeast assay system as described (Liu et al., 2013). A series of coding region fragments of *OsDRAP1* were amplified by PCR using *Nco*I and *Pst*I linker primers. The resultant PCR products were digested with *Nco*I and *Pst*I and then cloned into the *Nco*I and *Pst*I sites of pGBKT7, generating BD-OsDRAP1, BD-OsDRAP1ΔA, BD-OsDRAP1ΔAB, BD-OsDRAP1ΔD, BD-OsDRAP1ΔCD, BD-OsDRAP1ΔAD. An empty vector (BD) was used as a negative control. The constructs and the negative control BD were transformed into *AH109*, respectively according to the protocol of the manufacturer in the Leu-medium. About 2 days, the positive transformants verified by PCR were dropped on Leu- and Leu-His-Ade- medium, respectively. The transcriptional activation activities were evaluated according to their growth status.

Transient Transcription Dual-Luciferase (Dual-LUC) Assays

A previously described dual-luc method using *Nicotiana benthamiana* plants (Liu et al., 2008) was used for transient transcription assays. The effector plasmids, pMDC43-OsDRAP1 and pMDC43-OsDRAP1ΔD were constructed as described above. The reporter plasmid, pGreen-GCC/DRE-LUC, encodes two luciferases, the firefly luciferase controlled by the recombinant GCC box promoter or DRE *cis*-element, and the Renilla (REN) luciferase controlled by the constitutive 35S promoter. The recombinant GCC box and DRE *cis*-element promoters contain two wild-type GCC box (ATAAGAGCCG CCACTCATAAGAGCCGCCACT) and DRE *cis*-element (ATAC TACCGACATGAGATACTACCGACATGAG), respectively. Their mutant GCC box (mGCC, ATAAGATCCTCCACTCA TAAGATCCTCCACT) and DRE *cis*-element (mDRE, ATA CTACTGATATGAGATACTACTGATATGAG) fused to the minimum 35S promoter, were PCR-amplified from the 35S template and cloned into the *Apa*I and *Sac*II sites of the vector pGreen-0800-LUC, then transformed into *Agrobacterium* (strain EHA105) containing the helper plasmid, pSoup-P19, that also encodes a repressor of co-suppression. The *Agrobacterium* strain containing both the reporter pGreen-GCC/DRE-LUC and helper pSoup-P19 was used alone or mixed with the *Agrobacterium* strain containing the effector plasmids pMDC43-OsDRAP1 or pMDC43-OsDRAP1ΔD.

The reporter strain was either incubated alone or incubated as a mixture with the effector strain (at the reporter: effector ratio of 1:9 or 2:8). *Agrobacteria* suspension in a 10 ml syringe was carefully press-infiltrated manually onto healthy leaves of *Nicotiana benthamiana*. Plants were left for 3 days after infiltration. Leaf samples were collected for the dual-luc assay using commercial Dual-LUC reaction (DLR) reagents, according to the manufacturer's instruction (Promega). After measurement of the firefly luciferase activity, 40 ul of the Stop and Glow buffer (Promega) was added to the reaction to quench the firefly luciferase and to initiate the REN luciferase (REN) reaction.

Yeast Two-Hybrid Assay

The protein interaction analysis was performed using Matchmaker Two-Hybrid System 3 (Clontech, http://www.clontech.com/). A bait gene is expressed as a fusion to the GAL4 DNA-binding domain (DNA-BD), while cDNA is expressed as a fusion to the GAL4 activation domain-AD (Fields and Song, 1989; Chien et al., 1991). Construct pGBKT7-OsDRAP1ΔD above was used as a bait protein. An AD fusion library of rice leaves under drought condition (pGADT7-library) was constructed in Oebiotech (Shanghai). pGBKT7-OsDRAP1ΔD and pGADT7-library plasmids were co-transformed into *AH109*, and then were spread on SD/–Ade/–His/–Leu/–Trp/X-α-gal plates. These plates were incubated at 30°C until colonies appear. To identify the gene responsible for a positive

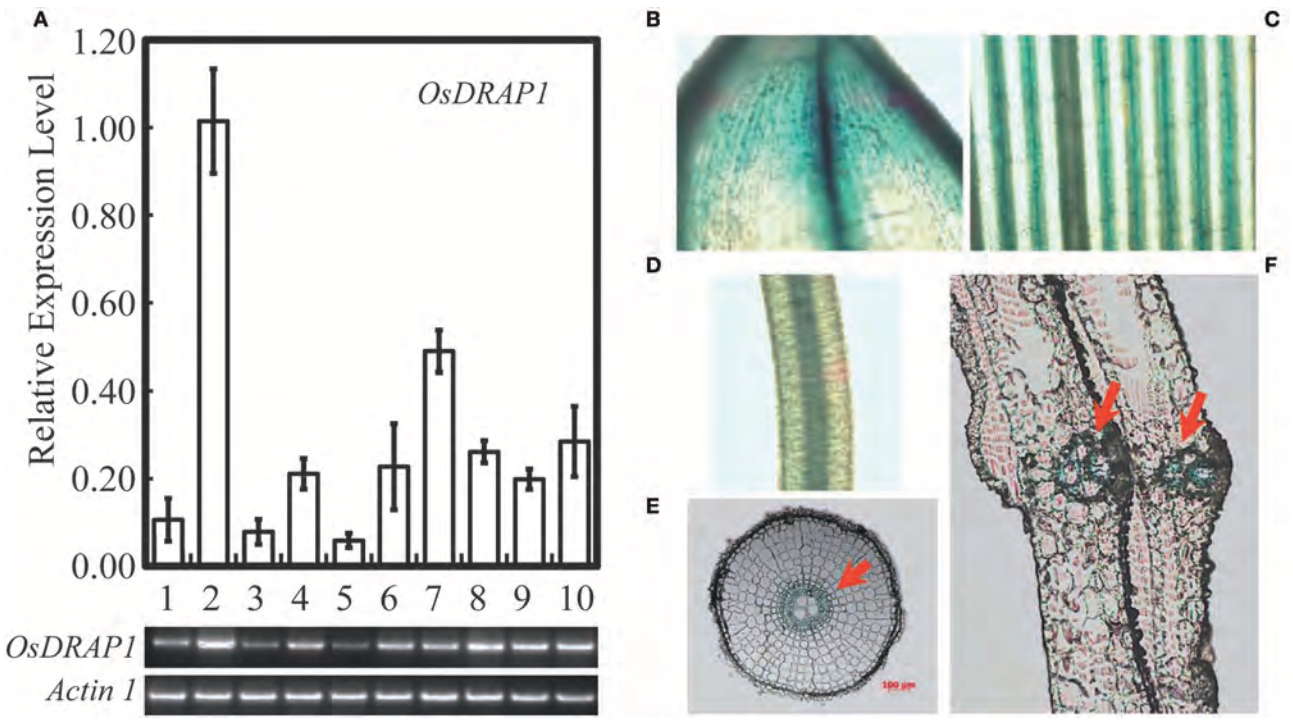

FIGURE 2 | Expression model of *OsDRAP1* in different tissues of rice, in which **(A)** the transcript levels were determined by qRT-PCR and semi RT-PCR, *OsDRAP1* transcript levels in young panicles (1), matured leaves (2), leaf sheaths (3), nodes (4), internodes (5), stem bases (6), matured roots (7), young leaves (8), young roots (9) and callus (10) with *Actin1* used as the reference gene. The *OsDRAP1* expression in different tissues of the OsDRAP1-Pro::GUS transgenic rice plants by GUS staining analysis, in the shell **(B)**, leaf blade **(C)**, root **(D)**, root cross section **(E)** and sheath cross section **(F)** with red arrows indicating the vascular bundles (the scale bars are in 100 μm).

two-hybrid interaction, we rescue the gene by PCR colony screening. After that, we sequenced the cDNA inserts and blast the sequences in NCBI databases. Finally, we retest the interaction by cotransformation into the *AH109*. In the same way, cotransformation mixtures were spread on SD/–Ade/–His/–Leu/–Trp/X-α-gal plates. These plates were incubated at 30°C until colonies appear.

Bimolecular Fluorescence Complementation (BiFC) Assay

Bimolecular fluorescence complementation (BiFC) assay analyses were performed as previously described (Sparkes et al., 2006). Complementary DNAs of OsDRAP1 and OsCBSX3 were cloned into BiFC vectors pnYFP-X and pcCFP-X, respectively. Pair of constructs was co-transformed into the leaves of 3-week-old tobacco (*Nicotiana benthamiana*) by *A. tumefaciens* infiltration as the above protocol in dual-LUC assays. Cells co-transformed with pnYFP-OsDRAP1/pcCFP-GUS, pnYFP-GUS/pcCFP-OsCBSX3, were used as negative controls. AHL22-mRFP was used as a nuclear localization marker protein (Xiao et al., 2009).

Protein Co-Immunoprecipitation (Co-IP) Assay

Recombinant constructs GFP-OsCBSX3 and Myc-OsDRAP1 were introduced into tobacco leaves as the above protocol in dual-LUC or BiFC assays, respectively, and protein extracts were prepared as described by Sawa et al. (2007). The protein extracts were precipitated with anti-Flag agarose beads (Abmart, http://www.ab-mart.com/) or anti-Myc agarose beads (CMC Scientific, http://www.cmcscientific.com) overnight. Then proteins bound to beads were resolved by SDS-PAGE and detected with Western blot using anti-GFP antibody (Sigma), and anti-Myc antibody (MBL, http://www.mblintl.com/).

RNA-Seq Analysis

Three top leaves for each sample (two replicates for each sample) were harvested for each genotype under 1 day and 3 days of drought stress and control conditions. The RNA-seq sequencing and assembly were performed by Beijing CapitalBio Corporation as described in previous study (Huang et al., 2014). The number of mapped clean reads for each gene was counted and normalized into the reads per kilo base per million value (Mortazavi et al., 2008); Cuffdiff (Trapnell et al., 2009) was then used to identify DEGs. Finally, genes with a $p \leq 0.001$ were designated as significantly differential expressed between each pair of samples. Gene function annotations were performed based on the Rice Genome Annotation Project version 7 (Kawahara et al., 2013). AgriGO was used to perform GO enrichment analysis (Du et al., 2010).The raw RNA-seq data are available in the Genome Sequence Archive in BIG Data Center (Beijing Institute of Genomics,

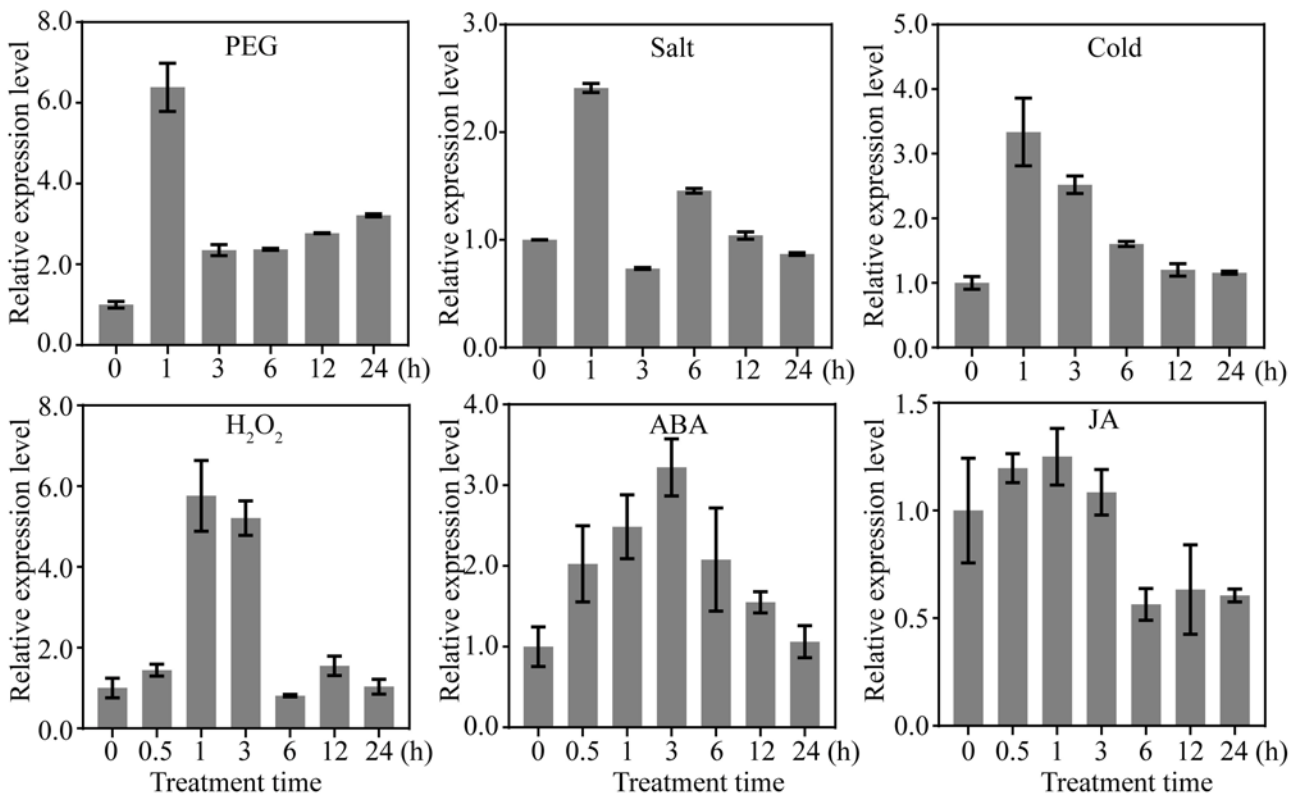

FIGURE 3 | Expression profiles of *OsDRAP1* in response to various abiotic stresses and exogenous hormones; in which 14-day-old seedlings of *Nipponbare* treated with PEG (20%), salt (150 mM), cold (4 C°), 100 mμ MeJA, 100 μM ABA and 20 mM H_2O_2, with *Actin 1* used as the endogenous control.

Chinese Academy of Sciences) under the accession number PRJCA000683.

RESULTS

Identification and Characterization of *OsDRAP1*

In our previous transcriptomic analyses (Wang D. et al., 2011), we identified a set of AP2/EREBP TF genes that were greatly up-regulated in leaves and panicles in drought tolerant pyramiding line DK151 under drought stress. One of these AP2/EREBP TF genes, designated as *OsDRAP1* (LOC_Os08g31580), was selected for further function confirmation in this study.

The *OsDRAP1* gene sequence has a full-length of 843 bp without any intron and encodes a polypeptide of 280 amino acids, consisting of an AP2 domain (103–166 aa) and four putative unknown domains (A: 25–38 aa, B: 82–100 aa, C: 190–201 aa, D: 210–239 aa; **Figure 1C**). The phylogenetic analysis indicated that *OsDRAP1* was closely related to members of the DREB2 subfamily in rice and wheat (**Figure S1**; Sharoni et al., 2011). *OsDRAP1* contains several stress- or hormone-responsive *cis*-elements in its promoter region (2.0 Kb upstream of the start codon), including 5 MYB binding sites (MBS), 6 ABA-responsive elements (ABRE), 2 gibberellin-responsive elements (GARE), and a CGTCA-motif for the MeJA-responsiveness (**Table 1**), implying that the expression of *OsDRAP1* could be regulated by phytohormones. Our results from cytological analyses (**Figures 1A,B**) indicated that *OsDRAP1* was localized in the nucleus and functioned as a nuclear protein, with its transactivation activity located primarily in region D (207-280 aa) (**Figures 1C,D**).

To determine if *OsDRAP1* is involved in the activation of multiple stress signaling pathways by interacting with GCC box or DRE element (Hao et al., 1998; Cheng et al., 2013), we performed a dual luciferase reporter assay by constructing reporter vectors containing GCC box mi35S-LUC, DRE mi35S-LUC, mutated GCC- and DRE-LUC (mGCC box mi35S-LUC, mDRE mi35S-LUC), and effector vectors containing 35S::*OsDRAP1* and 35S::*OsDRAP1*Δ*D*. The results (**Figures 1E,F**) showed that the full length of *OsDRAP1* could significantly enhance the LUC activity in the reporters of the GCC box mi35S-LUC and DRE mi35S-LUC, but had no effect on the two mutated reporters. The effector containing the truncated *OsDRAP1* with deletion of region D (*35S::OsDRAP1*Δ*D*) could not activate all reporters. All these results indicated that *OsDRAP1* was able to activate the

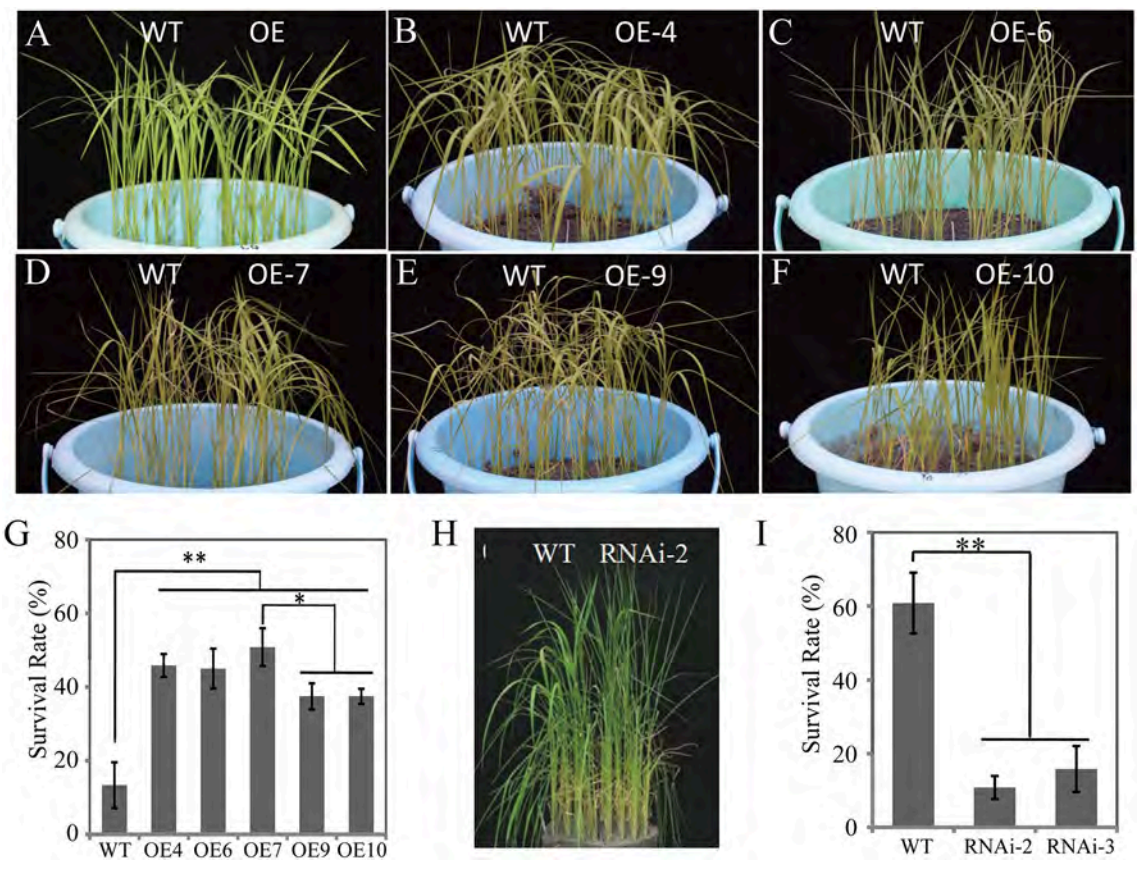

FIGURE 4 | The seedling phenotypes of *OsDRAP1* OE and RNAi lines at the seedling stage under the drought stress treatments: before drought **(A)** and 5 days after drought **(B–F,H)**, and the seedling survival rates **(G,I)** evaluated 7 days after re-watering, in which the error bars indicate SD based on data of 3 replicates and the asterisks (* or **) indicate the significant differences at $p < 0.05$ or $p < 0.01$ in *t*-tests when compared with WT ($n > 100$).

expression of downstream genes by binding *cis*-elements of the GCC box and DRE.

The Spatial-Temporal Pattern of *OsDRAP1* and Its Responses to Different Abiotic Stresses and Plant Hormones

Because *OsDRAP1* was differentially expressed under drought stress in a spatial-temporal manner (Wang D. et al., 2011), we examined its expression patterns in different tissues at different developmental stages using qRT-PCR. The results showed that *OsDRAP1* was highly expressed in the mature leaves and roots, but had relatively lower expression in young panicles, leaf sheaths and internodes (**Figure 2A**). The expression of *OsDRAP1* was induced by PEG-simulated drought, high salt, low temperature, H_2O_2, ABA (**Figure 3**). Generally, *OsDRAP1* showed similarly high expression in response to drought, salt and cold with the peak expression at 1 h after the treatments and maintaining a relatively high level of expression afterwards. Of the three plant hormones, *OsDRAP1* responded much more strongly to ABA and H_2O_2 than to JA, though it showed the highest expression at 1 or 3 h after the treatments and decline afterwards in the H_2O_2 and ABA treatments. All these results indicated that the *OsDRAP1* expression is induced by abiotic stresses, primarily by drought and salt, in a more H_2O_2 and/or ABA dependent manner.

Enhanced DT and Phenotypic Effects by Overexpression of *OsDRAP1* in Rice

To determine the biological function(s) of *OsDRAP1* in response to abiotic stresses, we constructed overexpressing and RNAi knockdown vectors including UbiPro::*OsDRAP1* and *OsDRAP1*-RNAi (see details in Materials and Methods). Thirteen *OsDRAP1*-overexpressing lines (OE-1 to 13) and four RNAi lines (RNAi-1 to 4) were obtained. The qRT-PCR results showed that the expression of *OsDRAP1* was up-regulated in OE lines, but down-regulated in RNAi lines to various extents when compared with WT under the normal growth conditions (**Figure S2**). The seedlings of the OE lines and WT plants showed no evident differences before the stress treatments and 5 d after drought (**Figures 4A–F**), but all transgenic OE lines exhibited improved DT compared to WT with significantly higher seedling survival rates 7 days after rewatering (**Figure 4G**). As expected, the two RNAi lines were more sensitive to drought stress with significantly decreased survival rates compared to WT

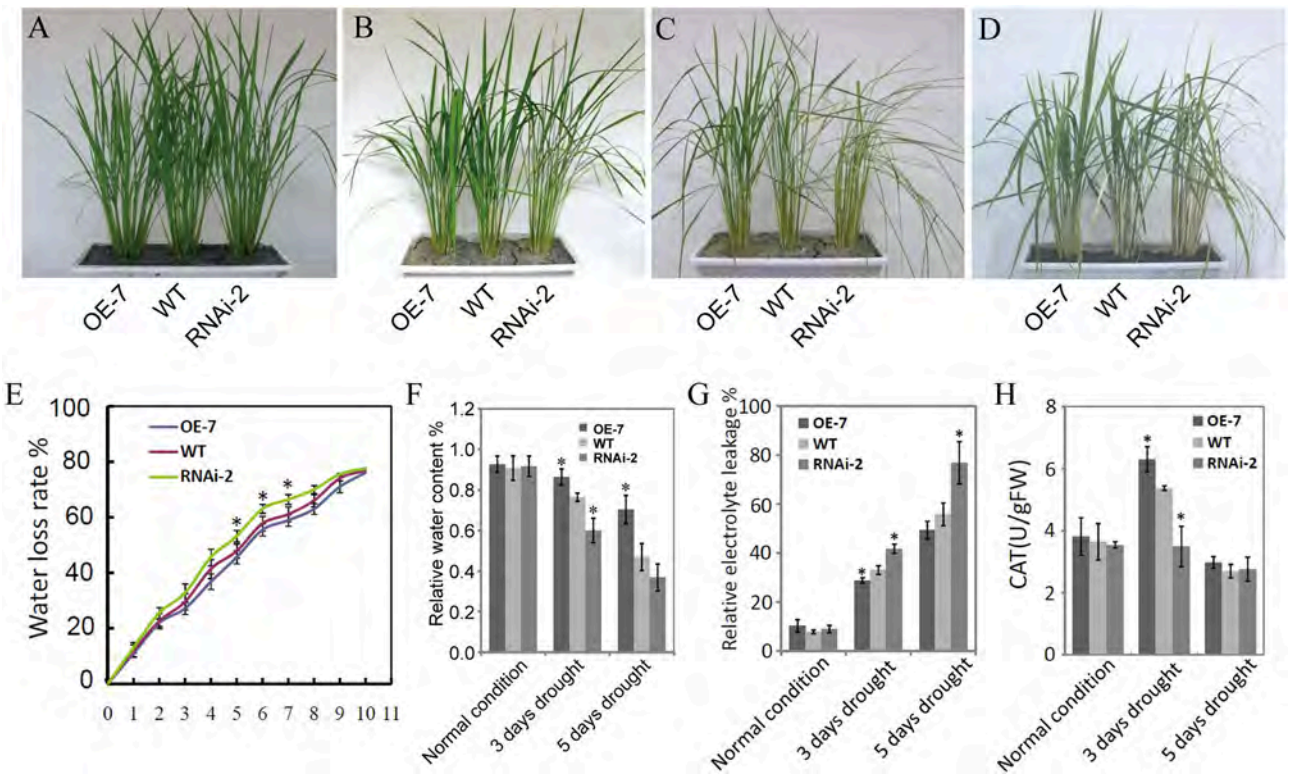

FIGURE 5 | Phenotypic and physiological trait performances of the *OsDRAP1* overexpression line (OE-7), RNAi line (RNAi-2) and wild type under drought stress; The seedling growth phenotypes of OE-7, RNAi-2 and WT under the normal irrigation **(A)**, 3d and 5d drought stress **(B,C)**, and 5d after re-watering **(D)**; **(E)** The assay of water loss rates of OE-7, WT and RNAi-2; **(F)** The relative leaf water content of OE-7, WT and RNAi-3 under normal control, 3d and 5d drought stress; **(G)** Detection of relative electrolyte leakage of OE-7, WT and RNAi-2 under control, 3d and 5d drought stress conditions; **(H)** Detection of activities of ROS-scavenging enzymes (CAT) in three rice genotypes subjected to drought stress, with each column representing mean ± SD (three replicates) and * indicating a significant difference at $p < 0.05$ vs. WT based on the Dunnett's multiple comparison tests in ANOVA.

(**Figures 4H,I**). These results showed that the expression of *OsDRAP1* was positively involved in DT. Based on these results, the transgenic lines, OE-7 and RNAi-2 were selected for further characterizing the functionality of *OsDRAP1* in the following experiments.

Figure 5 shows the results on the evaluation of the *OsDRAP1* overexpression line (OE-7), RNAi line (RNAi-2) and WT at the tillering stage for phenotypic and physiological trait performances under 3 and 5 days drought stress. There were no significant differences among three lines under the normal growth conditions. However, the WT and RNAi-2 plants started to show leaf rolling and wilting 3 d after drought stress, while the OE-7 was more viable than RNAi-2 and WT 5 days after drought stress and showed much better recovery 5 days after rewatering from the drought stress damage when the RNAi-2 plant was still wilted (**Figure 5D**). Furthermore, the OE-7 showed the lowest water loss, highest relative leaf water content, the lowest relative electrolyte leakage, and highest activities of ROS-scavenging enzymes during drought stress, while the opposite was true for the RNAi-2 plant (**Figures 5E–H**). All these results strongly suggested that *OsDRAP1* overexpression improved drought tolerance in rice by maintaining higher leaf water content and enhancing activities of ROS-scavenging enzymes. However, at the maturity, the OE-7 and RNAi-2 plants showed significantly reduced height by 6 cm and 16 cm when compared with the WT plant (**Figure S3**). In addition, when compared to the WT plant, the OE-7 plant showed significantly reduced spikelet fertility while the RNAi-2 plant showed significantly reduced panicle numbers/plant (**Figures S3C,E**). As a result, both the OE-7 and RNAi-2 plants had lower grain yield/plant than the WT plant (**Figure S3F**). All these results indicated that overexpression or repression of *OsDRAP1* had negative effects on the development and grain yield of rice, though the latter's effect was more severe.

GUS staining results of the OsDRAP1-Pro::GUS transgenic plants showed that OsDRAP1 was mainly expressed in rice vascular tissues, especially in the vascular bundle of glume, leaf vein, pericycle and sheaths (**Figures 2B–F**). Electron microscope scanning of the stem cross sections revealed significant differences in cell number and diameter of vascular bundle between of the RNAi-2 and WT or OE-7 rice plants. Specifically, the RNAi-2 plant had fewer vascular cells and smaller diameter of vascular bundle than the OE-7 and WT plants (**Figure 6**), suggesting that *OsDRAP1* may play an important role in vascular development.

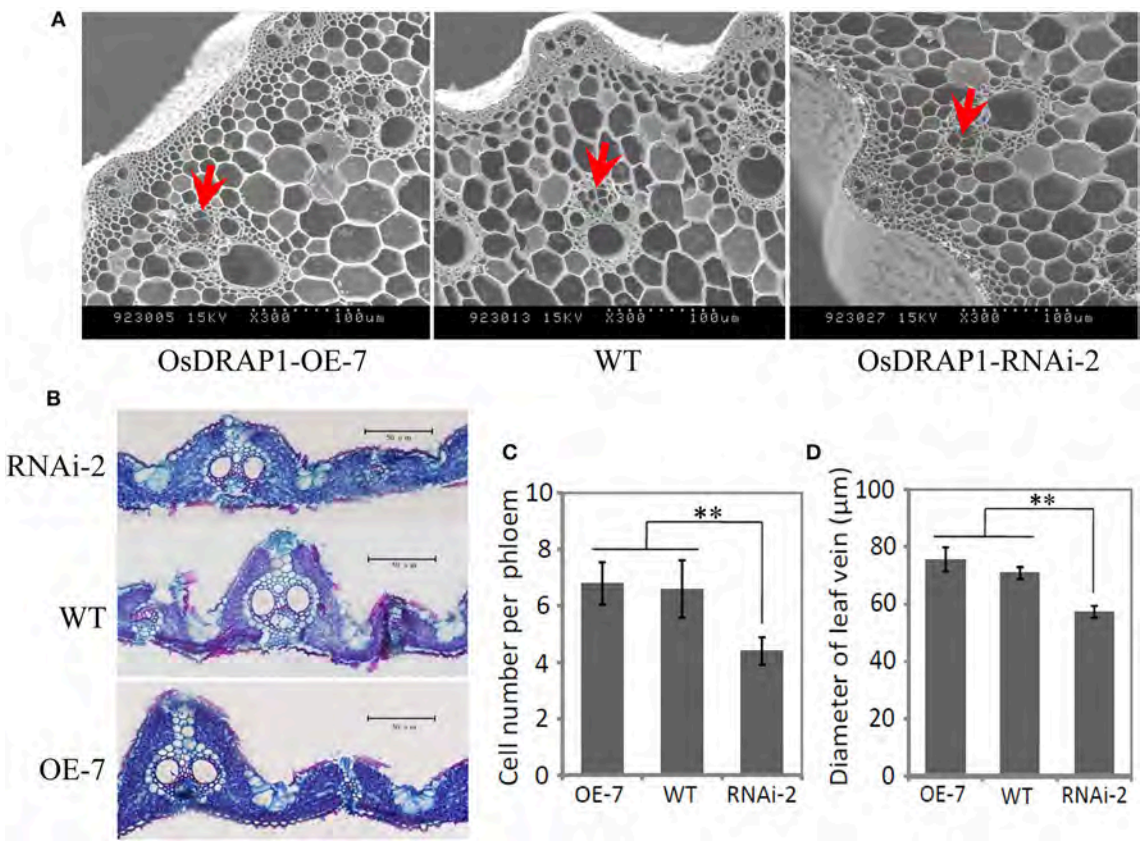

FIGURE 6 | The cellular observation of the vascular tissues in one overexpression line (OE-7), one RNAi line (RNAi-2) and non-transgenic wild type (WT) for *OsDRAP1*, **(A);** and the cross section of the stem and leaf blade **(B)** at the tillering stage. Red arrows indicate the vascular bundles (phloem), with scale bars in 100 μm; **(C)** The mean cell number per phloem in the vascular bundle of the OE-7, WT and RNAi-2 plants; and **(D)** The diameter of leaf veins of the OE-7, WT and RNAi-2 plants, with the asterisks (**) indicating significant differences at $p < 0.01$ in *t*-tests when compared with WT ($n > 10$).

Downstream Genes and Pathways Involved in DT Regulated by *OsDRAP1*

To gain insights into genes and pathways for DT regulated by *OsDRAP1*, we performed transcriptome sequencing to screen the differentially expressed genes in OE-7 compared to WT plants under normal growth and drought conditions, respectively. **Table S1** shows 42 and 46 genes that were up- and down-regulated in OE-7, respectively, when compared to WT under the normal growth conditions. GO analysis revealed that the majority of these genes were functionally related to "response to stress" and "metabolic process." After analyzing the *cis*-elements in the promoters of the 42 up-regulated genes in OE-7 using PLACE, we found that many of them have the binding sites of DREB TFs, GCC box and DRE *cis*-elements (**Table S1**), including GCCCOREC (S000430), DRECOREZMRAB17 (S000402) and DRECRTCOREAT (S000418), indicating that these genes were most likely directly regulated by *OsDRAP1* and function in pathway(s) contributing in the basal DT of rice.

Under drought stress, there were 85 and 53 genes up- and down-regulated in OE-7 as compared to WT (**Table S2**). Most of the up-regulated genes in OE-7 were functionally categorized in metabolic processes (19), response to stress (14) and transcription regulation (6). Several TFs (*OsEATB*, *OsERF5*, *OsMYB4*, and *OsWRKY89*) were evidently induced in OE-7 by drought stress. In addition, a gene encoding cellulose synthase-like family A (CSLA11) reportedly involved in cell wall biogenesis (Wang et al., 2010), was remarkably up-regulated in OE-7. Meanwhile, a set of genes related to the JA signaling pathway such as *OsJAZ8* (Yamada et al., 2012), *OsJAZ13* (Singh et al., 2015), *Jasmonate-zim-domain protein 1*, and *Jasmonate O-methyltransferase* were simultaneously induced in OE-7 under drought, indicating that JA was also involved in the *OsDRAP1* mediated regulating pathways of DT.

Identification of the Interacting Proteins of OsDRAP1

To identify proteins that directly interact with OsDRAP1, we performed yeast two-hybrid (Y2H) screening, which identified 30 interacting proteins from 45 positive clones screened according to their α-galactosidase activity (**Table S3**). Genes encoding these interacting proteins were predominant in function categories of response to stress (9), metabolic process (8) and nucleotide binding (7). These genes included several previously reported genes involved in response to abiotic stresses, such as *OsRZFP34* for stomata opening, *OsAPX2* and *OsCATC* involved in redox homeostasis under abiotic stress, *OsRACK1A* in ABA and H_2O_2 signaling pathways and *OsCBSX3* involved in biotic stress tolerance (Lin et al., 2012; Zhang et al., 2013, 2014; Hsu et al., 2014; Mou et al., 2015). Results from bimolecular fluorescence complementation and co-immunoprecipitation assays revealed the direct interaction between A CBS (cystathionine beta-synthase) domain containing protein (OsCBSX3) and OsDRAP1 in the nucleus (**Figure 7**), indicating that *OsCBSX3* is involved in the *OsDRAP1*-regulated pathway in rice.

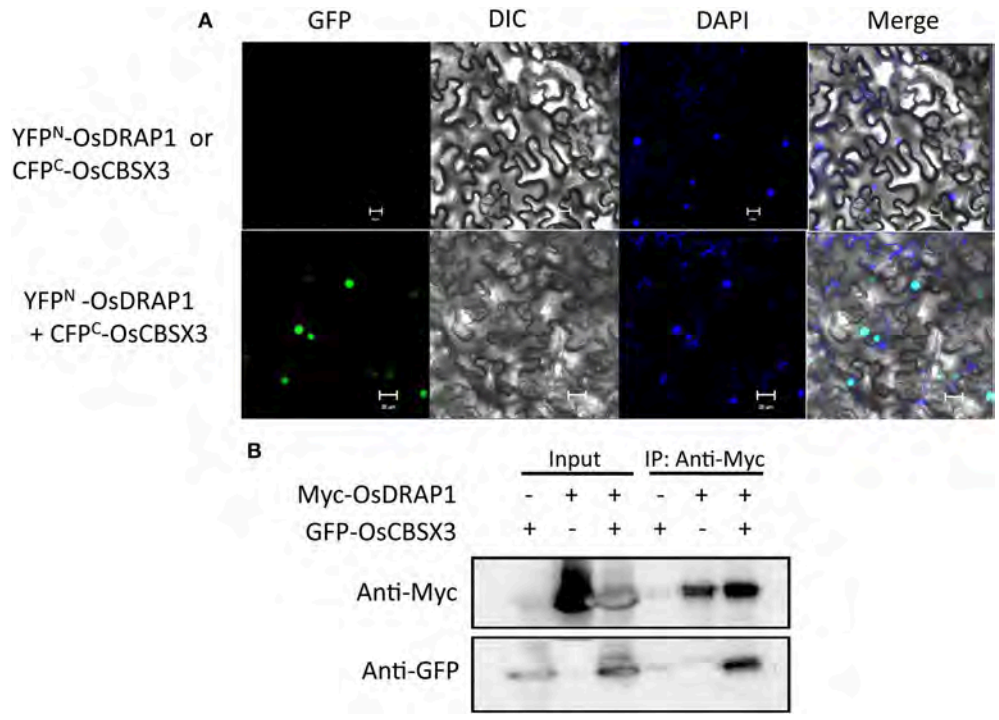

FIGURE 7 | Evidence of the interaction of OsDRAP1 with OsCBSX3. **(A)** the BiFC assay showing the interaction of OsDRAP1 with OsCBSX3 in the nuclei of *N. benthamiana* leaf cells with YFP^N-OsDRAP1 or CFP^C-OsCBSX3 co-transformed withCFP^C-GUS orYFP^N-GUSserved as the negative control and scale bars in 10 μm; **(B)** the Coimmunoprecipitation assays of OsDRAP1 and OsCBSX3 with GFP-OsCBSX3 or Myc-OsDRAP1 used as the negative control.

DISCUSSION

In plants, many DREB1 genes are known to be responsive to abiotic stresses and have been characterized, but only a few DREB2 genes have been functionally elucidated (Lata and Prasad, 2011). In this study, we have demonstrated that *OsDRAP1* in rice encodes a DREB2-like protein and functioned, as one of the DREB proteins in the AP2/ERF sub-family and plays an important role involved in several signal transduction pathways in response to different abiotic stresses, including drought, salt, cold and H_2O_2 stresses. *OsDRAP1* was previously characterized as a drought stress-induced AP2/EREBP gene (Wang D. et al., 2011). In this study, *OsDRAP1* was proved as a nuclear-localized protein and possessed transactivation activity which involved in ABA and JA transcriptional regulation, and *OsDRAP1* could activate the transcription of downstream genes by binding GCC box and DRE elements. The unique spatial expression pattern of *OsDRAP1* in vascular tissues and its

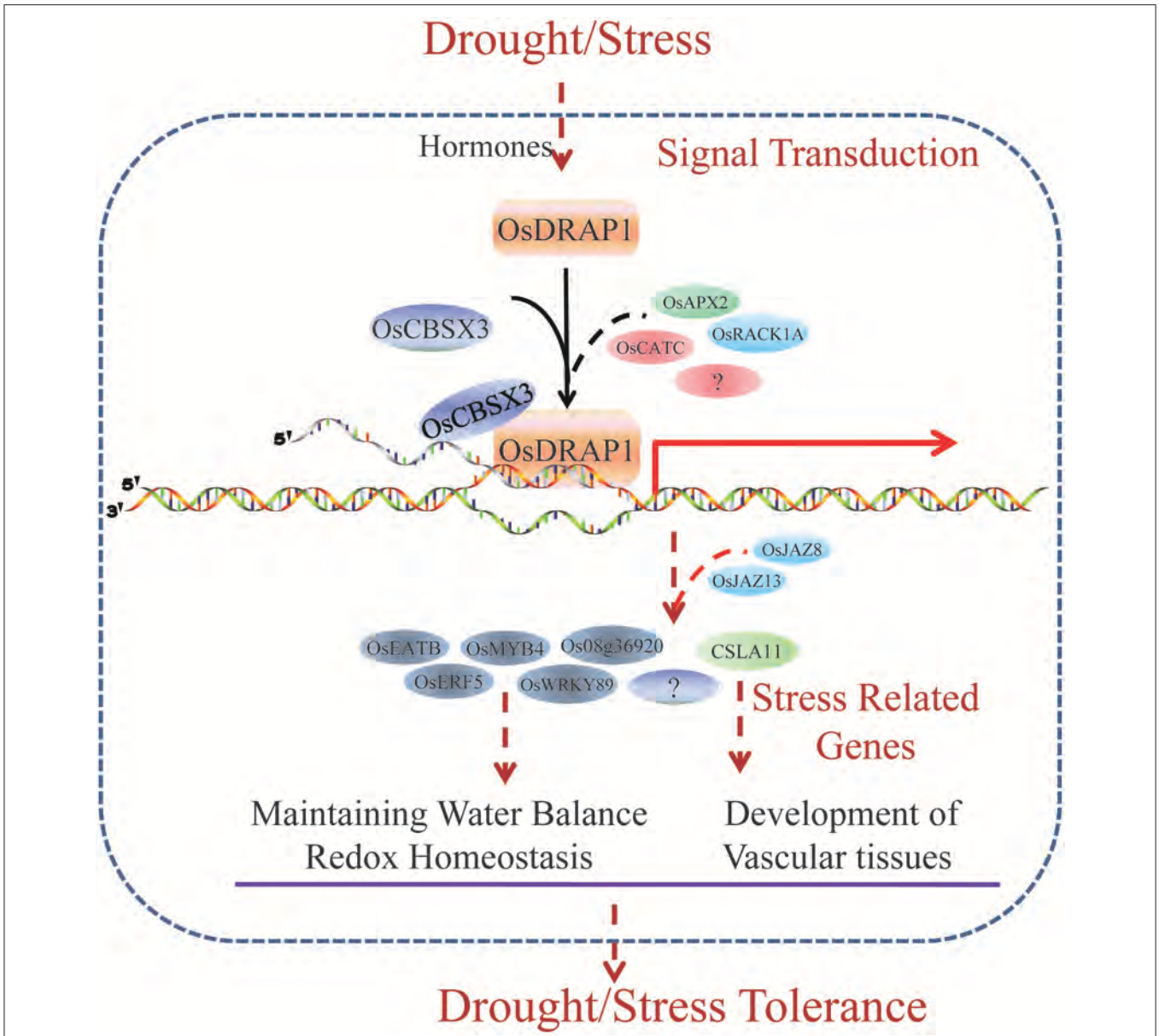

FIGURE 8 | A model for *OsDRAP1*-Mediated Stress Tolerance. Through a set of plant hormones pathways, the rice feels the stress signal and induce the expression of *OsDRAP1*. Interacting with other stress related proteins, including OsCBSX3, OsRACK1A, OsRZFP34, OsAPX2, and OsCATC, OsDRAP1 activate stress responsive genes which regulate water balance, redox homeostasis and vascular development directly or indirectly. Several stress responsive TFs (*OsEATB*, *OsERF5*, *OsMYB4*, and *OsWRKY89*) and a gene encoding cellulose synthase-like family A (CSLA11) induced by OsDRAP1 complex are likely to mediated by JA signaling pathway (*OsJAZ8*, *OsJAZ13*, *Jasmonate-zim-domain protein 1*, and *Jasmonate O-methyltransferase*). *OsDRAP1* mediate stress tolerance especially DT via its regulation of these stress responding genes.

effects causing reduced cell number and diameter of vascular bundle in RNAi plants suggest that *OsDRAP1* is involved in vascular bundle development. Although the vascular tissue is responsible the transport of water and nutrients in plants (Campbell and Turner, 2017), how vascular tissue responds to drought stress remains to be elucidated at the molecular level.

The presence of many different functional motifs in the promoter region of *OsDRAP1* suggests that *OsDRAP1* functions by mediating many downstream genes and pathways. Indeed, we were able to detect many genes functioning in response to stress and metabolic process were differentially expressed in the *OsDRAP1* OE lines, and most of these genes have GCC box and DRE elements in their promoters regulated by *OsDRAP1* (Cheng et al., 2013). Those genes also included a few TF genes such as *OsEATB*, *OsERF5*, *OsMYB4* and *OsWRKY89* that were previously reported to be involved in plant development or abiotic stress tolerance (Vannini et al., 2007; Wang et al., 2007; Zhou et al., 2010; Qi et al., 2011). Clearly, the *OsDRAP1* mediated DT genetic pathways underlying abiotic stress tolerances are involved in complex synergistic relationships with these TFs. Other important DT genes downstream of *OsDRAP1* included *CSLA11* that encodes a cellulose synthase-like family A protein. The CSLA gene family is reported to be involved in cell wall biogenesis (Wang et al., 2010; Liepman and Cavalier, 2012) and increased expression of *CSLA11* which might explain the strong effect of *OsDRAP1* on vascular development. We noted that several other genes the JA signaling pathway were strongly activated by *OsDRAP1* in the OE line, including *OsJAZ8*, *OsJAZ13*, Jasmonate-zim-domain protein 1 (LOC_Os03g08330) and Jasmonate O-methyltransferase (LOC_Os06g21820), implying that JA was involved in coordinate regulation of downstream genes in the *OsDRAP1* mediated drought stress responses, as reported previously (Ahmad et al., 2016). Other genes interacting with OsDRAP1 included OsCBSX3/OsBi1 (LOC_Os02g57280) and a CBS (cystathionine beta-synthase) domain containing protein (CDCPs). *OsCBSX3/OsBi1* was previously reported to be induced in rice by herbivore feeding and water deficit stress (Wang et al., 2004) and have a positive regulating role in rice resistance to *M. oryzae* in JA-mediated signaling pathways (Mou et al., 2015). CDCPs were reported to play an important role in plant responses to abiotic stresses by regulating many enzymes and maintaining the intracellular redox balance (Kushwaha et al., 2009; Yoo et al., 2011; Singh et al., 2012). OsCBSX3 might interact with OsDRAP1 and function positively in DT by maintaining the redox homeostasis under drought stress, however, the detailed molecular mechanisms how *OsCBSX3* is involved in the *OsDRAP1*-mediated DT genetic pathways remains to be elucidated.

Moreover, our results indicated that like many other plant DREB proteins, overexpression of *OsDRAP1* enhanced rice tolerance to drought and salinity, while knockdown of *OsDRAP1* lead to more sensitivity to drought in addition to significant negative effects on rice development and grain yield, as reported previously in overexpression experiments of other plant DREB genes (Kasuga et al., 1999, 2004; Ito et al., 2006). Clearly, this kind of fitness costs was much more severe in the *OsDRAP1*-knockdown plants than its constitutive overexpression-plants. This suggests it may be difficult to improve rice DT or salt tolerance by transgenic overexpression of *OsDRAP1*. Therefore, efficient utilization of *OsDRAP1* for improving rice tolerance to drought and salt requires more complete understanding of the *OsDRAP1* mediated gene networks and pathways and their related phenotypic effects.

CONCLUSIONS

OsDRAP1 is a DREB2-like TF gene which affects DT by maintaining water balance and redox homeostasis in rice under water deficit conditions. *OsDRAP1* appears to be involved in the regulation of the development of the vascular tissues. Constitutive overexpression of *OsDRAP1* could improve drought stress tolerance by affecting downstream genes with GCC and DRE *cis*-elements and synergistically regulating several TF genes including *OsERF5*, *OsMYB4,* and *OsWRKY89* and those related to JA pathways (**Figure 8**). The interaction protein OsCBSX3 could participate in the OsDRAP1-mediated regulation network in drought stress tolerance in rice.

AUTHOR CONTRIBUTIONS

LH and YW generated the transgenic materials, designed and performed the experiments, WW and ZcL analyzed RNA-Seq data, FS and QQ provided assistance on vector construction, XZ, FH, and YZ provided assistance on the drought phenotyping experiment, BF and ZL designed the experiments and wrote the manuscript.

FUNDING

This work was supported by grants from the National Natural Science Foundation of China (31571631 and 31501291), the Shenzhen Peacock Plan (20130415095710361), the CAAS Innovative Team Award, and the Bill & Melinda Gates Foundation (OPP1130530).

SUPPLEMENTARY MATERIAL

The Supplementary Material for this article can be found online at: https://www.frontiersin.org/articles/10.3389/fpls.2018.00094/full#supplementary-material

Figure S1 | The phylogenetic analysis of the DREB proteins in plants. The maximum parsimony tree of the DREB proteins from various plants **(A)** and rice **(B)**, based on the sequence database in UniProt Knowledgebase (UniProtKB): *Arabidopsis thaliana, At; Oryza sativa, Os; Zea mays, Zm; Phyllostachysedulis, Pe; Helianthus annuus, Ha; Oryzabrachyantha, Ob; Aegilopsbiuncialis, Ab; Nicotianabenthamiana, Nb; Poapratensis, Pp; Triticumaestivum, Ta; Glycine max, Gm; Solanumlycopersicum, Sl; Festucaarundinacea, Fa.*

Figure S2 | Expression analysis of *OsDRAP1* in the transgenic rice plants. With red and green columns indicating *OsDRAP1* overexpression (OsDRAP1-OE-1∼13) and *OsDRAP1* RNAi (OsDRAP1-RNAi-1∼4) in transgenic lines, respectively, the error bars indicating SD based on data of 3 replicates, *Actin*

1 used as the endogenous control and Arrows indicating the two lines (OE-7 and RNAi-2) that were used for further functional analysis.

Figure S3 | The negative effect on the plants overexpressing and knock-down of *OsDRAP1*. **(A)** The growth of *OsDRAP1*-OE-7, WT and *OsDRAP1*-RNAi-2 plants. Investigation of plant height **(B)**, number of tillering **(C)**, root performance **(D)**, fertility **(E)**, and grain yield **(F)** of the transgenic lines. The asterisk indicated the significant difference in *t*-test ($p < 0.05$ vs. WT, $n > 10$).

Table S1 | List of the differentially expressed gene in the *OsDRAP1* overexpression line compared with WT under normal growth conditions.

Table S2 | List of the differentially expressed gene in *OsDRAP1* overexpression line compared with WT under drought stress conditions.

Table S3 | List of interacting proteins of OsDRAP1 identified by yeast two-hybridization screening.

REFERENCES

Ahmad, P., Rasool, S., Gul, A., Sheikh, S. A., Akram, N. A., Ashraf, M., et al. (2016). Jasmonates: Multifunctional Roles in Stress Tolerance. *Front. Plant Sci.* 7:813. doi: 10.3389/fpls.2016.00813

Arora, R., Pitchay, D. S., and Bearce, B. C. (1998). Water-stress-induced heat tolerance in geranium leaf tissues: a possible linkage through stress proteins? *Plant Physiol.* 103, 24–34. doi: 10.1034/j.1399-3054.1998.1030104.x

Babu, R. C. (2010). Breeding for drought resistance in rice: an integrated view from physiology to genomics. *Electron. J. Plant Breed.* 1, 1133–1141.

Bart, R., Chern, M., Park, C. J., Bartley, L., and Ronald, P. C. (2006). A novel system for gene silencing using siRNAs in rice leaf and stem-derived protoplasts. *Plant Methods* 2:13. doi: 10.1186/1746-4811-2-13

Bonnecarrère, V., Borsani, O., Díaz, P., Capdevielle, F., Blanco, P., and Monza, J. (2011). Response to photoxidative stress induced by cold in japonica rice is genotype dependent. *Plant Sci.* 180, 726–732. doi: 10.1016/j.plantsci.2011.01.023

Campbell, L., and Turner, S. (2017). Regulation of vascular cell division. *J. Exp. Bot.* 68, 27–43. doi: 10.1093/jxb/erw448

Chen, J. Q., Meng, X. P., Zhang, Y., Xia, M., and Wang, X. P. (2008). Over- expression of *OsDREB* genes lead to enhanced drought tolerance in rice. *Biotechnol. Lett.* 30, 2191–2198. doi: 10.1007/s10529-008-9811-5

Cheng, M. C., Liao, P. M., Kuo, W. W., and Lin, T. P. (2013). The *Arabidopsis* ETHYLENE RESPONSE FACTOR1 regulates abiotic stress responsive gene expression by binding to different *cis*-acting elements in response to different stress signals. *Plant Physiol.* 162, 1566–1582. doi: 10.1104/pp.113.221911

Chien, C. T., Bartel, P. L., Sternglanz, R., and Fields, S. (1991). The two-hybrid system: a method to identify and clone genes for proteins that interact with a protein of interest. *Proc. Nati. Acad. Sci. U.S.A.* 88, 9578–9582. doi: 10.1073/pnas.88.21.9578

Cui, M., Zhang, W., Zhang, Q., Xu, Z., Zhu, Z., Duan, F., et al. (2011). Induced over-expression of the transcription factor *OsDREB2A* improves drought tolerance in rice. *Plant Physiol. Biochem.* 49, 1384–1391. doi: 10.1016/j.plaphy.2011.09.012

Curtis, M. D., and Grossniklaus, U. (2003). A Gateway TM cloning vector set for high-throughput functional analysis of genes in plants. *Plant Physiol.* 133, 462–469. doi: 10.1104/pp.103.027979

Du, Z., Zhou, X., Ling, Y., Zhang, Z., and Su, Z. (2010). agriGO: a GO analysis toolkit for the agricultural community. *Nucleic Acids Res.* 38, 64–70. doi: 10.1093/nar/gkq310

Duan, Y., Zhai, C., Li, H., Li, J., Mei, W., Gui, H., et al. (2012). An efficient and high-throughput protocol for *Agrobacterium*-mediated transformation based on phosphomannoseisomerase positive selection in Japonica rice (*Oryza sativa* L.). *Plant Cell Rep.* 31, 1611–1624. doi: 10.1007/s00299-012-1275-3

Dubouzet, J. G., Sakuma, Y., Ito, Y., Kasuga, M., Dubouzet, E. G., Miura, S., et al. (2003). *OsDREB* genes in rice, *Oryza sativa* L., encode transcription activators that function in drought-, high-salt- and cold-responsive gene expression. *Plant J.* 33, 751–763. doi: 10.1046/j.1365-313X.2003.01661.x

Fields, S., and Song, O. (1989). A novel genetic system to detect protein-protein interactions. *Nature* 340, 245–246. doi: 10.1038/340245a0

Hadiarto, T., and Tran, L. S. (2011). Progress studies of drought-responsive genes in rice. *Plant Cell Rep.* 30, 297–310. doi: 10.1007/s00299-010-0956-z

Hao, D., Ohme-Takagi, M., and Sarai, A. (1998). Unique mode of GCC box recognition by the DNA-binding domain of ethylene-responsive element-binding factor (ERF domain) in plant. *J. Biol. Chem.* 273, 26857–26861. doi: 10.1074/jbc.273.41.26857

Hsu, K. H., Liu, C. C., Wu, S. J., Kuo, Y. Y., Lu, C. A., Wu, C. R., et al. (2014). Expression of a gene encoding a rice RING zinc-finger protein, *OsRZFP34*, enhances stomata opening. *Plant Mol. Biol.* 86, 125–137. doi: 10.1007/s11103-014-0217-6

Huang, L., Zhang, F., Zhang, F., Wang, W., Zhou, Y., Fu, B., et al. (2014). Comparative transcriptome sequencing of tolerant rice introgression line and its parents in response to drought stress. *BMC Genomics* 15:1026. doi: 10.1186/1471-2164-15-1026

Ito, Y., Katsura, K., and Maruyama, K. (2006). Functional analysis of rice DREB1/CBF type transcription factors involved in cold-responsive gene expression in transgenic rice. *Plant Cell Physiol.* 47, 141–153. doi: 10.1093/pcp/pci230

Joshi, R., Wani, S. H., Singh, B., Bohra, A., Dar, Z. A., Lone, A. A., et al. (2016). Transcription factors and plants response to drought stress: current understanding and future directions. *Front. Plant Sci.* 7:1029. doi: 10.3389/fpls.2016.01029

Karimi, M., De Meyer, B., and Hilson, P. (2005). Modular cloning and expression of tagged fluorescent protein in plant cells. *Trends Plant Sci.* 10, 103–105. doi: 10.1016/j.tplants.2005.01.008

Kasuga, M., Liu, Q., Miura, S., Yamaguchi-Shinozaki, K., and Shinozaki, K. (1999). Improving plant drought, salt and freezing tolerance by gene transfer of a single stress-inducible transcription factor. *Nat. Biotechnol.* 17, 287–291. doi: 10.1038/7036

Kasuga, M., Miura, S., Shinozaki, K., and Yamaguchi-Shinozaki, K. (2004). A combination of *Arabidopsis DREB1A* gene and stress inducible *rd29A*promoter improved drought and low temperature stress tolerance in tobacco by gene transfer. *Plant Cell Physiol.* 45, 346–350. doi: 10.1093/pcp/pch037

Kawahara, Y., de la Bastide, M., Hamilton, J. P., Kanamori, H., McCombie, W. R., Ouyang, S., et al. (2013). Improvement of the *Oryza sativa* Nipponbare reference genome using next generation sequence and optical map data. *Rice* 6:4. doi: 10.1186/1939-8433-6-4

Kumar, A., Dixit, S., Ram, T., Yadaw, R. B., Mishra, K. K., and Mandal, N. P. (2014). Breeding high-yielding drought-tolerant rice: genetic variations and conventional and molecular approaches. *J. Exp. Bot.* 65, 6265–6278. doi: 10.1093/jxb/eru363

Kushwaha, H. R., Singh, A. K., Sopory, S. K., Singla-Pareek, S. L., and Pareek, A. (2009). Genome wide expression analysis of CBS domain containing proteins in *Arabidopsis thaliana* (L.) Heynh and *Oryza sativa* L. reveals their developmental and stress regulation. *BMC Genomics* 10:200. doi: 10.1186/1471-2164-10-200

Lata, C., and Prasad, M. (2011). Role of DREBs in regulation of abiotic stress responses in plants. *J. Exp. Bot.* 62, 4731–4748. doi: 10.1093/jxb/err210

Lenka, S. K., Katiyar, A., Chinnusamy, V., and Bansal, K. C. (2011). Comparative analysis of drought-responsive transcriptome in *indica* rice genotypes with contrasting drought tolerance. *Plant Biotechnol. J.* 9, 315–327. doi: 10.1111/j.1467-7652.2010.00560.x

Li, J., Han, Y., Liu, L., Chen, Y., Du, Y., Zhang, J., et al. (2015). *qRT9*, a quantitative trait locus controlling root thickness and root length in upland rice. *J. Exp. Bot.* 66, 2723–2732. doi: 10.1093/jxb/erv076

Li, Z. K., Fu, B. Y., Gao, Y. M., Xu, J. L., Ali, J., Lafitte, H. R., et al. (2005). Genome-wide introgression lines and their use in genetic and molecular dissection of complex phenotypes in rice (*Oryza sativa* L.). *Plant Mol. Biol.* 59, 33–52. doi: 10.1007/s11103-005-8519-3

Liepman, A. H., and Cavalier, D. M. (2012). The CELLULOSE SYNTHASE-LIKE A and CELLULOSE SYNTHASE-LIKE C families: recent advances and future perspectives. *Front. Plant Sci.* 3:109. doi: 10.3389/fpls.2012.00109

Lin, A., Wang, Y., Tang, J., Xue, P., Li, C., Liu, L., et al. (2012). Nitric oxide and protein S-nitrosylation are integral to hydrogen peroxide-induced leaf cell death in rice. *Plant Physiol.* 158, 451–464. doi: 10.1104/pp.111.184531

Liu, C. W., Fukumoto, T., Matsumoto, T., Gena, P., Frascaria, D., Kaneko, T., et al. (2013). Aquaporin OsPIP1;1 promotes rice salt resistance and seed germination. *Plant Physiol. Biochem.* 63, 151–158. doi: 10.1016/j.plaphy.2012.11.018

Liu, H. T., Yu, X. H., Li, K. W., Klejnot, J., Yang, H. Y., Lisiero, D., et al. (2008). Photoexcited CRY2 interacts with CIB1 to regulate transcription and floral initiation in *Arabidopsis*. *Science* 322, 1535–1539. doi: 10.1126/science.1163927

Liu, Q., Kasuga, M., Sakuma, Y., Abe, H., Miura, S., Yamaguchi-Shinozaki, K., et al. (1998). Two transcription factors, DREB1 and DREB2, with an EREBP/AP2 DNA binding domain separate two cellular signal transduction pathways in drought- and low-temperature-responsive gene expression, respectively, in *Arabidopsis*. *Plant Cell* 10, 1391–1406. doi: 10.1105/tpc.10.8.1391

Livak, K. J., and Schmittgen, T. D. (2001). Analysis of relative gene expression data using real-time quantitative PCR and the $2^{(-DeltaDeltaC(T))}$ method. *Methods* 25, 402–408. doi: 10.1006/meth.2001.1262

Matsukura, S., Mizoi, J., Yoshida, T., Todaka, D., Ito, Y., Maruyama, K., et al. (2010). Comprehensive analysis of rice DREB2-type genes that encode transcription factors involved in the expression of abiotic stress-responsive genes. *Mol. Genet. Genomics* 283, 185–196. doi: 10.1007/s00438-009-0506-y

Mizoi, J., Shinozaki, K., and Yamaguchi-Shinozaki, K. (2012). AP2/ERF family transcription factors in plant abiotic stress responses. *Biochim. Biophys. Acta.* 1819, 86–96. doi: 10.1016/j.bbagrm.2011.08.004

Mortazavi, A., Williams, B. A., McCue, K., Schaeffer, L., and Wold, B. (2008). Mapping and quantifying mammalian transcriptomes by RNA-Seq. *Nat. Methods* 5, 621–628. doi: 10.1038/nmeth.1226

Mou, S., Shi, L., Lin, W., Liu, Y., Shen, L., Guan, D., et al. (2015). Over-expression of rice CBS domain containing protein, OsCBSX3, confers rice resistance to *Magnaporthe oryzae* inoculation. *Int. J. Mol. Sci.* 16, 15903–15917. doi: 10.3390/ijms160715903

Pandey, S. (2009). Economic costs of drought and rice farmers' coping mechanisms. *Int. Rice Res. Notes* 1, 5–11. doi: 10.3860/irrn.v32i1.1078

Peng, H.,·Zhang, Q.,·Li, Y. D., Lei, C. L., Zhai, Y., Sun, X. H., et al. (2009). A putative leucine-rich repeat receptor kinase, OsBRR1, is involved in rice blast resistance. *Planta* 230, 377–385. doi: 10.1007/s00425-009-0951-1

Qi, W., Sun, F., Wang, Q., Chen, M., Huang, Y., Feng, Y., et al. (2011). Rice ethylene-response AP2/ERF factor OsEATB restricts internode elongation by down-regulating a gibberellin biosynthetic gene. *Plant Physiol.* 157, 216–228. doi: 10.1104/pp.111.179945

Riechmann, J. L., and Meyerowitz, E. M. (1998). The AP2/EREBP family of plant transcription factors. *Biol. Chem.* 379, 633–646.

Sakuma, Y., Liu,. Q., Dubouzet, J. G., Abe, H., Shinozaki, K., and Yamaguchi-Shinozaki, K. (2002). DNA-binding specificity of the ERF/AP2 domain of *Arabidopsis* DREBs, transcription factors involved in dehydration-and cold-inducible gene expression. *Biochem.Biophys. Res. Commun.* 290, 998–1009. doi: 10.1006/bbrc.2001.6299

Sawa, M., Nusinow, D. A., Kay, S. A., and Imaizumi, T. (2007). FKF1 and GIGANTEA complex formation is required for day-length measurement in *Arabidopsis*. *Science* 318, 261–265. doi: 10.1126/science.1146994

Sharoni, A. M., Nuruzzaman, M., Satoh, K., Shimizu, T., Kondoh, H., Sasaya, T., et al. (2011). Gene structures, classification and expression models of the AP2/EREBP transcription factor family in rice. *Plant Cell Physiol.* 52, 344–360. doi: 10.1093/pcp/pcq196

Shukla, N., Awasthi, R. P., Rawat, L., and Kumar, J. (2012). Biochemical and physiological responses of rice (*Oryza sativa* L.) as influenced by *Trichodermaharzianum* under drought stress. *Plant Physiol. Biochem.* 54, 78–88. doi: 10.1016/j.plaphy.2012.02.001

Singh, A. K., Kumar, R., Pareek, A., Sopory, S. K., and Singla-Pareek, S. L. (2012). Overexpression of rice CBS domain containing protein improves salinity, oxidative, and heavy metal tolerance in transgenic tobacco. *Mol. Biotechnol.* 52, 205–216. doi: 10.1007/s12033-011-9487-2

Singh, A. P., Pandey, B. K., Deveshwar, P., Narnoliya, L., Parida, S. K., and Giri, J. (2015). JAZ repressors: potential involvement in nutrients deficiency response in rice and chickpea. *Front. Plant Sci.* 6:975. doi: 10.3389/fpls.2015.00975

Sparkes, I. A., Kearns, A., and Hawes, C. (2006). Rapid, transient expression of fluorescent fusion proteins in tobacco plants and generation of stably transformed plants. *Nat. Protoc.* 1, 2019–2025. doi: 10.1038/nprot.2006.286

Srivastav, A., Mehta, S., Lindlof, A., and Bhargava, S. (2010). Over-represented promoter motifs in abiotic stress-induced DREB genes of rice and sorghum and their probable role in regulation of gene expression. *Plant Signal. Behav.* 5, 775–784. doi: 10.4161/psb.5.7.11769

Takemoto, Y., Coughlan, S. J., Okita, T. W., Satoh, H., Ogawa, M., and Kumamaru, T. (2002). The rice mutant *esp2* greatly accumulates the glutelin precursor and deletes the protein disulfide isomerase. *Plant Physiol.* 128, 1212–1222. doi: 10.1104/pp.010624

Todaka, D., Shinozaki, K., and Yamaguchi-Shinozaki, K. (2015). Recent advances in the dissection of drought-stress regulatory networks and strategies for development of drought-tolerant transgenic rice plants. *Front. Plant Sci.* 6:84. doi: 10.3389/fpls.2015.00084

Trapnell, C., Pachter, L., and Salzberg, S. L. (2009). TopHat: discovering splice junctions with RNA-Seq. *Bioinformatics* 25, 1105–1111. doi: 10.1093/bioinformatics/btp120

Uga, Y., Sugimoto, K., Ogawa, S., Rane, J., Ishitani, M., Hara, N., et al. (2013). Control of root system architecture by DEEPER ROOTING 1 increases rice yield under drought conditions. *Nat. Genet.* 45, 1097–1102. doi: 10.1038/ng.2725

Vannini, C., Campa, M., Iriti, M., Genga, A., Faoro, F., Carravieri, S., et al. (2007). Evaluation of transgenic tomato plants ectopically expressing the rice Osmyb4 gene. *Plant Sci.* 173, 231–239. doi: 10.1016/j.plantsci.2007.05.007

Wang, D., Pan, Y., Zhao, X., Zhu, L., Fu, B., and Li, Z. (2011). Genome-wide temporal-spatial gene expression profiling of drought responsiveness in rice. *BMC Genomics.* 12:149. doi: 10.1186/1471-2164-12-149

Wang, H., Hao, J., Chen, X., Hao, Z., Wang, X., Lou, U., et al. (2007). Overexpression of rice WRKY89 enhances *ultravioletB* tolerance and disease resistance in rice plants. *Plant Mol. Biol.* 65, 799–815. doi: 10.1007/s11103-007-9244-x

Wang, L., Guo, K., Li, Y., Tu, Y., Hu, H., Wang, B., et al. (2010). Expression profiling and integrative analysis of the CESA/CSL superfamily in rice. *BMC Plant Biol.* 10:282. doi: 10.1186/1471-2229-10-282

Wang, Q., Guan, Y., Wu, Y., Chen, H., Chen, F., and Chu, C. (2008). Overexpression of a rice OsDREB1F gene increases salt, drought, and low temperature tolerance in both *Arabidopsis* and rice. *Plant Mol. Biol.* 67, 589–602. doi: 10.1007/s11103-008-9340-6

Wang, W. S., Pan, Y. J., Zhao, X. Q., Dwivedi, D., Zhu, L. H., Ali, J., et al. (2011). Drought-induced site-specific DNA methylation and its association with drought tolerance in rice (*Oryza sativa* L.). *J. Exp. Bot.* 62, 1951–1960. doi: 10.1093/jxb/erq391

Wang, X., Ren, X., Zhu, L., and He, G. (2004). *OsBi1*, a rice gene, encodes a novel protein with a CBS-like domain and its expression is induced in responses to herbivore feeding. *Plant Sci.* 166, 1581–1588. doi: 10.1016/j.plantsci.2004.02.011

Xiao, C., Chen, F., Yu, X., Lin, C., and Fu, Y. F. (2009). Over-expression of an AT-hook gene, *AHL22*, delays flowering and inhibits the elongation of the hypocotyl in *Arabidopsis thaliana*. *Plant Mol. Biol.* 71, 39–50. doi: 10.1007/s11103-009-9507-9

Xu, Z., and Vision, T. J. (2005). Improving quantitative trait loci mapping resolution in experimental crosses by the use of genotypically selected samples. *Genetics* 170, 401–408. doi: 10.1534/genetics.104.033746

Yamada, S., Kano, A., Tamaoki, D., Miyamoto, A., Shishido, H., Miyoshi, S., et al. (2012). Involvement of *OsJAZ8* in jasmonate-induced resistance to bacterial blight in rice. *Plant Cell Physiol.* 53, 2060–2072. doi: 10.1093/pcp/pcs145

Yoo, K. S., Ok, S. H., Jeong, B. C., Jung, K. W., Cui, M. H., Hyoung, S., et al. (2011). Single cystathionine β-synthase domain-containing proteins modulate development by regulating the thioredoxin system in *Arabidopsis*. *Plant Cell* 23, 3577–3594. doi: 10.1105/tpc.111.089847

You, J., Zong, W., Li, X. K., Ning, J., Hu, H. H., Li, X. H., et al. (2013). The SNAC1-targeted gene *OsSRO1c* modulates stomatal closure and oxidative stress tolerance by regulating hydrogen peroxide in rice. *J. Exp. Bot.* 64, 569–583. doi: 10.1093/jxb/ers349

Zhang, D., Chen, L., Li, D., Lv, B., Chen, Y., Chen, J., et al. (2014). *OsRACK1* is involved in abscisic acid- and H_2O_2- mediated signaling to regulate seed germination in rice (*Oryza sativa*, L.). *PLoS ONE* 9:e97120. doi: 10.1371/journal.pone.0097120

Zhang, Z., Zhang, Q., Wu, J., Zheng, X., Zheng, S., Sun, X., et al. (2013). Gene knockout study reveals that cytosolic ascorbate peroxidase 2(OsAPX2) plays a critical role in growth and reproduction in rice under drought, salt and cold stresses. *PLoS ONE* 8:e57472. doi: 10.1371/journal.pone.0057472

Zhou, Y. L., Xu, M. R., Zhao, M. F., Xie, X. W., Zhu, L. H., Fu, B. Y., et al. (2010). Genome-wide gene responses in a transgenic rice line carrying the maize resistance gene *Rxo1* to the rice bacterial streak pathogen, *Xanthomonas oryzae* pv. oryzicola. *BMC Genomics* 11:78. doi: 10.1186/1471-2164-11-78

Conflict of Interest Statement: The authors declare that the research was conducted in the absence of any commercial or financial relationships that could be construed as a potential conflict of interest.

frontiers in Plant Science

ORIGINAL RESEARCH
published: 09 March 2018
doi: 10.3389/fpls.2018.00310

Overexpression of *OsNAC14* Improves Drought Tolerance in Rice

Jae Sung Shim[1†], *Nuri Oh*[1†], *Pil Joong Chung*[1†], *Youn Shic Kim*[1], *Yang Do Choi*[1,2] *and Ju-Kon Kim*[1*]

[1] *Graduate School of International Agricultural Technology and Crop Biotechnology Institute, GreenBio Science & Technology, Seoul National University, Pyeongchang, South Korea,* [2] *Department of Agricultural Biotechnology, Seoul National University, Seoul, South Korea*

Plants have evolved to have sophisticated adaptation mechanisms to cope with drought stress by reprograming transcriptional networks through drought responsive transcription factors. NAM, ATAF1-2, and CUC2 (NAC) transcription factors are known to be associated with various developmental processes and stress tolerance. In this study, we functionally characterized the rice drought responsive transcription factor *OsNAC14*. *OsNAC14* was predominantly expressed at meiosis stage but is induced by drought, high salinity, ABA, and low temperature in leaves. Overexpression of *OsNAC14* resulted in drought tolerance at the vegetative stage of growth. Field drought tests demonstrated that *OsNAC14* overexpressing transgenic rice lines exhibited higher number of panicle and filling rate compared to non-transgenic plants under drought conditions. RNA-sequencing analysis revealed that *OsNAC14* overexpression elevated the expression of genes for stress response, DNA damage repair, defense related, and strigolactone biosynthesis. In addition, chromatin immunoprecipitation analysis confirmed the direct interaction of OsNAC14 with the promoter of *OsRAD51A1*, a key component in homologous recombination in DNA repair system. Collectively, these results indicate that OsNAC14 mediates drought tolerance by recruiting factors involved in DNA damage repair and defense response resulting in improved tolerance to drought.

Keywords: NAC transcription factors, OsNAC14, transgenic rice, drought tolerance, RNA-sequencing, ChIP

OPEN ACCESS

Edited by:
Henry T. Nguyen, University of Missouri, United States

Reviewed by:
Ratna Karan, University of Florida, United States
Woo Taek Kim, Yonsei University, South Korea

***Correspondence:**
Ju-Kon Kim
jukon@snu.ac.kr

[†] *These authors have contributed equally to this work.*

Specialty section:
This article was submitted to Plant Breeding, a section of the journal Frontiers in Plant Science

Received: *01 November 2017*
Accepted: *22 February 2018*
Published: *09 March 2018*

Citation:
Shim JS, Oh N, Chung PJ, Kim YS, Choi YD and Kim J-K (2018) Overexpression of OsNAC14 Improves Drought Tolerance in Rice. Front. Plant Sci. 9:310. doi: 10.3389/fpls.2018.00310

INTRODUCTION

Drought is a major environmental stress adversely affecting crop yield worldwide. Recent climate change increases occurrence and severity of drought stress in field. Moreover, the need to utilize farmland with inadequate water supply has substantially increased, as a consequence of global warming and world population growth. Thus, improving crop performance under drought conditions is an important objective in agriculture to support world food requirements. To cope with drought stress, plants have been evolved to possess molecular mechanisms that coordinate expression of genes to protect them from water deficit stress and increase the chance of survival in arid regions (Yamaguchi-Shinozaki and Shinozaki, 2006; Zheng et al., 2009).

Transcriptional reprograming required for drought tolerance mechanism is largely regulated by drought induced-transcription factors (TFs) such as AP2/ERF, MYB, bZIP, and NAC families (Yamaguchi-Shinozaki and Shinozaki, 2006; Nakashima et al., 2007; Zheng et al., 2009; Jung et al., 2017). Several studies have shown that overexpression of drought induced transcription factors can enhance drought tolerance. For example, overexpression of drought induced *OsERF48*, *OsERF71*,

OsMYB2, *OsbZIP12,* and *OsbZIP71* enhance drought tolerance in rice (Yang et al., 2012; Joo et al., 2014; Liu et al., 2014; Lee et al., 2016; Jung et al., 2017). Thus, identification and characterization of drought induced TFs is useful approach to understand molecular mechanisms underlying in drought tolerance and generate plants showing enhanced performance under drought condition (Jung et al., 2017; Lee D. K. et al., 2017).

NAC transcription factor family is one of the largest families of plant-specific transcription factors, named from first three reported members of the family, petunia NO APICAL MERISTEM (NAM), Arabidopsis ACTIVATION FACTOR (ATAF), and CUP-SHAPED COTYLEDON (CUC) (Souer et al., 1996; Aida et al., 1997). Genome-wide analysis has identified 117 NACs in Arabidopsis, 151 in rice, 79 in grape, 163 in poplar, 152 each in soybean, and tobacco (Ooka et al., 2003; Nuruzzaman et al., 2010, 2013). NAC proteins contain a highly conserved N-terminal DNA-binding domain that can form either a homodimer or a heterodimer and a highly variable C-terminal region (Ooka et al., 2003; Zheng et al., 2009). NACs were originally identified as key regulators of development through forward genetic screens (Souer et al., 1996; Takada et al., 2001). Recently, NACs have been reported to regulate wide range of abiotic stress responses in plants (Nuruzzaman et al., 2013). In Arabidopsis, *AtNAC72* (*RD26*), *AtNAC19,* and *AtNAC55* are required for drought tolerance (Fujita et al., 2004; Tran et al., 2004). Overexpression of *ATAF1* enhances drought tolerance through stomatal closure in Arabidopsis (Wu et al., 2009). In rice, the members in stress-induced NAC (SNAC) subgroup are reported as key regulators of drought tolerance in rice. Overexpression of *OsNAC5, OsNAC6, OsNAC9,* and *OsNAC10* confers drought tolerance via root structural adaptation and up-regulation of genes involved in stress responses, redox homeostasis, defense responses, and ABA biosynthesis (Nakashima et al., 2007; Jeong et al., 2010, 2013; Takasaki et al., 2010; Redillas et al., 2012; Lee D. K. et al., 2017).

Maintenance of genome stability is another important process in plants under abiotic stress for survival and faithful transmission of genetic information to next generation (Tuteja et al., 2001; Roy, 2014). Plants are subjected to high levels of DNA damage resulting from exposure to environmental stresses such as cold, high temperature, UV-C, and drought (Tuteja et al., 2001; Roldan-Arjona and Ariza, 2009; Roy, 2014). Reactive oxygen species (ROS) generation is one potential cause of DNA damage under drought conditions because drought induced DNA damage is alleviated by exogenous application of ROS scavenger (Tuteja et al., 2001; Wang and Zhang, 2001). Among various forms of DNA lesions generated by drought stress, double strand breaks (DSBs) in DNA are considered as one of the major form of DNA damage (Yao et al., 2013; Roy, 2014). DSBs are repaired by homologous recombination mediated by Radiation sensitive 51 (RAD51) and Mre11-RAD50-Nbs1 (MRN) complex (Shinohara et al., 1992; Symington, 2002). Function of RAD51 in homologous recombination is highly conserved in various organisms (Shinohara et al., 1992; Li et al., 2004, 2007; Khoo et al., 2008). Failure of DNA repair leads to deterioration of cell function and cell death (Tuteja et al., 2001). Thus, proper regulation of DNA repair is required for drought tolerance. However, the underlying molecular mechanisms are still elusive.

In this study, we investigated the molecular mechanism of *OsNAC14*-mediated drought tolerance responses. OsNAC14 belongs to ONACII subgroup of Group A NAC TFs. Transgenic rice overexpressing *OsNAC14* exhibited enhanced drought tolerance at the vegetative and the reproductive stages of growth. We also identified downstream target genes constituting the OsNAC14-mediated drought tolerance pathway which are involved in stress response, DNA repair, defense-related and strigolactone biosynthesis. OsNAC14 was found to regulate DNA repair pathway by directly regulating the homologous recombination component *OsRAD51A1*. These data suggest that OsNAC14 regulates *OsRAD51A1* which in turn enhances drought tolerance of plants.

MATERIALS AND METHODS

Plasmid Construction and Rice Transformation

The coding region of *OsNAC14* (*Os01g0675800*) was amplified from rice (*Oryza sativa* cv. Nipponbare) total RNA using the Reverse Transcription System (Promega) and PrimeSTAR HS DNA polymerase (TAKARA). The amplified OsNAC14 coding sequence was cloned into rice transformation vector p700 carrying *PGD1* promoter for constitutive overexpression (Park et al., 2012). The final construct named *PGD1::OsNAC14* was transformed into rice (*Oryza sativa* cv. Nakdong) by Agrobacterium (LBA4404)-mediated co-cultivation, as described previously (Jang et al., 1999). Copy numbers *PGD1::OsNAC14* transgenic plants were determined by TaqMan Q-PCR (ThermoFisher) using probes specific for the bar gene. To analyze copy number of the transgenic rice plants, genomic DNA was extracted from 2-week-old rice seedlings. Genomic DNA extracted from transgenic plants previously confirmed as single inserted homozygous line was used as control. The single copy insertion lines self-fertilized and homozygous transgenic lines were selected from T_2 generations on MS media containing phosphinothricin (Duchefa).

For CRISPR/Cas9-mediated *OsNAC14* mutagenesis, the CRISPR/Cas9 expression vector was constructed using a rice codon-optimized *Streptococcus pyogenes* Cas9 (rCRISPR/Cas9) and guide RNA (gRNA) targeting CDS region (700–722 bp) of OsNAC14 in pSB11 vector through restriction enzyme-mediated excision and ligation reactions. To generate rice codon-optimized Cas9, the original Cas9 sequence was changed to a sequence suitable for translation in rice. Then, rice codon-optimized Cas9 was chemically synthesized (Bioneer, Korea), and used for further constructions. Nuclear localization sequence (NLS) was fused to both N-terminus and C-terminus of rCRISPR/Cas9, and self-cleaving 2A peptide (P2A), and GFP were inserted between rCRISPR/Cas9 and C-terminal NLS sequence. For the gRNA cassettes in these vectors, the rice *U6* promoter and a custom designed gRNA (5′- AAG

AGCTCTGGTGCAAGAAGGGG-3′) targeting CDS region (700–720 bp) of *OsNAC14* were introduced into pSB11 vector through following procedures. To minimize the possibility of off-target effects potentially caused by CRISPR/Cas9 mediated mutagenesis, we performed computational analysis to select unique and specific sequence which can be used for gRNA target site on *OsNAC14* coding sequence using CRISPRdirect software (https://crispr.dbcls.jp/). Rice *U6* promoter and 5′-region of gRNA was amplified by PCR reactions (F: 5′-CCCAAGCTT AAGGAATCTTTAAACATACGA-3′, R: 5′-CTTCTTGCA CCAGAGCTCTTGCCACGGATCATCTGCA). 3′-region of gRNA was amplified with 20 base overlap with 5′region of gRNA by PCR reactions (F:5′-AAGAGCTCTGGTGCAAGA AGGTTTTAGAGCTAGAAATAGG-3′, R:5′- TGCTCTAGA AAAACAAAAAAGCACCGACTCGGTGC-3′). Two PCR products were mixed and used as template for crossover PCR using primers recognizing 5′-region of *U6* promoter and 3′-region of gRNA (F: 5′-CCCAAGCTTAAGGAATCTTTA AACATACGA-3′, R:5′- TGCTCTAGAAAAACAAAAAAG CACCGACTCGGTGC-3′). Final PCR products were digested with HindIII and XbaI, and inserted into pSB11 vector by ligation. The plasmid was introduced into rice (*Oryza sativa* cv. Dongjin) using Agrobacterium-mediated co-cultivation method. Primer sequences used in this study are listed in Table S2.

Drought Stress Treatment and Tolerance Evaluation

Transgenic and NT (non-transgenic) (*Oryza sativa* cv. Nakdong) seeds were germinated on Murashige and Skoog (MS) medium (Duchefa Biochemie) with 3% sucrose in the dark for 3 days at 28°C, and transferred into light conditions for 1 day. Thirty Seedlings from each transgenic and NT plants were transplanted in soil pot (4 × 4 × 6 cm, three plants per pot) and grown for 5 weeks in the greenhouse (16 h-light/8 h-dark cycle) at 30°C. Drought stress was imposed by sequentially withholding water for 3 days and re-watering for 5 days. Drought-induced symptoms were visualized by imaging tested plants at indicated time point using an NEX-5N camera (Sony), and soil moisture was measured at indicated time point using a SM 150 soil moisture sensor (Delta T Devices).

Transient chlorophyll *a* fluorescence and the performance index were measured using a HANDY PEA fluorimeter (Hansatech Instruments), as described previously (Jung et al., 2017). Two-week-old plants were transplanted in soil pot (15 × 15 × 14 cm) and grown for 5 weeks. Chlorophyll fluorescence and the performance index were measured from longest leaves of each plant after 1 h of dark adaptation to ensure sufficient opening of the reaction center. Measurement was performed at apex, middle, and base regions of leaves using the Handy-pea fluorimeter (Hansatech Instrument). Thirty readings per line were averaged using the HANDY-PEA software (version 1.31). Fv/Fm value and the performance index were calculated according to the equations of the JIP test (Redillas et al., 2011).

Evaluation of the Agronomic Traits of Rice Plants Grown in the Field

To Evaluate yield components of transgenic and non-transgenic (NT) plants under normal field conditions, three independent T4 homozygous lines of the $OsNAC14^{OX}$ plants and NT plants were planted in the rice paddy field at Kyungpook National University, Gunwi (36°06′48.0″N,128°38038.0″E), Korea (RDA-A-2011-005, 2016). Yield parameters were scored from 30 plants collected from three different plots for normal field conditions. To evaluate yield components of the plants under drought field conditions, plants were grown in semi-field conditions under rain-off shelters before drought treatment. Intermittent drought stress was applied twice by withholding water during panicle development stage. Drought treatment was monitored by measuring soil water content using Soil Moisture Sensor (AT Delta-T Device). After two rounds of drought treatment, the plants were irrigated until harvesting. Yield components were scored from 18 plants for each line for drought field conditions. The results were compared between transgenic and NT plants using ANOVA ($p < 0.05$ level) with Fisher's least significant difference for multiple comparisons.

RNA-Sequencing Analysis

Total RNA was extracted from rice leaves (2 weeks old, grown soil) using Trizol reagent (Invitrogen) and purified on-colum DNase treatment with RNeasy Mini Kit (Qiagen). The libraries were prepared using the TruSeq RNA sample Prep Kit (v2) (Macrogen). RNA-sequencing was repeated twice with samples from NT and *PGD1::OsNAC14* transgenic plants. Single-end sequences were obtained using IRGSP (v 1.0) and raw sequence reads were trimmed to remove adaptor sequences, and those with a quality lower than Q20 were removed using the Trimmomatic 0.32 software (Bolger et al., 2014). To map the reads to reference genome, all reads were assembled with annotated genes from the Rap-DB database [http://rapdb.dna.affrc.go.jp; IRGSP (v 1.0)] using TopHat software (https://ccb.jhu.edu/software/tophat/index.shtml). After mapping reads to a reference genome differentially expressed genes were analyzed and validated by more than two-fold change value and independent *T*-test (p-value < 0.05), then 554 transcripts were selected for further analysis. The data set can be found at from GEO database with series accession number GSE106150 for RNA-sequencing data (http://www.ncbi.nlm.nih.gov/geo/).

Real-Time PCR Analysis

Total RNA was extracted from $OsNAC14^{OX}$ transgenic (Line 11) and NT plants grown for 2 weeks in soil using Trizol reagent (Invitrogen) according to the manufacturer's instructions. To generate first-strand complementary DNA (cDNA), 1 μg of total RNA was reverse-transcribed using RevertAid M-MuLV Reverse Transcriptase (Thermo Scientific). Subsequent quantitative real time PCR (qRT-PCR) was performed with 2X Real-Time PCR smart mix (SRH72-M10h, SolGent) and EvaGreen (31000-B500, SolGent). The PCR reactions were performed by initial denaturation at 95°C for 15 min, followed by 40 cycles of 95°C for 20 s, 60°C for 20 s, and 72°C for 30 s, using Strategene Mx300p real-time PCR machine (Stratagene). *UBIQUITIN1*

(Os06g0681400) was used as internal control for normalization. Three biological replicates were analyzed for quantitative experiments. The primer information used for qRT-PCR gene expression is listed in Table S2.

Protoplast Isolation and Transient Gene Expression

Polyethylene Glycol (PEG)-mediated protoplast transformation system was used to transiently express *OsNAC14* and verify the correlation between *OsNAC14* and its target genes (Chen et al., 2006; Yoo et al., 2007; Zhang Y. et al., 2011). Rice seedlings (*Oryza sativa* cv. Ilmi) were grown in the dark for 10 d and transferred to the light conditions for 8∼10 h. Leaf sheaths of 100 rice seedlings were cut into 0.5 mm pieces using a sharp blade on a glass. The pieces were transferred into 0.6 M mannitol solution and incubated for 30 min at room temperature in the dark conditions. After removal of mannitol solution, the pieces were soaked in enzyme solution [1.5% Cellulase R-10 (Yakult, Japan), 0.75% Macerozyme R-10 (Yakult, Japan), 0.5 M mannitol, 10 mM MES (pH 5.7), 0.1% BSA, 10 mM $CaCl_2$, and 5 mM β-mercaptoethanol] for cell wall degradation. Vacuum infiltration was applied to the enzyme solution for 15 min using desiccator and the digestion was carried out in the dark at 28°C for 4 h with gentle shaking. The enzyme solution was filtered twice through 70 μm and 40 μm nylon meshes (Falcon, USA). The flow-through was centrifuged at 300 g and the protoplast pellet was resuspended in W5 solution [154 mM NaCl, 125 mM $CaCl_2$, 5 mM KCl, 2 mM MES (pH 5.7)]. The protoplast concentration was measured under the microscope using a hemocytometer (Marienfeld) and adjusted to 7.0×10^7 protoplasts/mL. Fifty microliters of protoplasts (2.5×10^6 cells) was mixed with 15 μL of plasmids and 130 μL of PEG solution. The mixture was incubated for 15 min at 28°C in the dark. After incubation, 1 mL of W5 solution was added into mixture, and centrifuged at 300 g for 2 min to collect protoplasts. The protoplasts were resuspended in Incubation solution for 10 hr. Protoplasts were harvested by centrifugation at 300 g for 2 min and used for RNA extraction. Relative expression levels of genes in protoplasts were analyzed using qRT-PCR analysis. Detailed conditions for RNA extraction and qRT-PCR analysis are described in "Real-time PCR analysis" section.

Subcellular Localization of *OsNAC14*

The coding region of *OsNAC14* amplified from the cDNA was cloned into the pHBT vector carrying GFP-myc using the In-fusion system (Clonetech). The final construct (*35S::OsNAC14-GFP*) and the control vectors (*35S::GFP*) were transfected into protoplasts (*Oryza sativa* cv. Ilmi) using PEG-mediated protoplast transformation system. *35S::NF-YA7-GFP* was used as control for nuclear localization (Lee et al., 2015). GFP and mCherry signals were observed 12 h after transfection using SP8 STED confocal fluorescence microscope (Leica).

Chromatin Immunoprecipitation (ChIP) Assay

ChIP assay was performed according to Bowler et al. (2004) with minor modifications (Bowler et al., 2004). The transfected protoplasts ($5–7 \times 10^7$ protoplasts/one tube) were cross-linked with 1% formaldehyde by vacuum infiltration for 15 min, and the cross-linking reaction was stopped by the addition of 2 M glycine to a final concentration of 125 mM. The protoplasts pellet was resuspended in 10 ml of pre-chilled extraction buffer 1 [0.4 M Sucrose, 10 mM Tris-HCl (pH 8.0), 5 mM β-mercaptoethanol, protease inhibitors] for 30 min in the ice with gentle agitation. After centrifugation for 20 min at 2,880 g at 4°C, the pellet was resuspended in extraction buffer 2 [0.25 M Sucrose, 10 mM Tris-HCl (pH 8.0), 10 mM $MgCl_2$, 1% Triton X-100, 5 mM β-mercaptoethanol, protease inhibitors]. After subsequent centrifugation for 10 min at 12,000 g at 4°C, the pellet was resuspended in extraction buffer 3 [1.7 M Sucrose, 10 mM Tris-HCl (pH 8.0), 0.15% Triton X-100, 2 mM $MgCl_2$, 5 mM β-mercaptoethanol, 0.1 mM PMSF, protease inhibitors] and loaded on the extraction buffer 3 (300 ul). After centrifugation for 60 min at 16,000 g at 4°C, the chromatin pellet was resuspended in nuclei lysis buffer [50 mM Tris-HCl (pH 8.0), 10 mM EDTA, protease inhibitors]. To shear DNA to ∼100–200 bps DNA fragments, the chromatin solution was sonicated in ice using Bioruptor (Diagenode) for 20 min with 30 s ON and 30 s OFF cycle. The sonicated chromatin extract was centrifuged for 5 min at 12,000 g at 4°C, and the supernatant was diluted 10 times with ChIP dilution buffer [1.1% Triton X-100, 1.2 mM EDTA, 16.7 mM Tris-HCl (pH 8.0), 167 mM NaCl, protease inhibitors]. Diluted chromatin extract was incubated with anti-myc polyclonal antibody (sc789x, Santa Cruz) or without antibody overnight at 4°C, then, further incubated with protein A agarose beads with gentle agitation for 2 h. The beads were washed three times with low salt, high salt, LiCl, and TE wash buffers. The pellet was resuspended in elution buffer [1% SDS, 0.1 M $NaHCO_3$] and incubated at 65°C for 15 min. The resultant eluted DNAs were purified using the QIAquick PCR purification kit (Qiagen). The purified DNA was used in quantitative real-time PCR reactions using Mx3000P Real-Time PCR system (Agilent Technologies). To determine the positions of NAC binding motif on *OsRAD51A1* and *Piz-t* promoter region, the promoters were analyzed using A Database of Plant Cis-acting Regulatory DNA Elements (https://sogo.dna.affrc.go.jp/cgi-bin/sogo.cgi?lang=en&pj=640&action=page&page=newplace). Five sets of primers were designed based on the positions of NAC binding motif on *OsRAD51A1* and *Piz-t* promoter for ChIP-PCR analysis. The relative enrichment was normalized against the 1% of total input DNA.

RESULTS

OsNAC14 Is a Drought-Inducible Transcription Factor

Phylogenetic analysis revealed that OsNAC14 belongs to the ONACII family of group A. Members of this group are separated from the well-characterized stress-associated NAC (SNAC) family in terms of its diversity in NAC domain structure (Figure S1A) (Nuruzzaman et al., 2010). In group A, 29 members are responsive to water deficit conditions in leaves (Chung et al., 2016) suggesting that ONACII genes, including *OsNAC14*, may

be another component of the molecular pathway to regulate drought responses of plants.

To investigate the functions of *OsNAC14* in drought stress response, we shortlisted a number of genes from our previously reported microarray data on leaves of rice exposed to different stresses such as drought, high salinity, abscisic acid (ABA), and low temperature (Oh et al., 2009). From these, we found that *OsNAC14* was highly induced by drought and high-salinity treatments (Figure S1B). The drought-inducible expression pattern of *OsNAC14* was further confirmed from an independent RNA-sequencing experiment performed by Chung et al. (2016) (Figure S1C). Similarly, *OsNAC14* was up-regulated over a time course in response to drought stress (Figure S1C). *OsNAC*s belonging to SNAC subfamily (*OsNAC5*, *OsNAC6*, *OsNAC9,* and *OsNAC10*), previously reported as drought-inducible *OsNAC* transcription factors, were also up-regulated in response to drought stress (Figure S1C). Transcripts of *OsNAC9* and *OsNAC14* were increased later than that of *OsNAC5* and *OsNAC6* in response to drought stress (Figure S1C). The responses of *OsNAC14* transcription in stress conditions were further verified through quantitative real-time polymerase chain reaction (qRT-PCR) using total RNA from leaves and roots collected from 2-week-old rice seedlings (*Oryza sativa* L. cv. Ilmi) exposed to drought, high salt, abscisic acid (ABA), and low temperature (**Figure 1A** and Figure S2). *OsNAC14* expression was strongly induced within 2 h of exposure to drought, high salt, ABA, and low temperature stresses in leaves. The induction of *OsNAC14* expression in stress conditions were predominant in leaves (**Figure 1A**) than in root tissues (Figure S2).

To further characterize the function of OsNAC14, we performed a subcellular localization analysis to confirm its nuclear localization due to the nuclear localization sequence found at the C-terminal side of its sequence (Kosugi et al., 2009) (Figure S3). We generated a construct to express translationally fused OsNAC14 and GFP fluorescent protein (GFP) (OsNAC14-GFP) driven by the CaMV 35S promoter and transiently expressed in rice protoplasts together with OsNF-YA7-mcherry as positive control for nuclear localization (Lee et al., 2015) (**Figure 1B**). The fluorescence signals from both GFP and mCherry were co-localized in the nuclear region confirming that OsNAC14 is a nuclear-localized protein (**Figure 1C**). Taken together, these results suggest that OsNAC14 is responsive to drought stress and is localized in the nucleus of the cell.

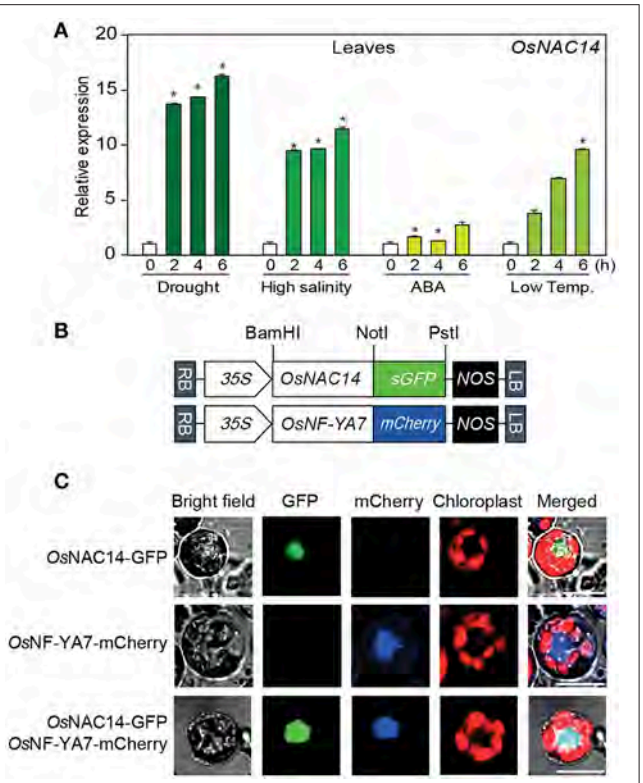

FIGURE 1 | Characterization of *OsNAC14*. **(A)** The relative expression patterns of *OsNAC14* in response to four different abiotic stresses. Two-week-old rice seedlings (*Oryza sativa*. L. Japonica cv. Ilmi) were exposed to air-drying (drought), 400 mM NaCl (high salinity), 100 μM abscisic acid (ABA), and 4°C (low-temperature). Leaves of rice plants were harvested at indicated time point after treatment. *OsUBIQUITIN1* (*OsUbi1*) was used as internal control for normalization. Data represent mean value + standard deviation (*SD*) ($n = 3$). Significant differences from non-treated control are indicated by asterisks (one-tailed Student's *t*-test, $^*P < 0.05$). **(B,C)** Subcellular localization of OsNAC14 in rice protoplast. **(B)** Schematic diagram of OsNAC14-GFP and OsNF-YA7-mCherry expression constructs **(C)** protoplasts were transiently co-transfected with OsNAC14-GFP and OsNF-YA7-mCherry expression constructs. Fluorescence was observed in protoplasts 12 h after transfection using a confocal microscope. Scale Bar = 10 μm.

Overexpression of *OsNAC14* Improves Drought Tolerance at the Vegetative Stage

To investigate the physiological functions of *OsNAC14* in plants in response to drought, transgenic rice plants overexpressing *OsNAC14* were generated by transforming *PGD1*::*OsNAC14* into *Nakdong* cultivar (designated as $OsNAC14^{OX}$). Thirty independent lines were produced and to avoid the effects of somaclonal variations, plants that grew normally without stunting were screened out. Based on the expression levels of *OsNAC14* (**Figures 2A,B**) we finally selected three independent homozygous lines (#8, #11, and #30).

To compare the performance of plants under drought conditions, the selected $OsNAC14^{OX}$ and non-transgenic plants (NT, Nakdong) were grown in a greenhouse for 5 weeks and exposed to drought conditions by withholding water for 3 days and monitored drought-induced visual symptoms (**Figures 2C–E**). Soil moisture contents showed a consistent rate of decrease among different pots indicating that stress treatments were uniformly applied to the plants (**Figure 2C**). Drought-associated symptoms, such as leaf rolling, wilting, and loss of chlorophyll appeared earlier in NT plants than in $OsNAC14^{OX}$ plants during drought treatment (**Figure 2D**). Transgenic plants also showed faster recovery compared to NT after being relieved from drought stress through re-watering (**Figures 2D,E**). $OsNAC14^{OX}$ plants scored 5 days after re-watering showed 83 to 92% survival rate whereas NT plants only showed 12% (**Figure 2E**). To further verify the stress tolerant phenotype of the

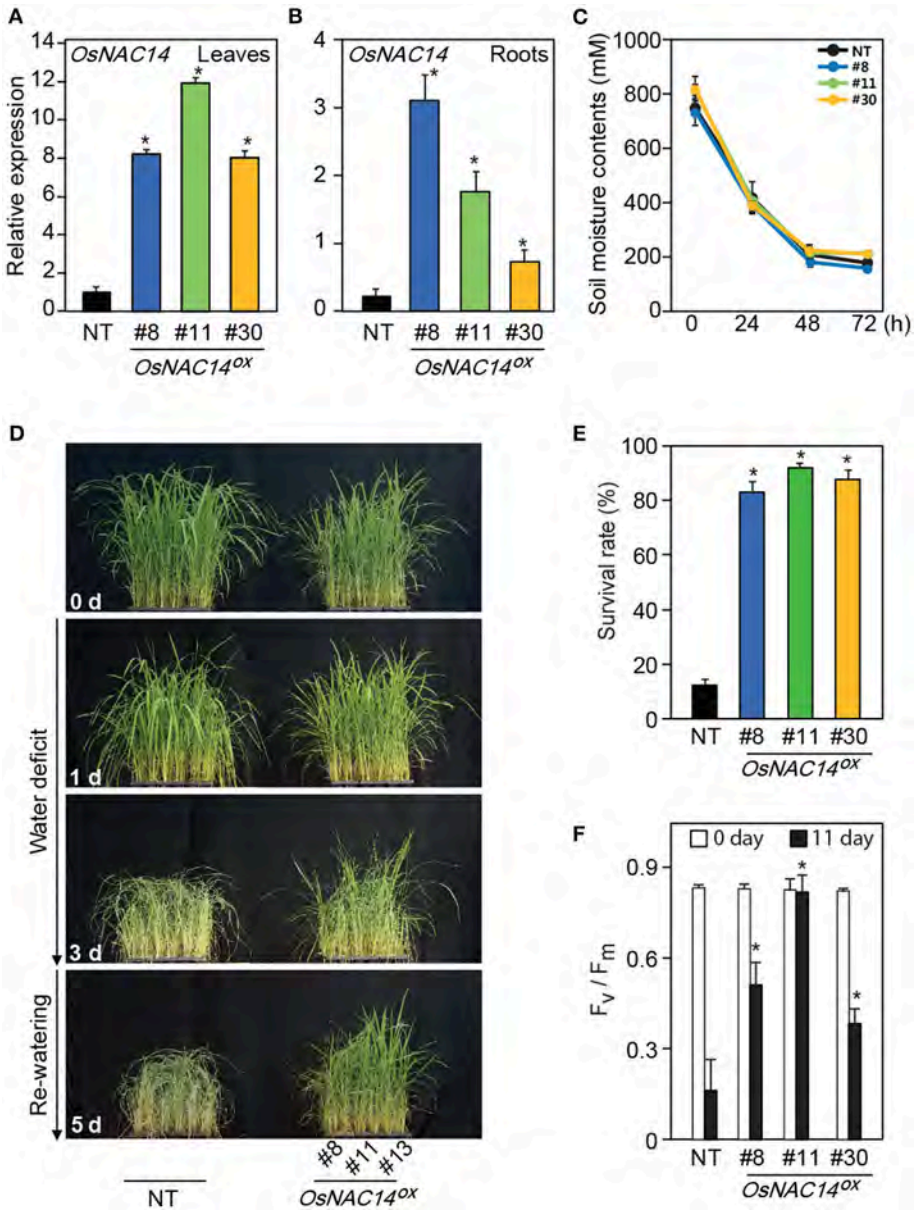

FIGURE 2 | *OsNAC14* overexpression in rice enhances drought resistance**. (A,B)** Relative expression levels of *OsNAC14* in non-transgenic (NT) and three independent T4 homozygous lines of *PGD1::OsNAC14* (*OsNAC14*^{OX}) plants. Total RNAs were extracted from leaves **(A)** and roots **(B)** of two-week-old rice seedlings. *OsUbi1* was used as internal control for normalization. Data represent mean value + *SD* ($n = 3$). **(C)** Measurement of soil moisture contents (mV). Data represent mean value ± *SD* of 30 measurements performed at different locations of soil. **(D)** The phenotype of transgenic rice plants during drought stress. Five-week-old three independent T4 homozygous lines of *OsNAC14*^{OX} plants and NT were exposed to drought stress for 3 days, followed by re-watering. Numbers on the image indicate duration of drought treatment and re-watering. **(E)** The survival rate of transgenic plants 5 days after re-watering. Data represent mean value + SD ($n = 30$). **(F)** Chlorophyll fluorescence (Fv/Fm) contents of plants under drought condition. Five-week-old three independent T4 homozygous lines of *OsNAC14*^{OX} and NT plants were exposed to drought stress for 11 days. Chlorophyll fluorescence was measured in the dark at indicated time point using a Pulse Amplitude Modulation (PAM) fluorometer. Data represent mean value + *SD* ($n = 20$). Significant differences from NT control are indicated by asterisks (one-tailed Student's *t*-test, $^*P < 0.05$).

plants, Fv/Fm values, an indicator of the photochemical efficiency of photosystem II, were measured in plants grown in bigger pots and exposed to drought for 11 days (**Figure 2F** and Figure S4). Similar gradual decrease in soil moisture contents between pots were observed showing uniform stress treatment (Figures S4A,B). The Fv/Fm values in NT plants showed a more rapid decrease than in *OsNAC14*^{OX} plants during drought treatments (**Figure 2F** and Figure S4C). Taken together, these results suggest that overexpression of *OsNAC14* enhances drought tolerance of plants when exposed to drought.

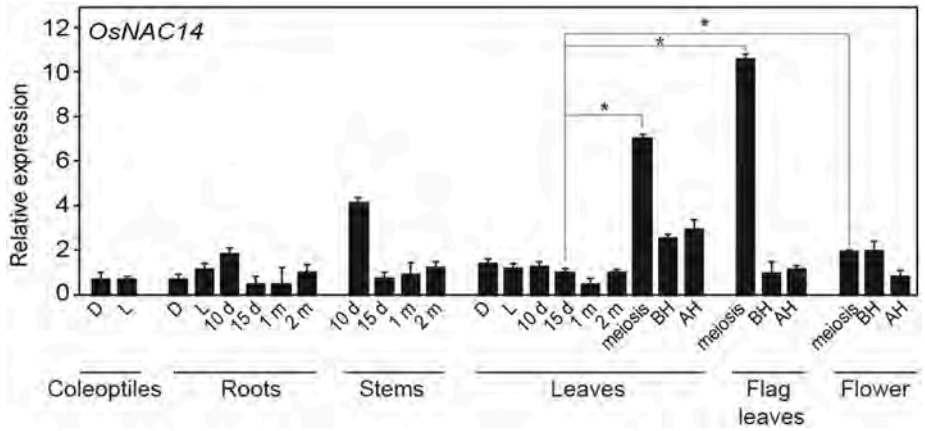

FIGURE 3 | *OsNAC14* expression at various developmental stages. qRT-PCR analysis of *OsNAC14* expression in rice tissues at different developmental stages (*Oryza sativa*. L. Japonica cv. Ilmi). d, day; D, Dark; BH, Before heading; AH, After heading. *OsUbi1* was used as internal control for normalization. Data represent mean value + standard deviation (*SD*) ($n = 3$). Significant differences from 15 days old leaves tissue are indicated by asterisks (one-tailed Student's *t*-test, $^*P < 0.05$).

OsNAC14 Is Significantly Expressed During Meiosis

Since NAC transcription factors are known to regulate various developmental processes in plants (Souer et al., 1996; Aida et al., 1997) we examined the expression levels of *OsNAC14* transcripts in various rice tissues at different developmental stages starting from coleoptile to flower formation (**Figure 3**). qRT-PCR analysis showed that *OsNAC14* transcripts were detected from all the tested tissues. The highest expression of *OsNAC14* was detected during meiosis stage in both leaves and flag leaves. These suggest the OsNAC14 might be involved in processes occurring during the meiosis stage.

Effect of *OsNAC14* Overexpression on Grain Yield Under Field Drought Conditions

Since grain production is seriously affected by drought stresses at the reproductive stage of growth, we evaluated yield components of $OsNAC14^{OX}$ plants in year 2016 in a rice paddy field. Three independent T_4 homozygous $OsNAC14^{OX}$ transgenic and NT plants were planted in a paddy field and grown to maturity. Under normal conditions, $OsNAC14^{OX}$ plants exhibited reductions in panicle length (−0.65 to −5.36%) and number of total grains (−2.24 to −17.93%) (**Table 1**). In the drought conditions, however, the overexpression of *OsNAC14* resulted in higher filling rate (12.25 to 36.64%) and number of panicles (5.88 to 18.62%) though there was a decrease in panicle length (−2.48 to −14.89%) and number of total grain (−2.24 to −27.34%) compared to NT (**Table 1**).

Identification of Genes Regulated by *OsNAC14*

To understand the transcriptional network regulated by the *OsNAC14* during drought, RNA-sequencing analysis was performed on 2-week-old $OsNAC14^{OX}$ plant (T4 generation, line 11) grown under normal growth conditions (**Table 2**). From the 37,972 differentially expressed genes (DEG) we then selected those that showed at least two-fold change (*p*-value < 0.05). The analysis revealed 122 up-regulated and 151 down-regulated genes following the overexpression of *OsNAC14* relative to NT (Table S1). These genes were then processed for Gene Ontology analysis using PANTHER Classification System (http://pantherdb.org) (Figure S5). Results revealed that majority of the genes were assigned to catalytic activity (62.7%) under the molecular function class and to metabolic process (32.0%) and cellular process (29.0%) pathway under the biological class. Among these, 23 up-regulated genes were further selected through their gene annotation and reported studies on stress response (**Table 2**). These up-regulated genes were associated with stress response, DNA damage repair, defense response, signal transduction, and metabolic process (**Table 2**). The expression patterns of *OsRAD51A1* (Os11g0615800), *Piz-t* (Os06g0286700), *Disease Resistance protein* (*DR*) (Os09g0357400), *20S PROTEASOME ALPHA SUBUNIT E1* (*OsPAE1*) (Os11g0615700), and *OsFbox341* (Os07g0158900) genes were analyzed in 2-week-old $OsNAC14^{OX}$ plants grown in normal conditions through qRT-PCR (**Figure 4**). Results showed that *OsNAC14* overexpression induces the expression of *OsRAD51A1*, *Piz-t*, *DR*, *OsPAE1,* and *OsFbox341*. To further confirm the role of *OsNAC14* in the regulation of the five induced genes, we performed another qRT-PCR on *OsNAC14* deletion mutant produced through CRISPR/Cas9 system. The mutant lacked seven nucleotides (712–718 bp) resulting in frame shift on its C-terminal region containing the NLS sequences (Figures S3, S6). Results showed that *OsNAC14* transcript was significantly reduced in *osnac14* relative to NT plants (**Figure 4**). In addition, expression of all the five genes induced by *OsNAC14* overexpression were significantly reduced in *osnac14* mutants confirming that *OsNAC14* is involved in the regulation of these genes.

TABLE 1 | Agronomic traits of *OsNAC14*^{OX} transgenic plants grown in the field.

Normal		Panicle length (cm)	No. of panicle (/hill)	No of total grain (/hill)	Filling rate (%)	1000 grain weight (g)
NT	Average	20.47	17.10	1688.19	87.62	24.60
OsNAC14^{OX} #8	Average	19.37	16.54	1385.44	87.12	24.24
	%Δ	−5.36	−3.28	−17.93	−0.57	−1.50
	p-value	0.00**	0.65	0.15	0.79	0.41
OsNAC14^{OX} #11	Average	20.33	14.17	1650.44	86.96	25.41
	%Δ	−0.65	−17.14	−2.24	−0.75	3.28
	p-value	0.74	0.01*	0.93	0.73	0.04*
OsNAC14^{OX} #30	Average	20.00	18.13	1468.33	90.55	23.85
	%Δ	−2.28	6.02	−13.02	3.34	−3.08
	p-value	0.25	0.38	0.31	0.13	0.35
Drought		**Panicle length (cm)**	**No. of panicle (/hill)**	**No of total grain (/hill)**	**Filling rate (%)**	**1000 seed weight**
NT	Average	17.63	19.13	1751.44	33.62	18.72
OsNAC14^{OX} #8	Average	15.00	21.63	1272.56	37.74	19.17
	%Δ	−14.89	13.07	−27.34	12.25	2.41
	p-value	0.00**	0.14	0.00**	0.24	0.02*
OsNAC14^{OX} #11	Average	17.19	20.25	1601.69	45.87	19.23
	%Δ	−2.48	5.88	−2.24	36.44	2.73
	p-value	0.49	0.51	0.93	0.03*	0.05
OsNAC14^{OX} #30	Average	16.5	22.69	1468.33	43.81	18.52
	%Δ	−6.38	18.62	−13.02	30.31	−1.07
	p-value	0.08	0.04*	0.13	0.08	0.01

Panicle length, number of panicle, number of grain, filling rate, and 1000 seed weight of three independent lines of OsNAC14^{OX} *transgenic rice plants. Percentage differences (%Δ) between the values for the OsNAC14*^{OX} *transgenic rice plants and NT controls are listed. An asterisk indicates a significant difference (*P < 0.05 and **P < 0.01).*

Identification of Genes Involved in *OsNAC14* Mediated Drought Responses

Next, we examined the expression pattern of five genes up-regulated by *OsNAC14* in drought conditions in order to identify downstream transcriptional network of *OsNAC14* involved in drought tolerance. qRT-PCR was performed using total RNA extracted from NT and *OsNAC14*^{OX} plants grown under normal and drought conditions. To confirm that drought treatment was properly applied to plants, expression of two drought-responsive marker genes, *Dehydration Stress-inducible Protein 1* (*OsDip1*, *Os02g0669100*) and *Small subunit of Rubisco* (*OsRbcS*, *Os12g0274700*), which show opposite expression patterns in response to drought stress (Jang et al., 2003) was examined. *OsDIP1* expression was induced while *OsRbcS* expression was reduced after 1 day of drought treatments validating successful induction of transcriptional reprograming turned on by drought stress (**Figure 5**). The induction of *OsDIP1* and reduction of *OsRbcS* in *OsNAC14*^{OX} plants were lower than NT plants suggesting that *OsNAC14*^{OX} plants are less sensitive to drought. In addition, the level of *OsNAC14* transcript induction due to drought treatment in NT was comparable with those of *PGD1* promoter under normal condition. Therefore, we aim to identify genes induced in both NT and *OsNAC14*^{OX} plants by drought treatment as downstream component of *OsNAC14* mediated drought tolerance pathway.

Results also showed that all five candidate genes showed higher expression levels in *OsNAC14*^{OX} than NT plants under both normal and drought conditions (**Figure 5**). However, after prolonged drought exposure (after 24 h) *Piz-t*, *OsFbox341,* and *DR* declined while *OsPAE1* expression was less affected by drought treatment. *OsRAD51A1*, on the other hand, was induced by both drought treatment and *OsNAC14* overexpression. Moreover, drought treatment and *OsNAC14* overexpression showed additive effects on expression of *OsRAD51A1* (**Figure 5**) indicating that the expression of *OsRAD51A1* is dependent on the expression of *OsNAC14.* Collectively, these results further suggest that *OsRAD51A1* is a possible direct downstream component of *OsNAC14*-mediated drought tolerance pathway.

OsNAC14 Directly Regulates *OsRAD51A1*, a Key Component in DNA Repair

To confirm whether *OsRAD51A1* is a direct target of OsNAC14, we performed chromatin immunoprecipitation (ChIP) coupled with qRT-PCR analysis on rice protoplast system. Protoplasts provide a good platform to perform functional characterization of genes and isolation of protein-DNA complex in plants (Zhang Y. et al., 2011; Lee J. H. et al., 2017). We first performed qRT-PCR on total RNA isolated from protoplasts of both NT and *OsNAC14*^{OX} plants (**Figure 6A**). Similar with stable transgenic plants, all five genes were up-regulated in protoplasts of *OsNAC14*^{OX} plants suggesting that the isolated protoplasts maintained transcriptional network of intact plants similar to what was observed by Lee J. H. et al. (2017) (**Figure 6A**). Next, we introduced *35S::OsNAC14-MYC* or *35S::GFP-MYC* effector

TABLE 2 | Up-regulated genes in *OsNAC14*^{OX} transgenic rice in comparison with non-transgenic plants.

Gene name	Loc_No* (IRGSP)	*OsNAC14*^{OX}/NT†	*p*-value**
OsNAC14	Os01g0675800	4.0	0.02
STRESS RESPONSE			
OsERF101	Os04g0398000	2.1	0.043
OsCIPK33	Os11g0134300	8.2	0.039
OsWRKY50	Os11g0117600	4.0	0.025
OsLEA14/WSI18	Os01g0705200	3.2	0.039
HSR201	Os12g0458100	2.3	0.005
OsRLCK66	Os02g0212900	2.3	0.033
DNA REPAIR			
OsRAD51A1	Os11g0615800	2.0	0.001
OsMSH4	Os07g0486000	10.4	0.008
DEFENSE RESPONSE			
Piz-t	Os06g0286700	4.1	0.027
Disease resistance protein	Os09g0357400	2.5	0.018
RPP13-like protein 3	Os11g0590700	3.6	0.043
Xa39	Os11g0588600	33.7	0.007
OsPAE1	Os11g0615700	16.0	0.011
OsPDR20	Os09g0332700	2.9	0.009
Oscyp71Z2	Os07g0217600	2.2	0.008
SIGNAL TRANSDUCTION			
OsFbox341	Os07g0158900	11.1	0.003
OsiWAK1	Os11g0691100	33.6	0.044
OsSTA127	Os04g0521600	3.9	0.001
OsRLCK66	Os02g0212900	2.3	0.033
OsCCD8a	Os01g0566500	2.0	0.020
METABOLIC PROCESS			
OsOSC11	Os11g0562100	30.7	0.006
OsTPS10	Os03g0348200	2.2	0.031
ILL8	Os07g0249800	2.1	0.029
OsAGP29	Os01g0607100	2.0	0.044

**Sequence identification numbers for the full-length cDNA sequences of the corresponding genes.*

† The mean of duplicate biological samples.

***P values were analyzed by one-way ANOVA (P < 0.01). Genes discussed in the text are in boldface. These microarray data sets can be found at http://www.ncbi.nlm.nih.gov/geo/ (Gene Expression Omnibus, accession number GSE106150).*

plasmids into protoplasts isolated from NT plants to verify that the transient expression of *OsNAC14* can induce similar response that was shown in stable *OsNAC14*^{OX} plants. As a result, *Piz-t* and *OsRAD51A1* were significantly induced in protoplasts after being transfected with *35S::OsNAC14-MYC* (**Figure 6A**). However, expression levels of *OsFbox341*, *DR,* and *OsPAE1* were not significantly increased by transient expression of *OsNAC14*. Among the five tested genes, *Piz-t* and *OsRAD51A1* were highly induced by transient expression of *PGD1::OsNAC14* compared to stable transformation. This could be due to a higher expression of *OsNAC14* in transient system but also indicates that expression of these two genes were tightly correlated with *OsNAC14* transcript level (**Figure 6A**). We therefore hypothesized that in addition to *OsRAD51A1*, *Piz-t* could also be a putative direct target of OsNAC14. To confirm this hypothesis, we performed chromatin-immunoprecipitation (ChIP) assay using transient protoplast system. Rice protoplasts transfected with *35S::OsNAC14-myc* were subjected for ChIP assay using anti-myc antibody. The *35S::GFP-myc* vector was independently transfected into rice protoplast as control. Enrichment of OsNAC14 on promoter regions was analyzed through ChIP-PCR analysis using genomic DNA isolated by ChIP assay (**Figure 6B**). Results showed very high enrichment on the promoter of *OsRAD51A1* but low in *Piz-t* confirming that OsNAC14 can strongly bind to the promoter of *OsRAD51A1* thereby regulating its expression (**Figure 6B**). Previous report has defined the 4 bps core sequence of the NAC binding motif as CACG (Olsen et al., 2005) which we found clustered in the promoter of *OsRAD51A1* while it was segregated in *Piz-t* promoter.

DISCUSSION

Here, we demonstrated that the rice *OsNAC14* transcription factor, a member of ONACII subgroup, is a regulator of drought tolerance pathway in rice. *OsNAC14* was induced by drought, high salinity, ABA and low temperature (**Figure 1A** and Figures S1B,C). Expression levels of *OsNAC14* are similar in roots and other aerial parts of plants under normal growth conditions (**Figure 3**); however, induced expression of *OsNAC14* by abiotic stresses was more predominant in leaves than in roots (**Figure 1A** and Figure S2). Other previously reported NACs belonging to the SNAC subgroup showed robust expression patterns in roots than leaves in response to abiotic stress (Redillas et al., 2012; Jeong et al., 2013; Lee D. K. et al., 2017). Thus, OsNAC14, unlike SNACs, acts as stress-induced transcription factor mainly in aerial parts of plants.

OsNAC14 overexpression induced drought tolerance in plants both at the vegetative and the reproductive stages of growth (**Figure 2**, Figure S4 and **Table 1**). We observed that overexpression of *OsNAC14* also affected the reproductive growth of plants such as the panicle length and number of total grains under normal growth conditions (**Table 1**). It is possible that constitutive overexpression of *OsNAC14* may have perturbed the reproductive development through alteration of its downstream gene expression. Introducing resistance (R) gene (e.g., *RPM1* in Arabidopsis and *Pi-ta* in rice) reported to cause yield penalties in plants due to a cost of resistance (Tian et al., 2003; Wang et al., 2015). A group of R genes up-regulated by *OsNAC14* overexpression including *Piz-t* (Os06g0286700) and *RPP13-like protein 3* (Os11g059700) similarly might have affected reproductive growth of *OsNAC14*^{OX} plants. Nevertheless, overexpression of *OsNAC14* can confer drought tolerance at the reproductive stage as evidenced by the higher filling rate over NT controls upon stress treatments (**Table 1**).

The RNA-seq analysis identified 122 up-regulated downstream genes in *OsNAC14*^{OX} plants (Table S1). The downstream genes could be divided into four groups: stress-inducible, defense related, DNA repair, and strigolactone biosynthesis genes. The stress-inducible genes include *LATE EMBRYOGENESIS ABUNDANT PROTEIN14/Water stress*

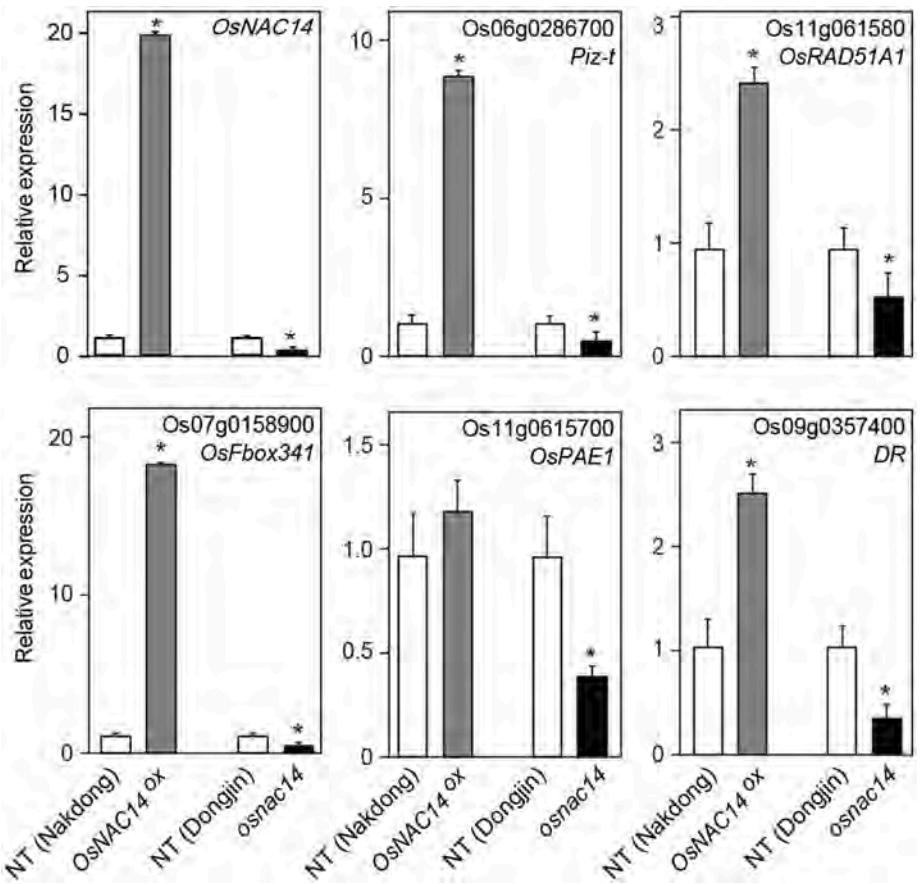

FIGURE 4 | Expression of differentially expressed genes (DEGs) isolated from RNA-sequencing data. qRT-PCR analysis of DEGs in NT, *OsNAC14*^{OX}, and *osnac14* mutant plants. *OsUbi1* was used as internal control for normalization. Data represent mean value + standard deviation (*SD*) ($n = 3$). Significant differences from NT control are indicated by asterisks (one-tailed Student's *t*-test, $^*P < 0.05$).

induced 18 (*LEA14/Wsi18*) which has been reported to improve drought tolerance of rice by increasing of proline and soluble sugar content and cell membrane stability (Kaur et al., 2017). Thus, the up-regulation of *OsLEA14/Wsi18* by *OsNAC14* overexpression contributed to enhanced drought tolerance of the plants. Defense relate proteins are also closely correlated with drought tolerance in plants. It has been reported that activation of plants defense against pathogens by expressing pathogen protein elicitors or R genes induces drought tolerance (Chini et al., 2004; Peng et al., 2015; Ma et al., 2017; Wang et al., 2017). Expression of *Magnaporthe oryzae* protein elicitors, *Hypersensitive response-inducing protein 1* and *2* (*MoHrip1* and *2*), can confer drought tolerance in rice together with enhanced blast resistance (Peng et al., 2015; Wang et al., 2017). The *NUCLEOTIDE BINDING SEQUENCE- LEUCINE-RICH REPEAT* (NBS-LRR) type *ACTIVATED DISEASE RESISTANCE* (*ADR1*) and grapevine (*Vitis amurensis*) *VaRGA1* also convey significant drought tolerance and disease resistance in plants (Chini et al., 2004). It remains elusive how activation of defense responses induces drought tolerance. Overexpression of *MoHrip1* and *2* up-regulates ABA biosynthetic (*OsNCED2, OsNCED3,* and *OsZEP1*) and signaling (*OsbZIP23*) genes. Moreover, exogenous application of harpin or overexpression of an *hrf1* gene in rice promotes stomatal closure through ABA signaling (Dong et al., 2005; Zhang L. et al., 2011). Overexpression of *OsNAC14* up-regulated the expression of *NBS-LRR* type genes including *Piz-t*, *RPP13-like protein* and *Disease resistance protein* (**Figure 4** and **Table 1**) that contributes to drought tolerance of *OsNAC14*^{OX} plants. Similarly, other *OsNAC*s involved in drought tolerance also induce expression of defense related genes. The overexpression of *OsNAC6* and *10* induces expression of *LRR* and *PATHOGEN-RELATED PROTEIN* (*PR*) genes, respectively (Nakashima et al., 2007; Jeong et al., 2010). The irreversible DNA damages generated by environmental stresses adversely affect plant growth and development. Thus, proper induction of DNA repair system in response to DNA damage facilitates plants to adapt to stress conditions (Roy, 2014). Drought stress causes DNA damage in plants (Mittler, 2002; Miller et al., 2010; Yao et al., 2013). Accumulation of ROS and oxidative damage generated by drought stress is regarded as inducer of DNA damage, such as double strand break (DSB), base deletion, and base

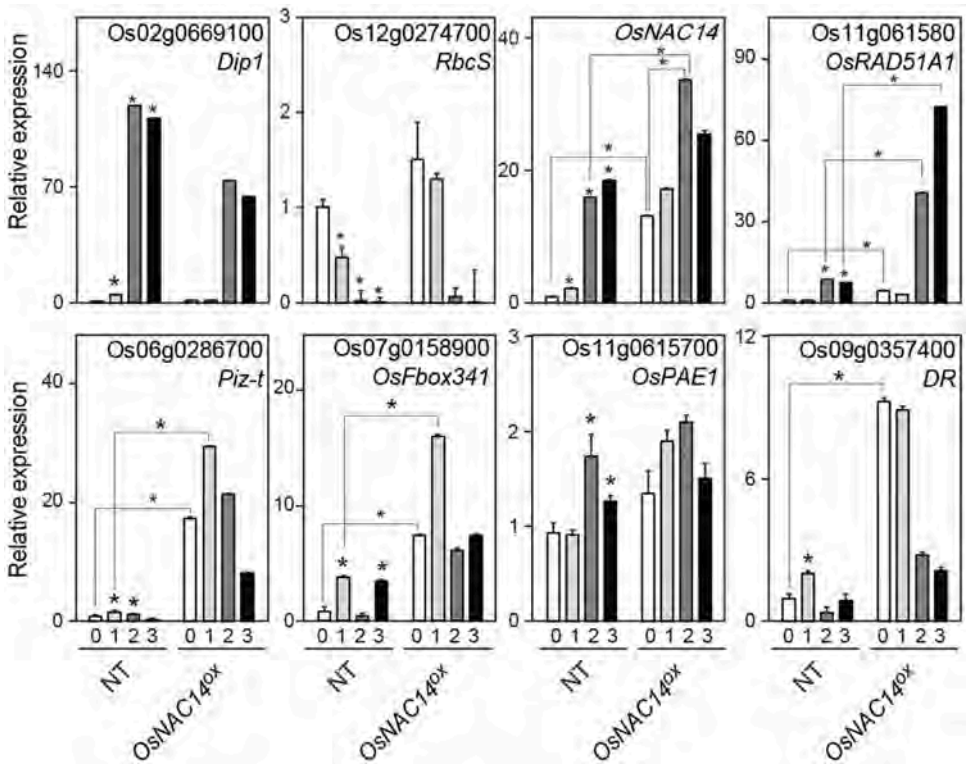

FIGURE 5 | The expression pattern of *OsNAC14* dependent genes in drought conditions. Total RNAs were extracted from 4-week-old rice NT and *OsNAC14*^{OX} plants exposed to drought conditions for indicated period. Relative expression of tested genes was determined by qRT-PCR analysis. Expression of two drought stress marker genes, *Dehydration stress-inducible protein 1* (*Dip1*) and *Small subunit of Rubisco* (*RbcS*), was analyzed to monitor progress of drought treatment. *OsUbi1* was used as internal control for normalization. Data represent mean value + standard deviation (*SD*) ($n = 3$). Significant differences from non-treated control or between samples are indicated by asterisks (one-tailed Student's *t*-test, $^*P < 0.05$).

modification (Tuteja et al., 2001; Mittler, 2002; Roldan-Arjona and Ariza, 2009; Miller et al., 2010). These lead to increased homologous recombination and mutation frequency in plants under drought conditions (Wang and Zhang, 2001; Yao and Kovalchuk, 2011; Yao et al., 2013). In this study, we found that expression of *OsRAD51A1*, a rice homolog of yeast *RAD51*, was not only highly induced under drought conditions (**Figure 5**) but also its expression was up-regulated by *OsNAC14*. *OsRAD51A1* expression was induced by both stable and transient overexpression of *OsNAC14* (**Figures 5**, **6**). Moreover, expression level of *OsRAD51A1* was reduced in *osnac14* mutants (**Figure 4**). Our ChIP-PCR analysis revealed that OsNAC14 was bound to *OsRAD51A1* promoter containing NAC binding elements (**Figure 6**). Taken together, OsNAC14 binds to *OsRAD51A1* promoter and activates its expression. *RAD51* is indispensable for successful homologous recombination to repair DSBs (Shinohara et al., 1992; Li et al., 2004, 2007; Rajanikant et al., 2008) and up-regulation of *OsRAD51* increases DNA repair efficiency and alleviates cell death, thereby conferring tolerance under salinity and genotoxic stress conditions in rice (Tripathi et al., 2016). Thus, regulation of *OsRAD51A1* expression offers another molecular mechanism for drought tolerance. Collectively, *OsNAC14*^{OX} plants activate DNA repair system via regulation of *OsRAD51A1*, which may alleviate drought-mediated DNA damage (**Figure 6**). Biosynthesis of strigolactone (SL) is reported to positively regulate drought response in plants (Ha et al., 2014). Expression of *CAROTENOID CLEAVAGE DIOXYGENASE 8a* (*OsCCD8a*) was up-regulated in the *OsNAC14*^{OX} plants (**Table 2**). SL is derived from carotenoids through multiple steps of enzymatic reactions. CAROTENOID CLEAVAGE DIOXYGENASE 7/MORE AXILLARY GROWTH 3 (CCD7/MAX3) and CCD8/MAX4 are two key enzymes to cleave 9-*cis*-β-carotene to carlactone, a precursor of SL (Alder et al., 2012). Compared with WT, SL-deficient mutants (*max3* and *max4*) exhibit increased water loss rate during dehydration. This phenotype is rescued by exogenous application of SL (Ha et al., 2014), indicating that SL is required for drought tolerance in plants. Biosynthesis of SL is positively regulated by both drought and ABA in plants. The transcript of *CCD7* and *CCD8* increases by drought stress and decreases by re-watering in soybean (Song et al., 2016). In addition, ABA deficient mutants *notabilis* (mutated in NCED) and *flacca* (mutated in aldehyde oxidase) showed reduced levels of SL, together with reduced expression of *LeCCD7* and *LeCCD8* in tomato (López-Ráez et al., 2010). Moreover, exogenous application of SL enhances drought tolerance through reduced water loss and enhanced antioxidant activity (Sedaghat et al., 2017). In this study, we found that expression of *OsCCD8a* was up-regulated in the *OsNAC14*^{OX}

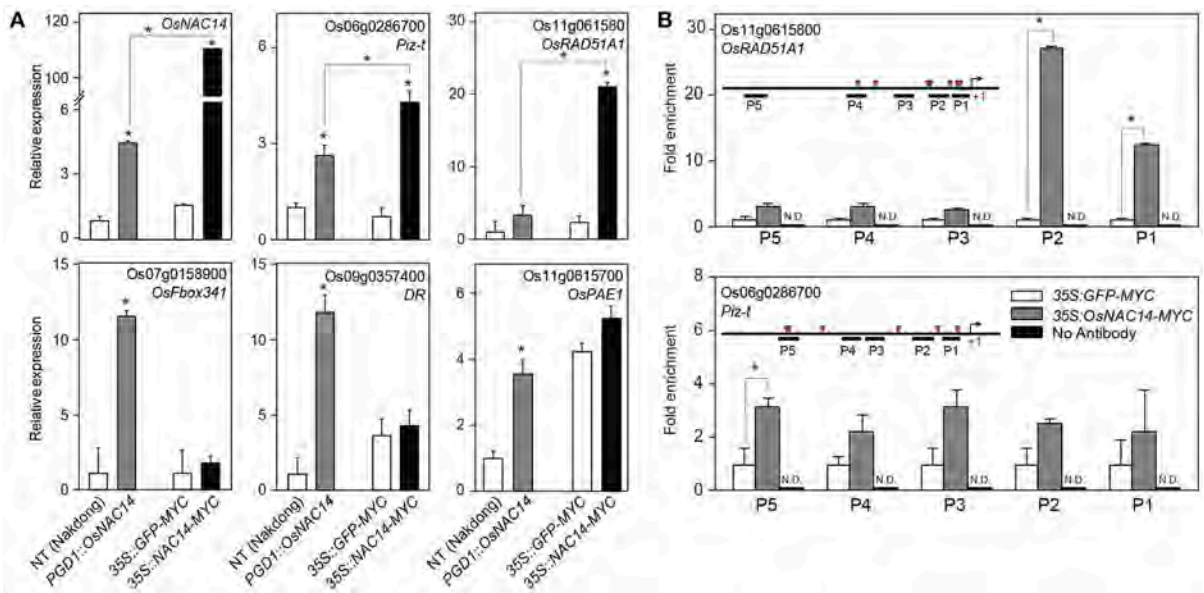

FIGURE 6 | Identification of direct target gene of OsNAC14. **(A)** The expression pattern of the candidate target genes of *OsNAC14* in rice protoplasts. Rice protoplasts were isolated from 2-week-old NT and *PGD1::OsNAC14* (*OsNAC14*^{OX}) plants (left two bars in each panel). The protoplasts isolated from NT plants were further transfected by plasmids harboring *35S::GFP* or *35S::OsNAC14* (right two bars in each panel). Total RNA was extracted from isolated protoplasts and applied for qRT-PCR analysis. *OsUbi1* was used as internal control for normalization. Data represent mean value + standard deviation (*SD*) ($n = 3$). Significant differences from NT or between samples are indicated by asterisks (one-tailed Student's *t*-test, $^*P < 0.05$). **(B)** Chromatin Immunoprecipitation (ChIP)-PCR analysis. Chromatins in rice protoplasts were precipitated using anti-MYC antibody and applied for qRT-PCR analysis. The structure of promoter and positions of tested region by qRT-PCR are illustrated in graph (left top). Red triangles represent distribution of NAC binding motif in the promoter regions. Rice protoplasts transfected with *35S::GFP-MYC* were used as negative control for *35S::OsNAC14-MYC*. ChIP experiment performed without anti-MYC antibody were applied as negative control for anti-MYC antibody. 1% input was used as control for normalization. Data represent mean value + standard deviation (**SD**) ($n = 3$). N.D., not detected. The information of primers used for ChIP-PCR was listed in Supplemental Table S2. Significant differences are indicated by asterisks (one-tailed Student's *t*-test, $^*P < 0.05$).

plants (**Table 2**) that accumulates SL, leading to drought tolerant phenotype.

In conclusion, the data presented here suggest that *OsNAC14* enhances drought tolerance in rice. Specifically, *OsNAC14* directly regulates the expression of *OsRAD51A1* and regulates other downstream target genes for stress response, DNA repair, defense related, and strigolactone biosynthesis, which together confers drought tolerance in rice.

ACCESSION NUMBERS

Gene from this article can be found in the National Center for Biotechnology Information (http://www.ncbi.nlm.nih.gov/) under following accession numbers: *OsNAC14* (Os01g0675800), *OsDIP1* (Os02g0669100), *OsRbcS* (Os12g0274700), *OsCIPK33* (Os11g0134300), *OsLEA14/WSI18* (Os01g0705200), *OsRAD51A1* (Os11g0615800), *OsMSH4* (Os07g0486000), *Piz-t* (Os06g0286700), *DR* (Os09g0357400), *RPP13-like protein 3* (Os11g0590700), *OsPAE1* (Os11g0615700), *OsFbox341* (Os07g0158900), *OsCCD8a* (Os01g0566500). The data set can be found at from GEO database with series accession number GSE106150 for RNA-sequencing data (http://www.ncbi.nlm.nih.gov/geo/).

AUTHOR CONTRIBUTIONS

JSS, NO, PJC, and J-KK designed experiment and JSS, NO, and PJC performed experiments. YSK performed field experiments and analyzed yield components in field conditions. JSS, YDC, and J-KK wrote the manuscript and prepared the figures.

ACKNOWLEDGMENTS

We thank the Rural Development Administration and Kyungpook National University for providing rice paddy fields, D.-K. Lee, S. W. Bang for discussion, M. C. F. R. Redillas for critical reading of the manuscript. This work was supported by the National Research Foundation of Korea Grant funded by the Korean Government (NRF-2013R1A6A3A04060627 to PJC). This work was also supported by the Rural Development Administration under the Next-Generation BioGreen 21 Program (Project No. PJ013666012018 to J-KK).

SUPPLEMENTARY MATERIAL

The Supplementary Material for this article can be found online at: https://www.frontiersin.org/articles/10.3389/fpls.2018.00310/full#supplementary-material

REFERENCES

Aida, M., Ishida, T., Fukaki, H., Fujisawa, H., and Tasaka, M. (1997). Genes involved in organ separation in Arabidopsis: an analysis of the cup-shaped cotyledon mutant. *Plant Cell* 9, 841–857. doi: 10.1105/tpc.9.6.841

Alder, A., Jamil, M., Marzorati, M., Bruno, M., Vermathen, M., Bigler, P., et al. (2012). The path from beta-carotene to carlactone, a strigolactone-like plant hormone. *Science* 335, 1348–1351. doi: 10.1126/science.1218094

Bolger, A. M., Lohse, M., and Usadel, B. (2014). Trimmomatic: a flexible trimmer for Illumina sequence data. *Bioinformatics* 30, 2114–2120. doi: 10.1093/bioinformatics/btu170

Bowler, C., Benvenuto, G., Laflamme, P., Molino, D., Probst, A. V., Tariq, M., et al. (2004). Chromatin techniques for plant cells. *Plant J.* 39, 776–789. doi: 10.1111/j.1365-313X.2004.02169.x

Chen, S., Tao, L., Zeng, L., Vega-Sanchez, M. E., Umemura, K., and Wang, G. L. (2006). A highly efficient transient protoplast system for analyzing defence gene expression and protein-protein interactions in rice. *Mol. Plant Pathol.* 7, 417–427. doi: 10.1111/j.1364-3703.2006.00346.x

Chini, A., Grant, J. J., Seki, M., Shinozaki, K., and Loake, G. J. (2004). Drought tolerance established by enhanced expression of the *CC-NBS-LRR* gene, *ADR1*, requires salicylic acid, EDS1 and ABI1. *Plant J.* 38, 810–822. doi: 10.1111/j.1365-313X.2004.02086.x

Chung, P. J., Jung, H., Jeong, D. H., Ha, S. H., Choi, Y. D., and Kim, J. K. (2016). Transcriptome profiling of drought responsive noncoding RNAs and their target genes in rice. *BMC Genomics* 17:563. doi: 10.1186/s12864-016-2997-3

Dong, H. P., Yu, H., Bao, Z., Guo, X., Peng, J., Yao, Z., et al. (2005). The ABI2-dependent abscisic acid signalling controls HrpN-induced drought tolerance in Arabidopsis. *Planta* 221, 313–327. doi: 10.1007/s00425-004-1444-x

Fujita, M., Fujita, Y., Maruyama, K., Seki, M., Hiratsu, K., Ohme-Takagi, M., et al. (2004). A dehydration-induced NAC protein, RD26, is involved in a novel ABA-dependent stress-signaling pathway. *Plant J.* 39, 863–876. doi: 10.1111/j.1365-313X.2004.02171.x

Ha, C. V., Leyva-González, M. A., Osakabe, Y., Tran, U. T., Nishiyama, R., Watanabe, Y., et al. (2014). Positive regulatory role of strigolactone in plant responses to drought and salt stress. *Proc. Natl. Acad. Sci. U.S.A.* 111, 851–856. doi: 10.1073/pnas.1322135111

Jang, I. C., Oh, S. J., Seo, J. S., Choi, W. B., Song, S. I., Kim, C. H., et al. (2003). Expression of a bifunctional fusion of the *Escherichia coli* genes for trehalose-6-phosphate synthase and trehalose-6-phosphate phosphatase in transgenic rice plants increases trehalose accumulation and abiotic stress tolerance without stunting growth. *Plant Physiol.* 131, 516–524. doi: 10.1104/pp.007237

Jang, I.-C., Nahm, B. H., and Kim, J.-K. (1999). Subcellular targeting of green fluorescent protein to plastids in transgenic rice plants provides a high-level expression system. *Mol. Breed.* 5, 453–461. doi: 10.1023/a:1009665314850

Jeong, J. S., Kim, Y. S., Baek, K. H., Jung, H., Ha, S. H., Do Choi, Y., et al. (2010). Root-specific expression of *OsNAC10* improves drought tolerance and grain yield in rice under field drought conditions. *Plant Physiol.* 153, 185–197. doi: 10.1104/pp.110.154773

Jeong, J. S., Kim, Y. S., Redillas, M. C., Jang, G., Jung, H., Bang, S. W., et al. (2013). OsNAC5 overexpression enlarges root diameter in rice plants leading to enhanced drought tolerance and increased grain yield in the field. *Plant Biotechnol. J.* 11, 101–114. doi: 10.1111/pbi.12011

Joo, J., Lee, Y. H., and Song, S. I. (2014). Overexpression of the rice basic leucine zipper transcription factor OsbZIP12 confers drought tolerance to rice and makes seedlings hypersensitive to ABA. *Plant Biotechnol. Rep.* 8, 431–441. doi: 10.1007/s11816-014-0335-2

Jung, H., Chung, P. J., Park, S. H., Redillas, M. C. F. R., Kim, Y. S., Suh, J. W., et al. (2017). Overexpression of OsERF48 causes regulation of *OsCML16*, a calmodulin-like protein gene that enhances root growth and drought tolerance. *Plant Biotechnol. J* 15, 1295–1308. doi: 10.1111/pbi.12716

Kaur, R., Chakraborty, A., Bhunia, R. K., Sen, S. K., and Ghosh, A. K. (2017). Tolerance to soil water stress by *Oryza sativa* cv. IR20 was improved by expression of *Wsi18* gene locus from *Oryza nivara*. *Biol. Plant.* 62, 129–139. doi: 10.1007/s10535-017-0742-7

Khoo, K. H. P., Jolly, H. R., and Able, J. A. (2008). The RAD51 gene family in bread wheat is highly conserved across eukaryotes, with RAD51A upregulated during early meiosis. *Funct. Plant Biol.* 35, 1267–1277. doi: 10.1071/FP08203

Kosugi, S., Hasebe, M., Tomita, M., and Yanagawa, H. (2009). Systematic identification of cell cycle-dependent yeast nucleocytoplasmic shuttling proteins by prediction of composite motifs. *Proc. Natl. Acad. Sci. U.S.A.* 106, 10171–10176. doi: 10.1073/pnas.0900604106

Lee, D. K., Chung, P. J., Jeong, J. S., Jang, G., Bang, S. W., Jung, H., et al. (2017). The rice OsNAC6 transcription factor orchestrates multiple molecular mechanisms involving root structural adaptions and nicotianamine biosynthesis for drought tolerance. *Plant Biotechnol. J.* 15, 754–764. doi: 10.1111/pbi.12673

Lee, D. K., Jung, H., Jang, G., Jeong, J. S., Kim, Y. S., Ha, S. H., et al. (2016). Overexpression of the *OsERF71* transcription factor alters rice root structure and drought resistance. *Plant Physiol.* 172, 575–588. doi: 10.1104/pp.16.00379

Lee, D. K., Kim, H. I., Jang, G., Chung, P. J., Jeong, J. S., Kim, Y. S., et al. (2015). The NF-YA transcription factor OsNF-YA7 confers drought stress tolerance of rice in an abscisic acid independent manner. *Plant Sci.* 241, 199–210. doi: 10.1016/j.plantsci.2015.10.006

Lee, J. H., Jin, S., Kim, S. Y., Kim, W., and Ahn, J. H. (2017). A fast, efficient chromatin immunoprecipitation method for studying protein-DNA binding in Arabidopsis mesophyll protoplasts. *Plant Methods* 13, 42. doi: 10.1186/s13007-017-0192-4

Li, J., Harper, L. C., Golubovskaya, I., Wang, C. R., Weber, D., Meeley, R. B., et al. (2007). Functional analysis of maize RAD51 in meiosis and double-strand break repair. *Genetics* 176, 1469–1482. doi: 10.1534/genetics.106.062604

Li, W., Chen, C., Markmann-Mulisch, U., Timofejeva, L., Schmelzer, E., Ma, H., et al. (2004). The *Arabidopsis AtRAD51* gene is dispensable for vegetative development but required for meiosis. *Proc. Natl. Acad. Sci. U.S.A.* 101, 10596–10601. doi: 10.1073/pnas.0404110101

Liu, C., Mao, B., Ou, S., Wang, W., Liu, L., Wu, Y., et al. (2014). OsbZIP71, a bZIP transcription factor, confers salinity and drought tolerance in rice. *Plant Mol. Biol.* 84, 19–36. doi: 10.1007/s11103-013-0115-3

López-Ráez, J. A., Kohlen, W., Charnikhova, T., Mulder, P., Undas, A. K., Sergeant, M. J., et al. (2010). Does abscisic acid affect strigolactone biosynthesis? *New Phytol.* 187, 343–354. doi: 10.1111/j.1469-8137.2010.03291.x

Ma, H., Chen, J., Zhang, Z., Ma, L., Yang, Z., Zhang, Q., et al. (2017). MAPK kinase 10.2 promotes disease resistance and drought tolerance by activating different MAPKs in rice. *Plant J.* 92, 557–570. doi: 10.1111/tpj.13674

Miller, G., Suzuki, N., Ciftci-Yilmaz, S., and Mittler, R. O. N. (2010). Reactive oxygen species homeostasis and signalling during drought and salinity stresses. *Plant Cell Environ.* 33, 453–467. doi: 10.1111/j.1365-3040.2009.02041.x

Mittler, R. (2002). Oxidative stress, antioxidants and stress tolerance. *Trends Plant Sci.* 7, 405–410. doi: 10.1016/S1360-1385(02)02312-9

Nakashima, K., Tran, L. S., Van Nguyen, D., Fujita, M., Maruyama, K., Todaka, D., et al. (2007). Functional analysis of a NAC-type transcription factor OsNAC6 involved in abiotic and biotic stress-responsive gene expression in rice. *Plant J.* 51, 617–630. doi: 10.1111/j.1365-313X.2007.03168.x

Nuruzzaman, M., Manimekalai, R., Sharoni, A. M., Satoh, K., Kondoh, H., Ooka, H., et al. (2010). Genome-wide analysis of NAC transcription factor family in rice. *Gene* 465, 30–44. doi: 10.1016/j.gene.2010.06.008

Nuruzzaman, M., Sharoni, A. M., and Kikuchi, S. (2013). Roles of NAC transcription factors in the regulation of biotic and abiotic stress responses in plants. *Front. Microbiol.* 4:248. doi: 10.3389/fmicb.2013.00248

Oh, S. J., Kim, Y. S., Kwon, C. W., Park, H. K., Jeong, J. S., and Kim, J. K. (2009). Overexpression of the transcription factor AP37 in rice improves grain yield under drought conditions. *Plant Physiol.* 150, 1368–1379. doi: 10.1104/pp.109.137554

Olsen, A. N., Ernst, H. A., Leggio, L. L., and Skriver, K. (2005). NAC transcription factors: structurally distinct, functionally diverse. *Trends Plant Sci.* 10, 79–87. doi: 10.1016/j.tplants.2004.12.010

Ooka, H., Satoh, K., Doi, K., Nagata, T., Otomo, Y., Murakami, K., et al. (2003). Comprehensive analysis of NAC family genes in *Oryza sativa* and *Arabidopsis thaliana*. *DNA Res.* 10, 239–247. doi: 10.1093/dnares/10.6.239

Park, S. H., Bang, S. W., Jeong, J. S., Jung, H., Redillas, M. C., Kim, H. I., et al. (2012). Analysis of the *APX*, *PGD1* and *R1G1B* constitutive gene promoters in various organs over three homozygous generations of transgenic rice plants. *Planta* 235, 1397–1408. doi: 10.1007/s00425-011-1582-x

Peng, X. C., Qiu, D. W., Zeng, H. M., Guo, L. H., Yang, X. F., and Liu, Z. (2015). Inducible and constitutive expression of an elicitor gene *Hrip1* from *Alternaria tenuissima* enhances stress tolerance in *Arabidopsis*. *Transgenic Res.* 24, 135–145. doi: 10.1007/s11248-014-9824-x

Rajanikant, C., Melzer, M., Rao, B. J., and Sainis, J. K. (2008). Homologous recombination properties of OsRad51, a recombinase from rice. *Plant Mol. Biol.* 68, 479–491. doi: 10.1007/s11103-008-9385-6

Redillas, M. C. F. R., Strasser, R. J., Jeong, J. S., Kim, Y. S., and Kim, J.-K. (2011). The use of JIP test to evaluate drought-tolerance of transgenic rice overexpressing OsNAC10. *Plant Biotechnol. Rep.* 5, 169–175. doi: 10.1007/s11816-011-0170-7

Redillas, M. C., Jeong, J. S., Kim, Y. S., Jung, H., Bang, S. W., Choi, Y. D., et al. (2012). The overexpression of *OsNAC9* alters the root architecture of rice plants enhancing drought resistance and grain yield under field conditions. *Plant Biotechnol. J.* 10, 792–805. doi: 10.1111/j.1467-7652.2012.00697.x

Roldán-Arjona, T., and Ariza, R. R. (2009). Repair and tolerance of oxidative DNA damage in plants. *Mutat. Res.* 681, 169–179. doi: 10.1016/j.mrrev.2008.07.003

Roy, S. (2014). Maintenance of genome stability in plants: repairing DNA double strand breaks and chromatin structure stability. *Front. Plant Sci.* 5:487. doi: 10.3389/fpls.2014.00487

Sedaghat, M., Tahmasebi-Sarvestani, Z., Emam, Y., and Mokhtassi-Bidgoli, A. (2017). Physiological and antioxidant responses of winter wheat cultivars to strigolactone and salicylic acid in drought. *Plant Physiol. Biochem.* 119, 59–69. doi: 10.1016/j.plaphy.2017.08.015

Shinohara, A., Ogawa, H., and Ogawa, T. (1992). Rad51 protein involved in repair and recombination in *S. cerevisiae* is a RecA-like protein. *Cell* 69, 457–470. doi: 10.1016/0092-8674(92)90447-K

Song, L., Prince, S., Valliyodan, B., Joshi, T., Maldonado dos Santos, J. V., Wang, J., et al. (2016). Genome-wide transcriptome analysis of soybean primary root under varying water-deficit conditions. *BMC Genomics* 17:57. doi: 10.1186/s12864-016-2378-y

Souer, E., van Houwelingen, A., Kloos, D., Mol, J., and Koes, R. (1996). The no apical meristem gene of Petunia is required for pattern formation in embryos and flowers and is expressed at meristem and primordia boundaries. *Cell* 85, 159–170.

Symington, L. S. (2002). Role of RAD52 epistasis group genes in homologous recombination and double-strand break repair. *Microbiol. Mol. Biol. Rev.* 66, 630–670. doi: 10.1128/MMBR.66.4.630-670.2002

Takada, S., Hibara, K., Ishida, T., and Tasaka, M. (2001). The *CUP-SHAPED COTYLEDON1* gene of Arabidopsis regulates shoot apical meristem formation. *Development* 128, 1127–1135.

Takasaki, H., Maruyama, K., Kidokoro, S., Ito, Y., Fujita, Y., Shinozaki, K., et al. (2010). The abiotic stress-responsive NAC-type transcription factor OsNAC5 regulates stress-inducible genes and stress tolerance in rice. *Mol. Genet. Genomics* 284, 173–183. doi: 10.1007/s00438-010-0557-0

Tian, D., Traw, M. B., Chen, J. Q., Kreitman, M., and Bergelson, J. (2003). Fitness costs of R-gene-mediated resistance in *Arabidopsis thaliana*. *Nature* 423, 74–77. doi: 10.1038/nature01588

Tran, L. S., Nakashima, K., Sakuma, Y., Simpson, S. D., Fujita, Y., Maruyama, K., et al. (2004). Isolation and functional analysis of Arabidopsis stress-inducible NAC transcription factors that bind to a drought-responsive *cis*-element in the *early responsive to dehydration stress 1* promoter. *Plant Cell* 16, 2481–2498. doi: 10.1105/tpc.104.022699

Tripathi, A. K., Pareek, A., and Singla-Pareek, S. L. (2016). A NAP-family histone chaperone functions in abiotic stress response and adaptation. *Plant Physiol.* 171, 2854–2868. doi: 10.1104/pp.16.00408

Tuteja, N., Singh, M. B., Misra, M. K., Bhalla, P. L., and Tuteja, R. (2001). Molecular mechanisms of DNA damage and repair: progress in plants. *Crit. Rev. Biochem. Mol. Biol.* 36, 337–397. doi: 10.1080/20014091074219

Wang, J., and Zhang, C. (2001). DNA damage and repair of two ecotypes of Phragmites communis subjected to water stress. *Acta Bot. Sin.* 43, 490–494.

Wang, X., Jia, M. H., Ghai, P., Lee, F. N., and Jia, Y. (2015). Genome-wide association of rice blast disease resistance and yield-related components of rice. *Mol. Plant Microbe Interact.* 28, 1383–1392. doi: 10.1094/MPMI-06-15-0131-R

Wang, Z., Han, Q., Zi, Q., Lv, S., Qiu, D., and Zeng, H. (2017). Enhanced disease resistance and drought tolerance in transgenic rice plants overexpressing protein elicitors from *Magnaporthe oryzae*. *PLoS ONE* 12:e0175734. doi: 10.1371/journal.pone.0175734

Wu, Y., Deng, Z., Lai, J., Zhang, Y., Yang, C., Yin, B., et al. (2009). Dual function of Arabidopsis ATAF1 in abiotic and biotic stress responses. *Cell Res.* 19, 1279–1290. doi: 10.1038/cr.2009.108

Yamaguchi-Shinozaki, K., and Shinozaki, K. (2006). Transcriptional regulatory networks in cellular responses and tolerance to dehydration and cold stresses. *Annu. Rev. Plant. Biol.* 57, 781–803. doi: 10.1146/annurev.arplant.57.032905.105444

Yang, A., Dai, X., and Zhang, W. H. (2012). A R2R3-type MYB gene, *OsMYB2*, is involved in salt, cold, and dehydration tolerance in rice. *J. Exp. Bot.* 63, 2541–2556. doi: 10.1093/jxb/err431

Yao, Y., and Kovalchuk, I. (2011). Abiotic stress leads to somatic and heritable changes in homologous recombination frequency, point mutation frequency and microsatellite stability in Arabidopsis plants. *Mut. Res.* 707, 61–66. doi: 10.1016/j.mrfmmm.2010.12.013

Yao, Y., Bilichak, A., Titov, V., Golubov, A., and Kovalchuk, I. (2013). Genome stability of Arabidopsis *atm*, *ku80* and *rad51b* mutants: somatic and transgenerational responses to stress. *Plant Cell Physiol.* 54, 982–989. doi: 10.1093/pcp/pct051

Yoo, S. D., Cho, Y. H., and Sheen, J. (2007). Arabidopsis mesophyll protoplasts: a versatile cell system for transient gene expression analysis. *Nat. Protoc.* 2, 1565–1572. doi: 10.1038/nprot.2007.199

Zhang, L., Xiao, S., Li, W., Feng, W., Li, J., Wu, Z., et al. (2011). Overexpression of a Harpin-encoding gene *hrf1* in rice enhances drought tolerance. *J. Exp. Bot.* 62, 4229–4238. doi: 10.1093/jxb/err131

Zhang, Y., Su, J., Duan, S., Ao, Y., Dai, J., Liu, J., et al. (2011). A highly efficient rice green tissue protoplast system for transient gene expression and studying light/chloroplast-related processes. *Plant Methods* 7:30. doi: 10.1186/1746-4811-7-30

Zheng, X., Chen, B., Lu, G., and Han, B. (2009). Overexpression of a NAC transcription factor enhances rice drought and salt tolerance. *Biochem. Biophys. Res. Commun.* 379, 985–989. doi: 10.1016/j.bbrc.2008.12.163

Conflict of Interest Statement: The authors declare that the research was conducted in the absence of any commercial or financial relationships that could be construed as a potential conflict of interest.

frontiers in Plant Science

ORIGINAL RESEARCH
published: 04 April 2018
doi: 10.3389/fpls.2018.00422

The Maize ABA Receptors ZmPYL8, 9, and 12 Facilitate Plant Drought Resistance

Zhenghua He[1,2†], Junwei Zhong[1†], Xiaopeng Sun[1], Bingcai Wang[1], William Terzaghi[3] and Mingqiu Dai[1]*

[1] National Key Laboratory of Crop Genetic Improvement, Huazhong Agricultural University, Wuhan, China, [2] Hubei Key Laboratory of Food Crop Germplasm and Genetic Improvement, Food Crops Institute, Hubei Academy of Agricultural Sciences, Wuhan, China, [3] Department of Biology, Wilkes University, Wilkes-Barre, PA, United States

Drought is one of the major abiotic stresses affecting world agriculture. Breeding drought-resistant crops is one of the most important challenges for plant biologists. *PYR1/PYL/RCARs*, which encode the abscisic acid (ABA) receptors, play pivotal roles in ABA signaling, but how these genes function in crop drought response remains largely unknown. Here we identified 13 *PYL* family members in maize (*ZmPYL1-13*). Changes in expression of these genes under different stresses indicated that *ZmPYLs* played important roles in responding to multiple abiotic stresses. Transgenic analyses of *ZmPYL genes* in Arabidopsis showed that overexpression of *ZmPYL3*, *ZmPYL9, ZmPYL10,* and *ZmPYL13* significantly enhanced the sensitivity of transgenic plants to ABA. Additionally, transgenic lines overexpressing *ZmPYL8*, *ZmPYL9,* and *ZmPYL12* were more resistant to drought. Accumulation of proline and enhanced expression of drought-related marker genes in transgenic lines further confirmed the positive roles of *ZmPYL* genes in plant drought resistance. Association analyses with a panel of 368 maize inbred lines identified natural variants in *ZmPYL8* and *ZmPYL12* that were significantly associated with maize drought resistance. Our results deepen the knowledge of the function of maize *PYL* genes in responses to abiotic stresses, and the natural variants identified in *ZmPYL* genes may serve as potential molecular markers for breeding drought-resistant maize cultivars.

Keywords: ABA receptors, drought resistance, natural variation, *Zea mays*, ABA response

OPEN ACCESS

Edited by:
Lijun Luo,
Shanghai Agrobiological Gene Center, China

Reviewed by:
Yang Zhao,
Shanghai Institutes for Biological Sciences (CAS), China
Charu Lata,
National Botanical Research Institute (CSIR), India
Caifu Jiang,
China Agricultural University, China

***Correspondence:**
Mingqiu Dai
mingqiudai@mail.hzau.edu.cn

† These authors have contributed equally to this work.

Specialty section:
This article was submitted to Plant Breeding, a section of the journal Frontiers in Plant Science

Received: *26 November 2017*
Accepted: *16 March 2018*
Published: *04 April 2018*

Citation:
He Z, Zhong J, Sun X, Wang B, Terzaghi W and Dai M (2018) The Maize ABA Receptors ZmPYL8, 9, and 12 Facilitate Plant Drought Resistance. Front. Plant Sci. 9:422. doi: 10.3389/fpls.2018.00422

INTRODUCTION

Due to their sessile lifestyle, plants cannot escape from environmental stresses which include biotic and abiotic stresses. Drought is one of the major abiotic stresses that negatively affect plant growth and development. Plants have evolved sophisticated mechanisms to respond to and survive drought. Generally, plants have two major mechanisms for drought resistance, drought avoidance and drought tolerance (Hu and Xiong, 2014). Drought avoidance includes increasing cuticular wax and abscisic acid (ABA) content, controlling relative water content and water potential, along with leaf rolling and stomatal aperture control. General criteria for drought tolerance are content of osmolytes such as proline and sugar, and membrane system stability (Hu and Xiong, 2014).

Abscisic acid is a phytohormone that plays critical roles in plant stress response. Under drought stress, plants increase the production of ABA, which initiates stomatal closure and thereby reduces

transpirational water loss, thus helping the plant avoid drought stress (Kim et al., 2010). Plants can perceive ABA via ABA receptors, the regulatory components of the ABA receptor (RCAR) or PYRABACTIN RESISTANCE 1 (PYR1)/PYR1-like protein (PYL) family of START proteins (Ma et al., 2009; Park et al., 2009). The clade A PP2C phosphatases and SnRK2 kinases are also important in mediating ABA signaling (Miyazono et al., 2009; Fujita et al., 2011; Joshi-Saha et al., 2011; Antoni et al., 2012; Nakashima et al., 2012, 2014; Rushton et al., 2012; Roychoudhury et al., 2013). A number of studies revealed the important roles of SnRK2 kinases and clade A PP2C phosphatases in regulation of plant drought resistance. Mutation of *SnRK2.6*/*OST1* caused constitutive stomatal opening and water loss (Mustilli et al., 2002). Triple mutants of *snrk2.2*/*3*/*6* lost the ability to respond to ABA and were hypersensitive to drought (Fujii and Zhu, 2009). Recent study has revealed that SnRK2.6 regulates the ubiquitin E3 ligase activity of RZFP34/CHYR1, a positive regulator of plant drought resistance (Ding et al., 2015). In Arabidopsis, the HAI PP2Cs function in drought responses by regulating the accumulation of osmoregulatory solutes such as proline (Bhaskara et al., 2012). *ZmPP2C-A10*, encoding a clade A PP2C phosphatase, negatively regulates maize drought response (Xiang et al., 2017).

There are 14 Arabidopsis genes encoding PYR/PYL/RCAR ABA receptors (Li et al., 2013). Recently, these Arabidopsis *PYR*/*PYL* genes have been extensively studied and reported to be important for plant drought responses. By using an ABA inducible promoter, researchers have revealed that overexpressing *PYL9* upon stress induction greatly enhanced drought resistance and drought-induced leaf senescence in transgenic Arabidopsis and rice plants (Zhao et al., 2016). Overexpression of *PYL5* also enhanced plant drought tolerance (Santiago et al., 2009). The A194T site mutant of *PYL4* formed stable complex with PP2CA in the absence of ABA, and 35S:*PYL4* (A194T) plants showed dramatically enhanced tolerance to drought and dehydration (Pizzio et al., 2013). In guard cells, PYL/RCAR ABA receptors interact with PP2C phosphatases, thus releasing active SnRK2 kinase to activate the SLAC1 channel which leads to stomatal closure by reducing guard cell turgor (Lee et al., 2013). This shows the involvement of PYL/RCAR ABA receptors in plant drought avoidance. In maize, a previous study reported the expression profiles of *ZmPYL* genes in response to ABA and dehydration stress (Fan et al., 2016). However, the function of *ZmPYL* genes in regulation of maize drought tolerance remains elusive.

Association analysis based on linkage disequilibrium (LD) is widely used for dissecting complex traits of crops (Wang and Qin, 2017). By using genome wide association analysis (GWAS), a number of loci involved in regulation of complex plant traits, such as flowering time, oil synthesis, salt tolerance, were indentified recently (Huang et al., 2011; Meyer et al., 2016; Fang et al., 2017). Maize is a model plant for genetic studies due to its huge genetic diversity among various accessions (Strable and Scanlon, 2009). Due to the fast LD decay, researchers can detect trait-locus associations in maize at single gene resolution. For example, recent studies used GWAS to detect two drought-tolerant genes, *ZmNAC111* and *ZmVPP1*, from a maize population consisting of 368 accessions (Mao et al., 2015; Wang et al., 2016). Based on the same maize population, we and another group identified two drought-resistance genes, *ZmPP2C-A10* and *ZmDREB2.7*, and their natural variations through candidate gene association analyses (Liu et al., 2013; Xiang et al., 2017). Although the function of PYL/RCAR ABA receptors in regulation of drought resistance has been revealed in several plant species, how the natural variations in *PYL*/*RCAR* genes are associated with plant drought responses remains essentially unknown.

In this study, we identified and cloned the maize *PYL* family genes. Expression analyses showed that *ZmPYL* genes responded to multiple abiotic stresses including ABA, drought and salt. Transgenic analyses revealed the roles of several *ZmPYLs* in regulation of plant ABA and drought responses. Association analysis with a large maize association population identified several favorable alleles of two *ZmPYL* genes, *ZmPYL8* and *ZmPYL12*, for maize drought resistance.

MATERIALS AND METHODS

Plant Material

Maize B73 seeds were used for gene cloning and expression analysis. The *Arabidopsis* ecotype Col-0 was used as the wild-type. The pRCS2(Bar)-*ZmPYLs* plasmids were introduced into *Agrobacterium tumefaciens* strain GV3101 and then transformed into Arabidopsis Col-0 ecotype using the floral dip method (Clough and Bent, 1998). Seeds of transformed Arabidopsis were selected on MS plates containing the appropriate antibiotics. Homozygous lines of T4 generations with one copy of inserted transgene were used for further analysis.

Plant Growth Conditions and Treatments

All maize seedlings were grown under 16 h light: 8 h dark photoperiod at 28°C. For drought treatment, maize seedlings were germinated and grown in soil under normal watering conditions until the three-leaf stage. Plants were then transferred onto filter paper and dried at 28°C. Shoot and root samples were harvested after 0, 1, 3, 6, 12, 24 h, respectively. For ABA and salt treatments, maize seeds were sown and grown in Hoagland's solution until the three-leaf stage. Then seedling roots were soaked in Hoagland's solution containing various concentrations of ABA (0, 1, 10, 50, 100, and 150 μM) for 3 h. For salt treatments, plant roots were immersed in Hoagland's solution containing 150 mM NaCl and sampled after 0, 1, 2, 3, and 4 days. Upon harvesting the samples were immediately frozen in liquid nitrogen for RNA extraction.

Arabidopsis seeds of wild-type and independent transgenic *ZmPYL*-overexpression lines were sterilized with 10% bleach and then kept at 4°C in the dark for 3 days. For the germination rate assay, sterilized seeds of wild-type and lines overexpressing *ZmPYLs* were sown on MS plates or MS plates supplemented with 1 μM ABA and grown under 16-h light: 8-h dark photoperiod at 22°C. Germination was first scored on the second day and counted continuously for 5 days. For the root growth assay, the seeds of wild-type and *ZmPYLs*-overexpression lines were sown perpendicularly on ½ MS agar medium and grown under 16-h

light: 8-h dark photoperiod at 22°C for 5 days, then transferred to ½ MS agar medium containing 0 or 10 μM ABA. They were then grown vertically for 7 days, after which root lengths and leaf weights were measured. For the drought treatment, sterilized seeds of wild-type and *ZmPYL*-overexpression lines were sown on MS growth medium for 9 days, then transferred to small pots containing potting soil. *Arabidopsis* plants grew under normal watering conditions with 12 h light: 12 h dark photoperiod at 22°C for about 3 weeks. Watering was then halted. Plants were sampled for marker gene assays after 10 days when they began to exhibit lethal effects of dehydration. Samples were taken for proline and malondialdehyde (MDA) assays after 12 days. Watering was then resumed and the fraction surviving was determined.

Identification and Analysis of *ZmPYLs*

All PYL protein sequences in Arabidopsis were obtained from the Ensemble Plants database[1]. To identify *ZmPYL* genes in maize, each Arabidopsis PYL sequence was analyzed by BLAST at maizeGDB[2] against the B73 working gene set translations 5a.59 for RefGen_v2. After removing redundant results, all sequences were submitted to SMART[3] to test whether the sequence had the Polyketide_cyc domain. Thirteen *ZmPYL* genes were retained for analysis in this study.

Constructs

For *Arabidopsis* transformation, the 13 *ZmPYL* genes were individually cloned from cDNA of maize line B73. The cDNAs were sequenced after insertion into pJET1.2 vector. The *ZmPYL* cDNAs were then released from the pJET vectors by digestion with E*coR* I and X*ho* I, and inserted into the pSAT6 vector to produce pSAT6-ZmPYLs. The expression cassettes using 2X35S promoters to drive expression of the *ZmPYL* cDNAs were released from the pSAT6 vectors by digestion with P*I-Psp* I and inserted into the pRCS2-Bar-OCS binary vector (Dai et al., 2012).

RNA Purification and Expression Analysis

Samples were collected after stress treatments. Total RNA was isolated using Trizol reagent (TransGen) from more than three seedlings for each treatment. RNA was treated with RNase-free DNase I (Thermo Scientific), and single-stranded cDNA was synthesized using recombinant M-MLV reverse transcriptase (Promega). The maize and Arabidopsis *Actin* genes were used as internal control to normalize the data.

Proline and Malondialdehyde (MDA) Content

Arabidopsis seedlings that were dehydrated for 12 days were used for MDA and proline assays. To assay proline, 50 mg fresh weight (FW) of leaves were shredded into 10 ml centrifuge tubes using scissors. Five milliliters of 3% sulfosalicylic acid solution were added to each sample and then the mixture was placed in boiling water for 10–30 min to obtain the extract solution. After cooling to room temperature, 2 ml of supernatant were pipetted into a new 10 ml centrifuge tube and mixed with 2 ml acetic acid and 2 ml ninhydrin. The mixture was placed in a boiling water bath for 30 min. Four milliliters of methylbenzene were added to the extract after cooling to room temperature, followed by centrifugation for 1 min and stewing for 10 min. The upper red solution was transferred to a 1.5 ml centrifuge tube. After centrifugation at 12000 rpm for 15 min, the upper proline solution was pipetted into a cuvette to measure absorbance at 520 nm by UV-vis spectrophotometry with methylbenzene as blank.

To assay MDA content, 50 mg FW of leaves were shredded using scissors and placed in 5 ml 5% TCA. After centrifugation at 3000 rpm and 4°C for 10 min, 2 ml of the supernatants were transferred into new 10 ml centrifuge tubes then 2 ml 0.67% thiobarbituric acid (TBA) were added and the extract was placed in a boiling water bath for 30 min. After cooling to room temperature, 1.5 ml of the extracts were transferred into 1.5 ml tubes and centrifuged at 12000 rpm and room temperature. Absorbance of the supernatants were measured at 440, 532, and 600 nm by UV-vis spectrophotometry. The MDA content was calculated as nmol/g FW tissue. $C/\text{umol/L} = 6.45\,(A_{532} - A_{600}) - 0.56A_{450}$

Association Analyses

Association analyses for the *ZmPYL* genes were performed using a maize association mapping population that contains 368 inbred lines and corresponding drought tolerance phenotypic data obtained in a previous study. Among 525105 high-quality SNPs data with Minor Allele Frequency (MAF) ≥ 0.05, 112 SNPs were found in the regions of *ZmPYL3*, *ZmPYL8*, *ZmPYL9*, *ZmPYL10*, and *ZmPYL12* genes. The mixed linear model (MLM) was used to detect SNPs significantly associated with drought tolerance using the program TASSEL5.0 (Bradbury et al., 2007).

Statistical Analyses

Statistical analyses were performed using Excel (Microsoft, United States). Figures were plotted by using Photoshop software (Adobe Systems, United States).

RESULTS

Sequence Analyses of *ZmPYL* Genes

To determine how many genes encoding ZmPYL proteins are in the maize genome, each Arabidopsis PYL sequence was used as a BlastP query against the maize genome database (version B73 working gene set translations 5a.59 for RefGen_V2). Thirteen genes encoding ZmPYLs (*ZmPYL1-13*) were identified (Supplementary Table S1). These genes are located on most of the chromosomes with 1 or 2 genes per chromosome, except that no *ZmPYL* gene was detected on chromosome 7 (Supplementary Figure S1). A previous study reported 11 *ZmPYL* genes (Fan et al., 2016). The involvement of *ZmPYL3* in ABA signaling has been reported (Wang et al., 2014). To

[1]http://plants.ensembl.org/

[2]http://www.maizegdb.org/

[3]http://smart.embl-heidelberg.de/

be consistent, the names of *ZmPYL1-11* in this study are same as those in the previous report (Fan et al., 2016). In our study, two more *ZmPYL* genes, GRMZM2G169695 (*ZmPYL13*, named in our study) and GRMZM2G405064 (*ZmPYL12*), were identified based on the conserved motifs and important amino acids of PYL family proteins (Li et al., 2013). Based on the protein sequences, a phylogenetic tree was generated using the NJ algorithm (**Figure 1A**). The ZmPYL proteins clustered into two subgroups, which is very similar to the Arabidopsis PYL proteins (**Figure 1A**; Li et al., 2013), suggesting the conservation of plant PYL proteins. Sequence analyses revealed that subgroup I genes had fewer introns than subgroup II *ZmPYL* genes (**Figure 1B**). In the promoter regions, a number of ABA responsive elements (ABREs) and MYB binding sites (MBS), which are involved in ABA and drought response (Seo et al., 2011; Singh and Laxmi, 2015), were detected in most *ZmPYL* genes except *ZmPYL8* and *ZmPYL10* (**Figure 1B**). The full-length coding sequences of the *ZmPYL* genes were cloned and confirmed by sequencing for further analyses.

Expression Analyses of *ZmPYL* Genes

In order to determine the functions of *ZmPYL* genes in plant development, we studied their tissue-specific expression patterns. An expression heatmap of *ZmPYL* genes was created using the publically available transcription data for fifteen maize tissues (**Figure 2A**). According to the heatmap, the expression levels of *ZmPYL* genes were divided into two patterns. Subgroup II genes showed higher expression levels than those of subgroup I in most tissues (**Figure 2A**), indicating that subgroup II *ZmPYL* genes may have more important roles in regulating plant development. There are no expression data for *ZmPYL2* and *ZmPYL3* in the public database, therefore these genes were not included in the heatmap. Next we measured the expression levels of these genes in maize seedlings subjected to various levels of drought stress. *ZmPYL4* was not detectable in our experiments, may be due to the extremely low expression of this gene in the tissues tested. Based on the expression patterns, the genes can be roughly divided into three types (**Figure 2B**). Type I genes (*ZmPYL1*, *ZmPYL3*, and *ZmPYL11*) were slightly down-regulated initially but up-regulated at later stages of drought stress in shoots, while in roots they were down-regulated. Type II genes (*ZmPYL5*, *ZmPYL6*, *ZmPYL7*, and *ZmPYL10)*, were down-regulated in both shoots and roots after drought stress. Type III genes (*ZmPYL2*, *ZmPYL8*, *ZmPYL9*, and *ZmPYL12*) were up-regulated by drought in shoots and slightly up-regulated or unchanged in roots. These results suggested different roles of *ZmPYL* genes in regulation of drought responses. We next tested the responses of *ZmPYL* genes to other abiotic stresses, including ABA and salt stress. The results showed that ABA inhibited the expression of most *ZmPYL* genes in shoots and roots except for *ZmPYL7* and *ZmPYL8,* whose expression levels were enhanced in either roots (*ZmPYL8*) or both shoots and roots (*ZmPYL7*) (Supplementary Figure S2). After salt stress, the expression levels of *ZmPYL1*, *ZmPYL2*, *ZmPYL3*, *ZmPYL5*, *ZmPYL6, ZmPYL7*, *ZmPYL10*, and *ZmPYL13* were down-regulated, while the expression levels of *ZmPYL8*, *ZmPYL9*, *ZmPYL11*, and *ZmPYL12* were slightly up-regulated or not changed (Supplementary Figure S3). Taken together, these results suggested diverse roles of *ZmPYL* genes in regulation of maize abiotic stress responses.

Roles of *ZmPYL* Genes in Regulation of ABA Responses

In order to decipher the biological functions of *ZmPYL* genes, we generated transgenic Arabidopsis plants overexpressing the *ZmPYL* genes. A total of 12 *ZmPYL* genes were introduced into and overexpressed in Arabidopsis plants except *ZmPYL4*. Our failure to clone *ZmPYL4* may be due to its extremely low expression in most of maize tissues. In order to determine

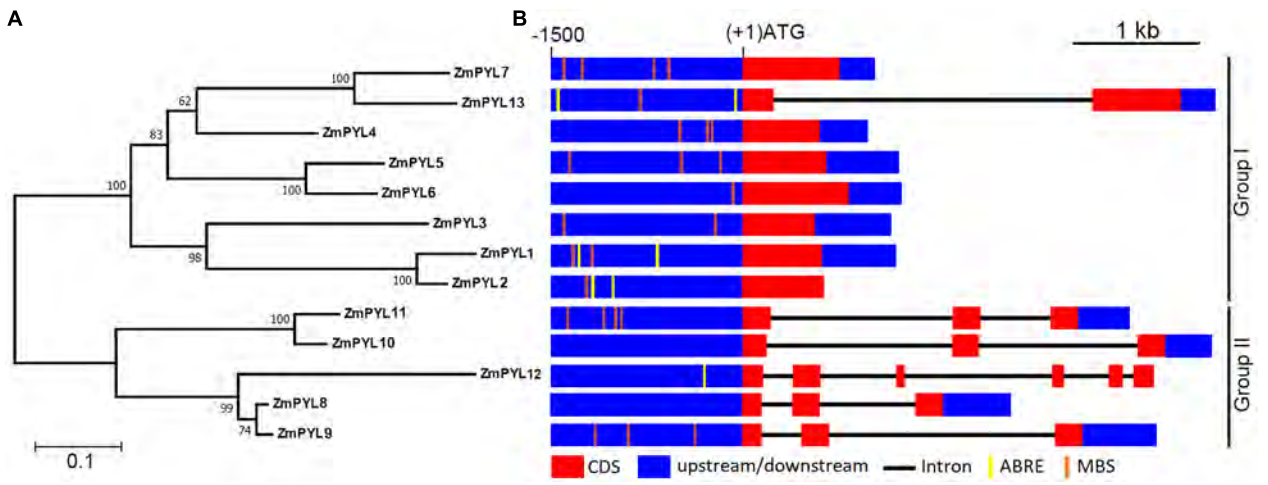

FIGURE 1 | Evolutionary relationships of taxa. **(A)** Phylogenetic tree of ZmPYL proteins. The phylogenetic tree was generated based on the alignments of the full-length ZmPYL protein sequences. Bootstrap values from 1,000 replicates are indicated at each node. The scale bar represents branch lengths. **(B)** *ZmPYL* gene structures. The upstream regions (0∼–1500 bp) of these genes were used to search the public data base (PlantCARE). Most of the *ZmPYLs* except *ZmPYL8* and *ZmPYL10* contain one or more drought response elements (MBS or ABRE) in the upstream regions. MBS, MYB binding site; ABRE, ABA responsive element.

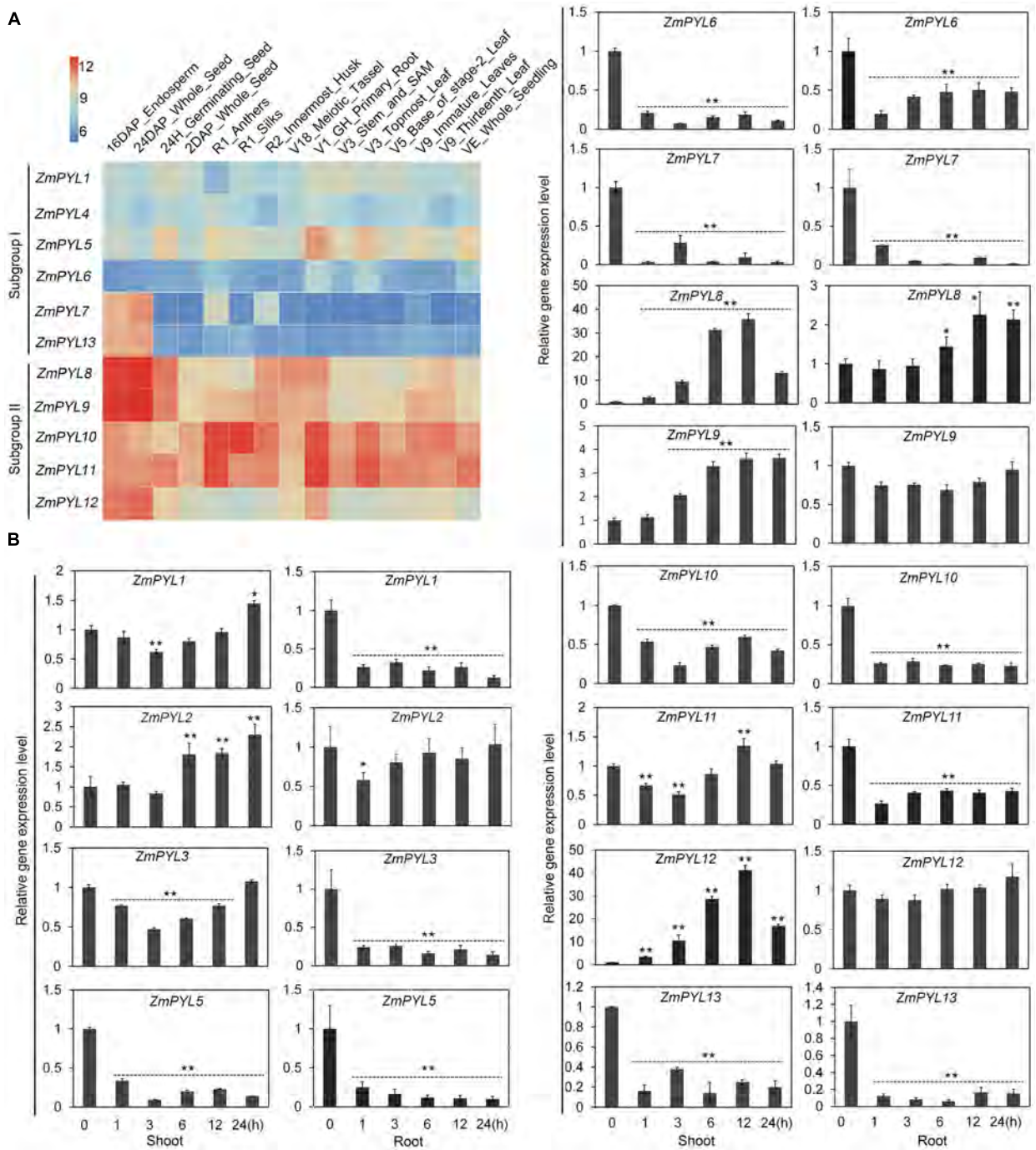

FIGURE 2 | Expression Patterns of Maize *ZmPYL* Genes. **(A)** Gene expression heat map of 11 *ZmPYL* genes in 15 different tissues from various developmental stages. Two *ZmPYL* genes have no available data. The gene expression levels are shown in different colors indicated by the scale bar. **(B)** Expression patterns of *ZmPYL* genes in maize B73 leaves and roots under normal and drought treatments. *ZmActin5* gene was used as an internal control. Both leaf and root tissues were collected after treatment at time points 0, 1, 3, 6, 12, and 24 h. Data represent the mean ± SD of three biological replicates. Asterisks indicate the significance of *T*-test, $*p < 0.05$, $**p < 0.01$.

how these *ZmPYL* genes function in regulating ABA responses, we germinated *ZmPYL* transgenic seeds on MS plates with or without ABA, and then measured the germination rates at various time points. To our surprise, we only observed that transgenic seeds overexpressing *ZmPYL3*, *ZmPYL9*, *ZmPYL10,* and *ZmPYL13* responded to ABA treatment (**Figure 3** and Supplementary Figure S4). These transgenic seeds were hypersensitive to ABA, suggesting negative roles of *ZmPYL3*,

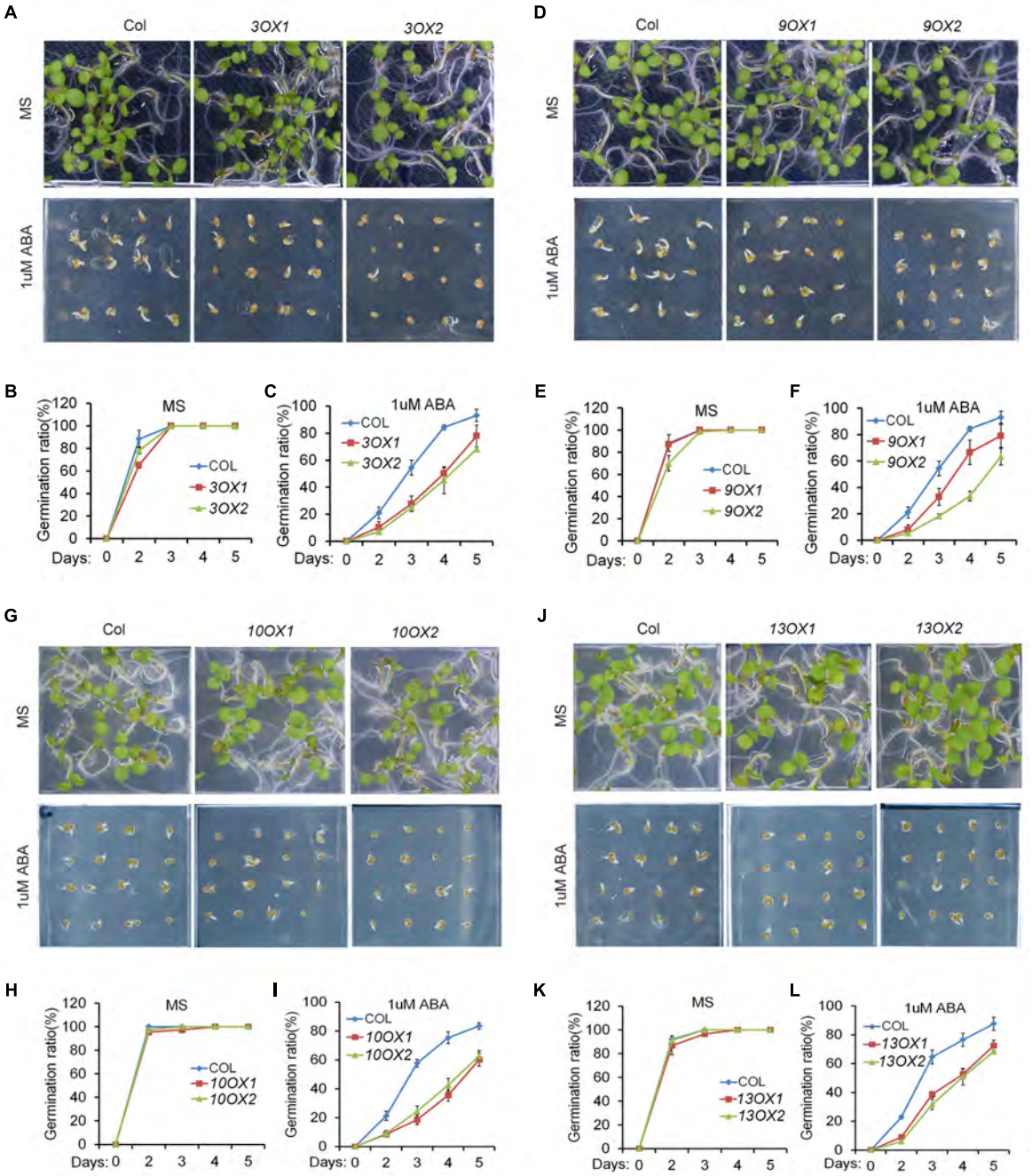

FIGURE 3 | Overexpression of *ZmPYL3*, *ZmPYL9*, *ZmPYL10*, *ZmPYL13* in *Arabidopsis* increased the sensitivity of seed germination to abscisic acid (ABA). **(A–C)** Germination phenotypes **(A)** and statistical analyses **(B,C)** of Col and two transgenic seeds overexpressing *ZmPYL3* sown on MS medium or MS medium supplemented with 1 μM ABA. **(D–F)** Germination phenotypes **(D)** and statistical analyses **(E,F)** of Col and two transgenic seeds overexpressing *ZmPYL9* sown on MS medium or MS medium supplemented with 1 μM ABA. **(G–I)** Germination phenotypes **(G)** and statistical analyses **(H,I)** of Col and two transgenic seeds overexpressing *ZmPYL10* sown on MS medium or MS medium supplemented with 1 μM ABA. **(J–L)** Germination phenotypes **(J)** and statistical analyses **(K,L)** of Col and two transgenic seeds overexpressing *ZmPYL13* sown on MS medium or MS medium supplemented with 1 μM ABA. Data represent the mean ± SD of three replicates in **(B)**, **(C)**, **(E)**, **(F)**, **(H)**, **(I)**, **(K)**, and **(L)**.

ZmPYL9, *ZmPYL10,* and *ZmPYL13* in regulation of ABA-mediated seed germination. It is well known that ABA inhibits plant growth (Luo et al., 2014). To determine how *ZmPYL3*, *ZmPYL9*, *ZmPYL10,* and *ZmPYL13* regulate plant growth in response to ABA, we grew the control and transgenic seedlings on MS plates with or without ABA, and then measured the root lengths and FW. The results showed that the transgenic seedlings overexpressing *ZmPYL3* or *ZmPYL9* had more severely

inhibited plant growth than the controls, suggesting that they were more sensitive to ABA than the controls (**Figure 4**). These results indicated that the activities of *ZmPYL3* and *ZmPYL9* were critical for both seed germination and post-germination growth. Intriguingly, we did not observe any phenotypic changes in *ZmPYL13* and *ZmPYL10* transgenic plants as compared to controls after ABA treatment (Data not shown), suggesting a specific role of *ZmPYL10* and *ZmPYL13* in regulating Arabidopsis seed germination rather than seedling growth.

Roles of *ZmPYL* Genes in Regulation of Drought Responses

Next, we performed experiments to test how *ZmPYL* genes regulate plant drought responses. All the transgenic lines overexpressing *ZmPYL* genes were subjected to severe drought stress. After stress, the plants were re-watered and survival rates of the transgenic lines were determined. We observed that most plants overexpressing *ZmPYL8* recovered upon rewatering after severe drought stress, whereas most control plants died (**Figures 5A,B**). The survival rates of plants overexpressing *ZmPYL8* were twofold higher than those of controls (**Figure 5C**). Further analyses showed that more than twofold higher of proline (**Figure 5D**), and 30% less of MDA accumulated in plants overexpressing *ZmPYL8* after drought stress as compared to controls (**Figure 5E**). These results suggested that *ZmPYL8* plays a positive role in regulation of plant drought tolerance. We observed similar phenotypic changes in plants overexpressing *ZmPYL9* and *ZmPYL12*. After drought stress, the transgenic plants overexpressing *ZmPYL9* and *ZmPYL12* had higher survival rates than the controls (Supplementary Figure S5), suggesting that *ZmPYL9* and *ZmPYL12* also have positive roles in plant drought tolerance.

When compared to control plants, we did not observe any phenotypic changes in transgenic plants overexpressing other *ZmPYL* genes in our drought stress experiments (Data not shown), suggesting these genes do not play major roles in regulating drought resistance of the transgenic plants. *ZmPYL8*, *ZmPYL9*, and *ZmPYL12* clustered together in the phylogenetic tree (**Figure 1A**), suggesting conserved roles of these genes at least in drought resistance. We therefore chose plants overexpressing *ZmPYL8* as representatives to measure the expression of drought-responsive marker genes. The results showed that the expression of all of these marker genes was enhanced in transgenic plants after drought stress (**Figure 6**). The increased expression of *ABA3*, *COR47*, *RD26*, *RD29A*, *RD29B*, *ABI1*, *ABI2*, *DREB2A*, which are known to respond to ABA, suggested enhanced ABA signaling in transgenic plants. P5CS1 is an enzyme responsible for proline biosynthesis (Kesari et al., 2012). The enhanced expression of *P5CS1* is consistent with the elevated accumulation of proline in *ZmPYL8* transgenic plants (**Figure 5D**). Taken together, these results suggested overexpression of *ZmPYL8* promoted ABA signaling, which, in turn, enhanced drought resistance of the transgenic plants.

Identification of Natural Variation in *ZmPYL* Genes Associated With Drought Resistance

Previous studies have identified one million SNPs in a maize panel consisting of 368 accessions (Fu et al., 2013). Using survival rates after severe drought stress as indices, the drought-resistance

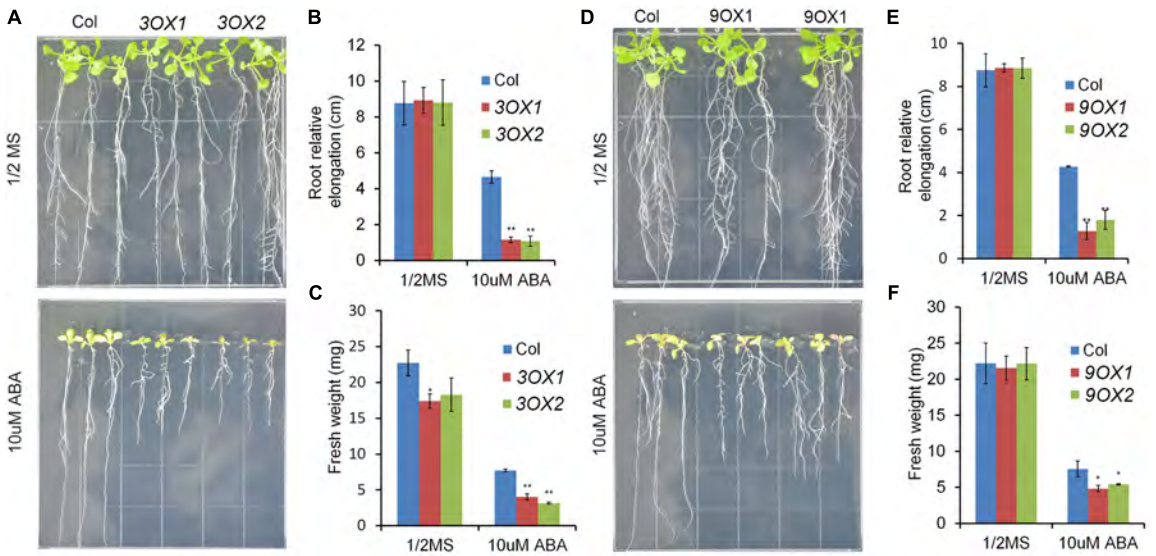

FIGURE 4 | Overexpression of *ZmPYL3*, *ZmPYL9* in *Arabidopsis* increased the sensitivity of plant growth to ABA. **(A–C)** Root growth phenotypes **(A)**, statistical analyses of root elongation **(B)**, and fresh weigh **(C)** of Col and *ZmPYL3* overexpression transgenic lines grown on ½ MS medium or ½ MS medium containing ABA (10 μM). **(D–F)** Root growth phenotypes **(D)**, statistical analyses of root elongation **(E),** and fresh weigh **(F)** of Col and *ZmPYL9* overexpression transgenic lines grown on ½ MS medium or ½ MS medium containing ABA (10 μM). Five-day seedlings were transferred from ½ MS medium to ½ MS medium containing ABA (10 μM), then grown vertically for 7 days before phenotype. Data represent the mean ± SD of three replicates for **(B)**, **(C)**, **(E)**, and **(F)**. Asterisks indicate the significance of *T*-test, $*p < 0.05$, $**p < 0.01$.

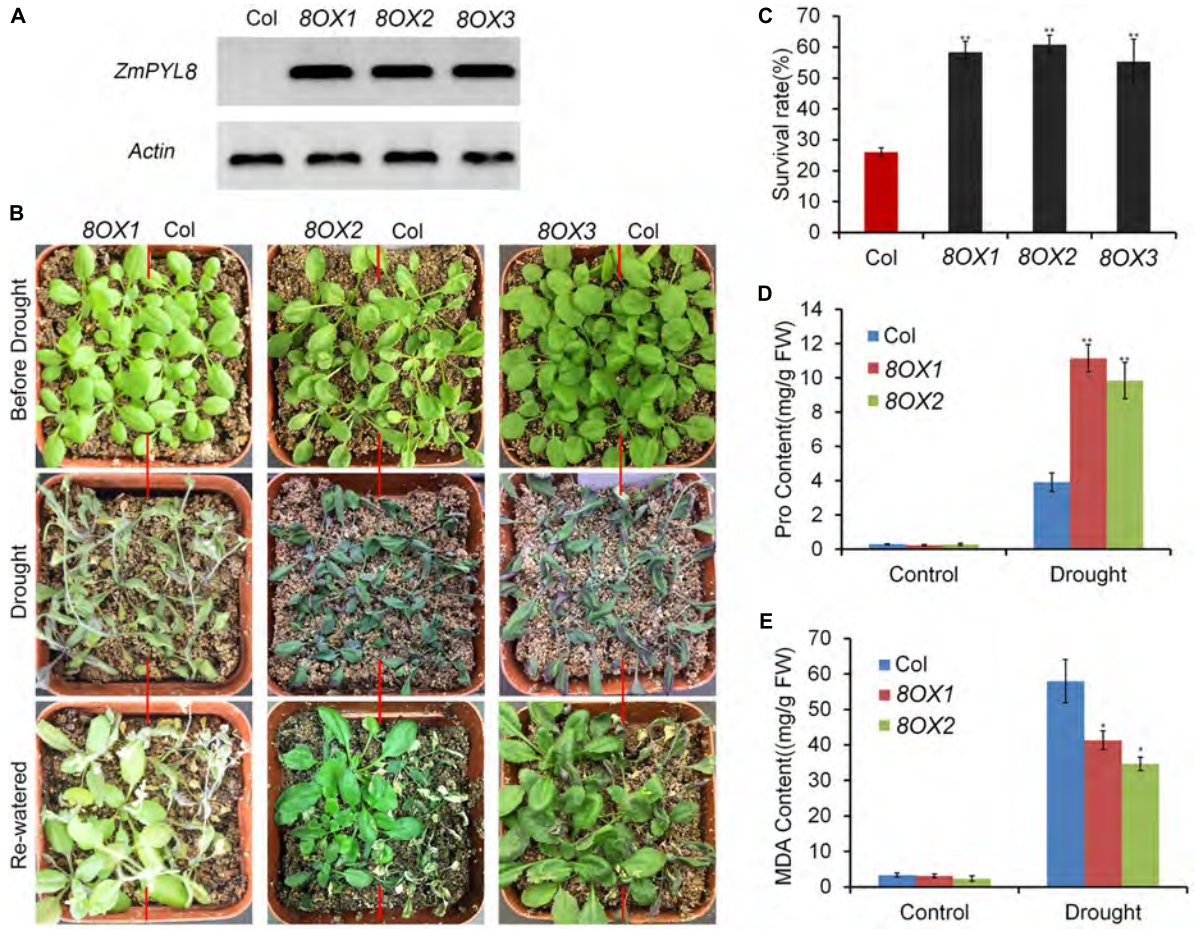

FIGURE 5 | Overexpression of *ZmPYL8* in *Arabidopsis* enhanced drought tolerance. **(A)** RT-PCR shows overexpression of *ZmPYL8* (8OX) in three independent transgenic lines. *Arabidopsis actin7* gene was used as control. **(B)** Drought tolerance assay of three transgenic lines overexpressing *ZmPYL8*. Three-week old plants were drought-stressed for 2 weeks and then rewatered for 1 day. **(C)** Survival rates of Col and *ZmPYL8* transgenic plants after drought stress. Data represent the mean ± SD of three replicates. **(D)** Proline contents of watered and drought-stressed Col and *ZmPYL8* transgenic plants. **(E)** Malondialdehyde (MDA) contents of watered and drought-stressed Col and *ZmPYL8* transgenic plants. Data represent the mean ± SD of three biological replicates. Asterisks indicate the significance of *T*-test, $*p < 0.05$, $**p < 0.01$.

phenotypes of these maize accessions were reported in several studies (Liu et al., 2013; Wang et al., 2016). To determine whether natural variation in *ZmPYL* genes was associated with maize drought resistance, we performed candidate gene association analyses with the MLM on *ZmPYL3*, *ZmPYL8*, *ZmPYL9*, *ZmPYL10*, *ZmPYL12*, which we identified as playing roles in regulation of ABA responses and/or drought resistance (**Figures 3–5** and Supplementary Figure S5). By using the genotypic and phenotypic data of the 368 accessions, we observed from association analyses that two genes, *ZmPYL8* and *ZmPYL12*, had natural variants that were significantly associated with drought resistance ($p \leq 0.01$, **Table 1**). The most significant *p*-value (lead *p*-value) was 0.00277 for *ZmPYL8* and 0.0018 for *ZmPYL12* (**Table 1**). Further analyses showed that the lead SNP (SNP1543, with lead *p*-value) in *ZmPYL8* was located in the third exon of this gene, and showed strong LD with another significant SNP (SNP1640) located downstream of the lead SNP (Supplementary Figure S6). The lead SNP of *ZmPYL12* (SNP415) was located in the second exon and showed strong LD with another significant SNP (SNP-52) located upstream of the lead SNP (**Figures 7A,B**). Further analyses identified the drought-resistant alleles of SNP415 and SNP-52 in *ZmPYL12* (**Figures 7C,D**). In the association populations, there were four major haplotypes (Hap), among which Hap4 was most drought-resistant (**Figure 7E**). In *ZmPYL8*, we did not detect drought-resistant alleles from the associated SNPs (data not shown).

DISCUSSION

Abscisic acid is well-known to be an important phytohormone regulating plant stress responses. A recent breakthrough in our understanding of ABA signaling came when two different groups identified the ABA receptors, the RCAR/PYL family proteins (Ma et al., 2009; Park et al., 2009). Subsequently, the functions of PYL

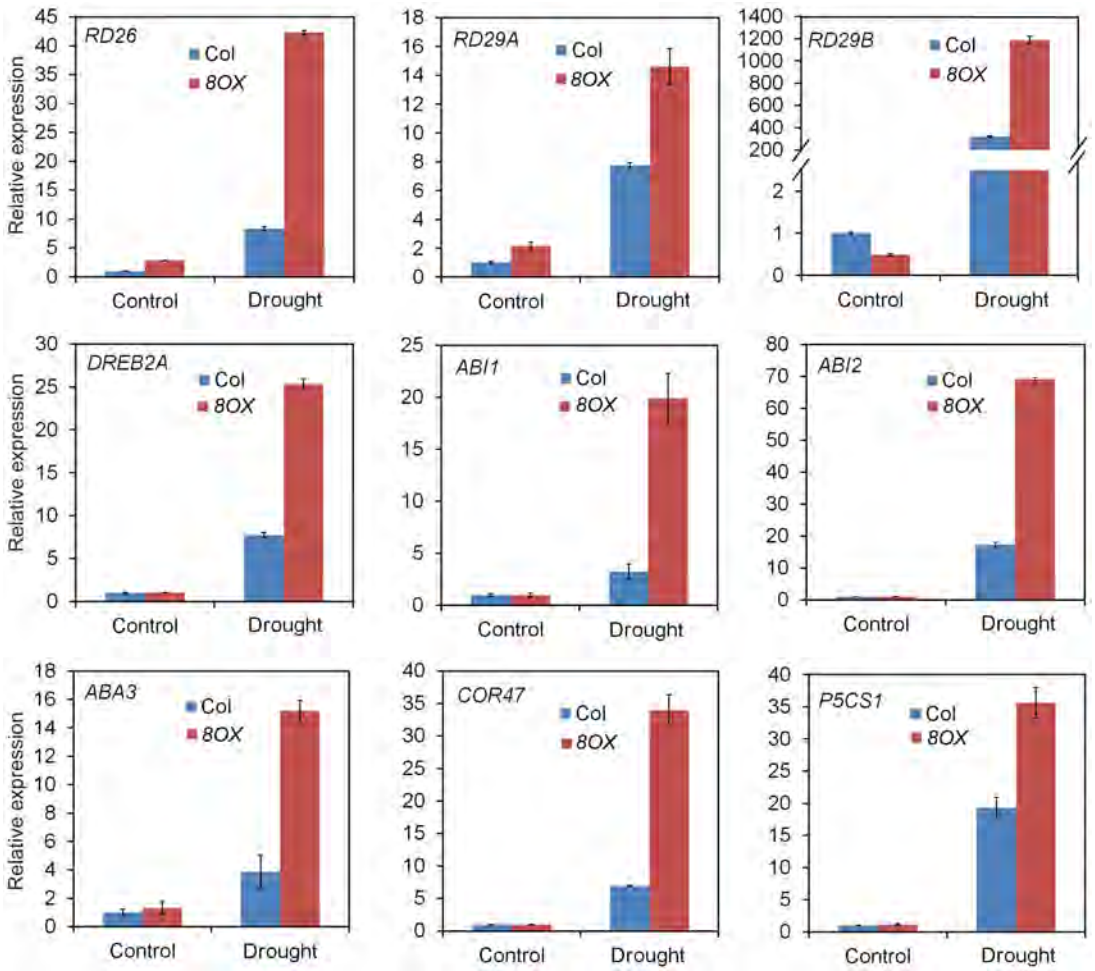

FIGURE 6 | Overexpression of *ZmPYL8* raised the expression of drought responsible marker genes. The expression of all marker genes under normal and drought conditions was examined by qRT-PCR. Three-week old plants were either watered or drought-stressed for 10 days.

TABLE 1 | Natural variations in *ZmPYL* genes associated with drought resistance in 368 maize inbred lines.

Gene ID	Name	Function	Polymorphic number*	MLM ($p \leq 0.01$)	Lead *p*-value
GRMZM2G154987	*ZmPYL3*	ABA	22	0	0.2909
GRMZM2G165567	*ZmPYL8*	Drought	40	2	0.00277
GRMZM2G133631	*ZmPYL9*	ABA, drought	26	0	0.04244
GRMZM2G063882	*ZmPYL10*	ABA	16	0	0.0436
GRMZM2G405064	*ZmPYL12*	Drought	8	2	0.0018

**MAF (Minor Allele Frequency) ≥ 0.05; ABA, abscisic acid; MLM, mixed linear model.*

receptors in regulation of ABA and stress responses have been widely studied (Klingler et al., 2010; Antoni et al., 2013; Liang et al., 2017; Pri-Tal et al., 2017). Maize is an important food and industrial crop worldwide and every year suffers yield losses due to drought. How ZmPYL ABA receptors are involved in maize drought resistance remains largely unknown. In this study, we comprehensively investigated the expression of *ZmPYL* genes in response to ABA and drought stresses, the roles of *ZmPYLs* in regulating ABA and drought responses and natural variants of *ZmPYL* genes associated with maize drought resistance.

Thirteen *ZmPYLs* genes were identified in this study. Analyses of the promoter sequences of these genes identified multiple *cis* elements, including ABRE and MBS, which have been reported to be involved in responses to ABA and drought stress (Seo et al., 2011; Singh and Laxmi, 2015). The changes in *ZmPYL* gene expression after ABA and drought stresses indicated the roles of these *cis* elements in regulation of gene expression. Intriguingly, most *ZmPYL* genes were down-regulated after drought treatment, whereas *ZmPYL8*, *ZmPYL9*, *ZmPYL2*, and *ZmPYL12* were up-regulated. After ABA treatment, most *ZmPYL*

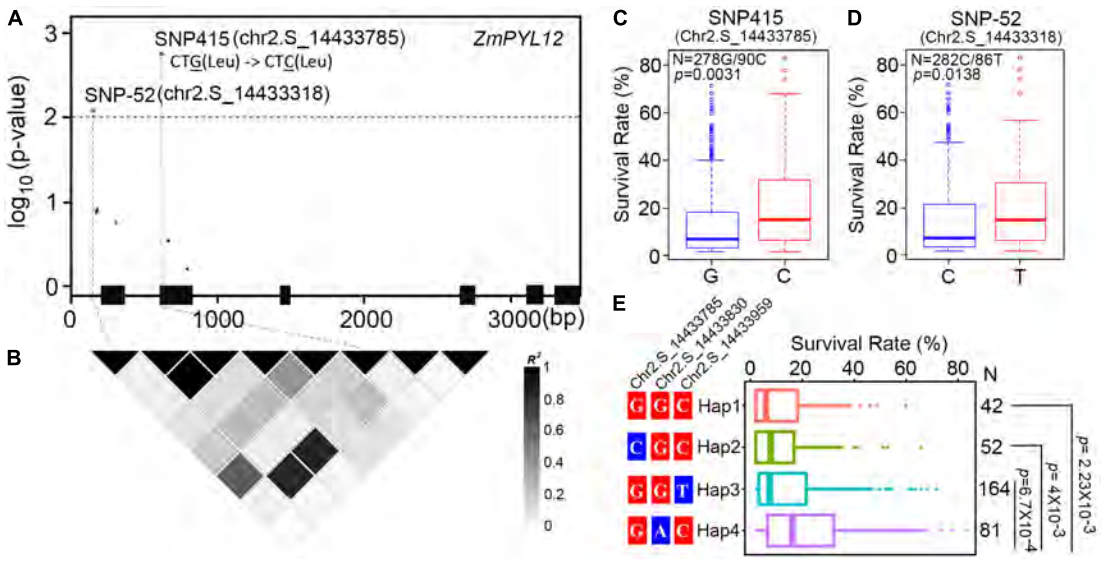

FIGURE 7 | Association analysis of genetic variations in *ZmPYL12* with maize drought tolerance. **(A)** Associations of *ZmPYL12* SNPs with drought tolerance. The gene structure is shown at the bottom. The significant associations are shown in red ($p < 0.01$). Exons and introns are shown as filled boxes and dark lines, respectively. SNP415 has G/C natural variations, but does not change the coding information of Leu. **(B)** LD map for *ZmPYL12* SNPs. Color in each block represents the R-squared value between two SNPs. **(C)** Association of two alleles in SNP415 with drought tolerance. **(D)** Association of two alleles in SNP-52 with drought tolerance. **(E)** Association of hyplotypes in *ZmPYL12* with drought tolerance.

genes were down-regulated, while *ZmPYL7* gene was up-regulated. Upon salt treatment, about 50% *ZmPYL* genes were down-regulated, while the rest were slightly affected or not changed. The different response patterns of *ZmPYL* genes after drought, ABA and salt treatments suggested diverse roles of *ZmPYLs* in regulation of plant abiotic stress responses. A previous study reported the expression of 11 *ZmPYLs* in response to ABA and PEG treatments (Fan et al., 2016). Both previous and this studies revealed very similar expression patterns of most *ZmPYL* genes in response to ABA, except *ZmPYL1-3* (Supplementary Figure S2; Fan et al., 2016). The various expression patterns of few *ZmPYLs* may be caused by different growth stages or environments for the experiments. Interestingly, *ZmPYLs* showed very different expression patterns in response to PEG or drought treatments. For instance, the expression of half of *ZmPYLs* was down-regulated under drought in this study, but the expression of most of *ZmPYLs* was up-regulated in response to PEG (**Figure 2**; Fan et al., 2016). These results suggested different effects of PEG and drought on *ZmPYL* expression.

To investigate the biological functions of *ZmPYLs*, we cloned all of the *ZmPYL* genes and overexpressed them in Arabidopsis plants, except *ZmPYL4* due to failure of detecting its expression in maize leaves. We observed that overexpression of four genes, *ZmPYL3*, *ZmPYL9*, *ZmPYL10*, and *ZmPYL13*, resulted in hypersensitivity to ABA treatment, suggesting negative roles of these genes in ABA responses in transgenic plants. This is very similar to what was observed in Arabidopsis, where *PYL* genes also played negative roles in ABA responses (Ma et al., 2009; Park et al., 2009), suggesting that the negative roles of these *PYL* genes in ABA responses are conserved across various plant species. There are 13 *ZmPYL* genes in maize, but surprisingly only four of them had roles in regulating ABA responses when ectopically expressed in Arabidopsis. One possibility is that the other *ZmPYL* genes have other roles rather than mediating ABA signaling. Considering that the expression levels of *ZmPYL1*, *ZmPYL4*, *ZmPYL5*, and *ZmPYL6* were also dramatically inhibited by ABA in maize but played no roles in regulation of ABA responses when ectopically expressed in Arabidopsis, another possible reason is that these *ZmPYL* genes may not function in Arabidopsis. Transgenic studies of these *ZmPYL* genes in maize may provide more precise evaluation of their roles in plant development and ABA responses.

In drought stress experiments, we observed that overexpressing *ZmPYL8*, *ZmPYL9*, and *ZmPYL12* in Arabidopsis, resulted in resistance of the transgenic plants to drought treatment, suggesting positive roles of these genes in drought responses. *ZmPYL8*, *ZmPYL9*, and *ZmPYL12* were clustered together in the phylogenetic tree (**Figure 1**). After drought treatment, *ZmPYL8*, *ZmPYL9*, and *ZmPYL12* showed very similar expression patterns in both shoots and roots (**Figure 2**). These observations indicated conserved roles of these genes in regulation of plant drought resistance. But the fact that only *ZmPYL9* was involved in regulation of both drought and ABA responses indicated functional diversity of these genes. A previous study reported the roles of Arabidopsis *PYLs* in plant drought stress responses by ectopically expressing these genes with various promoters, including the stress-inducible *RD29A* promoter, the *GC1* and *ROP11* promoters (guard cell-specific) and the *RBCS* promoter (green tissue-specific), as well as the constitutive 35S promoter (Zhao et al., 2016). Based on their experiments, different promoters resulted in different levels of drought resistance when these promoters were used to drive the

expression of various *PYL* genes (Zhao et al., 2016), indicating that the roles of plant *PYLs* in drought resistance depends on their temporal and spatial patterns of expression. In future, it will be worthwhile to use maize stress-inducible or tissue-specific promoters to study the functions of *ZmPYL* genes in regulation of drought resistance.

Developing new molecular markers is one of the most important topics in plant breeding. Thanks to the advances in high-throughput technologies, millions of SNP markers distributed throughout the whole genome at high density have been developed for various crops, including maize, rice, and other crops (Huang et al., 2011; Jiao et al., 2012; Fu et al., 2013; Zhou et al., 2015; Yano et al., 2016). Candidate gene association analyses, which are based on genetic variants and plant phenotypes, are widely used in dissecting the natural variation involved in plant drought resistance (Liu et al., 2013; Xiang et al., 2017). By using this association method, we detected natural variants of both *ZmPYL8* and *ZmPYL12* from a maize panel consisting of 368 natural accessions. Considering that these associations were most significant as compared to those detected in other *ZmPYL* genes which regulated ABA responses, and that *ZmPYL8* and *ZmPYL12* were proved to play positive roles in plant drought resistance, these associations are not false positive but real associations. Further analyses failed to detect resistant alleles in *ZmPYL8*, perhaps because they are not causal alleles of drought resistance. However, we detected resistant alleles in *ZmPYL12* (**Figure 7**), indicating that these alleles are causal alleles or have strong LD with the causal alleles.

Together, our results revealed the fundamental roles *ZmPYLs* in mediating ABA signaling and drought resistance in maize. Breeding of drought-resistant maize cultivars is an important goal for maize breeders. The drought-resistant *ZmPYLs* may be used as genetic resources in drought-tolerant breeding via transgenic approaches. Moreover, the resistant alleles or haplotypes detected in *ZmPYL12* have the potential to be used as molecular markers in genetic improvement of maize drought resistance.

AUTHOR CONTRIBUTIONS

MD and ZH designed the experiments. ZH and JZ conducted the experiments and analyzed the data. XS helped in the association and bioinformatic analyses. BW helped in the transgenic experiments. WT carefully edited the manuscript and analyzed the data. MD, ZH, and JZ wrote the manuscript. All authors revised the manuscript.

FUNDING

This study was supported by the Ministry of Science and Technology of China (2015BAD02B01), the Natural Science Foundation of China (31671256), the Fundamental Research Funds for the Central Universities of China (2662015PY170).

SUPPLEMENTARY MATERIAL

The Supplementary Material for this article can be found online at: https://www.frontiersin.org/articles/10.3389/fpls.2018.00422/full#supplementary-material

REFERENCES

Antoni, R., Gonzalez-Guzman, M., Rodriguez, L., Peirats-Llobet, M., Pizzio, G. A., Fernandez, M. A., et al. (2013). PYRABACTIN RESISTANCE1-LIKE8 plays an important role for the regulation of abscisic acid signaling in root. *Plant Physiol.* 161, 931–941. doi: 10.1104/pp.112.208678

Antoni, R., Gonzalez-Guzman, M., Rodriguez, L., Rodrigues, A., Pizzio, G. A., and Rodriguez, P. L. (2012). Selective inhibition of clade A phosphatases type 2C by PYR/PYL/RCAR abscisic acid receptors. *Plant Physiol.* 158, 970–980. doi: 10.1104/pp.111.188623

Bhaskara, G. B., Nguyen, T. T., and Verslues, P. E. (2012). Unique drought resistance functions of the *highly ABA-induced* clade A protein phosphatase 2Cs. *Plant Physiol.* 160, 379–395. doi: 10.1104/pp.112.202408

Bradbury, P. J., Zhang, Z., Kroon, D. E., Casstevens, T. M., Ramdoss, Y., and Buckler, E. S. (2007). TASSEL: software for association mapping of complex traits in diverse samples. *Bioinformatics* 23, 2633–2635. doi: 10.1093/bioinformatics/btm308

Clough, S. J., and Bent, A. F. (1998). Floral dip: a simplified method for *Agrobacterium*-mediated transformation of *Arabidopsis thaliana*. *Plant J.* 16, 735–743. doi: 10.1046/j.1365-313x.1998.00343.x

Dai, M., Zhang, C., Kania, U., Chen, F., Xue, Q., McCray, T., et al. (2012). PP6-type phosphatase holoenzyme directly regulates PIN phosphorylation and auxin efflux in *Arabidopsis*. *Plant Cell* 24, 2497–2514. doi: 10.1105/tpc.112.098905

Ding, S., Zhang, B., and Qin, F. (2015). *Arabidopsis* RZFP34/CHYR1, a ubiquitin E3 ligase, regulates stomatal movement and drought tolerance via SnRK2.6-mediated phosphorylation. *Plant Cell* 27, 3228–3244. doi: 10.1105/tpc.15.00321

Fan, W., Zhao, M., Li, S., Bai, X., Li, J., Meng, H., et al. (2016). Contrasting transcriptional responses of PYR1/PYL/RCAR ABA receptors to ABA or dehydration stress between maize seedling leaves and roots. *BMC Plant Biol.* 16:99. doi: 10.1186/s12870-016-0764-x

Fang, C., Ma, Y., Wu, S., Liu, Z., Wang, Z., Yang, R., et al. (2017). Genome-wide association studies dissect the genetic networks underlying agronomical traits in soybean. *Genome Biol.* 18:161. doi: 10.1186/s13059-017-1289-9

Fu, J., Cheng, Y., Linghu, J., Yang, X., Kang, L., Zhang, Z., et al. (2013). RNA sequencing reveals the complex regulatory network in the maize kernel. *Nat. Commun.* 4:2832. doi: 10.1038/ncomms3832

Fujii, H., and Zhu, J. K. (2009). Arabidopsis mutant deficient in 3 abscisic acid-activated protein kinases reveals critical roles in growth, reproduction, and stress. *Proc. Natl. Acad. Sci. U.S.A.* 106, 8380–8385. doi: 10.1073/pnas.0903144106

Fujita, Y., Fujita, M., Shinozaki, K., and Yamaguchi-Shinozaki, K. (2011). ABA-mediated transcriptional regulation in response to osmotic stress in plants. *J. Plant Res.* 124, 509–525. doi: 10.1007/s10265-011-0412-3

Hu, H., and Xiong, L. (2014). Genetic engineering and breeding of drought-resistant crops. *Annu. Rev. Plant Biol.* 65, 715–741. doi: 10.1146/annurev-arplant-050213-040000

Huang, X., Zhao, Y., Wei, X., Li, C., Wang, A., Zhao, Q., et al. (2011). Genome-wide association study of flowering time and grain yield traits in a worldwide collection of rice germplasm. *Nat. Genet.* 44, 32–39. doi: 10.1038/ng.1018

Jiao, Y., Zhao, H., Ren, L., Song, W., Zeng, B., Guo, J., et al. (2012). Genome-wide genetic changes during modern breeding of maize. *Nat. Genet.* 44, 812–815. doi: 10.1038/ng.2312

Joshi-Saha, A., Valon, C., and Leung, J. (2011). Abscisic acid signal off the STARting block. *Mol. Plant* 4, 562–580. doi: 10.1093/mp/ssr055

Kesari, R., Lasky, J. R., Villamor, J. G., Des Marais, D. L., Chen, Y. J., Liu, T. W., et al. (2012). Intron-mediated alternative splicing of *Arabidopsis P5CS1* and its association with natural variation in proline and climate adaptation. *Proc. Natl. Acad. Sci. U.S.A.* 109, 9197–9202.

Kim, T. H., Böhmer, M., Hu, H., Nishimura, N., and Schroeder, J. I. (2010). Guard cell signal transduction network: advances in understanding abscisic acid, CO_2, and Ca^{2+} signaling. *Annu. Rev. Plant Biol.* 61, 561–591. doi: 10.1146/annurev-arplant-042809-112226

Klingler, J. P., Batelli, G., and Zhu, J. K. (2010). ABA receptors: the START of a new paradigm in phytohormone signaling. *J. Exp. Bot.* 61, 3199–3210. doi: 10.1093/jxb/erq151

Lee, S. C., Lim, C. W., Lan, W., He, K., and Luan, S. (2013). ABA signaling in guard cells entails a dynamic protein-protein interaction relay from the PYL-RCAR family receptors to ion channels. *Mol. Plant* 6, 528–538. doi: 10.1093/mp/sss078

Li, W., Wang, L., Sheng, X., Yan, C., Zhou, R., Hang, J., et al. (2013). Molecular basis for the selective and ABA-independent inhibition of PP2CA by PYL13. *Cell Res.* 23, 1369–1379. doi: 10.1093/mp/sss078

Liang, C., Liu, Y., Li, Y., Meng, Z., Yan, R., Zhu, T., et al. (2017). *Activation* of ABA receptors gene *GhPYL9-11A* is positively correlated with cotton drought tolerance in transgenic *Arabidopsis*. *Front. Plant Sci.* 8:1453. doi: 10.3389/fpls.2017.01453

Liu, S., Wang, X., Wang, H., Xin, H., Yang, X., Yan, J., et al. (2013). Genome wide analysis of *ZmDREB* genes and their association with natural variation in drought tolerance at seedling stage of *Zea mays* L. *PLoS Genet.* 9:e1003790. doi: 10.1371/journal.pgen.1003790

Luo, X., Chen, Z., Gao, J., and Gong, Z. (2014). Abscisic acid inhibits root growth in Arabidopsis through ethylene biosynthesis. *Plant J.* 79, 44–55. doi: 10.1111/tpj.12534

Ma, Y., Szostkiewicz, I., Korte, A., Moes, D., Yang, Y., Christmann, A., et al. (2009). Regulators of PP2C phosphatase activity function as abscisic acid sensors. *Science* 324, 1064–1068. doi: 10.1126/science.1172408

Mao, H., Wang, H., Liu, S., Li, Z., Yang, X., Yan, J., et al. (2015). A transposable element in a *NAC* gene is associated with drought tolerance in maize seedlings. *Nat. Commun.* 6:8326. doi: 10.1038/ncomms9326

Meyer, R. S., Choi, J. Y., Sanches, M., Plessis, A., Flowers, J. M., Amas, J., et al. (2016). Domestication history and geographical adaptation inferred from a SNP map of African rice. *Nat. Genet.* 48, 1083–1088. doi: 10.1038/ng.3633

Miyazono, K., Miyakawa, T., Sawano, Y., Kubota, K., Kang, H. J., Asano, A., et al. (2009). Structural basis of abscisic acid signalling. *Nature* 462, 609–614. doi: 10.1038/nature08583

Mustilli, A. C., Merlot, S., Vavasseur, A., Fenzi, F., and Giraudat, J. (2002). Arabidopsis OST1 protein kinase mediates the regulation of stomatal aperture by abscisic acid and acts upstream of reactive oxygen species production. *Plant Cell* 14, 3089–3099. doi: 10.1105/tpc.007906

Nakashima, K., Takasaki, H., Mizoi, J., Shinozaki, K., and Yamaguchi-Shinozaki, K. (2012). NAC transcription factors in plant abiotic stress responses. *Biochim. Biophys. Acta* 1819, 97–103. doi: 10.1016/j.bbagrm.2011.10.005

Nakashima, K., Yamaguchi-Shinozaki, K., and Shinozaki, K. (2014). The transcriptional regulatory network in the drought response and its crosstalk in abiotic stress responses including drought, cold, and heat. *Front. Plant Sci.* 5:170. doi: 10.3389/fpls.2014.00170

Park, S. Y., Fung, P., Nishimura, N., Jensen, D. R., Fujii, H., Zhao, Y., et al. (2009). Abscisic acid inhibits type 2C protein phosphatases via the PYR/PYL family of START proteins. *Science* 324, 1068–1071.

Pizzio, G. A., Rodriguez, L., Antoni, R., Gonzalez-Guzman, M., Yunta, C., Merilo, E., et al. (2013). The PYL4 A194T mutant uncovers a key role of PYR1-LIKE4/PROTEIN PHOSPHATASE 2CA interaction for abscisic acid signaling and plant drought resistance. *Plant Physiol.* 163, 441–455. doi: 10.1104/pp.113.224162

Pri-Tal, O., Shaar-Moshe, L., Wiseglass, G., Peleg, Z., and Mosquna, A. (2017). Non-redundant functions of the dimeric ABA receptor BdPYL1 in the grass Brachypodium. *Plant J.* 92, 774–786. doi: 10.1111/tpj.13714

Roychoudhury, A., Paul, S., and Basu, S. (2013). Cross-talk between abscisic acid-dependent and abscisic acid-independent pathways during abiotic stress. *Plant Cell Rep.* 32, 985–1006. doi: 10.1007/s00299-013-1414-5

Rushton, D. L., Tripathi, P., Rabara, R. C., Lin, J., Ringler, P., Boken, A. K., et al. (2012). WRKY transcription factors: key components in abscisic acid signaling. *Plant Biotechnol. J.* 10, 2–11. doi: 10.1111/j.1467-7652.2011.00634.x

Santiago, J., Rodrigues, A., Saez, A., Rubio, S., Antoni, R., Dupeux, F., et al. (2009). Modulation of drought resistance by the abscisic acid receptor PYL5 through inhibition of clade A PP2Cs. *Plant J.* 60, 575–588. doi: 10.1111/j.1365-313X.2009.03981.x

Seo, P. J., Lee, S. B., Suh, M. C., Park, M. J., Go, Y. S., and Park, C. M. (2011). The MYB96 transcription factor regulates cuticular wax biosynthesis under drought conditions in *Arabidopsis*. *Plant Cell* 23, 1138–1152. doi: 10.1105/tpc.111.083485

Singh, D., and Laxmi, A. (2015). Transcriptional regulation of drought response: a tortuous network of transcriptional factors. *Front. Plant Sci.* 6:895. doi: 10.3389/fpls.2015.00895

Strable, J., and Scanlon, M. J. (2009). Maize (*Zea mays*): a model organism for basic and applied research in plant biology. *Cold Spring Harb. Protoc.* 2009:pdb.emo132. doi: 10.1101/pdb.emo132

Wang, H., and Qin, F. (2017). Genome-wide association study reveals natural variations contributing to drought resistance in crops. *Front. Plant Sci.* 8:1110. doi: 10.3389/fpls.2017.01110

Wang, X., Wang, H., Liu, S., Ferjani, A., Li, J., Yan, J., et al. (2016). Genetic variation in *ZmVPP1* contributes to drought tolerance in maize seedlings. *Nat. Genet.* 48, 1233–1241. doi: 10.1038/ng.3636

Wang, Y. G., Yu, H. Q., Zhang, Y. Y., Lai, C. X., She, Y. H., Li, W. C., et al. (2014). Interaction between abscisic acid receptor PYL3 and protein phosphatase type 2C in response to ABA signaling in maize. *Gene* 549, 179–185. doi: 10.1016/j.gene.2014.08.001

Xiang, Y., Sun, X., Gao, S., Qin, F., and Dai, M. (2017). Deletion of an endoplasmic reticulum stress response element in a *ZmPP2C-A* gene facilitates drought tolerance of maize seedlings. *Mol. Plant* 10, 456–469. doi: 10.1016/j.molp.2016.10.003

Yano, K., Yamamoto, E., Aya, K., Takeuchi, H., Lo, P. C., Hu, L., et al. (2016). Genome-wide association study using whole-genome sequencing rapidly identifies new genes influencing agronomic traits in rice. *Nat. Genet.* 48, 927–934. doi: 10.1038/ng.3596

Zhao, Y., Chan, Z., Gao, J., Xing, L., Cao, M., Yu, C., et al. (2016). ABA receptor PYL9 promotes drought resistance and leaf senescence. *Proc. Natl. Acad. Sci. U.S.A.* 113, 1949–1954. doi: 10.1073/pnas.1522840113

Zhou, Z., Jiang, Y., Wang, Z., Gou, Z., Lyu, J., Li, W., et al. (2015). Resequencing 302 wild and cultivated accessions identifies genes related to domestication and improvement in soybean. *Nat. Biotechnol.* 33, 408–414. doi: 10.1038/nbt.3096

Conflict of Interest Statement: The authors declare that the research was conducted in the absence of any commercial or financial relationships that could be construed as a potential conflict of interest.

frontiers in Plant Science

ORIGINAL RESEARCH
published: 26 July 2017
doi: 10.3389/fpls.2017.01314

Root Transcriptomic Analysis Revealing the Importance of Energy Metabolism to the Development of Deep Roots in Rice (*Oryza sativa* L.)

Qiaojun Lou[1,2†], Liang Chen[2†], Hanwei Mei[2], Kai Xu[2], Haibin Wei[2], Fangjun Feng[2], Tiemei Li[2], Xiaomeng Pang[2], Caiping Shi[3], Lijun Luo[2] and Yang Zhong[1*]*

[1] Department of Ecology and Evolutionary Biology, School of Life Sciences, Fudan University, Shanghai, China, [2] Shanghai Agrobiological Gene Center, Shanghai, China, [3] Shanghai Majorbio Bio-Pharm Technology Co., Ltd., Shanghai, China

Drought is the most serious abiotic stress limiting rice production, and deep root is the key contributor to drought avoidance. However, the genetic mechanism regulating the development of deep roots is largely unknown. In this study, the transcriptomes of 74 root samples from 37 rice varieties, representing the extreme genotypes of shallow or deep rooting, were surveyed by RNA-seq. The 13,242 differentially expressed genes (DEGs) between deep rooting and shallow rooting varieties (H vs. L) were enriched in the pathway of genetic information processing and metabolism, while the 1,052 DEGs between the deep roots and shallow roots from each of the plants (D vs. S) were significantly enriched in metabolic pathways especially energy metabolism. Ten quantitative trait transcripts (QTTs) were identified and some were involved in energy metabolism. Forty-nine candidate DEGs were confirmed by qRT-PCR and microarray. Through weighted gene co-expression network analysis (WGCNA), we found 18 hub genes. Surprisingly, all these hub genes expressed higher in deep roots than in shallow roots, furthermore half of them functioned in energy metabolism. We also estimated that the ATP production in the deep roots was faster than shallow roots. Our results provided a lot of reliable candidate genes to improve deep rooting, and firstly highlight the importance of energy metabolism to the development of deep roots.

Keywords: deep rooting, energy metabolism, *Oryza sativa* (rice), QTT (quantitative trait transcripts), RDR (ratio of deep roots), transcriptome, WGCNA (weighted gene co-expression network analysis)

OPEN ACCESS

Edited by:
Paul Christiaan Struik, Wageningen University and Research, Netherlands

Reviewed by:
Paola Leonetti, Consiglio Nazionale Delle Ricerche (CNR), Italy
Liezhao Liu, Southwest University, China

***Correspondence:**
Lijun Luo
lijun@sagc.org.cn
Yang Zhong
yangzhong@fudan.edu.cn

†These authors have contributed equally to this work.

Specialty section:
This article was submitted to Crop Science and Horticulture, a section of the journal Frontiers in Plant Science

Received: *02 May 2017*
Accepted: *12 July 2017*
Published: *26 July 2017*

Citation:
Lou Q, Chen L, Mei H, Xu K, Wei H, Feng F, Li T, Pang X, Shi C, Luo L and Zhong Y (2017) Root Transcriptomic Analysis Revealing the Importance of Energy Metabolism to the Development of Deep Roots in Rice (Oryza sativa L.). Front. Plant Sci. 8:1314. doi: 10.3389/fpls.2017.01314

INTRODUCTION

Drought stress is one of the most pressing issues inhibiting global agriculture today (Osakabe et al., 2014). But with the growing of world's population, more food must be produced with less fresh water (Fu et al., 2007; Zhang, 2007). Rice (*Oryza sativa* L.) is the main food for more than half of the world's population. Water deficit may reduce rice production seriously and threaten world food security (Serraj et al., 2009; Luo, 2010; Ahmadi et al., 2014). So, there is an urgent need to understand the underlying physiological and molecular mechanisms of drought resistance to sustain rice production in water-limiting areas (Nguyen et al., 1997; Lanceras et al., 2004; Rabello et al., 2008; Bernier et al., 2009; Serraj et al., 2011). As the main organ to uptake water in soil, root is the key contributor of plants' drought resistance (Kato et al., 2006; Henry et al., 2012). Therefore, recently root has become a hot area of research to improve drought resistance (Coudert et al., 2014).

Deep roots play important role in enhancing plants drought resistance, and it is an important component of roots architecture. According to the research of Uga (Uga et al., 2009; Uga, 2012), the roots distributing at 50–90° with the horizontal are recognized to be deep roots. The deep rooting varieties like upland rice usually have better drought resistance than shallow rooting varieties (Uga et al., 2013a; Lou et al., 2015). Over the course of evolution, the upland rice evolved a lot of adaptive mechanisms to cope with the environmental lack of water, like the feature of deep rooting possessing more and longer roots in deep soil (Kondo et al., 2003; Ding et al., 2011). Increasing deep roots ratio is a promising strategy to improving the drought resistance in rice. In recent years, progress has been made in detecting large effect quantitative trait loci (QTL) conferring the ratio of deep roots (RDR) in rice (Uga et al., 2011, 2012, 2013a,b, 2015; Kitomi et al., 2015; Lou et al., 2015). But, the knowledge about the genetics and molecular control of deep rooting in rice is still relatively limited, for example what genes control the deep rooting in rice and how these genes regulate the deep rooting in rice.

Comparative transcriptomes among specific samples is useful for exploring genes controlling various phenotypes and elucidating genetic mechanisms for plant's adaptation to adverse environments (Gan et al., 2011; Roberts et al., 2011; Yu et al., 2012). The current knowledge of transcriptome of drought resistance in plant mostly related to the comparative studies of different species with diverse genetic background and different ability of drought resistance (Moumeni et al., 2011). In this study, we investigated not only two groups of rice varieties with contrasting roots architecture but also 37 pairs of deep roots and shallow roots from one variety with the common genetic background. Differentially expressed genes (DEGs) were analyzed, and their expression patterns were further confirmed by microarray and qRT-PCR. Through weighted gene co-expression network analysis (WGCNA), we got some hub genes from the co-expressed DEGs, and found that the energy metabolism may play quite important role in the development of deep roots. Furthermore, to compare the difference of ATP synthesis between deep and shallow roots, we measured their oxygen consumption rates and found their rates were significantly different. Nowadays, association mapping has become an important bridge connecting phenotype and genotype to identify important genes controlling traits. So, besides the analysis of DEGs, the association mapping of the quantitative trait transcripts (QTT) with the phenotype was conducted. In our study, 10 QTTs genes associated to deep rooting were identified, and some of them also functioned in energy metabolism.

This study would help us to identify genes and mechanisms involved in the development of roots architecture. More importantly, this study could provide candidate genes to promote molecular breeding and genetic engineering projects for enhancing drought resistance in rice.

MATERIALS AND METHODS

Plant Materials and Growing Conditions

Through repeated phenotypic validation, 37 rice varieties were screened out from a set of more than 800 varieties (Lou et al., 2015). Fourteen of them are peculiar varieties with extremely deep rooting, fifteen peculiar varieties with extremely shallow rooting, and eight varieties with normally median root distribution (**Figure 1**, Table S1).

The experiment was conducted in the greenhouse at Shanghai Academy of Agricultural Sciences, Shanghai, China, in 2014 summer. In order to sample roots, the rice seedlings were cultured by hydroponic system using baskets placed in plastic boxes. The composition of nutrient solution was referred to the formula of International Rice Research Institute (IRRI), and the detailed parameters of the basket can be referred to our previous work (Lou et al., 2015). The roots emerging from the bottom and sides were regarded as deep roots (DR) and shallow roots (SR), respectively. For each variety, three baskets were used as replications and two seedlings were planted together in the center of each basket. After growing for 45 days, the tips about 1 cm long of roots were excised and immediately frozen in liquid nitrogen for RNA sampling. About 50 root tips from six plants of each variety were pooled as one sample. Thus, total mRNA of 74 samples (the deep roots sample and shallow roots sample were collected from each of the 37 varieties) was prepared for RNA-seq.

RNA Sequencing

Total RNA was extracted from root tips using Trizol reagent (Invitrogen, USA) and purified using Plant RNA Purification Reagent (Invitrogen, USA). The RNA quality was checked by Bioanalyzer 2100 (Aligent, USA), and the integrity number (RIN) of all these samples's RNA were >9.0.

According to the manufacturer's instructions (Illumina, USA), the sequencing libraries were prepared. Poly-A-containing mRNA was isolated from the total RNA by poly-T oligo-attached magnetic beads, and then fragmented by RNA fragmentation kit. The cDNA was synthesized using random primers through reverse transcription. After the ligation with adaptor, the cDNA were amplified by 15 cycles of PCR, and then 200-bp fragments were isolated using gel electrophoresis. At last, the products were sequenced by an Illumina HiSeq2500 instrument in Majorbio Co. Ltd. (China). The raw data had been submitted to NCBI Sequence Read Archive (SRA) with the Bioproject number PRJNA306542 from SRX1547421 to SRX1547494.

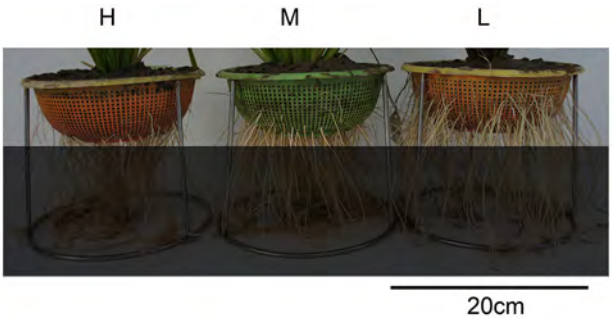

FIGURE 1 | Photos of three types of varieties with different root distribution. H is the deep rooting variety, M is the median rooting variety, and L is the shallow rooting variety.

RNA-Seq Data Analysis

After sequencing, we totally got 3,412,297,344 reads and about 345G bases raw data. After removing Illumina adapter sequences, and trimming low-quality bases, about 306G bases clean data was used in our analysis. Then, we mapped the reads to the Nipponbare MSU7.0 genomic reference (http://rice.plantbiology.msu.edu/index.shtml, Release 7) by the software TopHat v2.0.13 (http://tophat.cbcb.umd.edu/). According to the annotation of MSU7.0, there are 55,963 genes on the rice genome. The screening of DEGs was based on their FPKM (Reads per kilobase of exon model per million mapped reads) values (Mortazavi et al., 2008). The FPKM-value was calculated by the software of cufflinks from the website http://cole-trapnell-lab.github.io/cufflinks/ (Trapnell et al., 2012). The clustering of samples were carried out using the script of clust (method = "average") in R package. We compared the transcriptomic data in two levels: deep rooting varieties and shallow rooting varieties; and the deep roots and shallow roots from one variety. The comparative analysis of deep rooting varieties vs. shallow rooting varieties was carried out by Wilcox-test using R statistical software (https://www.r-project.org/). The paired comparative analysis of deep roots vs. shallow roots from one variety was conducted by the Cuffdiff software (http://cufflinks.cbcb.umd.edu/). A false discovery rate (FDR) of 0.05 was used for identifying significant DEGs. To inspect the functions of DEGs, the gene KEGG pathway enrichment analysis of the DEGs was performed by the software of KOBAS (http://kobas.cbi.pku.edu.cn/expression.php) and Fisher-test (Benjamini and Hochberg, 1995; Xie et al., 2011). Additionally, the software of Visual Genomics (http://www.vgenomics.cn/) was also used to data analysis and charting.

qRT-PCR and Microarray Confirmation

Some DEGs were selected for quantitative confirmation by quantitative real-time PCR (qRT-PCR) analysis with a BIO–RAD CFX96 Thermal Cycler (Bio-Rad, USA) (Livak and Schmittgen, 2001). After reversely transcription by PrimeScript RT reagent Kit (Takara, JP), we obtained the cDNA of the total mRNA. Then, the quantitative PCR reaction used SYBR Premix Ex Taq (Takara, JP). For each gene, the qPCR reactions were performed in biological triplicates.

Twelve 4*44K Agilent Rice Oligo Microarray (Agilent Technologies, Inc.) for six rice varieties were performed (Table S2). The samples were planted on June–July in the same place under the same growing condition as that operated in the experiment of RNA-Seq. The microarray experiments were conducted according to Agilent's manuals in SBC (Shanghai Biotechnology Corporation, China).

QTTs Analysis

The association mapping based on the four-omics datasets was called QTX mapping, including quantitative trait SNPs (QTS), QTT, quantitative trait proteins (QTP), and quantitative trait metabolites (QTM) (Zhou et al., 2013). In this study, QTT association mapping was conducted to detect QTT differences on phenotype. The prediction of random effects (q, qq) was obtained using QTXNetwork software based on GPU parallel computation (http://ibi.zju.edu.cn/software/QTXNetwork/). We calculated the QTTs using the transcriptome of deep roots and shallow roots, respectively. After normalized ($\log_2^{X+1}$), a total of 40,122 mRNA transcripts were used for QTTs mapping. The QTTs of three quantitative traits including SR, DR, and RDR were mapped.

WGCNA

WGCNA is a system biology method for describing the correlation patterns among genes across a group of special samples. WGCNA can be used for finding modules of highly correlated genes and hub genes with important effect. All the DEGs between shallow roots and deep roots from one variety by paired comparison with $P < 0.05$ were applied to WGCNA. The correlation of co-expressed genes in six different groups was analyzed: including the shallow roots sample (S); the deep roots sample (D); the group of deep rooting rice varieties (H); the group of shallow rooting rice varieties (L); and the group of median rooting rice varieties (M). In this study, the co-expressed genes involved in top 300 most correlated interactions were selected for further analysis (Aoki et al., 2007; Usadel et al., 2009).

Estimation of ATP Synthesis

Oxygen electrodes (Oxytherm, Hansatech) were set up and operated according to the manufacturer's instructions. The reaction solution is 2 ml K_2HPO_4 (20 mmolL^{-1}) solution at PH = 6.0 and full saturated by air before use. The reaction temperature was set at 25°C, and the speed of magnetic stirrer was set at 100. The reference sequence variety of Nipponbare was used in this experiment, and its fresh deep roots and shallow roots were sampled after 50 days cultivation in green house (25°C, dark 10 h; 35°C, light 14 h). Six pairs of samples of deep roots (D) and shallow roots (S) were replicated, and six intact root tips with 2 cm length were excised for each sample. Then the roots were soaked into reaction solution by injector to remove the surface oxygen and cut into 1 mm long pieces. Put the samples into electrode cuvette, about 5 min later, the oxygen depletion curves were generated to estimate the rates of oxygen consumption. The rate of oxygen consumption could be converted into rates of ATP production, because it was assumed that, in normoxic condition, the ATP:O_2 ratio was five, based on rates of phosphorylation completed in mitochondria (Chance and Williams, 1956; Gibbs and Greenway, 2003).

RESULTS

Gene Alignment and Sample Clustering

After RNA-sequencing, we totally got 295 billion pieces of clean reads, about 43 M reads for each sample (Table S3). On the average, about 92.60% of the reads could be mapped to the reference genomic sequence. And the Q20-values (the base-calling error probabilities = 99%) of the 74 samples are from 91.15 to 94.54%. After filtering, the expression profiles of 40,117 rice genes were used in further analysis.

Before clustering, the FPKM-values of the 40,117 genes were normalized by logarithm ($\log_2^{(FPKM+1)}$). Then, using these genes' expressing data (FPKM-values), the 74 samples were clustered into two groups (**Figure 2**). All the deep rooting samples were

FIGURE 2 | Clustering of the 74 samples by transcriptome data. H is the deep rooting rice varieties, L is the shallow rooting rice varieties, and M is the median rooting rice varieties. S indicates the shallow roots sample (the roots defined by an angle of 50° from the horizontal, centered on the stem of the rice plant), D indicates the deep roots sample (the roots defined by an angle of 40° from the vertical, centered on the stem of the rice plant).

clustered into one group (Cluster 1), while all the shallow rooting samples were clustered into another group (Cluster 2). Six median rooting varieties (M6, M5, M2, M3, M4, and M7) were located into Cluster 1 and only two median rooting varieties (M8, M9) were clustered into Cluster 2. The separate clustering of shallow and deep rooting varieties exhibited large difference at gene expression level between rice varieties with different root architectures.

Each pair of shallow roots and deep roots samples from the same variety was always stayed together in the clustering tree. This result was in full accordance with the clustering result by microarray (Figure S1). It indicated the genes' expression differences between roots with different spatial locations from the same variety were much smaller than the differences among roots from different varieties.

DEGs between the Deep and Shallow Rooting Varieties

Using the statistic method of Wilcox-test, we compared the transcriptomes of the deep rooting varieties to shallow rooting varieties with the criterion at FDR < 0.05. A total of 13,742 DEGs were detected between above-mentioned Cluster 1 vs. Cluster 2, while 13,242 DEGs were found between the deep rooting varieties compared with shallow rooting varieties (H vs. L) (**Figure 3A**). And there were 11,945 common DEGs that occupied about 90% of the total DEGs of H vs. L, so the comprehensive comparison between H and L could represent the comparison in all varieties. Furthermore, the DEGs of H vs. L, H vs. M (deep rooting varieties compared with median rooting varieties), and L vs. M (shallow rooting varieties compared with median rooting varieties) were pair-wise compared (**Figure 3B**).

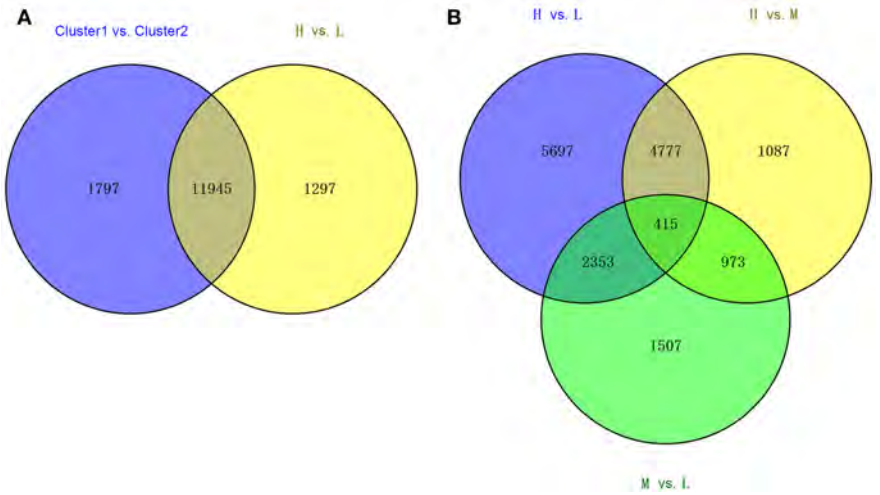

FIGURE 3 | The Venn diagram of the different collections of DEGs. **(A)** The overlaps of DEGS from Cluster1 vs. Cluster2 and the DEGs from H vs. L. **(B)** The overlaps of DEGs from three groups' comparison: H vs. L, H vs. M, and M vs. L. Cluster1 and Cluster2 was classified by clustering analysis referred to the **Figure 2**. H is the deep rooting rice varieties, L is the shallow rooting rice varieties, and M is the median rooting rice varieties.

The DEGs of H vs. L was more than the twice of L vs. M. There were 5,697 DEGs exclusively detected in H vs. L, while only 1,087 and 1,507 DEGs exclusively detected in H vs. M and L vs. M. The difference of gene expression pattern between deep rooting varieties and shallow rooting varieties was much greater than their difference with median rooting varieties.

Furthermore, we screened the DEGs using some criterions (**Table 1**). Firstly, the fold changes (average FPKM-values of H/L) were applied to screen candidate genes, and obtained 4,185 DEGs with fold changes >2: containing 1,634 DEGs with H/L < 0.5 and 2,551 DEGs with H/L > 2. It indicated more than half of the DEGs expressed higher in deep rooting varieties than shallow rooting varieties. Secondly, when considered the reliability of the data, the DEGS with high expression (average FPKM-values > 0.5) were selected for further analysis. There were 1,789 DEGs with average FPKM-values > 0.5 at least in one group (H and L): containing 1,403 DEGs with average FPKM-values > 0.5 in one of H or L group and 386 DEGs with average FPKM-values > 0.5 both in H and L group. In the end, these 1,789 genes most likely associated to roots' distribution were selected for enrichment analysis.

Based KEGG analysis (Kyoto Encyclopedia of Genes and Genomes, http://www.kegg.jp/), 10 pathways were significantly enriched using the 1,789 DEGs (**Table 2**). The first four all belong to the metabolism class involved in genetic information processing like DNA replication and mismatch repair. Another four pathways related to metabolism were significantly enriched too. Therefore, the difference in the genetic information processing and metabolism could distinct the deep rooting and shallow rooting varieties, and they contributed greatly to the differentiation of roots distribution in rice.

DEGs between the Deep and Shallow Roots from the Same Variety

In three group of rice varieties with deep, shallow and median rooting, totally 1,052 DEGs were detected with FDR < 0.05 between deep and shallow root samples (D vs. S) (Table S4). This number was far smaller than the DEG number of H vs. L. Only 599, 488, and 299 DEGs of D vs. S were identified in deep, shallow and median rooting varieties groups, respectively. Most of the DEGs have the same expression pattern in different varieties in the same group. In the deep rooting and median rooting group, more than half of the DEGs were up regulated especially in the median rooting varieties, while that was just the opposite in the shallow rooting varieties. These DEGs were enriched significantly in 18 KEGG pathways with $P < 0.05$, and 17 of them belong to metabolism pathways especially the energy metabolism (Table S5).

To narrow the candidate genes, the DEGs could be repeatedly detected in different rice varieties were chosen for further analysis. **Table 3** demonstrated the genes that could be repeatedly detected in more than three pairs of roots samples. More than half of the DEGs in **Table 3** were down regulated in H and L group, suggesting the repeatedly detected DEGs expressed higher in deep roots than in shallow roots in H and L rice groups. But in the median group (M), it was completely opposite because all the DEGs were expressed higher in shallow roots than in deep roots except LOC_Os11g24140. Nine genes in **Table 3** could be detected both in at least four deep and four shallow rooting varieties, and three genes can be detected both in more than three median and four shallow rooting varieties. The gene of LOC_Os02g37190 could be detected in all three groups. In Minghui 63 rice variety, LOC_Os02g37190 expressed higher in roots than all other tissues of plant (Wang et al., 2010). Four genes in **Table 3** (LOC_Os02g48710, LOC_Os05g48890,

TABLE 1 | The list of differentially expressed genes (DEGs) between deep rooting and shallow rooting varieties under different criteria.

			Number of DEGs
FDR < 0.05			13,242
	Fold changes > 2		4,185
	H/L > 2		2,551
	H/L < 0.5		1,634
		Average FPKM > 0.5	1,789
		H or L > 0.5	1,403
		Both H and L >0.5	386

TABLE 2 | KEGG pathway enrichment analysis of 1,789 genes differentially expressed between deep rooting and shallow rooting rice varieties.

KEGG pathway	ID	*P*-values	Classification
DNA replication	ko03030	0.000657	Genetic information processing
Mismatch repair	ko03430	0.000669	Genetic information processing
Nucleotide excision repair	ko03420	0.002917	Genetic information processing
Homologous recombination	ko03440	0.0041	Genetic information processing
Metabolism of xenobiotics by cytochrome P450	ko00980	0.007219	Metabolism
Drug metabolism—cytochrome P450	ko00982	0.007219	Metabolism
Plant-pathogen interaction	ko04626	0.021512	Organismal systems
MAPK signaling pathway	ko04010	0.028472	Environmental information processing
Phenylpropanoid biosynthesis	ko00940	0.045928	Metabolism
Phenylalanine, tyrosine and tryptophan biosynthesis	ko00400	0.049828	Metabolism

The DEGs used here meet three criteria: FDR < 0.05, fold changes > 2 and average FPKM > 0.5 as this table shows.

TABLE 3 | The number of differentially expressed genes (shallow roots vs. deep roots) that could be repeatedly detected in more than three varieties.

Gene ID	Ups^H	$Downs^H$	Ups^L	$Downs^L$	Ups^M	$Downs^M$
LOC_Os01g07850			4	0	4	0
LOC_Os01g22670					3	0
LOC_Os01g57958	0	10	0	5		
LOC_Os01g57968	0	8	0	6		
LOC_Os01g71340	3	3	1	3		
LOC_Os02g37190	4	0	4	0	3	0
LOC_Os02g37250					3	0
LOC_Os02g48710			4	0		
LOC_Os03g05640			0	4		
LOC_Os03g31750			0	6		
LOC_Os04g16722	0	10	0	7		
LOC_Os04g56100			7	0		
LOC_Os05g15880	0	5	1	3		
LOC_Os05g48200			0	7		
LOC_Os05g48890			5	0		
LOC_Os06g31960			4	0		
LOC_Os07g25050					3	0
LOC_Os07g25060					3	0
LOC_Os09g00999			0	8		
LOC_Os09g01000	0	7	0	7		
LOC_Os09g24370					4	0
LOC_Os10g21346			0	5		
LOC_Os10g21372	0	7	0	7		
LOC_Os11g24140	3	5	0	6	1	3
LOC_Osm1g00500	0	6				
LOC_Osp1g00770	0	4				
LOC_Osp1g01040			0	4		

Ups were the up regulated genes that expressed higher in shallow roots than in deep roots; Downs were just the opposite. Superscript H is the group of deep rooting rice varieties, superscript L is the group of shallow rooting rice varieties and superscript M is the group of median rooting rice varieties.

LOC_Os04g56100, and LOC_Os09g00999) appeared only in a single group. All of them were detected only in the shallow rooting varieties group, so these genes might exclusively function in the shallow rooting varieties. Furthermore, it was interesting to find almost all the genes expressed the same trend in different varieties within a group, no matter the deep rooting varieties or the shallow rooting ones. For example, LOC_Os01g57958 gene was down regulated both in 10 H varieties and in five L varieties. It suggested these genes have no variety-specificity, and they belong to organ-specificity genes.

DEGs Related to Root Development

According to the review of Jung and Mccouch (2013), totally about 1,380 candidate genes may control the architecture development of roots in rice. In this study, 1,052 DEGs were found between the shallow roots and the deep roots from the same variety as above analysis. And 75 of the DEGs were overlapped with the 1,380 genes that had been reported to be responsible for the roots architecture (Tables S6, S7). Through χ^2-test, we could found these DEGs were significantly enriched in the collection of the genes controlling the architecture of roots in rice, and the *P*-value (asymptotic significance two-sided) of Pearson Chi-Square-test was little to 8.04E-22.

To further study the 75 overlapped genes that related to roots architecture, we quantified the expression of these genes in two rice varieties: H32 and L16 using microarray and qRT-PCR. Forty-nine genes of the 75 overlap genes were detectable by at least two methods. **Table 4** indicated these 49 genes' expression ratio in shallow roots to deep roots (S/D) measured by RNA sequencing, qRT-PCR, and microarray. Almost all genes had the same expression trend among the three methods, and only a few genes' expressions measured by microarray were inconsistent. The correlation coefficients of these DEGs expression profiles obtained by different methods were all much larger than the significant threshold of 0.28 (Table S8). It suggested the reproducibility among these three methods of transcriptomic surveying was excellent, and the expression patterns of the DEGs were stable even using the samples cultured in different time. Between the deep rooting variety (H32) and the shallow rooting

TABLE 4 | Verification of 49 candidate genes relating to rice roots architecture by real time PCR quantification and RNA microarray.

	RNA-seq		qRT-PCR		Chip	
	H32s/d	L16s/d	H32s/d	L16s/d	H32s/d	L16s/d
LOC_Os01g04800	1.14	0.79	1.37	0.76	1.53	1.40
LOC_Os01g10040	1.28	1.18	1.84	1.55	1.70	1.06
LOC_Os01g42380	1.06	0.54	1.09	0.64	1.18	0.31
LOC_Os01g50820	0.66	0.87			0.71	0.44
LOC_Os01g58240	0.84	0.59	0.65	0.42	0.94	0.97
LOC_Os01g58290	1.23	2.17	1.20	1.89	2.13	0.75
LOC_Os01g63980	0.36	0.24	0.44	0.18	0.52	0.44
LOC_Os01g72140	0.62	0.74	0.31	0.46	0.39	0.56
LOC_Os01g72550			1.16	1.05	1.02	1.13
LOC_Os02g02190	0.31	3.47	0.25	1.02	1.76	0.55
LOC_Os02g11760	1.20	0.87	1.14	0.83	1.64	0.62
LOC_Os02g17900	0.51	0.12	0.25	0.14	1.74	0.28
LOC_Os02g20360	0.74	0.68	0.76	0.54	0.90	0.79
LOC_Os02g32590	0.69	0.57	0.55	0.67	0.35	0.38
LOC_Os02g40710	0.70	0.46			0.88	0.44
LOC_Os02g49440	1.03	1.45			0.79	1.01
LOC_Os03g08754	0.99	2.04	0.63	1.59	0.87	0.95
LOC_Os03g09880	0.49	0.59	0.18	0.23	0.77	0.72
LOC_Os03g49260	1.20	0.92	1.23	0.79	1.61	1.33
LOC_Os03g50960	0.49	0.41			0.66	0.60
LOC_Os03g52860	1.08	2.16	1.73	2.04	2.07	3.59
LOC_Os03g60570	0.78	0.57			0.33	0.34
LOC_Os04g08350	2.23	1.06	1.24	1.46	1.00	1.49
LOC_Os04g33900	1.60	3.29			0.67	0.48
LOC_Os04g44060	0.62	0.87	0.42	0.94	0.83	1.14
LOC_Os04g46810	1.74	2.31	1.56	1.17	3.33	4.95
LOC_Os04g46820	1.92	2.58	1.87	1.04	3.41	4.83
LOC_Os04g49150	0.00	2.59	0.09	2.73	1.03	2.32
LOC_Os04g51460	0.88	0.96	0.75	0.73	2.33	0.52
LOC_Os05g02070	0.96	0.86	0.58	0.67	0.54	0.52
LOC_Os05g45410	0.84	0.68	0.51	0.67	0.71	0.76
LOC_Os05g48890	1.72	2.16	1.89	1.75	1.40	1.93
LOC_Os06g06350	0.95	0.95	0.68	0.51	0.71	1.33
LOC_Os06g36850	0.00	1.45	0.14	1.60	0.54	1.34
LOC_Os06g48200	0.96	1.97	0.84	1.69	0.79	1.05
LOC_Os07g39320	1.68	0.79			1.65	0.90
LOC_Os08g02070	0.78	0.84	0.66	0.48	0.43	0.56
LOC_Os08g24790	0.97	1.32			0.47	0.97
LOC_Os08g37210	1.11	0.52	0.93	0.90	1.93	1.02
LOC_Os08g37250	0.63	0.91	0.47	0.74	0.87	0.64
LOC_Os08g41720	1.24	0.68	1.67	0.87	1.93	0.25
LOC_Os08g44270	0.78	1.36	0.56	0.86	0.74	0.69
LOC_Os10g07510	1.64	0.84			1.67	1.02
LOC_Os10g38740	0.83	1.14			1.09	5.28
LOC_Os10g39130	3.40	0.84	1.82	0.48	1.46	0.73
LOC_Os10g40520	1.38	1.16			1.58	1.06
LOC_Os11g16970	0.85	1.15			0.89	1.81
LOC_Os11g18366	0.78	2.94	0.70	1.88	0.92	1.12
LOC_Os11g45280	1.58	2.95	1.27	1.57	2.35	1.96
Average	1.03	1.26	0.90	1.01	1.22	1.21

s/d is the ratio of gene's expression in shallow roots contrast to deep roots.

variety (L16), some genes had different expression trend, for example LOC_Os10g39130 expressed significantly higher in the shallow roots of H32 than that in L16. The average values of all the genes' expression ratios of s/d were near 1, because the expression directions of the 49 DEGs were different and neutralized by each others. In the results of RNA-Seq and qRT-PCR, the average ratios of s/d in L16 (1.26 vs. 1.03) were a little larger than that in H32 (1.01 vs. 0.90), suggesting these genes might express higher in shallow roots of shallow rooting variety than that in deep rooting variety.

Quantitative Real-Time PCR Validation of Candidate Genes

To further verify and study the function of some putative genes, four DEGs were chosen for qRT-PCR-test. Two DEGs (LOC_Os01g47400 and LOC_Os01g08780) of H vs. L that were located on the known QTL intervals controlling RDR had been reported in our previous study (Lou et al., 2015) were carried out qRT-PCR-test in 14 rice varieties that were randomly chosen from all the rice varieties (**Figures 4A,B**). LOC_Os01g47400 is an Osman01-endo-beta-mannanase, belongs to glycosyl hydrolase superfamily. LOC_Os01g08780 contains the phosphatase family domain, behaving as an inositol polyphosphate 5-phosphatase I. LOC_Os01g47400 and LOC_Os01g08780 both expressed differently in H and L groups. Their mRNA levels were significantly higher in H group than in L group varieties. So the activity of these two enzymes in deep rooting varieties may be higher than that in shallow rooting varieties.

Two other DEGs (LOC_Os01g57968 and LOC_Os04g16722) of D vs. S from **Table 3** were selected for qRT-PCR-test in 28 RNA samples including 14 deep roots samples and 14 shallow roots samples (**Figures 4C,D**). The results of qRT-PCR coincided with the results of transcriptomic sequencing. In some rice varieties, those two genes both expressed differently in shallow roots and deep roots. The relative mRNA level of LOC_Os01g57968 in the deep roots was higher than its expression in the shallow roots, and their expression differences were especially dramatical in the shallow rooting group (L). But, for the gene of LOC_Os04g16722 with ycf68 domain, its transcriptomic difference was more significant in the deep rooting varieties group (H) than in the shallow rooting varieties group (L). Those candidate genes were in the process of genetic function verification by transgenic test.

QTT Mapping

The QTT module in QTXNetwork was applied to screen significant transcripts and to predict their effects on phenotype. There were a total of 10 QTTs that were detected to control the vertical distribution of roots in rice (**Table 5**). Four of them were overlapped with the DEGs between deep rooting and shallow rooting varieties. Seven QTTs were identified in the deep roots, and three QTTs were found in the shallow roots. There was no overlap between the QTTs of deep roots and shallow roots. Most of the QTTs detected in this study were single gene locus, and only one of them had qq interactions. The qq interaction

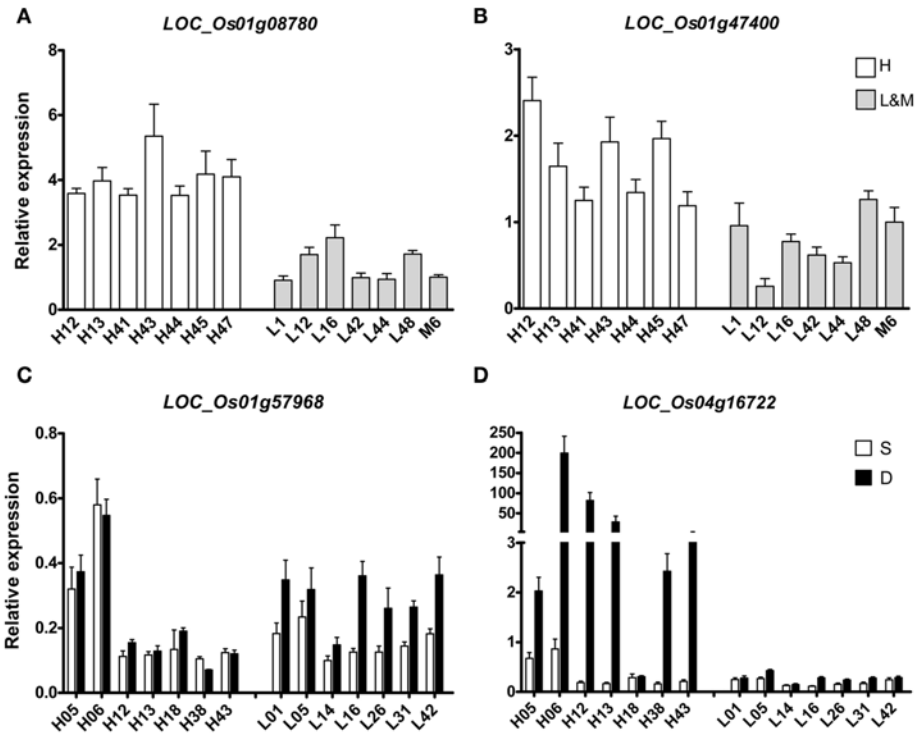

FIGURE 4 | qRT-PCR of four candidate DEGs in the roots of 14 rice varieties. **(A,B)** indicated two DEGs that differentially expressed between deep rooting and shallow rooting varieties; **(C,D)** indicated two DEGs that differentially expressed between deep roots and shallow roots from one variety.

TABLE 5 | Estimated heritability of QTTs for three traits of Root.

Transcriptome	Trait	Locus	Q/QQ	*P*-value	h^2
Deep roots	DR	LOC_Os01g15860× LOC_Os05g49980	122.22	1.60E-14	0.42
		LOC_Os01g02280	141.04	2.19E-18	0.56
	SR	LOC_Os01g65150	235.13	9.52E-05	0.29
		LOC_Os10g28400	353.52	1.51E-05	0.65
	RDR	LOC_Os01g42430	12.10	2.76E-03	0.23
		LOC_Os03g44840	15.69	1.66E-03	0.39
		LOC_Os08gG06810	−10.19	5.85E-04	0.17
Shallow roots	*SR*	*LOC_Os01g42140*	*543.71*	*3.89E-08*	*0.95*
	RDR	*LOC_Os03g08230*	*−33.02*	*8.20E-10*	*0.61*
		LOC_Os09g10860	*24.19*	*1.26E-05*	*0.33*

Q/QQ: Additive effect on the phenotype when the expression of the gene increasing two units. Two sets of transcriptome data were calculated in this study, the first half of the table showed the results of QTTs mapping using the deep roots transcriptomes, the second half of the table (italic effect) showed the results of QTTs mapping using the shallow roots transcriptomes.

of LOC_OS01G15860 × LOC_OS05G49980 might affect the DR (the number of deep roots) of rice with the h^2 of 42%.

RDR was the RDR, so it was decided by the number of deep roots and shallow roots. Three genes (LOC_OS01g42430, LOC_OS03g44840, and LOC_OS08g06810) in deep roots and two genes (LOC_OS03g08230 and LOC_OS09g10860) in shallow roots were identified to influence the RDR. Four genes of the QTTs (LOC_Os01g42430, LOC_Os01g65150, LOC_Os05g49980, and LOC_Os10g28400) were also found to be differentially expressed between deep rooting and shallow rooting varieties (Table S9), and two of them (LOC_Os01g42430 and LOC_Os01g65150) were annotated to be related to energy metabolism: LOC_Os01g42430 contributes to energy production while LOC_Os01g65150 relates to energy consumption.

Co-expressed Genes Network

WGCNA could find the network of associated genes with certain functions and identify new genes (Brown et al.,

2005). We analyzed the co-expression network of DEGs in 6 different groups of samples. Totally 9820 DEGs of D vs. S with $P < 0.05$ were used in WGCNA. After analysis, the top 300 interactions of correlated DEGs were chosen for further analysis (Table S10). The average weights of the top 300 co-expressed interactions in these six groups ranged from 0.44 to 0.65. In shallow rooting materials, the correlations among the DEGs were much closer than any other groups.

Through WGCNA analysis, one big module having comprehensive interaction was found, and almost all the genes were clustered into this big module (**Figure 5**). Inside of the module, there were some hub genes having many co-expressed genes. **Table 6** indicated the information of the hub genes with ≥7 significantly co-expressed genes. From this table, two obvious phenomena could be found: (1) half of the hub genes are from the mitochondria genome; (2) more than half of the hub genes relate to energy metabolism, especially relate to ATP biosynthesis. Furthermore, except LOC_Os12g34108, all the 17 hub genes in **Table 6** expressed significantly higher in deep roots than in shallow roots. So we can infer that the deep roots have stronger energy metabolism compared with the shallow roots. Besides the genes related to energy metabolism, the other hub genes belong to two other types: five hub genes of them act on transcription and translation, and three hub genes are uncharacterized proteins.

Estimation of ATP Synthesis

To estimate the rates of ATP synthesis, we measured the rate of oxygen consumption in roots for there were fixed ratio between the oxygen consumption and ATP synthesis in respiration reaction (Greenway and Gibbs, 2003; Edwards et al., 2012).

The rates of O_2 consumption between the deep roots and the shallow roots from the same plants were significantly different, and the deep roots used more oxygen than

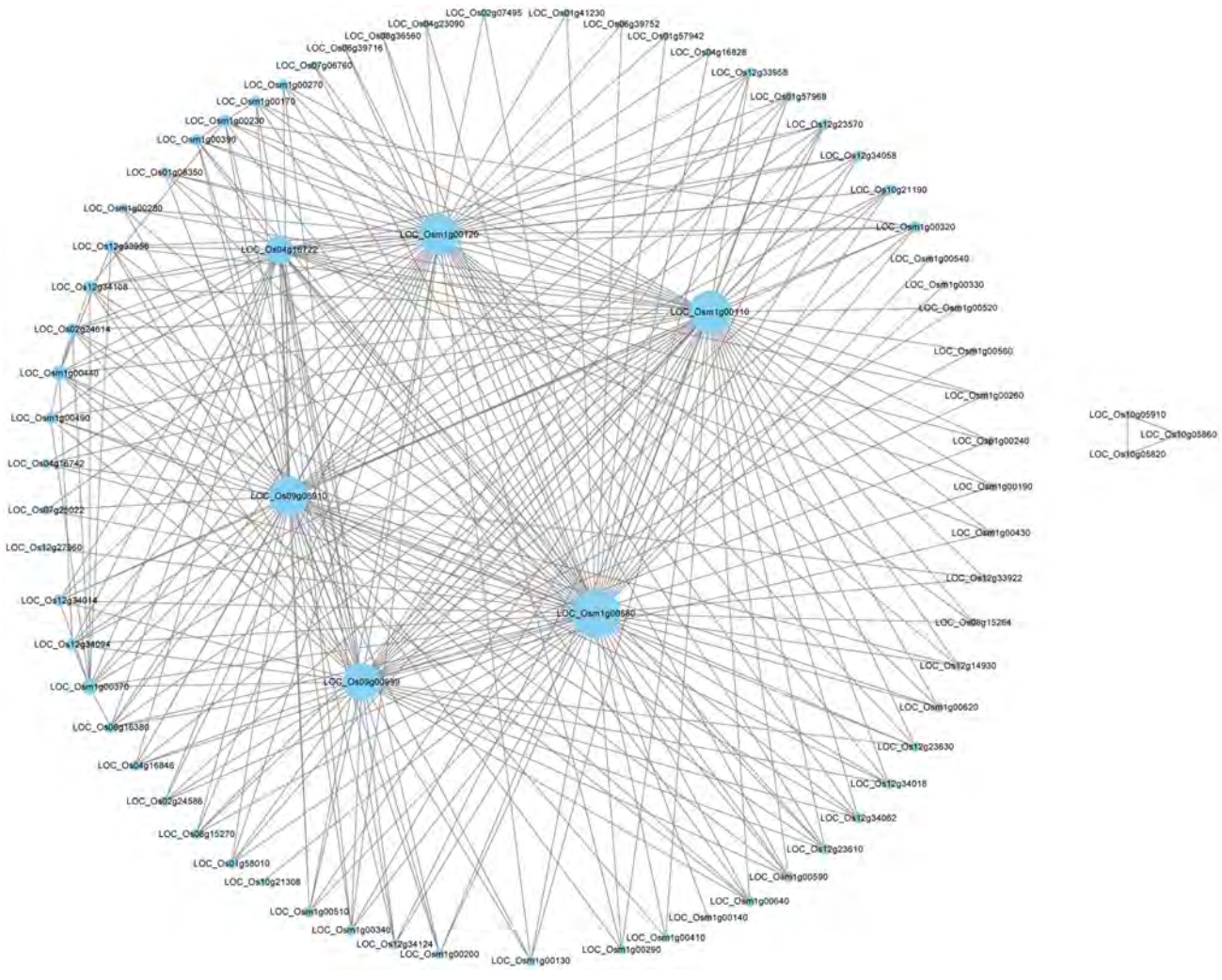

FIGURE 5 | The network of the top 300 co-expressed genes pairs from WGCNA. The WGCNA (weighted gene co-expression network analysis) used all DEGS of deep roots vs. shallow roots with $P < 0.05$ in whole samples.

TABLE 6 | The annotation of the hub genes with ≥7 co-expressed genes identified by WGCNA.

Node	Num	*P*-value	Fold change	Gene annotation	GO term
LOC_Osm1g00580	63	5.80E-03	6.14	ATP synthase F0 subunit 1	**ATP biosynthetic process**
LOC_Osm1g00110	54	4.40E-03	10.73	Cytochrome c oxidase subunit 3	**Respiratory electron transport chain**
LOC_Osm1g00120	52	7.90E-03	9.79	Hypothetical protein	**ATP synthesis coupled proton transport**
LOC_Os09g08910	48	3.42E-03	4.63	ATP synthase subunit alpha	**Response to stress**
LOC_Os09g00999	46	2.76E-03	4.62	Putative uncharacterized protein P0459B01.16	Unannotated
LOC_Os04g16722	32	2.17E-03	4.85	Uncharacterized protein ycf68	Unannotated
LOC_Osm1g00370	13	2.48E-03	6.77	ATP synthase F0 subunit 6	**ATP synthesis coupled proton transport**
LOC_Osm1g00440	12	1.80E-03	6.37	Ribosomal protein L2	*Translation*
LOC_Os12g34108	9	8.80E-02	1.39	ATP synthase protein 9	**Transporter activity**
LOC_Osm1g00230	9	8.73E-03	7.19	NADH dehydrogenase subunit 7	**Oxidation-reduction process**
LOC_Os02g24614	8	1.48E-02	3.53	DNA-directed RNA polymerase subunit beta	*Transferase activity*
LOC_Os12g33956	8	1.28E-02	3.19	Maturase	*Transferase activity*
LOC_Os12g34094	8	8.04E-03	4.66	NADH-ubiquinone oxidoreductase chain 4	**Generation of precursor metabolites and energy**
LOC_Os06g16380	7	7.97E-03	8.51	Expressed protein	Unannotated
LOC_Os12g34014	7	7.52E-03	10.62	NADH-ubiquinone oxidoreductase chain 6	**Generation of precursor metabolites and energy**
LOC_Osm1g00320	7	2.60E-02	5.29	NADH dehydrogenase subunit 4	**Oxidation-reduction process**
LOC_Osm1g00390	7	2.74E-02	10.18	Ribosomal protein S13	*Translation*
LOC_Osm1g00490	7	1.04E-02	3.03	Maturase-related protein	*mRNA processing*

The boldface in the "Node" column highlighted the genes located on the mitochondria genome. Num, is the number of co-expressed genes with the node gene in the first column; P-value, is the significance of the paired t-test of the gene expression between 37 pairs of deep roots and shallow roots in the same variety; Fold change, the average fold changes of the 37 pairs of gene expressions between the deep roots and shallow roots from the same variety. The boldface in the "GO Term" column highlighted the genes related to energy metabolism, and the italic highlighted the genes related to transcription and translation.

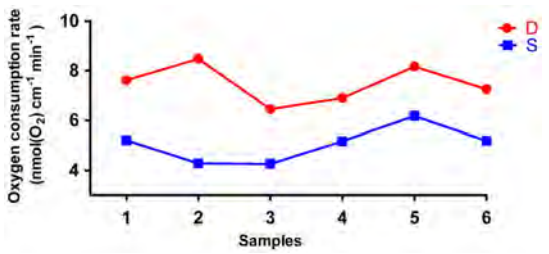

FIGURE 6 | The oxygen consumption rates of six pairs of deep roots and shallow roots. D is deep roots and S is shallow roots. The 1–6 at X-axis is the six replicates of the samples.

shallow roots in all six pairs of samples (**Figure 6**). The average rate of oxygen consumption of the deep roots was approximately 7.5 $\mathrm{nmol(O_2)\,cm^{-1}\,min^{-1}}$, and the average rate of oxygen consumption of the shallow roots was about 5.1 $\mathrm{nmol(O_2)\,cm^{-1}\,min^{-1}}$. The *P*-value of paired student test of the rates of oxygen consumption between deep and shallow roots is 0.001. So, we could conclude the rates of ATP production between deep roots and shallow roots were different, and the ATP production in the deep roots was faster than shallow roots.

DISCUSSION

Fresh water shortage is a global challenge for all countries. In China, agriculture used about 70% of the total water consumption of the country, 70% of which was used for rice production alone (Zhang, 2007). As the main water consumers, rice is more susceptible to drought stress than other crops. Enhancing crops' drought resistance through genetic improvement has proved to be practicable to obtain stable and adequate crop production in drought-prone areas (Wang et al., 2005; Gowda et al., 2011). The experiments of Uga et al. (2013a) suggested that increasing the RDR would contribute obviously to drought avoidance in rice. Some QTLs controlling RDR in rice have been reported (Uga et al., 2011, 2013b, 2015; Kitomi et al., 2015; Lou et al., 2015). Our research firstly profiled the transcriptions of root samples with diverse RDR and different spatial distribution underground. The DEGs of this study come from two levels of transcriptomic comparison: first comparison among the three groups of varieties with different roots distribution, second comparison between the paired roots samples (D vs. S) in the same variety. Compared with previous transcriptomic experiments, this experiment should be more accurate and meaningful, firstly because amounts of samples with different RDR were researched; secondly in the second comparison all the disturbances of background were removed. The paired samples had same genome, same growth environment and same development stage, so the positional difference was the only difference between them. Therefore, the DEGs identified here could provide breeders reliable candidate genes for plants' drought resistance improvement.

The transcriptome is the set of all messenger RNA molecules in a given organism at a given growth stage, and it is the most important part of genetic regulation in all living things.

The clustering result of the transcriptomic data was completely consistent with the phenotype of RDR (**Figure 2**, Table S1), which also could be found from the experiment of RNA microarrays assay (Table S2, Figure S1). It implied the difference of transcriptomes could represent the difference of varieties with diverse RDR phenotypes, so the transcriptomic analysis was suitable for deep rooting research. Furthermore, all the paired samples from the same variety were always clustered together in the minimum group, suggesting the differences derived from position-specificity were much less than the differences derived from genotype diversity.

The transcriptomic differences among different varieties were diverse. H vs. L contained 13,242 DEGs > H vs. M contained 7,252 DEGs> M vs. L contained 5,248 DEGs (**Figure 3B**). Therefore, compared with shallow and median rooting varieties, the deep rooting varieties H had the largest transcriptomic specificity. Furthermore, there were 5,192 DEGs could be both found in H vs. L and H vs. M, that was much more than the DEGs (1,507) could be exclusively found in M vs. L. It suggested the similarity between M and L is the largest one among three pair-wise comparisons. As a result, we could speculate the similarity between shallow rooting and median rooting varieties was quite high. From the **Figure 2**, we could also find most of the median varieties cluster with shallow rooting varieties. In a word, the deep rooting varieties were a special group compared with other rice varieties, and they might have experienced strict selection and developed a set of particular patterns of phenotype, genotype and transcriptome.

The DEGs of deep rooting varieties and shallow rooting varieties were enriched mainly in the pathway of genetic information processing and metabolism (**Table 2**). It suggested the divergence of deep rooting and shallow rooting rice varieties may be caused by their difference in the genetic information processing and metabolism. However, the DEGs from the paired comparison of shallow roots vs. deep roots were significantly enriched in the metabolism pathways especially energy metabolism (Table S5). It implied the importance of the metabolism process to the deep rooting. Meanwhile, the DEGs of D vs. S also enriched in the genes' collection controlling roots architecture with *P*-value 8.04E-22 (Table S6). It indicated the reliability of the DEGs identified in this study. Furthermore, we found 52 DEGs between deep and shallow roots from the same variety located on the intervals of QTLs controlling RDR that had been identified by our previous work (Lou et al., 2015). We also compared the 1,052 DEGs with the QTLs for root traits contributing to drought resistance like deep root rate, root volume, root length, and root weight in rice (Qu et al., 2008; Courtois et al., 2009; Obara et al., 2010; Uga et al., 2011, 2013b, 2015; Liang et al., 2013; Sthanumoorthy and Tamba, 2013; Wang et al., 2013), and we found 790 DEGs were located on the intervals of the 305 known QTLs reported to be related to the roots architecture and drought resistance. Therefore, the DEGs found here were quite reasonable and can be used for theoretical study and practical utility by roots architecture modification.

WGCNA is a useful way to analyze transcriptomic data to find the network of associated genes with certain functions and even identify new genes. In this study, through WGCNA using all the DEGs of D vs. S, a big module consisted of the top 300 genes' co-expressing network was found (**Figure 5**). Some hub genes had close correlations with many other genes in this big module. Through annotation, we surprisingly found half of them belong to mitochondria genes and involve in the energy metabolism, like the synthesis of ATP (**Table 6**). And all the hub genes expressed higher in deep roots than in shallow roots. Meanwhile, through QTTs mapping, two genes involved in the energy metabolism (LOC_Os01g42430 and LOC_Os07g23380) were also identified to be associated with the RDR (**Table 5**, Table S9). Almost all these hub genes have significantly higher expression in deep roots than that in shallow roots from the same variety. Through KEGG analysis of all the DEGs between deep roots and shallow roots from the same variety, the DEGs were significantly enriched in five energy metabolism pathways (Table S5). Besides the evidence of molecular data, we also found physiological evidence that the deep roots could produce more ATP than shallow roots. Therefore, we can infer the development of the roots may closely relate to energy metabolism. Deeper roots need more energy than shallow roots, or more energy could make roots grow deeper. The amount of energy could decide the distribution of roots. The further studies of these energy metabolism-related candidate genes and the map-based cloning of more RDR-related QTLs would provide more information to elucidate the relationship between energy metabolism and deep root growth.

DEPOSITED DATA

The RNA-seq datasets generated in this study have been submitted to NCBI Sequence Read Archive (SRA) with the Bioproject number PRJNA306542 from SRX1547421 to SRX1547494.

AUTHOR CONTRIBUTIONS

QL and LC performed the experiment, analyzed the data, and drafted the article. HM reviewed and edited the manuscript. KX, TL, and XP contributed to data acquisition. HW, FF, and CS participated in the data analysis and interpretation. LL and YZ conceived and designed the study.

FUNDING

This work was financially supported by the National Nature Science Youth Foundation (No. 31501293); the Youth Talent Development Plan of Shanghai Municipal Agricultural System, China (Grant No. 20160132); Shanghai Agriculture Applied Technology Development Program, China (Grant No. G2015060101); National 863 Program of modern agricultural technology (No. 2014AA10A603); Shared Platform of Crop Germplasm Resources in Shanghai (15DZ2290700) and Shanghai

Agriculture Applied Technology Development Program, China (Grant No. Z20160106).

ACKNOWLEDGMENTS

We are grateful to Dr. Jun Zhu (Department of Agronomy, Zhejiang University, Hangzhou 310058, China) and Shuang Xu (Horticultural Research Institute, Shanghai Academy of Agricultural Sciences, Shanghai, China) for their help to finish the experiments of QTT mapping and ATP estimation.

SUPPLEMENTARY MATERIAL

The Supplementary Material for this article can be found online at: http://journal.frontiersin.org/article/10.3389/fpls.2017.01314/full#supplementary-material

REFERENCES

Ahmadi, N., Audebert, A., Bennett, M. J., Bishopp, A., de Oliveira, A. C., Courtois, B., et al. (2014). The roots of future rice harvests. *Rice* 7:29. doi: 10.1186/s12284-014-0029-y

Aoki, K., Ogata, Y., and Shibata, D. (2007). Approaches for extracting practical information from gene co-expression networks in plant biology. *Plant Cell Physiol.* 48, 381–390. doi: 10.1093/pcp/pcm013

Benjamini, Y., and Hochberg, Y. (1995). Controlling the false discovery rate: a practical and powerful approach to multiple testing. *J. R. Statist. Soc.* 57, 289–300.

Bernier, J., Serraj, R., Kumar, A., Venuprasad, R., Impa, S., Gowda, R. P. V., et al. (2009). The large-effect drought-resistance qtl qtl12.1 increases water uptake in upland rice. *Field Crops Res.*110, 139–146. doi: 10.1016/j.fcr.2008.07.010

Brown, D., Zeef, L. J., Goodacre, R., and Turner, S. (2005). Identification of novel genes in arabidopsis involved in secondary cell wall formation using expression profiling and reverse genetics. *Plant Cell* 17, 2281–2295. doi: 10.1105/tpc.105.031542

Chance, B., and Williams, G. R. (1956). "The respiratory chain and oxidative phosphorylation," in *Advances in Enzymology and Related Areas of Molecular Biology*, ed A. Meister (New York, NY: John Wiley & Sons, Inc.), 65–134.

Coudert, Y., Le, V. A. T., Adam, H., Bès, M., Vignols, F., and Jouannic, S., et al. (2014). Identification of CROWN ROOTLESS1-regulated genes in rice reveals specific and conserved elements of postembryonic root formation. *N. Phytol.* 206, 243–254. doi: 10.1111/nph.13196

Courtois, B., Ahmadi, N., Khowaja, F., Price, A. H., Rami, J. F., and Frouin, J., et al. (2009). Rice root genetic architecture: meta-analysis from a drought QTL database. *Rice* 2, 115–128. doi: 10.1007/s12284-009-9028-9

Ding, X. P., Li, X. K., and Xiong, L. Z. (2011). Evaluation of near-isogenic lines for drought resistance QTL and fine mapping of a locus affecting flag leaf width, spikelet number, and root volume in rice. *Theor. Appl. Genet.* 123, 815–826. doi: 10.1007/s00122-011-1629-1

Edwards, J. M., Roberts, T. H., and Atwell, B. J. (2012). Quantifying ATP turnover in anoxic coleoptiles of rice (*Oryza sativa*) demonstrates preferential allocation of energy to protein synthesis. *J. Exp. Bot.* 63, 4389–4402. doi: 10.1093/jxb/ers114

Fu, B. Y., Xiong, J. H., Zhu, L. H., Zhao, X. Q., Xu, H. X., and Gao, Y. M., et al. (2007). Identification of functional candidate genes for drought tolerance in rice. *Mol. Genet. Genomics* 278, 599–609. doi: 10.1007/s00438-007-0276-3

Gan, X., Stegle, O., Behr, J., Steffen, J. G., Drewe, P., and Hildebrand, K. L., et al. (2011). Multiple reference genomes and transcriptomes for arabidopsis thaliana. *Nature* 477, 419–423. doi: 10.1038/nature10414

Gibbs, J., and Greenway, H. (2003). Review: mechanisms of anoxia tolerance in plants. *I.* Growth, survival and anaerobic catabolism. *Funct. Plant Biol.* 30, 1–47. doi: 10.1071/PP98095

Gowda, V. R. P., Henry, A., Yamauchi, A., Shashidhar, H. E., and Serraj, R. (2011). Root biology and genetic improvement for drought avoidance in rice. *Field Crops Res.*122, 1–13. doi: 10.1016/j.fcr.2011.03.001

Greenway, H., and Gibbs, J. (2003). Review: mechanisms of anoxia tolerance in plants. II. Energy requirements for maintenance and energy distribution to essential processes. *Funct. Plant Biol.* 30, 999–1036. doi: 10.1071/PP98096

Henry, A., Cal, A. J., Batoto, T. C., Torres, R. O., and Serraj, R. (2012). Root attributes affecting water uptake of rice (*Oryza sativa*) under drought. *J. Exp. Bot.* 63, 4751–4763. doi: 10.1093/jxb/ers150

Jung, J. K., and Mccouch, S. (2013). Getting to the roots of it: genetic and hormonal control of root architecture. *Front. Plant Sci.* 4:0186. doi: 10.3389/fpls.2013.00186

Kato, Y., Abe, J., Kamoshita, A., and Yamagishi, J. (2006). Genotypic variation in root growth angle in rice (*Oryza sativa* L.) and its association with deep root development in upland fields with different water regimes. *Plant Soil* 287, 117–129. doi: 10.1007/s11104-006-9008-4

Kitomi, Y., Kanno, N., Kawai, S., Mizubayashi, T., Fukuoka, S., and Uga, Y. (2015). QTLs underlying natural variation of root growth angle among rice cultivars with functional allele of DEEPER ROOTING 1. *Rice* 8, 1–12. doi: 10.1186/s12284-015-0049-2

Kondo, M., Pablico, P. P., Aragones, D. V., Agbisit, R., Abe, J., and Morita, S. (2003). Genotypic and environmental variations in root morphology in rice genotypes under upland field conditions. *Plant Soil* 255, 189–200. doi: 10.1023/A:1026142904714

Lanceras, J. C., Pantuwan, G., Jongdee, B., and Toojinda, T. (2004). Quantitative trait loci associated with drought tolerance at reproductive stage in rice. *Plant Physiol.* 135, 1–16. doi: 10.1104/pp.103.035527

Liang, Y. S., Zhan, X. D., Wang, H. M., Gao, Z. Q., Lin, Z. C., Chen, D. B., et al. (2013). Locating QTLs controlling several adult root traits in an elite Chinese hybrid rice. *Gene* 526:331. doi: 10.1016/j.gene.2013.04.010

Livak, K. J., and Schmittgen, T. D. (2001). Analysis of relative gene expression data using real-time quantitative PCR and the $2^{-\Delta\Delta CT}$ Method. *Methods* 25, 402–408. doi: 10.1006/meth.2001.1262

Lou, Q. J., Chen, L., Mei, H. W., Wei, H. B., Feng, F. J., Wang, P., et al. (2015). Quantitative trait locus mapping of deep rooting by linkage and association analysis in rice. *J. Exp. Bot.* 66, 4749–4757. doi: 10.1093/jxb/erv246

Luo, L. J. (2010). Breeding for water-saving and drought-resistance rice (WDR) in China. *J. Exp. Bot.* 61, 3509–3517. doi: 10.1093/jxb/erq185

Mortazavi, A., Williams, B. A., Mccue, K., Schaeffer, L., and Wold, B. (2008). Mapping and quantifying mammalian transcriptomes by RNA-Seq. *Nat. Methods* 5, 621–628. doi: 10.1038/nmeth.1226

Moumeni, A., Satoh, K., Kondoh, H., Asano, T., Hosaka, A., and Venuprasad, R., et al. (2011). Comparative analysis of root transcriptome profiles of two pairs of drought-tolerant and susceptible rice near-isogenic lines under different drought stress. *BMC Plant Biol.* 11:174. doi: 10.1186/1471-2229-11-174

Nguyen, H. T., Babu, R. C., and Blum, A. (1997). Breeding for drought resistance in rice: physiology and molecular genetics considerations. *Crop Sci.* 37, 1426–1434. doi: 10.2135/cropsci1997.0011183X003700050002x

Obara, M., Tamura, W., Ebitani, T., Yano, M., Sato, T., and Yamaya, T. (2010). Fine-mapping of qRL6.1, a major QTL for root length of rice seedlings grown under a wide range of NH4 (+) concentrations in hydroponic conditions. *Theor. Appl. Genet.* 121, 535–547. doi: 10.1007/s00122-010-1328-3

Osakabe, Y., Osakabe, K., Shinozaki, K., and Tran, L. S. P. (2014). Response of plants to water stress. *Front. Plant Sci.* 5:86. doi: 10.3389/fpls.2014.00086

Qu, Y. Y., Mu, P., Zhang, H. L., Chen, C. Y., Gao, Y. M., and Tian, Y., et al. (2008). Mapping qtls of root morphological traits at different growth stages in rice. *Genetica* 133, 187–200. doi: 10.1007/s10709-007-9199-5

Rabello, A. R., Guimarães, C. M., Rangel, P. H., Da, S. F., Seixas, D., and De, S. E., et al. (2008). Identification of drought-responsive genes in roots of upland rice (*Oryza sativa* L.). *BMC Genomics* 9:485. doi: 10.1186/1471-2164-9-485

Roberts, A., Pimentel, H., Trapnell, C., and Pachter, L. (2011). Identification of novel transcripts in annotated genomes using RNA-Seq. *Bioinformatics* 27, 2325–2329. doi: 10.1093/bioinformatics/btr355

Serraj, R., Kumar, A., Mcnally, K. L., Slametloedin, I., Bruskiewich, R., and Mauleon, R., et al. (2009). Improvement of drought resistance in rice. *Adv. Agron.* 103, 41–99. doi: 10.1016/S0065-2113(09)03002-8

Serraj, R., Mcnally, K. L., Slametloedin, I., Kohli, A., Haefele, S. M., and Atlin, G., et al. (2011). Drought resistance improvement in rice: an integrated genetic and resource management strategy. *Plant Prod. Sci.* 14, 1–14. doi: 10.1626/pps.14.1

Sthanumoorthy, N., and Tamba, M. (2013). Genetic variation, linkage mapping of QTL and correlation studies for yield, root, and agronomic traits for aerobic adaptation. *BMC Genet.* 14:104. doi: 10.1186/1471-2156-14-104

Trapnell, C., Roberts, A., Goff, L., Pertea, G., Kim, D., and Kelley, D. R., et al. (2012). Differential gene and transcript expression analysis of RNA-seq experiments with tophat and cufflinks. *Nat. Protoc.* 7, 562–578. doi: 10.1038/nprot.2012.016

Uga, Y. (2012). "Quantitative measurement of root growth angle by using the basket method," in *Methodologies for Root Drought Studies in Rice*, eds H. E. Shashidhar, A. Henry, and B. Hardy (Los Baños: International Rice Research Institute), 22–26.

Uga, Y., Ebana, K., Abe, J., Morita, S., Okuno, K., and Yano, M. (2009). Variation in root morphology and anatomy among accessions of cultivated rice (*Oryza sativa* L.) with different genetic backgrounds. *Breed. Sci.* 59, 87–93. doi: 10.1270/jsbbs.59.87

Uga, Y., Hanzawa, E., Nagai, S., Sasaki, K., Yano, M., and Sato, T. (2012). Identification of qSOR1, a major rice QTL involved in soil-surface rooting in paddy fields. *Theor. Appl. Genet.* 124, 75–86. doi: 10.1007/s00122-011-1688-3

Uga, Y., Kitomi, Y., Yamamoto, E., Kanno, N., and Kawai, S. (2015). A QTL for root growth angle on rice chromosome 7 is involved in the genetic pathway of DEEPER ROOTING 1. *Rice* 8, 1–8. doi: 10.1186/s12284-015-0044-7

Uga, Y., Okuno, K., and Yano, M. (2011). Dro1, a major QTL involved in deep rooting of rice under upland field conditions. *J. Exp. Bot.* 62, 2485–2494. doi: 10.1093/jxb/erq429

Uga, Y., Sugimoto, K., Ogawa, S., Ogawa, S., Rane, J., Ishitani, M., et al. (2013a). Control of root system architecture by DEEPER ROOTING 1 increases rice yield under drought conditions. *Nat. Genet.* 45, 1097–1102. doi: 10.1038/ng.2725

Uga, Y., Yamamoto, E., Kanno, N., Kawai, S., Mizubayashi, T., and Fukuoka, S. (2013b). A major qtl controlling deep rooting on rice chromosome 4. *Sci. Rep.* 3:3040. doi: 10.1038/srep03040

Usadel, B., Obayashi, T., Mutwil, M., Giorgi, F. M., Bassel, G. W., Tanimoto, M., et al. (2009). Co-expression tools for plant biology: opportunities for hypothesis generation and caveats. *Plant Cell Environ.* 32, 1633–1651. doi: 10.1111/j.1365-3040.2009.02040.x

Wang, H. M., Xu, X. M., Zhan, X. D., Zhai, R. R., Wu, W. M., Shen, X. H., et al. (2013). Identification of qrl7, a major quantitative trait locus associated with rice root length in hydroponic conditions. *Breed. Sci.* 63:267. doi: 10.1270/jsbbs.63.267

Wang, L., Xie, W., Chen, Y., Tang, W., Yang, J., Ye, R., et al. (2010). A dynamic gene expression atlas covering the entire life cycle of rice. *Plant J.* 61, 752–766. doi: 10.1111/j.1365-313X.2009.04100.x

Wang, X. S., Zhu, J., Locedie, M., and Richard, B. (2005). Identification of candidate genes for drought stress tolerance in rice by the integration of a genetic (QTL) map with the rice genome physical map. *J. Zhejiang Univ. Sci. B* 6, 382–388. doi: 10.1631/jzus.2005.B0382

Xie, C., Mao, X., Huang, J., Ding, Y., Wu, J., Dong, S., et al. (2011). Kobas 2.0: a web server for annotation and identification of enriched pathways and diseases. *Nucleic Acids Res.* 39, 316–322. doi: 10.1093/nar/gkr483

Yu, L. J., Luo, Y. F., Liao, B., Xie, L. J., Chen, L., Xiao, S., et al. (2012). Comparative transcriptome analysis of transporters, phytohormone and lipid metabolism pathways in response to arsenic stress in rice (*oryza sativa*). *N. Phytol.* 195, 97–112. doi: 10.1111/j.1469-8137.2012.04154.x

Zhang, Q. F. (2007). Strategies for developing green super rice. *Proc. Natl. Acad. Sci. U.S.A.* 104, 16404–16409. doi: 10.1073/pnas.0708013104

Zhou, L., Li, R., Fan, L., Shi, Y., Wang, Z., Xie, S., et al. (2013). Mapping epistasis and environment × qtx interaction based on four-omics genotypes for the detected qtx loci controlling complex traits in tobacco. *Crop J.* 1, 151–159. doi: 10.1016/j.cj.2013.09.001

Conflict of Interest Statement: The authors declare that the research was conducted in the absence of any commercial or financial relationships that could be construed as a potential conflict of interest.

frontiers in Plant Science

ORIGINAL RESEARCH
published: 26 June 2018
doi: 10.3389/fpls.2018.00893

Comparative Aerial and Ground Based High Throughput Phenotyping for the Genetic Dissection of NDVI as a Proxy for Drought Adaptive Traits in Durum Wheat

Giuseppe E. Condorelli[1], Marco Maccaferri[1], Maria Newcomb[2], Pedro Andrade-Sanchez[2], Jeffrey W. White[3], Andrew N. French[3], Giuseppe Sciara[1], Rick Ward[2] and Roberto Tuberosa[1]*

[1] Department of Agricultural Sciences, University of Bologna, Bologna, Italy, [2] Maricopa Agricultural Center, University of Arizona, Tucson, AZ, United States, [3] US Arid Land Agricultural Research Center, USDA-ARS, Maricopa, AZ, United States

OPEN ACCESS

Edited by:
Roberto Papa, Università Politecnica delle Marche, Italy

Reviewed by:
Pasquale De Vita, Consiglio per la Ricerca in Agricoltura e l'Analisi dell'Economia Agraria (CREA), Italy
Frédéric Marsolais, Agriculture and Agri-Food Canada (AAFC), Canada

***Correspondence:**
Marco Maccaferri
marco.maccaferri@unibo.it

Specialty section:
This article was submitted to Plant Breeding, a section of the journal Frontiers in Plant Science

Received: *10 January 2018*
Accepted: *07 June 2018*
Published: *26 June 2018*

Citation:
Condorelli GE, Maccaferri M, Newcomb M, Andrade-Sanchez P, White JW, French AN, Sciara G, Ward R and Tuberosa R (2018) Comparative Aerial and Ground Based High Throughput Phenotyping for the Genetic Dissection of NDVI as a Proxy for Drought Adaptive Traits in Durum Wheat. Front. Plant Sci. 9:893. doi: 10.3389/fpls.2018.00893

High-throughput phenotyping platforms (HTPPs) provide novel opportunities to more effectively dissect the genetic basis of drought-adaptive traits. This genome-wide association study (GWAS) compares the results obtained with two Unmanned Aerial Vehicles (UAVs) and a ground-based platform used to measure Normalized Difference Vegetation Index (NDVI) in a panel of 248 elite durum wheat (*Triticum turgidum* L. ssp. *durum* Desf.) accessions at different growth stages and water regimes. Our results suggest increased ability of aerial over ground-based platforms to detect quantitative trait loci (QTL) for NDVI, particularly under terminal drought stress, with 22 and 16 single QTLs detected, respectively, and accounting for 89.6 vs. 64.7% phenotypic variance based on multiple QTL models. Additionally, the durum panel was investigated for leaf chlorophyll content (SPAD), leaf rolling and dry biomass under terminal drought stress. In total, 46 significant QTLs affected NDVI across platforms, 22 of which showed concomitant effects on leaf greenness, 2 on leaf rolling and 10 on biomass. Among 9 QTL hotspots on chromosomes 1A, 1B, 2B, 4B, 5B, 6B, and 7B that influenced NDVI and other drought-adaptive traits, 8 showed *per se* effects unrelated to phenology.

Keywords: ***Triticum turgidum* L. subsp. *durum*, durum wheat, drought, high-throughput phenotyping, UAV, NDVI, GWAS, QTL**

INTRODUCTION

Global warming and the increasing frequency and severity of drought events unequivocally underline the urgency to select crops able to sustain growth in rainfed conditions, particularly when grown in Mediterranean countries, where climatic change is expected to exacerbate yield uncertainty (Ortiz et al., 2008; Kelley et al., 2015; Kyratzis et al., 2017). The selection of drought-resistant cultivars increasingly relies on the use of yield-related proxies selected either directly (Reynolds and Tuberosa, 2008) or via marker-assisted selection once the quantitative trait loci (QTLs) underpinning the variability of the relevant trait are identified (Langridge and Reynolds, 2015; Maccaferri et al., 2016; Mason et al., 2018).

The recent progress in high-throughput phenotyping platforms (HTTPs) based primarily on the use of ground-based and/or Unmanned Aerial Vehicles (UAVs) provides unprecedented opportunities to accurately measure proxy traits in hundreds of plots (Pauli et al., 2016; Duan et al., 2017; Shakoor et al., 2017; Shi et al., 2017; Trapp et al., 2017), as required in experiments to identify QTLs. In this respect, increasing attention is being devoted to the use of ground-based and aerial HTPPs that allow for such high-throughput phenotyping levels (Araus and Cairns, 2014; Zaman-Allah et al., 2015; Kefauver et al., 2017; Madec et al., 2017). A potential limitation of ground-based phenotyping platforms is the considerably longer time required to complete the measurements as compared to UAV-based remote sensing which allows phenotyping over a larger area in less time, an important prerequisite to minimize the effects due to daily fluctuations in environmental conditions, inevitable in large-scale experiments (Tuberosa, 2012). However, a potential advantage of ground-based platforms is the increased data resolution as result of shorter distances between sensors and plant targets. Empirical data are needed to compare benefits of the different platforms for different experimental objectives.

Because water shortage affects vegetative state and cover, drought-stress monitoring can be based on the use of vegetation indices (VIs). Normalized Difference Vegetation Index (NDVI) was found to be an effective indicator of vegetation response to drought based on the relationships between NDVI and a meteorologically based drought index (Ji and Peters, 2003). NDVI is based on the difference between the maximum absorption of radiation in the Red spectral region (from 620 to 690 nm) as result of chlorophyll pigments and the maximum reflectance in near infrared (NIR, from 760 to 900 nm) light as result of the leaf cellular structure (Tucker, 1979). Healthy and living canopies absorb most of the Red light by the photosynthetic pigments, while the NIR light is mostly reflected due to light scattering in leaf internal structure and canopy architecture. Therefore, NDVI-value, computed as (NIR – Red)/(NIR + Red), integrates biomass (or leaf area) and leaf chlorophyll content (Lukina et al., 1999), hence providing a proxy for grain yield (Labus et al., 2010). In wheat, NDVI has been shown to be associated with drought-adaptive traits as well as grain yield under stressed conditions (Bort et al., 2005; Marti et al., 2007; Reynolds et al., 2007; Lobos et al., 2014; Bowman et al., 2015; Tattaris et al., 2016; Yousfi et al., 2016), which ultimately allows for the identification of the relevant QTL governing the adaptive response to drought. In this case, it is important to account for the effects of the single QTLs on flowering time, a trait well known to influence drought adaptation (Tuberosa, 2012). A number of key genes (*PPD-A1*, *PPD-B1*, *FT-7A*-indel, *Rht-B1b,* and *VRN-A1*) affect flowering time and, consequently, NDVI and other drought-adaptive traits (Milner et al., 2016). Therefore, their effects should be accounted for when interpreting the results of QTL analyses, particularly when aiming at identifying loci that affect drought resistance on a *per se* basis, i.e., irrespectively of indirect effects due to differences in flowering time.

Although remote sensing based on the utilization of UAVs equipped with either conventional or hyperspectral and multispectral cameras is being increasingly adopted as an alternative to portable cameras and spectroradiometers to measure NDVI in wheat (Haghighattalab et al., 2016; Holman et al., 2016; Yang et al., 2016; Kyratzis et al., 2017) no study has yet compared the QTL results of a genome-wide association study (GWAS) for NDVI measured with both aerial- and ground-based phenotyping platforms in crops under both well-watered and water-deficit conditions of increasing severity. To our best knowledge, this study is the first to report on the use of UAV-based NDVI remote sensing for GWAS analysis in crops and to compare the results with those obtained via a ground-based HTPP. Importantly, GWAS of NDVI and other drought-adaptive traits allowed us to identify a number of QTL hotspots with *per se* effects that provide suitable targets for enhancing drought tolerance via marker-assisted selection.

MATERIALS AND METHODS

Plant Material and Field Management

The field trial was conducted at Maricopa Agricultural Center (33.070° N, 111.974° W, elevation 360 m) on a Casa Grande soil (fine-loamy, mixed, superactive, hyperthermic Typic Natrargids) (Supplementary Figure 1). The plant material included 248 accessions of durum wheat from the association mapping population UNIBO-Durum Panel (hereafter referred to as "Durum Panel") assembled at the University of Bologna (UNIBO), representing a large portion of the genetic diversity present in the most important improved durum wheat gene pools.

The Durum Panel includes Mediterranean-adapted accessions selected and released from breeding programs in Italy, the International Maize and Wheat Improvement Center (CIMMYT), the International Center for Agricultural Research in the Dry Areas (ICARDA), the National Institute for Agricultural Research (INRA, France) and the Institute of Agrifood Research and Technology (IRTA, Spain). The Durum Panel also includes accessions released by public breeding programs in the Northern Great Plains of the USA and Canada (North Dakota, Montana, Saskatchewan and Alberta), private French breeders and Australian breeding programs, as well as representative accessions from the Pacific Southwest of the US, commonly referred to as "Desert-Durum®" (Supplementary Table 1).

The 248 accessions were planted on 20 December 2016 according to a Randomized Complete Block Design (RCBD) with two replicates and border plots (cv. Orita). Each accession was evaluated in two-row plots (3.5 m long, 0.76 m apart) with a final density of 22 plants/m^2. Before planting, nitrogen at 112 kg ha^{-1} and phosphorus ($P_2 0_5$) at 56 kg ha^{-1} were incorporated into the soil and 28 days after sowing, irrigation was managed by a pressurized drip system using lines buried ∼10 cm deep. Drip irrigation was stopped on 16 March 2017 and from that date the accessions were subjected to a progressive drought stress until 3–4 April 2017 when plants were harvested to measure biomass.

Soil moisture data were collected for monitoring the water stress conditions using time domain reflectometry (TDR) probes (rod length: 15 cm) on 22 and 23 March 2017. TDR probes

worked in 8 equidistant field ranges by inserting the rods into the soil and within a few seconds the moisture value is presented on a display unit.

Plants were harvested on 105 days after planting (DAP) to allow for planting the next phenotyping experiment and therefore biomass data indicate the status at a point in time rather than direct estimates of final yields.

Disease and insect pest pressure were negligible throughout the crop.

Leaf Water Status

Relative Water Content (RWC) was measured in flag leaves collected from the two replicates for the cultivars "Gallareta," "Karim," "Mexicali 75," and "Svevo." Flag leaves were sampled on 24 March 2017 (DAP: 94), 27 March 2017 (DAP: 97) and 31 March 2017 (DAP: 101) placed in glass containers within a cooler and transported immediately to the laboratory to minimize water loss due to evaporation. Samples were weighed as fresh weight (FW) and then submerged in distilled water. After rehydration for 24 h at 4°C in the dark, the turgid leaves were rapidly blotted to remove surface water and weighed to obtain turgid weight (TW). Finally, the leaves were oven-dried at 60°C for 24 h and then the dry weight (DW) was obtained. RWC-values were computed as follows: $[(FW - DW)/(TW - DW)] \times 100$ (Barrs, 1968).

NDVI Measurements

NDVI was measured on progressive days after planting using two UAV-based and one tractor-based platforms and related phenology of each accession was evaluated on the basis of the Zadoks scale (Supplementary Table 2).

UAV-based NDVI was extracted from georeferenced orthomosaic GeoTIFFs generated from imagery captured from autopiloted flights of either a MicaSense RedEdge multi-spectral camera (MicaSense, Seattle, WA) carried on a hexacopter, or a Parrot Sequoia (Parrot, Paris, France) multi-spectral camera carried on an eBee (SenseFly, Lausanne) fixed wing aircraft. **Table 1** compares features of the two multispectral cameras in terms of band centers and bandwidths.

Flights were conducted at 40–42 m above ground level, resulting in ground sampling distances of ∼3 cm/pixel for the RedEdge, and 4.4 cm/pixel for the Sequoia. Mission planning was done with UgCS (UgCS, Riga) for the RedEdge camera, and either eMotion 3 (senseFly, Lausanne) or Atlas Flight (MicaSense, Seattle, WA) for the Sequoia camera. All flights were planned for 80% image overlap along flight corridors. Both the Sequoia and RedEdge cameras use global shutters.

Pix4DMapperPro desktop software (Pix4D SA, Switzerland, http://pix4d.com) was used to generate orthomosaics for each camera band. Six to eight ground control points (GCP) geolocated with Real Time Kinematic (RTK) survey precision were used to georeference the orthomosaics. Camera images were calibrated using manufactured supplied reflectance panels that were imaged at the beginning of each flight. The Pix4D processing options were essentially the same as those of Pix4D's "Ag Multispectral" template version 4.1.10, except that GeoTIFF tiles were merged to create the NDVI orthomosaic.

TABLE 1 | Properties of Sequoia, RedEdge, and GreenSeeker Normalized Difference Vegetation Index (NDVI) sensors and including type of recorded spectral band, bandcenter, and bandwidth.

Sensor	Spectral band	Band center (nm)	Band width (nm)
UAV-Sequoia[a]	Green	550	40
	Red	660	40
	Red Edge	735	10
	NIR	790	40
	Blue	475	20
Tractor-GreenSeeker[b]	Red	660	25
	NIR	770	25
UAV-RedEdge[c]	Green	560	20
	Red	668	10
	Red Edge	717	10
	NIR	840	40

[a] *https://www.micasense.com/parrotsequoia/*
[b] *https://agriculture.trimble.com/precision-ag/products/greenseeker/*
[c] *https://www.micasense.com/*

Plot-level NDVI means from UAV's were created in QGIS software version 2.18.3 (QGIS, US, http://www.qgis.org). Shape files containing annotated single plot polygons were generated with an R (r-project.org) script. Shape files with GCPs as features (points) were also employed based on RTK survey grade measuring devices. For all flights, the GeoTIFF with the NDVI orthomosaic from Pix4D was combined with the plot polygon and GCP shape files in a single QGIS project. Confirmation of proper geolocations of the Pix4D orthomosaics was achieved by visually confirming alignment of the visible GCPs with the corresponding points in the feature shape file. NDVI plot means were generated using the Zonal Statistics function in QGIS.

The tractor-based system was similar to that described by Andrade-Sanchez et al. (2013) but carried five GreenSeeker spectral sensors and RT200 communication module (Trimble, Inc., Sunnyvale, CA) mounted in a frame at the front of the vehicle. These active sensors are equipped with their own source of modulated white light, which is directed toward the top of the crop canopy with the platform in motion at an average speed of 0.84 m s^{-1}. A portion of the sensor-generated light reflects off the crop and is measured by Red and Near Infrared (NIR) wide-band filters located in the sensor head. The height position of the sensors was set to 1.32 m above ground in every event. Since the approximate view angle of this sensor model is 28°, the field-of-view (FOV) of each sensor was ∼50-cm at the soil surface. The ground platform was retrofitted with an ultra-precise RTK Global Navigation Satellite System (GNSS) receiver, AgGPS332 (Trimble, Inc., Sunnyvale, CA) to generate positioning data via "GGA" National Marine Electronics Association (NMEA) messages. The data acquisition system used in the tractor platform was a CR3000 micro-logger (Campbell Scientific, Logan, UT) programmed to record the NDVI output of all five spectral sensors plus latitude and longitude coordinates at a rate of 5 Hz. The combination of data sampling frequency

and platform speed of operation produced an average of 20 NDVI data points for each plot.

The lme4 package (r-project) and custom R scripts were used to conduct a spatial adjustment analysis of the raw NDVI plot data from aerial- and ground-based platforms using a mixed procedure including row and column random effects and a moving mean of variable size for optimizing spatial adjustment. Repeatability values and Pearson's correlation r coefficients among growth stages were also calculated in R.

Phenology Score (Zadoks System), Leaf Chlorophyll Content (SPAD), Leaf Rolling, and Dry Biomass Evaluation

Phenology of each accession was evaluated on the basis of the Zadoks scale (Zadoks et al., 1974) (Supplementary Table 2).

Flag leaf "greenness" on 101 DAP was assessed based on Soil-Plant Analysis Development (SPAD) estimates obtained with a non-destructive chlorophyll meter SPAD-502Plus (Konica Minolta Sensing, Inc., Japan) as an indicator of leaf photosynthetic activity, chlorophyll content and nitrogen (N) status. The hand-held SPAD meter operates by an illuminating system that emits Red (650 nm) and infrared (940 nm) light transmitted through a leaf to a receptor.

Leaf rolling (LR) was visually estimated on 99 DAP with a score from 0 (no leaf rolling) to 9 (severely rolled).

At the end of the field trial, plants within the entire two-row plots were cut with mechanical harvester (Carter mfg equipment) while subsamples of 2–3 plants were collected to evaluate moisture content in order to estimate dry biomass on 3–4 April 2017. Dry weight of the harvested plot assumed plot dimensions of 1.5 m width and 3.5 m length and was adjusted to 0% moisture. Plant moisture content (%) at harvest was estimated from a subsample of biomass either placed directly in a drying oven or stored temporarily in an uncooled greenhouse that reached a diurnal high temperature of 60°C before being transferred to an oven at 60°C for final drying.

SNP Genotyping, Population Structure, and GWAS Model

For each accession, genomic DNA was extracted using NucleoSpin® 8/96 Plant II Core Kit from Macherey Nagel and sent for SNP genotyping to TraitGenetics (http://www.traitgenetics.com/en/).

The Illumina iSelect 90K wheat SNP assay (Wang et al., 2014) was used and genotype calls were obtained as described in Maccaferri et al. (2015b). The tetraploid-consensus-2015 reported in Maccaferri et al. (2015a) was used to assign polymorphisms to chromosomes and map positions.

Linkage disequilibrium (LD) among markers was calculated in HaploView 4.2 software (Barrett et al., 2005), for each chromosome of A and B genomes and only SNPs with known position and with a minor allele frequency > 0.05 were considered. LD decay pattern as a function of consensus genetic distances was inspected considering squared allele frequency correlation (r^2) estimates obtained for all pairwise comparisons among intra-chromosomal SNPs. Curve fit and distance at which LD decays below r^2 0.3 were used to define the confidence intervals of QTLs detected in this study as already reported for the same germplasm by Liu et al. (2017) using a custom script in R following the methodology described in Rexroad and Vallejo (2009) and in Maccaferri et al. (2015a).

Population structure was assessed in STRUCTURE software 2.3.4 (Pritchard et al., 2000) using a reduced subset of 2,382 markers pruned for $r^2 = 0.5$ using the corresponding tagger function in Haploview 4.2 (Barrett et al., 2005).

The model-based quantitative assessment of subpopulation memberships of the accessions was carried out in STRUCTURE using inferences based on molecular SNP data only. STRUCTURE model included admixture and correlated allele frequencies among subpopulations. Numbers of hypothetical subpopulations ranging from $k = 2$ to 10 were assessed using 50,000 burn-in iterations followed by 100,000 recorded Markov-Chain iterations. To estimate the sampling variance (robustness) of population structure inference, five independent runs were carried out for each k.

The rate of change in the logarithm of the probability of likelihood [LnP(D)] value between successive k-values (Δk statistics, Evanno et al., 2005) together with the inspection of the rate of variation (decline) in number of accessions clearly attributed to subpopulations (no. of accessions with Q membership's coefficient ≥ 0.5 and ≥ 0.7) and meaningful grouping based on pedigree and accessions' passport data were used to predict the optimal number of subpopulations. Finally, to determinate the level of differentiation among subpopulations, we considered the Fixation Index (*Fst*) among all possible population pairwise combinations.

A maximum and optimal number of eight subpopulations with accession memberships consistent with the known pedigree and passport data was chosen for subsequent analysis and GWAS results interpretation based upon the integrated analysis of (i) the derivation of the variance of the maximum likelihood estimation of the model plotted vs. increasing k (Δk, Evanno et al., 2005) and (ii) analysis of pre-existing pedigree and passport information on the accessions included in the panel which provides an estimation of parentage among accessions. A kinship matrix of genetic relationships among individual accessions of the durum panel was calculated with all non-redundant SNP markers (7,723) using the Haploview 4.2 tagger function set to $r^2 = 1.0$. Kinship based on Identity-by-State (IBS) among accessions was calculated in TASSEL (Trait Analysis by aSSociation, Evolution and Linkage) 5.2.37.

Subsequently, 17,721 SNP markers with minor allele frequency (MAF) > 0.05, imputed with LinkImpute (LDkNNi) (Money et al., 2015) in TASSEL, were used in a GWAS of NDVI, leaf chlorophyll content, leaf rolling and phenology scores (Zadoks system) on 87 and 100 DAP. Marker-trait association (GWAS) analysis was implemented in the software package TASSEL 5.2.37 with a Mixed Linear Model (MLM; Yu et al., 2006; Bradbury et al., 2007) which included either the Kinship matrix (MLM-K) alone or STRUCTURE subpopulation membership estimates plus Kinship plus (MLM-Q+K) as random effect. Following Zhang et al. (2010), MLM was specified as follows: $y = X\beta + Zu + e$, where y is the phenotype value,

β is the fixed effect due to marker and u is a vector of random effects not accounted for by the markers; X and Z are incidence matrices that related y to β and u while e is the unobserved vector of random residual. Based on GWAS Q-Q (quantile-quantile) plot results (Supplementary Figure 2), the MLM-K was considered as the optimal model to control the *P*-value inflation associated to population structure while the MLM-Q+K model was noticed to lead to overcorrections. Thus, all GWAS analyses were subsequently carried out based on the MLM-K model. In addition, the allelic state of loci relevant for phenology (*PPD-A1*, *PPD-B1*, *FT-7A*-indel, *Rht-B1b,* and *VRN-A1*) was included as covariate in MLM analysis (Yu et al., 2006; Price et al., 2010). These genes are associated with the most important agronomic traits influencing NDVI and other drought-adaptive traits. GWAS *p*-values and R^2 effects were extracted and QTL selection criteria was carried-out based on standard conditions of significance: "highly significant" refers to $P < 0.0001$ and "significant" refers to $P < 0.001$. The average genetic distance at which LD decayed below r^2 of 0.3, a threshold frequently adopted in GWAS (Berger et al., 2013; Maccaferri et al., 2015a; Liu et al., 2017), was used to select the QTL confidence Interval (cM) in the association analysis in this study. By setting LD $r^2 = 0.3$, the corresponding inter-marker genetic distance was 3.0 cM as reported by Liu et al. (2017). Therefore, the confidence interval of ±3.0 cM based on map positions of QTL tag-SNPs was chosen. The proportion of variance for phenotypic traits explained by selected SNPs was calculated with Minitab[1]® 18.

RESULTS

Population Structure and LD Decay of the Elite Durum Panel

Out of the 17,721 polymorphic SNPs (minimum allele frequency ≥ 0.05) suitable for GWAS analysis, a representative reduced set of 2,382 SNPs obtained after pruning for LD at $r^2 = 0.50$ threshold was used to investigate the population structure of the elite durum panel of 248 elite accessions. STRUCTURE analysis indicated a strong population genetic structure, as reported in previous analyses of this durum wheat germplasm, using SSR, DArT, and SNP markers (Maccaferri et al., 2011; Letta et al., 2013; Liu et al., 2017). The number of optimal *k* subpopulations ranged from five to eight. With $k = 8$, 155 accessions (62.5%) were clearly grouped into one of the eight main gene pools (**Figure 1**) at a *Q* membership coefficient ≥0.5, while the remaining 93 were considered as admixed.

Subgroup S1 corresponded to native Mediterranean and North African germplasm. Subgroup S2 included germplasm specifically bred for dryland areas at ICARDA (Syria) from the early 1970s. Subgroup S3 included Spanish and Moroccan cultivars from early 1970s, and CIMMYT and ICARDA selections for temperate areas. Subgroup S4 mostly included ICARDA high-yielding lines/cultivars for temperate areas and contemporary (1970s) Italian accessions obtained from cv. Creso, an important Italian founder also related to CIMMYT materials. Subgroup S5 included accessions derived from widely adapted (photoperiod insensitive) CIMMYT germplasm released in the late 1970s to early 1980s. Subgroup S6 included accessions from the mid-1970s breeding program in Italy (Valnova group) while subgroup S7 included accessions from the high-yielding CIMMYT germplasm released in the late 1980s to early 1990s (founders Altar84 and Gallareta).Finally, subgroup S8 included 40 accessions from North Dakota (USA), Canada, France and Australia (Supplementary Table 3).

The division into eight subpopulations was supported by pairwise comparisons among and within subgroups based on the Fixation Index (*Fst*) which provides a measure of subpopulation diversity (Supplementary Table 4) and by Neighbor Joining tree (Saitou and Nei, 1987; **Figure 1**). High genetic diversity was detected between the old Italian cultivars (S1) and the French, North American, Canadian and Australian cultivars (S8), while a considerable admixture among subgroups characterized the ICARDA, CIMMYT, and Italian groups. As a further note, only a relatively small portion of the molecular variation was accounted for by the origin of the accessions, as expected based on the high exchange rate of germplasm among breeding programs.

Quantitative Trait Variation in Relation to Population Genetic Structure

Multiple linear regression was performed to estimate the impact of genetic population structure on the phenotypic traits (Supplementary Table 5). The R^2-values ranged from 0.02 to 0.11 for NDVI-UAV-Sequoia scores and from 0.08 to 0.09 for NDVI-tractor-GreenSeeker scores. R^2 for SPAD was higher ($R^2 = 0.17$), reflecting the selection for high flag leaf chlorophyll content in more recent germplasm groups such as S7, while R^2-values for leaf rolling and dry biomass were equal to 0.09 and 0.08, respectively. **Figure 2** shows violin-plot distributions in relation to the eight subpopulations.

Although multiple regression showed a limited relationship between population structure and NDVI, violin plots and median values based on the eight subgroups evidenced trends for increased NDVI and, even more pronounced, for SPAD from the oldest subgroups (S1-S2-S3) to the most recently improved groups S5-S6-S7. Notably, subgroup S8 showed the widest within-group variation for NDVI and SPAD-values, as expected based on the concomitant presence within the same genetically highly homogeneous group of conventional plant height accessions from the Northern Plains of the US and Canada and semidwarf (*RhtB1b*) accessions from France and Austria.

NDVI From UAV-Sequoia, UAV-Rededge, and Ground-Based Greenseeker Sensors

NDVI measurements from the aerial platforms included data from the Sequoia-sensor on four DAP associated with differing growing stages (GS), and from the RedEdge sensor on two DAP, the first of which coincided with the last measurement with the Sequoia. Phenotypic distributions approximated normality for both traits (**Figure 3**). Repeatability (h^2) values for NDVI were mostly high for both UAV-Sequoia (from 0.77 on 55 DAP to 0.89 on 83 DAP) and UAV-RedEdge (from 0.80 on

[1]Minitab Statistical Software release 9. Minitab Inc., 3081 Enterprise Drive, State College, PA 16801-3008.

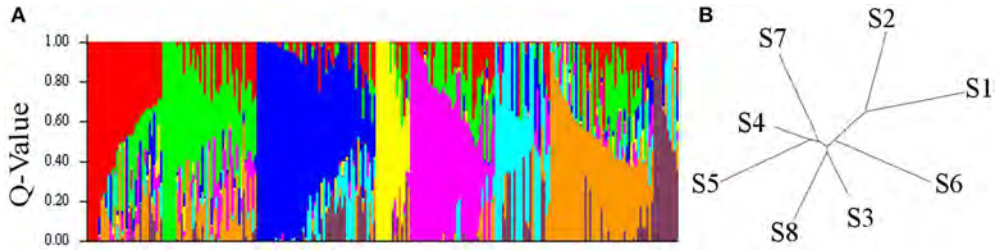

FIGURE 1 | Bar Plot **(A)** and Neighbor Joining Tree **(B)** using STRUCTURE 2.3.4. for the eight durum wheat subpopulations (S1-S8) sorted by Q and relative genetic distance.

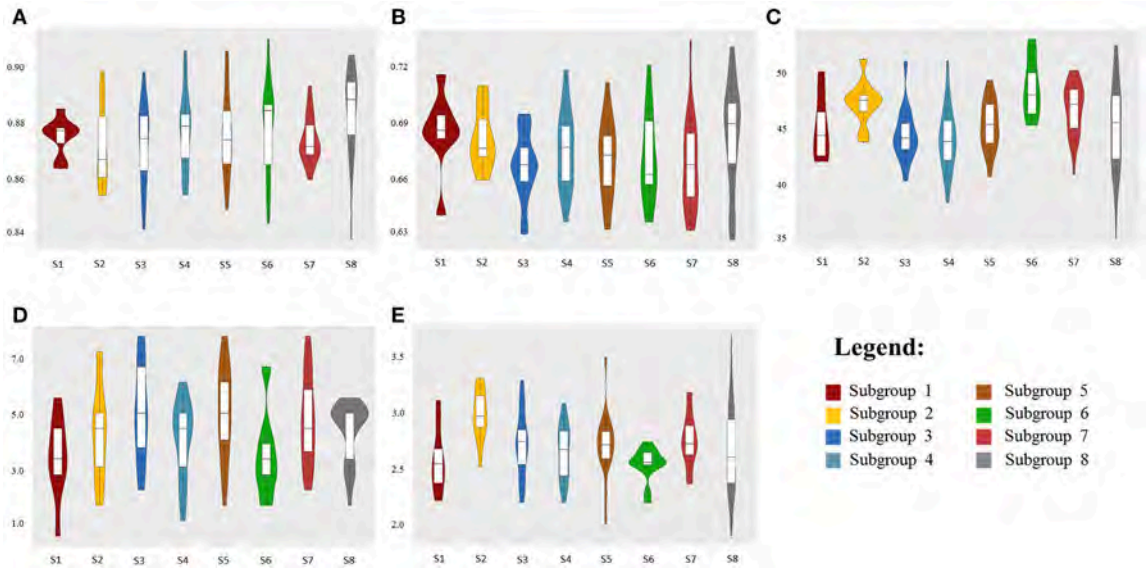

FIGURE 2 | Violin-plot distributions for the eight durum wheat subpopulations (S1-S8) related to NDVI-UAV-Sequoia at 91 DAP **(A)**, NDVI-tractor-GreenSeeker at 94 DAP **(B)**, leaf chlorophyll content (SPAD) at 101 DAP **(C)**, leaf rolling at 99 DAP **(D)**, and dry biomass (ton/ha) at 105 DAP **(E)**.

91 DAP to 0.89 on 98 DAP) and medium-high for ground-based GreenSeeker (from 0.61 on 58 DAP to 0.67.5 on 94 DAP).

NDVI-UAV-Sequoia mean values progressively increased during the time interval from 13 February (55 DAP) (NDVI from 0.40 to 0.63) to 21 March (91 DAP) (NDVI from 0.84 to 0.91). NDVI reached the highest mean value (0.87) at 21 March (91 DAP), the last measurement. NDVI-UAV-RedEdge measurements averaged 0.82 at 21 March (91 DAP) (comparable to NDVI-UAV-Sequoia) while at 29 March (98 DAP) the mean value decreased to 0.77. Summary statistics are reported in **Table 2**.

The NDVI data collected with the GreenSeeker showed distributions with lower mean values compared to the UAV-derived data and, most importantly, reached the plateau already at 6 March (76 DAP) (**Figure 3**). Similarly to NDVI-UAV-Sequoia, the mean values progressively increased from 16 February to 24 March (55 DAP to 91 DAP). NDVI on 58 DAP averaged 0.36 and on 76 DAP reached 0.64, considered as the plateau for this platform (**Figure 4**). **Table 3** reports Pearson's correlation coefficients among NDVI consecutive measurements, separately for UAV-Sequoia and tractor-GreenSeeker sensors.

Correlations reached medium to high values only for measurements taken at consecutive DAP, and were lower for non-consecutive DAP. **Table 4** shows the correlations between UAV-Sequoia and tractor-GreenSeeker at comparable DAP. The correlations were all highly significant and ranged from 0.42 to 0.61 ($P < 0.01$), with the latter observed for the two measurements taken on 91 and 94 DAP.

Leaf Chlorophyll Content (SPAD), Leaf Rolling (LR), Soil Moisture, RWC, and Dry Biomass

Leaf chlorophyll content (SPAD) and leaf rolling (LR) as assessed under terminal drought stress conditions showed a normal distribution (Supplementary Figure 3). SPAD measurements ranged from 35.3 to 53.7 with an average of 46.0 while leaf rolling had an average of 4.45. Repeatability values were equal to 0.88 for SPAD, 0.40 for LR and 0.64 for dry biomass (**Table 2**). RWC

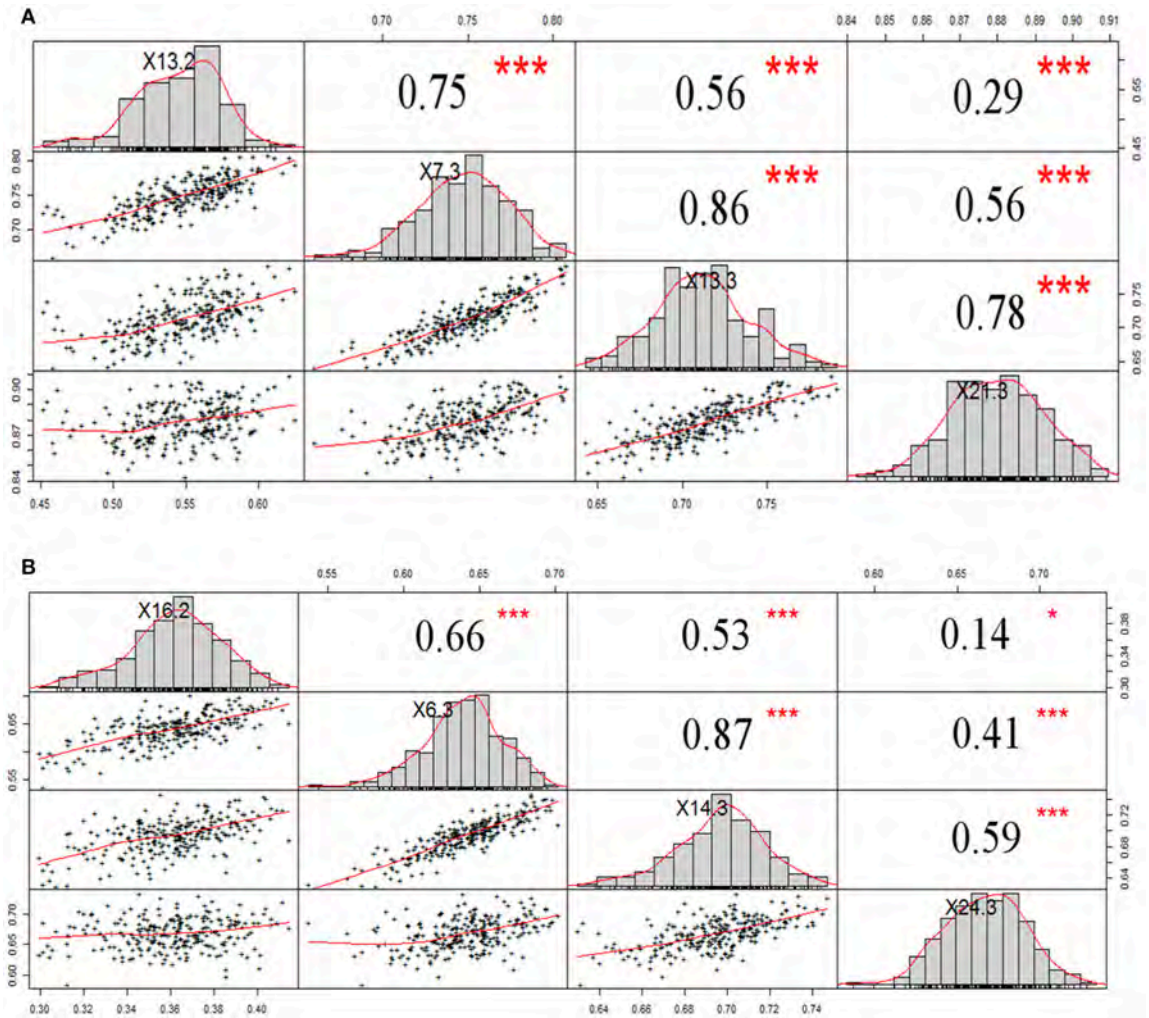

FIGURE 3 | Normal distribution curves and Pearson correlation coefficients for NDVI data from tractor-GreenSeeker **(A)** and UAV-Sequoia **(B)** at four different times. ***$P < 0.0001$, *$0.001 < P < 0.01$.

results show that the cessation of irrigation on March 16 resulted in progressively lower leaf RWC for the four tested varieties (Supplementary Figure 4). In addition, soil moisture data on volumetric basis ranged from 7.1 to 13.8% indicating high levels of drought stress.

Dry biomass showed a normal distribution with an average of 2.61 ton ha^{-1}. A positive correlation was observed between dry biomass and NDVI from aerial and tractor platforms with Pearson correlation coefficients ranging from 0.32 (91 and 94 DAP) to 0.53 (83 and 84 DAP) (Supplementary Figure 5).

Effect of Phenology-Relevant Loci on NDVI

Association testswere performed to investigate the effect of known phenology-relevant loci on the target traits (records of phenological stage and NDVI repeated measurements) (**Table 5**). *PPD-A1* had the strongest effect on phenology score, followed by *FT-7A* and *PPD-B1*. The photoperiod sensitive allele *PPD-A1-452* (Bentley et al., 2011), against all photoperiod-sensitive alleles had the strongest effects on phenology-score and NDVI measurements with –Log *P*-values equal to 9.69 and 12.16 for the two phenological scores and –Log *P*-values ranging from 2.46 to 7.52 for ground-based NDVI. The photoperiod-insensitive allele *PPD-A1-380* showed only a mildly significant effect compared to the insensitive allele *PPD-A1-452*. Also *FT-7A* showed significant effects on phenological scores and on both UAV- and ground-based NDVI on 91, 94, and 98 DAP. *PPD-B1* showed mild effects on phenology scores only, while *VRN-A1* had no effect on any of the drought-adaptive traits. In addition, *Rht-B1b* had a significant effect on dry biomass with –Log *P*-value equal to 3.14. The phenology-relevant loci did not affect the manually scored SPAD. Based on these results, the loci relevant for phenology/plant development were used as covariates in GWAS analysis for NDVI traits.

TABLE 2 | Summary statistics for Normalized Difference Vegetation Index (NDVI), leaf chlorophyll content (SPAD), phenology score (PHENO-score 1 and PHENO-score 2), leaf rolling (LR), and dry biomass on different days after planting (DAP) in a panel of 248 durum wheat elite advanced lines and cultivars from worldwide.

Trait	DAP	Range	Mean	St. dev.	h^2(%)
NDVI-UAV (Sequoia)	55	0.40–0.63	0.54	0.012	77.2
	77	0.66–0.81	0.74	0.029	83.9
	83	0.64–0.79	0.71	0.026	88.5
	91	0.84–0.91	0.87	0.032	87.3
NDVI-tractor (GreenSeeker)	58	0.30–0.42	0.36	0.025	61.1
	76	0.54–0.70	0.64	0.022	66.3
	84	0.63–0.75	0.69	0.028	66.9
	94	0.58–0.73	0.66	0.023	67.5
NDVI-UAV (RedEdge)	91	0.78–0.87	0.82	0.016	80.0
	98	0.64–0.84	0.77	0.029	88.6
Leaf cholorophyll content (SPAD)	101	35.3–53.65	45.9	3.04	87.5
PHENO-score 1	87	37.00–51.50	43.06	3.99	66.2
PHENO-score 2	100	37.00–75.00	59.49	10.3	69.3
Leaf rolling (LR)	99	1.00–8.00	4.45	1.44	40.4
Dry biomass (ton/ha)	105	1.9–3.7	2.6	0.29	63.5

GWAS for NDVI, Dry Biomass, Leaf Chlorophyll Content (SPAD), Leaf Rolling, and Phenology Score

A total of 55 single NDVI QTLs were detected for the UAV-Sequoia platform on 55, 77, 83 and 91 DAP (detailed results reported in Supplementary Table 6), while for the similar DAP (58, 76, 84, and 94) the tractor-mounted platform identified 41 QTLs, about 25% fewer than with the UAV platform (Supplementary Tables 6, 7). In total, 28 QTLs were identified exclusively with the UAV-Sequoia platform while 15 QTLs were uniquely detected the tractor-mounted platform. When overlapping QTLs across platforms and GSs were considered as single identities, a total of 46 unique NDVI QTLs were identified (Supplementary Table 12). MLM-Q+K analysis detected 17 out of 46 unique NDVI QTLs on chromosomes 1A, 1B, 2B, 4A, 4B, 5A, 6A, 6B and 7A (Supplementary Table 13).

As to NDVI-UAV-Sequoia, the global R^2 of multiple QTL models ranged from 24.2% on 77 DAP (6 QTLs) to 89.6% on 91 DAP (22 QTLs), as shown in Supplementary Table 6. For NDVI-tractor-GreenSeeker at the same growth stages, the global R^2 of multiple QTL models ranged from 15.1% on 76 DAP (11 QTLs) to 64.7% on 94 DAP (16 QTLs). Notably, 19 of the 46 unique NDVI QTLs were consistently detected by both Sequoia-UAV and tractor-mounted platforms (41.30%, Supplementary Table 8). A common feature of both platforms was that the number of detectable NDVI QTLs and the global R^2 of multiple QTL models sharply increased from 55–77 DAP (14 QTLs for UAV-Sequoia and 9 QTLs for tractor-GreenSeeker) to 76–94 DAP (41 QTLs for UAV-Sequoia and 32 QTLs for tractor-GreenSeeker), in coincidence with and/or after anthesis. Twelve QTLs (52% of all 23 QTLs) were detected by both platforms for 55–77 DAP and 41 of 73 NDVI QTLs (56%) were detected at 76–94 DAP.

As expected from the medium to low correlation value, NDVI QTLs were detected at each of the four DAP herein considered. Specific QTLs were found particularly on 76–77 DAP and 91–94 DAP. **Table 6** reports the QTLs, commonly detected over at least two of the following inter-related traits: NDVI-UAV-Sequoia, NDVI-tractor-GreenSeeker, leaf chlorophyll content (SPAD), and dry biomass. A strong *per se* QTL influencing all eight NDVI measurements, SPAD and dry biomass was identified on chromosome 2B (*QNDVI.ubo-2B.1*), positioned at 5.9 cM on the tetraploid consensus map of Maccaferri et al. (2015a). R^2-values for this QTL were 5.38% for NDVI-UAV-Sequoia (91 DAP), 6.29% for SPAD, and 5.67% for dry biomass. Importantly, the confidence interval of this QTL did not overlap with that of *PPD-B1* (mapped at 51.3 cM on chromosome 2B of the consensus map) and can thus be considered as a valuable constitutive *per se* QTL affecting NDVI from the vegetative stage under well-watered conditions up to late-milk grain filling under water-deficit conditions. Additional QTLs consistently detected for NDVI, SPAD and dry biomass mapped on chromosomes 4A and 4B (*QNDVI.ubo-4A.2* and *QNDVI.ubo-4B.1*), with the latter closely mapping to the well-known *RhtB1b* locus. At least nine additional QTLs on chromosomes 1A, 2B, 3A, 4B, 5B, 6B, 7A, and 7B (*QNDVI.ubo-1A.1, QNDVI.ubo-2B.1, QNDVI.ubo-2B.4, QNDVI.ubo-3A.1, QNDVI.ubo-4B.1, QNDVI.ubo-5B.4, QNDVI.ubo-6B.6, QNDVI.ubo-7A.4,* and *QNDVI.ubo-7B.1*) affected NDVI concomitantly with both SPAD and dry biomass (chr. 1A, 2B, 4B, 5B, 6B, and 7B) or dry biomass only (chr. 2B, 3A, and 7A), suggesting that these QTLs affected biomass accumulation during the fast-growing stage or during the remobilization/translocation phases. In all cases, eight out of nine QTLs had no effects on phenology, hence suggesting *per se* effects on NDVI unrelated to growth stage.

Additionally, QTLs showed concurrent effects on NDVI (**Table 7**), and SPAD as well. However, for these QTLs no significant effects were detected on dry biomass, suggesting a prevalence of effects on chlorophyll content and/or senescence at the grain-filling stage without an appreciable impact on total biomass. Examples of these NDVI QTLs are *QNDVI.ubo-1B.3,-2A.1,-2A.2,-3A.2,-3B.1, -3B.3,-3B.4,-3B.5, -4A.1,-4A.2,-4B.2, -5B.1,-5B.3,-7A.2,* and *-7B.4*. Several QTLs affected only a single NDVI measurement and were therefore considered of marginal interest. UAV-RedEdge platform on 91 and 98 DAP identified 45 single QTLs for NDVI (Supplementary Table 9). A major *per se* NDVI locus (*QNDVI.ubo-6B.5*), not detectable by SPAD, was detected on 91 DAP (R^2 = 8.43%) and on 98 DAP (R^2 = 6.71%). However, this QTL was then ascertained to be coincident with a QTL for visual leaf rolling. The UAV-based platforms identified 13 common NDVI QTLs out of the 22 that were detected with at least one of the UAV-based platforms (Supplementary Table 9).

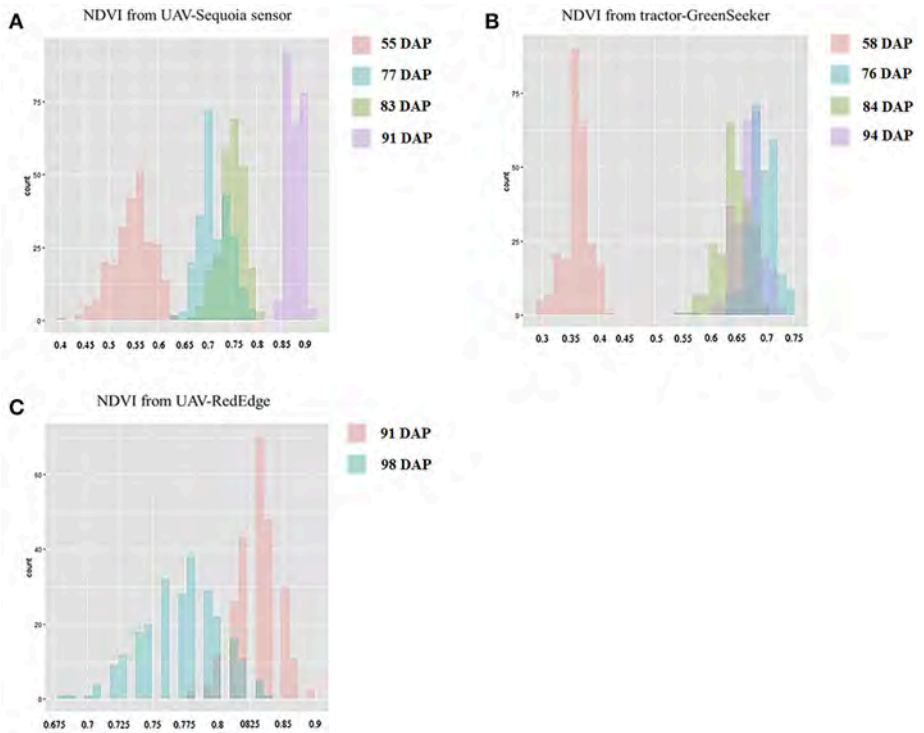

FIGURE 4 | Histograms for NDVI-UAV-Sequoia **(A)**, NDVI-tractor-GreenSeeker **(B)**, and NDVI-UAV-RedEdge **(C)** at different days after planting (DAP).

TABLE 3 | Broad-sense heritability and Pearson correlation coefficient for NDVI by UAV-Sequoia and tractor-GreenSeeker platforms on different days after planting (DAP).

NDVI-UAV-Sequoia	h^2**(%)**	**55**	**77**	**83**	**91**
55	77.2	1	–	–	–
77	83.2	0.747***	1	–	–
83	88.5	0.562***	0.859***	1	–
91	87.3	0.291***	0.555***	0.782***	1
NDVI-Tractor-GreenSeeker	h^2**(%)**	**58**	**76**	**84**	**94**
58	61.1	1	–	–	–
76	66.3	0.661***	1	–	–
84	66.9	0.535***	0.869***	1	–
94	67.5	0.142*	0.415***	0.590***	1

****P <0.001, *0.01< P <0.05.*

TABLE 4 | Pearson correlation coefficient for NDVI between UAV-Sequoia and tractor-GreenSeeker platforms on different days after planting (DAP).

NDVI	**Tractor-GreenSeeker**				
	DAP	**58**	**76**	**84**	**94**
UAV-Sequoia	55	0.506***	0.469***	0.384***	0.189**
	77	0.467***	0.507***	0.376***	0.243***
	83	0.357***	0.435***	0.423***	0.383***
	91	0.105***	0.219**	0.397***	0.614***

****P < 0.001, **0.001< P <0.01.*

Most of the NDVI-QTLs were detected from 76 to 94 DAP, with 12 out of 19 QTLs common to UAV- and tractor-mounted platforms, in contrast to only 3 QTLs detected on 55–58 DAP. As reported in **Table 6**, R^2 of multiple QTL models for common NDVI QTLs showed a himasongher percentage of explained variance (PEV) for UAV-Sequoia than for NDVI-tractor-GreenSeeker. PEV was 45.0% on 55 DAP for UAV-Sequoia and considerably lower (15.4%) on 58 DAP for tractor-GreenSeeker. UAV-Sequoia and tractor-GreenSeeker showed a PEV of 59.5% (77 DAP) and 42.1% (76 DAP), respectively, while PEV was 89.6% (91 DAP) and 64.7% (94 DAP), respectively. In addition, PEV was equal to 73.9 and 91.8% for NDVI-UAV-RedEdge on 91 and 98 DAP, respectively.

A total of 39 significant QTLs were detected for SPAD, particularly on chromosomes 1A (R^2 = 9.7%), 3B (R^2 = 6.8%), 5A (R^2 =10.3%), 5B (R^2 =8.0%), and 7A (R^2 = 9.3%). Out of the 39 SPAD-QTLs, a total of 22 loci (56%) overlapped between SPAD and NDVI. Among these 22 loci, 19 were not related to phenology. Selected SNPs associated to SPAD showed a very high global R^2 of 97.2% (**Table 6**), most likely overestimated due to residual population structure effects not accounted for.

Leaf rolling (LR) was associated to nine significant QTLs with one with the largest effect on chromosome 3A (R^2 = 6.34%), while selected SNPs associated to LR showed a global R^2 of 36.0% (Supplementary Table 11). Co-localization was observed

TABLE 5 | Significance and associated effect for major loci known to affect phenology and plant height *PPD-A1*-452 (sensitivity vs. insensitivity), *PPD-A1*-380/290 (insensitivity alleles), *PPD-B1* (copy number variation polymorphism), *Rht-B1* (RhtB1b semi-dwarfism allele) and *FT-7A* (indel in promoter region) on phenology score (17.3.2017 and 30.3.2017), NDVI and dry biomass on different days after planting (DAP).

Traits	DAP	*PPD-A1-452*		*PPD-A1-380/290*		*PPD-B1*		*Rht-B1*		*FT-7A*	
		–Log *P*	Effect	–Log *P*	Effect	–Log *P*	Effect	–Log *P*	Effect	–Log *P*	Effect
NDVI-UAV-Sequoia	91	**6.40**[a]	−9a[b]							**3.45**	−9a
NDVI-tractor-GreenSeeker	76							2.99	20a		
	84	2.46	−9a					2.79	10a		
	94	**7.52**	−9a							**4.11**	−1a
NDVI-UAV-RedEdge	91	**3.08**	−7a								
	98	**6.11**	−21a							**3.31**	−1a
PHENO-score1	87	**12.16**	8.65			2.76	2.05			**6.15**	2.71
PHENO-score2	100	**9.69**	3.79	2.12	3.57	2.56	8.65			**6.78**	7.46
Dry biomass	105							**3.14**	0.24		

[a]*GWAS significance P < 0.0001 (corresponding to Bonferroni P 0.05 multiple test significance threshold) correspond to a bold underlined font, 0.0001 < P < 0.001 to a bold font and 0.001 < P <0.01 to a regular font;* [b]*Effect: a = E−03.*

for LR and NDVI at *QNDVI.ubo-5B.2* and *QNDVI.ubo-6B.5*. In particular, the first locus was related to NDVI measured with both UAV- and ground-mounted platforms under drought stress. *QNDVI.ubo-6B.5* was even more interesting as it was strongly associated to NDVI signals from all three platforms and to LR but not SPAD nor biomass. In addition, LR co-mapped with leaf chlorophyll content (SPAD) measured on 101 DAP on chromosome 2B.

GWAS for dry biomass identified 19 significant QTLs (Supplementary Table 11) with the strongest effects shown by those on chromosomes 2B (R^2 = 6.3%), 4B (R^2 = 6.5%), 6A (R^2 = 7.2%), and 7B (R^2 = 6.4%). Nine of these QTLs were linked to NDVI (47% of UAV-detected QTLs) with *QNDVI.ubo-5A.3* (R^2 = 5.8%) and *QNDVI.ubo-5B.4* (R^2 = 5.7%) only detected with UAV-based platforms. Selected SNPs associated to dry biomass QTLs accounted for 64% of the phenotypic variance.

The full QTL list for NDVI, dry biomass, leaf chlorophyll content (SPAD), LR and phenology scores is available in Supplementary Tables 6, 7, 11. For comparative analysis of our results with previously published work, all QTLs identified in this study were positioned on the tetraploid-consensus map assembled by Maccaferri et al. (2015a) and are reported in **Figure 5**, including also NDVI QTLs gathered from the literature, mainly identified in the hexaploid wheat germplasm with hand-held portable instruments such as the classic GreenSeeker. Notably, 23 of the 46 NDVI QTLs did not overlap with growth stage QTLs, hence suggesting a prevalence of effects on a *per se* basis.

Based on the results reported herein, eight QTL hotspots for NDVI and/or chlorophyll content (SPAD), leaf rolling (LR) and biomass unrelated to phenology were detected on chromosomes 1A (*QNDVI.ubo-1A.1*), 1B (*QNDVI.ubo-1B.3*), 2B (*QNDVI.ubo-2B.1*), 4B (*QNDVI.ubo-4B.1*), 5B (*QNDVI.ubo-5B.*1), 6B (*QNDVI.ubo-6B.5* and *QNDVI.ubo-6B.6*), and 7B (*QNDVI.ubo-7B.1*).

DISCUSSION

NDVI Measurements by UAV- and Ground-Based Platforms

To our best knowledge, this study is the first to report on the use of UAV-based NDVI remote sensing for GWAS analysis in crops and to compare the results to those obtained using a ground-based platform. We compared two UAV- and one ground-based platforms to search for NDVI QTLs in a field trial first conducted under well-watered conditions until flowering, then followed by 2 weeks of progressively increasing water-deficit conditions that decreased leaf relative water content (RWC) to 53%. The rapid decrease in RWC after stopping irrigation was consequent to the high evaporative demand typical of the environment where the field trial was conducted. During the time interval from 16 to 31 March when irrigation was terminated and plants experienced an increasing water-deficit stress, the average mean daily and average maximum temperatures were 20.9 and 29.7°C, respectively while the average reference daily evapotranspiration using the standardized Penman-Monteith method was 5.41 mm.

It is well known that NDVI devices/platforms show different sensitivity features and, consequently, differ in their capacities to discriminate genotypes, specifically depending on the crop developmental stage and/or agronomic management (Marti et al., 2007; Cabrera-Bosquet et al., 2011; Christopher et al., 2016). Sensitivity of commonly used ground-based sensors such as GreenSeeker is maximum at early growth stages and then at the grain-filling/senescence stage while the sensitivity of UAV-based sensors, particularly for GWAS-QTL analysis, has not been assessed. Based on the known relationships of NDVI (as an integrative measure) with chlorophyll content and total plant/canopy biomass, a time-series of consecutive NDVI measurements were cross-referenced with flag leaf relative chlorophyll content (SPAD), leaf rolling and dry biomass data in order to identify the growth stage when NDVI and its relevant QTLs were most informative.

TABLE 6 | NDVI GWAS-QTLs for UAV-Sequoia (DAP: 55, 77, 83, and 91) and Tractor-GreenSeeker platforms (DAP: 58, 76, 84, and 94), leaf chlorophyll content (SPAD) (101 DAP) and dry biomass (105 DAP), commonly detected for at least two traits. QTL significance, tagging-marker R^2-value and co-localization with previously known NDVI QTLs are reported.

QTL	Marker	Position	NDVI UAV-Sequoia				NDVI Tractor-GreenSeeker				SPAD	Dry biomass	NDVI QTL from literature
		cM[1]	55	77	83	91	58	76	84	94	101	105	QTL[2]
QNDVI.ubo-1A.1	IWB72019	59.7			4.9[3]	4.6			4.74	3.92	5.03	5.13	e
QNDVI.ubo-1B.2	IWA8557	25.4							6.56				a,d
QNDVI.ubo-1B.3	IWA6917	67.6			5.99	**6.99**				6.99	**7.07**		
QNDVI.ubo-2A.3	IWB8175	107.0				**7.21**				3.90			
QNDVI.ubo-2B.1	IWB47560	5.9	3.41	4.53	4.82	5.38	5.35	**2.69**	**5.24**	5.37	**6.29**	5.67	
QNDVI.ubo-2B.4	wPt-2929	170.6			5.35			6.08				**6.3**	
QNDVI.ubo-3A.1	IWA5039	64.3			4.95				2.91			4.21	e,f
QNDVI.ubo-3B.1	IWB6062	2.4			4.84						**6.84**		e
QNDVI.ubo-3B.3	IWB8435	41.3				5.37				3.95	4.84		
QNDVI.ubo-3B.4	IWB24050	147.2							4.86		**8.45**		
QNDVI.ubo-3B.5	IWB22805	204.5	**4.2**				4.6				**6.79**		b
QNDVI.ubo-4A.1	IWB73476	22.2								7.83	4.63		b,f,g
QNDVI.ubo-4A.2	IWB60692	167.6	4.73	6.59	5.38	5.35			5.23	5.23	3.13		
QNDVI.ubo-4B.1	IWB70795	2.8	**8.01**	**5.02**	4.48	4.79		5.25			5.11	4.34	b
QNDVI.ubo-4B.2	IWB56078	32.9								3.00	**7.56**		b,d
QNDVI.ubo-4B.3	IWB72120	92.9				**5.98**				4.15	**6.63**		
QNDVI.ubo-5A.3	IWA3583	112.1				4.23						5.76	
QNDVI.ubo-5B.1	IWB73979	14.7				**5.89**				5.00	5.72		b,d,e
QNDVI.ubo-5B.2	IWB59038	48.9			4.75								c,d
QNDVI.ubo-5B.3	IWB54773	93.9									4.79		f
QNDVI.ubo-5B.4	wPt-0498	109				5.35					3.2	5.67	
QNDVI.ubo-6B.6	IWB45581	155.1			3.14	4.59			3.24	4.08	4.75	2.9	
QNDVI.ubo-7A.2	IWB44791	59.8				2.61				4.21	5.78		e
QNDVI.ubo-7A.3	IWB58341	131.3		4.90	**7.18**	**4.32**			4.63				
QNDVI.ubo-7A.4	IWB28063	181.8	3.30		4.37	**5.73**	**6.91**					4.61	
Global QTL model (R^2, %)		-	45.0	24.2	59.5	89.6	15.4	15.1	42.1	64.7	97.2	64.0	

The full list of GWAS-QTLs is reported in Supplementary Table 12. [1]Chromosomes of QTL regions based on the tetraploid wheat consensus map (Maccaferri et al., 2015a); [2]a: (Shi et al., 2017); b: (Pinto et al., 2016); c: (Sukumaran et al., 2015); d: (Gao et al., 2015); e: (Li et al., 2014); f: (Bennett et al., 2012); g: (Pinto et al., 2010); [3]Tagging-marker R^2-values are reported. GWAS significance P < 0.0001 (corresponding to Bonferroni P 0.05 multiple test significance threshold) correspond to a bold underlined font, 0.0001 < P <0.001 to a bold font and 0.001 < P <0.01 to a regular font.

When compared to the two UAV-based platforms, NDVI-values collected with the ground-based platform plateaued earlier from 76 to 84 DAP, indicating its lower capacity to monitor plant biomass accumulation and leaf greenness during the reproductive stage of the wheat growth cycle. Additionally, UAV-mounted platforms allowed us to measure hundreds of plots in very short time, hence minimizing the confounding effects due to time-related environmental variation, which inevitably affect the results of studies conducted with ground-based platforms (Haghighattalab et al., 2016). Whether differences between the ground-based platform and UAV-based platforms are due to the means of locomotion or the nature of the sensors employed, they could not be assessed with these data.

NDVI has long been recognized for its ability to estimate crop biomass and grain yield (Lewis et al., 1998; Araus et al., 2001; Chuvieco Salinero, 2002) and this correlation becomes stronger when estimated with UAV platforms (Kyratzis et al., 2015). In our study, the two UAV-based platforms showed a markedly higher repeatability for NDVI measurements as compared to those collected with the ground-based platform. High repeatability, hence heritability, is critical to effectively identify and eventually clone QTLs (Tuberosa, 2012). Therefore, from a methodological perspective on the use of the aerial vs. ground-based HTPPs to detect QTL for NDVI, our results show the increased ability of the former, particularly under terminal drought stress, as shown by the considerably higher number of QTLs and overall R^2-values detected with the UAV-based platforms. Accordingly, a recent study conducted in barley grown under 10 different nitrogen treatments has also shown an increased sensitivity of aerial vs. ground-based platforms to measure NDVI using RGB (conventional digital cameras), multispectral and thermal aerial imagery in combination with a matching suite of ground sensors (Kefauver et al., 2017). The relative benefits and comparison

TABLE 7 | Highly-significant GWAS-QTLs for NDVI ($P < 0.0001$) from UAV-RedEdge (DAP: 91 and 98), UAV-Sequoia (DAP: 55, 77, 83, and 91) and tractor-GreenSeeker (DAP: 58, 76, 84, and 94).

Platform	DAP	QTL	Marker	Chr.	Position (cM)[1]	CI (cM)	Alleles	Effect	–Log *P*	R^2 (%)
UAV-Sequoia	55	*QNDVI.ubo-4B.1*	IWB70795	4B	7.95	4.95-10.95	**A**/G[3]	9.9c[2]	4.89	8.01
	77	*QNDVI.ubo-4B.1*	IWB70795	4B	16	13-19	**A**/G	−6.2a	4.15	5.02
	83	*QNDVI.ubo-7A.3*	IWB58341	7A	124.1	121.1-127.1	**A**/G	−1.5b	4.57	7.18
	91	*QNDVI.ubo-1B.3*	IWA6917	1B	58.5	55.5-61.5	**A**/G	−5.9a	4.90	6.99
		QNDVI.ubo-2A.1	IWB34575	2A	46.6	43.6-49.6	**A**/G	0.09	4.43	7.21
UAV-RedEdge	91	*QNDVI.ubo-1B.3*	IWB31673	1B	59.1	56.1-62.1	**C**/T	−1.2b	4.07	5.89
		QNDVI.ubo-6B.5	IWB71546	6B	94.8	91.8-97.8	**A**/G	−1.5b	5.53	8.43
		QNDVI.ubo-7A.4	IWB28063	7A	181.8	178.8-184.8	**A**/G	0.01	4.62	6.83
	98	*QNDVI.ubo-1B.2*	IWB8612	1B	43.6	40.6–46.6	**G**/T	0.02	4.98	6.61
		QNDVI.ubo-3B.3	IWB1757	3B	32	29–35	**A**/C	−2.1b	4.89	6.47
		QNDVI.ubo-6B.5	IWB71546	6B	94.8	91.8–97.8	**A**/G	−2.3b	5.05	6.71
Tractor	58	*QNDVI.ubo-7A.4*	IWA8393	7A	183.2	180.2–186.2	**C**/T	0.03	4.11	6.91
	76	*QNDVI.ubo-2B.1*	IWB47560	2B	5.9	2.9–8.9	**C**/T	0.02	4.45	2.69
	84	*QNDVI.ubo-2B.1*	IWB47560	2B	5.9	2.9–8.9	**C**/T	0.01	4.29	5.24
	94	*QNDVI.ubo-4A.2*	wPt-3449	4A	161.5	158.5–164.5	**A**/T	0.01	5.35	4.25

QTL regions were defined based on a confidence interval of ±3.0 cM from the map positions of the QTL tagging-SNPs. [1]Chromosomes of QTL regions based on the tetraploid wheat consensus map (Maccaferri et al., 2015a); [2]Allele effect: a = E+01, b = E+02, and c = E−04; [3]The estimate of the effect is referred to the allele highlighted in bold.

of UAV- and ground-based platforms remain to be empirically evaluated for other phenotypic variables beyond NDVI.

Notably, the NDVI measurements from UAV-RedEdge on 91 DAP showed a decrease in NDVI average values under water shortage, most likely consequent to the cumulative effects of senescence and drought stress severity. As reported by Peters et al. (2002), NDVI can indicate vegetation response to water stress and could be used as a proxy to evaluate drought effects (Kyratzis et al., 2015; Liu et al., 2016).

GWAS Analysis for NDVI and Other Drought-Adaptive Traits

It is known that spectrometers to measure NDVI and other vegetative indexes show different sensitivities. Consequently, sensors/platforms are also characterized by different capacity to discriminate among genotypes, depending on the developmental stage and/or agronomic management. In wheat, sensitivity of commonly used ground-based active sensors such as GreenSeeker is maximum at early growth stages while progressively decreasing approaching heading/anthesis (canopy closure) and then increasing again with the onset of the grain-filling/senescence phase (Marti et al., 2007; Christopher et al., 2016). While several GWAS studies have reported on the dissection of genetic inheritance of NDVI data collected with traditional ground-based sensors (as detailed below), no specific study has so far addressed the effectiveness of UAV-based sensors in providing NDVI scores suitable for QTL discovery. In our study, the UAV-based (Sequoia) NDVI data allowed for the identification of a considerably larger number (58%) of NDVI QTLs as compared to the ground-based platform (42%). Moreover, the use of the UAV-based platforms allowed us to increase the level of QTL significance and repeatability across growth stages. As expected, grain-filling stages appeared the most valuable for detecting NDVI-related genetic differences among genotypes (61.2% of which were identified at the grain-filling stage) in response to the progressive onset of senescence and drought stress related to the water-shortage treatment. Along this line, breeding strategies for enhancing drought tolerance are increasingly adopting remote-sensing of NDVI and other spectral technologies (Monneveux et al., 2012; Araus and Cairns, 2014; Ramya et al., 2016; Trapp et al., 2017).

Two main loci identified on chromosomes 2A (R^2 from 6.40 to 7.21%) and 6B (R^2 from 6.13 to 8.43%) were associated to NDVI QTLs as per UAV-based (Sequoia and RedEdge sensors) data during the water-stressed treatment (Supplementary Table 10). Based on the known relationships of NDVI (as integrative measure) with chlorophyll content and total plant biomass, NDVI measurements were cross-referenced to leaf chlorophyll content (SPAD) and dry biomass accumulation data. Among the 39 significant loci mapped for SPAD, 22 (56%) overlapped with NDVI QTLs from aerial and ground-based platforms.

QTL Hotspots for NDVI and Other Drought-Related Proxy Traits

The major loci known to influence photoperiod, vernalization, flowering time, and plant height (Milner et al., 2016) significantly affected phenology score, NDVI, leaf rolling and dry biomass. In particular, *PPD-A1* and *FT-7A* influenced phenology score, UAV- and ground-based NDVI, especially under water-deficit stress. The strong effect on phenology score and adaptation of *PPD-A1* allelic variants is well documented (Snape et al., 2001) while the effects of variants at *PPD-B1* (copy number variation) and at *FT-7A* have been less explored. *PPD-A1* (452-bp allele) influenced UAV-based NDVI on 91 and 98 DAP as well as ground-based NDVI on 84 and 94 DAP, while *FT-7A* influenced UAV-based NDVI on 91 and 98 DAP as well as NDVI-tractor-GreenSeeker on 94 DAP (**Table 5**). Accounting for the effects (as covariates) of these major loci in the GWAS

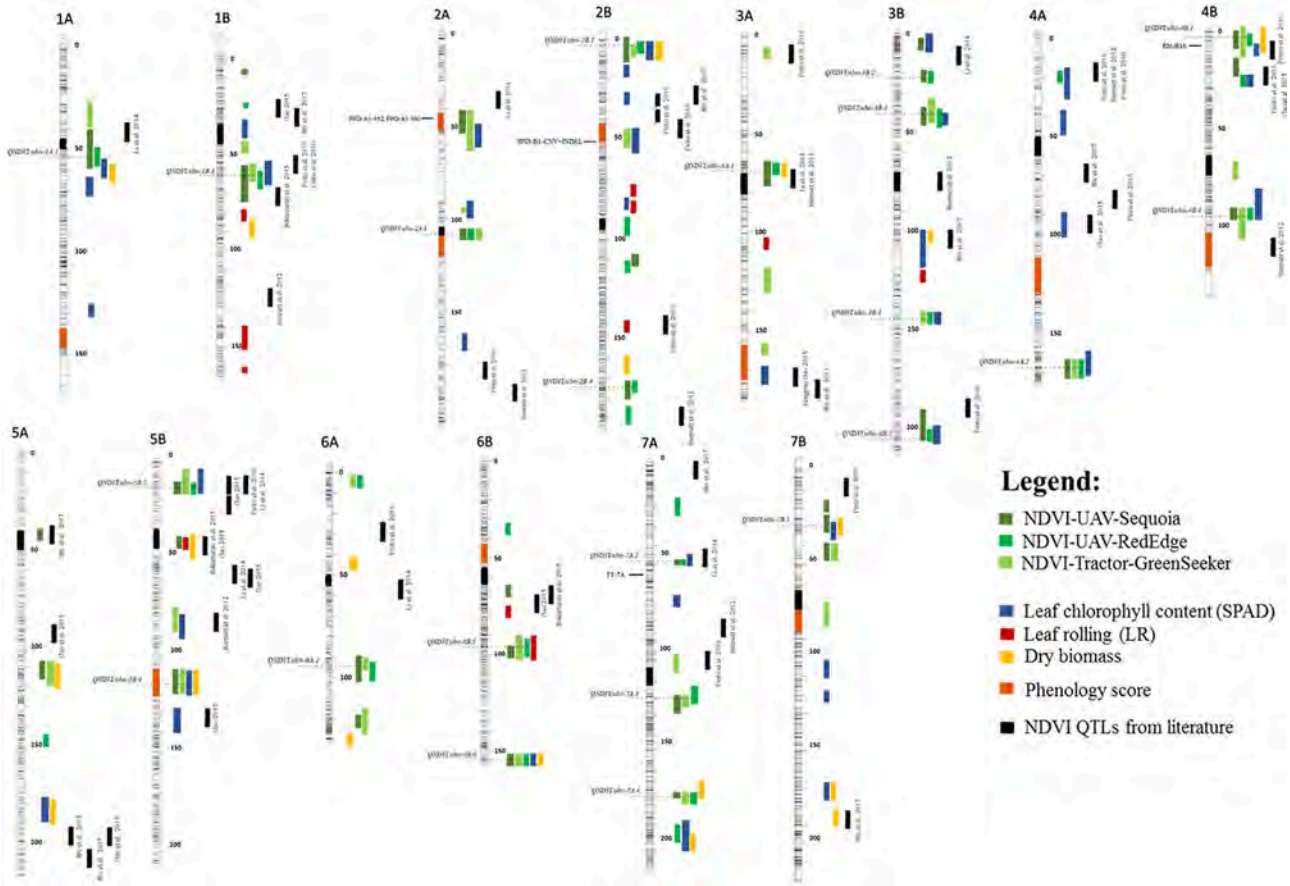

FIGURE 5 | Chromosome position on the durum consensus map (Maccaferri et al., 2015a) of (i) QTLs identified in this study, (ii) previously mapped NDVI QTLs and (iii) main genes for phenology. NDVI QTLs significant for UAV-Sequoia are highlighted with a dark-green vertical bar, NDVI QTLs significant for UAV-RedEdge with a light-green bar, NDVI QTLs significant for tractor-GreenSeeker with a green-bar. QTLs highlighted with a yellow bar were significant for dry biomass, QTLs with a blue bar are significant for SPAD, QTLs with a red bar were significant for leaf rolling (LR) and QTLs indicated with an orange bar (shown directly on the chromosomes) are significant for phenology score. Black vertical bars indicate NDVI QTLs identified from the literature. Horizontal gray-dotted lines indicate the QTL peak positions.

mixed model allowed us to markedly increase the power of QTL detection while providing more accurate estimates of their effects and identifying QTLs influencing drought-adaptive traits on a *per se* basis. After covariance analysis based on the molecular genotypes of accessions at the major *PPD*, *VRN*, and *FT* loci, six QTLs were still found to influence both NDVI and phenology score (Zadoks system). This notwithstanding, our study also highlighted the presence of eight hotspot QTLs affecting NDVI and/or chlorophyll content (SPAD), leaf rolling (LR), biomass and/or visual response to water shortage independently from phenology, further supported by co-location with NDVI QTLs reported in bread wheat.

The leaves of many important cereal crops (maize, rice, sorghum, and wheat) show a tendency to roll up into a cylinder in response to drought conditions and then unroll when leaf water balance improves (Sirault et al., 2015). Apart from mutant genetic stocks showing a constitutively high leaf rolling (LR), this trait in cultivated wheat germplasm is associated with leaf water loss and thus provides a proxy of drought stress over a certain degree of relative water loss. In this regard, the negative relationship observed between NDVI and LR, particularly evident with subgroup S1 (ancient Italian accessions) which showed the lowest NDVI (98 DAP) and the highest LR-values, suggests that modern durum wheat varieties for Mediterranean countries have been selected for both enhanced chlorophyll content and improved drought-response.

Comparative Analysis With Other QTL Studies in Wheat

Although recent studies have identified significant NDVI QTLs in cereals (Pinto et al., 2010, 2016; Bennett et al., 2012; Li et al., 2014; Gao et al., 2015; Sukumaran et al., 2015; Shi et al., 2017; **Figure 5**), none of these studies deployed UAV-mounted cameras to collect multi-spectral images.

Among the five NDVI QTLs detected by Pinto et al. (2010) in elite Seri/Babax recombinant inbred lines (RILs) at vegetative and grain-filling stages, two overlapped with our QTLs on chromosomes 1B and 4A for ground-based NDVI. More recently, Pinto et al. (2016) detected the major QTL for NDVI at the vegetative stage in Seri/Babax wheat mapping population on

chromosome 1B and other NDVI loci on chromosomes 1A, 2A, 4A, 5B, and 7A, all of which overlapped with each locus of this study, except for the QTL on chromosome 2A.

In particular, the NDVI QTL on chromosome 1B is of great interest, since it showed the highest LOD score and percentage explained variance (PEV) in Seri/Babax (Pinto et al., 2016) and it has been consistently detected across three NDVI phenotyping methods in our experiment, within a coincident confidence interval of <10 cM. Most notably, this QTL did not affect phenology. Therefore, this chromosome region represents an important hotspot for NDVI and leaf greenness and is a good candidate for marker-assisted selection as well as positional cloning (Salvi and Tuberosa, 2015). Studying the inheritance of this region in tetraploid wheat and eventually cloning the underlining functional polymorphism would also be a good complement toward the dissection of drought-adaptive traits in hexaploid wheat, in view of the simplified genetics of tetraploid wheats and, particularly, the recent assembly of a high-quality assembly in emmer wheat (*T. turgidum* ssp. *dicoccum* Schrank; Avni et al., 2017), the tetraploid progenitor of both durum and bread wheat.

Bennett et al. (2012) identified four significant loci for NDVI in RAC875/Kukri doubled-haploid population under heat and drought treatments and two of those overlapped with our QTLs for UAV-based NDVI on chromosomes 2B and 5B. Gao et al. (2015) reported NDVI QTLs in the Chinese Wheat Cross Zhou 8425b/Chinese Spring at anthesis and at 10 days post-anthesis, eight of which co-mapped with NDVI QTLs detected in this study and, in particular, a strong overlapping was identified on chromosomes 3B and 5B. Additionally, Li et al. (2014) detected NDVI QTLs in bread wheat (Jingdong 8/Aikang 5) overlapping with QTLs on chromosomes 1A, 3A, 3B, 5B, and 7A also identified in the present work. Additionally, according to the markers shared with the tetraploid consensus map (Maccaferri et al., 2015a), two significant NDVI QTLs were identified on chromosomes 1B and 5B at 13 and 7 cM, respectively, from the QTLs previously identified by Sukumaran et al. (2015) for NDVI at vegetative and grain-filling stages using GreenSeeker portable sensors on spring hexaploid wheat lines. According to Kyratzis et al. (2017), there is a close association between NDVI and leaf/canopy greenness in durum wheat. Moreover, SPAD provides an estimation of grain yield (Islam et al., 2014; Monostori et al., 2016) and grain protein concentration (Le Bail et al., 2005). As reported by Kyratzis et al. (2015), NDVI represents also a proxy for biomass and the efficient application of this technology in large breeding programs has become the next challenge. We identified 19 significant GWAS QTLs for dry biomass, nine of which (47.3%) co-mapped with NDVI from both aerial and ground-based platforms, hence confirming the usefulness of this vegetation index for predicting final wheat biomass (Marti et al., 2007; Pantazi et al., 2016). Notably, nine of these loci on chromosomes 1B, 2B, 3B, 4B, 6A, 6B, and 7B overlapped with QTLs for field thousand grain weight (TGW) and/or grain yield (GY) from data published in Maccaferri et al. (2011) and reanalyzed for GWAS based on the same SNP platform (Maccaferri et al., 2016) considered herein. In addition *QNDVI.ubo.5A.3* and *QNDVI.ubo.5B.4* were linked to both dry biomass and NDVI captured only from aerial platforms with a R^2 of 5.76 and 5.67%, respectively (**Table 6**). Among the four main QTLs mapped for LR on chromosomes 1B, 3A, 3B, and 6B, the last one overlapped with the LR QTL reported by Peleg et al. (2009) in durum wheat × wild emmer RIL evaluated under drought stress.

In summary, eight QTL hotspots for NDVI and/or chlorophyll content (SPAD), leaf rolling (LR) and biomass unrelated to phenology were detected on chromosomes 1A (*QNDVI.ubo-1A.1*), 1B (Q*NDVI.ubo-1B.3*), 2B (*QNDVI.ubo-2B.1*), 4B (*QNDVI.ubo-4B.1*), 5B (*QNDVI.ubo-5B.1*), 6B (*QNDVI.ubo-6B.5* and *QNDVI.ubo-6B.6*) and 7B (*QNDVI.ubo-7B.1*). Notably, *QNDVI.ubo-2B.1*, *QNDVI.ubo-4B.1* and *QNDVI.ubo-6B.6* overlapped with QTLs for TGW and/or GY (Maccaferri et al., 2016).

CONCLUSIONS

This study compared NDVI field phenotyping based on the emerging UAV-based platforms vs. the standard ground-based methods targeting an elite durum wheat collection suitable for GWAS analysis and representative of global durum breeding. The results reported herein demonstrated the great potential and effectiveness of both fixed-wing and multi-rotor UAV-based platforms to gather rapid, precise, and detailed NDVI measurements, which in turn considerably improved trait repeatability estimates, QTL identification and considerably increasing the portion of phenotypic variation accounted for by the multiple-QTL models. NDVI phenotypes and NDVI QTLs were cross-referenced by parallel leaf greenness (SPAD) and final biomass evaluation. The durum panel proved informative for the identification of QTLs for NDVI, SPAD, LR, and biomass. Strong effect NDVI QTLs were consistently detected across phenotyping platforms, with concomitant QTL effects on SPAD, LR and/or biomass. One major *per se* NDVI QTL detected on chromosome 1B (*QNDVI.ubo-1B.4*) across the three NDVI phenotyping platforms and for SPAD co-mapped in a 10-cM interval with a major NDVI QTL described in the CIMMYT spring hexaploid wheat germplasm. Therefore, this QTL is worth considering for further characterization as well as positional cloning. Moreover, three additional *per se* NDVI QTLs were detected across measurements, consistently expressed from the end of fast-growth stage on 91 DAP (*QNDVI.ubo-2B.1*, *QNDVI.ubo-4A.2* and *QNDVI.ubo-4B.1*) in addition to several specific NDVI QTLs were also detected, particularly for the grain-filling drought-stressed stages. Importantly, our results demonstrate that UAV-based platforms allow phenotypic data to be collected in high-throughput and with precision capable of discerning genetic differences to facilitate the detection of QTLs for drought-adaptive traits.

AUTHOR CONTRIBUTIONS

MN and PA-S provided overall coordination of the field experiments including manual, ground, and aerial phenotyping. JW, MN, RW, MM, and RT designed the experiment.

GC, JW, and MN conducted the field and laboratory measurements. RW and AF managed the UAV workflow including photogrammetry and zonal statistics. PA-S and JW managed ground-based data workflows. GC and MM conducted genotyping experiments. GC and MM analyzed the data, interpreted the results, and wrote the manuscript, under the supervision of RT and with contributions from all the other authors.

ACKNOWLEDGMENTS

This study is the result of the collaborative project among the Department of Agricultural Sciences of University of Bologna (Italy), Maricopa Agricultural Center (MAC) of University of Arizona (USA) and US Arid-Land Agricultural Research Center of USDA ARS (USA). USDA is an equal opportunity provider and employer. Mention of trade names or commercial products in this publication is solely for the purpose of providing specific information and does not imply recommendation or endorsement by the U.S. Department of Agriculture.

Technical assistance was provided by John T. Heun and Sara J. Harders. UAV flights were conducted by Mark Yori (Phoenix Drone Services).

TERRA REF project, funded by the Advanced Research Projects Agency-Energy (ARPA-E), U.S. Department of Energy, under award number DE-AR0000594.

SUPPLEMENTARY MATERIAL

The Supplementary Material for this article can be found online at: https://www.frontiersin.org/articles/10.3389/fpls.2018.00893/full#supplementary-material

REFERENCES

Andrade-Sanchez, P., Gore, M. A., Heun, J. T., Thorp, K. R., Carmo-Silva, A. E., French, A. N., et al. (2013). Development and evaluation of a field-based high-throughput phenotyping platform. *Funct. Plant Biol.* 41, 68–79. doi: 10.1071/FP13126

Araus, J. L., and Cairns, J. (2014). Field high-throughput phenotyping: the new crop breeding frontier. *Trends Plant Sci.* 19, 52–61. doi: 10.1016/j.tplants.2013.09.008

Araus, J. L., Casadesus, J., and Bort, J. (2001). "Recent tools for the screening of physiological traits determining yield," in *Application of Physiology in Wheat Breeding,* eds M. P. Reynolds, J. I. Ortiz-Monasterio, and A. McNab (Mexico: CIMMYT), 59–77.

Avni, R., Nave, M., Barad, O., Baruch, K., Twardziok, S. O., Gundlach, H., et al. (2017). Wild emmer genome architecture and diversity elucidate wheat evolution and domestication. *Science* 357, 93–97. doi: 10.1126/science.aan0032

Barrett, J. C., Fry, B., Maller, J., and Daly, M. J. (2005). Haploview: analysis and visualization of LD and haplotype maps. *Bioinformatics* 21, 263–265. doi: 10.1093/bioinformatics/bth457

Barrs, H. D. (1968). "Determination of water deficits in plant tissues," in *Water Deficits and Plant Growth,* ed T. T. Kozolvski (New Delhi: Academic Press), 235–368.

Bennett, D., Reynolds, M., Mullan, D., Izanloo, A., Kuchel, H., Langridge, P., et al. (2012). Detection of two major grain yield QTL in bread wheat (*Triticum aestivum* L.) under heat, drought and high yield potential environments. *Theor. Appl. Genet.* 125, 1473–1485. doi: 10.1007/s00122-012-1927-2

Bentley, A. R., Turner, A. S., Gosman, N., Leigh, F. J., Maccaferri, M., Dreisigacker, S., et al. (2011). Frequency of photoperiod-insensitive *Ppd-A1a* alleles in tetraploid, hexaploid and synthetic hexaploid wheat germplasm. *Plant Breed.* 130, 10–15. doi: 10.1111/j.1439-0523.2010.01802.x

Berger, G. L., Liu, S., Hall, M. D., Brooks, W. S., Chao, S., Muehlbauer, G. J., et al. (2013). Marker-trait associations in Virginia Tech winter barley identified using genome-wide mapping. *Theor. Appl. Genet.* 126, 693–710. doi: 10.1007/s00122-012-2011-7

Bort, J., Casadesus, J., Nachit, M. M., and Araus, J. L. (2005). Factors affecting the grain yield predicting attributes of spectral reflectance indices in durum wheat: growing conditions, genotype variability and date of measurement. *Int. J. Remote Sens.* 26, 2337–2358. doi: 10.1080/01431160512331337808

Bowman, B. C., Chen, J., Zhang, J., Wheeler, J., Wang, Y., Zhao, W., et al. (2015). Evaluating grain yield in spring wheat with canopy spectral reflectance. *Crop Sci.* 55, 1881–1890. doi: 10.2135/cropsci2014.08.0533

Bradbury, P. J., Zhang, Z., Kroon, D. E., Casstevens, T. M., Ramdoss, Y., and Buckler, E. S. (2007). TASSEL: software for association mapping of complex traits in diverse samples. *Bioinformatics* 23, 2633–2635. doi: 10.1093/bioinformatics/btm308

Cabrera-Bosquet, L., Sánchez, C., Rosales, A., Palacios-Rojas, N., and Araus, J. L. (2011). Near-Infrared Reflectance Spectroscopy (NIRS) assessment of delta O18 and nitrogen and ash contents for improved yield potential and drought adaptation in maize. *J. Agric. Food Chem.* 59, 467–474. doi: 10.1021/jf103395z

Christopher, J. T., Christopher, M. J., Borrell, A. K., Fletcher, S., and Chenu, K. (2016). Stay-green traits to improve wheat adaptation in well-watered and water-limited environments. *J. Exp. Bot.* 67, 5159–5172. doi: 10.1093/jxb/erw276

Chuvieco Salinero, E. (2002). *Analisis de Imagenes: Extraccion de Informacion Tematica. Teledeteccion Ambiental.* Barcelona: Ariel, La observacion de la tierra desde el espacio.

Duan, T., Chapman, S. C., Guo, Y., and Zheng, B. (2017). Dynamic monitoring of NDVI in wheat agronomy and breeding trials using an unmanned aerial vehicle. *Field Crops Res.* 210, 71–80. doi: 10.1016/j.fcr.2017.05.025

Evanno, G., Regnaut, S., and Goudet, J. (2005). Detecting the number of clusters of individuals using the software STRUCTURE: a simulation study. *Mol. Ecol.* 14, 2611–2620. doi: 10.1111/j.1365-294X.2005.02553.x

Gao, F., Wen, W., Liu, J., Rasheed, A., Yin, G., Xia, X., et al. (2015). Genome-wide linkage mapping of QTL for yield components, plant height and yield-related physiological traits in the Chinese Wheat Cross Zhou 8425B/Chinese Spring. *Front. Plant. Sci.* 6:1099. doi: 10.3389/fpls.2015.01099

Haghighattalab, A., González Pérez, L., Mondal, S., Singh, D., Schinstock, D., Rutkoski, J., et al. (2016). Application of unmanned aerial systems for high throughput phenotyping of large wheat breeding nurseries. *Plant Methods.* 12:35. doi: 10.1186/s13007-016-0134-6

Holman, F. H., Riche, A. B., Michalski, A., Castle, M., Wooster, M. J., and Hawkesford, M. J. (2016). High throughput field phenotyping of wheat plant height and growth rate in field plot trials using UAV based remote sensing. *Remote Sens.* 8:1031. doi: 10.3390/rs8121031

Islam, M. R., Sham sul Haque, K. M., Akter, N., and Abdul Karim, M. (2014). Leaf chlorophyll dynamics in wheat based on SPAD meter reading and its relationship with grain yield. *Sci. Agric.* 4, 13–18. doi: 10.15192/PSCP.SA.2014.4.1.1318

Ji, L., and Peters, A. J. (2003). Assessing vegetation response to drought in the northern Great Plains using vegetation and drought indices. *Remote Sens. Environ.* 87, 85–98. doi: 10.1016/S0034-4257(03)00174-3

Kefauver, S. C., Vicente, R., Vergara-Díaz, O., Fernandez-Gallego, J. A., Kerfal, S., Lopez, A., et al. (2017). Comparative UAV and field phenotyping to assess yield and nitrogen use efficiency in hybrid and conventional barley. *Front. Plant. Sci.* 8:1733. doi: 10.3389/fpls.2017.01733

Kelley, C. P., Mohtadi, S., Cane, M. A., Seager, R., and Kushnir, Y. (2015). Climate change in the Fertile Crescent and implications of the recent Syrian drought. *Proc. Natl. Acad. Sci. U.S.A.* 112, 3241–3246. doi: 10.1073/pnas.1421533112

Kyratzis, A. C., Skarlatos, D. P., Fotopoulos, V., Vamvakousis, V. F., and Katsiotis, A. (2015). Investigating correlation among NDVI index derived by unmanned

aerial vehicle photography and grain yield under late drought stress conditions. *Proc. Env. Sci.* 29, 225–226. doi: 10.1016/j.proenv.2015.07.284

Kyratzis, A. C., Skarlatos, D. P., Menexes, G. C., Vamvakousis, V. F., and Katsiotis, A. (2017). Assessment of vegetation indices derived by UAV imagery for durum wheat phenotyping under a water limited and heat stressed mediterranean environment. *Front. Plant. Sci.* 8:1114. doi: 10.3389/fpls.2017.01114

Labus, M. P., Nielsen, G. A., Lawrence, R. L., Engel, R., and Long, D. S. (2010). Wheat yield estimates using multi-temporal NDVI satellite imagery. *Int. J. Remote Sens.* 23, 4169–4180. doi: 10.1080/01431160110107653

Langridge, P., and Reynolds, M. P. (2015). Genomic tools to assist breeding for drought tolerance. *Curr. Opin. Biotechnol.* 32, 130–135. doi: 10.1016/j.copbio.2014.11.027

Le Bail, M., Jeuffroy, M. H., Bouchard, C., and Barbottin, A. (2005). Is it possible to forecast grain protein content and yield of several varieties from chlorophyll meter measurements? *Eur. J. Agron.* 23, 379–391. doi: 10.1016/j.eja.2005.02.003

Letta, T., Maccaferri, M., Badebo, A., Ammar, K., Ricci, A., Crossa, J., et al. (2013). Searching for novel sources of field resistance to Ug99 and Ethiopian stem rust races in durum wheat via association mapping. *Theor. Appl. Genet.* 126, 1237–1256. doi: 10.1007/s00122-013-2050-8

Lewis, J. E., Rowland, J., and Nadeau, A. (1998). Estimating maize production in Kenya using NDVI: some statistical considerations. *Int. J. Remote Sens.* 19, 2609–2617. doi: 10.1080/014311698214677

Li, X., Chen, X., Xiao, Y., Xia, X., Wang, D., He, Z., et al. (2014). Identification of QTLs for seedling vigor in winter wheat. *Euphytica* 198, 199–209. doi: 10.1007/s10681-014-1092-6

Liu, W., Maccaferri, M., Bulli, P., Rynearson, S., Tuberosa, R., Chen, X., et al. (2017). Genome-wide association mapping for seedling and field resistance to *Puccinia striiformis* f. *sp. tritici* in elite durum wheat. *Theor. Appl. Genet.* 130, 649–667. doi: 10.1007/s00122-016-2841-9

Liu, Z., Li, C., Zhou, P., and Chen, X. (2016). A probabilistic assessment of the likelihood of vegetation drought under varying climate conditions across China. *Sci. Rep.* 6:35105. doi: 10.1038/srep35105

Lobos, G. A., Matus, I., Rodriguez, A., Romero-Bravo, S., Araus, J. L., and Del Pozo, A. (2014). Wheat genotypic variability in grain yield and carbon isotope discrimination under Mediterranean conditions assessed by spectral reflectance. *J. Integr. Plant Biol.* 56, 470–479. doi: 10.1111/jipb.12114

Lukina, E. V., Stone, M. L., and Rann, W. R. (1999). Estimating vegetation coverage in wheat using digital images. *J. Plant Nutr.* 22, 341–350. doi: 10.1080/01904169909365631

Maccaferri, M., El-Feki, W., Nazemi, G., Salvi, S., Canè, M. A., Colalongo, M. C., et al. (2016). Prioritizing quantitative trait loci for root system architecture in tetraploid wheat. *J. Exp. Bot.* 67, 1161–1178. doi: 10.1093/jxb/erw039

Maccaferri, M., Ricci, A., Salvi, S., Milner, S. G., Noli, E., Martelli, P. L., et al. (2015a). A high-density, SNP-based consensus map of tetraploid wheat as a bridge to integrate durum and bread wheat genomics and breeding. *Plant Biotechnol. J.* 13, 648–663. doi: 10.1111/pbi.12288

Maccaferri, M., Sanguineti, M. C., Demontis, A., El Ahmed, A., Garcia del Moral, L., Maalouf, F., et al. (2011). Association mapping in durum wheat grown across a broad range of water regimes. *J. Exp. Bot.* 62, 409–438. doi: 10.1093/jxb/erq287

Maccaferri, M., Zhang, J., Bulli, P., Abate, Z., Chao, S., Cantu, D., et al. (2015b). A genome-wide association study of resistance to stripe rust (*Puccinia striiformis* f. sp. *tritici*) in a worldwide collection of hexaploid spring wheat (*Triticum aestivum* L.). *G3* 5, 449–465. doi: 10.1534/g3.114.014563

Madec, S., Baret, F., de Solan, B., Thomas, S., Dutartre, D., Jezequel, S., et al. (2017). High-throughput phenotyping of plant height: comparing unmanned aerial vehicles and ground LiDAR estimates. *Front. Plant Sci.* 8:2002. doi: 10.3389/fpls.2017.02002

Marti, J., Bort, J., Slafer, G. A., and Araus, J. L. (2007). Can wheat yield be assessed by early measurements of NDVI? *Ann. Appl. Biol.* 150, 253–257. doi: 10.1111/j.1744-7348.2007.00126.x

Mason, R. E., Addison, C. K., Babar, A., Acuna, A., Lozada, D., Subramanuan, N., et al. (2018). Diagnostic markers for vernalization and photoperiod loci improve genomic selection for grain yield and spectral reflectance in wheat. *Crop Sci.* 58, 242–252. doi: 10.2135/cropsci2017.06.0348

Milner, S. G., Maccaferri, M., Huang, B. E., Mantovani, P., Massi, A., Frascaroli, E., et al. (2016). A multiparental cross population for mapping QTL for agronomic traits in durum wheat (*Triticum turgidum* ssp. *durum*). *Plant Biotechnol. J.* 14, 735–748. doi: 10.1111/pbi.12424

Money, D., Gardner, K., Migicovsky, Z., Schwaninger, H., Zhong, G. Y., and Myles, S. (2015). LinkImpute: fast and accurate genotype imputation for nonmodel organisms. *G3* 5, 2383–2390. doi: 10.1534/g3.115.021667

Monneveux, P., Jing, R., and Misra, S. C. (2012). Phenotyping for drought adaptation in wheat using physiological traits. *Front. Physiol.* 3:429. doi: 10.3389/fphys.2012.00429

Monostori, L., Kadar, B., Bauernhansl, T., Kondoh, S., Kumara, S., Reinhart, G., et al. (2016). Cyber-physical systems in manufacturing. *CIRP Ann. Manuf. Technol.* 65, 621–641. doi: 10.1016/j.cirp.2016.06.005

Ortiz, R., Sayre, K. D., Govaerts, B., Gupta, R., and Subbarao, G. V., Ban, et al. (2008). Climate change: can wheat beat the heat? *Agric. Ecosyst. Environ.* 126, 46–58. doi: 10.1016/j.agee.2008.01.019

Pantazi, X. E., Moshou, D., Alexandridis, T., Whetton, R. L., and Mouazen, A. M. (2016). Wheat yield prediction using machine learning and advanced sensing techniques. *Comput. Electron. Agric.* 121, 57–65. doi: 10.1016/j.compag.2015.11.018

Pauli, D., Andrade-Sanchez, P., Carmo-Silva, A. E., Gazave, E., French, A. N., Heun, J., et al. (2016). Field-based high-throughput plant phenotyping reveals the temporal patterns of quantitative trait loci associated with stress-responsive traits in cotton. *G3* 6, 865–879. doi: 10.1534/g3.115.023515

Peleg, Z., Fahima, T., Krugman, T., Abbo, S., Yakir, D., Korol, A. B., et al. (2009). Genomic dissection of drought resistance in durum wheat × wild emmer wheat recombinant inbred line population. *Plant Cell Environ.* 32, 758–779. doi: 10.1111/j.1365-3040.2009.01956.x

Peters, J. A., Elizabeth, A., Shea, W., Lel, J. I., Vliia, A., Hayes, M., et al. (2002). Drought monitoring with NDVI-based standardized vegetation index. *Photogramm. Eng. Remote Sens.* 68, 71–75.

Pinto, R. S., Lopes, M. S., Collins, N. C., and Reynolds, M. P. (2016). Modelling and genetic dissection of staygreen under heat stress. *Theor. Appl. Genet.* 129:2055. doi: 10.1007/s00122-016-2757-4

Pinto, R. S., Reynolds, M. P., Mathews, K. L., McIntyre, C. L., Olivares-Villegas, J. J., and Chapman, S. C. (2010). Heat and drought adaptive QTL in a wheat population designed to minimize confounding agronomic effects. *Theor. Appl. Genet.* 121, 1001–1021. doi: 10.1007/s00122-010-1351-4

Price, A. L., Zaitlen, N. A., Reich, D., and Patterson, N. (2010). New approaches to population stratification in genome-wide association studies. *Nat. Rev. Genet.* 11, 459–463. doi: 10.1038/nrg2813

Pritchard, J. K., Stephens, M., and Donnelly, P. (2000). Inference of population structure using multilocus genotype data. *Genetics* 155, 945–959.

Ramya, P., Singh, G. P., Jain, N., Singh, P. K., Pandey, M. K., Sharma, K., et al. (2016). Effect of recurrent selection on drought tolerance and related morpho-physiological traits in bread wheat. *PLoS ONE* 11:e0156869. doi: 10.1371/journal.pone.0156869

Rexroad, C. E., and Vallejo, R. L. (2009). Estimates of linkage disequilibrium and effective population size in rainbow trout. *BMC Genet.* 10:83. doi: 10.1186/1471-2156-10-83

Reynolds, M., and Tuberosa, R. (2008). Translational research impacting on crop productivity in drought-prone environments. *Curr. Opin. Plant. Biol.* 11, 171–179.. doi: 10.1016/j.pbi.2008.02.005

Reynolds, M., Dreccer, F., and Trethowan, R. (2007). Drought-adaptive traits derived from wheat wild relatives and landraces. *J. Exp. Bot.* 58, 177–186. doi: 10.1093/jxb/erl250

Saitou, N., and Nei, M. (1987). The neighbour-joining method: a new method for reconstructing phylogenetic trees. *Mol. Biol. Evol.* 4, 406–426.

Salvi, S., and Tuberosa, R. (2015). The crop QTLome comes of age. *Curr. Opin. Biotechnol.* 32, 179–185. doi: 10.1016/j.copbio.2015.01.001

Shakoor, N., Lee, S., and Mockler, T. C. (2017). High throughput phenotyping to accelerate crop breeding and monitoring of diseases in the field. *Curr. Opin. Plant Biol.* 38, 184–192. doi: 10.1016/j.pbi.2017.05.006

Shi, S., Azam, F. I., Li, H., Chang, X., Li, B., and Jing, R. (2017). Mapping QTL for stay-green and agronomic traits in wheat under diverse water regimes. *Euphytica* 213, 1–19. doi: 10.1007/s10681-017-2002-5

Sirault, X. R., Condon, A. G., Wood, J. T., Farquhar, G. D., and Rebetzke, G. J. (2015). "Rolled-upness": phenotyping leaf rolling in cereals using

computer vision and functional data analysis approaches. *Plant Methods*. 11:52. doi: 10.1186/s13007-015-0095-1

Snape, J., Butterworth, K., Whitechurch, E., and Worland, A. J. (2001). Waiting for fine times: genetics of flowering time in wheat. *Euphytica* 119, 185–190. doi: 10.1023/A:1017594422176

Sukumaran, S., Dreisigacker, S., Lopes, M., Chavez, P., and Reynolds, M. P. (2015). Genome-wide association study for grain yield and related traits in an elite spring wheat population grown in temperate irrigated environments. *Theor. Appl. Genet.* 128, 353–363. doi: 10.1007/s00122-014-2435-3

Tattaris, M., Reynolds, M. P., and Chapman, S. C. (2016). A direct comparison of remote sensing approaches for high-throughput phenotyping in plant breeding. *Front. Plant Sci.* 7:1131. doi: 10.3389/fpls.2016.01131

Trapp, J. J., Urrea, C. A., Zhou, J., Khot, L. R., Sankaran, S., and Miklas, P. N. (2017). Selective phenotyping traits related to multiple stress and drought response in dry bean. *Crop Sci.* 56, 1460–1472. doi: 10.2135/cropsci2015.05.0281

Tuberosa, R. (2012). Phenotyping for drought tolerance of crops in the genomics era. *Front. Physiol.* 3:347. doi: 10.3389/fphys.2012.00347

Tucker, C. J. (1979). Red and photographic infrared linear combinations for monitoring vegetation. *Remote Sens. Environ.* 8, 127–150. doi: 10.1016/0034-4257(79)90013-0

Wang, S., Wong, D., Forrest, K., Allen, A., Chao, S., Huang, B., et al. (2014). Characterization of polyploid wheat genomic diversity using a high-density 90,000 single nucleotide polymorphism array. *Plant Biotechnol. J.* 12, 787–796. doi: 10.1111/pbi.12183

Yang, D., Liu, Y., Cheng, H., Chang, L., Chen, J., Chai, S., et al. (2016). Genetic dissection of flag leaf morphology in wheat (*Triticum aestivum* L.) under diverse water regimes. *BMC Genetics* 17:94. doi: 10.1186/s12863-016-0399-9

Yousfi, S., Márquez, A. J., Betti, M., Araus, J. L., and Serret, M. D. (2016). Gene expression and physiological responses to salinity and water stress of contrasting durum wheat genotypes. *J. Integr. Plant Biol.* 58, 48–66. doi: 10.1111/jipb.12359

Yu, J., Pressoir, G., Briggs, W. H., Vroh Bi, I., Yamasaki, M., Doebley, J. F., et al. (2006). A unified mixed-model method for association mapping that accounts for multiple levels of relatedness. *Nat. Genet.* 38, 203–208. doi: 10.1038/ng1702

Zadoks, J. C., Chang, T. T., and Konzak, C. F. (1974). A decimal code for the growth stages of cereals. *Weed Res.* 14, 415–421. doi: 10.1111/j.1365-3180.1974.tb01084.x

Zaman-Allah, M., Vergara, O., Araus, J. L., Tarekegne, A., Magorokosho, C., Zarco-Tejada, P. J., et al. (2015). Unmanned aerial platform-based multispectral imaging for field phenotyping of maize. *Plant Methods* 11:35. doi: 10.1186/s13007-015-0078-2

Zhang, Z., Ersoz, E., Lai, C. Q., Todhunter, R. J., Tiwari, H. K., Gore, M. A., et al. (2010). Mixed linear model approach adapted for genome-wide association studies. *Nat. Genet.* 42, 355–360. doi: 10.1038/ng.546

Conflict of Interest Statement: The authors declare that the research was conducted in the absence of any commercial or financial relationships that could be construed as a potential conflict of interest.

frontiers in Plant Science

ORIGINAL RESEARCH
published: 04 January 2018
doi: 10.3389/fpls.2017.02180

Interactive Effects of CO_2 Concentration and Water Regime on Stable Isotope Signatures, Nitrogen Assimilation and Growth in Sweet Pepper

*María D. Serret[1], Salima Yousfi[1], Rubén Vicente[1], María C. Piñero[2], Ginés Otálora-Alcón[2], Francisco M. del Amor[2] and José L. Araus[1]**

[1] Departament de Biologia Evolutiva, Ecologia i Ciències Ambientals, Universitat de Barcelona, Barcelona, Spain, [2] Departamento de Hortofruticultura, Instituto Murciano de Investigación y Desarrollo Agrario y Alimentario, La Alberca-Murcia, Spain

OPEN ACCESS

Edited by:
Roberto Tuberosa,
Università di Bologna, Italy

Reviewed by:
Iker Aranjuelo,
Instituto de Agrobiotecnología (IDAB), Spain
Pedro Revilla,
Misión Biológica de Galicia (CSIC), Spain

***Correspondence:**
José L. Araus
jaraus@ub.edu

Specialty section:
This article was submitted to Plant Breeding, a section of the journal Frontiers in Plant Science

Received: 26 July 2017
Accepted: 12 December 2017
Published: 04 January 2018

Citation:
Serret MD, Yousfi S, Vicente R, Piñero MC, Otálora-Alcón G, del Amor FM and Araus JL (2018) Interactive Effects of CO_2 Concentration and Water Regime on Stable Isotope Signatures, Nitrogen Assimilation and Growth in Sweet Pepper. Front. Plant Sci. 8:2180. doi: 10.3389/fpls.2017.02180

Sweet pepper is among the most widely cultivated horticultural crops in the Mediterranean basin, being frequently grown hydroponically under cover in combination with CO_2 fertilization and water conditions ranging from optimal to suboptimal. The aim of this study is to develop a simple model, based on the analysis of plant stable isotopes in their natural abundance, gas exchange traits and N concentration, to assess sweet pepper growth. Plants were grown in a growth chamber for near 6 weeks. Two [CO_2] (400 and 800 μmol mol^{-1}), three water regimes (control and mild and moderate water stress) and four genotypes were assayed. For each combination of genotype, [CO_2] and water regime five plants were evaluated. Water stress applied caused significant decreases in water potential, net assimilation, stomatal conductance, intercellular to atmospheric [CO_2], and significant increases in water use efficiency, leaf chlorophyll content and carbon isotope composition, while the relative water content, the osmotic potential and the content of anthocyanins did change not under stress compared to control conditions support this statement. Nevertheless, water regime affects plant growth via nitrogen assimilation, which is associated with the transpiration stream, particularly at high [CO_2], while the lower N concentration caused by rising [CO_2] is not associated with stomatal closure. The stable isotope composition of carbon, oxygen, and nitrogen ($\delta^{13}C$, $\delta^{18}O$, and $\delta^{15}N$) in plant matter are affected not only by water regime but also by rising [CO_2]. Thus, $\delta^{18}O$ increased probably as response to decreases in transpiration, while the increase in $\delta^{15}N$ may reflect not only a lower stomatal conductance but a higher nitrogen demand in leaves or shifts in nitrogen metabolism associated with decreases in photorespiration. The way that $\delta^{13}C$ explains differences in plant growth across water regimes within a given [CO_2], seems to be mediated through its direct relationship with N accumulation in leaves. The changes in the profile and amount of amino acids caused by water stress and high [CO_2] support this conclusion. However, the results do not support the use of $\delta^{18}O$ as an indicator of the effect of water regime on plant growth.

Keywords: [CO_2], nitrogen, sweet pepper, photosynthesis, water stress, $\delta^{13}C$, $\delta^{15}N$, $\delta^{18}O$

INTRODUCTION

After tomato, sweet pepper is the second largest horticultural product cultivated in the Mediterranean basin in terms of area (del Amor, 2007). Moreover, a significant area is devoted to its cultivation under cover (greenhouses of different categories), and is frequently combined with the application of CO_2 fertilization (Piñero et al., 2016). Essentially, a high CO_2 concentration ([CO_2]) stimulates photosynthesis and may contribute to increasing productivity in greenhouses while palliating environmental problems such as water stress or high temperature. Nevertheless, plant responses to elevated [CO_2] may be affected in one or another way as a result of photosynthetic acclimation (Long et al., 2004) or due to differences in growing conditions such as water regime (O'Leary et al., 2015). Thus, some degree of water stress may increase the efficiency of water use, and at the same time positively affect the quality of the final product (López-Marín et al., 2017). However, the interaction of elevated [CO_2] with water stress has not been widely studied and there are studies supporting either the positive or the negative effects of elevated [CO_2] on water stress tolerance (Medina et al., 2016). Exposure to elevated [CO_2] may mitigate the inhibition of photosynthesis under water stress and improve water use efficiency by a positive synergistic effect of both factors on stomatal closure, but can also stimulate oxidative stress and not affect plant growth (Erice et al., 2007, 2014; Bencze et al., 2014; Medina et al., 2016). In addition, plant size may limit the direct physiological effects of elevated [CO_2] (Xu et al., 2016). Moreover, some studies indicated that this interaction is highly dependent on the genotypic variability and the severity of water stress (Erice et al., 2014; Medina et al., 2016; Xu et al., 2016).

Therefore, a better understanding of the interactions between high [CO_2] and water stress is important for predicting the agricultural consequences of the expected increase in [CO_2]. In the case of sweet pepper the genotypic performance and the specific responses to the combinations of [CO_2] and water conditions have usually been monitored through photosynthetic and transpirative gas exchange traits (Peñuelas et al., 1995; del Amor et al., 2010). However, the use of methodologies that are able to integrate physiological processes on a larger temporal scale is an alternative that needs exploration. The analysis of the natural abundances of stable isotopes in plant matter may represent an alternative (Dawson et al., 2002; Araus et al., 2008) that is worth exploring.

Carbon isotope composition ($\delta^{13}C$), frequently expressed as discrimination ($\Delta^{13}C$) against the surrounding air, provides information on the effect of growing conditions on photosynthetic carbon assimilation (Farquhar et al., 1982; Condon et al., 1990). Plants discriminate against the heavier carbon isotope (^{13}C) during photosynthesis and the extent of this discrimination depends on the ratio of the intercellular vs. the atmospheric [CO_2] (C_i/C_a) in photosynthetic organs (Farquhar et al., 1982, 1989). Since the C_i/C_a ratio depends on the balance between the photosynthetic activity and the stomatal conductance (A/g_s) of the plant (Farquhar et al., 1982, 1989; Rebetzke et al., 2002; Condon et al., 2004), when analyzed in plant dry matter $\Delta^{13}C$ becomes a time-integrated indicator of the A/g_s ratio and therefore of water use efficiency of the plant (Farquhar and Richards, 1984). Under drought stress, the $\Delta^{13}C$ (or $\delta^{13}C$) is also a good predictor of stomatal conductance (Condon et al., 2002) and of water input received by the crop (Araus et al., 2003). For growing conditions where the water regime is not the main environmental variable, it remains challenging to assess whether variation in the carbon isotope signature is the result of changes in intrinsic photosynthetic capacity or stomatal conductance (Scheidegger et al., 2000; Farquhar et al., 2007). Due to this, the analysis of the stable oxygen isotope signature in plants may contribute toward understanding the nature of the changes in $\delta^{13}C$ (Barbour and Farquhar, 2000).

The oxygen isotope composition ($\delta^{18}O$) in plant tissues can be influenced by three main factors. The first factor is the isotopic composition of the source water taken up by the plant (Roden and Ehleringer, 1999). The second factor is the enrichment in ^{18}O in the leaves due to evaporation in comparison to source water (Pande et al., 1995). The third factor is the fractionation of oxygen isotopes during biochemical reactions involved in the synthesis of organic matter (Farquhar and Lloyd, 1993). Sugars and other metabolites formed in leaves incorporate the leaf water isotopic signal, which is then retained in structural organic compounds, such as cellulose (Barbour, 2007; Gessler et al., 2014). Stomatal conductance plays a crucial role in regulating the water balance of the plant. Providing there is constancy in the $\delta^{18}O$ of the water taken up by the plant, the $\delta^{18}O$ of plant matter integrates evaporative conditions throughout the life cycle of the plant, and this is largely unaffected by photosynthesis (Barbour and Farquhar, 2000; Farquhar et al., 2007). Therefore, $\delta^{18}O$ has been proposed for estimating stomatal conductance and transpiration and thus plant water use in different species (Barbour and Farquhar, 2000; Barbour et al., 2000; Sheshshayee et al., 2005; Farquhar et al., 2007; Cabrera-Bosquet et al., 2009a, 2011; Cernusak et al., 2009a).

Nitrogen is the most growth-limiting nutrient element for plants (Piñero et al., 2016). In fact, the nitrogen isotope composition ($\delta^{15}N$) in plant matter is an indicator of the effect of growing conditions on the nitrogen metabolism of the plant, even though a complete knowledge of the underlying biochemical mechanisms is lacking (Cernusak et al., 2009b; Tcherkez, 2010; Yousfi et al., 2012). The natural abundance of $\delta^{15}N$ has been used in sweet pepper to assess the source of nitrogen fertilization (Flores et al., 2007; del Amor and Navarro, 2008). However, to the best of our knowledge, studies on the interactive effect of [CO_2] and water regime on the $\delta^{15}N$ and $\delta^{18}O$ of the plant are scarce.

This study compared the $\delta^{13}C$, $\delta^{18}O$, and $\delta^{15}N$, together with N concentration, of the leaf dry matter of sweet pepper plants growing under different [CO_2] and water regimes. Further the stable isotope signatures of these three elements were correlated with plant growth. Moreover, gas exchange and amino acid profiles were measured on similar leaves. The final aim of this study is to produce a single conceptual model, integrating different key physiological traits, that explains the variability in sweet pepper biomass due to growing conditions and genotypic variability. To that end, plants were grown under hydroponic conditions at a relatively low light intensity

and mild to moderate water stress, resembling the growing conditions usually experienced, in a mild Mediterranean climate, by sweet pepper plants within commercial plastic/polycarbonate greenhouses adapted to CO_2 fertilization and which often include a shadow sheet (Dueck et al., 2006; del Amor and Gómez-López, 2009; del Amor et al., 2010; Pérez-Jiménez et al., 2016).

MATERIALS AND METHODS

Plant Material and Growth Conditions

The experiment was carried at the Instituto Murciano de Investigación y Desarrollo Agrario y Alimentario (IMIDA), La Alberca, Murcia, Spain. Four sweet pepper (*Capsicum annuum* L.) cultivars were studied: Tallante (Ta; De Ruiter Vegetable Seeds, Inc.), Coyote (Co; Syngenta Seeds SA), Herminio (He; Syngenta Seeds SA), and Velez (Ve; Enza Zaden BV). These cultivars are commonly used in commercial greenhouses in SE Spain (Almeria and Murcia regions). Seedlings were transplanted to 5-l black containers filled with coconut coir fiber (Pelemix, Alhama de Murcia, Murcia, Spain) and acclimated during 5 days to the new conditions. Then three irrigation treatments were applied for 41 days: the control (an amount of 500 ml of nutrient solution was applied every day), mild stress (same amount every 2 days), and moderate stress (same amount every 3 days). Plants were irrigated with a modified Hoagland solution with the following composition in meq L^{-1}; NO_3^-: 12.0; $H_2PO_4^-$: 1.0; SO_4^{2-}: 3.5; K^+: 7.0; Ca^{2+}: 4.5; Mg^{2+}: 2.0. Irrigation was supplied via pressure-compensating and anti-drain drippers (2 l h^{-1}) and fresh nutrient solution was applied to avoid salt accumulation, with a minimum of 35% drainage (del Amor and Gómez-López, 2009).

Plants were grown in a climate chamber designed to mimic usual environmental conditions experienced by pepper plants within greenhouses (del Amor et al., 2010), with fully-controlled environmental parameters: 70% RH, 16/8 h day/night photoperiod, 28/16°C and a photosynthetically-active radiation (PAR) of 250 μmol m^{-2} s^{-1} provided by a combination of fluorescent lamps (TL-D Master reflex 830 and 840, Philips, the Netherlands) and high-pressure sodium lamps (Son-T Agro, Philips, the Netherlands). Plants were grown at [CO_2] of 400 μmol mol^{-1} (atmospheric [CO_2]) and 800 μmol mol^{-1} (high [CO_2]). The [CO_2] was regulated by injection of external compressed CO_2 (bottle [CO_2] ≥ 99.9%), controlled by an infrared gas analyser (Dräger Politron IR CO_2, Sweden). For each cultivar within a specific water regime and [CO_2], five replications (each consisting in a single plant) were run. Thus, 24 treatments were studied, corresponding to the combination of four cultivars, three irrigation levels, and two [CO_2], totalling 120 plants. All the study was done in the same growth chamber. Therefore, the experiment was done consecutively, with the only difference being [CO_2]. We carefully verified that the germination and seedling growth conditions were the same (by using a small growth chamber (BINDER KBWF 240, BINDER GmbH, Tuttlingen, Germany), with light, temperature, and RH control. Plants were grown under a randomized complete block design ($n = 60$).

Photosynthetic and Transpirative Gas Exchange and Chlorophyll Content

At the end of the experimental period, net CO_2 assimilation, stomatal conductance, transpiration, and the C_i/C_a ratio were measured in the youngest fully-expanded leaf of five plants per treatment, using a CIRAS-2 portable photosynthesis system (PP Systems, Amesbury, MA, USA) with a PLC6 (U) Automatic Universal Leaf Cuvette of 1.7 cm^2. The cuvette provided light (LED) with a photon flux of 800 μmol m^{-2} s^{-1}, 400 or 800 μmol mol^{-1} [CO_2] and a leaf temperature of 22°C. Water use efficiency (WUE) was determined as the ratio of net CO_2 assimilation to transpiration.

The leaf chlorophyll content on an area basis was determined in the same leaves used for gas exchange with a SPAD-502 (Konica-Minolta Sensing, Japan) portable meter. Three measurements were made on each leaf.

Measurement of Tissue Anthocyanins

Anthocyanins were extracted from oven-dried (after a minimum of 72 h at 65°C), ground tissue samples of plant leaves, suspended in acidified methanol (methanol:water:HCl, 79:20:1, by vol.), autoextracted at 0°C for 72 h, centrifuged and absorbance measured at 530 and 657 nm for each supernatant (Mirecki and Teramura, 1984). Anthocyanin concentration was calculated as Ab_{530} nm-1/3 Ab_{657} nm g^{-1} dry matter (Lindoo and Caldwell, 1978).

Leaf Water and Osmotic Potentials and Relative Water Content

The leaf water potential (Ψ_w) was measured in the same leaves used for gas exchange determinations, using a Scholander pressure chamber (model 3000, Soil Moisture Equipment Corp., Santa Barbara, USA) as reported elsewhere (Turner, 1988). Measurements were performed after gas exchange determinations and then the leaves were put in Eppendorf tubes with holes at the bottom and rapidly frozen. These tubes were then centrifuged twice, at 4,000 g for 4 min (4°C), using an Eppendorf centrifuge so that all sap was extracted from the samples. The osmotic potential ($\Psi\pi$) of the leaf sap was assessed with a vapor pressure osmometer (Wescor 5500, Logan, Utah, USA) used to measure the osmolality (mmol kg^{-1}) of the expressed sap; this was converted to osmotic potential according to the Van't Hoff equation: $\Psi\pi$ (MPa) = −RTC, where R is the gas constant (0.008321 MPa K^{-1} mol^{-1}), T is the temperature (293 K) and C is the number of moles of solute in 1 kg of water (= 1 l at 293 K). The leaf relative water content (RWC) was measured on same-age leaves as those used for $\Psi\pi$. Three small disks (2.07 cm^2) per leaf from each of the six plants were cut and weighed immediately to obtain fresh mass (FM), and then they were placed for 24 h in the dark in a beaker (30 cm^3) filled with distilled water. After this, they were reweighed to obtain turgid fresh mass (TM), and dry mass (DM) after drying at 80°C for 48 h. The relative water content (RWC), expressed as a percentage, was calculated as RWC = [(FM–DM)/(TM–DM)] ×100%.

Shoot Biomass

Plants were harvested at the end of the experiment (41 days after transplanting), and 120 plants (five plants per treatment) were analyzed. The aerial parts (thereafter referred as shoot biomass, including leaves plus stems and petioles) were dried and the dry weight determined after a minimum of 72 h at 65°C. The specific leaf area (SLA) was calculated as the ratio between the area and the dry weight of leaf discs of 6.91 cm^2.

Leaf N-Total Concentration and Stable Carbon, Nitrogen, and Oxygen Isotope Composition

Total nitrogen concentration and the stable carbon ($^{13}C/^{12}C$) and ($^{15}N/^{14}N$) isotope ratios in the whole pool of shoot leaves were measured using an elemental analyser (Flash 1112 EA, ThermoFinnigan, Germany) coupled with an isotope ratio mass spectrometer (Delta C IRMS, ThermoFinnigan, Germany), operating in continuous mode. Samples of 1 mg and reference materials were weighed into tin capsules, sealed, and then loaded into an automatic sampler (ThermoFinnigan, Germany) prior to EA-IRMS analysis. Measurements were carried out at the CCiT (Centres Científics i Tecnològics) of the University of Barcelona. Nitrogen was expressed as a concentration (percent of dry weight). The $^{13}C/^{12}C$ ratios were expressed in δ notation (Coplen, 2008): $\delta^{13}C$ (‰) = $(^{13}C/^{12}C)_{sample}/(^{13}C/^{12}C)_{standard} - 1$, where "sample" refers to plant material and "standard" to international secondary standards of known $^{13}C/^{12}C$ ratios (IAEA CH7 polyethylene foil, IAEA CH6 sucrose, and USGS 40 L-glutamic acid) calibrated against Vienna Pee Dee Belemnite calcium carbonate (VPDB) with an analytical precision (*SD*) of 0.10‰. The same δ notation was used for the $^{15}N/^{14}N$ ratio ($\delta^{15}N$), but in this case using international secondary standards of known $^{15}N/^{14}N$ ratios (IAEA N_1 and IAEA N_2 ammonium sulfate and IAEA NO_3 potassium nitrate) referred to N_2 in air, with an analytical precision of 0.18‰.

For the $\delta^{18}O$, the $^{18}O/^{16}O$ was determined by an on-line pyrolysis technique using a Thermo-Chemical Elemental Analyser (TC/EA Thermo Quest Finnigan, Germany) coupled with an IRMS (Delta C Finnigan MAT, Germany). Samples of 1 mg were weighed into silver capsules, sealed and oven-dried at 60°C for not less than 72 h to remove moisture and loaded into an automatic sampler. Results were expressed as $\delta^{18}O$ values, using two secondary standards (IAEA 601 and IAEA 602) calibrated against Vienna Standard Mean Oceanic Water (VSMOW) (Coplen, 2011); the analytical precision was ≈ 0.25%. Analyses were conducted at Iso-Analytical Limited (Crewe, Cheshire, UK).

Free Amino Acids

The free amino acids were extracted from leaves (frozen at −80°C): the sap was extracted, after vortexing at 5,000 rpm (10 min, 4°C), and analyzed by the AccQ·Tag-ultra ultraperformance liquid chromatography (UPLC) method (Waters, UPLC Amino Acid Analysis Solution, 2006). For derivatization, 70 µl of borate buffer was added to 10 µl of the fruit sap and 20 µl of reagent solution. The reaction mixture was mixed instantly and heated at 55°C for 10 min. After the temperature was lowered, an aliquot of the reaction mixture was used for injection. The column was an Acquity BEH C18 1.7 µm, 2.1–100 mm (Waters), and the wavelengths were set at 266 nm (excitation) and 473 nm (emission). The solvent system consisted of two eluents: (A) AccQ·Tag-ultra eluent A concentrate (5%, v/v) and water (95%, v/v); and (B) AccQ·Tag-ultra eluent B. The following elution gradient procedure was used for the analysis: 0–0.54 min, 99.9% A−0.1% B; 5.74 min, 90.9% A− 9.1% B; 7.74 min, 78.8% A−21.2% B; 8.04 min, 40.4% A−59.6% B; 8.05–8.64 min, 10% A−90% B; 8.73–10 min, 99.9% A−0.1% B. The injection volume was 1 µl, with a flow rate of 0.7 ml min^{-1}. The temperature of the column was maintained at 55°C. External standards (Thermo Scientific) were used for the quantification of the amino acids, and Empower 2 (Waters) software for data acquisition and processing.

Statistical Analysis

Data were subjected to factorial ANOVA to test the effects of the growing conditions ([CO_2] and water regime), genotype, and their interactions. Mean comparisons were performed using Tukey's honestly significant difference (HSD) test. A bivariate correlation procedure was used to calculate the Pearson correlation coefficients between the different traits measured. Multiple linear regression (stepwise) analysis was used to analyse the criterion included to explain variation in shoot biomass under different growing conditions. Principal component analysis was produced to analyse the interrelationships among the shoot biomass, leaf nitrogen concentration, and chlorophyll content, the stable isotope composition of C, O, and N, and the gas exchange variables. Data were analyzed using IBM SPSS Statistics 24 (SPSS Inc., Chicago, IL, USA). Figures were created using a Sigma-Plot 11.0 program for Windows (Systat Software Inc., Point Richmond, CA, USA). Finally, we performed path analyses (Li, 1975) to quantify the relative contributions of direct and indirect effects of stable isotopes and other key traits on aboveground biomass. This methodology offers the possibility of building associations between variables that is based on prior knowledge. A path analysis determines simple correlations between independent factors (in this case $\delta^{13}C$), and regresses them on each intermediary (C_i/C_a, g_s, $\delta^{15}N$ and N concentration) or dependent factor (shoot biomass) to obtain direct effects in the form of partial regression coefficients (i.e., path coefficients). This model was aimed at understanding biomass responses to genotypic differences across water regimes under different levels of [CO_2]. A model with a comparative fit index (CFI) (Arbuckle, 1997) with values > 0.9 was taken as indicative of a good fit. Data were analyzed using the Amos Graphics package (IBM SPSS Amos, USA). A clustered heat map of amino acid profile was built using the R statistics environment (R Development Core Team, Vienna, Austria). Additionally, after generating a correlation matrix of all parameters analyzed in R, we performed a network analysis of significant correlations (Pearson correlation coefficient cut-off of 0.7 and $P < 0.05$) under

ambient and elevated [CO_2] using Cytoscape software (Shannon et al., 2003).

RESULTS

Effect of Growing Conditions and Genotype on Shoot Biomass

Compared with control plants water stress negatively affected shoot biomass (SB), plant height (PH), and the leaf water potential (Ψ_w), whereas leaf chlorophyll (LC) content slightly increased and no differences existed in the specific leaf area (SLA), relative water content (RWC), leaf osmotic potential ($\Psi\pi$), and anthocyanin content (**Table 1**). Increasing ambient [CO_2] significantly increased SB, PH, LC, anthocyanin, and $\Psi\pi$, whereas all the other traits reported in **Table 1** decreased. A genotypic effect was significant for all the traits except RWC, anthocyanin, and $\Psi\pi$.

The interactions between water regime (WR) and [CO_2] were significant for all the traits of **Table 1** except RWC, anthocyanin, and Ψ_w, meaning that, except for these two traits, the response to water regime differed depending on [CO_2]. Most of the interactions of genotypes with growing conditions were not significant, even when it is worth to mention the significant interaction between genotype and [CO_2] for SB.

Effect of Growing Conditions and Genotype on Gas Exchange and Stable Isotope Signatures

Water stress significantly decreased the leaf net CO_2 assimilation (A), stomatal conductance (g_s), the intercellular to ambient CO_2 concentration (C_i/C_a), the stable oxygen isotope composition ($\delta^{18}O$) and the nitrogen concentration (N), whereas the water use efficiency (WUE), the stable carbon isotope composition ($\delta^{13}C$), and the stable nitrogen isotope composition ($\delta^{15}N$) increased and no significant differences existed for the transpiration (T) (**Table 2**). Rising [CO_2] significantly increased A, g_s, T, C_i/C_a, WUE, and $\delta^{18}O$, whereas N, $\delta^{13}C$ and $\delta^{15}N$ decreased. The genotypic effect was significant for all traits except A and T. The interaction between WR and [CO_2] was significant for all the traits except $\delta^{18}O$ ($P = 0.060$) and T. The interactions between genotype and [CO_2] were significant for A, g_s, C_i/C_a, and WUE, and near significant for T ($P = 0.056$), whereas the interaction between genotype and WR were also significant for g_s, C_i/C_a, and WUE. Except for an interaction between genotype and WR for $\delta^{15}N$, no interactions between genotype and growing conditions were found.

Given the significance of the interactions between WR and [CO_2] for most of the traits in **Tables 1**, **2**, a subset of traits in these tables was analyzed across water regimes within each [CO_2]

TABLE 1 | Water regime, CO_2 concentration and genotype effects on biomass, growth parameters, anthocyanin content, and leaf water status of four sweet pepper genotypes grown under different combinations of CO_2 concentration and water supply.

	SB	PH	SLA	LC	anthocyanin	RWC	Ψ_w	$\Psi\pi$
WATER REGIME								
Control	$10.48^{a} \pm 0.18$	$39.80^{a} \pm 0.59$	$946.58^{a} \pm 22.50$	$44.12^{b} \pm 0.46$	$0.17^{a} \pm 0.03$	$85.88^{a} \pm 0.74$	$-3.88^{c} \pm 0.18$	$-7.17^{a} \pm 0.16$
Mild water stress	$8.65^{b} \pm 0.19$	$36.40^{b} \pm 0.61$	$920.83^{ab} \pm 23.24$	$46.20^{a} \pm 0.47$	$0.24^{a} \pm 0.04$	$85.04^{a} \pm 0.77$	$-5.18^{b} \pm 0.18$	$-6.87^{a} \pm 0.16$
Moderate water stress	$6.35^{c} \pm 0.20$	$35.09^{b} \pm 0.64$	$860.20^{b} \pm 25.54$	$45.71^{a} \pm 0.52$	$0.18^{a} \pm 0.02$	$85.87^{a} \pm 0.85$	$-6.52^{a} \pm 0.20$	$-6.98^{a} \pm 0.18$
CO_2 CONCENTRATION								
400 ppm	7.78 ± 0.14	35.90 ± 0.46	996.30 ± 17.63	43.89 ± 0.36	0.13 ± 0.01	88.70 ± 0.58	-4.90 ± 0.14	-7.72 ± 0.12
800 ppm	9.52 ± 0.17	38.88 ± 0.55	822.62 ± 21.07	47.15 ± 0.43	0.27 ± 0.03	81.87 ± 0.70	-5.49 ± 0.16	-6.21 ± 0.15
GENOTYPES								
Coyote	$7.93^{d} \pm 0.21$	$37.30^{b} \pm 0.67$	$919.52^{ab} \pm 25.66$	$46.32^{ab} \pm 0.52$	$0.22^{a} \pm 0.04$	$85.53^{a} \pm 0.85$	$-5.32^{ab} \pm 0.20$	$-7.02^{a} \pm 0.18$
Herminio	$8.76^{bc} \pm 0.22$	$40.20^{a} \pm 0.70$	$867.48^{b} \pm 26.92$	$46.87^{a} \pm 0.55$	$0.21^{a} \pm 0.03$	$86.48^{a} \pm 0.89$	$-5.21^{ab} \pm 0.21$	$-7.10^{a} \pm 0.19$
Tallante	$8.38^{cd} \pm 0.22$	$34.27^{c} \pm 0.72$	$965.42^{a} \pm 27.36$	$43.36^{c} \pm 0.56$	$0.16^{a} \pm 0.05$	$85.96^{a} \pm 0.91$	$-5.40^{a} \pm 0.21$	$-7.03^{a} \pm 0.19$
Velez	$9.31^{a} \pm 0.24$	$37.05^{b} \pm 0.78$	$886.92^{ab} \pm 29.79$	$44.66^{bc} \pm 0.61$	$0.19^{a} \pm 0.03$	$84.40^{a} \pm 0.99$	$-4.60^{b} \pm 0.23$	$-6.89^{a} \pm 0.21$
LEVEL OF SIGNIFICANCE								
Water regime (WR)	214.01^{***}	455.48^{***}	38058^{ns}	60.31^{**}	0.15^{ns}	0.95^{ns}	76.42^{***}	2.54^{ns}
CO_2 concentration (CO_2)	52.15^{***}	153.01^{***}	521286^{***}	183.80^{***}	0.32^{***}	806.83^{***}	5.86^{**}	49.06^{***}
Genotype (G)	9.12^{*}	370.48^{***}	155183^{*}	116.74^{***}	0.03^{ns}	25.87^{ns}	7.60^{*}	1.79^{ns}
WR x CO_2	33.36^{***}	260.37^{***}	109438^{*}	48.09^{*}	0.03^{ns}	9.69^{ns}	0.77^{ns}	8.16^{ns}
WR x G	3.82^{ns}	12.88^{ns}	352201^{***}	20.45^{ns}	0.52^{*}	50.87^{ns}	3.27^{ns}	13.23^{*}
CO_2 x G	16.57^{***}	29.27^{ns}	53189^{ns}	32.64^{ns}	0.03^{ns}	149.20^{*}	2.01^{ns}	6.09^{ns}
WR x CO_2 x G	9.37^{ns}	15.75^{ns}	316187^{**}	56.05^{ns}	0.25^{ns}	122.07^{ns}	10.96^{ns}	8.16^{ns}

SB, shoot biomass (g DW); PH, plant height (cm); SLA, specific leaf area (cm^2/g); LC, leaf chlorophyll content (SPAD units); anthocyanin content (absorbance g^{-1} dry matter); RWC, leaf relative water content (%); Ψ_w, leaf water potential (bar); $\Psi\pi$, leaf osmotic potential (bar).Values within each water regime are the means ± SE of 40 measurements (two levels of CO_2 concentration, four genotypes, and five replicates per genotype), CO_2 concentration values are the means ± SE of 60 measurements (three water regimes, four genotypes, and five replicates per genotype), while genotypic values are the means of 30 ± SE measurements (two CO_2 concentrations, three water regimes, and five replicates per genotype). For each replicate a single plant was used. Means followed by different letters are significantly different ($P < 0.05$) according to Tukey's honestly significant difference (HSD) test. Analysis of variance for the same variables is shown for the water regime (WR), CO_2 concentration (CO_2), genotype (G), and interaction (WR x CO_2), (WR x G), (CO_2 x G), (WR x CO_2 x G) effects. The associated percentage of the sum of squares and probabilities (ns, not significant; $^{*}P < 0.05$; $^{**}P < 0.01$ and $^{***}P < 0.001$) are shown.

TABLE 2 | Water regime, CO_2 concentration, and genotype effects on gas-exchange parameters, carbon, oxygen, and nitrogen isotope composition, and nitrogen concentration of four sweet pepper genotypes grown under different combinations of CO_2 concentration and water supply.

	A	g_s	C_i/C_a	*T*	WUE	N (%)	$\delta^{13}C$ (‰)	$\delta^{18}O$ (‰)	$\delta^{15}N$ (‰)
WATER REGIME									
Control	$13.03^{a} \pm 0.18$	$314.51^{a} \pm 10.71$	$0.79^{a} \pm 0.01$	$4.16^{a} \pm 0.39$	$3.34^{b} \pm 0.15$	$6.06^{a} \pm 0.06$	$-42.46^{b} \pm 0.10$	$26.55^{a} \pm 0.09$	$2.35^{b} \pm 0.06$
Mild stress	$13.01^{a} \pm 0.20$	$211.84^{b} \pm 11.66$	$0.74^{b} \pm 0.02$	$3.15^{a} \pm 0.42$	$4.27^{a} \pm 0.27$	$5.41^{b} \pm 0.06$	$-41.45^{a} \pm 0.10$	$26.21^{b} \pm 0.09$	$2.42^{ab} \pm 0.07$
Moderate stress	$11.68^{b} \pm 0.20$	$169.32^{c} \pm 11.48$	$0.69^{c} \pm 0.02$	$3.38^{a} \pm 0.41$	$4.50^{a} \pm 0.25$	$4.66^{c} \pm 0.06$	$-41.17^{a} \pm 0.10$	$26.20^{b} \pm 0.09$	$2.60^{a} \pm 0.07$
CO_2 CONCENTRATION									
400 ppm	10.12 ± 0.20	222.02 ± 13.09	0.69 ± 0.01	3.11 ± 0.30	3.51 ± 0.11	5.54 ± 0.05	-35.32 ± 0.08	26.12 ± 0.07	3.12 ± 0.05
800 ppm	15.01 ± 0.21	251.56 ± 13.21	0.78 ± 0.01	4.01 ± 0.31	4.55 ± 0.22	5.27 ± 0.05	-48.03 ± 0.08	26.56 ± 0.07	1.79 ± 0.05
GENOTYPES									
Coyote	$12.58^{a} \pm 0.21$	$206.02^{b} \pm 12.60$	$0.71^{b} \pm 0.02$	$3.95^{a} \pm 0.45$	$4.07^{a} \pm 0.18$	$5.53^{ab} \pm 0.07$	$-41.89^{b} \pm 0.12$	$26.34^{ab} \pm 0.11$	$2.67^{a} \pm 0.08$
Herminio	$12.96^{a} \pm 0.23$	$213.01^{b} \pm 13.47$	$0.73^{b} \pm 0.01$	$3.02^{a} \pm 0.49$	$4.57^{a} \pm 0.35$	$5.10^{c} \pm 0.06$	$-41.74^{b} \pm 0.12$	$26.48^{a} \pm 0.10$	$2.43^{ab} \pm 0.07$
Tallante	$12.27^{a} \pm 0.23$	$280.78^{a} \pm 13.54$	$0.77^{a} \pm 0.02$	$3.85^{a} \pm 0.49$	$3.38^{b} \pm 0.12$	$5.65^{a} \pm 0.07$	$-42.17^{b} \pm 0.12$	$26.50^{a} \pm 0.11$	$2.24^{b} \pm 0.08$
Velez	$12.56^{a} \pm 0.22$	$244.13^{ab} \pm 12.52$	$0.73^{b} \pm 0.02$	$3.52^{a} \pm 0.45$	$4.06^{a} \pm 0.30$	$5.32^{bc} \pm 0.06$	$-41.13^{a} \pm 0.11$	$26.03^{b} \pm 0.10$	$2.47^{ab} \pm 0.07$
LEVEL OF SIGNIFICANCE									
Water regime (WR)	59.20^{***}	389424^{***}	0.16^{***}	18.27^{ns}	27.84^{***}	32.21^{***}	22.12^{***}	2.82^{*}	1.07^{*}
CO_2 concentration (CO_2)	701.39^{***}	22051^{*}	0.20^{***}	20.67^{*}	30.60^{***}	1.90^{***}	4143.95^{***}	5.02^{***}	45.24^{***}
Genotype (G)	0.52^{ns}	73058^{***}	0.05^{***}	10.02^{ns}	18.26^{***}	4.35^{***}	7.02^{***}	3.75^{**}	1.84^{**}
WR x CO_2	11.44^{*}	36743^{*}	0.03^{**}	27.02^{ns}	8.99^{**}	10.72^{***}	13.73^{***}	1.71^{ns}	4.86^{***}
WR x G	12.84^{ns}	68741^{*}	0.04^{*}	31.11^{ns}	9.29^{***}	0.13^{ns}	3.20^{ns}	1.81^{ns}	2.44^{*}
CO_2 x G	51.42^{***}	93735^{***}	0.07^{***}	36.72^{ns}	26.51^{***}	0.08^{ns}	1.93^{ns}	0.77^{ns}	0.27^{ns}
WR x CO_2 x G	13.55^{ns}	$34002.^{ns}$	0.03^{*}	27.71^{ns}	12.51^{*}	0.46^{ns}	1.95^{ns}	3.87^{ns}	1.11^{ns}

A, leaf net CO_2 assimilation (μmol CO_2 m^{-2} s^{-1}); g_s, stomatal conductance (mmol CO_2 m^{-2} s^{-1}); C_i/C_a, intercellular to ambient CO_2 concentration; T, transpiration rate (mmol H_2O m^{-2} s^{-1}); WUE, water use efficiency (μmol CO_2 mmol H_2O^{-1}); N, nitrogen concentration (% DW); $\delta^{13}C$, stable carbon isotope composition (‰), $\delta^{18}O$ stable oxygen isotope composition (‰); $\delta^{15}N$, stable nitrogen isotope composition (‰). Values within each water regime are the means ± SE of 40 measurements (two levels of CO_2 concentration, four genotypes, and five replicates per genotype), CO_2 concentration values are the means ± SE of 60 measurements (three water regimes, four genotypes, and five replicates per genotype), while genotypic values are the means ± SE of 30 measurements (two CO_2 concentrations, three water regimes, and five replicates per genotype). For each replicate a single plant was used. Means followed by different letters are significantly different ($P < 0.05$) according to Tukey's honestly significant difference (HSD) test. Analysis of variance for the same variables is shown for the water regime (WR), CO_2 concentration (CO_2), genotype (G), and interaction (WR x CO_2), (WR x G), (CO_2 x G), (WR x CO_2 x G) effects. The associated percentage of the sum of squares and probabilities (ns, not significant; $^{*}P < 0.05$; $^{**}P < 0.01$ and $^{***}P < 0.001$) are shown.

(**Table 3**). At atmospheric [CO_2] the water regime significantly affected SB, A, g_s, C_i/C_a, N, and $\delta^{18}O$, and the effect for $\delta^{13}C$ ($P = 0.068$) and $\delta^{15}N$ ($P = 0.057$) approached significance, whereas at high [CO_2] the water regime significantly affected all the traits except $\delta^{18}O$. The genotypic effect at atmospheric [CO_2] was significant for all the traits, except $\delta^{15}N$ ($P = 0.057$) and SB, whereas at high [CO_2] the genotypic effect was significant for all the traits except $\delta^{15}N$ and $\delta^{18}O$. Interactions of genotypes with WR at atmospheric [CO_2] were only significant for A, C_i/C_a and $\delta^{18}O$, whereas at high [CO_2] no interactions were detected.

Relationships of Shoot Biomass with Gas Exchange and Stable Isotopes

The range of A rates measured across the different water conditions at the end of the experiment was only weakly correlated with SB ($r = 0.34$, $P < 0.05$) at atmospheric [CO_2] and was not correlated at high [CO_2] (data not shown). In fact, while A and g_s were less affected by water limitation at high compared to atmospheric [CO_2], the opposite occurred for leaf growth, where the greatest decrease in biomass occurred at high [CO_2].

The single correlations between the signatures of the different isotopes against SB were plotted for each [CO_2] level across the three water regimes. $\delta^{13}C$ correlated negatively against SB at high [CO_2], whereas the negative relationship at atmospheric [CO_2] did not reach significance (**Figure 1A**). By contrast $\delta^{18}O$ correlated with SB in a weak, albeit significant, positive manner at atmospheric [CO_2], whereas the positive relationship did not reach significance at high [CO_2] (**Figure 1B**). $\delta^{15}N$ correlated negatively with SB at high [CO_2],whereas no correlation existed at atmospheric [CO_2] (**Figure 1C**). The nitrogen concentration correlated positively with SB at both [CO_2] levels (**Figure 2C**) in a stronger manner than any of the three stable isotopes. In addition, the N concentration correlated negatively with $\delta^{13}C$ at atmospheric [CO_2] and in a far stronger way at high [CO_2] (**Figure 2A**). Moreover, $\delta^{13}C$ correlated with the total shoot nitrogen content (calculated as a SB x N/100) in a weaker manner ($r = -0.43$ and -0.64, both $P < 0.01$, for 400 and 800 μmol mol^{-1} [CO_2], respectively) than the nitrogen concentration alone (**Figure 2A**). In contrast the N concentration correlated negatively with $\delta^{15}N$ only at high [CO_2] (**Figure 2B**) and a weak positive correlation existed between nitrogen concentration and $\delta^{18}O$ at atmospheric [CO_2] ($r = 0.33$, $P < 0.05$; data not shown). Moreover, g_s correlated positively with the N concentration at

TABLE 3 | Effect of water regime treatments in each CO_2 concentration (400 and 800 ppm) on shoot biomass, gas-exchange parameters, nitrogen content, and carbon, oxygen, and nitrogen stable composition.

		SB	A	g_s	C_i/C_a	N (%)	$\delta^{13}C$ (‰)	$\delta^{18}O$ (‰)	$\delta^{15}N$ (‰)
CO_2 400 ppm	Control	$9.58^{a} \pm 1.26$	$10.99^{a} \pm 1.28$	$317.36^{a} \pm 87.93$	$0.76^{a} \pm 0.03$	$6.09^{a} \pm 0.24$	$-35.61^{a} \pm 0.31$	$26.38^{a} \pm 0.41$	$3.12^{a} \pm 0.44$
	Mild stress	$7.25^{b} \pm 0.59$	$10.88^{a} \pm 1.51$	$225.64^{b} \pm 61.92$	$0.71^{a} \pm 0.05$	$5.22^{b} \pm 0.57$	$-35.13^{a} \pm 0.70$	$25.86^{b} \pm 0.25$	$3.27^{a} \pm 0.33$
	Moderate stress	$6.57^{b} \pm 0.56$	$8.65^{b} \pm 1.29$	$126.65^{c} \pm 51.86$	$0.62^{b} \pm 0.07$	$5.27^{b} \pm 0.31$	$-35.12^{a} \pm 0.83$	$26.08^{ab} \pm 0.21$	$2.98^{a} \pm 0.26$
Level of significance	Water regime (WR)	77.59***	49.23***	258979***	0.14***	7.13***	1.83^{ns}	1.71***	0.74^{ns}
	Genotype (G)	1.23^{ns}	19.42**	39535*	0.04***	1.92**	4.87**	2.51***	0.098^{ns}
	WR x G	3.21^{ns}	19.46*	29874^{ns}	0.04**	0.57^{ns}	3.50^{ns}	1.47*	0.47^{ns}
CO_2 800 ppm	Control	$11.99^{a} \pm 2.06$	$15.68^{a} \pm 1.20$	$312.90^{a} \pm 84.00$	$0.82^{a} \pm 0.04$	$6.04^{a} \pm 0.25$	$-48.59^{b} \pm 0.61$	$26.69^{a} \pm 0.60$	$1.67^{b} \pm 0.47$
	Mild stress	$10.23^{b} \pm 0.92$	$14.86^{a} \pm 1.47$	$217.38^{b} \pm 92.96$	$0.77^{ab} \pm 0.07$	$5.63^{b} \pm 0.46$	$-48.55^{b} \pm 0.65$	$26.68^{a} \pm 0.75$	$1.39^{b} \pm 0.48$
	Moderate stress	$6.23^{c} \pm 1.03$	$14.63^{a} \pm 1.22$	$203.60^{b} \pm 77.78$	$0.75^{b} \pm 0.08$	$4.14^{c} \pm 0.40$	$-46.88^{a} \pm 0.83$	$26.36^{a} \pm 0.80$	$2.23^{a} \pm 0.38$
Level of significance	Water regime (WR)	257.65***	10.59*	110428***	0.03**	30.50***	30.78***	1.19^{ns}	4.26***
	Genotype (G)	23.08**	23.67***	111626***	0.07***	2.53***	4.11*	1.39^{ns}	0.59^{ns}
	WR x G	13.96^{ns}	11.36^{ns}	54817^{ns}	0.02^{ns}	0.24^{ns}	2.35^{ns}	3.17^{ns}	1.90^{ns}

Means followed by different letters are significantly different ($P < 0.05$) according to Tukey's honestly significant difference (HSD) test. Analysis of variance for the same variables is shown for the water regime (WR), genotype (G), and interaction (WR x G) effects. The associated percentage of the sum of squares and probabilities (ns, not significant; $^{*}P < 0.05$; $^{**}P < 0.01$ and $^{***}P < 0.001$) are shown. Values within each water regime are the means ± SE of 20 measurements (four genotypes and five replicates per genotype). For each replicate a single plant was used.SB, shoot biomass (g DW); A, leaf net CO_2 assimilation (μmol CO_2 m^{-2} s^{-1}); g_s, stomatal conductance (mmol CO_2 m^{-2} s^{-1}); C_i/C_a, intercellular to ambient CO_2 concentration; N, nitrogen concentration (%, DW); $\delta^{13}C$, stable carbon isotope composition (‰), $\delta^{18}O$ stable oxygen isotope composition (‰); $\delta^{15}N$, stable nitrogen isotope composition.

both [CO_2] levels, and while it also correlated with SB, this was only at atmospheric [CO_2] (Figure S1). C_i/C_a correlated with the N concentration and SB in a similar way, but in a somewhat weaker manner than g_s.

In order to get an overall view of the relationships between shoot biomass and all the different physiological traits, a principal component analysis (PCA) was undertaken that included SB and LC together with the gas exchange traits and stable isotope signatures in **Table 2**. For all the water regimes and [CO_2] combined, the two first components explained 60% of variability. SB was placed nearly opposite to $\delta^{13}C$ and $\delta^{15}N$ and surrounded, at a certain distance, by $\delta^{18}O$, N and the A, g_s, C_i/C_a, and T gas-exchange parameters, whereas LC was placed further away (**Figure 3A**). For the three water regimes at atmospheric [CO_2] the two first component axes of the PCA accounted for more than 62% variability. In this case SB, and particularly N, were placed clearly opposite to $\delta^{13}C$, LC and $\delta^{15}N$, with the first isotope the furthest away and the second the closest to the center (**Figure 3B**), whereas C_i/C_a (together with N) surrounded SB. The rest of the gas exchange traits were placed more (g_s, and T) or less (A) close to C_i/C_a, while $\delta^{18}O$ had the least alignment to SB. In the case of the PCA for the three water regimes at high [CO_2], the two first component axes explained around 55% of variability. As in the previous PCAs, $\delta^{13}C$ and $\delta^{15}N$ were placed opposite to SB, whereas for the rest of the parameters only N was placed relatively near SB and all the gas exchange traits, together with $\delta^{18}O$ and LC, were placed on the same side of the representation as SB but far away from it (**Figure 3C**).

The relationships between SB with the different traits of **Table 2** in combination were assessed through a stepwise regressions analysis (**Table 4**). At atmospheric [CO_2] and the three water regimes combined, the first variable chosen by the model was g_s, which on its own explained 30% of the variability in SB. The second variable chosen by the model was N, with the two variables explaining together 44% of the variability in SB. At elevated [CO_2] and the three water regimes combined, the first variable chosen by the model was N concentration, which on its own explained 51% of the variability in SB. The second variable chosen by the model was Ci with the two variables explaining 58% of the variability in SB. In control conditions and both [CO_2] combined, the first variable chosen by the model was $\delta^{13}C$, explaining 34% of the variability in SB. The second variable chosen by the model was g_s; the two variables together explaining 44% of the variability in SB. Under mild stress and both [CO_2] combined, the first variable chosen by the model was also $\delta^{13}C$, which on its own explained 76% of the variability; the second variable chosen by the model was N concentration, with the two variables together explaining 81% of the variability in SB. Concerning the moderate stress, only T was chosen by the model and it explained merely 16% of the variability in SB.

Path Analysis

Further, we used the traits best correlated with shoot biomass to develop a conceptual model via a path-analysis. Besides SB, the model included $\delta^{13}C$ and $\delta^{15}N$, (as time-integrated indicators of water conditions and nitrogen metabolism, respectively), together with the N concentration and the gas exchange traits, g_s and C_i/C_a (**Figure 4**). In this case only the models across water regimes within each of the two [CO_2] levels were assayed, but excluding the model combining the two [CO_2], because the different $\delta^{13}C$ of the ambient air and the compressed CO_2. At atmospheric [CO_2], both the g_s and N concentration had quite

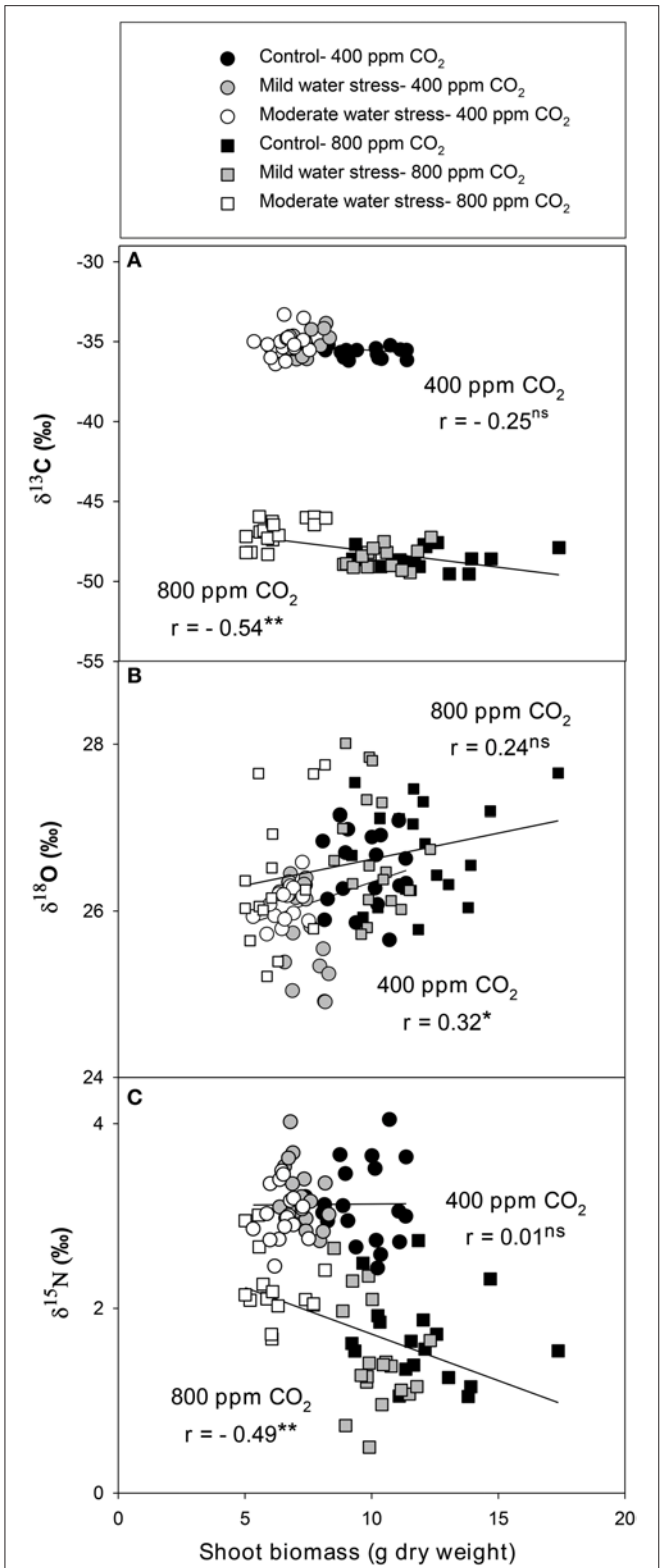

FIGURE 1 | Relationships of shoot biomass with the stable isotope compositions of **(A)** carbon ($\delta^{13}C$), **(B)** oxygen ($\delta^{18}O$), and **(C)** nitrogen ($\delta^{15}N$) analyzed in the leaves of sweet pepper grown hydroponically under different [CO_2] and water regimes. Levels of significance: ns, no significant; $^{*}P < 0.05$ and $^{**}P < 0.01$.

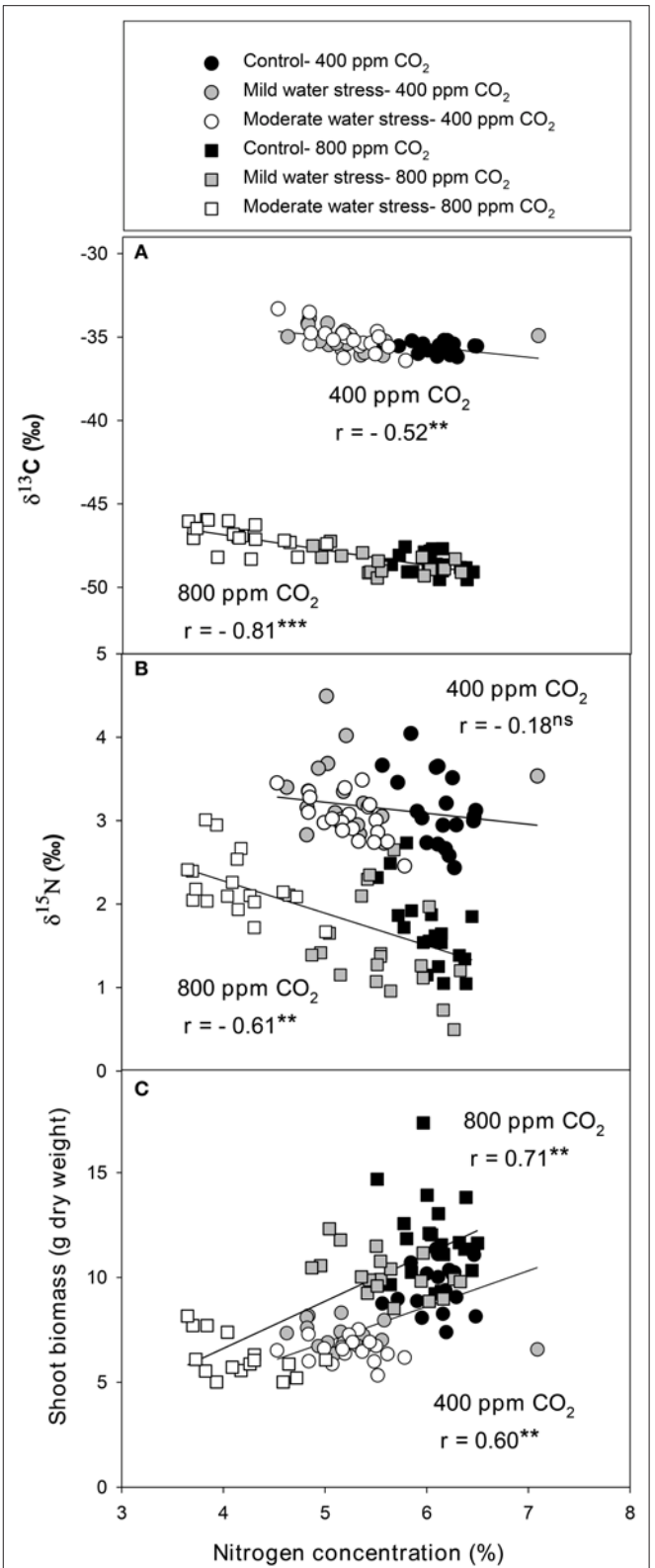

FIGURE 2 | Relationships of leaf nitrogen concentration with the stable isotope compositions of **(A)** carbon ($\delta^{13}C$) and **(B)** nitrogen ($\delta^{15}N$) and the **(C)** shoot biomass of sweet pepper grown hydroponically under different [CO_2] and water regimes. Levels of significance: $^{**}P < 0.01$ and $^{***}P < 0.001$.

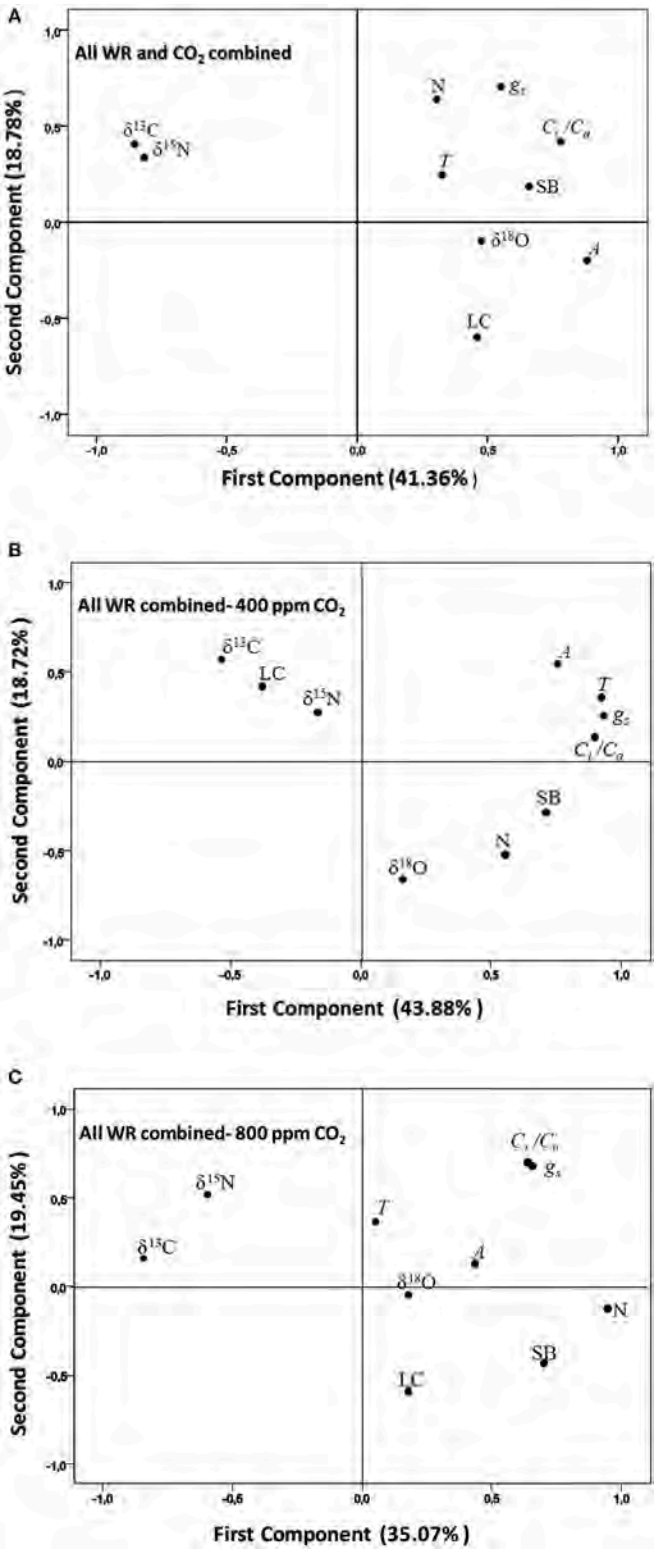

FIGURE 3 | Principal component analysis of shoot biomass (SB) and different physiological traits related to the photosynthetic, transpirative, and nitrogen status of the plant were set for four sweet pepper varieties grown under **(A)** three different water regimes (WR) and two [CO_2] combined, **(B)**, three water regimes at atmospheric [CO_2], and **(C)** three water regimes at high [CO_2]. The physiological traits included as variables are: the stable carbon, oxygen and nitrogen isotope compositions ($\delta^{13}C$, δ^{18} O, $\delta^{15}N$), the nitrogen concentration (N), the chlorophyll content (LC), and the net CO_2 Assimilation (A), transpiration (T), stomatal conductance (g_s), and the ratio of the intercellular vs. the atmospheric [CO_2] (C_i/C_a) of leaves.

TABLE 4 | Multiple linear regressions (stepwise) explaining shoot biomass (SB) variation across genotypic groups in each CO_2 concentration and all water regimes (WR) combined and in each water regime condition and all [CO_2] combined as a dependent variable, and all the gas exchange traits and stables isotope signatures and nitrogen concentration in the same growing conditions as independent variables.

Dependent variable	Growing condition	Variable chosen	R^2	Final stepwise model
SB	CO_2 400 ppm (all WR combined)	g_s	0.30***	SB = 0.006 g_s + 1.06 N + 0.53
		g_s; N	0.44***	
SB	CO_2 800 ppm (all WR combined)	N	0.51***	SB = 2.73 N−0.02 C_i+ 4.86
		N; C_i/C_a	0.58***	
SB	Control (all CO_2 combined)	$\delta^{13}C$	0.34***	SB = −0.18 $\delta^{13}C$ − 0.008 g_s + 5.49
		$\delta^{13}C$; g_s	0.44***	
SB	Mild stress (all CO_2 combined)	$\delta^{13}C$	0.76***	SB = −0.24 $\delta^{13}C$ −0.76 N + 2.76
		$\delta^{13}C$; N	0.81***	
SB	Moderate stress (all CO_2 combined)	*T*	0.16*	SB = −0.08 *T* + 6.67

*Levels of significance: *P < 0.05 and ***P < 0.001. Abbreviations for variables are as defined in* ***Table 2****.*

similar direct positive effects on the shoot biomass. However, g_s also indirectly affected N concentration through its strong direct effect on C_i/C_a and $\delta^{13}C$. Thus, $\delta^{13}C$ was negatively related with the N concentration in dry matter. The relationship of $\delta^{13}C$ on $\delta^{15}N$ was small, whereas there was no direct relation of $\delta^{15}N$ on the N concentration. At high [CO_2] most of the direct effect on shoot biomass corresponded to the N concentration, whereas the effect of g_s was minor and apparently negative. The direct effect of g_s on C_i/C_a was very strong but its direct effect on $\delta^{13}C$ was minor. However, the effect of $\delta^{13}C$ on N concentration was stronger than atmospheric [CO_2] and included a direct negative effect, together with an indirect effect mediated through changes in $\delta^{15}N$.

Amino Acid Profile and Network Analysis

The profile of 17 amino acids were assayed in the leaves of the four sweet pepper genotypes grown under contrasting [CO_2] and water regimes and plotted in a hierarchically clustered heat map (**Figure 5**). The significance of the three main factors and their interactions revealed that water regime, [CO_2] and the CO_2 x water stress interaction were the most relevant conditions affecting amino acid contents (all of them except lysine, methionine, and histidine). Although genotypic variability was only significant for three amino acids (proline, glycine, and glutamate), the interaction genotype by [CO_2] affected nine amino acids, almost exactly the amino acids that were altered under the CO_2 x water regime. CO_2 enrichment significantly decreased the content of 8 amino acids (serine, asparagine, glutamate, threonine, proline, cysteine, and valine), and tended to decrease the content of other amino acids, and only increased the levels of tyrosine. Water stress, regardless of the severity, decreased the contents of eight amino acid (serine, glycine, asparagine, threonine, alanine, proline, cysteine, and valine). In spite of some genotypic differences the [CO_2] x water regime interaction highlighted that, although elevated CO_2 and water stress led to a decrease of amino acid levels, this decrease was less clear under mild compared with the most severe water stress.

Based on significant correlations between trait pairs we built a correlation network for ambient and elevated [CO_2] treatments, including amino acid content (Figure S2). They showed similar number of nodes (32 and 31, respectively) and edges (128), although there were some differences with more negative correlations under elevated [CO_2]. In both networks amino acid levels were positively correlated between them. However, most amino acids correlated positively with shoot biomass under elevated [CO_2], while at ambient [CO_2] only cysteine and tyrosine did. In ambient [CO_2] network (Figure S2A) amino acids levels were also positively associated with SLA, N content, and $\delta^{18}O$ and negatively with $\delta^{15}N$. By contrast, in elevated [CO_2] network (Figure S2B) amino acids levels were associated with more traits: positively with PH, A, and N content and negatively with RWC, Ψ_w, $\delta^{13}C$, T, and $\delta^{15}N$.

DISCUSSION

Water stress affected negatively plant growth as compared with control conditions and regardless the [CO_2] assayed. Water stress also decreased Ψ_w but did not have any effect on RWC and $\Psi\pi$. These kinds of responses do not support osmotic adjustment, which contrasts with the available literature (e.g., Wullschleger and Oosterhuis, 1991; del Amor et al., 2010), and may be due to the mild to moderate nature of the water stress applied. In fact, the relatively small (but significant) changes in A rates, g_s, LC, and $\delta^{13}C$ and the lack of differences for SLA and anthocyanins under stress compared to control conditions support this statement. Moreover, although anthocyanins have protective functions during drought stress, their contribution to osmotic regulation might be low (Manetas, 2006).

The effects of high [CO_2] on increasing plant growth and biomass have been widely reported in many plant species including pepper (del Amor et al., 2010), with the positive effect being less evident at the most severe water stress (Peñuelas et al., 1995; Medina et al., 2016). The decrease in SLA has also been reported following increases in [CO_2] (Peñuelas et al., 1995; Piñero et al., 2016) and as a consequence of water stress (Xu et al., 2014). These results suggest that the leaf thickness of mesophyll packing increased in response to high [CO_2] (Oberbauer et al., 1985). The LC and anthocyanins also increased in response to high [CO_2]. Previous results in pepper only exhibited a trend toward higher chlorophyll content following exposure to high [CO_2] (Peñuelas et al., 1995). The increase of anthocyanins under elevated [CO_2], as it was also observed in Takatani et al. (2014) in response to higher carbon/nitrogen balance observed under these growth conditions. Indeed, the accumulation of anthocyanins is an indicative of nitrogen limitation in the plant according to these authors. The high sucrose levels usually reported under elevated [CO_2] might stimulate the expression of MYB75/PAP1 transcription factor that further enhances the

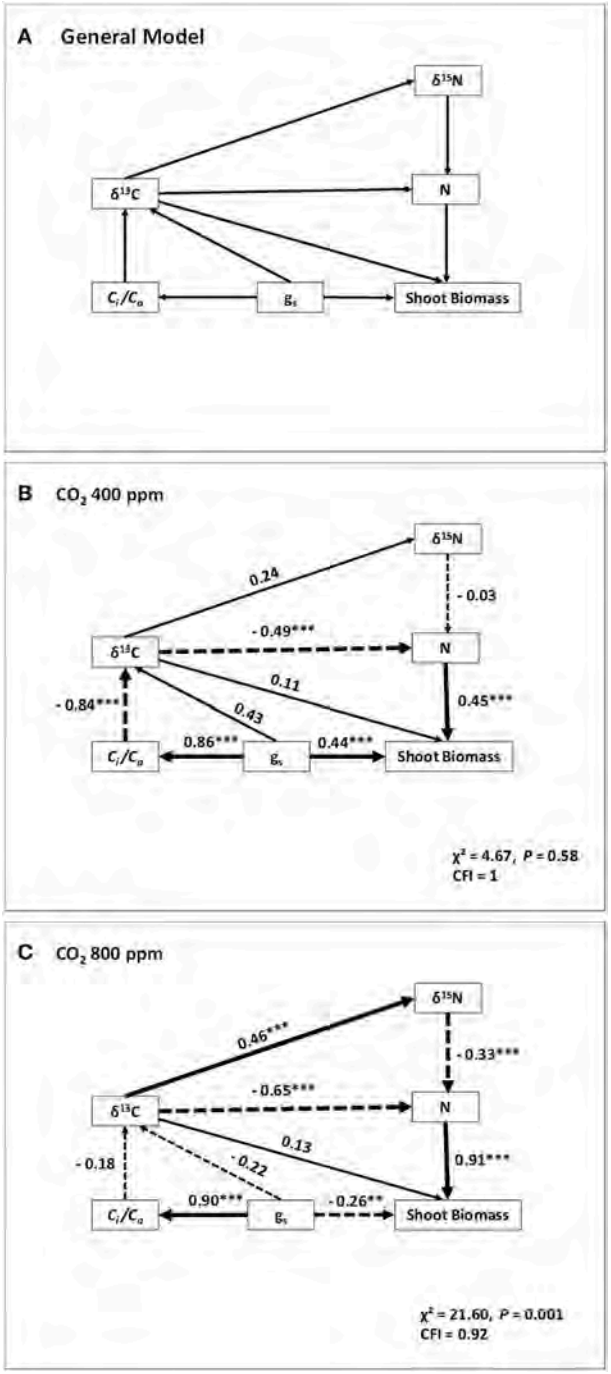

FIGURE 4 | Path analyses of four sweet pepper varieties grown under different water regimes and two [CO_2]. The conceptual model quantifying the relative strengths of direct and indirect relationships of gas exchange, stable isotope compositions and nitrogen concentration on shoot biomass (SB) is shown in **(A)**. Physiological parameters included in the model are: g_s, stomatal conductance; C_i/C_a, the ratio of the intercellular vs. the atmospheric [CO_2]; $\delta^{13}C$, carbon isotope composition; $\delta^{15}N$, nitrogen isotope composition and N concentration of leaves. The width of arrows is proportional to the path coefficient values. Dashed lines indicate negative relationships. Overall fit statistics for each path model (x^2 and comparative fit index, CFI), the latter useful for small sample sizes (with values >0.9 taken as indicative of a good fit), are shown at the bottom right of each panel. $^{**}P < 0.01$, $^{***}P < 0.001$.

production of anthocyanins (Tzin and Galili, 2010). Moreover, the levels of tyrosine, a precursor of anthocyanins, were induced under elevated [CO_2] and they could also induce the anthocyanin biosynthesis, as showed in *Arabidopsis thaliana* (Zhou et al., 2014). Regarding the genotype x water regime interaction, we observed that in most of the genotypes anthocyanin content increased with water stress as a response to water limitation. However, in the case of Coyote we observed a reduction of anthocyanins with water stress; that could suggest a limitation of the protective functions of anthocyanins in response to water stress in this genotype, which in part accounts for the lowest shoot biomass of this genotype.

In addition, high [CO_2] decreased leaf RWC and Ψ_w, and increased $\Psi\pi$. A previous study in pepper found a tendency to lower Ψ_w in response to high [CO_2] under well-watered conditions, whereas the RWC increased regardless of the water regime considered, and the $\Psi\pi$ increased but only under water stress (del Amor et al., 2010). However, the high [CO_2] concentration assayed in this paper was nearly three times higher than in the present study. The effect of high [CO_2] decreasing water status seems fairly surprising, but it may be due to a larger transpiration area compared with plants grown under normal [CO_2].

As expected high [CO_2] increased A and WUE compared with atmospheric [CO_2], but surprisingly did not decrease g_s and transpiration under control and mild-stress conditions, and even these rates increased under moderate water stress. A small number of studies have noted similar patterns, including work on sweet pepper (del Amor et al., 2010; del Amor, 2013), other herbaceous crops (Morison, 1998; Medina et al., 2016) and in tree species that were not acclimated (Medlyn et al., 2001). The results of the current study suggest that there was no acclimation of g_s to elevated [CO_2]. Moreover, the response of photosynthesis to growth in elevated [CO_2] is commonly tested by comparing the gas exchange of plants grown at atmospheric- and high-[CO_2] at the same [CO_2] across both sets of plants (e.g., Drake et al., 1997; Curtis and Wang, 1998).

Effect of [CO_2] and Water Regime on $\delta^{13}C$, $\delta^{18}O$, and $\delta^{15}N$

The increase in $\delta^{13}C$ under water stress is in line with earlier work (Farquhar et al., 1982, 1989). However, the effect was more evident at high [CO_2], which agrees with the findings of del Amor (2013) for sweet pepper plants that were subjected to different levels of salinity under these two different [CO_2]. This may be due to the $\delta^{13}C$ dilution effect of the CO_2 used to raise the air [CO_2] up to 800 ppm (i.e., the industrial CO_2 is a by-product of combusting fossil fuels and therefore its $\delta^{13}C$ is far more negative than atmospheric CO_2). Indeed, $\delta^{13}C$ decreased around 3‰ for each 100 μmol mol^{-1} of increase in [CO_2], which is in line with previous reports (Schubert and Jahren, 2012; del Amor, 2013). Therefore at high [CO_2], water stress slows the increase of new biomass with lower $\delta^{13}C$. The effect (pointed out above) of high [CO_2] decreasing water status due to a larger transpiration area, compared with plants grown under normal [CO_2], may be also involved in the larger range of $\delta^{13}C$ values as

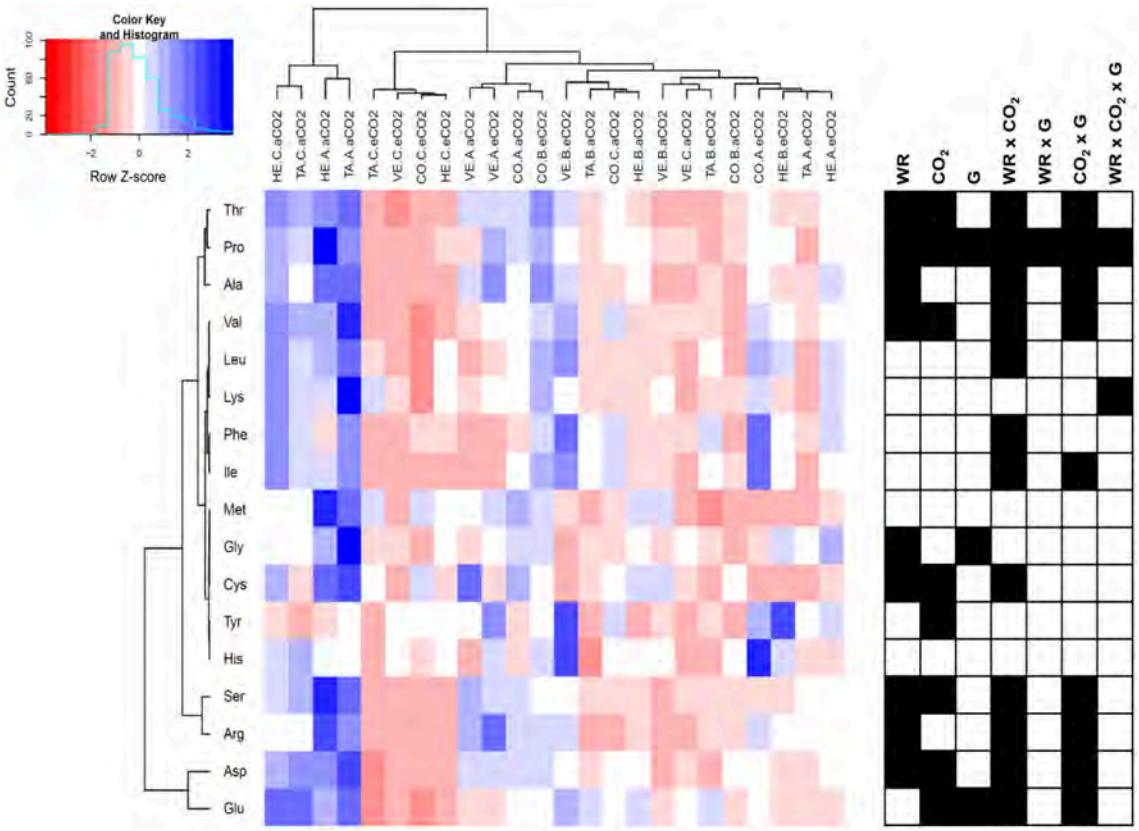

FIGURE 5 | Hierarchically clustered heat map of amino acid content of four sweet pepper genotypes (TA, Tallante; CO, Coyote; HE, Herminio; VE, Velez) grown hydroponically under different [CO_2] (aCO_2, ambient [CO_2]; eCO_2, elevated [CO_2]) and water regimes (A, control; B, mild water stress; C, moderate water stress). Values were scaled in the row direction as presented in the color key. Significance of main factors (WR, water regime; CO_2, [CO_2]; and G, genotype) and their interactions are shown as black cells ($P < 0.05$).

response to water stress. Thus, at high [CO_2] the absolute changes in $\delta^{13}C$ were more in parallel with the SB than with the net assimilation or C_i/C_a. In that regard, $\delta^{13}C$ correlated negatively with SB across water regimes at high [CO_2], but the negative relationship did not reach significance at atmospheric [CO_2]. Significantly, stronger negative relationships between $\delta^{13}C$ and SB at high vs. atmospheric [CO_2] have been reported before for sweet pepper when plants growing across different levels of salinity were compared (del Amor, 2013). Moreover, genotypic effects on $\delta^{13}C$ were significant at both [CO_2]. To the best of our knowledge there are no studies reporting on the genotypic variability in $\delta^{13}C$ of sweet pepper under different levels of water stress and [CO_2].

Water stress slightly decreased $\delta^{18}O$ but only at high [CO_2]. Such decreases in $\delta^{18}O$ in response to water stress and a lower transpiration are opposite to most of the reports (Barbour and Farquhar, 2000; Farquhar et al., 2007; Cabrera-Bosquet et al., 2009a, 2011). The increase in $\delta^{18}O$ in plant material exposed to high [CO_2] has been reported before and may be caused by increases in the $\delta^{18}O$ of the leaf water (Cooper and Norby, 1994). Although it has been shown that the oxygen isotopic content of atmospheric carbon dioxide has little direct influence on the $\delta^{18}O$ of either leaf water or cellulose (DeNiro and Epstein, 1979), increasing atmospheric carbon dioxide concentrations may have significant indirect effects on heavy stable isotope enrichment in leaf water. This would result from the expected decreases in transpiration and increases in WUE by plants as [CO_2] levels increase (Eamus and Jarvis, 1989). The processes leading to concentration of the heavy isotopes ^{18}O in leaf water are similar in many respects to evaporation, which alters the isotopic composition of terrestrial surface waters (Cooper and Norby, 1994). Alternative explanations for the increase in $\delta^{18}O$ at high [CO_2] are not supported by our results. Indeed, a higher CO_2 release due to photorespiration at atmospheric compared with high [CO_2] levels would cause an increase in $\delta^{18}O$ at atmospheric [CO_2] levels (Farquhar et al., 1993), which does not agree with the increase we found in $\delta^{18}O$ at high [CO_2]. Changes in g_s do not seem to be involved because, regardless of the presence or absence of differences in g_s within a given water regime between the atmospheric and high [CO_2], all water regimes at high [CO_2] exhibited higher $\delta^{18}O$ than the corresponding water regimes at atmospheric [CO_2]. Moreover, genotypic variability was only significant at atmospheric [CO_2]. In spite of some positive results (Barbour et al., 2000; Cabrera-Bosquet et al., 2009b), the weak performance of $\delta^{18}O$ in correlating with biomass and yield has been extensively reported (Araus et al., 2013; Bort et al., 2014;

Foulkes et al., 2016; Munjonji et al., 2016). This poor performance appears to be caused by post photosynthetic fractionations of the ^{18}O signature in the photoassimilates (Sánchez-Bragado et al., 2016). The same reasoning may be extended for the weak and erratic correlations of $\delta^{18}O$ with gas exchange traits and $\delta^{13}C$ that we found.

Plants under the strongest water stress exhibited slightly lower $\delta^{15}N$ values than the other two treatments at atmospheric [CO_2], and the opposite occurred at high [CO_2]. Decreases in $\delta^{15}N$ following water limitation (Araus et al., 2013; Bort et al., 2014) or growing conditions causing water stress, such as salinity (Yousfi et al., 2009, 2012), have been reported before. The effect of rising [CO_2] on $\delta^{15}N$ was clearer than the effect of the water regime; in this case decreasing the isotopic composition, irrespective of the water regime considered. Depletion of the heavier N isotope in plants grown under high [CO_2] and water deficit conditions has been reported before in a study with alfalfa (Ariz et al., 2015), whereas another recent study, this time in durum wheat, concluded that elevated [CO_2] was the main factor that increased $\delta^{15}N$ (Medina et al., 2016). The decrease in $\delta^{15}N$ under elevated [CO_2] may reflect decreased g_s, but could also be related to a higher nitrogen demand in leaves, as suggested by the decreased in leaf N (Ariz et al., 2015) or shifts in nitrogen metabolism associated with decreases in photorespiration (Tcherkez, 2010).

The photorespiratory nitrogen cycle extending over different plant compartments implicates several reactions related to nitrogen recycling that may have ^{15}N-kinetic isotope effects (Yu and Woo, 1991; Werner and Schmidt, 2002). Normally, the kinetic isotope effects on these reactions should not become evident when there is a total recycling of the intermediates without input or net production of substrates and products (Werner and Schmidt, 2002). However, plants can excrete gaseous ammonia (Francis et al., 1997; Pearson et al., 1998) as a consequence of photorespiration. If the uptake/loss of NH_3 from plant stomata is rate-limited by the diffusion of NH_3 in air, the transported NH_3 will be depleted in ^{15}N by around 18‰ relative to the $\delta^{15}N$ of the source (Farquhar et al., 1980; Tcherkez and Hodges, 2008). As a consequence an increase in $\delta^{15}N$ may be expected as a response to photorespiration, which may be the case for plants exposed to atmospheric [CO_2] compared to enhance [CO_2].

The correlation of $\delta^{15}N$ with SB across water regimes was only significant (and negative) at the high [CO_2]. The lack of correlation at atmospheric [CO_2] may be due, as for $\delta^{13}C$, to the relatively narrow range of variability in SB associated with the response to water regimes at atmospheric [CO_2]. Negative relationships between $\delta^{15}N$ and SB and yield at atmospheric [CO_2] have been frequently reported (Robinson et al., 2000; Yousfi et al., 2009; Raimanová and Haberle, 2010; Araus et al., 2013).

Growing Conditions, N Concentration, and Plant Growth

The effects of water stress decreasing the N concentration in leaves have been extensively reported (Shangguan et al., 2000; Yousfi et al., 2012). In accordance with this, the N concentration was positively correlated with the g_s ($r = 0.36$, $P < 0.01$; $r = 0.51$, $P < 0.001$, at atmospheric and high [CO_2], respectively), suggesting that the N concentration in leaves depends to some extent on the transpirative stream (Dalla Costa and Gianquinto, 2002). This may be the case for plants growing under hydroponic conditions in particular, where water and nitrogen are provided together through the nutrient solution (Peñuelas et al., 1995) and the transpiration stream largely determines the availability of mineral N in the rhizosphere (Gonzalez-Dugo et al., 2010). In support of that, our results show a general decrease in the content of the different amino acids as response to water stress. Such decrease is nonspecific, as shown by the fact these amino acids belong to different metabolic pathways (Galili et al., 2016). This may highlight that primary substrate(s) for the synthesis of all amino acids were reduced, involving the provision of C skeletons or N. It has been reported for Arabidopsis plants that a reduction in the levels of transpiration, decreased the capacity for nitrogen uptake and the shoot nitrogen concentration of the plant but only when water availability was not restricted (Hepworth et al., 2015).

Increasing the [CO_2] had a significant, albeit minor effect, decreasing the N concentration. In fact, the results of an increase in [CO_2] decreasing N concentration were only significant at the strongest water stress. A decrease in nitrogen concentration has been widely reported in non-leguminous plants following increases in [CO_2] (Jablonski et al., 2002), irrespective of the water regime (Medina et al., 2016). In fact, the predicted growth response to elevated [CO_2] is reduced at low N availability (McMurtrie et al., 2008; Vicente et al., 2016b). In our study, water deficit combined with high [CO_2] caused the lowest SB and N concentration in the leaves among the six different growing conditions.

As expected at elevated [CO_2], the levels of photorespiratory intermediates, glycine and serine decreased (Geiger et al., 1998, 1999; Yu et al., 2012; Aranjuelo et al., 2013; Noguchi et al., 2015). However, different to previous studies (Fritz et al., 2006; Krapp et al., 2011; Noguchi et al., 2015), the levels of (other) major amino acids (e.g., aspartate, asparagine, glutamate, and alanine) decreased. Such decrease has been reported as response to insufficient nitrogen conditions; specifically under NO_3^- and ambient [CO_2] conditions (Noguchi et al., 2015; Vicente et al., 2016b). This pattern suggests that in our system some limitation of N availability may be present. Nevertheless, the relative decrease of glycine as response to inhibition of photorespiration (i.e., at high compared with ambient [CO_2]) was much lower than that of serine which is against a low N availability (Sulpice et al., 2013; Noguchi et al., 2015). On the other hand in agreement with previous studies the amount of minor amino acids (e.g., threonine, valine, cysteine, methionine, lysine, leucine, etc.) decrease at elevated [CO_2] (Noguchi et al., 2015).

Summarizing the decrease in the amount of several amino acids under elevated CO_2, reported in our study may have several causes. Some of them, decreased probably due to the inhibition of photorespiration under elevated CO_2 (glycine and serine). The rest of the amino acids could have been reduced due to the inhibition of N assimilation; this has been reported in several plants under elevated CO_2, such as Arabidopsis and wheat (Aranjuelo et al., 2013; Noguchi et al., 2015; Vicente et al.,

2016b). The inhibition of N assimilation under elevated CO_2 is not completely understood, but it could be due, as reported in Vicente et al. (2016b) and in agreement with previous studies (Bloom et al., 2010; Aranjuelo et al., 2013), to (i) lower rates of photorespiration in elevated CO_2 that decrease the availability of reductant in the cytosol, and inhibition of NO_2^- influx into chloroplasts; or to increased demand for NO_3^- to match the increase in net photosynthetic assimilation in elevated CO_2, leading to a decline of the metabolic NO_3^- pool that restricts induction of nitrate reductase and thus NO_3^- assimilation.

Interestingly tyrosine was the only amino acid clearly increasing as response to a high [CO_2]. Moreover, under water stress, high [CO_2] also increased phenylalanine. Both are aromatic amino acids, which have low N/C ratios, involved as precursors in the synthesis of anthocyanin. In fact an increase in both amino acids has been reported in Arabidopsis leaves at elevated [CO_2] in $NH_4^+ + NO_3^-$ media (Noguchi et al., 2015) which is our case (i.e., nutrient solution). Cysteine was strongly decreased under elevated [CO_2] regardless of water regime. It constitutes the first stable product of the sulfur assimilation, and acts as precursor of the majority of organic sulfur compounds (Hawkesford et al., 2012).

Independently of [CO_2], the levels of all amino acids were correlated (Supplementary Material Figure S2). However, the relationships between amino acids with other physiological traits varied depending on [CO_2]. It was especially remarkable that amino acid contents correlated positively with SB under high [CO_2] and negatively with traits related to water status (RWC, Ψ_w, $\delta^{13}C$, and T), while under atmospheric [CO_2] the correlations between amino acids and other traits were scarce. These findings suggest that amino acid pool greatly influences biomass accumulation under elevated [CO_2] and its amount is influenced by leaf and plant water status in a highly-dependent manner.

Decreases in transpiration associated with mass flow of soil solution, have been proposed to limit plant N acquisition. In an experiment with cottonwood, where relative humidity and atmospheric [CO_2] were manipulated to alter the transpirative stream, N gain was positively correlated across all treatments with root mass, and a significant portion of the remaining variation (44%) was positively related to transpiration per unit root mass (McDonald et al., 2002). Thus, decreases in plant N concentration under water stress are attributable in part to associated decreases in g_s and transpiration. However, other mechanisms may be involved for the decrease in plant N under [CO_2] enrichment. Thus, in our study no clear differences existed in the rates of g_s measured at different [CO_2] and even transpiration was increased at high [CO_2] relative to atmospheric [CO_2]. Besides the potential effect of diminishing transpirative stream, [CO_2] enrichment is reported to inhibit the assimilation of nitrate into organic nitrogen compounds (Bloom et al., 2010; Vicente et al., 2016b). This inhibition may be largely responsible for [CO_2] acclimation, that is, the decrease in photosynthesis and growth of C_3 plants after long exposures to [CO_2] enrichment. Different studies have shown that the effect of elevated [CO_2] on reducing N content was related at the transcript level to a down-regulation of genes encoding for Rubisco subunits and N-assimilation enzymes (GS1 and GS2), indicating a co-regulation of primary C and N metabolism (Stitt and Krapp, 1999; Vicente et al., 2015, 2016a,b; Medina et al., 2016).

As a consequence of the effect of water regime on N concentration, the trait best correlated with total biomass within each of the two [CO_2] was the total leaf N concentration (and amino acid contents), although the correlation was stronger at high [CO_2]. Overall, the results showed that greater plant growth across water regimes was linked to an increase in shoot N concentration associated to a higher transpiration stream, even when changes in N metabolism appear also involved (Hirel et al., 2007; Medina et al., 2016). A study of Peñuelas et al. (1995) on sweet pepper also found that the effect of [CO_2] and water regime was dependent on the accumulated N supply. All these studies have plants grown under hydroponic conditions in common, where irrigation and fertilization are provided together through the nutrient solution under relatively low photosynthetic photon flux density.

The leaf N concentration was negatively correlated with $\delta^{13}C$ within each [CO_2] across water regimes, whereas nitrogen concentration and g_s correlated positively (but in a weaker manner). Moreover, $\delta^{13}C$ correlated with the total shoot nitrogen content in a weaker manner than the nitrogen concentration alone. In fact, both the $\delta^{13}C$ and nitrogen concentration were expressed on a dry matter basis, which may explain their better correlation. $\delta^{13}C$ is not just an indicator of water use efficiency (Farquhar et al., 1982, 1989) but it is also strongly negatively affected by the amount of available water (Araus et al., 1997, 2003) and therefore when analyzed on a dry matter basis it may be considered an indicator on the total (i.e., through time) water used by the plant. Moreover, in the Principal Component Analysis the nitrogen concentration was placed clearly opposite to $\delta^{13}C$. In other words, the negative relationship between $\delta^{13}C$ and nitrogen concentration on a dry leaf basis may be understood as the nitrogen concentration in the leaves being, at least in part, the consequence of the amount of water transpired by the plant. The Path Analysis further supported the direct contribution of the nitrogen concentration in determining total biomass as well as the positive role of an increased water use (assessed through a lower $\delta^{13}C$ of the dry matter) on the N accumulation. This model worked better under high [CO_2]. In sweet pepper growing under hydroponic conditions, strong negative correlations across salinity levels for leaf $\delta^{13}C$ with both g_s and nitrate accumulation have been reported, with the correlations being higher at elevated [CO_2] compared with atmospheric [CO_2] (del Amor, 2013).

CONCLUSION

The signatures of the three different stable isotopes are significantly affected by water regime, [CO_2], and genotypic effects. However, the results do not support the use of $\delta^{18}O$ as an indicator of the effect of growing conditions and genotypes on plant growth. This study proves that the effect of water regime on sweet pepper growth in a hydroponic system is caused by changes in the amount of nitrogen assimilated, which is associated with the plant's water use. In that sense, the role of $\delta^{13}C$

in explaining differences in plant growth across water regimes appears mediated via its direct relationship with N accumulation in leaves, particularly at high [CO_2]. However, our study does not support stomatal closure as being associated with an elevated [CO_2]-induced reduction in N concentration in the shoot.

AUTHOR CONTRIBUTIONS

FdA and JA conceived and designed the experiments. MP, MS, and GO-A contributed to the experimental work. SY and RV contributed to the data analysis and preparation of tables and figures. MS wrote the paper under the supervision of FdA and JA and all three revised the manuscript. All authors read and approved the final manuscript.

ACKNOWLEDGMENTS

This study was supported in part by the European Regional Development Fund (ERDF) 80%—Región de Murcia (FEDER 1420-07) and the 2014-SGR-628 AGAUR project, Generalitat de Catalunya, Spain. MP is the recipient of a pre-doctoral fellowship from INIA. The authors thank Miguel Marín for his technical assistance.

SUPPLEMENTARY MATERIAL

The Supplementary Material for this article can be found online at: https://www.frontiersin.org/articles/10.3389/fpls.2017.02180/full#supplementary-material

REFERENCES

Aranjuelo, I., Sanz-Sáez, A., Jáuregui, I., Irigoyen, J. J., Araus, J. L., Sánchez-Díaz, M., et al. (2013). Harvest index, a parameter conditioning responsiveness of wheat plants to elevated CO_2. *J. Exp. Bot.* 64, 1879–1892. doi: 10.1093/jxb/ert081

Araus, J. L., Buxo, R., Febrero, A., Camalich, M. D., Martin, D., Molina, F., et al. (1997). Identification of ancient irrigation practices based on the carbon isotope discrimination of plant seeds: a case study from the Southeast Iberian Peninsula. *J. Archaeol. Sci.* 24, 729–740. doi: 10.1006/jasc.1997.0154

Araus, J. L., Serret, M. D., Bort, J., and Nieto-Taladriz, M. T. (2013). Comparative performance of $\delta^{13}C$, $\delta^{18}O$ and $\delta^{15}N$ for phenotyping durum wheat adaptation to a dryland environment. *Funct. Plant Biol.* 40, 595–608. doi: 10.1071/FP12254

Araus, J. L., Slafer, G., Royo, C., and Serret, M. D. (2008). Breeding for yield potential and stress adaptation in cereals. *Crit. Rev. Plant Sci.* 27, 377–412. doi: 10.1080/07352680802467736

Araus, J. L., Villegas, D., Aparicio, N., Garcia del Moral, L. F., El Hani, S., Rharrabti, Y., et al. (2003). Environmental factors determining carbon isotope discrimination and yield in durum wheat under Mediterranean conditions. *Crop Sci.* 43, 170–180. doi: 10.2135/cropsci2003.1700

Arbuckle, J. L. (1997). *Amos Users' Guide; v. 3.6*. Chicago, IL: Small Waters Corporation.

Ariz, I., Cruz, C., Neves, T., Irigoyen, J. J., García-Olaverri, C., Nogués, S., et al. (2015). Leaf $\delta^{15}N$ as a physiological indicator of the responsiveness of N_2-fixing alfalfa plants to elevated [CO_2], temperature and low water availability. *Front. Plant Sci.* 6:574. doi: 10.3389/fpls.2015.00574

Barbour, M. M. (2007). Stable oxygen isotope composition of plant tissue: a review. *Funct. Plant Biol.* 34, 83–94. doi: 10.1071/FP06228

Barbour, M. M., and Farquhar, G. D. (2000). Relative humidity –and ABA- induced variation in carbon and oxygen isotope ratios of cotton leaves. *Plant Cell Environ.* 23, 473–485. doi: 10.1046/j.1365-3040.2000.00575.x

Barbour, M. M., Fischer, R. A., Sayre, K. D., and Farquhar, G. D. (2000). Oxygen isotope radio of leaf and grain material correlates with stomatal conductance and grain yield in irrigated wheat. *Aust. J. Plant Physiol.* 27, 625–637. doi: 10.1071/PP99041

Bencze, S., Bamberger, Z., Janda, T., Balla, K., Varga, B., Bedo, Z., et al. (2014). Physiological response of wheat varieties to elevated atmospheric CO_2 and low water supply levels. *Photosynthetica* 52, 71–82. doi: 10.1007/s11099-014-0008-y

Bloom, A. J., Burger, M., Rubio Asensio, J. S., and Cousins, A. B. (2010). Carbon dioxide enrichment inhibits nitrate assimilation in wheat and Arabidopsis. *Science* 328, 899–903. doi: 10.1126/science.1186440

Bort, J., Belhaj, M., Latiri, K., Kehel, Z., and Araus, J. L. (2014). Comparative performance of the stable isotope signatures of carbon, nitrogen and oxygen in assessing early vigour and grain yield in durum wheat. *J. Agric. Sci.* 152, 408–426. doi: 10.1017/S0021859613000269

Cabrera-Bosquet, L., Albrizio, R., Nogués, S., and Araus, J. L. (2011). Dual $\Delta^{13}C/\delta^{18}O$ response to water and nitrogen availability and its relationship with yield in field-grown durum wheat. *Plant Cell Environ.* 34, 418–433. doi: 10.1111/j.1365-3040.2010.02252.x

Cabrera-Bosquet, L., Molero, G., Nogués, S., and Araus, J. L. (2009a). Water and nitrogen conditions affect the relationship of $\Delta^{13}C$ and $\Delta^{18}O$ to gas exchange and growth in durum wheat. *J. Exp. Bot.* 60, 1633–1644. doi: 10.1093/jxb/erp028

Cabrera-Bosquet, L., Sanchez, C., and Araus, J. L. (2009b). Oxygen isotope enrichment ($\Delta^{18}O$) reflects yield potential and drought resistance in maize. *Plant Cell Environ.* 32, 1487–1499. doi: 10.1111/j.1365-3040.2009.02013.x

Cernusak, L. A., Winter, K., and Turner, B. L. (2009a). Physiological and isotopic ($\delta^{13}C$ and $\delta^{18}O$) responses of three tropical tree species to water and nutrient availability. *Plant Cell Environ.* 32, 1441–1455. doi: 10.1111/j.1365-3040.2009.02010.x

Cernusak, L. A., Winter, K., and Turner, B. L. (2009b). Plant $\delta^{15}N$ correlates with the transpiration efficiency of nitrogen acquisition in tropical trees. *Plant Physiol.* 151, 1667–1676. doi: 10.1104/pp.109.145870

Condon, A. G., Farquhar, G. D., and Richards, R. A. (1990). Genotypic variation in carbon isotope discrimination and transpiration efficiency in wheat. Leaf gas exchange and whole plant studies. *Aust. J. Plant Physiol.* 17, 9–22. doi: 10.1071/PP9900009

Condon, A. G., Richards, R. A., Rebetzke, G. J., and Farquhar, G. D. (2002). Improving intrinsic water use efficiency and crop yield. *Crop Sci.* 42, 122–131. doi: 10.2135/cropsci2002.1220

Condon, A. G., Richards, R. A., Rebetzke, G. J., and Farquhar, G. D. (2004). Breeding for high water-use efficiency. *J. Exp. Bot.* 55, 2447–2460. doi: 10.1093/jxb/erh277

Cooper, L. W., and Norby, R. J. (1994). Atmospheric CO_2 enrichment can increase the ^{18}O content of leaf water and cellulose: paleoclimatic and ecophysiological implications. *Clim. Res.* 4, 1–11. doi: 10.3354/cr004001

Coplen, T. B. (2008). *Explanatory Glossary of Terms Used in Expression of Relative Isotope Ratios and Gas Ratios.* IUPAC Recommendations 2008. International Union of Pure and Applied Chemistry Inorganic Chemistry Division, Commission on Isotopic Abundances and Atomic Weights: Research Triangle Park, NC, USA. Available online at: https://old.iupac.org/reports/provisional/abstract08/coplen_310508.html

Coplen, T. B. (2011). Guidelines and recommended terms for expression of stable-isotope-ratio and gas-ratio measurement results. *Rapid Commun. Mass Spectrom.* 25, 2538–2560. doi: 10.1002/rcm.5129

Curtis, P. S., and Wang, X. (1998). A meta-analysis of elevated CO_2 effects on woody plant mass, form, and physiology. *Oecologia* 113, 299–313. doi: 10.1007/s004420050381

Dalla Costa, L., and Gianquinto, G. (2002). Water stress and watertable depth influence yield, water use efficiency, and nitrogen recovery in bell pepper: Lysimeter studies. *Aust. J. Agric. Res.* 53, 201–210. doi: 10.1071/AR00133

Dawson, T. E., Mambelli, S., Plamboeck, A. H., Templer, P. H., and Tu, K. P. (2002). Stable isotopes in plant ecology. *Annu. Rev. Ecol. Syst.* 33, 507–559. doi: 10.1146/annurev.ecolsys.33.020602.095451

del Amor, F. M. (2007). Yield and fruit quality response of sweet pepper to organic and mineral fertilization. *Renew. Agric. Food Syst.* 22, 233–238. doi: 10.1017/S1742170507001792

del Amor, F. M. (2013). Variation in the leaf $\delta^{13}C$ is correlated with salinity tolerance under elevated CO_2 concentration. *J. Plant Physiol.* 170, 283–290. doi: 10.1016/j.jplph.2012.10.019

del Amor, F. M., and Gómez-López, M. D. (2009). Agronomical response and water use efficiency of sweet pepper plants grown in different greenhouse substrates. *Hortscience* 44, 810–814.

del Amor, F. M., and Navarro, J. (2008). Isotopic discrimination as a tool for organic farming certification in sweet pepper. *J. Environ. Qual.* 37, 182–185. doi: 10.2134/jeq2007.0329

del Amor, F. M., Cuadra-Crespo, P., Walker, D. J., Cámara, J. M., and Madrid, R. (2010). Effect of foliar application of antitranspirant on photosynthesis and water relations of pepper plants under different levels of CO_2 and water stress. *J. Plant Physiol.* 167, 1232–1238. doi: 10.1016/j.jplph.2010.04.010

DeNiro, M. J., and Epstein, S. (1979). Relationship between the oxygen isotope ratios of terrestrial plant cellulose, carbon dioxide, and water. *Science* 204, 51–53. doi: 10.1126/science.204.4388.51

Drake, B. G., Gonzalez-Meler, M. A., and Long, S. P. (1997). More efficient plants: a consequence of rising atmospheric CO_2? *Annu. Rev. Plant Physiol. Plant Mol. Biol.* 48, 609–639. doi: 10.1146/annurev.arplant.48.1.609

Dueck, T. A., Grashoff, C., Broekhuijsen, G., and Marcelis, L. F. M. (2006). Efficiency of light energy used by leaves situated in different levels of a sweet pepper canopy. *Acta Horticult.* 711, 201–206. doi: 10.17660/ActaHortic.2006.711.25

Eamus, D., and Jarvis, P. J. (1989). The direct effects of increase in the global atmospheric CO_2 concentration on natural and commercial temperate trees and forests. *Adv. Ecol. Res.* 19, 1–55. doi: 10.1016/S0065-2504(08)60156-7

Erice, G., Aranjuelo, I., Irigoyen, J. J., and Sánchez-Díaz, M. (2007). Effect of elevated CO_2, temperature and limited water supply on antioxidant status during regrowth of nodulated alfalfa. *Physiol. Plant.* 130, 33–45. doi: 10.1111/j.1399-3054.2007.00889.x

Erice, G., Sanz-Sáez, A., Urdiain, A., Araus, J. L., Irigoyen, J. J., and Aranjuelo, I. (2014). Harvest index combined with impaired N availability constrains the responsiveness of durum wheat to elevated CO_2 concentration and terminal water stress. *Funct. Plant. Biol.* 41, 1138–1147. doi: 10.1071/FP14045

Farquhar, G. D., and Lloyd, J. (1993). "Carbon and oxygen isotope effects in the exchange of carbon dioxide between terrestrial plants and the atmosphere," in *Stable Isotopes and Plant-Carbon Water Relations*, eds J. R. Ehleringer, A. E. Hall, and G. D. Farquhar (San Diego, CA: Academic Press), 47–70.

Farquhar, G. D., and Richards, R. A. (1984). Isotopic composition of plant carbon correlates with water-use efficiency of wheat genotypes. *Aust. J. Plant Physiol.* 11, 539–552. doi: 10.1071/PP9840539

Farquhar, G. D., Cernusak, L. A., and Barnes, B. (2007). Heavy water fractionation during transpiration. *Plant Physiol.* 143, 11–18. doi: 10.1104/pp.106.093278

Farquhar, G. D., Ehleringer, J. R., and Hubick, K. T. (1989). Carbon isotope discrimination and photosynthesis. *Annu. Rev. Plant Physiol. Mol. Biol.* 40, 503–537. doi: 10.1146/annurev.pp.40.060189.002443

Farquhar, G. D., Firth, P. M., Wetselaar, R., and Weir, B. (1980). On the gaseous exchange of ammonia between leaves and the environment: determination of the ammonia compensation point. *Plant Physiol.* 66, 710–714. doi: 10.1104/pp.66.4.710

Farquhar, G. D., Lloyd, J., Taylor, J. A., and Ehleringer, J. R. (1993). Vegetation effects on the oxygen isotopic composition of atmospheric CO_2. *Nature* 363, 439–443. doi: 10.1038/363439a0

Farquhar, G. D., O'Leary, M. H., and Berry, J. A. (1982). On the relationship between carbon isotope discrimination and intercellular carbon dioxide concentration in leaves. *Aust. J. Plant Physiol.* 9, 121–137.

Flores, P., Fenoll, J., and Hellín, P. (2007). The feasibility of using $\delta^{15}N$ and $\delta^{13}C$ values for discriminating between conventionally and organically fertilized pepper (*Capsicum annuum* L.). *J. Agric. Food Chem.* 55, 5740–5745. doi: 10.1021/jf0701180

Foulkes, M. J., DeSilva, J., Gaju, O., and Carvalho, P. (2016). Relationships between $\delta^{13}C$, $\delta^{18}O$ and grain yield in bread wheat genotypes under favourable irrigated and rain-fed conditions. *Field Crops Res.* 196, 237–250. doi: 10.1016/j.fcr.2016.07.006

Francis, D. D., Schepers, J. S., and Sims, A. L. (1997). Ammonia exchange from corn foliage during reproductive growth. *Agron. J.* 89, 941–946. doi: 10.2134/agronj1997.00021962008900060015x

Fritz, C., Mueller, C., Matt, P., Feil, R., and Stitt, M. (2006). Impact of the C–N status on the amino acid profile in tobacco source leaves. *Plant Cell Environ.* 29, 2055–2076. doi: 10.1111/j.1365-3040.2006.01580.x

Galili, G., Amir, R., and Fernie, A. R. (2016). The regulation of essential amino acid synthesis and accumulation in plants. *Annu. Rev. Plant Biol.* 67, 153–178. doi: 10.1146/annurev-arplant-043015-112213

Geiger, M., Haake, V., Ludewig, F., Sonnewald, U., and Stitt, M. (1999). The nitrate and ammonium nitrate supply have a major influence on the response of photosynthesis, carbon metabolism, nitrogen metabolism and growth to elevated carbon dioxide in tobacco. *Plant Cell Environ.* 22, 1177–1199. doi: 10.1046/j.1365-3040.1999.00466.x

Geiger, M., Walch-Liu, P., Engels, C., Harnecker, J., Schulze, E. D., Ludewig, F., et al. (1998). Enhanced carbon dioxide leads to a modified diurnal rhythm of nitrate reductase activity in older plants, and a large stimulation of nitrate reductase activity and higher levels of amino acids in young tobacco plants. *Plant Cell Environ.* 21, 253–268. doi: 10.1046/j.1365-3040.1998.00277.x

Gessler, A., Ferrio, J. P., Hommel, R., Treydte, K., Werner, R. A., and Monson, R. K. (2014). Stable isotopes in tree rings: towards a mechanistic understanding of isotope fractionation and mixing processes from the leaves to the wood. *Tree Physiol.* 34, 796–818. doi: 10.1093/treephys/tpu040

Gonzalez-Dugo, V., Durand, J. L., and Gastal, F. (2010). Water deficit and nitrogen nutrition of crops. *Rev. Agron. Sustain. Dev.* 30, 529–544. doi: 10.1051/agro/2009059

Hawkesford, M., Horst, W., Kichey, T., Lambers, H., Schjoerring, J., Møller, I. S., et al. (2012). "Functions of macronutrients," in *Marschner's Mineral Nutrition of Higher Plants, 3rd Edn*, ed P. Marschner (San Diego,CA: Academic Press), 135-189.

Hepworth, C., Doheny-Adams, T., Hunt, L., Cameron, D. D., and Gray, J. E. (2015). Manipulating stomatal density enhances drought tolerance without deleterious effect on nutrient uptake. *New Phytol.* 208, 336–341. doi: 10.1111/nph.13598

Hirel, B., Le Gouis, J., Ney, B., and Gallais, A. (2007). The challenge of improving nitrogen use efficiency in crop plants: towards a more central role for genetic variability and quantitative genetics within integrated approaches. *J. Exp. Bot.* 58, 2369–2387. doi: 10.1093/jxb/erm097

Jablonski, L. M., Wang, X., and Curtis, P. S. (2002). *Rapid report.* Plant reproduction under elevated CO_2 conditions: a meta-analysis of reports on 79 crop and wild species. *New Phytol.* 156, 9–26. doi: 10.1046/j.1469-8137.2002.00494.x

Krapp, A., Berthomeo, R., Orsel, M., Mercey-Boutet, S., Yu, A., Castaings, L., et al. (2011). *Arabidopsis* roots and shoots show distinct temporal adaptation patterns toward nitrogen starvation. *Plant Physiol.* 157, 1255–1282. doi: 10.1104/pp.111.179838

Li, C. C. (1975). *Path Analysis. A Primer*. Pacific Grove, CA: The Boxwood Press.

Lindoo, S. J., and Caldwell, M. M. (1978). Ultraviolet-B radiation-induced inhibition of leaf expansion and promotion of anthocyanin production. *Plant Physiol.* 61, 278–282. doi: 10.1104/pp.61.2.278

Long, S. P., Ainsworth, E. A., Rogers, A., and Ort, D. R. (2004). Rising atmospheric carbon dioxide: plants FACE the future. *Annu. Rev. Plant Biol.* 55, 591–628. doi: 10.1146/annurev.arplant.55.031903.141610

López-Marín, J., Gálvez, A., del Amor, F. M., Albacete, A., Fernández, J. A., Egea-Gilabert, C., et al. (2017). Selecting vegetative/generative/dwarfing rootstocks for improving fruit yield and quality in water stressed sweet peppers. *Sci. Hortic.* 214, 9–17. doi: 10.1016/j.scienta.2016.11.012

Manetas, Y. (2006). Why some leaves are anthocyanic and why most anthocyanic leaves are red? *Flora* 201, 163–177. doi: 10.1016/j.flora.2005.06.010

McDonald, E. P., Erickson, J. E., and Kruger, E. L. (2002). Research note: can decreased transpiration limit plant nitrogen acquisition in elevated CO_2? *Funct. Plant Biol.* 29, 1115–1120. doi: 10.1071/FP02007

McMurtrie, R. E., Norby, R. J., Medlyn, B. E., Dewar, R. C., Pepper, D. A., Reich, P. B., et al. (2008). Why is plant-growth response to elevated CO_2 amplified when water is limiting, but reduced when nitrogen is limiting? A growth-optimisation hypothesis. *Funct. Plant Biol.* 35, 521–534. doi: 10.1071/FP08128

Medina, S., Vicente, R., Amador, A., and Araus, J. L. (2016). Interactive effects of elevated [CO_2] and water stress on physiological traits and gene expression during vegetative growth in four Durum Wheat genotypes. *Front. Plant Sci.* 7:1738. doi: 10.3389/fpls.2016.01738

Medlyn, B. E., Barton, C. V. M., Broadmeadow, M. S. J., Ceulemans, R., De Angelis, P., Forstreuter, M., et al. (2001). Stomatal conductance of forest species after long-term exposure to elevated CO_2 concentration: a synthesis. *New Phytol.* 149, 247–264. doi: 10.1046/j.1469-8137.2001.00028.x

Mirecki, R. M., and Teramura, A. H. (1984). Effects of ultraviolet-B irradiance on soybean.V. The dependence of plant sensitivity on the photosynthetic photon flux density during and after leaf expansion. *Plant Physiol.* 74, 478–480. doi: 10.1104/pp.74.3.475

Morison, J. I. L. (1998). Stomatal response to increased CO_2 concentration. *J. Exp. Bot.* 49, 443–452. doi: 10.1093/jxb/49.Special_Issue.443

Munjonji, L., Ayisi, K. K., Vandewalle, B., Haesaert, G., and Boeck, P. (2016). Combining carbon-13 and oxygen-18 to unravel triticale grain yield and physiological response to water stress. *Field Crops Res.* 195, 36–49. doi: 10.1016/j.fcr.2016.06.001

Noguchi, K., Watanabe, C. K., and Terashima, I. (2015). Effects of elevated atmospheric CO_2 on primary metabolite levels in *Arabidopsis thaliana* Col-0 leaves: an examination of metabolome data. *Plant Cell Physiol.* 56, 2069–2078. doi: 10.1093/pcp/pcv125

Oberbauer, S. F., Strain, B. R., and Fetcher, N. (1985). Effect of CO_2-enrichment on seedling physiology and growth of two tropical tree species. *Physiol. Plant.* 65, 352–356. doi: 10.1111/j.1399-3054.1985.tb08658.x

O'Leary, G. J., Christy, B., Nuttall, J., Huth, N., Cammarano, D., Stöckle, C., et al. (2015). Response of wheat growth, grain yield and water use to elevated CO_2 under a Free-Air CO_2 Enrichment (FACE) experiment and modelling in a semi-arid environment. *Glob. Chang. Biol.* 21, 2670–2686. doi: 10.1111/gcb.12830

Pande, P., Datta, P., Bhattacharya, S., and Tyagi, S. (1995). Post-anthesis metabolic-enrichment of $H2^{18}O$ in wheat grain. *Indian J. Exp. Biol.* 33, 394–396.

Pearson, J., Clough, E. C. M., Woodall, J., Havill, D. C., and Zhang, X. H. (1998). Ammonia emissions to the atmosphere from leaves of wild plants and *Hordeum vulgare* treated with methionine sulphoximine. *New Phytol.* 138, 37–48. doi: 10.1046/j.1469-8137.1998.00880.x

Peñuelas, J., Biel, C., and Estiarte, M. (1995). Growth, biomass allocation, and phenology responses of pepper to elevated CO_2 concentrations and different water and nitrogen supply. *Photosynthetica* 31, 91–99.

Pérez-Jiménez, M., Pazos-Navarro, M., Piñero, M. C., Otálora-Alcón, G., López-Marín, J., and del Amor, F. M. (2016). Regulation of the drought response of sweet pepper (*Capsicum annuum* L.) by foliar-applied hormones, in Mediterranean-climate greenhouse conditions. *Plant Growth Reg.* 80, 159–169. doi: 10.1007/s10725-016-0153-3

Piñero, M. C., Pérez-Jiménez, M., López-Marín, J., and del Amor, F. M. (2016). Changes in the salinity tolerance of sweet pepper plants as affected by nitrogen form and high CO_2 concentration. *J. Plant Physiol.* 200, 18–27. doi: 10.1016/j.jplph.2016.05.020

Raimanová, I., and Haberle, J. (2010). The effects of differentiated water supply after anthesis and nitrogen fertilization on $\delta^{15}N$ of wheat grain. *Rapid Commun. Mass Spectrom.* 24, 261–266. doi: 10.1002/rcm.4382

Rebetzke, G. J., Condon, A. G., Richards, R. A., and Farquhar, G. D. (2002). Selection for reduced carbon isotope discrimination increases aerial biomass and grain yield of rainfed bread wheat. *Crop Sci.* 42, 739–745. doi: 10.2135/cropsci2002.0739

Robinson, D., Handley, L. L., Scrimgeour, C. M., Gordon, C., Forster, B. P., and Ellis, R. P. (2000). Using stable isotope natural abundances ($\delta^{15}N$ and $\delta^{13}C$) to integrate the stress responses of wild barley (*Hordeum spontaneum* C Koch.) genotypes. *J. Exp. Bot.* 51, 41–50. doi: 10.1093/jexbot/51.342.41

Roden, J. S., and Ehleringer, J. R. (1999). Observations of hydrogen and oxygen isotopes in leaf water confirm the Craig-Gordon model under wide-ranging environmental conditions. *Plant Physiol.* 120, 1165–1173. doi: 10.1104/pp.120.4.1165

Sánchez-Bragado, R., Araus, J. L., Scheerer, U., Cairns, J. E., Rennenberg, H., and Ferrio, J. P. (2016). Factors preventing the performance of oxygen isotope ratios as indicators of grain yield in maize. *Planta* 243, 355–368. doi: 10.1007/s00425-015-2411-4

Scheidegger, Y., Saurer, M., Bahn, M., and Siegwolf, R. (2000). Linking stable oxygen and carbon isotopes with stomatal conductance and photosynthetic capacity: a conceptual model. *Oecologia* 125, 350–357. doi: 10.1007/s004420000466

Schubert, B. A., and Jahren, A. H. (2012). The effect of atmospheric CO_2 concentration on carbon isotope fractionation in C_3 land plants. *Geochim. Cosmochim. Acta* 96, 29–43. doi: 10.1016/j.gca.2012.08.003

Shangguan, Z. P., Shao, M. A., and Dyckmans, J. (2000). Nitrogen nutrition and water stress effects on leaf photosynthetic gas exchange and water use efficiency in winter wheat. *Environ. Exp. Bot.* 44, 141–149. doi: 10.1016/S0098-8472(00)00064-2

Shannon, P., Markiel, A., Ozier, O., Baliga, N. S., Wang, J. T., Ramage, D., et al. (2003). Cytoscape: a software environment for integrated models of biomolecular interaction networks. *Genome Res.* 13, 2498–2504. doi: 10.1101/gr.1239303

Sheshshayee, M. S., Bindumadhava, H., Ramesh, R., Prasad, T. G., Lakshminarayana, M. R., and Udayakumar, M. (2005). Oxygen isotope enrichment (Delta O-18) as a measure of time averaged transpiration rate. *J. Exp. Bot.* 56, 3033–3039. doi: 10.1093/jxb/eri300

Stitt, M., and Krapp, A. (1999). The interaction between elevated carbon dioxide and nitrogen nutrition: the physiological and molecular background. *Plant Cell Environ.* 22, 583–621. doi: 10.1046/j.1365-3040.1999.00386.x

Sulpice, R., Nikoloski, Z., Tschoep, H., Antonio, C., Kleessen, S., Larhlimi, A., et al. (2013). Impact of the carbon and nitrogen supply on relationships and connectivity between metabolism and biomass in a broad panel of Arabidopsis accessions. *Plant Physiol.* 162, 347–363. doi: 10.1104/pp.112.210104

Takatani, N., Ito, T., Kiba, T., Mori, M., Miyamoto, T., Maeda, S., et al. (2014). Effects of high CO_2 on growth and metabolism of Arabidopsis seedlings during growth with a constantly limited supply of nitrogen. *Plant Cell Physiol.* 55, 281–292. doi: 10.1093/pcp/pct186

Tcherkez, G. (2010). Natural $^{15}N/^{14}N$ isotope composition in C^3 leaves: are enzymatic isotope effects informative for predicting the ^{15}N- abundance in key metabolites? *Funct. Plant Biol.* 38, 1–12. doi: 10.1071/FP10091

Tcherkez, G., and Hodges, M. (2008). Special issue opinion paper. How stable isotopes may help to elucidate primary nitrogen metabolism and its interaction with (photo)respiration in C^3 leaves. *J. Exp. Bot.* 59, 1685–1693. doi: 10.1093/jxb/erm115

Turner, N. C. (1988). Measurement of plant water status by the pressure chamber technique. *Irrigation Sci.* 9, 289–308.

Tzin, V., and Galili, G. (2010). New insights into the shikimate and aromatic amino acids biosynthesis pathways in plants. *Mol. Plant* 3, 956–972. doi: 10.1093/mp/ssq048

Vicente, R., Martínez-Carrasco, R., Pérez, P., and Morcuende, R. (2016a). An association network reveals co-regulation of carbon and nitrogen metabolism-related parameters in durum wheat grown under different environmental conditions. *New Biotechnol.* 33:414. doi: 10.1016/j.nbt.2015.10.079

Vicente, R., Pérez, P., Martínez-Carrasco, R., Feil, R., Lunn, J. E., Watanabe, M., et al. (2016b). Metabolic and transcriptional analysis of durum wheat responses to elevated CO_2 at low and high nitrate supply. *Plant Cell Physiol.* 57, 2133–2146. doi: 10.1093/pcp/pcw131

Vicente, R., Pérez, P., Martínez-Carrasco, R., Usadel, B., Kostadinova, S., and Morcuende, R. (2015). Quantitative RT-PCR platform to measure transcript levels of C and N metabolism-related genes in durum wheat: transcript profiles in elevated [CO_2] and high temperature at different nitrogen supplies. *Plant Cell Physiol.* 56, 1556–1573. doi: 10.1093/pcp/pcv079

Werner, R. A., and Schmidt, H. L. (2002). The *in vivo* nitrogen isotope discrimination among organic plant compounds. *Phytochemistry* 61, 465–484. doi: 10.1016/S0031-9422(02)00204-2

Wullschleger, S. D., and Oosterhuis, D. M. (1991). Osmotic adjustment and the growth response of seven vegetable crops following water-deficit stress. *Horstscience* 26, 1210–1212.

Xu, Z., Jiang, Y., Jia, B., and Zhou, G. (2016). Elevated-CO_2 response of stomata and its dependence on environmental factors. *Front. Plant Sci.* 7:657. doi: 10.3389/fpls.2016.00657

Xu, Z., Shimizu, H., Ito, S., Yagasaki, Y., Zou, C., Zhou, G., et al. (2014). Effects of elevated CO_2, warming and precipitation change on plant growth, photosynthesis and peroxidation in dominant species from North China grassland. *Planta* 239, 421–435. doi: 10.1007/s00425-013-1987-9

Yousfi, S., Serret, M. D., and Araus, J. L. (2009). Shoot $\delta^{15}N$ gives a better reflection than ion concentration or $\Delta^{13}C$ of genotypic differences in the response of durum wheat to salinity. *Funct. Plant Biol.* 36, 144–155. doi: 10.1071/FP08135

Yousfi, S., Serret, M. D., Márquez, A. J., Voltas, J., and Araus, J. L. (2012). Combined use of $\delta^{13}C$, $\delta^{18}O$ and $\delta^{15}N$ tracks nitrogen metabolism and genotypic adaptation of durum wheat to salinity and water deficit. *New Phytol.* 194, 230–244. doi: 10.1111/j.1469-8137.2011.04036.x

Yu, J., and Woo, K. C. (1991). Correlation between the development of photorespiration and the change in activities of NH_3 assimilation enzymes in greening oat leaves. *Aust. J. Plant Physiol.* 18, 583–588.

Yu, J., Du, H., Xu, M., and Huang, B. (2012). Metabolic responses to heat stress under elevated atmospheric CO_2 concentration in a cool-season grass species. *J. Am. Soc. Hortic. Sci.* 137, 221–228. Available online at: http://journal.ashspublications.org/content/137/4/221.abstract

Zhou, Z., Zhi, T., Liu, Y., Chen, Y., and Ren, C. (2014). Tyrosine induces anthocyanin biosynthesis in *Arabidopsis thaliana*. *Am. J. Plant Sci.* 5, 328–331. doi: 10.4236/ajps.2014.53045

Conflict of Interest Statement: The authors declare that the research was conducted in the absence of any commercial or financial relationships that could be construed as a potential conflict of interest.

frontiers in Plant Science

ORIGINAL RESEARCH
published: 01 May 2018
doi: 10.3389/fpls.2018.00563

Optimizing Winter Wheat Resilience to Climate Change in Rain Fed Crop Systems of Turkey and Iran

Marta S. Lopes[1], Conxita Royo[2], Fanny Alvaro[2], Miguel Sanchez-Garcia[3], Emel Ozer[4], Fatih Ozdemir[4], Mehmet Karaman[5], Mozaffar Roustaii[6], Mohammad R. Jalal-Kamali[7] and Diego Pequeno[8]*

[1] The International Maize and Wheat Improvement Center (CIMMYT), Ankara, Turkey, [2] Sustainable Field Crops Program, Institute for Food and Agricultural Research and Technology (IRTA), Lleida, Spain, [3] International Centre for Agricultural Research in Dry Areas, Rabat, Morocco, [4] Bahri Dagdas International Agricultural Research Institute, Konya, Turkey, [5] GAP Uluslararası Tarımsal Araştırma Ve Eğitim Merkezi Müdürlüğü (GAPUTAEM), Diyarbakir, Turkey, [6] Dryland Agricultural Research Institute (DARI), AREEO, Maragheh, Iran, [7] Global Wheat Program, The International Maize and Wheat Improvement Center (CIMMYT), Seed and Plant Improvement Institute Campus, Karaj, Iran, [8] Socioeconomics Program, The International Maize and Wheat Improvement Center (CIMMYT), Texcoco, Mexico

OPEN ACCESS

Edited by:
Hui Xia,
Shanghai Agrobiological Gene Center, China

Reviewed by:
Robert John French, Department of Primary Industries and Regional Development of Western Australia (DPIRD), Australia
José Luis Araus, Universitat de Barcelona, Spain

***Correspondence:**
Marta S. Lopes
m.dasilva@cgiar.org

Specialty section:
This article was submitted to Plant Breeding, a section of the journal Frontiers in Plant Science

Received: *23 November 2017*
Accepted: *10 April 2018*
Published: *01 May 2018*

Citation:
Lopes MS, Royo C, Alvaro F, Sanchez-Garcia M, Ozer E, Ozdemir F, Karaman M, Roustaii M, Jalal-Kamali MR and Pequeno D (2018) Optimizing Winter Wheat Resilience to Climate Change in Rain Fed Crop Systems of Turkey and Iran. Front. Plant Sci. 9:563. doi: 10.3389/fpls.2018.00563

Erratic weather patterns associated with increased temperatures and decreasing rainfall pose unique challenges for wheat breeders playing a key part in the fight to ensure global food security. Within rain fed winter wheat areas of Turkey and Iran, unusual weather patterns may prevent attaining maximum potential increases in winter wheat genetic gains. This is primarily related to the fact that the yield ranking of tested genotypes may change from one year to the next. Changing weather patterns may interfere with the decisions breeders make about the ideotype(s) they should aim for during selection. To inform breeding decisions, this study aimed to optimize major traits by modeling different combinations of environments (locations and years) and by defining a probabilistic range of trait variations [phenology and plant height (PH)] that maximized grain yields (GYs; one wheat line with optimal heading and height is suggested for use as a testing line to aid selection calibration decisions). Research revealed that optimal phenology was highly related to the temperature and to rainfall at which winter wheat genotypes were exposed around heading time (20 days before and after heading). Specifically, later winter wheat genotypes were exposed to higher temperatures both before and after heading, increased rainfall at the vegetative stage, and reduced rainfall during grain filling compared to early genotypes. These variations in exposure to weather conditions resulted in shorter grain filling duration and lower GYs in long-duration genotypes. This research tested if diversity within species may increase resilience to erratic weather patterns. For the study, calculated production of a selection of five high yielding genotypes (if grown in five plots) was tested against monoculture (if only a single genotype grown in the same area) and revealed that a set of diverse genotypes with different phenologies and PHs was not beneficial. New strategies of progeny selection are discussed: narrow range of variation for phenology in families may facilitate the discovery and selection of new drought-resistant and avoidant wheat lines targeting specific locations.

Keywords: heading, low rainfall, reproductive stage, vegetative stage, within species diversity

INTRODUCTION

Water shortage (drought) and extremes in temperature (cold and heat) are common abiotic stresses worldwide (e.g., Zampieri et al., 2017). Although the wheat breeding and research community focuses on developing high yielding varieties with improved adaptation to drought and heat, annual genetic gains during the last three decades have been poor in low yielding environments (around 0.5% year, see, e.g., Lopes et al., 2012 and more recently quantified in heat stressed environments in Crespo-Herrera et al., 2017). The small amount of progress achieved to improve heat and drought adaptation and resistance is at least partially related to methodological obstacles such as: (i) the confounding effects caused by phenology (or crop stage at which the crop experiences the stress) when evaluating a diverse set of wheat genotypes and (ii) the erratic nature of weather (rainfall and temperature vary importantly from year to year). One good example of the first obstacle is that cereal genotypes of short duration will yield more than long-duration genotypes when grown under terminal drought conditions (also known as drought escape mechanism; Fischer and Wood, 1979; Mitchell et al., 1996; Lopes et al., 2014). Meiosis, the most stress sensitive stage of reproduction in wheat (Saini and Westgate, 1999) generally coincides with the booting stage (Zadoks et al., 1974) and escape of exposure to drought and heat at this stage is crucial for survival and grain set. Additionally, early flowering is an evolutionary mechanism for adaptation to warm and drought environments (Royo et al., 2014). Blum (2009) citing Mitchell et al. (1996) explained that short-term growth duration dictates moderate water-use and the escape of terminal drought stress, whereas long-duration genotypes generally have greater water use and larger deep root systems that allow deep soil moisture extraction – if indeed deep soil moisture is available. Therefore, exposure of genotypes with long and short duration to drought or heat conditions at the same developmental stage would likely reveal different effects on grain yield (GY). While the literature indicates several explanations for the better performance of short duration genotypes, exposure of these genotypes to weather variables in comparison to late duration genotypes has not been determined.

Fischer and Wood (1979) and Mitchell et al. (1996) have suggested reducing the confounding effect of phenology to explore other mechanisms of drought avoidance and tolerance. Despite these early efforts, looking at the literature, a very large number of published research studies (e.g., Araki et al., 1999; Kirigwi et al., 2007; Kuchel et al., 2007; Honsdorf et al., 2014) related to responses to drought or heat (both phenotyping and genetics) completely ignored the effect of phenology that Fischer took into consideration in his early work to improve screening methodologies for drought adaptation (Fischer and Maurer, 1978). This oversight is unfortunate and at least partially hampers our progress to increase GYs under low rainfall and warm environments. Fortunately, there have been a few significant efforts to remove the confounding effects of phenology in various wheat populations for gene discovery at the International Maize and Wheat Improvement Center (CIMMYT; Olivares-Villegas et al., 2007; Pinto et al., 2010; Lopes et al., 2013, 2015). The removal of confounding effects of phenology must be fully encouraged when developing new populations for gene discovery or other purposes related to studies of drought or heat adaptation (the evident exception would be for populations developed for the discovery of new phenology genes or related studies). In a scenario of increased temperatures in dry areas, as projected in the last IPCC report (available at: http://www.ipcc.ch/ipccreports/tar/wg2/index.php?idp=378), these considerations become even more relevant due to the increased difficulty of breeding for a combination of stresses.

Some researchers have proposed that synchronizing growth duration with the expected or predicted seasonal moisture supply takes place as the first and foremost step in breeding for water-limited environments (Blum, 2009). Although this categorization is simple, the types of rainfall patterns found in many parts of the world are becoming more erratic which makes it difficult to define the synchronization that best suits a particular environment and a specific year. Therefore, this study aims to find the most probable optimal synchronization for low rainfall winter wheat areas across years and locations. By extension, this research also aims to determine optimal plant height (PH) for this region, since height together with heading are probably the highest contributors to improved GY when not optimized and fixed by breeders (e.g., Lopes et al., 2014). For PH, both positive and negative correlations with GY have been reported depending on environmental factors. In high yielding environments (either with high rainfall or irrigated), tall genotypes will lodge and will have a GY penalty. However, in low yielding environments where PH may decrease as a response to water stress and high temperatures, increased PH (up to a certain limit) is important for creating a source of biomass and assimilates to feed grains and increase GYs (Lopes et al., 2014). Moreover, PH is not just a positive trait in terms of securing pre-anthesis reserves to filling grain but may also confer a proper pre-anthesis canopy architecture optimizing radiation interception (Miralles and Slafer, 1997).

One possible way to ensure increased plasticity to erratic weather conditions would be by planting several genotypes with various flowering times and PHs. Hypothetically, this variation would have the potential to increase resilience of the crop across years and to increase GYs. Crop variety mixtures, in which several genotypes are sown together in the same field, have been proposed as a mechanism for increasing yield stability in situations of environmental biotic and abiotic stress (Wolfe, 2000; Zhu et al., 2000; Creissen et al., 2016). This approach has proven efficiency against crop diseases (Zhu et al., 2000) and it is expected that compensation processes will also increase crop performance under low rainfall environments; however, this needs assessment.

In this context, particularly for the winter wheat rain fed areas of Turkey and Iran, a series of trials were conducted across several locations with the following objectives: (i) evaluate the contribution of cycle length to heading and PH to improve GY in rain fed winter wheat grown in low rainfall regions of both countries; (ii) explain the drought escape mechanisms

in the region using environmental variables measured at key developmental stages; (iii) bridge environmental variables at key developmental stages with height and GY; (iv) define optimal phenology and PH and develop new strategies to facilitate the discovery of germplasm with adaptation and resistance to water shortage; and (v) test total production of a diverse and a mono-varietal crop setup.

MATERIALS AND METHODS

Plant Material

One wheat population containing 250 modern wheat varieties and breeding lines (named here genotypes) from the CIMMYT International Winter Wheat Improvement Program (IWWIP) was assembled from international nurseries distributed every year (released from the early 1990s to 2011).

Experimental Design and Environments

Field experiments were conducted at three locations (Konya, Turkey; Diyarbakir, Turkey; and Maragheh, Iran) during four growth cycles (2012–2013, 2013–2014, 2014–2015, and 2015–2016) using an alpha lattice design with two replications. In Diyarbakir, trials were conducted at the International Agricultural Research and Training Center (GAPUTAEM), with Xerosols (Calcic Xerosols) and sown on November 20,' 2012 and January 24,' 2015. In Konya, trials were sown at the Bahri Dagdas International Agricultural Research Institute with Xerosols (Calcic Xerosols) on October 31,' 2012, October 24,' 2013, and October 20,' 2014. In Maragheh, trials were established at the Dryland Agricultural Research Institute (DARI) with Xerosols (Haplic Xerosols) on October 12,' 2012, October 10,' 2013, and October 12, 2015 for growth cycles in 2012–2013, 2013–2014, and 2015–2016, respectively. Plot size was 1.5 m long with three rows and approximately 200 seeds per m^{-2} in 2012–2013 and 4 m long with six rows at the same seed density, for the remaining years in all locations.

Phenotypic Trait Evaluation

Grain yield was determined by manually harvesting the middle row of each plot in 2012–2013 and by mechanically harvesting the entire plot in 2013–2014, 2014–2015, and 2015–2016. For the manual harvest, each middle row containing straw and grain was weighed and threshed. Days to heading (DH) were determined as the number of days from the sowing date until the point when more than 50% of plants were displaying heads (Zadoks Stage 59, Zadoks et al., 1974). Days to physiological maturity (DM) were measured as the time when 50% of the spikes in a plot showed a total loss of green color, corresponding to Zadoks stage 89 (Zadoks et al., 1974). PH was determined by measuring the distance from the base of the stem to the top of the spike, excluding awns.

Statistical Analysis and Calculations

Analysis of variance was conducted for each year and combined years using an alpha lattice design, where genotype was considered as a fixed effect and the effect of block nested within replicate was considered as a random effect, with the PROC GLM of SAS statistical package (Sas Institute Inc., 2009). Broad-sense heritability (H^2) was estimated for each trait individually to determine their reproducibility across years and within each field trial (by removing the year variance component) as: $H^2 = Vg/[Vg + (Vge/e) + (V/re)]$, where r = number of replications, e = number of locations/years, V = error variance, Vg = genotypic variance, and Vge = genotype by locations/years interaction variance. To better understand the dependence and tradeoffs among agronomic traits and their mechanisms of operation in different wheat populations, Pearson correlation coefficients on the estimated means and associated probabilities were determined with the PROC CORR from SAS (Sas Institute Inc., 2009).

To determine the range of DH and PH where GY is maximized, all genotypes were grouped into seven categories based on DH grand means across locations and years: for DH very early (1, with average 192 days), early (2, with average 194 days), early medium (3, with average 195 days), medium (4, with average 196 days), medium late (5, with average 197 days), and late (6, with average 198 days), very late (7, with average 200 days); and for PH very short (1, with average 66 cm), short (2, with average 70 cm), short medium (3, with average 73 cm), medium (4, with average 75 cm), medium tall (5, with average 77 cm), tall (6, with average 82 cm), and very tall (7, with average 89 cm). Twenty random sets of 10 genotypes (for each set, different combinations of genotypes were randomly selected out from the 250 genotypes) were assembled for each DH and PH category. Average GY in each one of the seven phenology and height categories (average of 10 genotypes in each category) was determined for all the sets and non-linear regression equations relating GY to DH and PH were fitted using Microsoft Excel (2013). The DH and PH at which GY was maximum (optima DH and PH) were calculated as $x = -b/2a$ from the quadratic functions $y = ax^2+bx+c$.

To determine the effects of temperature at one of the most sensitive stages to abiotic stresses (around heading), the average mean (TA), maximum (TM), and minimum daily temperature (Tm) were calculated 20 days before (TA20BH, TM20BH, and Tm20BH) and after heading (TA20AH, TM20AH, and Tm20AH) for each genotype. Given the stress sensitivity of booting stage, the effect of temperature and rainfall at this developmental stage has a considerable impact on final GY. Moreover, booting stage and meiosis occur at different points in time for wheat genotypes differing in phenology, and the exact moment of that stage is difficult to assess in the field, particularly when several hundred wheat genotypes need to be evaluated. To predict approximate temperature during this sensitive period, average temperatures during the 20-day period before and after heading were calculated for each genotype in each location and year. To calculate the amount of rainfall before and after heading instead of the 20-day period, the entire vegetative (between sowing and heading, R_{VEG}) and grain filling (between heading and maturity, R_{GF}) stages were used (as shown in Araus et al., 2002). This calculation was related to the erratic patterns of rain in all locations and years where rain following just before or after the 20-day period is still available to the crop, but would

not be included if calculated based on this short period. The total amount of rainfall (from sowing to maturity, *Rt*) was also calculated.

Finally, the hypothesis that growing several wheat genotypes may contribute to increase resilience of GY in environments with erratic weather patterns was tested. To do so, calculation of grain production of five wheat genotypes was compared to production of one single genotype or "mega-variety." For this exercise, three sets of data were used: 250 modern winter wheat varieties and breeding lines described above and data generated from international nurseries distributed worldwide by CIMMYT, the 23rd ESWYT (Elite Selection Wheat Yield Trials), and the 21st SAWYT (Semi-Arid Wheat Yield Trial). The data can be found at: https://www.cimmyt.org/international-wheat-improvement-network-iwin/. First, environments were named "training environments" if used for selection of genotypes based on mean GY and "testing environments" if used to test performance of genotypes previously selected in the "training environments." Then, one or five genotypes with the highest mean yield over six "training environments" were tested for their performance in two other random environments or "testing environments." In total, 28 combinations of environments were developed using six random "training environments" and two "testing environments." For each combination, total production of different selections was calculated: (i) total grain production of one genotype grown in two "testing environments" (total of 20 ha), and previously showing the highest mean yield, in six "training environments" (or "mega-variety"); (ii) total grain production of five genotypes grown in two "testing environments" (total of 20 ha) previously showing the top five highest mean yields in six "training environments"; and (iii) total grain production of the genotype showing the highest mean yield in all eight environments in a total of 20 ha.

The total grain production resulting from growing one genotype in *e* "testing environments" (*TiGP*) was calculated by multiplying GY in the *i*th environment (*iGY*) in gm^{-2} to total production in tonnes in 10 ha by multiplying by 0.1 (100,000 m^2 divided by 1,000,000 g) and summing grain production of that particular genotype in *e* "testing environments," as indicated in the equation below.

$$TiGP = \sum_{i=1}^{e2} (0.1 * iGY)$$

The total grain production resulting from growing five genotypes in "testing environments" (*TiiGP*) was calculated as the sum grain production of each of the five genotypes in 2 ha (corresponding to five genotypes in 10 ha). The grain production of the *i*th genotype was calculated by multiplying GY of the *i*th genotype (*iGY*) in gm^{-2} to total production in tonnes in 2 ha by multiplying by 0.02 (20,000 m^2 and divided by 1,000,000 g) and summing grain production for the five genotypes, as indicated in the equation below.

$$TiiGP = \sum_{i=1}^{5} (0.02 * iGY)$$

Finally, *TiiGP* resulting from each of the *e* "testing environments" were summed together to obtain total production of five genotypes in 10 ha and in *e* environments. Analysis of variance was conducted with all 28 combinations (treating combinations as replicates) to determine if differences between production of one genotype or five genotypes were significant.

The same exercise was carried out in two other sets of data from the 23rd ESWYT (grown in 64 environments, 32 were used as "training environments" and other 32 used as "testing environments") and 21st SAWYT (grown in 66 environments, 33 were used as "training environments" and other 33 used as "testing environments"). For these two sets of data, a sample of 10 random combinations of "training" and "testing environments" was used and the number of environments in equation *TiGP* was increased to 32 (total of 320 ha) and 33 (total of 330 ha) for the 23rd ESWYT and 21st SAWYT, respectively.

RESULTS

Characterization of Environmental Conditions of Field Trials

Meteorological data of all trials conducted in Turkey and Iran are shown in **Table 1**. Environments where trials were conducted have shown typical conditions of winter wheat low-moderate rainfall environments (mega-environment 12, Braun et al., 2010). Experiments in Diyarbakir showed the highest minimum, maximum, and average temperatures and total rainfall (**Table 1**). These environments were also the most productive. Similar temperatures were observed in Konya and Maragheh throughout all seasons, although Konya tended to be warmer with slightly higher average and maximum temperatures (**Table 1**). Overall, Tm and Rainfall significantly explain variations in GY across locations and years (R^2 of 65 and 62%, respectively, when regressing Tm and Rainfall with GY in all eight environments using data in **Table 1**).

In more detail, **Supplementary Figures S1A–H** show the window of variation for heading date and maturity in each location and year tested for this study together with daily rainfall and temperature. Overall, these environments are characterized by cold winters, progressively higher temperatures, and a decrease in rainfall at around heading time continuing to maturity (**Supplementary Figures S1A–H**). In all trials (locations and years), heading of all genotypes occurred when temperatures were rising (**Supplementary Figures S1A–H**). On a daily basis, rainfall patterns were erratic across locations and years (**Supplementary Figures S1A–H**). However, overall, the amount of rainfall at the grain filling stage (R_{GF}) was on average (across locations and years) around 12% of the amount falling at the vegetative stage (**Table 2**).

Contributions of DH and PH to Grain Yield in Turkey and Iran

Since one of the main objectives of this study is to determine optimal DH and PH to maximize GY, correlations between these two traits were calculated per trial (**Table 1**). Significant

negative correlations between DH and GY were reported in Diyarbakir 2013, Konya 2013, Maragheh 2014, Diyarbakir 2015, and Maragheh 2016 (**Table 1**). Correlations (linear associations) between GY and DH in other trials were not significant (**Table 1**). PH correlated positively with GY (and statistically significant) in Konya 2013, Maragheh 2013, Konya 2014, Maragheh 2014, and Konya 2015, being those also the environments with lower rainfall (**Table 1**). Correlations between GY and PH in other trials were not significant (**Table 1**). Using the means of each genotype across locations and years, DH and PH correlated negatively with GY ($r = -0.40$ and $r = -0.15$; **Table 3**).

Characterization of Temperature 20 Days Before and After Heading and Rainfall at the Vegetative and Grain Filling Stages

Average, maximum, and minimum temperatures during the 20-day period before and after heading (TA20BH, TA20AH,

TABLE 1 | Meteorological data of the field trials conducted in Konya and Diyarbakir (Turkey) and Maragheh (Iran) between 2012 and 2016.

LOC	Harvest Year	ENV#	Tm °C	TA °C	TM °C	TMO	Rain mm	GY (g m^{-2})	DH (days)	CORR GY-DH	CORR GY-PH
Diyarbakir	2013	1	8.1	12.5	17.2	41.8	578	384	154	**−0.37*** **	−0.09, NS
Konya		2	4.3	10.8	17.0	34.9	254	339	191	**−0.34*** **	**0.15** **
Maragheh		3	3.5	8.2	12.8	34	282	180	228	0.03, NS	**0.14***
Konya	2014	4	2.3	9.5	16.3	37	225	136	205	0.05, NS	**0.50*** **
Maragheh		5	2.3	7.2	12.2	35	209	223	234	**−0.37*** **	**0.27*** **
Diyarbakir	2015	6	7.3	13.8	20.3	43.4	556	415	113	**−0.47*** **	0.10, NS
Konya		7	2.5	8.4	14.7	33.3	288	295	214	0.01, NS	**0.29*** **
Maragheh	2016	8	3.5	8.3	13.2	35.5	338	287	227	**−0.22*** **	−0.03, NS

*Average minimum temperature (Tm), average mean temperature (TA), average maximum temperature (TM), maximum temperature observed (TMO), rainfall (Rain) from sowing to physiological maturity, average grain yield (GY), and cycle length to heading (DH) are presented. Pearson correlation coefficients between GY and DH (CORR GY-DH) and between GY and PH (CORR GY-PH) are shown for each trial. ***, significant at $p < 0.0005$; **, significant at $p < 0.005$; *, significant at $p < 0.05$; NS, non-significant. Significant correlations are shown in bold values.*

TABLE 2 | Basic statistics [heritability (H^2), standard error of mean (SEM), standard error of difference (SED), least significant difference (LSD), average (avg), maximum (max), and minimum (min)] of agronomic and weather traits measured in a winter wheat population (250 varieties and breeding lines) grown in eight trials between 2012 and 2016 in Turkey and Iran.

	DH	DM	GFD	GY	PH	TA_{20BH}	TA_{20AH}	TM_{20BH}	TM_{20AH}	Tm_{20BH}	Tm_{20AH}	R_{VEG}	R_{GF}	R_t
H^2	0.91	0.83	0.47	0.48	0.89	0.80	0.76	0.79	0.65	0.73	0.82	0.70	0.67	0.00
SEM	0.52	0.83	0.78	625	5.5	0.03	0.03	0.05	0.05	0.03	0.02	1.7	2.5	1.2
SED	1.0	1.3	1.2	35	3.3	0.2	0.2	0.3	0.3	0.2	0.2	7.8	2.2	1.5
LSD	2.0	2.6	2.5	71	6.7	0.5	0.5	0.6	0.6	0.5	0.4	3.6	4.5	3.1
avg	196	231	35	261	76	15	18	22	26	7.8	10	251	39	291
max	205	239	38	335	100	16	20	24	27	9.3	12	262	45	293
min	191	226	32	144	58	14	17	20	25	7.1	9.6	246	31	288
G	***	***	***	***	***	***	***	***	***	***	***	***	***	NS
E	***	***	***	***	***	***	***	***	***	***	***	***	***	***
GxE	***	***	***	***	***	***	***	***	***	***	***	***	***	***
E Avg														
1	155	195	40	384	92	14	17	21	26	7.1	9.5	384	105	489
2	191	225	34	339	78	15	17	22	24	5.9	9.3	217	34	251
3	228	268	40	120	76	12	17	16	24	7.6	10	272	6.7	279
4	205	243	37	136	57	16	19	24	26	7.8	9.8	150	38	188
5	234	268	34	221	66	15	18	20	25	9.5	11	206	3.0	209
6	113	145	31	311	99	18	21	26	29	9.9	12	209	42	252
7	214	244	30	295	67	14	17	23	24	6.2	9.1	217	23	240
8	227	263	36	287	72	14	19	20	26	8.4	1.0	355	61	417

*Analysis of variance with trial (E), genotype (G), and genotype by trial interaction (G × E) effects are shown. Average per environment is shown (E AVG) for each trait. Environment (E) 1–8 correspond to locations and years as shown in **Table 1**; days to heading (DH), days to maturity (DM), grain filling duration (GFD), grain yield (GY), and plant height (PH) measured in a population containing 250 varieties and breeding lines grown in eight trials between 2012 and 2016 in Turkey and Iran. Exposure of genotypes to weather conditions is shown: average temperature 20 days before (TA_{20BH}) and after heading (TA_{20AH}); average maximum temperature 20 days before (TM_{20BH}) and after heading (TM_{20AH}); average minimum temperature 20 days before (Tm_{20BH}) and after heading (Tm_{20AH}); rain from sowing to heading (R_{VEG}); rain from heading to maturity (R_{GF}); and total rain from sowing to maturity (R_t). ***, significant at $p < 0.0005$; **, significant at $p < 0.005$; *, significant at $p < 0.05$; NS, non-significant.*

TABLE 3 | Correlation matrix with Pearson correlation coefficient and associated probability of overall weather and agronomic traits as means across all tested trials in Turkey and Iran.

***N* = 250**	**DM**	**GFD**	**GY**	**PH**	**TA_{20BH}**	**TA_{20AH}**	**TM_{20BH}**	**TM_{20AH}**	**Tm_{20BH}**	**Tm_{20AH}**	**R_{VEG}**	**R_{GF}**
DH	**0.87** ***	**−0.49** ***	**−0.40** ***	−0.04 NS	**0.97** ***	**0.95** ***	**0.96** ***	**0.93** ***	**0.96** ***	**0.96** ***	**0.93** ***	**−0.93** ***
DM		−0.01 NS	**−0.29** ***	−0.03 NS	**0.85** ***	**0.84** ***	**0.85** ***	**0.82** ***	**0.83** ***	**0.86** ***	**0.79** ***	**−0.78** ***
GFD			**0.31** ***	0.02 NS	**−0.46** ***	**−0.46** ***	**−0.45** ***	**−0.45** ***	**−0.49** ***	**−0.43** ***	**−0.49** ***	**0.50** ***
GY				**−0.15** **	**−0.39** ***	**−0.42** ***	**−0.39** ***	**−0.40** ***	**−0.40** ***	**−0.36** ***	**−0.37** ***	**0.36** ***
PH					−0.04 NS	−0.02 NS	−0.03 NS	−0.03 NS	−0.06 NS	−0.06 NS	−0.10 NS	0.08 NS
TA_{20BH}						**0.95** ***	**0.94** ***	**0.97** ***	**0.98** ***	**0.94** ***	−0.11 NS	**−0.39** ***
TA_{20AH}							**0.93** ***	**0.93** ***	**0.96** ***	**0.93** ***	−0.10 NS	**−0.38** ***
TM_{20BH}								**0.93** ***	**0.96** ***	**0.93** ***	−0.10 NS	**−0.38** ***
TM_{20AH}									**0.95** ***	**0.95** ***	−0.09 NS	**−0.40** ***
Tm_{20BH}										**0.93** ***	**−0.14** **	**−0.40** ***
Tm_{20AH}											−0.12 NS	**−0.36** ***
R_{VEG}												**−0.94** ***

*All traits were measured in a wheat population containing 250 varieties and breeding lines grown in eight trials between 2012 and 2016 in Turkey and Iran. Days to heading (DH), days to maturity (DM), grain filling duration (GFD), grain yield (GY), and plant height (PH). Exposure of genotypes to weather conditions is shown: average temperature 20 days before (TA_{20BH}) and after heading (TA_{20AH}); maximum temperature 20 days before (TM_{20BH}) and after heading (TM_{20AH}); minimum temperature 20 days before (Tm_{20BH}) and after heading (Tm_{20AH}); rainfall between sowing and heading (R_{VEG}); and rainfall between heading and maturity (R_{GF}). ***, significant at $p < 0.0005$; **, significant at $p < 0.005$; *, significant at $p < 0.05$; NS, non-significant. Significant correlations are shown in bold values.*

TM20BH, TM20AH, Tm20BH, and Tm20AH, respectively) were calculated in each trial and across all trials (**Table 2**). Different genotypes (varying in DH for more than 10 days, see maximum and minimum across locations and years in **Table 2**) were consistently exposed to different temperatures in the time period of 20 days before and after heading (**Table 2**) as shown by significant "genotype" effects and medium to high heritability (0.65–0.82) across trials for TA20BH, TA20AH, TM20BH, TM20AH, Tm20BH, and Tm20AH. Moreover, for total rainfall at the vegetative and grain filling stages (R_{VEG} and R_{GF}), significant "genotype" effects were observed across locations and years and heritability of 0.67–0.70 showing that different genotypes are exposed to different amount of rainfall in a consistent manner across locations and years. Moreover, the "genotype" effect for total rainfall (R_t, corresponding to the sum of $R_{VEG} + R_{GF}$) across locations and years was not significant with 0.00 reproducibility (H^2) showing that the total amount of rainfall received by all genotypes was the same.

After the overall analysis revealed that genotypes with variable phenology were exposed to different temperatures and rainfall at specific stages of development, simple correlations were calculated (**Table 3**). In the type of environments and wheat genotypes tested herein, GY correlated negatively with DH ($r = -0.40$) and DM ($r = -0.29$) and positively with grain filling duration (GFD, $r = 0.31$; **Table 3**). Moreover, DH and DM correlated positively with temperature 20 days before and after heading ($r > 0.90$ and $r > 0.80$, respectively). The amount of rainfall at the vegetative stage (R_{VEG}) correlated positively with DH and DM ($r = 0.93$ and $r = 0.79$, respectively), whereas R_{GF} correlated negatively with DH and DM ($r = -0.93$ and $r = -0.78$, respectively; **Table 3**). Temperature 20 days before and after heading and R_{VEG} correlated negatively with GY ($r > -0.36$ and $r = -0.37$); however, R_{GF} correlated positively with GY ($r = 0.36$; **Table 3**). Correlations between temperature and GY were not consistent when each environment was taken individually (**Supplementary Table S1**). Sometimes temperature had a positive effect (e.g., Diyarbakir 2013 and Maragheh 2013); however, in Maragheh 2014, Diyarbakir 2015, and Maragheh 2016, temperature had a negative effect on GY. Correlations per locations and years of R_{VEG} and R_{GF} with GY when significant were consistently negative and positive, respectively (**Supplementary Table S1**). To better illustrate the tradeoffs between DH and GFD as explained by R_{GF}, R_{VEG}, and temperature, regressions are represented in **Figure 1**.

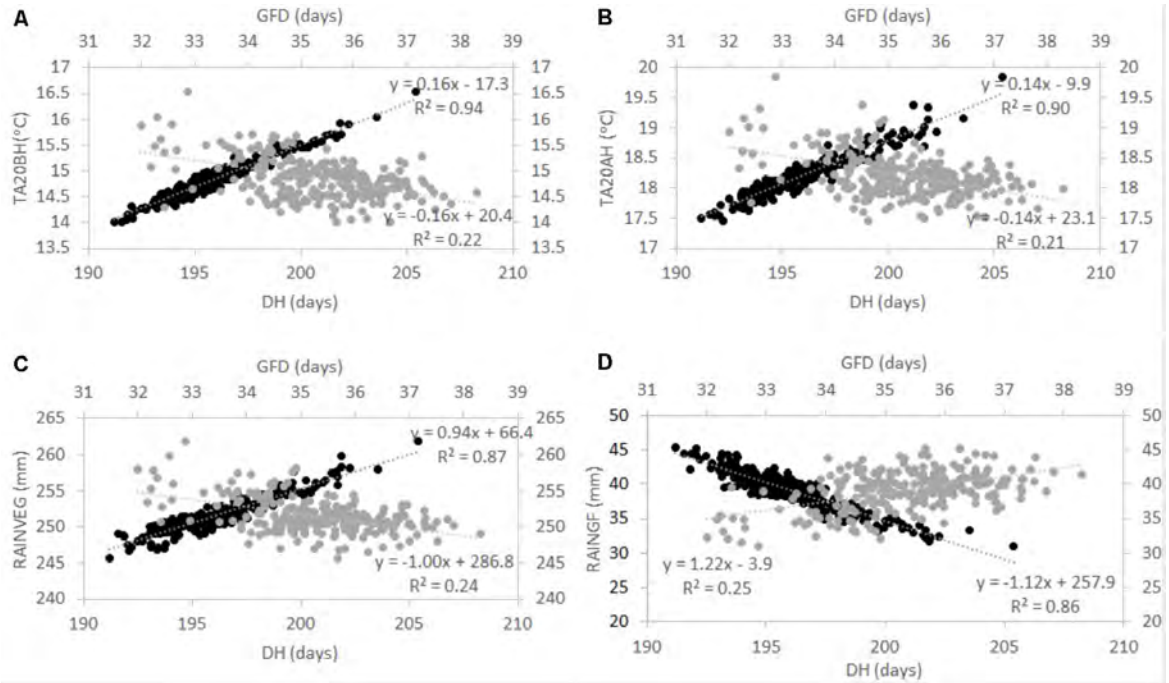

FIGURE 1 | Tradeoff between days to heading (DH) and grain filling duration (GFD) as explained by average temperature 20 days before (TA20BH) and after (TA20AH) heading (**A** and **B**, respectively), and rainfall at the vegetative ($RAIN_{VEG}$) and grain filling (RAINGF) stages (**C** and **D**, respectively) in a winter wheat population grown in Turkey and Iran between 2012 and 2016. Grand means across environments for each genotype are shown. Dark circles represent DH and gray circles represent GFD (shown in secondary axes). Regression equations and R^2 are shown. Correlations are all significant at $P < 0.005$ as shown in **Table 3**.

Calculating Optimal DH and PH to Maximize Grain Yield in a Changing Environment

With the objective of finding the DH and PH that maximize GY across locations and years, all genotypes were classified according to seven DH and PH categories (as described in Section "Materials and Methods"). After categorization, random genotypes were selected from each category and used to plot with GY as shown in **Figures 2**, **3**. Each line in **Figures 2A**, **3A** corresponds to average GY of 10 genotypes randomly selected and falling within seven DH and PH categories. This exercise was repeated 20 times corresponding to 20 lines in **Figures 2A**, **3A** (each time using different genotypes from the entire population consisting of 250 winter wheat breeding lines and varieties). The quadratic function shown in **Figure 2B** and representing the relationship DH with GY revealed that maximum yields were obtained at 194.9 DH. The maximum of the function in each location was also calculated for DH and is shown in **Supplementary Table S2**. For PH, the quadratic function shown in **Figure 3** revealed that maximum yields were obtained at 76.0 cm average height across all locations and years (**Figure 3B**). Moreover, the maximum of the quadratic function was also calculated for PH, in each location and is shown in **Supplementary Table S2**. Finally, one modern wheat breeding line with optima DH and PH was selected for each location which can be used in testing blocks for calibration during selection procedures (**Supplementary Table S3**). Moreover, major functional genes are shown for the selected genotypes (**Supplementary Table S3**). Since optima DH and PH were different in each location (**Supplementary Tables S2**, **S3**), the differences in GY obtained by selecting for specific adaptation to each location or by selecting for adaptation to all locations together were calculated (**Supplementary Table S4**). These calculations have shown, that by selecting wheat breeding lines with optima DH and PH in each location provided on average an increase of 18.6% GY compared to selection based on all locations and years (average of %CHANGE_GY in **Supplementary Table S4**).

Testing Resilience and Total Production of a Diverse and a Mono-Varietal Crop Setup

Three sets of germplasm and data were used to test if several wheat varieties grown together would buffer the effects of erratic weather patterns: (i) wheat population used herein (grown in eight environments); (ii) 23rd ESWYT (grown in 64 environments most of them irrigated and high yielding); and (iii) 21st SAWYT (grown in 66 semi-arid environments with little or no irrigation and low yielding). One of the objectives of this exercise was to identify the selection methodology that will permit the identification of the best possible genotype(s) for a specific type of environment. Therefore, genotypes for (i)–(iii) were selected based on GY performance in "training environments" and then the selected genotypes were evaluated

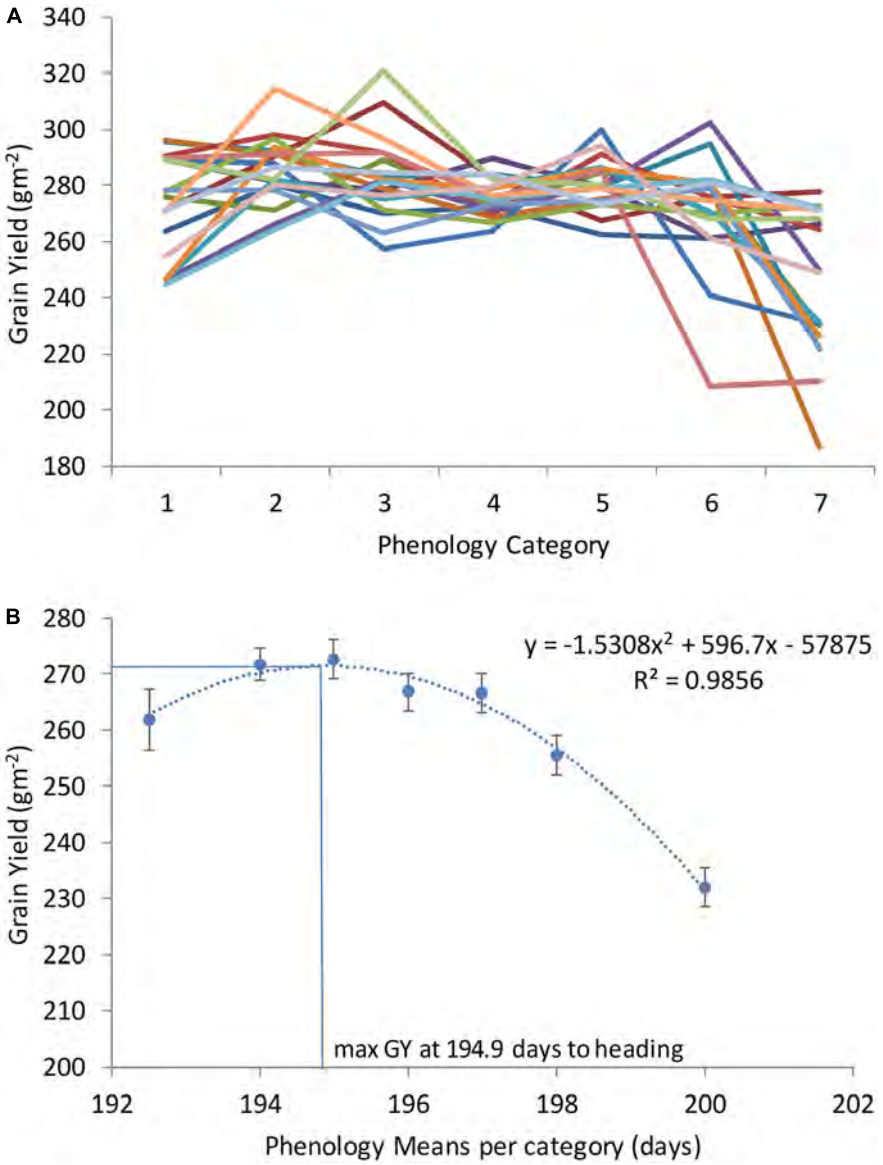

FIGURE 2 | Grain yield (GY) of seven phenology categories in a winter wheat population of 250 varieties and breeding lines grown in Turkey and Iran (1, very early; 2, early; 3, early-medium; 4, medium; 5, medium late; 6, late; and 7, very late). Twenty sets of 10 genotypes were randomly selected of each phenology category to model phenology and associated grain yield **(A)**. Average grain yield associated with each phenology category was calculated as an average of all sets (assembled with 10 genotypes of each category in **B**).

in a set of "testing environments," which correspond to the GY shown in **Figures 4A–C**. This scenario would simulate what generally happens when breeders make a selection of new promising wheat lines based on their best performance (highest GY) in international trials, and farmers adopt those selected lines. Second, this exercise aimed to test whether instead of using one single wheat genotype, five genotypes would boost resilience and total grain production across environments and years. The results revealed that the best genotype in monoculture always demonstrated higher production than a group of the five best genotypes provided that the number of environments was sufficient enough to find the genotype showing the highest yield (**Figure 4A**). However, the best selected genotype in "six training environments" showed similar grain production to five genotypes. Given the fact that the number of trials conducted for this population was relatively low, the same hypothesis was tested in spring wheat where data from international nurseries are available at CIMMYT. In the two sets of data for the 23rd ESWYT and 21st SAWYT, always the selection of the best unique genotypes gave the highest GY and the group of five genotypes showed no benefit comparatively. In the 23rd ESWYT (**Figure 4B**), the best-selected genotype in 32 training environments had lower GY than the best-selected unique genotype across all 64 environments. However, in the 21st

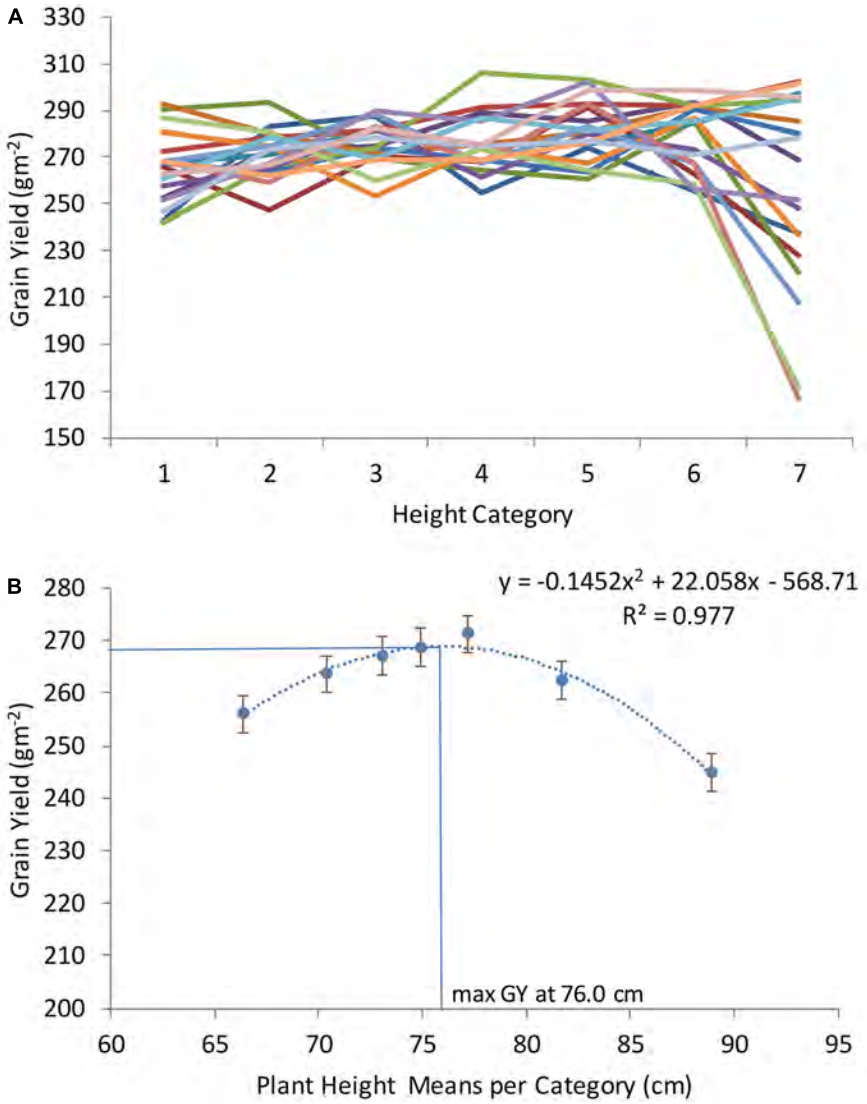

FIGURE 3 | Grain yield (GY) of seven plant height categories in a winter wheat population of 250 varieties and breeding lines grown in Turkey and Iran (1, very short; 2, short; 3, short-medium; 4, medium; 5, medium tall; 6, tall; and 7, very tall). Twenty sets of 10 genotypes were randomly selected of each height category to model height and associated grain yield **(A)**. Average grain yield associated with each height category was calculated as an average of all sets (assembled with 10 genotypes of each category in **B**).

SAWYT (**Figure 4C**), the best-selected unique wheat genotype in 33 training environments had similar GY to the best-selected genotype in all 66 field trials.

DISCUSSION

Contributions of DH and PH to Improve Grain Yield in Rain Fed Winter Wheat Grown in Turkey and Iran

Manipulation of DH and PH in wheat has probably had the highest impact on wheat GY globally and both are also responsible for the adoption of wheat in a wide range of environments (Reynolds and Bourlag, 2006; Lopes et al., 2014, 2015; Royo et al., 2017). Cycle length to heading and PH together may explain up to 68% of GY variation in low yielding environments (Lopes et al., 2014) although this largely depends on the genetic background of the wheat genotypes, range of variation of DH and PH, and the environments being tested. Given the importance of these two traits and the simplicity of detection in the field during selection of progenies in breeding programs, the optimal expression of these traits was evaluated and calculated to maximize GY. For this study, DH and PH were determined in a series of experimental field trials in three locations for 4 years. This wheat population was intentionally designed for expressing a wide range of variation for phenology to understand more

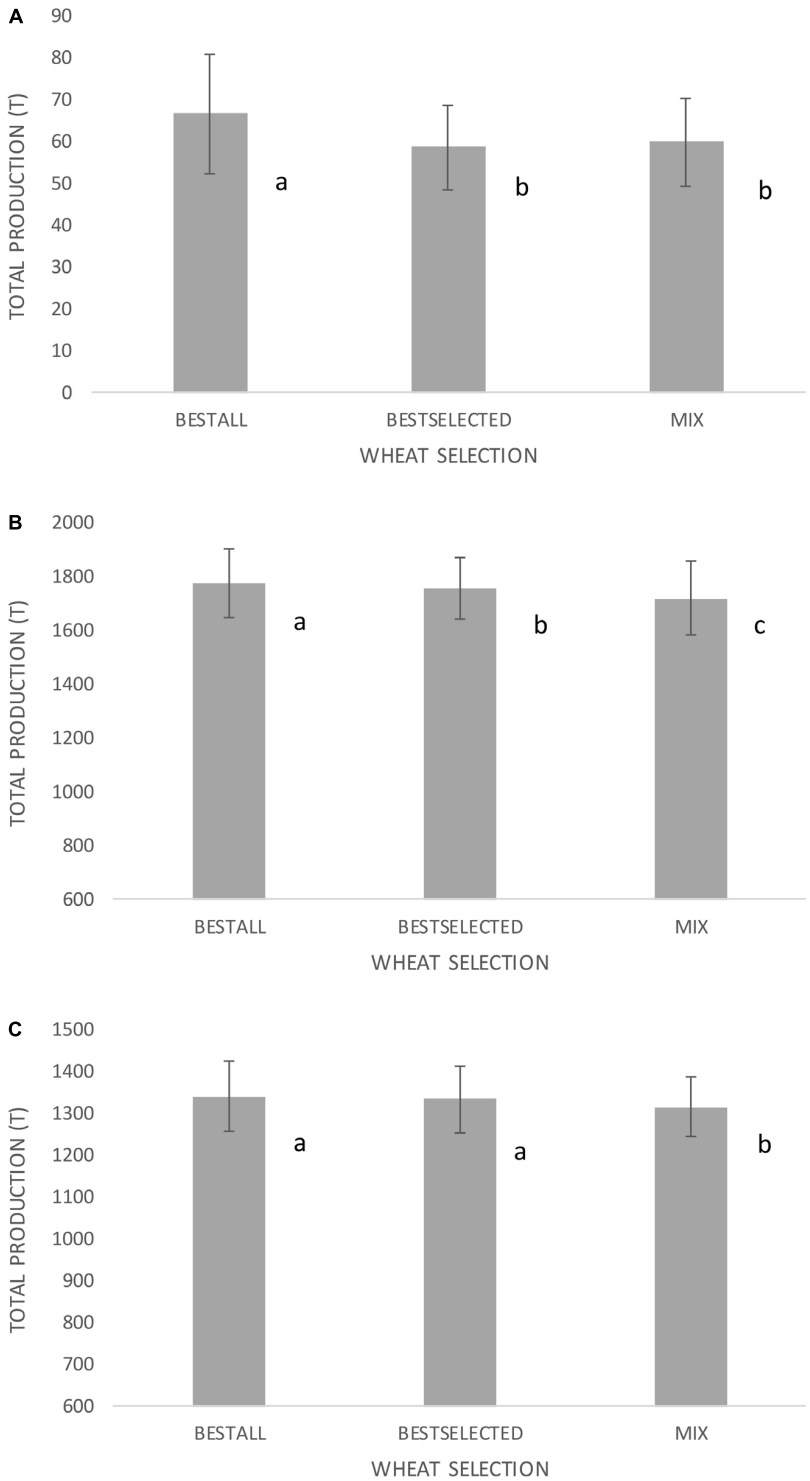

FIGURE 4 | Grain production using three sets of international trials including **(A)** Turkey and Iran for 4 years (eight trials with low yielding environments) in a total of 20 ha, **(B)** 64 trials across the globe for the international nursery 23rd ESWYT (Elite Selection Wheat Yield Trials- high yielding environments) in a total of 320 ha, and **(C)** 66 trials across the globe for the international nursery 21st SAWYT (Semi-Arid Wheat Yield Trial – low yielding environments) in a total of 330 ha. BESTALL is the actual best wheat genotype in the whole set of environments (based on grand means across all environments), BESTSELECTED corresponds to the best wheat genotype selected in a subset of training environments (based on grand means across half of the environments), and MIX corresponds to the best five selected genotypes in a subset of training environments and grown together in 2 ha plots side by side. Different letters indicate significant differences using LSD test at $p < 0.05$. Error bars indicate SD across random sets of environments.

about how different mechanisms of adaptation and stress escape of early and late genotypes in rain fed winter wheat areas of Turkey and Iran. Cycle length to heading and GY correlated negatively and significantly in most trials tested. However, PH correlated positively and significantly with GY in most field trials, but overall PH correlated negatively with GY when means across locations and years for each genotype were used (but with weak Pearson Correlation coefficient $r = -0.15$). These results are in accordance with previous observations because weather conditions partially contribute to changes in optimal DH and PH, and PH contributions to GY (Lopes et al., 2012, 2013). For the type of locations and years studied (winter wheat region of Turkey and Iran), some level of earliness has been identified as important to escape periods of water shortage during grain filling. To better explain the mechanisms related to this response, the environmental conditions to which different DH and PH winter wheat genotypes are exposed are analyzed below.

Drought Escape Mechanisms in Winter Wheat Grown Under Low Rainfall Regions of Turkey and Iran

Grain yield across trials was primarily and significantly affected by rainfall and Tm as shown by the significant correlations between GY and the former weather variables. As described in Section "Introduction," Fischer and Wood (1979) and Mitchell et al. (1996) highlighted the discrimination against long-duration genotypes in poor-yielding environments, and the resulting confounding effects hindering the discovery of genotypes with drought avoidance and resistance. While these confounding effects have been reported and cited in the literature, the mechanisms associated with this response are poorly understood in the context of winter wheat rain fed regions of Turkey and Iran. When comparing different wheat genotypes (particularly with variable phenology) in one specific field trial, it is assumed that all genotypes are exposed to the same environmental conditions. While this is correct if an average of all environmental traits is taken from sowing to harvest, it may not be when temperature and rainfall are determined at specific developmental stages. Since different genotypes attain a certain developmental stage at different points in time, weather data were collected and calculated for each genotype at key developmental stages. Specifically, temperature and rainfall were quantified and evaluated for the period 20 days before and after heading in a series of genotypes. The results presented here show that genotypes differing in their phenology were exposed to different temperatures and rainfall 20 days before and after heading. Primarily, DH positively correlated with temperature TA, TM, and Tm 20 days before and after heading. On average across locations and years, the effect of delaying heading by 1 day resulted in an increase of 0.16 and 0.14°C in temperature 20 days before and after heading, respectively (as shown by the regression line in **Figures 1A,B**). This means that two genotypes with a 10-day difference in heading may be exposed to a difference in temperature of up to 1.6 and 1.4°C (on average across locations and years) 20 days before or after heading. This increase in temperature of late genotypes led to shorter grain filling duration (**Figures 1A,B**) as shown by a negative correlation of temperature with GFD and DH with GFD. This is in agreement with Bruckner and Frohberg (1987) where increasing temperature during grain filling in different genotypes tended to stop grain growth prematurely and to hasten physiological maturity.

In the field trials conducted here, even if the total amount of rainfall from sowing to maturity received by each genotype was similar, the distribution of this rainfall changed across genotypes at a specific growth stage. Non-significant "genotype" effects showed this for *Rt* (total rainfall from sowing to maturity) in the analysis of variance across locations and years and significant "genotype" effects for R_{VEG} (total rainfall during the vegetative stage for each genotype) and R_{GF} (total rainfall during the grain filling stage for each genotype) across locations and years. Moreover, R_{VEG} and R_{GF} correlated positively and negatively with DH (**Table 3**), respectively (*Rt* did not show "genotype" effects and was not included for correlation analysis). On average across locations and years, the effect of delaying heading by 1 day resulted in an increase of 0.94 mm in R_{VEG} (as shown by the regression line in **Figure 1C**) and a decrease of 1.12 mm in R_{GF}. This shows that on average across the type of locations and years tested, late genotypes were exposed to more rainfall during the vegetative stage, but were also exposed to less rainfall at the grain filling stage compared to earlier genotypes, and as demonstrated by the regression lines of both periods (**Figures 1C,D**). In conclusion, increased temperature at around heading and less rainfall during the grain filling period explain the lower success of late winter wheat genotypes in the type of locations and years tested.

Bridging Temperature and Rainfall Exposures of Different Genotypes With Height and GY

Temperature at around heading and R_{VEG} and R_{GF} across genotypes were not correlated with PH, although PH had an effect on GY as shown by positive correlations in several field trials. This indicated that mechanisms through which PH affected GY in these environments were not driven by the differences observed in temperature and rainfall at a specific developmental stage across genotypes. However, the correlation of PH with GY across genotypes was a function of total rainfall in each year and location, with correlations trending negative to null with high rainfall and correlation trending positive with low rainfall. This result is in accordance with Lopes et al. (2014) where the success of taller wheat genotypes was associated with low yielding low rainfall environments. Other studies have explained the success of taller wheat varieties in dry environments through longer coleoptiles and larger roots systems compared with the semi-dwarfs, where deep sowing ensures contact with available soil moisture (Rebetzke and Richards, 2000), improved pre-anthesis radiation interception (Miralles and Slafer, 1997), and decreased canopy temperature (Lopes et al., 2012a). Mathews et al. (2006) analyzed 81 trials around the world and concluded that tall and semi-dwarf lines had similar adaptation to stressed environments and showed the highest GY. It is also worth noting that tall varieties may be desirable for reasons other than high

yield, including high biomass and longer straw lengths (can be used as animal feed).

Fitting DH and PH to the Environment as a Major Goal to Increase Adaptation and Maximize Grain Yield

One challenge for future wheat breeding is to modify the reproductive stage timing to suit local climatic conditions while maintaining or even increasing yield potential (Langer et al., 2014). In most instances, wheat breeders have been guided by a set of highly productive wheat check lines or genotypes that in principle have optimal DH and PH. However, optimal synchronization has not always been achieved in rain fed winter wheat. In this study, a major objective was to define optimal DH and PH for winter wheat grown under low rainfall cold temperature (ME12, Braun et al., 2010) and fit the most sensitive stages of crop development to the most favorable time and weather conditions of the wheat cycle. A method of calculation was used to categorize genotypes into different DH and PH groups, and random genotypes were selected from each category to determine how these influenced GY. Optima DH and PH were calculated across all locations and years together and GY was maximized at 194.9 DH and at 76.0 cm PH. However, optima DH and PH varied with location. Specifically, Diyarbakir is warmer and wetter (higher temperatures and total amount of rainfall) than Konya and Maragheh and earlier genotypes are better adapted to Diyarbakir. Konya and Maragheh are cooler and winter wheat (later genotypes) is better adapted to these regions. These specificities and requirements in each location studied herein showed that to improve GY, selection must target various optima DH and PH. This was shown by a 18.6% increase in GY when selection targeted optima DH and PH obtained from Diyarbakir, Konya, and Maragheh separately compared to targeting one overall (across all locations and years) optima DH and PH. A wheat breeding line with optima DH and PH for each location was selected and these can be used as checks in the field in demonstration plots for calibration during selection procedures (**Supplementary Table S2**). Moreover, in international breeding programs targeting many different regions, multiple optimal DH and PH ranges must be identified according to the target regions to avoid the risks of limiting the amount of progress in those regions.

Testing Resilience and Total Production of a Diverse and a Mono-Varietal Crop Setup

Crop biodiversity has been proposed as a possible solution to the vulnerability of monoculture crops to disease (Zhu et al., 2000) and climate variability (Lin, 2011). Crop diversity and the coexistence of multiple species have been used as an example for improved resilience (Lin, 2011). However, limited information is available on the resilience within species diversity to increase resilience of wheat systems to climate change. In theory, it would be beneficial for wheat production to have a set of a few highly productive wheat genotypes grown in one particular farm over a period of years to increase wheat resilience through compensation and adaptation mechanisms of different traits. This hypothesis was tested for this study by selecting the best wheat genotypes in sets of environments, and comparing the best selected genotype in monoculture (hypothetical defined in 10 ha) and in groups of five genotypes grown in 2 ha per genotype (in a total of 10 ha). The results revealed that the best-selected genotype in monoculture always demonstrated higher production than a group of the five best genotypes. The results were unexpected given that different phenology, PH, and other traits in the diverse set (five genotypes) would help minimize the losses caused by one "bad year" for one specific genotype. Probably, crop variety mixtures are not the solution for water and heat stresses in the tested environments, given the fact these stresses may occur too late in the crop cycle, when crop plasticity (in terms of tillering, for example) is already accomplished. It may have more sense for environments when water stress occurs during the first stages of crop cycle and this needs further testing. Moreover, this hypothesis was tested for this study by also using data from international nurseries released each year by CIMMYT. This data were used to select the five best genotypes in 32 and 33 training environments (used for genotype selection) for the ESWYT and SAWYT, respectively, and then by testing those selected genotypes in other 32 and 33 testing environments (not used for genotype selection). Using a diverse setup of five genotypes always resulted in lower yields compared to a monoculture with the highest yielding genotype and this was mainly due to the fact that the total crop area also contained lower yielding genotypes. Moreover, the best-selected genotype in a set of 33 training environments was at least for the 21st SAWYT the best genotype in 33 testing environments. However, for the 23rd ESWYT, the best-selected genotype in the training environments was not always the best genotype in the testing environments. This indicated a gap between highest potential GY attainable, i.e., if the highest GY genotype can be identified and adopted and genotypes actually obtained by selection and eventually adopted by farmers. To close this gap, more than 30 training environments must be used to ensure that the best-selected variety will actually perform well in a wide range of environments. For this reason, international nurseries at CIMMYT are planted in at least 60 environments to ensure the best possible selection.

CONCLUSION

For many years, researchers have realized the slow yield progress of less productive wheat areas in the world where irrigation is not an option or where water resources are becoming scarce. To date, research efforts to tackle this bottleneck have not been sufficient to reverse the slow progress. The results presented from this study helped to define the aspects of wheat breeding that need attention, and are preventing our progress in environments with low rainfall and cold temperature in Turkey and Iran. To increase genetic gains in rain fed winter, wheat the adoption of phenology that synchronizes with rainfall distribution typical from a specific region at the vegetative and grain filling stages is necessary. It was shown that genotypes with different phenologies received different rainfall and temperatures at a specific key

developmental stage. Late-duration genotypes received more rainfall during the vegetative stage and less rainfall at the grain filling stage compared to short-duration genotypes. Moreover, the late-duration genotypes were exposed to higher temperature at around heading, and both rainfall and temperature shortened the grain filling duration and penalized yields. Optimal DH and PH that maximize GY in rain fed winter wheat areas of Turkey and Iran have now been defined. After that, parental lines with similar synchronization with rainfall and temperature (similar optimal heading dates) but differing for other traits should be crossed. Alternatively, even if parental lines are very different, early generation selection must be conducted toward optimal DH and PH so that in subsequent generations, the difference is minimized. By keeping progenies within the same optimal phenology, environmental selection will naturally follow toward drought and heat avoidance and resistance strategies (and drought escape will be ruled out). In this case, breeders will not be misleading selection toward escaping stress exclusively and will open and explore a new window of genetic variation. Similarly, any marker discovery efforts toward drought resistance and avoidance must use phenology controlled populations for adequate gene discovery.

Overall, to avoid the risk of limiting wheat yield progress in specific regions while exploring more than just drought escape in many parts of the world, the following strategy is suggested: (i) first define optimal heading and height ranges for the different target regions; (ii) select new progenies based on optimal heading and height defined in (i); (iii) compose yield trials compartmentalized in groups of wheat lines having optimal heading and height for the target regions defined in (i); and (iv) within each optimal heading and height group, identify the highest yielding lines which correspond to most resistant and avoidant lines.

Finally, this research revealed that the use of groups of genotypes (e.g., five genotypes) did not increase wheat resilience through compensation and adaptation mechanisms of different traits associated with different genotypes. In all tested sets of field trials, it was concluded that monoculture of the best selected genotype always demonstrated higher production.

AUTHOR CONTRIBUTIONS

ML: conception and design of the research, data collection with analysis and interpretation, critical revision of the article, and overall responsibility. CR, FA, MS-G, FO, MJ-K, and DP: critical revision of the article. MK, EO, and MR: conducted field trials, collected data, and critical revision of the article.

FUNDING

This research was funded by a European Union project titled "Addressing the challenges of climate change for sustainable food security in Turkey, Iran, and Morocco, through the creation and dissemination of an international database to promote the use of wheat genetic resources and increase genetic gains," CFP 2014/2015-W3B-PR-18-Turkey. Additional funds were received from CGIAR Research Program (CRP) WHEAT. CERCA Programme/Generalitat de Catalunya is also acknowledged.

ACKNOWLEDGMENTS

The authors would like to thank Susanne Dreisigacker, Head of the Wheat Molecular Breeding Laboratory at CIMMYT, for providing information on functional markers presented in **Supplementary Table S2**. Seeds were provided by the International Winter Wheat Improvement Program (IWWIP), a Turkey-CIMMYT-ICARDA coalition. Editing assistance was received from Julie Mollins.

SUPPLEMENTARY MATERIAL

The Supplementary Material for this article can be found online at: https://www.frontiersin.org/articles/10.3389/fpls.2018.00563/full#supplementary-material

FIGURE S1 | Heading and maturity date of a collection of 250 winter wheat varieties and breeding lines grown in eight trials conducted between 2012 and 2016 in Turkey (Diyarbakir and Konya) and Iran (Maragheh) (location and year indicated in the lower right corner of each diagram) during the wheat cycle (*xx* axes date). Daily maximum temperature (dark solid line), daily average temperature (dashed dark line), and daily minimum temperature (gray solid line) are all indicated in the primary *yy* axes and daily rain (light gray bars) are indicated in the secondary *yy* axes. Sowing time is indicated by the symbol "S," days to heading of the entire population "H," and days to maturity "M."

TABLE S1 | Pearson correlation coefficients and probability between grain yield (GY) and average temperature 20 days before and after heading (TA20AH and TA20BH), maximum temperature 20 days before and after heading (TM20AH and TM20BH), and minimum temperature 20 days before and after heading (Tm20BH and Tm20AH). Eight trials were conducted as indicated in **Table 1**. ***, significant at $p < 0.0005$; **, significant at $p < 0.005$; *, significant at $p < 0.05$, NS, non-significant. Significant correlations are shown in bold values.

TABLE S2 | Range of variation of optima (where grain yield is maximized) days to heading (DH OPTIM) and plant height (PH OPTIM) determined in each location at Diyarbakir for two growth seasons (DIY), Konya for three growth seasons (KON), Maragheh for three growth seasons (MAR), and across all (ALL) environments (from **Figures 3**, **4**).

TABLE S3 | Selection of wheat breeding lines showing optima combination of days to heading and plant height in Diyarbakir (DIY SEL) for 2 years ("U1275-1-4-2-2/KS85W663-7-4-2//JAGGER" accession number, ACCN# 30961), in Konya (KON SEL) for 3 years ("MADSEN/TAM-202//TX89V4138," ACCN# 40662), and in Maragheh (MAR SEL) for 3 years ("WO405D/HGF112//W7469C/HCF012," ACCN# 70546) and across all environments (ALL SEL) and years ("TAM 105/3/NE70654/BBY//BOW"S"/4/Century*3/TA2450"ACC# 70554). Functional genes present (1) and absent (0) are shown. DHAVG, PHAVG, GYAVG: days to heading (DHAVG), plant height (PHAVG), and grain yield (GYAVG) average across all environments and years.

TABLE S4 | Grain yield (GY) of genotypes selected based on optima days to heading (DH) and plant height (PH) in each location (Diyarbakir-DIY SEL for two seasons, Konya-KON SEL with for three seasons, and Maragheh-MAR SEL for three seasons) and across all locations and years (ALL). As a reference, the highest yielding genotype in each location is shown (HGY_ENV). Changes in GY between the two types of selection (selected in each location versus selected across all locations and years) are also shown in absolute values and in percentage (CHANGE_GY and % GY CHANGE, respectively).

REFERENCES

Araki, E., Miura, H., and Sawada, S. (1999). Identification of genetic loci affecting amylase content and agronomic traits on chromosome 4A of wheat. *Theor. Appl. Genet.* 98, 977–984. doi: 10.1007/s001220051158

Araus, J. L., Slafer, G. A., Reynolds, M. O., and Royo, C. (2002). Plant breeding and drought in C3 cereals: what should we breed for? *Ann. Bot.* 89, 925–940. doi: 10.1093/aob/mcf049

Blum, A. (2009). Effective use of water (EUW) and not water-use efficiency (WUE) is the target of crop yield improvement under drought stress. *Field Crops Res.* 113, 119–123. doi: 10.1016/j.fcr.2009.03.009

Braun, H. J., Atlin, G., and Payne, T. (2010). "Multi-location testing as a tool to identify plant response to global climate change," in *Climate Change and Crop Production*, ed. M. P. Reynolds (Oxfordshire: CABI), 115–138. doi: 10.1079/9781845936334.0115

Bruckner, P. L., and Frohberg, R. C. (1987). Rate and duration of grain fill in spring wheat1. *Crop Sci.* 27, 451–455. doi: 10.2135/cropsci1987.0011183X002700030005x

Creissen, H. E., Jorgensen, T. H., and Brown, J. K. M. (2016). Increased yield stability of field-grown winter barley (*Hordeum vulgare* L.) varietal mixtures through ecological processes. *Crop Prot.* 85, 1–8. doi: 10.1016/j.cropro.2016.03.001

Crespo-Herrera, L. A., Crossa, J., Huerta-Espino, J., Autrique, E., Mondal, S., Velu, G., et al. (2017). Genetic yield gains in CIMMYT's International elite spring wheat yield trials by modeling the genotype x environment interaction. *Crop Sci.* 57, 789–801. doi: 10.2135/cropsci2016.06.0553

Fischer, R. A., and Maurer, R. (1978). Drought resistance in spring wheat cultivars. I grain yield responses. *Aust. J. Agric. Res.* 29, 897–912. doi: 10.1071/AR9780897

Fischer, R. A., and Wood, J. T. (1979). Drought resistance in spring wheat cultivars. III. Yield association with morpho-physiological traits. *Aust. J. Agric. Res.* 30, 1001–1020. doi: 10.1071/AR9791001

Honsdorf, N., March, T. J., Berger, B., Tester, M., and Pillen, K. (2014). High-Throughput phenotyping to detect drought tolerance QTL in wild barley introgression lines. *PLoS One* 9:e97047. doi: 10.1371/journal.pone.0097047

Kirigwi, F. M., Van Ginkel, M., Brown-Guedira, G., Gill, B. S., Paulsen, G. M., and Fritz, A. K. (2007). Markers associated with a QTL for grain yield in wheat under drought. *Mol. Breed.* 20, 401–413. doi: 10.1007/s11032-007-9100-3

Kuchel, H., Williams, K. J., Langridge, P., Eagles, H. A., and Jefferies, S. P. (2007). Genetic dissection of grain yield in bread wheat. *I. QTL analysis. Theor. Appl. Genet.* 115, 1029–1041. doi: 10.1007/s00122-007-0629-7

Langer, S. M., Longin, F. H., and Wurschum, T. (2014). Flowering time control in European winter wheat. *Front. Plant Sci.* 5:537. doi: 10.3389/fpls.2014.00537

Lin, B. B. (2011). Resilience in agriculture through crop diversification: adaptive management for environmental change. *BioScience* 61, 183–193. doi: 10.1525/bio.2011.61.3.4

Lopes, M. S., Dreisigacker, S., Pena, R. J., Sukumaran, S., and Reynolds, M. P. (2015). Genetic characterization of the wheat association mapping initiative (WAMI) panel for dissection of complex traits in spring wheat. *Theor. Appl. Genet.* 128, 453–464. doi: 10.1007/s00122-014-2444-2

Lopes, M. S., Reynolds, M. P., Jalal-Kamali, M. R., Moussa, M., Feltaous, Y., Tahir, I. S. A., et al. (2012). The yield correlations of selectable physiological traits in a population of advanced spring wheat lines grown in warm and drought environments. *Field Crops Res.* 128, 129–136. doi: 10.1016/j.fcr.2011.12.017

Lopes, M. S., Reynolds, M. P., Manes, Y., Singh, R. P., Crossa, J., and Braun, H. J. (2012a). Genetic yield gains and changes in associated traits of CIMMYT spring bread wheat in a "Historic" set representing 30 years of breeding. *Crop Sci.* 52, 1123–1131. doi: 10.2135/cropsci2011.09.0467

Lopes, M. S., Reynolds, M. P., McIntyre, C. L., Mathews, K. L., Jalal Kamali, M. R., Mossad, M., et al. (2013). QTL for yield and associated traits in the Seri/Babax population grown across several environments in Mexico, in the West Asia, North Africa, and South Asia regions. *Theor. Appl. Genet.* 6, 974–981. doi: 10.1007/s00122-012-2030-4

Lopes, M. S., Saglam, D., Ozdogan, M., and Reynolds, M. (2014). Traits associated with winter wheat grain yield in Central and West Asia. *J. Integr. Plant Biol.* 7, 673–683. doi: 10.1111/jipb.12172

Mathews, K. L., Chapman, S. C., Trethowan, R., Singh, R., Crossa, J., Pfeiffer, W., et al. (2006). Global adaptation of spring bread and durum wheat lines near-isogenic for major reduced height genes. *Crop Sci.* 46, 603–613. doi: 10.2135/cropsci2005.05-0056

Miralles, D. J., and Slafer, G. A. (1997). Radiation interception and radiation use efficiency of near-isogenic wheat lines with different height. *Euphytica* 97, 201–208. doi: 10.1023/A:1003061706059

Mitchell, J., Fukai, S., and Cooper, M. (1996). Influence of phenology on grain yield variation among barley cultivars grown under terminal drought. *Aust. J. Agric. Res.* 47, 757–774. doi: 10.1071/AR9960757

Olivares-Villegas, J. J., Reynolds, M. P., and McDonald, G. K. (2007). Drought-adaptive attributes in the Seri/Babax hexaploid wheat population. *Funct. Plant Biol.* 34, 189–203. doi: 10.1071/FP06148

Pinto, R. S., Reynolds, M. P., Mathews, K. L., McIntyre, C. L., Villegas, J. J. O., and Chapman, S. C. (2010). Heat and drought adaptive QTL in a wheat population designed to minimize confounding agronomic effects. *Theor. Appl. Genet.* 121, 1001–1021. doi: 10.1007/s00122-010-1351-4

Rebetzke, G. J., and Richards, R. A. (2000). Gibberellic acid-sensitive dwarfing genes reduce plant height to increase kernel number and grain yield of wheat. *Aust. J. Agric. Res.* 51, 235–245. doi: 10.1071/AR99043

Reynolds, M. P., and Bourlag, N. E. (2006). Impacts of breeding on international collaborative wheat improvement. *J. Agric. Sci.* 144, 3–17. doi: 10.1017/S0021859606005867

Royo, C., Ammar, K., Alfaro, C., Dreisigacker, S., Garcia del Moral, L., and Villegas, D. (2017). Effect of *Ppd-1* photoperiod sensitivity genes on dry matter production and allocation in durum Wheat. *Field Crop. Res.* 221, 358–367. doi: 10.1016/j.fcr.2017.06.005

Royo, C., Nazco, R., and Villegas, D. (2014). The climate of the zone of origin of Mediterranean durum wheat (*Triticum durum* Desf.) landraces affects their agronomic performance. *Genet. Resour. Crop Evol.* 61, 1345–1358. doi: 10.1007/s10722-014-0116-3

Saini, H. S., and Westgate, M. E. (1999). Reproductive development in grain crops during drought. *Adv. Agron.* 68, 59–96. doi: 10.1016/S0065-2113(08)60843-3

Sas Institute Inc. (2009). *SAS/STAT® 9.2. User's Guide*, 2nd Edn. Cary, NC: SAS Institute Inc.

Wolfe, M. S. (2000). Crop strength through diversity. *Nature* 406, 681–682. doi: 10.1038/35021152

Zadoks, J. C., Chang, T. T., and Konzak, C. F. (1974). A decimal code for the growth stages of cereals. *Weed Res.* 14, 415–421. doi: 10.1111/j.1365-3180.1974.tb01084.x

Zampieri, M., Ceglar, A., Dentener, F., and Toreti, A. (2017). Wheat yield loss attributable to heat waves, drought and water excess at the global, national and subnational scales. *Environ. Res. Lett.* 12:064008. doi: 10.1088/1748-9326/aa723b

Zhu, Y., Chen, H., Fan, J., Wang, Y., Li, Y., Chen, J., et al. (2000). Genetic diversity and disease control in rice. *Nature* 406, 718–722. doi: 10.1038/35021046

Conflict of Interest Statement: The authors declare that the research was conducted in the absence of any commercial or financial relationships that could be construed as a potential conflict of interest.

frontiers in Plant Science

REVIEW
published: 11 April 2018
doi: 10.3389/fpls.2018.00361

Genomics-Enabled Next-Generation Breeding Approaches for Developing System-Specific Drought Tolerant Hybrids in Maize

Thirunavukkarsau Nepolean, Jyoti Kaul, Ganapati Mukri and Shikha Mittal*

Maize Research Lab, Division of Genetics, ICAR-Indian Agricultural Research Institute, New Delhi, India

Breeding science has immensely contributed to the global food security. Several varieties and hybrids in different food crops including maize have been released through conventional breeding. The ever growing population, decreasing agricultural land, lowering water table, changing climate, and other variables pose tremendous challenge to the researchers to improve the production and productivity of food crops. Drought is one of the major problems to sustain and improve the productivity of food crops including maize in tropical and subtropical production systems. With advent of novel genomics and breeding tools, the way of doing breeding has been tremendously changed in the last two decades. Drought tolerance is a combination of several component traits with a quantitative mode of inheritance. Rapid DNA and RNA sequencing tools and high-throughput SNP genotyping techniques, trait mapping, functional characterization, genomic selection, rapid generation advancement, and other tools are now available to understand the genetics of drought tolerance and to accelerate the breeding cycle. Informatics play complementary role by managing the big-data generated from the large-scale genomics and breeding experiments. Genome editing is the latest technique to alter specific genes to improve the trait expression. Integration of novel genomics, next-generation breeding, and informatics tools will accelerate the stress breeding process and increase the genetic gain under different production systems.

Keywords: accelerated line breeding, big data, breeding informatics, drought, genomics, maize, next-generation breeding, rainfed

OPEN ACCESS

Edited by:
Lijun Luo,
Shanghai Agrobiological Gene Center, China

Reviewed by:
Shabir Hussain Wani,
Michigan State University, United States
Tibor Janda,
Centre for Agricultural Research (MTA), Hungary

****Correspondence:***
Thirunavukkarsau Nepolean
tnepolean@gmail.com;
tnepolean@yahoo.com

Specialty section:
This article was submitted to Plant Breeding, a section of the journal Frontiers in Plant Science

Received: *30 October 2017*
Accepted: *05 March 2018*
Published: *11 April 2018*

Citation:
Nepolean T, Kaul J, Mukri G and Mittal S (2018) Genomics-Enabled Next-Generation Breeding Approaches for Developing System-Specific Drought Tolerant Hybrids in Maize. Front. Plant Sci. 9:361. doi: 10.3389/fpls.2018.00361

INTRODUCTION

Increasing the food production is a challenge to feed the global population that is expected to reach about 9 billion by 2050. Maize (*Zea mays* L.) is one of the important crops and its acreage is increasing considerably especially in Asia and Africa. The world productivity of maize was 5.5 ton/ha whereas in developing economies it is about 2.5 ton/ha (https://apps.fas.usda.gov/psdonline/circulars/production.pdf). The Intergovernmental Panel on Climate Change (IPCC) prediction says that the mean temperatures around the planet may rise between 2 and 5°C or more by 2050 (www.ipcc.ch). Among other hurdles, the changes in the climate followed by its consequences are the major threats to different crop production systems. The tropical and subtropical climates occupying 160 million hectares are most vulnerable, since climate changes, adversely affect the dynamics of temperature and water availability. And it is also important to note that most of the thickly populated and developing countries are located in these climates,

any adversity in agriculture production will cause greater damage to the food security of millions of people. The common production system in tropical and subtropical climates is rain-fed (Edmeades, 2008) and the global yield loss is nearly 25% in the rain-fed system. About 19 million hectares of the tropical Asia is rain-fed of which 80% is drought-prone. More losses are expected in the tropical system owing to the unpredictable rainfall condition (Mhike et al., 2012).

From the "Mendelian era" of nineteenth century we have now reached the stage of "Genomics era" in twenty-first century where several new tools and techniques are available to understand the genetics of traits and accelerate the breeding process. The growth of "genomics" has become rapid in the last two decades. Sequencing of DNA and RNA are no longer the constraints and millions of SNPs can be generated in no time with the help of modern sequencers. Identification and understanding the function of genes are possible with the help of *omics* which include genome, transcriptome, and proteome and so on. The large-scale data from such genome-scale studies also ushered in new branches in bio-informatics called big-data management.

At the same time, new "breeding techniques" have rapidly emerged to reduce the breeding cycles and improve the genetic gain. Linkage and linkage-disequilibrium based QTL mapping approaches were revolutionized the way of understanding the genetics of traits. Introgressing QTLs into the target genotypes through marker-assisted breeding has improved several traits. New line breeding and whole-genome based selection approaches such as genomic selection (GS) has come up to further accelerate the breeding cycle and improve the genetic gain in the breeding programme. Currently genome editing techniques are available to develop customized genotypes.

Results from various genomics and novel breeding experiments on drought tolerance in maize have started coming up in the public domain. The review has compiled those experiments as well as explained the strategies and opportunities to breed drought tolerant hybrids for different maize production systems.

PRODUCTION SYSTEM-BASED STRESS BREEDING

Breeding for drought tolerance specific to the target production systems would provide more dividends since the systems decide the type of traits to be phenotyped to breed effective maize hybrids and to maximize the genetic gain. Drought stress is predominant in the low input rain-fed system which occupies more than 70% of the maize production systems in the developing world. Several component traits that belong to morpho-physiological categories include seedling vigor, root traits (volume, deepness, spread, primary, and secondary structures, hairs), leaf traits (hair, rolling, chlorophyll, delayed senescence), synchronized male-female flowering, stomatal regulation, evapo-transpiration, relative-water content, canopy temperature, hormones, osmotic adjustment, anti-oxidants, enzymes, etc. have been proposed to understand and improve the drought tolerance in maize. In the rain-fed system of sub-tropical regions, the seeds are sown after the first shower of the rain. Early emergence and seedling vigor are the important traits so the plants could emerge fast and reach to the vegetative stage. The next critical stage is flowering where male and female flowering should be synchronized for the effective pollination. Hence, breeding for reducing anthesis and silking interval (ASI) assumes great significance under rain-fed system (Araus et al., 2012). Positive correlation between ASI and grain yield in maize has been reported previously (Monneveux et al., 2006). During the seed setting stage, the plant survives with the existing soil moisture and maximizes its grain filling efficiency. Green leaves with delayed senescence (stay green) retain the moisture and help better in photosynthesis during grain filling stage (Lee and Tollenaar, 2007). Breeding genotypes with the ability to convert the source to the sink rapidly is another preferable approach, so effective grain filling is possible in shorter duration. Since efficient mining of moisture is vital for survival and reproduction, a better deep root system will be supportive throughout the plant life cycle in rain-fed condition. Breeding medium maturity hybrids by considering the above-mentioned traits is necessary to sustain the productivity.

Maize is also cultivated in high-input irrigated system with assured resources and clear-cut management. The use-efficiency of irrigation water is often low and around 50% of the increase in demand for water could be saved by increasing the effectiveness of irrigation (Seckler et al., 1998). What is necessary in the irrigated system is to reduce the quantity of water per irrigation or to reduce the number of irrigations per crop cycle with optimized water-use-efficiency. The aerial parts of the plant play an important role in deciding water-requirement of the plant. Plant types with better osmotic adjustments (OA) and less evapo-transpiration rate are the efficient ones under this condition. Genotypes that can save the water at least to the tune of 10–20% will greatly reflect in the environmental sustainability. The efforts in reducing the water consumption and improving the environmental sustainability in the irrigated system will also lead to the reduction of carbon foot prints.

On the other hand, it is very difficult to differentiate micro traits such as hormone levels, enzymes, signaling molecules, ROS scavenging mechanisms, etc. and their possible interactions unique to the production systems. Since many drought-associated traits are interrelated across systems, selecting system-specific macro traits by keeping other micro traits in common would be a plausible strategy. Additionally, it is imperative to understand the correlation between drought tolerant genes with grain yield components. While breeding for drought tolerance, caution should be taken since the tolerant genes operating in different pathways may lead to yield penalty. Breaking the negative association between tolerant genes and yield components, if any, is an important strategy to sustain the grain yield in any production system.

UTILIZATION OF MAIZE GERMPLASM

Over 50,000 global maize accessions conserved at several gene banks (Hoisington et al., 1999) including 28,000 accessions in

CIMMYT (http://www.cimmyt.org/germplasm-bank/) explain the quantum of genetic variability available in maize germplasm. The artificial selection over the period of time caused genetic drift and reduced the allelic diversity in the elite gene pool (Xu et al., 2009). It has to be increased by incorporating exotic wild germplasm and landraces into the elite germplasm pool to tape-out the new genes including the stress tolerant genes. Mining novel alleles for drought tolerance from the unutilized germplasm is possible since only 5% of the germplasm is globally used in commercial breeding (Hoisington et al., 1999). Core sets in maize have been developed from different kinds of germplasm to capture the maximum allelic diversity with minimum number of genotypes (Wang et al., 2008; Wen et al., 2012).

Trait-specific core set such as "drought-core" is necessary to exploit the genetic variability that exists in the wild and cultivated germplasm. Phenotyping a large set of genetically diverse maize germplasm under drought stress would be helpful to understand the variability as well as to develop a core set. The "drought-core" could provide an opportunity to identify novel genes using genomic approaches. Additionally, drought tolerant populations in maize have been developed using drought tolerance with good combining ability. Similarly, drought-specific pools have been developed using ASI, leaf senescence, and leaf rolling traits (Edmeades et al., 1999; Monneveux et al., 2006). Such pools are useful for enriching the drought tolerant alleles and genotypes extracted from the pool could be for further used in stress breeding programmes.

ACCELERATED LINE BREEDING

Development of potential parental lines, which is a vital component of a maize breeding programme, is challenging and time consuming process. Through conventional pedigree and bulk methods, 7–8 generations are required to get complete homozygous lines from heterozygous founder stocks. Development of homozygous lines through accelerated line breeding (ALB) approaches is expected to save resources as well as speed-up the product delivery.

Doubled-haploid (DH) production has become a routine technology in maize genetics and breeding (Rober et al., 2005; Geiger and Gordillo, 2009). It is credited with significantly shortening of the breeding cycle by development of completely homozygous lines in two generations as well as simplifying logistics (Geiger and Gordillo, 2009), including requirement of less time, labor, and financial resources; the time and resources thus saved could be potentially channelized for implementing more effective selections and for accelerated release of elite cultivars. Tested genetic stocks are now used for rapid development of homozygous lines. Using Haploid inducers (HI) in maize, only two generations are required to generate homozygous lines (De La Fuente et al., 2013). Earlier, genetic stock 6 was used to produce haploids in maize (Coe, 1959). New generation inducer lines derived from genetic stock 6 with higher induction rates are now available. RWS is one of such inducing lines (Rober et al., 2005) and its sister line RWS-76 (Geiger and Gordillo, 2009) has a haploid induction rate of 8–10% in tropical maize (Prigge et al., 2012). DH technology in maize has become a huge success both in public and private sectors (De La Fuente et al., 2013). The haploid inducers are useful in developing homozygous inbreds from heterozygous and heterogeneous populations, converting male fertile lines into cytoplasmic sterile lines, development of homozygous QTL mapping populations, development of trait mapping panels from landraces, marker-assisted backcross breeding (MABC) and, development of genetic stocks such as isogenic lines and segmental substitution lines.

Rapid generation advancement (RGA) is a new technique to reduce the life cycle of the plant so that inbreds can be rapidly obtained. Unlike DH where lethal alleles also fixed in the population, the population developed from RGS has less likely to contain recessive alleles due to natural and artificial selection. Similar to recombinant inbred line (RIL) development procedure, more recombinant events are allowed in RGA technique. The principle behind the technique is that many generations per year could be obtained by following different strategies. For example, by reducing the life cycle of a full season maize that matures in 100 to 110 days by 30–50%, may enable the breeders to take many crops per year thereby accelerating the line breeding process. In RGA, strategies such as seed treatment, nutrient management, application of hormones, accelerated-flowering, temperature control, breaking seed dormancy, embryo rescue, and combinations thereof are involved in reducing the life cycle. RGA has been attempted in several crops to shorten the breeding cycle (Chickpea-Gaur et al., 2007; Sorghum-Rizal et al., 2014; Rice-Tanaka et al., 2016). Once the RGA technique in maize is standardized, it could play a major role in hybrid breeding programme as well as in rapid generation of genetic stocks for genomics studies.

PRECISION PHENOTYPING

Phenotyping is an integral part of the drought breeding that contributes in understanding the genetics of drought tolerance and product development. The target traits need to be measured rapidly and precisely. Since many component traits of drought tolerance are controlled quantitatively, therefore improving the accuracy of phenotyping has acquired much attention to improve the heritability of the traits. Selection of primary and secondary traits (Monneveux et al., 2008) is the way to achieve drought tolerance in maize. Agronomically important traits such as grain yield and yield contributing traits are the primary traits considered for direct selection. ASI, root architecture and stay green are the important secondary traits to impart drought tolerance and contribute indirectly to yield (Nepolean et al., 2013). Hormones, free-radical scavengers, signaling molecules, enzymes, osmotic adjustment, leaf water potential (Thirunavukkarasu et al., 2014) are the molecular and physiological traits to be included in the selection process. Though the traits are classified in different categories, the agro-morpho-physiological traits should complement to each other for better productivity. Since the yield traits are the manifestation of several secondary traits, identification and selection of traits

that are highly heritable, amenable for HTP phenotyping and positively correlated with yield traits is the key issue to achieve target level of drought tolerance (Maazou et al., 2016).

Precision phenotyping of direct and indirect traits is a challenging task in drought breeding programmes. Plant architecture including primary and secondary traits under drought stress could precisely be phenotyped in controlled conditions through newly emerged high-throughput and non-destructive techniques. Imaging techniques are widely used to phenotype the traits of maize. These have been used to phenotype the whole or specific part/s of the plant. Visible light imaging for whole part of the plant (Grift et al., 2011; Nagel et al., 2012), thermal imaging for whole shoot or leaf tissues (Araus et al., 2012), near infrared imaging for whole part of the plant (Spielbauer et al., 2009; Cook et al., 2012) and 3D imaging for shoot (Klose et al., 2009) have been reported in maize. The "phenotyping under controlled conditions" is helpful in large-scale phenotyping including trait mapping experiments. However, caution needs to be taken while deciphering the solution for drought tolerance since the controlled environment might not mimic the actual field condition as well as be less useful to study the genotype × environment interactions which are very crucial to understand the drought tolerance mechanisms. Alternatively, dynamic phenotyping in the controlled condition could be developed to reflect the actual field conditions. In the dynamic phenotyping the weather parameters are not static but variable all-through the plant life cycle akin to the target production systems.

Remotely-controlled unmanned aerial vehicles (UAVs) with appropriate instruments are also used to phenotype under open-field conditions. UAVs fly on the field and measure the target traits throughout the cropping period. Aerial phenotyping in maize using thermal images provide the normalized difference vegetation index (NDVI) and RGB data which can be further useful to measure a series of traits (Frank et al., 2015; Zaman-Allah et al., 2015).

MAIZE GENOMIC RESOURCES

With the advent of next-generation sequencing (NGS) technologies, genotyping is moving from amplicon-based low-throughput (LTP) to SNP-based high-throughput (HTP) systems (**Figure 1**). The abundance and cost-effective assays made SNP as the preferred marker choice for the genomic studies. The throughput of the SNPs can be modulated based on the purpose of genotyping. High-density SNPs are needed for high resolution fingerprinting, genome-wide association mapping (GWAS) and genomic selection (GS). Low to medium density SNPs are needed for genetic diversity analysis, QTL/trait mapping, marker-assisted selection (MAS), marker-assisted recurrent selection (MARS) and candidate gene-based selections.

Till recent past, NGS-based sequencing technologies were used to capture the SNPs at whole genome level. Now, third-generation sequencing technologies (Jiao and Schneeberger, 2017; Lee et al., in review) have emerged with a capability of generating long-read sequences. Pacific Biosciences (PacBio)

FIGURE 1 | The trends in flow of information in genomics and molecular breeding in the last two decades.

Single Molecule Real Time (SMRT) sequencing, the Illumina Tru-seq Synthetic Long-Read technology and the Oxford Nanopore Technologies sequencing platform offer third-generation chemistries to capture the SNPs. The draft genome of the elite maize inbred line "Ph207" has been recently developed through Illumina Tru-seq Synthetic Long-Read technology (Hirsch et al., 2016).

Whole-genome sequencing will comprehensively reveal the structural architecture of a genome. Genome assemblies of 10 maize lines are available including reference lines B73, W22 and Mo17 (www.maizegdb.org). Close to 40,000 protein coding genes have been identified using B73 genome. The whole-genome sequencing also provides functional information on genes and SNPs. A total of 6,385,011 SNPs from 15 maize inbreds was identified by aligning the respective sequences against the maize reference B73 genome (Xu et al., 2014). Genome-wide SNPs will be eventually used in identification of haplotypes and in genetic mapping. The first generation haplotype map in maize called Hapmap1 was developed in 2009 (Gore et al., 2009) followed by second generation HapMap2 in 2012 (Chia et al., 2012). About 55 million SNPs have been identified in the HapMap2 set which comprises 103 lines from pre-domesticated and domesticated maize varieties. Now, the third generation Hapmap3 is available with the size of 3.83 million SNPs and InDels identified based on 1,218 maize germplasms (Bukowski et al., 2015).

Among restriction enzyme (RE)-based SNP identification, genotype-by-sequencing (GBS) (Elshire et al., 2011) has evolved as a cost-effective HTP method. Identification and utilization of SNPs through GBS have been performed in maize for various purposes. More than 100 SNPs were identified for root traits under drought stress condition from 955,690 SNPs generated though GBS (Zaidi et al., 2016). Genomic prediction of SNPs developed through GBS was studied from a diverse panel of 296 maize inbreds and 504 DH lines (Crossa et al., 2013) by phenotyping in controlled water-stress condition. GBS data has been used in identification of QTLs and SNPs in the maize nested association mapping (NAM) population for ASI and other drought-related traits under water-stress condition (Li et al.,

2016). Through GBS, a total 383,145 putative SNPs have been identified from 21 diverse inbreds (7 flints and 14 dents) to assess the biomass production in maize (Muraya et al., 2015) and 261,055 SNPs were detected in an association mapping panel consisting of 282 genotypes to map tar leaf spot in maize (Cao et al., 2017). Another RE-based low cost rapid SNP discovery is restriction site-associated DNA sequencing (RADseq) (Baird et al., 2008). Using this technique, a total of 14,384 polymorphic SNPs was identified based on 34 maize inbreds (Tamaki et al., 2016).

In 2009, Illumina developed a golden gate assay Illumina® 1536 SNP chip and later it developed a high-density Illumina® MaizeSNP50 Beadchip (Lu et al., 2009; Wu et al., 2014). Using Affymetrix® Axiom® platform, a very high density Maize Genotyping Array has been developed to a level of 600K SNPs (MaizeSNP600K) (Unterseer et al., 2014). A lesser density array was also recently developed from the same platform with a density of 55,229 SNPs which covers variants from both tropical and temperate germplasms (Xu et al., 2017). These SNP chips have been used in genetic characterization of maize inbreds (Lorenz and Hoegemeyer, 2013; Thirunavukkarasu et al., 2013; Tian et al., 2015) and in GWAS (Cook et al., 2012; Li et al., 2013; Thirunavukkarasu et al., 2014).

Pre-selected and validated SNPs are necessary in tracking genotypes in MAS, MARS and GS. KASP™ offers customisable genotyping assay to run selected SNPs in applied breeding programmes (Thompson et al., 2014). A set of 275 SNPs through KASP assay was used to improve the drought tolerance of maize population through MARS (Abdulmalik et al., 2017). Testcross genotypes were selected based on the GEBVs of 1,214 SNPs using KASP assay (Vivek et al., 2017). Array Tape™ by Douglas Scientific, the OpenArray system from Life Technologies and Dynamic Arrays™ from Fluidigm are the other flexible systems available for HTP genotyping of selected SNPs (Thompson et al., 2014).

TRAIT MAPPING

Bi-parental populations such as F_2-derived, RILs, near-isogenic lines (NILs), etc. which follow the principle of linkage are used for coarse and fine mapping of QTLs. QTLs for grain yield and its component traits, ASI, abscisic acid (ABA) were identified under water-stressed conditions using F_2-derived and RIL populations (Lebreton et al., 1995; Agrama and Moussa, 1996; Ribaut et al., 1997; Tuberosa et al., 1998a,b; Frova et al., 1999; Guo et al., 2008; Messmer et al., 2009; Almeida et al., 2013). A meta-QTL approach was used to identify QTLs for grain yield under drought condition from the data of 18 bi-parental mapping populations (Semagn et al., 2013).

Multi-parents population such as GWAS panel are developed by exploiting the principle of linkage disequilibrium (LD) (Thirunavukkarasu et al., 2013). They help in reducing the time taken for population development and provide an opportunity to test more alleles. GWAS is similar to that of fine mapping approach since it has the ability to identify genes when genome-wide SNPs are used in genetically diverse genotypes. GWAS has been employed in maize to understand the inheritance of complex traits. Using a GWAS panel, gene *ZmVPP1*, encoding a vacuolar-type H^+ pyrophosphatase, identified as the most significantly contributing gene to the drought tolerance along with 42 candidate genes by exposing the seedlings to drought stress (Wang et al., 2016). The GWAS results were validated through linkage mapping, expression assays and candidate gene-based mapping experiments to employ the results in the selection programmes. The QTLs identified on chromosome 2, 7, and 8 for tar leaf spot using an association mapping approach were validated through linkage mapping using DH populations (Cao et al., 2017). A combined linkage and association mapping were performed to validate the QTLs for plant height and ear height in maize (Li et al., 2016).

Unequal allele frequencies in the members of GWAS panel produce false-positives which is considered as a major limitation of GWAS approach. The NAM population (Yu et al., 2008) was proposed to overcome the limitations of linkage mapping and association mapping. A large population created by systematic crossing of a common line with many founder lines provides an opportunity to exploit both linkage and linkage-disequilibrium models to map QTLs. NAM population has been used to identify QTLs for flowering time (Buckler et al., 2009), southern leaf blight (Kump et al., 2011), northern leaf blight (Poland et al., 2011) and drought tolerance (Li et al., 2016). MAGIC population (Kover et al., 2009), a balanced multi-parent cross design has been proposed in maize with higher resolution, power and elevated minor allele frequency (Dell'Acqua et al., 2015) against NAM population. The current statistical models based on multi-parent population approaches still have the limitation of including minor alleles in the analysis. New models are needed to include minor alleles present among the genotypes to understand their role in trait expression.

FUNCTIONAL CHARACTERIZATION OF DROUGHT TOLERANCE

Characterizing downstream events of QTLs is important to understand the functional mechanisms of the QTLs. Post transcriptional and post-translational changes have to be looked upon to understand the gene regulation process. mRNAs can be captured by exposing the genotypes under specific drought stress condition and by comparing with the control and/or sensitive genotypes. The differentially expressed genes (DEGs) will be functionally classified and annotated to realize their role in drought tolerance.

RNA sequencing (RNA-Seq) is the HTP NGS technique to sequence and quantify the abundance of mRNAs at whole genome level. RNA-Seq has been performed in various tissues and at different growth stages in maize under water stress condition. DEGs involved in cell wall biosynthesis, transmembrane, ROS scavenging, and ABA have been identified by subjecting the maize seedlings of the RIL population to drought stress (Min et al., 2016). By treating the leaf, stem and root of maize under well-watered and drought-stress conditions, 5,866 DEGs including eight MAPKKK genes responsive to

drought stress have been identified (Liu et al., 2015). They also found that DEGs involved in oxidation, photosynthesis, starch, proline, ethylene, and salicylic acid metabolisms were co-expressed with the MAPKKK genes. Drought treatment to *Zea mays* ssp. *mexicana* L. (a member of teosinte, a wild relative of the *Zea mays* spp. *mays* L.) generated 614 DEGs through RNA-Seq analysis. Functional enrichment analyses showed that these DEGs were related to ABA, trehalose synthesis and ICE1-CBF pathways (Lu et al., 2017). Affymterix GenChip maize genome array, a hybridisation-based technique, comprising 17,555 probes has been used for identification of DEGs under drought stress (Zhang et al., 2010; Thirunavukkarasu et al., 2017). Customized oligo arrays having 1000 genes were used to identify the DEGs under drought stress in maize (Marino et al., 2009). HTP methods opened-up new possibilities to understand the expression of DEGs involved in various pathways under stress condition at genome-scale. The selected drought-responsive DEGs will be systematically validated in an independent set of genotypes, or in candidate-gene mapping experiments to further exploit them in breeding programmes. A set 52 drought–responsive candidate genes collected from the public data base and from the GWAS (Shikha et al., 2017) was validated in five maize hybrids and seven parental lines. Differential regulation and interactions of genes in various biological functions explained the basis of drought tolerance in subtropical maize hybrids (Van Gioi et al., 2017). A set of genes and their characteristics identified for drought tolerance through genomics and functional genomics approaches is presented in **Table 1**.

Small RNAs called micro RNAs are the class of regulatory RNAs and their role in drought stress response through regulating the target mRNAs has been reported in maize. Genome-wide survey of miRNAs provided 150 high-confidence genes within 26 miRNA families (Zhang et al., 2009). A total of 192 mature miRNAs including 68 potential novel miRNA candidates was identified by constructing small RNA libraries at genome-scale from a set of contrasting maize genotypes to drought response. Five of these were differentially expressed under drought stress and played an important role in photosynthesis under drought stress (Sheng et al., 2015). A set of 13 drought-associated miRNA families regulating 42 unique target mRNAs were identified from drought-exposed seedlings of maize. The expression analysis revealed that miRNAs had both positive and negative regulations with their respective target mRNAs under stress (Aravind et al., 2017). RNA-Seq coupled with transcriptome re-assembly, a total of 13,387 long non-coding RNAs (lncRNAs) was identified under water-stress condition using maize seedlings. The identification of non-coding RNAs also revealed the role of epigenetic mechanism responsible for stress tolerance (Forestan et al., 2016).

Information on proteins and post translational modification under drought stress provide better knowledge on trait expression and selection of QTLs/genes for tolerance. Rapid quantification of proteins at genome-level is possible with the help of modern proteomics techniques such as shotgun proteomics [multidimensional protein identification technology (MudPIT)], isotope-code affinity tags (ICATs), targeted mass tags (TMTs), isobaric tags for relative and absolute quantitation (iTRAQ) (Ghatak et al., 2017). A set of 61 drought-associated proteins were identified at eight-leaf stage after exposing the maize plant to drought stress through iTRAQ approach. Functional characterization of these proteins revealed that chaperone proteins, proteases, ethylene responsive proteins and ripening-related proteins played a major role in drought tolerance (Zhao et al., 2016a). Using the same technique, 150 ABA-dependent proteins were identified from a set of ABA-deficient maize mutant Vp5 and its wild-type under drought stress (Zhao et al., 2016b). Using multiplex iTRAQ-based quantitative proteomic and LC-MS/MS methods, 149 differentially phosphorylated peptides were identified at five-leaf stage of maize under drought stress (Hu et al., 2015). Leaf proteome of maize under moderate drought were analyzed by two independent approaches, 2D gel electrophoresis and iTRAQ, revealed the importance of detoxification proteins in drought tolerance (Benešová et al., 2012).

The role of specific proteins have been identified and characterized under drought stress conditions in maize. Up-regulation of RAB 17, phosphoribulokinase, caffeate *O*-methyltransferase, COMT, glutamate semialdehyde aminotransferase (GSAAT), β-glucosidase, chloroplastic fructose bisphosphate aldolase, and ferritin proteins under drought stress condition were identified from the maize leaf tissue (Riccardi et al., 1998). Changes in the expression of oxygen evolving enhancer (OEE) protein 1, malate dehydrogenase and ABA stress ripening (ASR) proteins were identified from the leaf proteome under drought stress (Riccardi et al., 2004). Non accumulation of two isoforms (acidic protein COMT 1 and less acidic protein COMT 2) of caffeic acid/5-hydroxyferulic 3-Omethyltransferase in the drought-stressed maize leaves was identified as the cause for reduced leaf elongation under stress (Vincent et al., 2005).

Metabolites react with environmental changes and are the better candidates to study the drought response. Recent studies indicated that metabolites have a positive correlation with drought tolerance. Metabolic traits could be used as an additional selection tool along with other genomic tools to improve drought tolerance in maize. Gas chromatography-mass spectroscopy (GC-MS)-based metabolite profiling revealed 41 metabolites under drought stress of which glysine and myoinositol were significantly correlated with grain yield in maize (Obata et al., 2015). Tryptophan, proline, histidine, and several intermediates from the TCA cycle analyzed through GC–TOF–MS method showed significant difference in the maize hybrids under drought stress condition. These metabolites also had a strong relationship with phenotypic traits (Witt et al., 2012). A mass spectrometer analysis detected different levels of abscisic acid, jasmonate, salicylic acid, and other hormones in herbicide tolerant maize varieties under control and drought-stress conditions (Benevenuto et al., 2017).

The functional genomics approaches play important role to understand the identification of genes operating in stress tolerant pathways, interaction of key genes in various pathways and contribution of genes to final trait expression under stress condition. Together with genomics, functional genomics approaches are useful in selection of better genotypes in stress breeding programmes.

TABLE 1 | List of drought stress-responsive genes and their characteristics controlling various important traits in maize.

Trait	Gene ID	Gene name	Chr	Gene start	Gene end	Functional mechanism	References
Stomatal regulation	GRMZM2G407181	*nced2*	1	174550907	174553815	ABA-dependent pathway	Iuchi et al., 2001; Thompson et al., 2007
	GRMZM2G089619	*zhd 15*	2	50140925	50142374	ABA-dependent pathway	Davletova et al., 2005
	GRMZM2G053384	*PRC protein*	2	227347436	227349815	RNA binding	Thirunavukkarasu et al., 2014; Van Gioi et al., 2017
	GRMZM2G102429	*u-box*	2	226617615	226619360	Catalytic activity	Thompson et al., 2007; Thirunavukkarasu et al., 2014
	GRMZM5G858784	*nced3*	3	87358369	87360132	ABA-dependent pathway	Iuchi et al., 2001; Thompson et al., 2007
	GRMZM2G159724	*me6*	3	201756751	201761835	Nucleotide binding, protein binding	Thirunavukkarasu et al., 2014; Van Gioi et al., 2017
	GRMZM2G069365	*zhd 17*	4	160153804	160155930	ABA-dependent pathway	Davletova et al., 2005
	GRMZM2G122479	*me2*	6	139464390	139470075	Ion homeostasis-dependent pathway	Laporte et al., 2002
	GRMZM2G161680	*ca5p3*	6	93659875	93665056	Stomatal conductance	Song et al., 2017
	GRMZM2G071112	*zhd 13*	7	112658777	112661470	ABA-dependent pathway	Davletova et al., 2005
Root developoment	GRMZM2G003466	*ereb101*	1	20094963	20096296	Dessication tolerance	Liu et al., 2013
	GRMZM2G124037	*dbf3*	2	194479918	194481002	Dessication tolerance	Liu et al., 2013
	GRMZM2G060465	*ereb155*	4	185036196	185037019	DNA binding	Thirunavukkarasu et al., 2014
	GRMZM2G090576	*nac3*	5	20815035	20817354	Auxin transport	Hund et al., 2009
	GRMZM2G432571	*NBS-IRR partial*	5	20914992	20918282	Nucleotide binding	Thirunavukkarasu et al., 2014; Van Gioi et al., 2017
	GRMZM2G028648	*nac2*	6	115935425	115937455	Auxin transport	Hund et al., 2009
	GRMZM2G104400	*nactf38*	8	102056994	102060989	Auxin transport	Hund et al., 2009
	GRMZM2G134073	*nac68*	8	160424732	160426914	DNA binding	Thirunavukkarasu et al., 2014; Van Gioi et al., 2017
	GRMZM2G015605	*nac1*	10	87283919	87284844	Auxin transport	Hund et al., 2009
	GRMZM2G091819	*Flavin monoxygenase*	10	16522572	16525775	Auxin biosynthesis	Overvoorde et al., 2010
	GRMZM2G371345	*V-type PPase H+ pump*	10	46790874	46793155	Auxin transport	Overvoorde et al., 2010
ROS	GRMZM2G066120	*mkkk11*	1	37470728	37476121	Reactive oxygen species homeostasis	Zhu, 2002
	GRMZM2G172322	*gsr1*	1	12985602	12991971	H_2O_2 metabolism	Galle et al., 2013
	GRMZM2G140667	*apx2*	2	219258176	219261097	Reactive oxygen species homeostasis	Badawi et al., 2004
	GRMZM2G054559	*pld1*	3	12195404	12200349	Phospholipid hydrolysis	Zhu, 2002
	GRMZM2G071021	*aldh3*	3	221771183	221775333	Reactive oxygen species homeostasis	Miao et al., 2006; Chen et al., 2012
	GRMZM2G367411	*mkk6*	5	12679871	12707265	Kinase activity, nucleotide binding	Thirunavukkarasu et al., 2014; Van Gioi et al., 2017
	GRMZM2G059991	*sod3*	6	136070517	136074741	Oxygen radical detoxification	McKersie et al., 1996; Castillejo et al., 2008
	GRMZM2G025992	*sod2*	7	171775019	171778224	Oxygen radical detoxification	McKersie et al., 1996; Castillejo et al., 2008
	GRMZM5G884600	*GPx*	10	138607002	138608876	Catalytic activity	Thirunavukkarasu et al., 2014; Van Gioi et al., 2017
	GRMZM5G822829	*BHLH*	10	138462252	138463015	DNA binding	Thirunavukkarasu et al., 2014; Van Gioi et al., 2017
Hormone Signaling	GRMZM2G083717	*wrky14*	1	299282977	299288556	Sequence-specific DNA binding	Thirunavukkarasu et al., 2014; Van Gioi et al., 2017
	GRMZM2G008250	*NFY-A*	1	174845979	174849344	Sequence-specific DNA binding	Thirunavukkarasu et al., 2014; Van Gioi et al., 2017
	GRMZM2G117851	*bzip1*	3	212179339	212194812	Sequence-specific DNA binding	Thirunavukkarasu et al., 2014; Van Gioi et al., 2017

(Continued)

TABLE 1 | Continued

Trait	Gene ID	Gene name	Chr	Gene start	Gene end	Functional mechanism	References
	GRMZM2G056120	*artf11*	3	196638145	196644110	ABA-inducible TFs triggering stomatal closure	Furihata et al., 2006; Kim et al., 2012
	GRMZM2G172327	*myb14*	7	150087003	150088438	DNA binding,chromatin binding	Thirunavukkarasu et al., 2014; Van Gioi et al., 2017
	GRMZM2G152661	*camta5*	10	109572710	109580177	DNA binding, protein binding	Thirunavukkarasu et al., 2014; Van Gioi et al., 2017
Photosynthesis	GRMZM2G414192	*umc1383*	1	247786615	247788296	Chlorophyll A-B binding protein	Song et al., 2017
	GRMZM2G078409	*ploc2*	2	24166809	24167435	Electron transfer	Efeoglu et al., 2009
	GRMZM2G162200	*rca1*	4	693736	696087	Role in photosynthesis	Rollins et al., 2013
	GRMZM2G162282	*rca3*	4	691410	693139	Role in photosynthesis	Rollins et al., 2013
	GRMZM2G568636	*ferredoxin–nitrite reductase*	4	56335735	56340792	photosynthetic electron transport	Min et al., 2016
	GRMZM2G122337	*Ferredoxin 1*	6	1340417	1341388	Oxidation reduction process	Kimata and Hase, 1989
	GRMZM2G033885	*light harvesting complex photosystem II*	7	157314547	157315990	Photosynthesis antenna2	Min et al., 2016
	GRMZM2G012397	*psa6*	7	5134217	5135120	Photosystem I reaction center 6	Li et al., 2011
	GRMZM2G033208	*Transketolase*	9	22790749	22795294	Carbon fixation in photosynthetic organisms	Min et al., 2016
Sucrose metabolism	GRMZM2G175423	*sodh1*	1	197301249	197304338	Cellulose hydrolysis	Mei et al., 2009
	GRMZM2G391936	*ADP glucose pyrophosphorylase large subunit 1*	1	273514151	273518985	Starch synthesis	Min et al., 2016
	GRMZM2G028353	*cellulose synthase 6*	2	170393027	170398878	Cellulose synthase	Min et al., 2016
	GRMZM2G018241	*Cellulose synthase 9*	2	161757546	161763704	Cellulose synthase	Min et al., 2016
	GRMZM2G130043	*ss5*	4	172635729	172706662	Hydrolysis of sucrose	Ruan et al., 2010
	GRMZM2G122277	*cellulose-synthase like D2*	4	31271742	31278123	Cellulose synthase	Min et al., 2016
	GRMZM2G046587	*pyrophosphorylase 1*	5	200881599	200885907	starch synthesis	Min et al., 2016
	GRMZM2G089836	*invertase2*	5	67537393	67540691	Response to drought stress	Zhang et al., 2017
	GRMZM2G058310	*amyb5*	7	155396510	155399710	Starch degradation	Rizhsky et al., 2004
	GRMZM2G152908	*sus1*	9	122479052	122485725	Sucrose metabolism	Gonzalez et al., 1995
	GRMZM2G016890	*Sbe2A*	10	34240659	34246077	Starch biosynthesis	Hurkman et al., 2003
ABA-mediated ignaling	GRMZM2G057935	*phyC1*	1	277059620	277064623	Signaling network	Sheehan et al., 2004
	AC198979.4_FG009	*ereb95*	1	10988032	10988424	ABA-dependent signaling pathway	Zhang et al., 2017
	GRMZM2G082487	*ZmPP2C-A5*	2	176186305	176187719	ABA signaling	Xiang et al., 2017
	GRMZM2G019819	*ZmPP2C-A8*	2	103675901	103679774	ABA signaling	Xiang et al., 2017
	GRMZM2G059453	*ZmPP2C-A1*	3	180096139	180098099	ABA signaling	Xiang et al., 2017
	GRMZM5G867568	*MAPKK3*	3	111079872	111080021	ABA signaling	Zhang et al., 2012
	GRMZM2G122228	*ZmPP2C-A6*	3	212913668	212919667	ABA signaling	Xiang et al., 2017
	GRMZM2G134628	*ZmPP2C-A11*	3	220928320	220934085	ABA signaling	Xiang et al., 2017
	GRMZM2G112240	*prh1*	4	170944444	170947965	ABA signaling network	Zheng et al., 2010
	GRMZM2G137046	*bzip61*	5	112670143	112675317	ABA signaling	Song et al., 2017
	GRMZM2G066867	*snrkII10*	5	18469442	18472522	ABA signaling network	Schafleitner et al., 2007; Mao et al., 2010
	GRMZM2G177386	*ZmPP2C-A10*	6	161744096	161747484	ABA signaling	Xiang et al., 2017
	GRMZM2G102255	*ZmPP2C-A12*	6	167604993	167607983	ABA signaling	Xiang et al., 2017
	GRMZM2G308615	*ZmPP2C-A4*	7	89059718	89061311	ABA signaling	Xiang et al., 2017
	GRMZM2G069146	*ereb115*	7	141174421	141175245	ABA-dependent signaling pathway	Song et al., 2017

(Continued)

TABLE 1 | Continued

Trait	Gene ID	Gene name	Chr	Gene start	Gene end	Functional mechanism	References
	GRMZM2G305066	*MKKK18*	8	152510200	152511639	Signaling network	Shou et al., 2004
	GRMZM2G166297	*ZmPP2C-A2*	8	168030486	168032471	ABA signaling	Xiang et al., 2017
	GRMZM5G818101	*ZmPP2C-A7*	8	72141439	72143820	ABA signaling	Xiang et al., 2017
	GRMZM2G383807	*ZmPP2CA-13*	8	77501631	77504702	ABA signaling	Xiang et al., 2017
	GRMZM2G180555	*MKKK10*	9	141628047	141638073	Signaling network	Shou et al., 2004
	GRMZM2G159811	*ZmPP2C-A9*	10	101377174	101382475	ABA signaling	Xiang et al., 2017
	GRMZM2G142718	*dof41*	10	147844469	147845926	ABA-dependent signaling pathway	Song et al., 2017
Aquaporins	GRMZM2G081843	*PIP1;4*	4	170004633	170006133	Aquarins	Min et al., 2016
	GRMZM2G154628	*PIP2.1*	5	195239679	195242694	Aquarins	Min et al., 2016
	GRMZM2G137108	*NOD26-like intrinsic protein 4*	6	113136258	113140405	Aquarins	Min et al., 2016
Delayed flowering time	GRMZM2G021777	*col3*	5	183418226	183419769	Delay flowering time	Song et al., 2017
	GRMZM2G004483	*cct2*	9	115786897	115789787	Delay flowering time	Song et al., 2017
Plant development	GRMZM2G336533	*nactf60*	5	2887335	2889124	DNA- binding	Zhang et al., 2017
	GRMZM2G024973	*d9*	5	11793473	11795945	Modulator of plant development	Zhang et al., 2017
	GRMZM2G126566	*myb159*	7	108815110	108818213	DNA binding,chromatin binding	Zhang et al., 2017
	GRMZM2G042666	*C2H2*	7	146276397	146281153	Plant development	Zhang et al., 2017
	GRMZM2G140355	*bzip80*	9	85130086	85132905	Sequence-specific DNA binding	Song et al., 2017
Signal transduction	GRMZM2G466563	–	1	220901789	220904352	Signal transduction	Alam et al., 2010
	GRMZM2G428554	–	1	210641732	210645615	Signal transduction	Perruc et al., 2004

MARKER-BASED SELECTION APPROACHES

QTLs and genes are identified and validated by various trait mapping and functional studies. For the validated QTLs and genes, QTL-flanking and gene-specific markers can be designed. The markers are further used in applied breeding through MAS, MARS and GS to improve the trait expression.

MAS

QTL-based selection techniques largely follow marker-assisted backcrossing (MABC) or MARS. Although several QTL mapping experiments are reported in maize little has been published on the successful introgression of QTLs especially for drought tolerance. A successful MABC programme by introgressing five QTLs for ASI in maize for drought tolerance has been reported (Ribaut and Ragot, 2007).

The success of MAS programmes for drought tolerance depends upon two components: 1. Identification of true QTLs for the component traits, 2. Introgression of the identified QTLs in MAS. Drought is a combination of several quantitative traits with a high level of epistatic and environmental interactions. Quantifying the phenotypic variation explained by the QTLs and their possible interactions are important issues since the effects are confounded with study design, selection of component traits, challenges involved in phenotyping, marker coverage, genotyping, QTL mapping models and so on. Any fluctuation on the above-mentioned factors would significantly alter the QTL numbers and their phenotypic contribution. Apart from this, though true QTLs are identified, practically, chasing too many QTLs through MABC remains a daunting task. So during the introgression programme, transferring one or two major QTLs do not provide the expected level of trait expression since a QTL identified with epistatic interaction lose the effect in the absence of its counterparts. All above-mentioned factors are to be considered while performing QTL mapping experiments since a successful MAS programme depends upon the QTL mapping results.

MARS

MARS allows simultaneous identification and improvement of polygenic traits by stacking favorable alleles at a large number of the loci. MARS can be either used by inter-mating the marker genotypes in random (Hospital et al., 1997; Moreau et al., 1998) or directed recombination of the selected genotypes of a segregating population (Charmet et al., 1999). MARS was successfully employed in maize to improve the complex quantitative traits such as yield and stover quality (Massman et al., 2013) and drought tolerance (Beyene et al., 2015). Through MARS, the number of favorable alleles for the drought tolerance

has been increased from 114 in C_0 to 124 in C_3 (Abdulmalik et al., 2017). The frequency of favorable alleles of drought tolerance was increased from 0.510 at C_0 to 0.515 at C_2 with a genetic gain of 3% by practicing MARS in maize (Bankole et al., 2017).

GS

In the recent past, the genetics of traits was studied with the help of QTLs based on bi-parental mapping populations. This approach provides information on two alleles per locus. Later association mapping approach came up with a possibility of studying several alleles to the range of 30-40 depends upon the genetic variability present in the GWAS panel. Now, we have reached an era from studying a few loci to all loci of the genome (**Figure 1**). The GS models assume that all marker loci of the genome contribute to the trait-expression (Meuwissen et al., 2001) either positively or negatively, so small-effect marker loci will also be effectively included in the model (Heffner et al., 2009; Guo et al., 2012). This approach is quite useful to develop lines with best SNP combinations by combining SNPs from genetically diverse population. The cumulative effect of SNPs called as genomic estimated breeding value (GEBV) decides the expression of the trait. GS has two components: 1. Prediction of GEBVs and 2. Utilization of GEBVs in the selection programme. GEBVs can be predicted with the help of GS models using genome-wide SNPs and comprehensive phenotypic data. The best model was predicted using seven GS models in drought-phenotyped genotypes and compared the GS results with GWAS results (Shikha et al., 2017). Improvement of populations for drought tolerance through GS approach has been already reported in maize. About 7.3% higher grain yield in maize was obtained through GS over conventional selection under drought stress (Beyene et al., 2015). From 10 to 20% of GS was achieved over conventional phenotypic selection under drought conditions in the testcrosses from bi-parental populations using 1,214 SNP markers (Vivek et al., 2017).

The combination of ALB with GS selection approaches is expected to reduce the breeding cycles and deliver the products rapidly in maize (**Figure 2**). The lines developed from ALB approach would feed back to the GS selection cycle to generate GEBVs. The GEBVs in turn would help in selection of better lines with drought tolerance developed through ALB. The selected elite lines would be used in hybrid breeding programme to develop drought-tolerant high-yielding hybrids.

GENOME EDITING

Targeted genome editing is the latest approach to manipulate the gene function. Of several approaches, clustered regularly interspaced short palindromic repeats (CRISPR) and CRISPR-associated protein9 nuclease (Cas9) are the effective genome editing technologies used in plant system (Gasiunas et al., 2012; Cong et al., 2013). Several modifications to the CRISPR/Cas9 system are now available for site-directed modifications such as truncated-gRNAs (tru-gRNAs) with no off-target effect (Osakabe et al., 2016). Zinc-finger nuclease (Kim et al., 1996) and transcription activator-like effector nucleases (TALENS) (Boch et al., 2009; Moscou and Bogdanove, 2009) are the other techniques used in editing the genes.

Through genome editing approaches, point mutation (deletion or insertion), gene knockouts, activation or repression of genes and epigenetic changes are possible (Kamburova et al., 2017). Many gene editing experiments are successful since the

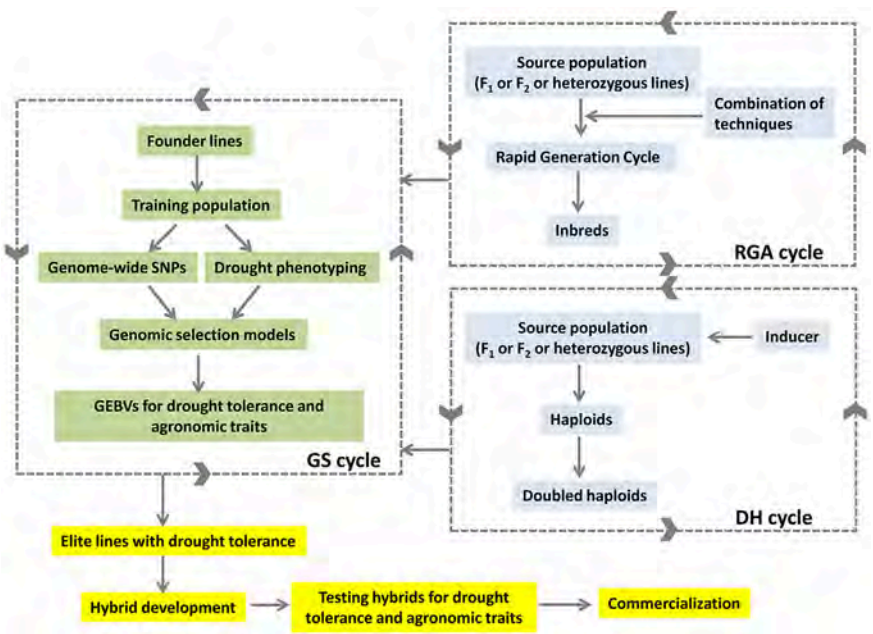

FIGURE 2 | Accelerated development of drought tolerant hybrids by combining DH, RGA and GS approaches.

target traits are governed by a single gene. In maize upstream of the liguleless1 (LIG1) gene, male fertility genes (Ms26 and Ms45), and acetolactate synthase (ALS) genes (ALS1 and ALS2) have been successfully altered through targeted mutagenesis, precise gene editing, and site-specific gene insertion using Cas9 and guide RNA (Svitashev et al., 2015). A CRISPR/Cas9 binary vector set was developed as a toolkit to perform multiplex genome editing in a variety of plant species including maize (Xing et al., 2014). Biolistic delivery of pre-assembled Cas9–gRNA ribonucleoproteins into embryo cells, and DNA- and selectable marker-free recovery of plants with mutated alleles at high frequencies was demonstrated in maize (Svitashev et al., 2016). Recently, RNA editing using programmable single-effector RNA-guided RNases Cas13 has been reported (Cox et al., 2017). Through RNA editing the structure of the DNA remains intact whereas the function of genes is altered. The utility of RNA editing is yet to be explored in maize for drought tolerance.

Genome editing is currently akin to MAS where one or few genes are being modified for a given trait. Since drought tolerance is a complex trait, many genes need to be targeted to achieve the desired level of tolerance. Mutant lines can be created for various drought-responsive genes and through pyramiding approaches those genes can be introgressed into a single genotype. However, pyramiding approach is laborious and resource intensive. Hence, up-gradation or modification in the existing genome editing approaches is needed to alter several genes operating in various pathways in a genome at one go. Such an advanced approach will be useful to manipulate several target genes of individual and component traits to develop drought tolerant genotypes rapidly.

Combining genomics and gene editing techniques would accelerate the trait improvement at desired level. Through genomics one can understand the structure and function of the genes that are controlling simple and complex traits. The number, location, phenotypic contribution of genes to the trait expression should be elucidated in advance in order to use them in genome editing approaches. Since drought is controlled by several genes with variable level of phenotypic expression the epistatic interactions of genes should be thoroughly studied. This would help in selecting combination of genes to be targeted for editing experiment. Selection of genes that are working in tandem would be a good option for trait improvement program rather working on individual genes to realize improved genetic gain. Identification of candidate genes for drought through genomics followed by editing of those target genes is necessary to improve the genetic gain rapidly.

GENOME AND BREEDING INFORMATICS, AND BIG-DATA

The cost-effective ever-growing genomics approaches generated data in the form of DNA and RNA sequences, proteins, metabolites and etc. to the scale of 100's of terabytes. The large scale data produced from such genomic techniques is called as "Big data." The large-scale genomics data will pose computational challenges thus new techniques need to be developed (Stephens et al., 2015). The management of big data includes storage, compilation, curation, processing, complex data analyses, visualization, retrieval and sharing. High-power local server- or cloud-based computing systems are necessary to manage the big data.

The genome-level big data developed from omics techniques are complementary to each other to understand the structural architecture of genome and functional complexities of gene regulation at intra and inter species level. Customised informatics platforms are needed to integrate the big data to get meaningful information and decisions. Genomics Open-source Breeding Informatics Initiative (GOBII) is one of such open-source platforms to develop and implement genomics data management tools (http://cbsugobii05.tc.cornell.edu/wordpress/).

The decisions from the big data will be exploited in the applied breeding programmes such as MAS, MARS, and GS. These selection programmes have several activities including phenotyping, genotyping, backcross breeding, testing the product and etc. Breeding informatics tools play handy to streamline the activities of the selection programmes and help in effective management of the breeding processes.

Integration of big data management tools, decision making tools and down-stream molecular breeding activities are become necessary to practice the next-generation breeding efficiently and to accelerate the product delivery. Various commercial and open-source platforms are available to combine genomics, data management and breeding activities. Integrated Breeding Platform (www.integratedbreeding.net) has provided various informatics tools to manage genomics and breeding data. Complex trait breeding such as drought tolerance will be benefitted when various genomics, novel breeding, and informatics tools are combined effectively (**Figure 3**).

CONCLUSIONS

Breeding for climate-resilient drought tolerant maize is important owing to changing climatic conditions. Though it is an important trait, but its complex inheritance poses a major challenge to the researchers. Several morpho-physiological traits have been reported for drought tolerance in maize. Since maize growing in different agro-climatic conditions, system-specific approach would be relevant to choose target traits for improvement. Genomics and breeding tools have come-up in the last two decades for better understanding of the inheritance of traits. Cost-effective third-generation sequencing technologies are now available to capture the SNPs as well as customize the genotyping. The identification and functional characterization of genes involved in various drought tolerance mechanisms can be performed with the help of expression and protein assays. Combining approaches such as DH technology with GS would be useful to accelerate the drought breeding in maize. The genomics and breeding approaches should be sufficiently complemented and supported with sophisticated informatics tools. Big data management and informatics tools have become necessary in applied breeding programmes. Genome editing approaches are going to play a big role in future in developing customized genotypes for the target environment. Identification of key genes

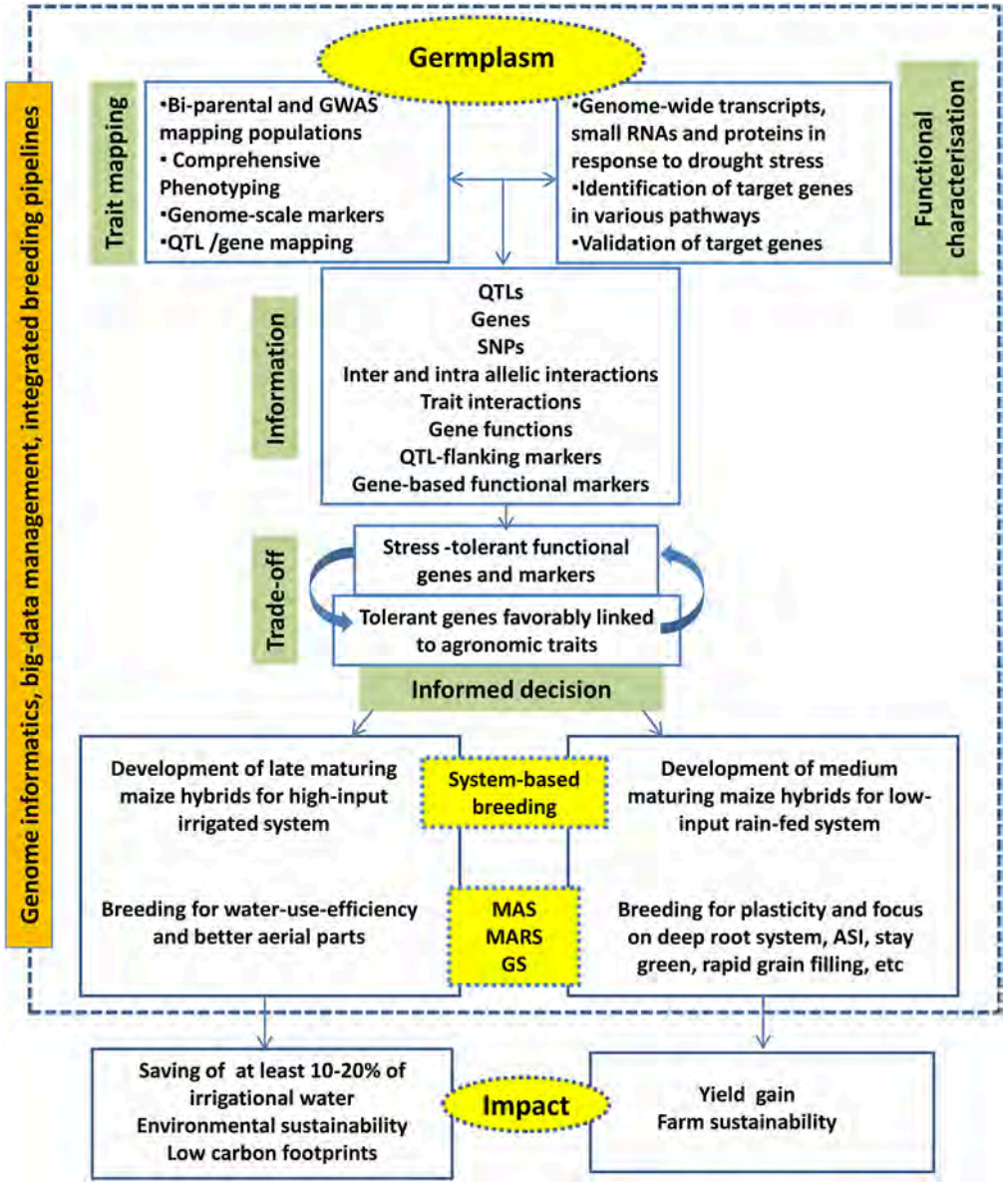

FIGURE 3 | The next generation drought breeding involves utilization of various genome-level techniques, decision from different informatics pipelines to deliver products for system-specific hybrids.

operating in different pathways through QTL/gene mapping and gene expression assays remains important to exploit them in genome editing experiments. The editing of target genes could provide desired level of drought tolerance and sustain the grain yield in hybrids for different production systems. Although several advancements have happened in the field of genomics, knowledge on inter- and intra -allelic interactions need to be focussed to improve the heritability. In order to maximise the genetic gain in the selection programmes for drought tolerance, focus has to be given to elucidate the inter-trait interaction at molecular level. Precision breeding of drought tolerant maize hybrids is possible by strategic integration of modern genomics approaches with advanced breeding methods.

AUTHOR CONTRIBUTIONS

TN conceived the concept; TN, JK, GM, and SM wrote the manuscript.

ACKNOWLEDGMENTS

The corresponding author was funded by the Computational Biology and Agricultural Bioinformatics (Agril.Edn.14(44)/2014-A&P) and the ICAR Network Project on Transgenics in Crop Plants (Maize Functional Genomics Component, 21-22). The funders had no role in study design, data collection and analysis, decision to publish, or preparation of the manuscript.

REFERENCES

Abdulmalik, R. O., Menkir, A., Meseka, S. K., Unachukwu, N., Ado, S. G., Olarewaju, J. D., et al. (2017). Genetic gains in grain yield of a maize population improved through marker assisted recurrent selection under stress and non-stress conditions in West Africa. *Front. Plant Sci.* 8:841. doi: 10.3389/fpls.2017.00841

Agrama, H. A., and Moussa, M. E. (1996). Mapping QTLs in breeding for drought tolerance in maize (*Zea mays L.*). *Euphytica* 91, 89–97. doi: 10.1007/BF00035278

Alam, M. M., Sharmin, S., Nabi, Z., Mondal, S. I., Islam, M. S., Nayeem, S. B., et al. (2010). A putative leucine-rich repeat receptor-like kinase of jute involved in stress response. *Plant Mol. Biol. Report.* 28, 394–402. doi: 10.1007/s11105-009-0166-4

Almeida, G. D., Makumbi, D., Magorokosho, C., Nair, S., Borém, A., Ribaut, J. M., et al. (2013). QTL mapping in three tropical maize populations reveals a set of constitutive and adaptive genomic regions for drought tolerance. *Theor. Appl. Genet.* 126, 583–600. doi: 10.1007/s00122-012-2003-7

Araus, J. L., Serret, M. D., and Edmeades, G. O. (2012). Phenotyping maize for adaptation to drought. *Front. Physiol.* 3:305. doi: 10.3389/fphys.2012.00305

Aravind, J., Rinku, S., Pooja, B., Shikha, M., Kaliyugam, S., Mallikarjuna, M. G., et al. (2017). Identification, characterization, and functional validation of drought-responsive microRNAs in subtropical maize inbreds. *Front. Plant Sci.* 8:941. doi: 10.3389/fpls.2017.00941

Badawi, G. H., Kawano, N., Yamauchi, Y., Shimada, E., Sasaki, R., Kubo, A., et al. (2004). Over-expression of ascorbate peroxidase in tobacco chloroplasts enhances the tolerance to salt stress and water deficit. *Physiol. Plant.* 121, 231–238. doi: 10.1111/j.0031-9317.2004.00308.x

Baird, N. A., Etter, P. D., Atwood, T. S., Currey, M. C., Shiver, A. L., Lewis, Z. A., et al. (2008). Rapid SNP discovery and genetic mapping using sequenced RAD markers. *PLoS ONE* 3:e3376. doi: 10.1371/journal.pone.0003376

Bankole, F., Menkir, A., Olaoye, G., Crossa, J., Hearne, S., Unachukwu, N., et al. (2017). Genetic gains in yield and yield related traits under drought stress and favorable environments in a maize population improved using marker assisted recurrent selection. *Front. Plant Sci.* 8:808. doi: 10.3389/fpls.2017.00808

Benešová, M., Holá, D., Fischer, L., Jedelský, P. L., Hnilička, F., Wilhelmová, N., et al. (2012). The physiology and proteomics of drought tolerance in Maize: early stomatal closure as a cause of lower tolerance to short-term dehydration? *PLoS ONE* 7:e38017. doi: 10.1371/journal.pone.0038017

Benevenuto, R. F., Agapito-Tenfen, S. Z., Vilperte, V., Wikmark, O. G., van Rensburg, P. J., and Nodari, R. O. (2017). Molecular responses of genetically modified maize to abiotic stresses as determined through proteomic and metabolomic analyses. *PLoS ONE* 12:e0173069. doi: 10.1371/journal.pone.0173069

Beyene, Y., Semagn, K., Mugo, S., Tarekegne, A., Babu, R., Meisel, B., et al. (2015). Genetic gains in grain yield through genomic selection in eight bi-parental maize populations under drought stress. *Crop Sci.* 55, 154–163. doi: 10.2135/cropsci2014.07.0460

Boch, J., Scholze, H., Schornack, S., Landgraf, A., Hahn, S., Kay, S., et al. (2009). Breaking the code of DNA binding specificity of TAL-Type III Effectors. *Science* 80, 1509–1512. doi: 10.1126/science.1178811

Buckler, E. S., Holland, J. B., Bradbury, P. J., Acharya, C. B., Brown, P. J., Browne, C., et al. (2009). The genetic architecture of maize flowering time. *Science* 80, 714–718. doi: 10.1126/science.1174276

Bukowski, R., Guo, X., Lu, Y., Zou, C., He, B., Rong, Z., et al. (2015). Construction of the third generation *Zea mays* haplotype map. *bioRxiv* 26963. doi: 10.1101/026963

Cao, S., Loladze, A., Yuan, Y., Wu, Y., Zhang, A., Chen, J., et al. (2017). Genome-wide analysis of tar spot complex resistance in maize using genotyping-by-sequencing SNPs and whole-genome prediction. *Plant Genome* 10, 1–14. doi: 10.3835/plantgenome2016.10.0099

Castillejo, M. Á., Maldonado, A. M., Ogueta, S., and Jorrín, J., V (2008). Proteomic analysis of responses to drought stress in sunflower (*Helianthus annuus*) leaves by 2DE gel electrophoresis and mass spectrometry. *Open Proteomics J.* 1, 59–71. doi: 10.2174/1875039700801010059

Charmet, G., Robert, N., Perretant, M. R., Gay, G., Sourdille, P., Groos, C., et al. (1999). Marker-assisted recurrent selection for cumulating additive and interactive QTLs in recombinant inbred lines. *Theor. Appl. Genet.* 99, 1143–1148. doi: 10.1007/s001220051318

Chen, L., Song, Y., Li, S., Zhang, L., Zou, C., and Yu, D. (2012). The role of WRKY transcription factors in plant abiotic stresses. *Biochim. Biophys. Acta* 1819, 120–128. doi: 10.1016/j.bbagrm.2011.09.002

Chia, J. M., Song, C., Bradbury, P. J., Costich, D., de Leon, N., Doebley, J., et al. (2012). Maize HapMap2 identifies extant variation from a genome in flux. *Nat. Genet.* 44, 803–807. doi: 10.1038/ng.2313

Coe, E. H. (1959). A line of maize with high haploid frequency. *Am. Nat.* 93, 381–382. doi: 10.1086/282098

Cong, L., Ran, F. A., Cox, D., Lin, S., Barretto, R., Habib, N., et al. (2013). Multiplex genome engineering using CRISPR/Cas systems. *Science* 339, 819–823. doi: 10.1126/science.1231143

Cook, J. P., McMullen, M. D., Holland, J. B., Tian, F., Bradbury, P., Ross-Ibarra, J., et al. (2012). Genetic architecture of maize kernel composition in the nested association mapping and inbred association panels. *Plant Physiol.* 158, 824–834. doi: 10.1104/pp.111.185033

Cox, D. B. T., Gootenberg, J. S., Abudayyeh, O. O., Franklin, B., Kellner, M. J., Joung, J., et al. (2017). *Science* 358, 1019–1027. doi: 10.1126/science.aaq0180

Crossa, J., Beyene, Y., Kassa, S., Pérez, P., Hickey, J. M., Chen, C., et al. (2013). Genomic prediction in maize breeding populations with genotyping-by-sequencing. G3 3, 1903–1926. doi: 10.1534/g3.113.008227

Davletova, S., Schlauch, K., Coutu, J., and Mittler, R. (2005). The zinc-finger protein Zat12 plays a central role in reactive oxygen and abiotic stress signaling in arabidopsis. *Plant Physiol.* 139, 847–856. doi: 10.1104/pp.105.068254

Dell'Acqua, M., Gatti, D. M., Pea, G., Cattonaro, F., Coppens, F., Magris, G., et al. (2015). Genetic properties of the MAGIC maize population: a new platform for high definition QTL mapping in *Zea mays*. *Genome Biol.* 16:167. doi: 10.1186/s13059-015-0716-z

De La Fuente, G. N., Frei, U. K., and Lübberstedt, T. (2013). Accelerating plant breeding. *Trends Plant Sci.* 18, 667–672. doi: 10.1016/j.tplants.2013.09.001

Edmeades, G. (2008). *Drought tolerance in maize: an emerging reality. A Feature In James, Clive. 2008. Global Status of Commercialized Biotech/GM Crops: 2008. Glob. Status Commer. Biotech/GM Crop. ISAAA Br. No. 39*. Available online at: http://www.salmone.org/wp-content/uploads/2009/02/droughtmaize.pdf

Edmeades, G. O., Bolaños, J., Chapman, S. C., Lafitte, H. R., and Bänziger, M. (1999). Selection improves drought tolerance in tropical maize populations: I. gains in biomass, grain yield, harvest index. *Crop Sci.* 39, 1306–1315. doi: 10.2135/cropsci1999.3951306x

Efeoglu, B., Ekmekci, Y., and Cicek, N. (2009). Physiological responses of three maize cultivars to drought stress and recovery. *South Afr.J. Bot.* 75, 34–42. doi: 10.1016/j.sajb.2008.06.005

Elshire, R. J., Glaubitz, J. C., Sun, Q., Poland, J. A., Kawamoto, K., Buckler, E. S., et al. (2011). A robust, simple genotyping-by-sequencing (GBS) approach for high diversity species. *PLoS ONE* 6:e19379. doi: 10.1371/journal.pone.0019379

Forestan, C., Aiese Cigliano, R., Farinati, S., Lunardon, A., Sanseverino, W., Varotto, S., et al. (2016). Stress-induced and epigenetic-mediated maize transcriptome regulation study by means of transcriptome reannotation and differential expression analysis. *Sci. Rep.* 6:30446. doi: 10.1038/srep30446

Frova, C., Krajewski, P., di Fonzo, N., Villa, M., and Sari-Gorla, M. (1999). Genetic analysis of drought tolerance in maize by molecular markers I. Yield components. *Theor. Appl. Genet.* 99, 280–288. doi: 10.1007/s001220051233

Furihata, T., Maruyama, K., Fujita, Y., Umezawa, T., Yoshida, R., Shinozaki, K., et al. (2006). Abscisic acid-dependent multisite phosphorylation regulates the activity of a transcription activator AREB1. *Proc. Natl. Acad. Sci .U.S.A.* 103, 1988–1993. doi: 10.1073/pnas.0505667103

Gallé, Á., Csiszar, J., Benyo, D., Laskay, G., Leviczky, T., Erdei, L., et al. (2013). Isohydric and anisohydric strategies of wheat genotypes under osmotic stress: biosynthesis and function of ABA in stress responses. *J. Plant Physiol.* 170, 1389–1399. doi: 10.1016/j.jplph.2013.04.010

Gasiunas, G., Barrangou, R., Horvath, P., and Siksnys, V. (2012). Cas9-crRNA ribonucleoprotein complex mediates specific DNA cleavage for adaptive immunity in bacteria. *Proc. Natl. Acad. Sci. U.S.A.* 109, E2579–E2586. doi: 10.1073/pnas.1208507109

Gaur, P. M., Srinivasan, S., Gowda, C. L. L., and Rao, B. V (2007). Rapid generation advancement in chickpea. *J. SAT Agric. Res.* 3, 1–3.

Geiger, H. H., and Gordillo, G. A. (2009). Double haploids in hybrid maize breeding. *Maydica* 54, 485–499.

Ghatak, A., Chaturvedi, P., and Weckwerth, W. (2017). Cereal crop proteomics: systemic analysis of crop drought stress responses towards marker-assisted selection breeding. *Front. Plant Sci.* 8:757. doi: 10.3389/fpls.2017.00757

Gonzalez, E. M., Gordon, A. J., James, C. L., and Arrese-lgor, C. (1995). The role of sucrose synthase in the response of soybean nodules to drought. *J. Exp. Bot.* 46, 1515–1523. doi: 10.1093/jxb/46.10.1515

Gore, M. A., Chia, J.-M., Elshire, R. J., Sun, Q., Ersoz, E. S., Hurwitz, B. L., et al. (2009). A first-generation haplotype map of maize. *Science* 80, 1115–1117. doi: 10.1126/science.1177837

Grift, T. E., Novais, J., and Bohn, M. (2011). High-throughput phenotyping technology for maize roots. *Biosyst. Eng.* 110, 40–48. doi: 10.1016/j.biosystemseng.2011.06.004

Guo, J., Su, G., Zhang, J., and Wang, G. (2008). Genetic analysis and QTL mapping of maize yield and associate agronomic traits under semi-arid land condition. *Afr. J. Biotechnol.* 7, 1829–1838. doi: 10.5897/AJB2008.000-5031

Guo, Z., Tucker, D. M., Lu, J., Kishore, V., and Gay, G. (2012). Evaluation of genome-wide selection efficiency in maize nested association mapping populations. *Theor. Appl. Genet.* 124, 261–275. doi: 10.1007/s00122-011-1702-9

Heffner, E. L., Sorrells, M. E., and Jannink, J. (2009). Genomic selection for crop improvement. *Crop Sci.* 49, 1–12. doi: 10.2135/cropsci2008.08.0512

Hirsch, C. N., Hirsch, C. D., Brohammer, A. B., Bowman, M. J., Soifer, I., Barad, O., et al. (2016). Draft assembly of elite inbred line PH207 provides insights into genomic and transcriptome diversity in maize. *Plant Cell* 28, 2700–2714. doi: 10.1105/tpc.16.00353

Hoisington, D., Khairallah, M., Reeves, T., Ribaut, J. M., Skovmand, B., Taba, S., et al. (1999). Plant genetic resources: what can they contribute toward increased crop productivity? *Proc. Natl. Acad. Sci. U.S.A.* 96, 5937–5943. doi: 10.1073/pnas.96.11.5937

Hospital, F., Moreau, L., Lacoudre, F., Charcosset, A., and Gallais, A. (1997). More on the efficiency of marker-assisted selection. *Theor. Appl. Genet.* 95, 1181–1189. doi: 10.1007/s001220050679

Hu, X., Wu, L., Zhao, F., Zhang, D., Li, N., Zhu, G., et al. (2015). Phosphoproteomic analysis of the response of maize leaves to drought, heat and their combination stress. *Front. Plant Sci.* 6:298. doi: 10.3389/fpls.2015.00298

Hund, A., Trachsel, S., and Stamp, P. (2009). Growth of axile and lateral roots of maize: I development of a phenotying platform. *Plant Soil* 325, 335–349. doi: 10.1007/s11104-009-9984-2

Hurkman, W. J., McCue, K. F., Altenbach, S. B., Korn, A., Tanaka, C. K., Kothari, K. M., et al. (2003). Effect of temperature on expression of genes encoding enzymes for starch biosynthesis in developing wheat endosperm. *Plant Sci.* 164, 873–881. doi: 10.1016/S0168-9452(03)00076-1

Iuchi, S., Kobayashi, M., Taji, T., Naramoto, M., Seki, M., Kato, T., et al. (2001). Regulation of drought tolerance by gene manipulation of 9-cis-epoxycarotenoid dioxygenase, a key enzyme in abscisic acid biosynthesis in Arabidopsis. *Plant J.* 27, 325–333. doi: 10.1046/j.1365-313x.2001.01096.x

Jiao, W. B., and Schneeberger, K. (2017). The impact of third generation genomic technologies on plant genome assembly. *Curr. Opin. Plant Biol.* 36, 64–70. doi: 10.1016/j.pbi.2017.02.002

Kamburova, V. S.,Nikitina, E. V., Shermatov, S. E., Buriev, Z. T., Kumpatla, S. P., Emani, C., et al. (2017). Genome editing in plants: an overview of tools and applications. *Int. J. Agron.* 2017:15. doi: 10.1155/2017/7315351

Kim, M. J., Park, M.-J., Seo, P. J., Song, J.-S., Kim, H.-J., and Park, C.-M. (2012). Controlled nuclear import of the transcription factor NTL6 reveals a cytoplasmic role of SnRK2.8 in the drought-stress response. *Biochem. J.* 448, 353–363. doi: 10.1042/BJ20120244

Kim, Y. G., Cha, J., and Chandrasegaran, S. (1996). Hybrid restriction enzymes: zinc finger fusions to Fok I cleavage domain. *Proc. Natl. Acad. Sci. U.S.A.* 93, 1156–1160. doi: 10.1073/pnas.93.3.1156

Kimata, Y., and Hase, T. (1989). Localization of ferredoxin isoproteins in mesophyll and bundle sheath cells in maize leaf. *Plant Physiol.* 89, 1193–1197. doi: 10.1104/pp.89.4.1193

Klose, R., Penlington, J., and Ruckelshausen, A. (2009). Usability of 3D time-of-flight cameras for automatic plant phenotyping. *Bornimer Agrartech. Berichte* 69, 93–105.

Kover, P. X., Valdar, W., Trakalo, J., Scarcelli, N., Ehrenreich, I. M., Purugganan, M. D., et al. (2009). A multiparent advanced generation inter-cross to fine-map quantitative traits in *Arabidopsis thaliana*. *PLoS Genet.* 5:e1000551. doi: 10.1371/journal.pgen.1000551

Kump, K. L., Bradbury, P. J., Wisser, R. J., Buckler, E. S., Belcher, A. R., Oropeza-Rosas, M. A., et al. (2011). Genome-wide association study of quantitative resistance to southern leaf blight in the maize nested association mapping population. *Nat. Genet.* 43, 163–168. doi: 10.1038/ng.747

Laporte, M. M., Shen, B., and Tarczynski, M. C. (2002). Engineering for drought avoidance: expression of maize NADP malic enzyme in tobacco results in altered stomatal function. *J. Exp. Bot.* 53, 699–705. doi: 10.1093/jexbot/53.369.699

Lebreton, C., Lazic-Jancic, V., Steed, A., Pekic, S., and Quarrie, S. A. (1995). Identification of QTL for drought responses in maize and their use in testing causal relationships between traits. *J. Exp. Bot.* 46:853. doi: 10.1093/jxb/46.7.853

Lee, E. A., and Tollenaar, M. (2007). Physiological basis of successful breeding strategies for maize grain yield. *Crop Sci.* 47(Suppl. 3):S-202–S-215. doi: 10.2135/cropsci2007.04.0010IPBS

Li, C., Li, Y., Sun, B., Peng, B., Liu, C., Liu, Z., et al. (2013). Quantitative trait loci mapping for yield components and kernel-related traits in multiple connected RIL populations in maize. *Euphytica* 193, 303–316. doi: 10.1007/s10681-013-0901-7

Li, J., Zhang, Y., Gu, J., Guo, C., Wen, S., Liu, G., et al. (2011). Molecular characterization and roles of AP2 transcription factors on drought tolerance in plants. *Front. Agric. China* 5, 463–472. doi: 10.1007/s11703-011-1148-5

Li, X., Zhou, Z., Ding, J., Wu, Y., Zhou, B., Wang, R., et al. (2016). Combined linkage and association mapping reveals qtl and candidate genes for plant and ear height in maize. *Front. Plant Sci.* 7:833. doi: 10.3389/fpls.2016.00833

Liebisch, F., Kirchgessner, N., Schneider, D., Walter, A., and Hund, A. (2015). Remote, aerial phenotyping of maize traits with a mobile multi-sensor approach. *Plant Methods* 11, 9. doi: 10.1186/s13007-015-0048-8

Liu, S., Wang, X., Wang, H., Xin, H., Yang, X., Yan, J., et al. (2013). Genome-wide analysis of ZmDREB genes and their association with natural variation in drought tolerance at seedling stage of *Zea mays* L. *PLoS Genet.* 9:e1003790. doi: 10.1371/journal.pgen.1003790

Liu, Y., Zhou, M., Gao, Z., Ren, W., Yang, F., He, H., et al. (2015). RNA-seq analysis reveals MAPKKK family members related to drought tolerance in maize. *PLoS ONE* 10:0143128. doi: 10.1371/journal.pone.0143128

Lorenz, A., and Hoegemeyer, T. (2013). The phylogenetic relationships of US maize germplasm. *Nat. Genet.* 45, 844–845. doi: 10.1038/ng.2697

Lu, G., Gao, C., Zheng, X., and Han, B. (2009). Identification of OsbZIP72 as a positive regulator of ABA response and drought tolerance in rice. *Planta* 229, 605–615. doi: 10.1007/s00425-008-0857-3

Lu, X., Zhou, X., Cao, Y., Zhou, M., McNeil, D., Liang, S., et al. (2017). RNA-seq analysis of cold and drought responsive transcriptomes of *Zea mays* ssp. *mexicana L. Front. Plant Sci.* 8:136. doi: 10.3389/fpls.2017.00136

Maazou, A. S., Jialu, T., Qiu, J., and Liu, Z. (2016). Breeding for drought tolerance in maize (*Zea mays* L.). *Am. J. Plant Sci.* 7:13. doi: 10.4236/ajps.2016.714172

Mao, X., Zhang, H., Tian, S., Chang, X., and Jing, R. (2010). TaSnRK2.4, an SNF1-type serine/threonine protein kinase of wheat (*Triticum aestivum* L.), confers enhanced multistress tolerance in Arabidopsis. *J. Exp. Bot.* 61, 683–696. doi: 10.1093/jxb/erp331

Marino, R., Ponnaiah, M., Krajewski, P., Frova, C., Gianfranceschi, L., Pè, M. E., et al. (2009). Addressing drought tolerance in maize by transcriptional profiling and mapping. *Mol. Genet. Genomics* 281, 163–179. doi: 10.1007/s00438-008-0401-y

Massman, J. M., Jung, H. J. G., and Bernardo, R. (2013). Genomewide selection versus marker-assisted recurrent selection to improve grain yield and stover-quality traits for cellulosic ethanol in maize. *Crop Sci.* 53, 58–66. doi: 10.2135/cropsci2012.02.0112

McKersie, B. D., Bowley, S. R., Harjanto, E., and Leprince, O. (1996). Water-deficit tolerance and field performance of transgenic alfalfa overexpressing superoxide dismutase. *Plant Physiol.* 111, 1177–1181. doi: 10.1104/pp.111.4.1177

Mei, C., Park, S. H., Sabzikar, R., Qi, C., Ransom, C., and Sticklen, M. (2009). Green tissue-specific production of a microbial endo-cellulase in maize (*Zea mays* L.) endoplasmic-reticulum and mitochondria converts cellulose into fermentable sugars. *J. Chem. Technol. Biotechnol.* 84, 689–695. doi: 10.1002/jctb.2100

Messmer, R., Fracheboud, Y., Bänziger, M., Vargas, M., Stamp, P., and Ribaut, J. M. (2009). Drought stress and tropical maize: QTL-by-environment interactions and stability of QTLs across environments for yield components and secondary traits. *Theor. Appl. Genet.* 119, 913–930. doi: 10.1007/s00122-009-1099-x

Meuwissen, T. H., Hayes, B. J., and Goddard, M. E. (2001). Prediction of total genetic value using genome-wide dense marker maps. *Genetics* 157, 1819–1829.

Mhike, X., Okori, P., Magorokosho, C., and Ndlela, T. (2012). Validation of the use of secondary traits and selection indices for drought tolerance in tropical maize (*Zea mays* L.). *Afr. J. Plant Sci.* 6, 96–102. doi: 10.5897/AJPS11.179

Miao, Y., Lv, D., Wang, P., Wang, X.-C., Chen, J., Miao, C., et al. (2006). An Arabidopsis glutathione peroxidase functions as both a redox transducer and a scavenger in abscisic acid and drought stress responses. *Plant Cell* 18, 2749–2766. doi: 10.1105/tpc.106.044230

Min, H., Chen, C., Wei, S., Shang, X., Sun, M., Xia, R., et al. (2016). Identification of drought tolerant mechanisms in maize seedlings based on transcriptome analysis of recombination inbred lines. *Front. Plant Sci.* 7:1080. doi: 10.3389/fpls.2016.01080

Monneveux, P., Sanchez, C., and Tiessen, A. (2008). Future progress in drought tolerance in maize needs new secondary traits and cross combinations. *J. Agric. Sci.* 146, 287–300. doi: 10.1017/S0021859608007818

Monneveux, P., Sánchez, C., Beck, D., and Edmeades, G. O. (2006). Drought tolerance improvement in tropical maize source populations: evidence of progress. *Crop Sci.* 46, 180–191. doi: 10.2135/cropsci2005.04-0034

Moreau, L., Charcosset, A., Hospital, F., and Gallais, A. (1998). Marker-assisted selection effciency in populations of finite size. *Genetics* 148, 1353–1365.

Moscou, M. J., and Bogdanove, A. J. (2009). A simple cipher governs dna recognition by TAL effectors. *Science* 80, 1501–1501. doi: 10.1126/science.1178817

Muraya, M. M., Schmutzer, T., Ulpinnis, C., Scholz, U., and Altmann, T. (2015). Targeted sequencing reveals large-scale sequence polymorphism in maize candidate genes for biomass production and composition. *PLoS ONE* 10:e0132120. doi: 10.1371/journal.pone.0132120

Nagel, K. A., Putz, A., Gilmer, F., Heinz, K., Fischbach, A., Pfeifer, J., et al. (2012). GROWSCREEN-Rhizo is a novel phenotyping robot enabling simultaneous measurements of root and shoot growth for plants grown in soil-filled rhizotrons. *Funct. Plant Biol.* 39, 891–904. doi: 10.1071/FP12023

Nepolean, T., Singh, I., Hossain, F., Pandey, N., and Gupta, H. S. (2013). Molecular characterization and assessment of genetic diversity of inbred lines showing variability for drought tolerance in maize. *J. Plant Biochem. Biotechnol.* 22, 71–79. doi: 10.1007/s13562-012-0112-7

Obata, T., Witt, S., Lisec, J., Palacios-Rojas, N., Florez-Sarasa, I., Yousfi, S., Luis Araus, J., et al. (2015). Metabolite profiles of maize leaves in drought, heat, and combined stress field trials reveal the relationship between metabolism and grain yield. *Plant Physiol.* 169, 2665–2683. doi: 10.1104/pp.15.01164

Osakabe, Y., Watanabe, T., Sugano, S. S., Ueta, R., Ishihara, R., Shinozaki, K., et al. (2016). Optimization of CRISPR/Cas9 genome editing to modify abiotic stress responses in plants. *Sci. Rep.* 6:26685. doi: 10.1038/srep26685

Overvoorde, P., Fukaki, H., and Beeckman, T. (2010). Auxin control of root development. *Cold Spring Harb. Perspect. Biol.* 2:a001537. doi: 10.1101/cshperspect.a001537

Perruc, E., Charpenteau, M., Ramirez, B. C., Jauneau, A., Galaud, J.-P., Ranjeva, R., et al. (2004). A novel calmodulin-binding protein functions as a negative regulator of osmotic stress tolerance in *Arabidopsis thaliana* seedlings. *Plant J.* 38, 410–420. doi: 10.1111/j.1365-313X.2004.02062.x

Poland, J. A., Bradbury, P. J., Buckler, E. S., and Nelson, R. J. (2011). Genome-wide nested association mapping of quantitative resistance to northern leaf blight in maize. *Proc. Natl. Acad. Sci. U.S.A.* 108, 6893–6898. doi: 10.1073/pnas.1010894108

Prigge, V., Schipprack, W., Mahuku, G., Atlin, G. N., and Melchinger, A. E. (2012). Development of *in vivo* haploid inducers for tropical maize breeding programs. *Euphytica* 185, 481–490. doi: 10.1007/s10681-012-0657-5

Ribaut, J. M., and Ragot, M. (2007). Marker-assisted selection to improve drought adaptation in maize: the backcross approach, perspectives, limitations, and alternatives. *J. Exp. Bot.* 58, 351–360. doi: 10.1093/jxb/erl214

Ribaut, J.-M., Jiang, C., Gonzalez-de-Leon, D., Edmeades, G. O., and Hoisington, D. (1997). Identification of quantitative trait loci under drought conditions in tropical maize. 2. Yield components and marker-assisted selection strategies. *Theor. Appl. Genet.* 94, 887–896. doi: 10.1007/s001220050492

Riccardi, F., Gazeau, P., de Vienne, D., and Zivy, M. (1998). Protein changes in response to progressive water deficit in maize. *Plant Physiol.* 117, 1253–1263. doi: 10.1104/pp.117.4.1253

Riccardi, F., Gazeau, P., Jacquemot, M. P., Vincent, D., and Zivy, M. (2004). Deciphering genetic variations of proteome responses to water deficit in maize leaves. *Plant Physiol. Biochem.* 42, 1003–1011. doi: 10.1016/j.plaphy.2004.09.009

Rizal, G., Karki, S., Alcasid, M., Montecillo, F., Acebron, K., Larazo, N., et al. (2014). Shortening the breeding cycle of sorghum, a model crop for research. *Crop Sci.* 54, 520–529. doi: 10.2135/cropsci2013.07.0471

Rizhsky, L., Davletova, S., Liang, H., and Mittler, R. (2004). The zinc finger protein Zat12 is required for cytosolic ascorbate peroxidase 1 expression during oxidative stress in Arabidopsis. *J. Biol. Chem.* 279, 11736–11743. doi: 10.1074/jbc.M313350200

Rober, F. K., Gordillo, G. A., and Geiger, H. H. (2005). *In vivo* haploid induction in maize - performance of new inducers and significance of doubled haploid lines in hybrid breeding. *Maydica* 50, 275–283.

Rollins, J. A., Habte, E., Templer, S. E., Colby, T., Schmidt, J., and Von Korff, M. (2013). Leaf proteome alterations in the context of physiological and morphological responses to drought and heat stress in barley (*Hordeum vulgare* L.). *J. Exp. Bot.* 64, 3201–3212. doi: 10.1093/jxb/ert158

Ruan, Y. L., Jin, Y., Yang, Y. J., Li, G. J., and Boyer, J. S. (2010). Sugar input, metabolism, and signaling mediated by invertase: roles in development, yield potential, and response to drought and heat. *Mol. Plant* 3, 942–955. doi: 10.1093/mp/ssq044

Schafleitner, R., Gutierrez Rosales, R. O., Gaudin, A., Alvarado Aliaga, C. A., Martinez, G. N., Tincopa Marca, L. R., et al. (2007). Capturing candidate drought tolerance traits in two native Andean potato clones by transcription profiling of field grown plants under water stress. *Plant Physiol. Biochem.* 45, 673–690. doi: 10.1016/j.plaphy.2007.06.003

Seckler, D., Amarasinghe, U., Molden, D., De Silva, R., and Barker, R. (1998). *World Water Demand and Supply, 1990 to 2025: Scenarios and Issues.* Colombo: International Water Management Institute, 1–40.

Semagn, K., Beyene, Y., Warburton, M. L., Tarekegne, A., Mugo, S., Meisel, B., et al. (2013). Meta-analyses of QTL for grain yield and anthesis silking interval in 18 maize populations evaluated under water-stressed and well-watered environments. *BMC Genomics* 14:313. doi: 10.1186/1471-2164-14-313

Sheehan, M. J., Farmer, P. R., and Brutnell, T. P. (2004). Structure and expression of maize phytochrome family homeologs. *Genetics* 167, 1395–1405. doi: 10.1534/genetics.103.026096

Sheng, L., Chai, W., Gong, X., Zhou, L., Cai, R., Li, X., et al. (2015). Identification and characterization of novel maize mirnas involved in different genetic background. *Int. J. Biol. Sci.* 11, 781–793. doi: 10.7150/ijbs.11619

Shikha, M., Kanika, A., Rao, A. R., Mallikarjuna, M. G., Gupta, H. S., and Nepolean, T. (2017). Genomic selection for drought tolerance using genome-wide SNPs in maize. *Front. Plant Sci.* 8:550. doi: 10.3389/fpls.2017.00550

Shou, H., Bordallo, P., and Wang, K. (2004). Expression of the Nicotiana protein kinase (NPK1) enhanced drought tolerance in transgenic maize. *J. Exp. Bot.* 55, 1013–1019. doi: 10.1093/jxb/erh129

Song, K., Kim, H. C., Shin, S., Kim, K.-H., Moon, J.-C., Kim, J. Y., et al. (2017). Transcriptome analysis of flowering time genes under drought stress in maize leaves. *Front. Plant Sci.* 8:267. doi: 10.3389/fpls.2017.00267

Spielbauer, G., Armstrong, P., Baier, J. W., Allen, W. B., Richardson, K., Shen, B., et al. (2009). High-throughput near-infrared reflectance spectroscopy for predicting quantitative and qualitative composition phenotypes of individual maize kernels. *Cereal Chem.* 86, 556–564. doi: 10.1094/CCHEM-86-5-0556

Stephens, Z. D., Lee, S. Y., Faghri, F., Campbell, R. H., Zhai, C., Efron, M. J., et al. (2015). Big data: astronomical or genomical? *PLoS Biol.* 13:e1002195. doi: 10.1371/journal.pbio.1002195

Svitashev, S., Schwartz, C., Lenderts, B., Young, J. K., and Mark Cigan, A. (2016). Genome editing in maize directed by CRISPR–Cas9 ribonucleoprotein complexes. *Nat. Commun.* 7:13274. doi: 10.1038/ncomms13274

Svitashev, S., Young, J. K., Schwartz, C., Gao, H., Falco, S. C., and Cigan, A. M. (2015). Targeted mutagenesis, precise gene editing, and site-specific gene insertion in maize using Cas9 and guide RNA. *Plant Physiol.* 169, 931–945. doi: 10.1104/pp.15.00793

Tamaki, H., Mitsuhashi, S., Kudoh, H., Nagano, A. J., and Yasugi, M. (2016). Genomewide molecular polymorphisms among maize (*Zea mays* L.) inbred lines found from restriction-associated dna tag sequencing (RAD-Seq) analysis

as a preliminary study on " genomewide selection " for breeding by japanese public sectors. *Bull. NARO Inst. Livest. Grassl. Sci.* 16, 1–9.

Tanaka, J., Hayashi, T., and Iwata, H. (2016). A practical, rapid generation-advancement system for rice breeding using simplified biotron breeding system. *Breed. Sci.* 66, 542–551. doi: 10.1270/jsbbs.15038

Thirunavukkarasu, N., Hossain, F., Kaliyugam, S., Swati, M., Kanika, A., Abhishek, A., et al. (2013). Unraveling the genetic architecture of subtropical maize (*Zea mays* L.) lines and their utility in breeding programs. *BMC Genomics* 14:877. doi: 10.1186/1471-2164-14-877

Thirunavukkarasu, N., Hossain, F., Arora, K., Sharma, R., Shiriga, K., Mittal, S., et al. (2014). Functional mechanisms of drought tolerance in subtropical maize (*Zea mays* L.) identified using genome-wide association mapping. *BMC Genomics* 15:1182. doi: 10.1186/1471-2164-15-1182

Thirunavukkarasu, N., Sharma, R., Singh, N., Shiriga, K., Mohan, S., Mittal, S., et al. (2017). Genomewide expression and functional interactions of genes under drought stress in maize. *Int. J. Genomics* 2017, 1–14. doi: 10.1155/2017/2568706

Thompson, A. J., Mulholland, B. J., Jackson, A. C., McKee, J. M. T., Hilton, H. W., Symonds, R. C., et al. (2007). Regulation and manipulation of ABA biosynthesis in roots. *Plant Cell Environ.* 30, 67–78. doi: 10.1111/j.1365-3040.2006.01606.x

Thompson, A. M., Crants, J., Schnable, P. S., Yu, J., Timmermans, M. C. P., Springer, N. M., et al. (2014). Genetic control of maize shoot apical meristem architecture. G3 4, 1327–1337. doi: 10.1534/g3.114.011940

Tian, H.-L., Wang, F.-G., Zhao, J.-R., Yi, H.-M., Wang, L., Wang, R., et al. (2015). Development of maizeSNP3072, a high-throughput compatible SNP array, for DNA fingerprinting identification of Chinese maize varieties. *Mol. Breed.* 35:136. doi: 10.1007/s11032-015-0335-0

Tuberosa, R., Parentoni, S., Kim, T. S., Sanguineti, M. C., and Phillips, R. L. (1998a). Mapping QTLs for ABA concentration in leaves of a maize cross segregating for anthesis date. *Maize Genet. Coop. Newslett* 72, 72–73.

Tuberosa, R., Sanguineti, M. C., Landi, P., Salvi, S., Casarini, E., and Conti, S. (1998b). RFLP mapping of quantitative trait loci controlling abscisic acid concentration in leaves of drought-stressed maize (*Zea Mays* L.). *TAG Theor. Appl. Genet.* 97, 744–755. doi: 10.1007/s001220050951

Unterseer, S., Bauer, E., Haberer, G., Seidel, M., Knaak, C., Ouzunova, M., et al. (2014). A powerful tool for genome analysis in maize: development and evaluation of the high density 600 k SNP genotyping array. *BMC Genomics* 15:823. doi: 10.1186/1471-2164-15-823

Van Gioi, H., Mallikarjauna, M. G., Shikha, M., Pooja, B., Jha, S. K., Dash, P. K., et al. (2017). Variable level of dominance of candidate genes controlling drought functional traits in maize hybrids. *Front. Plant Sci.* 8:940. doi: 10.3389/fpls.2017.00940

Vincent, D., Lapierre, C., Pollet, B., Cornic, G., Negroni, L., and Zivy, M. (2005). Water De cits affect caffeate O-Methyltransferase, Ligni cation, and Related Enzymes In Maize Leaves. a proteomic investigation. *Plant Physiol.* 137, 949–960. doi: 10.1104/pp.104.050815

Vivek, B. S., Krishna, G. K., Vengadessan, V., Babu, R., Zaidi, P. H., Kha, L. Q., et al. (2017). Use of genomic estimated breeding values results in rapid genetic gains for drought tolerance in maize. *Plant Genome* 10, 1–8. doi: 10.3835/plantgenome2016.07.0070

Wang, R., Yu, Y., Zhao, J., Shi, Y., Song, Y., Wang, T., et al. (2008). Population structure and linkage disequilibrium of a mini core set of maize inbred lines in China. *Theor. Appl. Genet.* 117, 1141–1153. doi: 10.1007/s00122-008-0852-x

Wang, X., Wang, H., Liu, S., Ferjani, A., Li, J., Yan, J., et al. (2016). Genetic variation in ZmVPP1 contributes to drought tolerance in maize seedlings. *Nat. Genet.* 48, 1233–1241. doi: 10.1038/ng.3636

Wen, W., Franco, J., Chavez-Tovar, V. H., Yan, J., and Taba, S. (2012). Genetic characterization of a core set of a tropical maize race Tuxpeño for further use in maize improvement. *PLoS ONE* 7:e32626. doi: 10.1371/journal.pone.0032626

Witt, S., Galicia, L., Lisec, J., Cairns, J., Tiessen, A., Araus, J. L., et al. (2012). Metabolic and phenotypic responses of greenhouse-grown maize hybrids to experimentally controlled drought stress. *Mol. Plant* 5, 401–417. doi: 10.1093/mp/ssr102

Wu, X., Li, Y., Shi, Y., Song, Y., Wang, T., Huang, Y., et al. (2014). Fine genetic characterization of elite maize germplasm using high-throughput SNP genotyping. *Theor. Appl. Genet.* 127, 621–631. doi: 10.1007/s00122-013-2246-y

Xiang, Y., Sun, X., Gao, S., Qin, F., and Dai, M. (2017). Deletion of an endoplasmic reticulum stress response element in a ZmPP2C-A gene facilitates drought tolerance of maize seedlings. *Mol. Plant* 10, 456–469. doi: 10.1016/j.molp.2016.10.003

Xing, H.-L., Dong, L., Wang, Z.-P., Zhang, H.-Y., Han, C.-Y., Liu, B., et al. (2014). A CRISPR/Cas9 toolkit for multiplex genome editing in plants. *BMC Plant Biol.* 14:327. doi: 10.1186/s12870-014-0327-y

Xu, C., Ren, Y., Jian, Y., Guo, Z., Zhang, Y., Xie, C., et al. (2017). Development of a maize 55 K SNP array with improved genome coverage for molecular breeding. *Mol. Breed.* 37:20. doi: 10.1007/s11032-017-0622-z

Xu, J., Yuan, Y., Xu, Y., Zhang, G., Guo, X., Wu, F., et al. (2014). Identification of candidate genes for drought tolerance by whole-genome resequencing in maize. *BMC Plant Biol.* 14:83. doi: 10.1186/1471-2229-14-83

Xu, Y., Skinner, D. J., Wu, H., Palacios-Rojas, N., Araus, J. L., Yan, J., et al. (2009). Advances in maize genomics and their value for enhancing genetic gains from breeding. *Int. J. Plant Genomics* 2009:30. doi: 10.1155/2009/957602

Yu, J., Holland, J. B., McMullen, M. D., and Buckler, E. S. (2008). Genetic design and statistical power of nested association mapping in maize. *Genetics* 178, 539–551. doi: 10.1534/genetics.107.074245

Zaidi, P. H., Seetharam, K., Krishna, G., Krishnamurthy, L., Gajanan, S., Babu, R., et al. (2016). Genomic regions associated with root traits under drought stress in tropical maize (*Zea mays* L.). *PLoS ONE* 11:e0164340. doi: 10.1371/journal.pone.0164340

Zaman-Allah, M., Vergara, O., Araus, J. L., Tarekegne, A., Magorokosho, C., Zarco-Tejada, P. J., et al. (2015). Unmanned aerial platform-based multi-spectral imaging for field phenotyping of maize. *Plant Methods* 11:35. doi: 10.1186/s13007-015-0078-2

Zhang, G., Guo, G., Hu, X., Zhang, Y., Li, Q., Li, R., et al. (2010). Deep RNA sequencing at single base-pair resolution reveals high complexity of the rice transcriptome. *Genome Res.* 20, 646–654. doi: 10.1101/gr.100677.109

Zhang, L., Chia, J. M., Kumari, S., Stein, J. C., Liu, Z., Narechania, A., et al. (2009). A genome-wide characterization of microRNA genes in maize. *PLoS Genet.* 5:e1000716. doi: 10.1371/journal.pgen.1000716

Zhang, M., Pan, J., Kong, X., Zhou, Y., Liu, Y., Sun, L., et al. (2012). ZmMKK3, a novel maize group B mitogen-activated protein kinase kinase gene, mediates osmotic stress and ABA signal responses. *J. Plant Physiol.* 169, 1501–1510. doi: 10.1016/j.jplph.2012.06.008

Zhang, X., Liu, X., Zhang, D., Tang, H., Sun, B., Li, C., et al. (2017). Genome-wide identification of gene expression in contrasting maize inbred lines under field drought conditions reveals the significance of transcription factors in drought tolerance. *PLoS ONE* 12:e0179477. doi: 10.1371/journal.pone.0179477

Zhao, F., Zhang, D., Zhao, Y., Wang, W., Yang, H., Tai, F., et al. (2016a). The difference of physiological and proteomic changes in maize leaves adaptation to drought, heat, and combined both stresses. *Front. Plant Sci.* 7:1471. doi: 10.3389/fpls.2016.01471

Zhao, Y., Wang, Y., Yang, H., Wang, W., Wu, J., and Hu, X. (2016b). Quantitative proteomic analyses identify aba-related proteins and signal pathways in maize leaves under drought conditions. *Front. Plant Sci.* 7:1827. doi: 10.3389/fpls.2016.01827

Zheng, J., Fu, J., Gou, M., Huai, J., Liu, Y., Jian, M., et al. (2010). Genome-wide transcriptome analysis of two maize inbred lines under drought stress. *Plant Mol. Biol.* 72, 407–421. doi: 10.1007/s11103-009-9579-6

Zhu, J. K. (2002). Salt and drought stress signal transduction in plants. *Annu. Rev. Plant Biol.* 53, 247–273. doi: 10.1146/annurev.arplant.53.091401.143329

Conflict of Interest Statement: The authors declare that the research was conducted in the absence of any commercial or financial relationships that could be construed as a potential conflict of interest.

frontiers in Plant Science

REVIEW
published: 22 August 2018
doi: 10.3389/fpls.2018.01143

Is Nitrogen a Key Determinant of Water Transport and Photosynthesis in Higher Plants Upon Drought Stress?

Lei Ding[1,2], Zhifeng Lu[1], Limin Gao[1], Shiwei Guo[1] and Qirong Shen[1]*

[1] *Jiangsu Provincial Key Lab for Organic Solid Waste Utilization, National Engineering Research Center for Organic-based Fertilizers, Jiangsu Collaborative Innovation Center for Solid Organic Waste Resource Utilization, Nanjing Agricultural University, Nanjing, China,* [2] *Louvain Institute of Biomolecular Science and Technology, Université catholique de Louvain, Louvain-la-Neuve, Belgium*

Drought stress is a major global issue limiting agricultural productivity. Plants respond to drought stress through a series of physiological, cellular, and molecular changes for survival. The regulation of water transport and photosynthesis play crucial roles in improving plants' drought tolerance. Nitrogen (N, ammonium and nitrate) is an essential macronutrient for plants, and it can affect many aspects of plant growth and metabolic pathways, including water relations and photosynthesis. This review focuses on how drought stress affects water transport and photosynthesis, including the regulation of hydraulic conductance, aquaporin expression, and photosynthesis. It also discusses the cross talk between N, water transport, and drought stress in higher plants.

Keywords: drought stress, water transport, photosynthesis, nitrogen, aquaporin

OPEN ACCESS

Edited by:
Lijun Luo,
Shanghai Agrobiological Gene Center, China

Reviewed by:
Claudio Lovisolo,
Università degli Studi di Torino, Italy
Kazuo Nakashima,
Japan International Research Center for Agricultural Sciences, Japan
Lizhong Xiong,
Huazhong Agricultural University, China

****Correspondence:***
Shiwei Guo
sguo@njau.edu.cn

Specialty section:
This article was submitted to Plant Breeding, a section of the journal Frontiers in Plant Science

Received: *08 March 2018*
Accepted: *17 July 2018*
Published: *22 August 2018*

Citation:
Ding L, Lu Z, Gao L, Guo S and Shen Q (2018) Is Nitrogen a Key Determinant of Water Transport and Photosynthesis in Higher Plants Upon Drought Stress? Front. Plant Sci. 9:1143. doi: 10.3389/fpls.2018.01143

INTRODUCTION

Crop production is facing threats from both biotic and abiotic stresses. Drought stress is considered to be one of the most devastating abiotic stresses, and it decreases crop yield, particularly in arid and semiarid areas (Chaves et al., 2003; Parry et al., 2007; Lambers et al., 2008). The decrease in yield varies from 13 to 94% in the investigated crops that were under drought stress (Farooq et al., 2009). Rice is traditionally cultivated in waterlogged conditions, and in China, 80% of the freshwater used in agriculture is for rice production, indicating that rice production would suffer more drought stress due to water shortages (Guo et al., 2007a). It is expected that drought stress would be more severe because of global warming (Chang, 2007).

In higher plants, drought stress induces an array of physiological and biochemical adaptations of metabolism for survival by increasing the drought resistance through three strategies, namely, "drought escape," "drought avoidance," and "drought tolerance" (Morgan, 1984; Xu et al., 2010; Vilagrosa et al., 2012). Strategies of drought escape include reducing life span and inducing vegetative dormancy to escape severe drought stress (Geber and Dawson, 1990; Vilagrosa et al., 2012). Strategies of drought avoidance include increasing water uptake ability and water use efficiency, for example, stomatal closure, extensive root systems, high capacity for water transport from roots to leaves, and high leaf mass to leaf area ratio (Schulze, 1986; Jackson et al., 2000). Strategies of drought tolerance mainly include improving osmotic adjustment ability, increasing cell wall elasticity to maintain tissue turgidity, increasing antioxidant metabolism, increasing compatible solutes, and enhancing the resistance to xylem cavitation (Morgan, 1984).

In this review, we present an overview on how drought stress affects water uptake, transport, and photosynthesis in higher plants. In particular, we summarize that nitrogen (N) supply may regulate drought tolerance in higher plants with different N forms and/or N levels. Nitrogen is an essential macronutrient for plants, and it can affect many aspects of plant growth and metabolic pathways (Guo et al., 2007b; Xu et al., 2012; Wang et al., 2014). Ammonium and nitrate are two major N sources in higher plants. It is well-documented that these N forms regulate drought tolerance through root water uptake and photosynthesis in rice (Li et al., 2009a, 2012; Yang et al., 2012; Ding et al., 2016b), French beans (Guo et al., 2002, 2007b), and maize (Mihailović et al., 1992).

DROUGHT STRESS AFFECTS WATER UPTAKE AND TRANSPORT

In soil-plant-atmosphere continuum system, water travels from soil to the atmosphere. Two water flow pathways are included in this process: axial movement (water flow from root xylem to leaf vessels) and radial movement (water flow from soil to root xylem and from leaf xylem vessels to mesophyll cells) (Sade and Moshelion, 2017). The whole plant hydraulic conductance is determined by radial conductance, that is, root hydraulic conductivity (Lpr) and leaf hydraulic conductance (K_{leaf}), since water must pass through apoplastic barriers, which resist the water flow (Steudle and Peterson, 1998; Sack and Holbrook, 2006). During drought stress, both Lpr and K_{leaf} are affected in higher plants (Aroca and Ruiz-Lozano, 2012; Sade and Moshelion, 2017).

Drought Stress Affects Lpr and K_{leaf}

Root hydraulic conductivity tends to decrease during drought stress (North et al., 2004; Aroca et al., 2012; Grondin et al., 2016; Meng and Fricke, 2017). The decrease in Lpr (1) causes a decrease in transpiration and an increase in water use efficiency (Iuchi et al., 2001) and (2) evades water leakage from root back into soil while soil water content decreases progressively (Jackson et al., 2000). Nonetheless, an increase in Lpr was observed after short-term water stress treatment with polyethylene glycol (PEG) 6000 in rice (Ding et al., 2016b) and maize (Hose et al., 2000). In other studies, decrease in Lpr was detected after short-term water stress treatment (with PEG) in cucumber (Qian et al., 2015) and tobacco (Mahdieh et al., 2008). The response of Lpr to drought stress varies among species, indicating that there are different strategies for water uptake regulation. It can be seen that water distribution is non-uniform when the soil becomes dry. McLean et al. (2011) demonstrated that one half of the roots increased the capacity of water uptake in a wet zone, whereas the other half of the roots decreased water uptake in a dry zone.

Vandeleur et al. (2009) showed that, in grapevine under drought stress, Lpr decreased while cell hydraulic conductivity (Lpc) increased. Similar result was obtained by Hachez et al. (2012) in maize, and it was demonstrated that Lpc increased after 2 h of PEG treatment, without any further change in Lpr. Such an increase of Lpc might be helpful for osmotic adjustment. It was postulated that Lpr was controlled by the conductivity of exo- and endodermis cells, while not cortical cells (Lpc) under water stress, since large resistance was expected for water flow passing exo- and endodermis due to the deposition of lignin and suberine in these cells (Hachez et al., 2012).

In leaves, drought stress induced the decrease of both leaf water potential (Ψ_{leaf}) and K_{leaf} in many plants, including woody species (Johnson et al., 2009; Scoffoni et al., 2011a), grapevine (Pou et al., 2013), Arabidopsis (Shatil-Cohen et al., 2011), and sunflower (Nardini and Salleo, 2005). Water movement inside leaves includes two pathways (1) water movement through leaf xylem (i.e., petiole and venation) and (2) water movement outside the xylem (i.e., bundle sheath and mesophyll) (Sack and Holbrook, 2006). When plants suffer from drought stress, both water flow pathways are affected (Scoffoni et al., 2011b) and aquaporins play an important role in regulating water movement outside the xylem (Buckley, 2015). Decrease in K_{leaf} was associated with the downregulation of aquaporin expression and/or activity in bundle sheath cells under drought stress (Shatil-Cohen et al., 2011). Additionally, it was demonstrated that abscisic acid (ABA) accumulation inside leaves induced the downregulation of aquaporin activity in bundle sheath cells, which further induced the decrease of K_{leaf} under drought stress. Indeed, overexpressing the aquaporin gene (*NtAQP1*) in bundle sheath cells reduced the effect of ABA on K_{leaf} (Sade et al., 2015). On the other hand, leaf xylem embolism by cavitation formation decreased K_{leaf} under drought stress (Johnson et al., 2009; Scoffoni et al., 2011b; Vilagrosa et al., 2012).

Drought Stress Affects Lpr Through the Regulation of Aquaporin

In the "composite transport model" (Steudle and Peterson, 1998; Steudle, 2000a), water flows from soil to root xylem in two parallel pathways, namely, apoplastic pathway and cell-to-cell pathway. Apoplastic water flow is blocked by apoplastic barriers in exodermis and endodermis, and the flow must proceed through the cell-to-cell pathway, which has large resistance for water movement (Maurel, 1997). Yet, aquaporins located on the membrane reduce the resistance. Aquaporins play an important role in regulating Lpr (Javot and Maurel, 2002; Gambetta et al., 2017). Vandeleur et al. (2014) showed that shoot topping decreased Lpr by 50–60%, through the downregulation of aquaporin gene expression (five to tenfold decrease). Gambetta et al. (2017) reviewed that the contribution of aquaporin to Lpr is highly variable across species, ranging from 0∼90%, and the variability depends on the type of aquaporin inhibitor and the method used to measure Lpr. Genetically modified aquaporin expression is used to change Lpr, which was decreased by 42% in *NtAQP1* knockouts, antisense tobacco plants deficient in the tobacco aquaporin NtAQP1, and by 20∼30% in *AtPIP1;2* knockouts, *Arabidopsis thaliana* plants deficient in the aquaporin AtPIP1;2 (Postaire et al., 2010).

Under drought stress, the change in Lpr is associated with the regulation of aquaporin expression (Steudle, 2000b; Aroca and Ruiz-Lozano, 2012; Aroca et al., 2012; Henry et al., 2012). The contribution of aquaporins to Lpr was up to 85% under

drought stress in rice (Grondin et al., 2016). Four rice genotypes showed increased contribution, whereas two showed decreased contribution after long-term drought treatment in comparison with well-watered treatment. Our results demonstrated that ammonium nutrition enhanced drought tolerance in rice seedlings when compared with nitrate nutrition (Guo et al., 2007a; Li et al., 2009a), which is associated with the regulation of aquaporin expression (see **Figure 1**; Gao et al., 2010; Yang et al., 2012; Ding et al., 2015, 2016b). After 24 h of water stress treatment with PEG 6000, the expression and activity of aquaporins were enhanced in plants supplied with ammonium when compared with normal water treatment, whereas no increase was observed in plants supplied with nitrate (Ding et al., 2015, 2016b). Furthermore, it was observed that ABA accumulation was much faster in roots supplied with ammonium than with nitrate during 24 h drought treatment, which supported the increase in aquaporin expression (Ding et al., 2016b). Abscisic acid had a positive effect on Lpr and aquaporin expression (Aroca et al., 2006; Mahdieh and Mostajeran, 2009; Parent et al., 2009). Parent et al. (2009) demonstrated that a higher aquaporin expression and Lpr was observed in the maize line producing more ABA than in the line producing less ABA.

Drought Stress Affects Lpr Through the Regulation of Root Anatomy and Morphology

The decrease in Lpr could be explained by increased or accelerated deposition of root suberin under drought stress (Gambetta et al., 2017), and the accumulation of suberin leads to the formation of apoplastic barriers. Vandeleur et al. (2009) demonstrated that the diminution of Lpr was caused by suberin and lignin depositions, which restricts the apoplastic water flow under drought stress. In rice plants, suberization of the endodermis increased under drought stress (Henry et al., 2012). On the other hand, more aerenchyma formation could restrict the passage of water through cortical cells in rice roots (Ranathunge et al., 2003, 2004; Yang et al., 2012; Ren et al., 2015). Yang et al. (2012) observed that drought induced more root aerenchyma formation and restricted root water uptake in rice plants supplied with nitrate.

Additionally, Lpr is regulated by the change in root morphology under drought stress. Plants tend to develop a deeper root system to obtain more water, since the drying rate is more pronounced in superficial soil layers than in the deeper ones (Pinheiro et al., 2005; Alsina et al., 2010). In rice plants, lateral root growth was enhanced by water stress treatment with PEG 6000 in plants supplied with ammonium (Ding et al., 2015).

DROUGHT STRESS AFFECTS PHOTOSYNTHESIS

Drought stress decreases photosynthetic rate (A), restricts plant growth, and reduces crop yield (Farooq et al., 2009). The decrease in A is associated with stomatal closure (Flexas and Medrano, 2002; Flexas et al., 2006a) and metabolic impairment (Tezara et al., 1999; Tang et al., 2002). In most studies, the decrease in A was due to stomatal closure and increase in resistance to CO_2 diffusion (Xu et al., 2010; Flexas et al., 2012; Perez-Martin et al., 2014). Under drought stress, ABA accumulated in leaf apoplast and induced stomatal closure (Seki et al., 2007; Skirycz and Inzé, 2010; Rodrigues et al., 2017). Photosynthesis was restored after elevating CO_2 concentration in leaves (Kaiser, 1987; Gallé et al., 2007) or stripping the epidermis (Schwab et al., 1989), indicating that stomatal closure is the main factor causing the decline in A. The ways to evaluate photosynthesis limitation under drought stress are discussed by Flexas et al. (2012). Drought stress intensity was divided into three levels based on stomatal conductance (g_s): (1) mild drought stress ($g_s > 0.15$ mol H_2O m^{-2} s^{-1}), (2) moderate drought stress (0.05 mol H_2O m^{-2} s^{-1} $< g_s < 0.15$ mol H_2O m^{-2} s^{-1}), and (3) severe drought stress ($g_s < 0.05$ mol H_2O m^{-2} s^{-1}) (Medrano et al., 2002; Cano et al., 2014). During mild drought stress, decrease in g_s was the only cause for the decline in photosynthetic rate. During moderate drought stress, the decrease in g_s and meshophyll conductance (g_m) caused the decline in A. After severe drought stress photosynthetic capacity is impaired, inhibiting photosynthetic enzymes and decreasing chlorophyll and protein content. The plants also suffer oxidative stress under severe drought stress (Zhou et al., 2007; Farooq et al., 2009). However, the decrease in g_s and g_m accounts for more than 90% of total A reduction from mild to severe drought stress in tobacco (Galle et al., 2009) and eucalyptus (Cano et al., 2014).

In C_3 plants, light-saturated photosynthetic rate is restricted by chloroplastic CO_2 concentration (Cc) under present ambient CO_2 level, and Cc is unsaturated (Li et al., 2009b; Ding et al., 2016a). The Cc depends on the regulation of g_s and g_m (Flexas et al., 2008; Evans et al., 2009; Kaldenhoff, 2012). Under drought stress, even less Cc is predicted owing to stomatal closure, the increase in diffusion resistance, and the activity of Rubisco (key enzyme for carboxylation), which decreases due to insufficient CO_2 (Flexas et al., 2006a). In comparison with stomatal closure, which is regulated by ABA and/or hydrogen peroxide (H_2O_2) (Zhang et al., 2001; Rodrigues et al., 2017), the regulation of g_m is more complex under drought stress. It was demonstrated that the decrease in Ψ_{leaf} resulted in chloroplast downsizing and subsequently decreased g_m in plants supplied with nitrate under water stress treatment with PEG 6000 (Li et al., 2012). Chloroplast shrinking induced the decrease in total chloroplast surface area and the surface area of chloroplasts exposed to intercellular airspace per unit leaf area (Sc), which are positively correlated to g_m (Evans et al., 2009; Li et al., 2009b; Xiong et al., 2017).

In other studies, the decrease in g_s and g_m has been associated with the regulation of aquaporin expression (Flexas et al., 2006b; Miyazawa et al., 2008; Pou et al., 2013; Perez-Martin et al., 2014). In olive, the downregulation of two aquaporin gene expression, *OePIP1;1* and *OePIP2;1*, explained the decrease in both g_s and g_m under drought stress (Perez-Martin et al., 2014). Pou et al. (2013) observed that the expression of *VvTIP2;1*, a grapevine tonoplast aquaporin, was highly correlated with g_s, and the downregulated expression might partially cause g_s decline under drought stress. However, they also found that there was no decrease in the expression of the other aquaporin genes under drought stress,

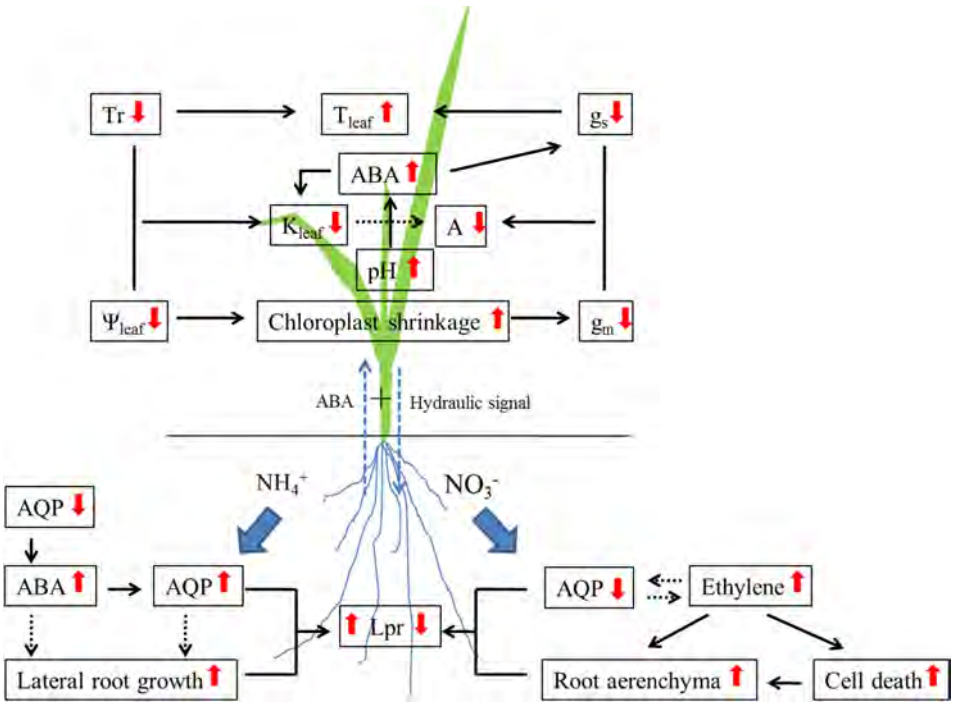

FIGURE 1 | The mechanism of nitrogen form affecting drought tolerance in rice plants. NH_4^+, Ammonium; NO_3^-, Nitrate; AQP, Aquaporin; ABA, Abscisic acid; Lpr, Root hydraulic conductivity; Tr, Transpiration rate; Ψ_{leaf}, Leaf water potential; T_{leaf}, Leaf temperature; K_{leaf}, Leaf hydraulic conductance; A, Photosynthetic rate; g_s, Stomatal conductance; g_m, Mesophyll conductance. Up arrows, increase; down arrows, decrease.

for example, *VvPIP2;1* (a grapevine root-specific aquaporin) and *VvTIP1;1* (an isoform of the grapevine tonoplast aquaporin). This result suggests that the aquaporin members play different roles in regulating leaf water relations and photosynthesis. Indeed, some aquaporin genes are located in stomatal complexes [guard cells, Hachez et al. (2017)], and they are involved in controlling the stomatal movement. Rodrigues et al. (2017) showed that AtPIP2;1, an aquaporin in Arabidopsis, facilitated H_2O_2 entry into guard cells and induced stomatal closure under ABA treatment. Evidence elucidates that the inhibition of aquaporin expression in bundle sheath cells was due to ABA accumulation in leaf under drought stress (Shatil-Cohen et al., 2011). Mizokami et al. (2015) observed that g_m decreased with the increase in leaf ABA content in wild type plants under drought stress, whereas both ABA and g_m were unchanged in *aba*1, an ABA-deficient mutant, indicating that ABA plays a major role in the regulation of g_m under drought stress by affecting aquaporin expression.

Full recovery of A after rewatering was observed in many studies (Izanloo et al., 2008; Xu et al., 2009; Cano et al., 2014). However, the recovery speed varied among these studies, which depended on the degree and velocity of decline in A during stress imposition (Flexas et al., 2012). In severe drought stress plants, the recovery of A was only 40–60% on the first day of rewatering, but the recovery continued in the next few days. When A was 36% in control plants before rewatering, the total recovery of A occurred in 4 days. When A was 23% in control plants, full recovery took up to 6 days, and when A was 3% in control plants, full recovery required 18 days (Flexas et al., 2012). Besides, the recovery of A depends on the change in g_s and g_m after rewatering. Cano et al. (2014) observed that full recovery of A was associated with quick recovery of g_m in eucalyptus, whereas g_s recovery was slower than g_m. Stomatal conductance might not be fully recovered after rewatering, which aims to increase intrinsic water use efficiency (Gallé et al., 2007; Galmés et al., 2007; Xu et al., 2009).

THE COORDINATED DECLINE IN K_{leaf} WITH A UNDER DROUGHT STRESS

The coordination between K_{leaf} and A played an important role in the evolution of leaves (Sack and Holbrook, 2006; Scoffoni et al., 2016). Many studies have demonstrated that positive correlations exist among species between hydraulic conductance of stem; leaf; the whole plant; and g_s, g_m, and A (Sack and Holbrook, 2006; Brodribb et al., 2007; Flexas et al., 2013; Scoffoni et al., 2016; Xiong et al., 2017).

Under drought stress, coordinated decline of K_{leaf} and A was observed in maize (Gleason et al., 2017), rice (Tabassum et al., 2016), and woodland species (Skelton et al., 2017). In rice plants, the decrease in major venation thickness induced the decline of both A and K_{leaf} (Tabassum et al., 2016). In other studies, it has been shown that ABA plays an important role in the coordinated decline of K_{leaf} and A under drought stress (Shatil-Cohen et al., 2011; Mizokami et al., 2015; Coupel-Ledru et al., 2017), through the regulation of aquaporins (Shatil-Cohen et al.,

2011; Pou et al., 2013). Abscisic acid induced the deactivation of aquaporins in bundle sheath cells under drought stress, which caused the decrease in Ψ_{leaf} and K_{leaf} (Shatil-Cohen et al., 2011). The deactivation of aquaporins could directly downregulate g_m by affecting CO_2 transport (Flexas et al., 2006b; Evans et al., 2009; Kaldenhoff, 2012).

CROSS TALK OF N, WATER TRANSPORT, AND DROUGHT STRESS

Nitrogen Supply Affects Root Water Uptake

Nitrogen is an essential macronutrient for plants, and it affects many aspects of plant growth and metabolic pathways (Guo et al., 2007c; Xu et al., 2012; Wang et al., 2014). Ammonium and nitrate are two major sources of N uptake by higher plants. The N form and the levels of N available affect root water uptake (Tyerman et al., 2017). Gorska et al. (2008a) found that the increase in root water uptake was associated with high nitrate supply (5 mM) in cucumber and tomato. Further analysis demonstrated that the increase in root hydraulic conductivity resulted from the change in Lpc, which was measured with a cell pressure probe. The Lpc decreased after inhibition of nitrate uptake by cucumber roots with nitrate reductase inhibitor tungstate, whereas Lpc was able to recover after direct injection of nitrate into the cells (Gorska et al., 2008a). Additionally, it was demonstrated that the capacity for nitrate regulation of Lpr correlated with the species' nitrate uptake rates (Górska et al., 2010). High nitrate supply significantly increased the nitrate uptake rate, as well as root water uptake rate in maize plants, whereas the increase was not found in *Populus trichocarpa*, which is insensitive to high nitrate supply. Similar result was obtained by Li G. et al. (2016), although they showed a strong positive relationship between Lpr and nitrate accumulation in shoots rather than in roots. In *NRT2.1*, mutant of a high-affinity nitrate transporter, there was 30% reduction in Lpr. The results revealed that synergetic transport exists between nitrate and water uptake in roots. In plants supplied with N in both ammonium and nitrate forms, the high N supply also increased Lpr in rice (Ishikawa-Sakurai et al., 2014; Ren et al., 2015). Nitrogen deprivation decreased Lpr, resulting from the downregulation of aquaporin genes in roots, as well as the increased aerenchyma formation. On the contrary, high ammonium (3 mM) supply induced more apoplastic barrier formation and decreased Lpr when compared with low ammonium supply (0.03 mM) in rice seedlings (Ranathunge et al., 2016). Nonetheless, when we compared root water uptake in plants supplied with ammonium or nitrate, a higher expression of aquaporin genes (*PIPs* and *TIPs*) was observed in rice plants supplied with ammonium than with nitrate (2.86 mM) (Ding et al., 2016b; Wang et al., 2016), indicating a higher water uptake ability (symplastic pathway flux) in rice plants under similar conditions. But, this was not observed in other species, such as maize (Gorska et al., 2008b) and French bean (Guo et al., 2007b). Instead, they observed higher root water uptake or aquaporin expression in plants supplied with nitrate than with ammonium.

With different forms of N supply, the regulation of root hydraulics/aquaporins could be through (1) local and systemic signaling induced by nitrate (Cramer et al., 2009; Li G. et al., 2016), (2) root anatomy development, i.e., the depositions of lignin and suberin, regulated by ammonium and nitrate (Ren et al., 2015; Barberon et al., 2016; Ranathunge et al., 2016; Gao et al., 2017), or (3) the transport of N-containing molecules (Wang et al., 2016). Firstly, there is a strong correlation between soil N mobility and water mass flow. More nitrate could reach the root surface with increasing total water flow through the plant when nitrate is sensed (Gorska et al., 2008a,b; Cramer et al., 2009). Both high and low affinity nitrate transporters were involved in this sensing and signaling (Tyerman et al., 2017). In *NRT2.1* knock out plants, Lpr was reduced and under different N concentration treatments, Lpr was positively correlated with the nitrate content in leaves (Li G. et al., 2016). However, when the nitrate concentration was above 2 mM inside xylem, stomatal conductance decreased in an ABA-dependent manner in maize (Wilkinson et al., 2007). It could be expected that less water and nitrate were acquired. Secondly, it's well known that two parallel pathways, namely, apoplastic and cell-to-cell pathway, exist for radial water movement in root. Basically, water flow in apoplastic pathway is blocked by apoplastic barriers, and water flow continues through the cell-to-cell pathway. The deposition of lignin and suberin may affect Lpr and the expression of aquaporins. Ranathunge et al. (2016) demonstrated that high ammonium supply increased the deposition of lignin and suberin; furthermore, Lpr decreased in comparison with low ammonium supply in rice. Unfortunately, they didn't examine the difference between ammonium and nitrate supply. In a previous study, we observed that the expression of *PIPs* and *TIPs* was higher in rice plants supplied with ammonium than with nitrate (Ding et al., 2016b). We could expect a higher deposition of lignin and/suberin in roots supplied with ammonium than with nitrate, since no difference in Lpr was observed between ammonium and nitrate treatments (Yang et al., 2012; Ding et al., 2015). Moreover, the production of ethylene and ABA was regulated by the different N forms available in rice (Ding et al., 2015, 2016b; Gao et al., 2017). Ethylene may reduce the suberisation, whereas ABA increases the suberisation (Barberon et al., 2016). Thirdly, some aquaporin genes are involved in NH_4^+/NH_3 transport but not in nitrate transport in plants (Wang et al., 2016). The correlation between nitrogen fixation and aquaporins is discussed in the next section. From this correlation, it becomes clear that the expression of aquaporins is regulated by ammonium/nitrate supply. Aquaporins could be regulated at many levels, including transcription, protein amount, localization, and by gating (Chaumont and Tyerman, 2014), and it remains unclear how N supply affects these regulations.

The Correlation Between N Metabolism and Aquaporins

Nitrogen is acquired by plants through either nitrogen fixation from atmosphere, carried out by the Leguminosae family

plants, or by utilization of N sources present in soil, including ammonium, nitrate, urea, and other organic N forms. During N absorption, assimilation, and remobilization, aquaporins play important roles, and the two main subfamilies involved are nodulin 26-like intrinsic proteins (NIPs) and tonoplast intrinsic proteins (TIPs).

Nodulin 26-Like Intrinsic Protein (NIPs) and Nitrogen Fixation

Nitrogen is fixed by Leguminosae family plants, through nodulin. Symbiosomes are established between nitrogen fixing bacteria and root by exchange of carbon and nitrogen through symbiosome membrane in the nodulin (Roth and Stacey, 1989; Mylona et al., 1995; Udvardi and Poole, 2013). Nodulin 26-like intrinsic protein is a superfamily of aquaporins (aquaglyceroporin), and it was named based on nodulin 26, which is the major protein component of the mature soybean symbiosome membrane (Fortin et al., 1987; Weaver et al., 1991; Kaldenhoff and Fischer, 2006). It was observed that, nodulin 26 was able to facilitate the transport of water and glycerol (Rivers et al., 1997; Dean et al., 1999) and the efflux of NH_3/NH_4^+ from the symbiosome membrane based on stopped flow measurement with symbiosome membrane vesicles (Niemietz and Tyerman, 2000) and proteoliposomes by reconstituting nodulin 26 protein (Hwang et al., 2010). Nodulin 26 showed a fivefold preference in the transport rate of ammonia when compared with water (Hwang et al., 2010). Moreover, Masalkar et al. (2010) observed that nodulin 26 formed a complex with soybean nodule cytosolic glutamine synthetase (GS), which catalyzes the assimilation of ammonia. GS interacts with the carboxyl terminal domain of nodulin 26, by regulating the activity, trafficking, and stability of nodulin 26. The results suggested that nodulin 26 plays a major role in nitrogen fixation by Leguminosae plants. Phosphorylation of nodulin 26 was induced by osmotic drought stress (Guenther et al., 2003) and flooding/hypoxia stress (Hwang, 2013), by affecting the activity of water and/or ammonia transport.

Additionally, the expression of NIPs was induced by arbuscular mycorrhizal (AM) fungi infection in *Lotus japonicas* (Giovannetti et al., 2012) and *Medicago truncatula* (Uehlein et al., 2007), which benefits the utilization of phosphate and nitrogen (Smith and Smith, 2011). It could be assumed that NIPs are involved in both rhizobial and AM symbiosis for nutrient delivery and water transport.

During the evolution of plants, NIPs were present in all land plants (Roberts and Routray, 2017), such as maize (Chaumont et al., 2001), Arabidopsis (Johanson et al., 2001), rice (Sakurai et al., 2005), grapevine (Fouquet et al., 2008), cotton (Park et al., 2010), and soybean (Zhang et al., 2013). Apart from their function as ammonia channels, NIPs are also characterized as channels for metalloids (Bienert and Bienert, 2017), including boron (Takano et al., 2008), silicon (Ma and Yamaji, 2015), arsenic (Ma et al., 2008), aluminum (Wang Y. et al., 2017), antimony, and germanium (Bienert and Bienert, 2017). For more details, the function and classification of NIPs were reviewed by Roberts and Routray (2017).

Aquaporin Facilitates the Transport of Ammonium, Ammonia, and Urea

Urea is the most widely used nitrogen fertilizer in agricultural crop production and also an important N metabolite in plants. Urea is degraded to ammonium by urease in soil and then utilized by plants. However, urea can be taken up by roots directly, mediated by two types transporters, namely, aquaporins (Liu et al., 2003b; Yang et al., 2015) and DUR3 orthologs (Liu et al., 2003a; Witte, 2011). Wang et al. (2016), in a review, showed that two main subfamilies of aquaporins were involved in the transport of urea, including NIPs and TIPs. Nodulin 26-like proteins facilitate the entry of urea into cells via the plasma membrane, followed by vacuolar loading through TIPs. Vacuolar loading is beneficial for the storage of excess urea, and vacuolar unloading can remobilize the urea under nitrogen starvation (Kojima et al., 2006). Zhang et al. (2016) demonstrated that CsNIP2;1, a plasma membrane transporter from *Cucumis sativus*, was able to transport urea through the plasma membrane when expressed in yeast. The expression of *CsNIP2;1* was induced by nitrogen deficiency. Additionally, they found that ectopic expression of *CsNIP2;1* improved the growth of Arabidopsis and rescued the growth of *atdur3-3* mutant on medium with urea as the sole N source. These results suggested that urea was transported by aquaporins of NIPs, which were localized in the plasma membrane. On the contrary, a lower expression of *AtNIP5;1* and *AtNIP6;1*, two urea transporters, was observed in Arabidopsis supplied with urea than with ammonium nitrate, although a higher expression of DUR3 was observed in the plants under similar conditions (Yang et al., 2015). It was postulated that the downregulation of *AtNIP5;1* and *AtNIP6;1* was involved in the detoxicification of urea/ammonia under excessive urea level. Besides, it was demonstrated that urea uptake decreased in *nip5;1* when compared with the wild type under boron deficient conditions. The remobilization of urea from vacuoles is regulated by TIPs. ZmTIP4;4, a maize aquaporin gene, was shown to facilitate the transport of urea, and the expression of the gene was upregulated under N deficiency in expanded leaves (Gu et al., 2012), suggesting that ZmTIP4;4 played an important role in unloading vacuolar urea across tonoplast under N deficient conditions. Soto et al. (2010) demonstrated that two urea transporters were involved in N recycling in pollen tubes in Arabidopsis.

Urea is degraded to ammonium by the enzyme urease present in soil. Ammonia (NH_4^+/NH_3) is taken up by roots mainly through ammonium transporters (Xu et al., 2012). Transport of NH_4^+/NH_3 into vacuole would allow N storage and eliminate toxicity, and the stored N could be remobilized by passive and low-affinity transport pathways. Both the influx and efflux of NH_4^+/NH_3 into vacuole are regulated by TIPs (Wang et al., 2016).

Nitrogen Supply Affects Drought Tolerance in Plants

Despite the high nitrate supply, increased root water uptake was observed under normal water condition, and the high

TABLE 1 | Drought tolerance was affected by the deregulation of a single aquaporin gene.

Deregulation	Drought tolerance	Species	Genes	Reference
Over-expression	Drought tolerant	Arabidopsis	JcPIP2;7/JcTIP1;3	Khan et al., 2015
		Arabidopsis	AvNIP5;1	Yu et al., 2015
		Arabidopsis	FaPIP2;1	Zhuang et al., 2015
		Arabidopsis	MaPIP1;1	Xu et al., 2014
		Arabidopsis	PgTIP1	Peng et al., 2007
		Tobacco	BjPIP1	Zhang et al., 2008
		Tobacco	BnPIP1	Yu et al., 2005
		Banana	MusaPIP1;2	Sreedharan et al., 2013
		Tomato	MdPIP1;3	Wang L. et al., 2017
		Tomato	SlPIP2;1/SlPIP2;5 /SlPIP2;7	Li R. et al., 2016
		Tomato	SlTIP2;2	Sade et al., 2009
		Rice	RWC3	Lian et al., 2004
		Soybean	GmTIP2;1	Zhang et al., 2017
Down-regulation	Drought sensitive	Arabidopsis	PIP1/PIP2	Martre et al., 2002
		Tobacco	NtAQP1	Siefritz et al., 2002
		Tobacco	BnPIP1	Yu et al., 2005
		Poplar	PIP1	Secchi and Zwieniecki, 2014

nitrate supply may decrease drought tolerance in plants under drought stress. Wilkinson et al. (2007) observed that the decrease in stomatal closure and leaf elongation rates were more sensitive to drought stress in maize plants supplied with high nitrate. Stomatal conductance decreased by 30% in plants supplied with high nitrate after 3 days of drought stress, whereas only 10% decrease in g_s was found in control plants (supplied with water). Further evidence showed that the effect of nitrate on growth inhibition under drought stress was associated with pH based ABA redistribution. Drought stress may induce the alkalinization of leaf apoplast, in tomato (Jia and Davies, 2007) and hop (Korovetska et al., 2014), and especially in plants supplied with high nitrate (Wilkinson et al., 2007). While pH increases under drought stress, more ABA is activated in leaf apoplast, which further induces stomatal closure (Zhang et al., 2006) and decrease in K_{leaf} (Shatil-Cohen et al., 2011).

On the other hand, nitrogen supply might affect plant drought tolerance through regulation of root water uptake (**Figure 1**). In plants supplied with ammonium nutrition, drought stress induced a rapid decrease in aquaporin expression (including PIPs and TIPs), meanwhile ABA started to accumulate in the roots (Ding et al., 2016b). After 24 h water stress treatment with PEG 6000, an increase in aquaporin expression was observed, and ABA accumulation reached a peak. Both increase in aquaporin expression and Lpr were regulated by ABA accumulation (Ding et al., 2015, 2016b). In plants supplied with nitrate, root water uptake and transport were restricted by lower aquaporin expression and/or activity, more aerenchyma formation was observed when compared with plants supplied with ammonium under water stress treatment with PEG 6000. Yang et al. (2012) investigated that more aerenchyma formation would restrict radial water transport in roots supplied with nitrate than with ammonium, and aerenchyma formation was regulated by ethylene production (Gao et al., 2017). Additionally, ethylene may inhibit ABA production (Sharp, 2002), which could further affect aquaporin expression.

Interestingly, increased root ABA content and higher stomatal conductance were found in rice plants supplied with ammonium than with nitrate under water stress treatment with PEG 6000 (Ding et al., 2016b). It's well known that drought stress induces stomatal closure, regulated by ABA; yet, this ABA may be not from roots. Christmann et al. (2007) showed that this ABA was biosynthesized in shoots and it further induced stomatal closure.

IMPLICATIONS

Many efforts have been made to increase crop drought resistance through identification of genetic, transcriptomic, metabolomic, and epigenetic aspects. Water uptake and photosynthesis are the two key traits that enhance crop drought tolerance. In this review, two approaches have been highlighted for enhancing crop drought tolerance:

(1) Deregulation of aquaporin expression. Many researchers have demonstrated that over-expressing a single aquaporin gene could enhance plant drought tolerance and silence the genes that result in drought sensitivity in plants (**Table 1**). There are plenty of aquaporin members in plant species (Fox et al., 2017), and they play important roles in controlling water relations (Chaumont and Tyerman, 2014), nutrient uptake (Wang et al., 2016), and photosynthesis (Groszmann et al., 2017; Uehlein et al., 2017). In the future, more aquaporin genes should be characterized and their expression should be genetically modified in specific tissues and/or organs to enhance plant drought tolerance.

(2) Ammonium fertilizer application for rice water saving culture. Rice is traditionally cultivated in waterlogged

conditions, and 80% of the freshwater used in agriculture is for rice production in China (Guo et al., 2007a). With increase in the severity of water shortage, water saving culture (non-flooded mulching cultivation) has become popular now. The main nutritional change that occurs when rice is cultivated in aerobic soil is the N form, i.e., from ammonium in waterlogged condition, to nitrate and/or the mixture of ammonium and nitrate in aerobic condition. It was well documented that ammonium nutrition could enhance rice seedling drought tolerance (Guo et al., 2007a; Li et al., 2009a). In non-flooded mulching cultivation of rice, we recommend using ammonium fertilizer to enhance drought tolerance in rice seedlings.

AUTHOR CONTRIBUTIONS

LD and SG wrote the manuscript. ZL, LG, and QS contributed to the discussion and revision of the manuscript.

FUNDING

This work was financially supported by the National Natural Science Foundation of China (31401941), the National Key Research and Development Plan of China (2016YFD0200900), and the Special Fund for Agriculture Profession of China (20150312205).

REFERENCES

Alsina, M. M., Smart, D. R., Bauerle, T., De Herralde, F., Biel, C., Stockert, C., et al. (2010). Seasonal changes of whole root system conductance by a drought-tolerant grape root system. *J. Exp. Bot.* 62, 99–109. doi: 10.1093/jxb/erq247

Aroca, R., Ferrante, A., Vernieri, P., and Chrispeels, M. J. (2006). Drought, abscisic acid and transpiration rate effects on the regulation of PIP aquaporin gene expression and abundance in *Phaseolus vulgaris* plants. *Ann. Bot.* 98, 1301–1310. doi: 10.1093/aob/mcl219

Aroca, R., Porcel, R., and Ruiz-Lozano, J. M. (2012). Regulation of root water uptake under abiotic stress conditions. *J. Exp. Bot.* 63, 43–57. doi: 10.1093/jxb/err266

Aroca, R., and Ruiz-Lozano, J. M. (2012). "Regulation of root water uptake under drought stress conditions," in *Plant Responses to Drought Stress*, ed. R. Aroca (Berlin: Springer), 113–127.

Barberon, M., Vermeer, J. E. M., De Bellis, D., Wang, P., Naseer, S., Andersen, T. G., et al. (2016). Adaptation of root function by nutrient-induced plasticity of endodermal differentiation. *Cell* 164, 447–459. doi: 10.1016/j.cell.2015.12.021

Bienert, M. D., and Bienert, G. P. (2017). "Plant aquaporins and metalloids," in *Plant Aquaporins*, F. Chaumont and S. D. Tyerman (Cham: Springer), 297–332.

Brodribb, T. J., Feild, T. S., and Jordan, G. J. (2007). Leaf maximum photosynthetic rate and venation are linked by hydraulics. *Plant Physiol.* 144, 1890–1898. doi: 10.1104/pp.107.101352

Buckley, T. N. (2015). The contributions of apoplastic, symplastic and gas phase pathways for water transport outside the bundle sheath in leaves. *Plant Cell Environ.* 38, 7–22. doi: 10.1111/pce.12372

Cano, F. J., López, R., and Warren, C. R. (2014). Implications of the mesophyll conductance to CO2 for photosynthesis and water-use efficiency during long-term water stress and recovery in two contrasting *Eucalyptus* species. *Plant Cell Environ.* 37, 2470–2490. doi: 10.1111/pce.12325

Chang, C. (2007). "Impacts, Adaptation and Vulnerability," in *Proceedings of the Contribution of Working Group II to the Fourth Assessment Report of the Intergovernmental Panel on Climate Change/ML Parry*, eds O. F. Canziani, J. P. Palutikof et al., (Cambridge: Cambridge University Press), 976.

Chaumont, F., Barrieu, F., Wojcik, E., Chrispeels, M. J., and Jung, R. (2001). Aquaporins constitute a large and highly divergent protein family in maize. *Plant Physiol.* 125, 1206–1215. doi: 10.1104/pp.125.3.1206

Chaumont, F., and Tyerman, S. D. (2014). Aquaporins: highly regulated channels controlling plant water relations. *Plant Physiol.* 164, 1600–1618. doi: 10.1104/pp.113.233791

Chaves, M. M., Maroco, J. P., and Pereira, J. S. (2003). Understanding plant responses to drought—from genes to the whole plant. *Funct. Plant Biol.* 30, 239–264. doi: 10.1071/FP02076

Christmann, A., Weiler, E. W., Steudle, E., and Grill, E. (2007). A hydraulic signal in root-to-shoot signalling of water shortage. *Plant J.* 52, 167–174. doi: 10.1111/j.1365-313X.2007.03234.x

Coupel-Ledru, A., Tyerman, S., Masclef, D., Lebon, E., Christophe, A., Edwards, E. J., et al. (2017). Abscisic acid down-regulates hydraulic conductance of grapevine leaves in isohydric genotypes only. *Plant Physiol.* 175, 1121–1134. doi: 10.1104/pp.17.00698

Cramer, M. D., Hawkins, H.-J., and Verboom, G. A. (2009). The importance of nutritional regulation of plant water flux. *Oecologia* 161, 15–24. doi: 10.1007/s00442-009-1364-3

Dean, R. M., Rivers, R. L., Zeidel, M. L., and Roberts, D. M. (1999). Purification and functional reconstitution of soybean nodulin 26. An aquaporin with water and glycerol transport properties. *Biochemistry* 38, 347–353. doi: 10.1021/bi982110c

Ding, L., Gao, C., Li, Y., Li, Y., Zhu, Y., Xu, G., et al. (2015). The enhanced drought tolerance of rice plants under ammonium is related to aquaporin (AQP). *Plant Sci.* 234, 14–21. doi: 10.1016/j.plantsci.2015.01.016

Ding, L., Gao, L., Liu, W., Wang, M., Gu, M., Ren, B., et al. (2016a). Aquaporin plays an important role in mediating chloroplastic CO2 concentration under high-N supply in rice (*Oryza sativa*) plants. *Physiol. Plant.* 156, 215–226. doi: 10.1111/ppl.12387

Ding, L., Li, Y., Wang, Y., Gao, L., Wang, M., Chaumont, F., et al. (2016b). Root ABA accumulation enhances rice seedling drought tolerance under ammonium supply: interaction with aquaporins. *Front. Plant Sci.* 7:1206. doi: 10.3389/fpls.2016.01206

Evans, J. R., Kaldenhoff, R., Genty, B., and Terashima, I. (2009). Resistances along the CO2 diffusion pathway inside leaves. *J. Exp. Bot.* 60, 2235–2248. doi: 10.1093/jxb/erp117

Farooq, M., Wahid, A., Kobayashi, N., Fujita, D., and Basra, S. (2009). *Plant Drought Stress: Effects, Mechanisms and Management Sustainable Agriculture*. Berlin: Springer), 153–188.

Flexas, J., Gallé, A., Galmés, J., Ribas-Carbo, M., and Medrano, H. (2012). "The response of photosynthesis to soil water stress," in *Plant Responses to Drought Stress*, ed. R. Aroca (Berlin: Springer), 129–144. doi: 10.1007/978-3-642-32653-0_5

Flexas, J., and Medrano, H. (2002). Drought-inhibition of photosynthesis in C3 plants: stomatal and non-stomatal limitations revisited. *Ann. Bot.* 89, 183–189. doi: 10.1093/aob/mcf027

Flexas, J., Ribas-Carbo, M., Diaz-Espejo, A., Galmes, J., and Medrano, H. (2008). Mesophyll conductance to CO2: current knowledge and future prospects. *Plant Cell Environ.* 31, 602–621. doi: 10.1111/j.1365-3040.2007.01757.x

Flexas, J., Ribas-Carbó, M., Bota, J., Galmés, J., Henkle, M., Martínez-Cañellas, S., et al. (2006a). Decreased Rubisco activity during water stress is not induced by decreased relative water content but related to conditions of low stomatal conductance and chloroplast CO2 concentration. *New Phytol.* 172, 73–82. doi: 10.1111/j.1469-8137.2006.01794.x

Flexas, J., Ribas-Carbo, M., Hanson, D. T., Bota, J., Otto, B., Cifre, J., et al. (2006b). Tobacco aquaporin NtAQP1 is involved in mesophyll conductance to CO2 *in vivo*. *Plant J.* 48, 427–439. doi: 10.1111/j.1365-313X.2006.02879.x

Flexas, J., Scoffoni, C., Gago, J., and Sack, L. (2013). Leaf mesophyll conductance and leaf hydraulic conductance: an introduction to their measurement and coordination. *J. Exp. Bot.* 64, 3965–3981. doi: 10.1093/jxb/ert319

Fortin, M. G., Morrison, N. A., and Verma, D. P. S. (1987). Nodulin-26, a peribacteroid membrane nodulin is expressed independently of the

development of the peribacteroid compartment. *Nucleic Acids Res.* 15, 813–824. doi: 10.1093/nar/15.2.813

Fouquet, R., Léon, C., Ollat, N., and Barrieu, F. (2008). Identification of grapevine aquaporins and expression analysis in developing berries. *Plant Cell Rep.* 27, 1541–1550. doi: 10.1007/s00299-008-0566-1

Fox, A. R., Maistriaux, L. C., and Chaumont, F. (2017). Toward understanding of the high number of plant aquaporin isoforms and multiple regulation mechanisms. *Plant Sci.* 264, 179–187. doi: 10.1016/j.plantsci.2017.07.021

Galle, A., Florez-Sarasa, I., Tomas, M., Pou, A., Medrano, H., Ribas-Carbo, M., et al. (2009). The role of mesophyll conductance during water stress and recovery in tobacco (*Nicotiana sylvestris*): acclimation or limitation? *J. Exp. Bot.* 60, 2379–2390. doi: 10.1093/jxb/erp071

Gallé, A., Haldimann, P., and Feller, U. (2007). Photosynthetic performance and water relations in young pubescent oak (*Quercus pubescens*) trees during drought stress and recovery. *New Phytol.* 174, 799–810. doi: 10.1111/j.1469-8137.2007.02047.x

Galmés, J., Medrano, H., and Flexas, J. (2007). Photosynthetic limitations in response to water stress and recovery in Mediterranean plants with different growth forms. *New Phytol.* 175, 81–93. doi: 10.1111/j.1469-8137.2007.02087.x

Gambetta, G. A., Knipfer, T., Fricke, W., and Mcelrone, A. J. (2017). "Aquaporins and Root Water Uptake," in *Plant Aquaporins: From Transport to Signaling*, eds F. Chaumont and S. D. Tyerman(Cham: Springer), 133–153. doi: 10.1007/978-3-319-49395-4_6

Gao, C., Ding, L., Li, Y., Chen, Y., Zhu, J., Gu, M., et al. (2017). Nitrate increases ethylene production and aerenchyma formation in roots of lowland rice plants under water stress. *Funct. Plant Biol.* 44, 430–442. doi: 10.1071/FP16258

Gao, Y. X., Li, Y., Yang, X. X., Li, H. J., Shen, Q. R., and Guo, S. W. (2010). Ammonium nutrition increases water absorption in rice seedlings (*Oryza sativa* L.) under water stress. *Plant Soil* 331, 193–201. doi: 10.1007/s11104-009-0245-1

Geber, M. A., and Dawson, T. E. (1990). Genetic variation in and covariation between leaf gas exchange, morphology, and development in *Polygonum arenastrum*, an annual plant. *Oecologia* 85, 153–158. doi: 10.1007/BF00319396

Giovannetti, M., Balestrini, R., Volpe, V., Guether, M., Straub, D., Costa, A., et al. (2012). Two putative-aquaporin genes are differentially expressed during arbuscular mycorrhizal symbiosis in *Lotus japonicus*. *BMC Plant Biol.* 12:186. doi: 10.1186/1471-2229-12-186

Gleason, S. M., Wiggans, D. R., Bliss, C. A., Comas, L. H., Cooper, M., Dejonge, K. C., et al. (2017). Coordinated decline in photosynthesis and hydraulic conductance during drought stress in *Zea mays*. *Flora* 227, 1–9. doi: 10.1016/j.flora.2016.11.017

Górska, A., Lazor, J. W., Zwieniecka, A. K., Benway, C., and Zwieniecki, M. A. (2010). The capacity for nitrate regulation of root hydraulic properties correlates with species' nitrate uptake rates. *Plant Soil* 337, 447–455. doi: 10.1007/s11104-010-0540-x

Gorska, A., Ye, Q., Holbrook, N. M., and Zwieniecki, M. A. (2008a). Nitrate control of root hydraulic properties in plants: translating local information to whole plant response. *Plant Physiol.* 148, 1159–1167. doi: 10.1104/pp.108.122499

Gorska, A., Zwieniecka, A., Holbrook, N. M., and Zwieniecki, M. A. (2008b). Nitrate induction of root hydraulic conductivity in maize is not correlated with aquaporin expression. *Planta* 228, 989–998. doi: 10.1007/s00425-008-0798-x

Grondin, A., Mauleon, R., Vadez, V., and Henry, A. (2016). Root aquaporins contribute to whole plant water fluxes under drought stress in rice (*Oryza sativa* L.). *Plant Cell Environ.* 39, 347–365. doi: 10.1111/pce.12616

Groszmann, M., Osborn, H. L., and Evans, J. R. (2017). Carbon dioxide and water transport through plant aquaporins. *Plant Cell Environ.* 40, 938–961. doi: 10.1111/pce.12844

Gu, R., Chen, X., Zhou, Y., and Yuan, L. (2012). Isolation and characterization of three maize aquaporin genes, ZmNIP2; 1, ZmNIP2; 4 and ZmTIP4; 4 involved in urea transport. *BMB Rep.* 45, 96–101. doi: 10.5483/BMBRep.2012.45.2.96

Guenther, J. F., Chanmanivone, N., Galetovic, M. P., Wallace, I. S., Cobb, J. A., and Roberts, D. M. (2003). Phosphorylation of soybean nodulin 26 on serine 262 enhances water permeability and is regulated developmentally and by osmotic signals. *Plant Cell* 15, 981–991. doi: 10.1105/tpc.009787

Guo, S., Bruck, H., and Sattelmacher, B. (2002). Effects of supplied nitrogen form on growth and water uptake of French bean (*Phaseolus vulgaris* L.) plants - Nitrogen form and water uptake. *Plant Soil* 239, 267–275. doi: 10.1023/A:1015014417018

Guo, S., Chen, G., Zhou, Y., and Shen, Q. R. (2007a). Ammonium nutrition increases photosynthesis rate under water stress at early development stage of rice (*Oryza sativa* L.). *Plant Soil* 296, 115–124. doi: 10.1007/s11104-007-9302-9

Guo, S., Kaldenhoff, R., Uehlein, N., Sattelmacher, B., and Brueck, H. (2007b). Relationship between water and nitrogen uptake in nitrate- and ammonium-supplied *Phaseolus vulgaris* L. plants. *J. Plant Nutr. Soil Sci.* 170, 73–80. doi: 10.1002/jpln.200625073

Guo, S., Zhou, Y., Shen, Q., and Zhang, F. (2007c). Effect of ammonium and nitrate nutrition on some physiological processes in higher plants - Growth, photosynthesis, photorespiration, and water relations. *Plant Biol.* 9, 21–29. doi: 10.1055/s-2006-924541

Hachez, C., Milhiet, T., Heinen, R. B., and Chaumont, F. (2017). "Roles of Aquaporins in Stomata," in *Plant Aquaporins*, eds F. Chaumont and S. Tyerman (Cham: Springer), 167–183. doi: 10.1007/978-3-319-49395-4_8

Hachez, C., Veselov, D., Ye, Q., Reinhardt, H., Knipfer, T., Fricke, W., et al. (2012). Short-term control of maize cell and root water permeability through plasma membrane aquaporin isoforms. *Plant Cell Environ.* 35, 185–198. doi: 10.1111/j.1365-3040.2011.02429.x

Henry, A., Cal, A. J., Batoto, T. C., Torres, R. O., and Serraj, R. (2012). Root attributes affecting water uptake of rice (*Oryza sativa*) under drought. *J. Exp. Bot.* 63, 4751–4763. doi: 10.1093/jxb/ers150

Hose, E., Steudle, E., and Hartung, W. (2000). Abscisic acid and hydraulic conductivity of maize roots: a study using cell-and root-pressure probes. *Planta* 211, 874–882. doi: 10.1007/s004250000412

Hwang, J. H. (2013). *Soybean Nodulin 26: A Channel for Water and Ammonia at the Symbiotic Interface of Legumes and Nitrogen-Fixing Rhizobia Bacteria*. Ph.D. dissociation, Knoxville, TN, University of Tennessee.

Hwang, J. H., Ellingson, S. R., and Roberts, D. M. (2010). Ammonia permeability of the soybean nodulin 26 channel. *FEBS Lett.* 584, 4339–4343. doi: 10.1016/j.febslet.2010.09.033

Ishikawa-Sakurai, J., Hayashi, H., and Murai-Hatano, M. (2014). Nitrogen availability affects hydraulic conductivity of rice roots, possibly through changes in aquaporin gene expression. *Plant Soil* 379, 289–300. doi: 10.1007/s11104-014-2070-4

Iuchi, S., Kobayashi, M., Taji, T., Naramoto, M., Seki, M., Kato, T., et al. (2001). Regulation of drought tolerance by gene manipulation of 9-*cis*-epoxycarotenoid dioxygenase, a key enzyme in abscisic acid biosynthesis in Arabidopsis. *Plant J.* 27, 325–333. doi: 10.1046/j.1365-313x.2001.01096.x

Izanloo, A., Condon, A. G., Langridge, P., Tester, M., and Schnurbusch, T. (2008). Different mechanisms of adaptation to cyclic water stress in two South Australian bread wheat cultivars. *J. Exp. Bot.* 59, 3327–3346. doi: 10.1093/jxb/ern199

Jackson, R. B., Sperry, J. S., and Dawson, T. E. (2000). Root water uptake and transport: using physiological processes in global predictions. *Trends Plant Sci.* 5, 482–488. doi: 10.1016/S1360-1385(00)01766-0

Javot, H., and Maurel, C. (2002). The role of aquaporins in root water uptake. *Ann. Bot.* 90, 301–313. doi: 10.1093/aob/mcf199

Jia, W., and Davies, W. J. (2007). Modification of leaf apoplastic pH in relation to stomatal sensitivity to root-sourced abscisic acid signals. *Plant Physiol.* 143, 68–77. doi: 10.1104/pp.106.089110

Johanson, U., Karlsson, M., Johansson, I., Gustavsson, S., Sjövall, S., Fraysse, L., et al. (2001). The complete set of genes encoding major intrinsic proteins in Arabidopsis provides a framework for a new nomenclature for major intrinsic proteins in plants. *Plant Physiol.* 126, 1358–1369. doi: 10.1104/pp.126.4.1358

Johnson, D. M., Meinzer, F. C., Woodruff, D. R., and Mcculloh, K. A. (2009). Leaf xylem embolism, detected acoustically and by cryo-SEM, corresponds to decreases in leaf hydraulic conductance in four evergreen species. *Plant Cell Environ.* 32, 828–836. doi: 10.1111/j.1365-3040.2009.01961.x

Kaiser, W. M. (1987). Effects of water deficit on photosynthetic capacity. *Physiol. Plant.* 71, 142–149. doi: 10.1111/j.1399-3054.1987.tb04631.x

Kaldenhoff, R. (2012). Mechanisms underlying CO2 diffusion in leaves. *Curr. Opin. Plant Biol.* 15, 276–281. doi: 10.1016/j.pbi.2012.01.011

Kaldenhoff, R., and Fischer, M. (2006). Functional aquaporin diversity in plants. *Biochim. Biophys. Acta* 1758, 1134–1141. doi: 10.1016/j.bbamem.2006.03.012

Khan, K., Agarwal, P., Shanware, A., and Sane, V. A. (2015). Heterologous expression of two Jatropha aquaporins imparts drought and salt tolerance and improves seed viability in transgenic *Arabidopsis thaliana*. *PLoS One* 10:e0128866. doi: 10.1371/journal.pone.0128866

Kojima, S., Bohner, A., and Von Wirén, N. (2006). Molecular mechanisms of urea transport in plants. *J. Membr. Biol.* 212, 83–91. doi: 10.1007/s00232-006-0868-6

Korovetska, H., Novák, O., Jùza, O., and Gloser, V. (2014). Signalling mechanisms involved in the response of two varieties of *Humulus lupulus* L. to soil drying: I. changes in xylem sap pH and the concentrations of abscisic acid and anions. *Plant Soil* 380, 375–387. doi: 10.1007/s11104-014-2101-1

Lambers, H., Chapin, F. III, and Pons, T. (2008). *Plant Physiological Ecology*, 2nd Edn. New York, NY: Springer-Verlag. doi: 10.1007/978-0-387-78341-3

Li, G., Tillard, P., Gojon, A., and Maurel, C. (2016). Dual regulation of root hydraulic conductivity and plasma membrane aquaporins by plant nitrate accumulation and high-affinity nitrate transporter NRT2. 1. *Plant Cell Physiol.* 57, 733–742. doi: 10.1093/pcp/pcw022

Li, R., Wang, J., Li, S., Zhang, L., Qi, C., Weeda, S., et al. (2016). Plasma membrane intrinsic proteins *SlPIP2; 1*, *SlPIP2; 7* and *SlPIP2; 5* conferring enhanced drought stress tolerance in tomato. *Sci. Rep.* 6:31814. doi: 10.1038/srep31814

Li, Y., Gao, Y. X., Ding, L., Shen, Q. R., and Guo, S. W. (2009a). Ammonium enhances the tolerance of rice seedlings (*Oryza sativa* L.) to drought condition. *Agric. Water Manag.* 96, 1746–1750. doi: 10.1016/j.agwat.2009.07.008

Li, Y., Gao, Y. X., Xu, X. M., Shen, Q. R., and Guo, S. W. (2009b). Light-saturated photosynthetic rate in high-nitrogen rice (*Oryza sativa* L.) leaves is related to chloroplastic CO2 concentration. *J. Exp. Bot.* 60, 2351–2360. doi: 10.1093/jxb/erp127

Li, Y., Ren, B. B., Yang, X. X., Xu, G. H., Shen, Q. R., and Guo, S. W. (2012). Chloroplast downsizing under nitrate nutrition restrained mesophyll conductance and photosynthesis in rice (*Oryza sativa* L.) under drought conditions. *Plant Cell Physiol.* 53, 892–900. doi: 10.1093/pcp/pcs032

Lian, H.-L., Yu, X., Ye, Q., Ding, X.-S., Kitagawa, Y., Kwak, S.-S., et al. (2004). The role of aquaporin RWC3 in drought avoidance in rice. *Plant Cell Physiol.* 45, 481–489. doi: 10.1093/pcp/pch058

Liu, L.-H., Ludewig, U., Frommer, W. B., and Von Wirén, N. (2003a). AtDUR3 encodes a new type of high-affinity urea/H+ symporter in Arabidopsis. *Plant Cell* 15, 790–800. doi: 10.1105/tpc.007120

Liu, L.-H., Ludewig, U., Gassert, B., Frommer, W. B., and Von Wirén, N. (2003b). Urea transport by nitrogen-regulated tonoplast intrinsic proteins in Arabidopsis. *Plant Physiol.* 133, 1220–1228. doi: 10.1104/pp.103.027409

Ma, J. F., and Yamaji, N. (2015). A cooperative system of silicon transport in plants. *Trends Plant Sci.* 20, 435–442. doi: 10.1016/j.tplants.2015.04.007

Ma, J. F., Yamaji, N., Mitani, N., Xu, X.-Y., Su, Y.-H., Mcgrath, S. P., et al. (2008). Transporters of arsenite in rice and their role in arsenic accumulation in rice grain. *Proc. Natl. Acad. Sci. U.S.A.* 105, 9931–9935. doi: 10.1073/pnas.0802361105

Mahdieh, M., and Mostajeran, A. (2009). Abscisic acid regulates root hydraulic conductance via aquaporin expression modulation in *Nicotiana tabacum*. *J. Plant Physiol.* 166, 1993–2003. doi: 10.1016/j.jplph.2009.06.001

Mahdieh, M., Mostajeran, A., Horie, T., and Katsuhara, M. (2008). Drought stress alters water relations and expression of PIP-type aquaporin genes in *Nicotiana tabacum* plants. *Plant Cell Physiol.* 49, 801–813. doi: 10.1093/pcp/pcn054

Martre, P., Morillon, R., Barrieu, F., North, G. B., Nobel, P. S., and Chrispeels, M. J. (2002). Plasma membrane aquaporins play a significant role during recovery from water deficit. *Plant Physiol.* 130, 2101–2110. doi: 10.1104/pp.009019

Masalkar, P., Wallace, I. S., Hwang, J. H., and Roberts, D. M. (2010). Interaction of cytosolic glutamine synthetase of soybean root nodules with the C-terminal domain of the symbiosome membrane nodulin 26 aquaglyceroporin. *J. Biol. Chem.* 285, 23880–23888. doi: 10.1074/jbc.M110.135657

Maurel, C. (1997). Aquaporins and water permeability of plant membranes. *Annu. Rev. Plant Biol.* 48, 399–429. doi: 10.1146/annurev.arplant.48.1.399

McLean, E. H., Ludwig, M., and Grierson, P. F. (2011). Root hydraulic conductance and aquaporin abundance respond rapidly to partial root-zone drying events in a riparian *Melaleuca* species. *New Phytol.* 192, 664–675. doi: 10.1111/j.1469-8137.2011.03834.x

Medrano, H., Escalona, J., Bota, J., Gulias, J., and Flexas, J. (2002). Regulation of photosynthesis of C3 plants in response to progressive drought: stomatal conductance as a reference parameter. *Ann. Bot.* 89, 895–905. doi: 10.1093/aob/mcf079

Meng, D., and Fricke, W. (2017). Changes in root hydraulic conductivity facilitate the overall hydraulic response of rice (*Oryza sativa* L.) cultivars to salt and osmotic stress. *Plant Physiol. Biochem.* 113, 64–77. doi: 10.1016/j.plaphy.2017.02.001

Mihailović, N., Jelić, G., Filipović, R., Djurdjević, M., and Dželetović, Ž. (1992). Effect of nitrogen form on maize response to drought stress. *Plant Soil* 144, 191–197. doi: 10.1007/BF00012875

Miyazawa, S. -I., Yoshimura, S., Shinzaki, Y., Maeshima, M., and Miyake, C. (2008). Deactivation of aquaporins decreases internal conductance to CO2 diffusion in tobacco leaves grown under long-term drought. *Funct. Plant Biol.* 35, 553–564. doi: 10.1071/FP08117

Mizokami, Y., Noguchi, K., Kojima, M., Sakakibara, H., and Terashima, I. (2015). Mesophyll conductance decreases in the wild type but not in an ABA-deficient mutant (*aba1*) of *Nicotiana plumbaginifolia* under drought conditions. *Plant Cell Environ.* 38, 388–398. doi: 10.1111/pce.12394

Morgan, J. M. (1984). Osmoregulation and water stress in higher plants. *Annu. Rev. Plant Physiol.* 35, 299–319. doi: 10.1146/annurev.pp.35.060184.001503

Mylona, P., Pawlowski, K., and Bisseling, T. (1995). Symbiotic nitrogen fixation. *Plant Cell* 7, 869–885. doi: 10.1105/tpc.7.7.869

Nardini, A., and Salleo, S. (2005). Water stress-induced modifications of leaf hydraulic architecture in sunflower: co-ordination with gas exchange. *J. Exp. Bot.* 56, 3093–3101. doi: 10.1093/jxb/eri306

Niemietz, C. M., and Tyerman, S. D. (2000). Channel-mediated permeation of ammonia gas through the peribacteroid membrane of soybean nodules. *FEBS Lett.* 465, 110–114. doi: 10.1016/S0014-5793(99)01729-9

North, G., Martre, P., and Nobel, P. (2004). Aquaporins account for variations in hydraulic conductance for metabolically active root regions of *Agave deserti* in wet, dry, and rewetted soil. *Plant Cell Environ.* 27, 219–228. doi: 10.1111/j.1365-3040.2003.01137.x

Parent, B., Hachez, C., Redondo, E., Simonneau, T., Chaumont, F., and Tardieu, F. (2009). Drought and abscisic acid effects on aquaporin content translate into changes in hydraulic conductivity and leaf growth rate: a trans-scale approach. *Plant Physiol.* 149, 2000–2012. doi: 10.1104/pp.108.130682

Park, W., Scheffler, B. E., Bauer, P. J., and Campbell, B. T. (2010). Identification of the family of aquaporin genes and their expression in upland cotton (*Gossypium hirsutum* L.). *BMC Plant Biol.* 10:142. doi: 10.1186/1471-2229-10-142

Parry, M., Canziani, O., Palutikof, J., Van Der Linden, P. J., and Hanson, C. E. (2007). *Climate Change 2007: Impacts, Adaptation and Vulnerability*. Cambridge: Cambridge University Press.

Peng, Y., Lin, W., Cai, W., and Arora, R. (2007). Overexpression of a *Panax ginseng* tonoplast aquaporin alters salt tolerance, drought tolerance and cold acclimation ability in transgenic Arabidopsis plants. *Planta* 226, 729–740. doi: 10.1007/s00425-007-0520-4

Perez-Martin, A., Michelazzo, C., Torres-Ruiz, J. M., Flexas, J., Fernandez, J. E., Sebastiani, L., et al. (2014). Regulation of photosynthesis and stomatal and mesophyll conductance under water stress and recovery in olive trees: correlation with gene expression of carbonic anhydrase and aquaporins. *J. Exp. Bot.* 65, 3143–3156. doi: 10.1093/jxb/eru160

Pinheiro, H. A., Damatta, F. M., Chaves, A. R., Loureiro, M. E., and Ducatti, C. (2005). Drought tolerance is associated with rooting depth and stomatal control of water use in clones of *Coffea canephora*. *Ann. Bot.* 96, 101–108. doi: 10.1093/aob/mci154

Postaire, O., Tournaire-Roux, C., Grondin, A., Boursiac, Y., Morillon, R., Schaffner, A. R., et al. (2010). A PIP1 aquaporin contributes to hydrostatic pressure-induced water transport in both the root and rosette of Arabidopsis. *Plant Physiol.* 152, 1418–1430. doi: 10.1104/pp.109.145326

Pou, A., Medrano, H., Flexas, J., and Tyerman, S. D. (2013). A putative role for TIP and PIP aquaporins in dynamics of leaf hydraulic and stomatal conductances in grapevine under water stress and re-watering. *Plant Cell Environ.* 36, 828–843. doi: 10.1111/pce.12019

Qian, Z. J., Song, J. J., Chaumont, F., and Ye, Q. (2015). Differential responses of plasma membrane aquaporins in mediating water transport of cucumber seedlings under osmotic and salt stresses. *Plant Cell Environ.* 38, 461–473. doi: 10.1111/pce.12319

Ranathunge, K., Kotula, L., Steudle, E., and Lafitte, R. (2004). Water permeability and reflection coefficient of the outer part of young rice roots are differently affected by closure of water channels (aquaporins) or blockage of apoplastic pores. *J. Exp. Bot.* 55, 433–447. doi: 10.1093/jxb/erh041

Ranathunge, K., Schreiber, L., Bi, Y.-M., and Rothstein, S. J. (2016). Ammonium-induced architectural and anatomical changes with altered suberin and lignin levels significantly change water and solute permeabilities of rice (*Oryza sativa* L.) roots. *Planta* 243, 231–249. doi: 10.1007/s00425-015-2406-1

Ranathunge, K., Steudle, E., and Lafitte, R. (2003). Control of water uptake by rice (*Oryza sativa* L.): role of the outer part of the root. *Planta* 217, 193–205.

Ren, B., Wang, M., Chen, Y., Sun, G., Li, Y., Shen, Q., et al. (2015). Water absorption is affected by the nitrogen supply to rice plants. *Plant Soil* 396, 397–410. doi: 10.1007/s11104-015-2603-5

Rivers, R. L., Dean, R. M., Chandy, G., Hall, J. E., Roberts, D. M., and Zeidel, M. L. (1997). Functional analysis of nodulin 26, an aquaporin in soybean root nodule symbiosomes. *J. Biol. Chem.* 272, 16256–16261. doi: 10.1074/jbc.272.26.16256

Roberts, D. M., and Routray, P. (2017). "The nodulin 26 intrinsic protein subfamily," in *Plant Aquaporins*, eds F. Chaumont and S. Tyerman (Cham: Springer), 267–296.

Rodrigues, O., Reshetnyak, G., Grondin, A., Saijo, Y., Leonhardt, N., Maurel, C., et al. (2017). Aquaporins facilitate hydrogen peroxide entry into guard cells to mediate ABA-and pathogen-triggered stomatal closure. *Proc. Natl. Acad. Sci. U.S.A.* 114, 9200–9205. doi: 10.1073/pnas.1704754114

Roth, L., and Stacey, G. (1989). Bacterium release into host cells of nitrogen-fixing soybean nodules: the symbiosome membrane comes from three sources. *Eur. J. Cell Biol.* 49, 13–23.

Sack, L., and Holbrook, N. M. (2006). Leaf hydraulics. *Annu. Rev. Plant Biol.* 57, 361–381. doi: 10.1146/annurev.arplant.56.032604.144141

Sade, N., and Moshelion, M. (2017). "Plant aquaporins and abiotic stress," in *Plant Aquaporins*, eds F. Chaumont and S. D. Tyerman (Berlin: Springer), 185–206.

Sade, N., Shatil-Cohen, A., and Moshelion, M. (2015). Bundle-sheath aquaporins play a role in controlling Arabidopsis leaf hydraulic conductivity. *Plant Signal. Behav.* 10:e1017177. doi: 10.1080/15592324.2015.1017177

Sade, N., Vinocur, B. J., Diber, A., Shatil, A., Ronen, G., Nissan, H., et al. (2009). Improving plant stress tolerance and yield production: is the tonoplast aquaporin SlTIP2; 2 a key to isohydric to anisohydric conversion? *New Phytol.* 181, 651–661. doi: 10.1111/j.1469-8137.2008.02689.x

Sakurai, J., Ishikawa, F., Yamaguchi, T., Uemura, M., and Maeshima, M. (2005). Identification of 33 rice aquaporin genes and analysis of their expression and function. *Plant Cell Physiol.* 46, 1568–1577. doi: 10.1093/pcp/pci172

Schulze, E. (1986). Carbon dioxide and water vapor exchange in response to drought in the atmosphere and in the soil. *Annu. Rev. Plant Physiol.* 37, 247–274. doi: 10.1146/annurev.pp.37.060186.001335

Schwab, K., Schreiber, U., and Heber, U. (1989). Response of photosynthesis and respiration of resurrection plants to desiccation and rehydration. *Planta* 177, 217–227. doi: 10.1007/BF00392810

Scoffoni, C., Chatelet, D. S., Pasquet-Kok, J., Rawls, M., Donoghue, M. J., Edwards, E. J., et al. (2016). Hydraulic basis for the evolution of photosynthetic productivity. *Nat. Plants* 2:16072. doi: 10.1038/nplants.2016.72

Scoffoni, C., Mckown, A. D., Rawls, M., and Sack, L. (2011a). Dynamics of leaf hydraulic conductance with water status: quantification and analysis of species differences under steady state. *J. Exp. Bot.* 63, 643–658. doi: 10.1093/jxb/err270

Scoffoni, C., Rawls, M., Mckown, A., Cochard, H., and Sack, L. (2011b). Decline of leaf hydraulic conductance with dehydration: relationship to leaf size and venation architecture. *Plant Physiol.* 156, 832–843. doi: 10.1104/pp.111.173856

Secchi, F., and Zwieniecki, M. A. (2014). Down-regulation of plasma intrinsic protein1 aquaporin in poplar trees is detrimental to recovery from embolism. *Plant Physiol.* 164, 1789–1799. doi: 10.1104/pp.114.237511

Seki, M., Umezawa, T., Urano, K., and Shinozaki, K. (2007). Regulatory metabolic networks in drought stress responses. *Curr. Opin. Plant Biol.* 10, 296–302. doi: 10.1016/j.pbi.2007.04.014

Sharp, R. E. (2002). Interaction with ethylene: changing views on the role of abscisic acid in root and shoot growth responses to water stress. *Plant Cell Environ.* 25, 211–222. doi: 10.1046/j.1365-3040.2002.00798.x

Shatil-Cohen, A., Attia, Z., and Moshelion, M. (2011). Bundle-sheath cell regulation of xylem-mesophyll water transport via aquaporins under drought stress: a target of xylem-borne ABA? *Plant J.* 67, 72–80. doi: 10.1111/j.1365-313X.2011.04576.x

Siefritz, F., Tyree, M. T., Lovisolo, C., Schubert, A., and Kaldenhoff, R. (2002). PIP1 plasma membrane aquaporins in tobacco from cellular effects to function in plants. *Plant Cell* 14, 869–876. doi: 10.1105/tpc.000901

Skelton, R. P., Brodribb, T. J., Mcadam, S. A., and Mitchell, P. J. (2017). Gas exchange recovery following natural drought is rapid unless limited by loss of leaf hydraulic conductance: evidence from an evergreen woodland. *New Phytol.* 215, 1399–1412. doi: 10.1111/nph.14652

Skirycz, A., and Inzé, D. (2010). More from less: plant growth under limited water. *Curr. Opin. Biotechnol.* 21, 197–203. doi: 10.1016/j.copbio.2010.03.002

Smith, S. E., and Smith, F. A. (2011). Roles of arbuscular mycorrhizas in plant nutrition and growth: new paradigms from cellular to ecosystem scales. *Annu. Rev. Plant Biol.* 62, 227–250. doi: 10.1146/annurev-arplant-042110-103846

Soto, G., Fox, R., Ayub, N., Alleva, K., Guaimas, F., Erijman, E. J., et al. (2010). TIP5; 1 is an aquaporin specifically targeted to pollen mitochondria and is probably involved in nitrogen remobilization in *Arabidopsis thaliana*. *Plant J.* 64, 1038–1047. doi: 10.1111/j.1365-313X.2010.04395.x

Sreedharan, S., Shekhawat, U. K., and Ganapathi, T. R. (2013). Transgenic banana plants overexpressing a native plasma membrane aquaporin MusaPIP1; 2 display high tolerance levels to different abiotic stresses. *Plant Biotechnol. J.* 11, 942–952. doi: 10.1111/pbi.12086

Steudle, E. (2000a). Water uptake by plant roots: an integration of views. *Plant Soil* 226, 45–56. doi: 10.1023/A:1026439226716

Steudle, E. (2000b). Water uptake by roots: effects of water deficit. *J. Exp. Bot.* 51, 1531–1542. doi: 10.1093/jexbot/51.350.1531

Steudle, E., and Peterson, C. A. (1998). How does water get through roots? *J. Exp. Bot.* 49, 775–788. doi: 10.1093/jxb/49.322.775

Tabassum, M. A., Zhu, G., Hafeez, A., Wahid, M. A., Shaban, M., and Li, Y. (2016). Influence of leaf vein density and thickness on hydraulic conductance and photosynthesis in rice (*Oryza sativa* L.) during water stress. *Sci. Rep.* 6:36894. doi: 10.1038/srep36894

Takano, J., Miwa, K., and Fujiwara, T. (2008). Boron transport mechanisms: collaboration of channels and transporters. *Trends Plant Sci.* 13, 451–457. doi: 10.1016/j.tplants.2008.05.007

Tang, A. C., Kawamitsu, Y., Kanechi, M., and Boyer, J. S. (2002). Photosynthetic oxygen evolution at low water potential in leaf discs lacking an epidermis. *Ann. Bot.* 89, 861–870. doi: 10.1093/aob/mcf081

Tezara, W., Mitchell, V., Driscoll, S., and Lawlor, D. (1999). Water stress inhibits plant photosynthesis by decreasing coupling factor and ATP. *Nature* 401, 914–917. doi: 10.1038/44842

Tyerman, S. D., Wignes, J. A., and Kaiser, B. N. (2017). "Root Hydraulic and Aquaporin Responses to N Availability," in *Plant Aquaporins*, eds F. Chaumont and S. Tyerman (Cham: Springer), 207–236.

Udvardi, M., and Poole, P. S. (2013). Transport and metabolism in legume-rhizobia symbioses. *Annu. Rev. Plant Biol.* 64, 781–805. doi: 10.1146/annurev-arplant-050312-120235

Uehlein, N., Fileschi, K., Eckert, M., Bienert, G. P., Bertl, A., and Kaldenhoff, R. (2007). Arbuscular mycorrhizal symbiosis and plant aquaporin expression. *Phytochemistry* 68, 122–129. doi: 10.1016/j.phytochem.2006.09.033

Uehlein, N., Kai, L., and Kaldenhoff, R. (2017). "Plant Aquaporins and CO2," in *Plant Aquaporins*, eds F. Chaumont and S. Tyerman (Cham: Springer), 255–265. doi: 10.1007/978-3-319-49395-4_12

Vandeleur, R. K., Mayo, G., Shelden, M. C., Gilliham, M., Kaiser, B. N., and Tyerman, S. D. (2009). The role of plasma membrane intrinsic protein aquaporins in water transport through roots: diurnal and drought stress responses reveal different strategies between isohydric and anisohydric cultivars of grapevine. *Plant Physiol.* 149, 445–460. doi: 10.1104/pp.108.128645

Vandeleur, R. K., Sullivan, W., Athman, A., Jordans, C., Gilliham, M., Kaiser, B. N., et al. (2014). Rapid shoot-to-root signalling regulates root hydraulic conductance via aquaporins. *Plant Cell Environ.* 37, 520–538. doi: 10.1111/pce.12175

Vilagrosa, A., Chirino, E., Peguero-Pina, J. -J., Barigah, T. S., Cochard, H., and Gil-Pelegrin, E. (2012). "Xylem cavitation and embolism in plants living in water-limited ecosystems," in *Plant Responses to Drought Stress*, ed. R. Aroca (Berlin: Springer), 63–109.

Wang, L., Li, Q.-T., Lei, Q., Feng, C., Zheng, X., Zhou, F., et al. (2017). Ectopically expressing *MdPIP1; 3*, an aquaporin gene, increased fruit size and enhanced drought tolerance of transgenic tomatoes. *BMC Plant Biol.* 17:246. doi: 10.1186/s12870-017-1212-2

Wang, Y., Li, R., Li, D., Jia, X., Zhou, D., Li, J., et al. (2017). NIP1; 2 is a plasma membrane-localized transporter mediating aluminum uptake, translocation, and tolerance in Arabidopsis. *Proc. Natl. Acad. Sci. U.S.A.* 114, 5047–5052. doi: 10.1073/pnas.1618557114

Wang, M., Ding, L., Gao, L., Li, Y., Shen, Q., and Guo, S. (2016). The Interactions of aquaporins and mineral nutrients in higher plants. *Int. J. Mol. Sci.* 17:E1229. doi: 10.3390/ijms17081229

Wang, M., Shen, Q. R., Xu, G. H., and Guo, S. W. (2014). New insight into the strategy for nitrogen metabolism in plant cells. *Int. Rev. Cell Mol. Biol.* 310, 1–37. doi: 10.1016/B978-0-12-800180-6.00001-3

Weaver, C. D., Crombie, B., Stacey, G., and Roberts, D. M. (1991). Calcium-dependent phosphorylation of symbiosome membrane proteins from nitrogen-fixing soybean nodules: evidence for phosphorylation of nodulin-26. *Plant Physiol.* 95, 222–227. doi: 10.1104/pp.95.1.222

Wilkinson, S., Bacon, M. A., and Davies, W. J. (2007). Nitrate signalling to stomata and growing leaves: interactions with soil drying, ABA, and xylem sap pH in maize. *J. Exp. Bot.* 58, 1705–1716. doi: 10.1093/jxb/erm021

Witte, C.-P. (2011). Urea metabolism in plants. *Plant Sci.* 180, 431–438. doi: 10.1016/j.plantsci.2010.11.010

Xiong, D., Flexas, J., Yu, T., Peng, S., and Huang, J. (2017). Leaf anatomy mediates coordination of leaf hydraulic conductance and mesophyll conductance to CO2 in Oryza. *New Phytol.* 213, 572–583. doi: 10.1111/nph.14186

Xu, G., Fan, X., and Miller, A. J. (2012). Plant nitrogen assimilation and use efficiency. *Annu. Rev. Plant Biol.* 63, 153–182. doi: 10.1146/annurev-arplant-042811-105532

Xu, Y., Hu, W., Liu, J., Zhang, J., Jia, C., Miao, H., et al. (2014). A banana aquaporin gene, *MaPIP1; 1*, is involved in tolerance to drought and salt stresses. *BMC Plant Biol.* 14:59. doi: 10.1186/1471-2229-14-59

Xu, Z., Zhou, G., and Shimizu, H. (2009). Are plant growth and photosynthesis limited by pre-drought following rewatering in grass? *J. Exp. Bot.* 60, 3737–3749. doi: 10.1093/jxb/erp216

Xu, Z., Zhou, G., and Shimizu, H. (2010). Plant responses to drought and rewatering. *Plant Signal. Behav.* 5, 649–654. doi: 10.4161/psb.5.6.11398

Yang, H., Menz, J., Häussermann, I., Benz, M., Fujiwara, T., and Ludewig, U. (2015). High and low affinity urea root uptake: involvement of NIP5; 1. *Plant Cell Physiol.* 56, 1588–1597. doi: 10.1093/pcp/pcv067

Yang, X. X., Li, Y., Ren, B. B., Ding, L., Gao, C. M., Shen, Q. R., et al. (2012). Drought-induced root aerenchyma formation restricts water uptake in rice seedlings supplied with nitrate. *Plant Cell Physiol.* 53, 495–504. doi: 10.1093/pcp/pcs003

Yu, G., Li, J., Sun, X., Zhang, X., Liu, J., and Pan, H. (2015). Overexpression of AcNIP5; 1, a novel nodulin-like intrinsic protein from halophyte *Atriplex canescens*, enhances sensitivity to salinity and improves drought tolerance in Arabidopsis. *Plant Mol. Biol. Rep.* 33, 1864–1875. doi: 10.1007/s11105-015-0881-y

Yu, Q., Hu, Y., Li, J., Wu, Q., and Lin, Z. (2005). Sense and antisense expression of plasma membrane aquaporin BnPIP1 from *Brassica napus* in tobacco and its effects on plant drought resistance. *Plant Sci.* 169, 647–656. doi: 10.1016/j.plantsci.2005.04.013

Zhang, D. Y., Ali, Z., Wang, C. B., Xu, L., Yi, J. X., Xu, Z. L., et al. (2013). Genome-wide sequence characterization and expression analysis of major intrinsic proteins in soybean (*Glycine max* L.). *PLoS One* 8:e56312. doi: 10.1371/journal.pone.0056312

Zhang, D.-Y., Kumar, M., Xu, L., Wan, Q., Huang, Y.-H., Xu, Z.-L., et al. (2017). Genome-wide identification of major intrinsic proteins in *Glycine soja* and characterization of GmTIP2; 1 function under salt and water stress. *Sci. Rep.* 7:4106. doi: 10.1038/s41598-017-04253-z

Zhang, J., Jia, W., Yang, J., and Ismail, A. M. (2006). Role of ABA in integrating plant responses to drought and salt stresses. *Field Crops Res.* 97, 111–119. doi: 10.1016/j.fcr.2005.08.018

Zhang, L., Yan, J., Vatamaniuk, O. K., and Du, X. (2016). CsNIP2; 1 is a plasma membrane transporter from *Cucumis sativus* that facilitates urea uptake when expressed in *Saccharomyces cerevisiae* and *Arabidopsis thaliana*. *Plant Cell Physiol.* 57, 616–629. doi: 10.1093/pcp/pcw018

Zhang, X., Zhang, L., Dong, F., Gao, J., Galbraith, D. W., and Song, C.-P. (2001). Hydrogen peroxide is involved in abscisic acid-induced stomatal closure in *Vicia faba*. *Plant Physiol.* 126, 1438–1448. doi: 10.1104/pp.126.4.1438

Zhang, Y., Wang, Z., Chai, T., Wen, Z., and Zhang, H. (2008). Indian mustard aquaporin improves drought and heavy-metal resistance in tobacco. *Mol. Biotechnol.* 40, 280–292. doi: 10.1007/s12033-008-9084-1

Zhou, Y., Lam, H. M., and Zhang, J. (2007). Inhibition of photosynthesis and energy dissipation induced by water and high light stresses in rice. *J. Exp. Bot.* 58, 1207–1217. doi: 10.1093/jxb/erl291

Zhuang, L., Liu, M., Yuan, X., Yang, Z., and Huang, B. (2015). Physiological effects of aquaporin in regulating drought tolerance through overexpressing of *Festuca arundinacea* aquaporin gene FaPIP2; 1. *J. Am. Soc. Hortic. Sci.* 140, 404–412.

Conflict of Interest Statement: The authors declare that the research was conducted in the absence of any commercial or financial relationships that could be construed as a potential conflict of interest.

Advantages of publishing in Frontiers

OPEN ACCESS
Articles are free to read for greatest visibility and readership

FAST PUBLICATION
Around 90 days from submission to decision

HIGH QUALITY PEER-REVIEW
Rigorous, collaborative, and constructive peer-review

TRANSPARENT PEER-REVIEW
Editors and reviewers acknowledged by name on published articles

Frontiers
Avenue du Tribunal-Fédéral 34
1005 Lausanne | Switzerland

Visit us: www.frontiersin.org
Contact us: info@frontiersin.org | +41 21 510 17 00

REPRODUCIBILITY OF RESEARCH
Support open data and methods to enhance research reproducibility

DIGITAL PUBLISHING
Articles designed for optimal readership across devices

FOLLOW US
@frontiersin

IMPACT METRICS
Advanced article metrics track visibility across digital media

EXTENSIVE PROMOTION
Marketing and promotion of impactful research

LOOP RESEARCH NETWORK
Our network increases your article's readership